United Nations Scientific Committee on the Effects of Atomic Radiation

SOURCES, EFFECTS AND RISKS OF IONIZING RADIATION

UNSCEAR 2024 Report

Volume II

SCIENTIFIC ANNEX B:

Evaluation of public exposure to ionizing radiation

UNITED NATIONS

SOURCES, EFFECTS AND RISKS OF IONIZING RADIATION

United Nations Scientific Committee on the Effects of Atomic Radiation

UNSCEAR 2024
Report to the General Assembly with Scientific Annexes

VOLUME II
Scientific Annex B

UNITED NATIONS
New York, 2025

NOTE

The report of the Committee without its annexes appears as *Official Records of the General Assembly*, Seventy-ninth Session, Supplement No. 46 (A/79/46).

The designations employed and the presentation of material in this publication do not imply the expression of any opinion whatsoever on the part of the Secretariat of the United Nations concerning the legal status of any country, territory, city or area, or of its authorities, or concerning the delimitation of its frontiers or boundaries.

The country names used in this document are, in most cases, those that were in use at the time the data were collected or the text prepared. In other cases, however, the names have been updated, where this was possible and appropriate, to reflect political changes.

The attachments cited in this annex are electronically available from the UNSCEAR website.

UNITED NATIONS PUBLICATION
Sales No. E.25.IX.2
ISBN: 978-92-1-003331-2
eISBN: 978-92-1-106874-0

ANNEX B

EVALUATION OF PUBLIC EXPOSURE TO IONIZING RADIATION

CONTENTS

The attachments cited in this annex and its appendices are electronically available for download from https://www.unscear.org/unscear/en/publications/2024_2_Attachments.html

LIST OF ABBREVIATIONS

AGR	Advanced gas cooled reactor
AM	Arithmetic mean
BWR	Boiling-water reactors
CT	Computed tomography
CTBTO	Comprehensive Nuclear-Test-Ban Treaty Organization
DC	Dose coefficient
DPRK	Democratic People's Republic of Korea
DU	Depleted uranium
EC	European Commission
EEC	Equilibrium equivalent concentration
EHV	Extreme high values
EXPACS	Excel-based program for calculating atmospheric cosmic-ray spectrum
EURT	East Urals radioactive trace
GLE	Ground level enhancements
GM	Geometric mean
GSD	Geometric standard deviation
HBRA	High background radiation area
HDI	Human development index
IAEA	International Atomic Energy Agency
ICAO	International Civil Aviation Organization
ICRP	International Commission on Radiological Protection
ICRU	International Commission on Radiation Units and Measurements
ISL	In-situ leaching
LLWR	Low-level waste repository
NCP	National Contact Person
NEA	Nuclear Energy Agency
NNSS	Nevada National Security Site
NORM	Naturally occurring radioactive material
NPP	Nuclear power plant
OECD	Organisation for Economic Co-operation and Development
PDF	Probability density function
PPGHO	Priargunsky Mining and Chemical Production Association
REE	Rare earth elements

RPK	Revenue passenger kilometres
RTG	Radioisotope thermoelectric generator
SD	Standard deviation
UNEP	United Nations Environment Programme
UNSCEAR	United Nations Scientific Committee on the Effects of Atomic Radiation
WHO	World Health Organization

I. INTRODUCTION

1. Exposure of the public to ionizing radiation from natural and human-made sources was firstly evaluated by the Committee in the UNSCEAR 1958 Report [U8]. Further evaluations have been carried out at regular intervals over the years since then [U10]. This annex presents an updated evaluation of public exposure to ionizing radiation that takes account of several developments since the last comprehensive assessment undertaken by the Committee and published in the UNSCEAR 2008 Report, annex B [U19]. Since that report, the Committee has evaluated radiation exposure of the public arising from electricity generation considering the principal relevant commercial technologies, both nuclear and non-nuclear, in the UNSCEAR 2016 Report [U24]. In doing so, the Committee reviewed and revised its methodology for estimating public exposure due to radioactive discharges to the environment. The Committee also updated the methodology for estimating public exposure from radon and its decay products in the UNSCEAR 2019 Report, annex B [U27], and published its final report related to the accident at the Fukushima Daiichi Nuclear Power Station (NPS) in 2022 [U29]. In addition, the Committee has been exploring ways to improve the collection, analysis and dissemination of data on radiation exposure from natural and human-made sources of ionizing radiation. This annex also draws on the experience gained from the UNSCEAR 2012 Report, annex B [U23] and 2017 Report, annex A [U25] in developing quality criteria for the evaluation of public exposure data.

2. Public exposure to ionizing radiation varies across the world because of differences in natural sources and in the uses of both natural and human-made sources. Two categories of data on public exposures vary over time and were reviewed and analysed: changes in public exposures over time resulting from the introduction of new or improved practices, technologies and revised regulations and new data from studies on public exposure carried out in many countries since the publication of the UNSCEAR 2008 Report, annex B [U19].

A. Scope and objectives of the annex

3. The objectives of this annex are:

(a) To provide a comprehensive and independent evaluation of public exposures to natural and human-made sources of radiation. More specifically:

i. To identify sources and radiation levels worldwide of public exposures to naturally occurring ionizing radiation and assess relevant doses to the public;

ii. To identify sources and radiation levels worldwide of public exposures to human-made sources of ionizing radiation, including past radiological accidents, and assess relevant doses to the public;

iii. To review and update, as appropriate, parameters included in the methodology for the evaluation of public exposures from radioactive discharges presented in the UNSCEAR 2016 Report [U24] and used to estimate public exposures from electricity generation from nuclear power. Public exposures from other forms of electricity generation have not, however, been reevaluated in this annex;

iv. To assess the variability and uncertainties of public exposures worldwide to different sources to the extent possible;

v. To allow readers to derive benchmarks for comparison purposes and to manage exposures.

(b) To identify and analyse temporal and spatial trends in exposures from natural and human-made sources of ionizing radiation. More specifically:

i. To identify contributions of different sources to overall public exposure;

ii. To evaluate temporal variations in public exposure since the UNSCEAR 2008 Report;

iii. To assess dependence of exposures to geographical and environmental features.

(c) To identify essential data and develop quality requirements and quality criteria for data evaluation for public exposure from natural and human-made radiation sources.

4. The annex also identifies areas where improvements in global assessments of public exposure to ionizing radiation and further research in the development of environmental models are needed to better analyse the sources and levels of exposure of the public and their potential impact on the public.

5. This annex focuses on the evaluation of exposure of the public to ionizing radiation from natural and human-made sources distributed across an environment and human habitat, or present in various types of facilities where exposures occur as part of everyday life. Occupational exposures of radiation workers and medical exposures of patients to ionizing radiation are not subjects of this annex as they were evaluated in UNSCEAR 2020/2021 Report, annex A and annex D, respectively [U30, U31].

6. For practical reasons, the Committee uses quantities and concepts recommended by the International Commission on Radiological Protection (ICRP) and the International Commission on Radiation Units and Measurements (ICRU) for purposes of radiation protection. Both ICRP and ICRU have developed a comprehensive system of radiation protection dosimetry that allows the determination of doses to members of the public from exposure to both external and internal irradiation and the quantities and units recommended by these organizations are widely used and reported around the world. Furthermore, continuing use of these quantities enables comparison with previous UNSCEAR reports.

7. This annex does not cover exposures of the public previously described in detail in other UNSCEAR reports; where appropriate, new information is provided alongside summary of information provided in those annexes. In particular, exposures associated with accidental releases are not dealt with extensively because the Committee evaluated these exposures in the UNSCEAR 2008 Report, annexes C and D [U20]; and UNSCEAR 2020/2021 Report, annex B [U29].

8. There are many uncertainties associated with the information provided in this annex, owing to the different ways countries collect, analyse, and manage their data. These uncertainties reflect differences in the methodologies for sampling, measuring, treating, and reporting data, as well as differences in assessment approaches. The Committee recognizes that standardized methodologies need to be used to improve the comparison and analysis of reported data and to draw more reliable conclusions. To address some of the uncertainties and to provide for consistency in the treatment of data, quality criteria were established for the selection of the information to be considered. The quality criteria, including unified statistical procedures, are presented in detail in electronic attachment A-7.

B. Sources of public exposure to ionizing radiation

9. The world population is exposed to ionizing radiation from sources of two types: natural and human-made. The following radiation sources of public exposure are considered in this annex:

(a) Natural sources of ionizing radiation:

i. Radon and thoron;

ii. Natural radionuclides other than radon and thoron;

iii. Enhanced sources of naturally occurring radioactive material.

(b) Human-made sources of ionizing radiation:

i. Nuclear power production and related nuclear fuel cycle facilities;

ii. Radioactive waste management;

iii. Applications other than nuclear power production;

iv. Military use of nuclear and radioactive materials;

v. Exposure from radiological accidents and past peaceful practices;

vi. Transport of nuclear and radioactive material.

10. This categorization is considered to be the most consistent with the Committee's earlier evaluations [U15, U19] and facilitates the comparison of the results and the assessment of trends. The methodologies adopted by the Committee for the assessment of public doses in this annex are described in detail in appendix A, and in electronic attachments A-1 to A-6, while a general summary is given in chapter II.

1. Natural sources of ionizing radiation

11. Exposure of the public to ionizing radiation from natural sources is a ubiquitous feature of life on Earth and is influenced by many human factors, such as the proportion of time people spend outdoors or indoors, the type and material of buildings where people reside or work, the ventilation of these premises, and the dietary habits of people.

12. For most individuals, exposure to sources of natural radiation is higher than that from all human-made radiation sources combined. Notable exceptions include elevated exposures through medical diagnostic or radiotherapy procedures, radiological incidents involving environmental release of radionuclides, and occupational exposure in specific work environments. Nevertheless, natural background radiation is used as the reference level against which all additional exposures are measured and evaluated.

13. There are two main contributors to exposures from natural sources of radiation:

(a) High-energy cosmic ray particles incident on the Earth's atmosphere;

(b) Radionuclides that originated in the Earth's crust at its formation and are present everywhere in the environment and in the human body.

14. The most significant source of public exposure to ionizing radiation is natural radon and its decay products that are inhaled by people from both indoor and outdoor air. Radon originates from the decay of radium present in the ground and in building materials; radium is part of the uranium and thorium decay chains which are present in all soils and rocks in various amounts.

15. The evaluation of doses from natural sources mostly focused on exposures to typical levels of the natural radiation background, but data are also presented for areas designated in the literature as high background radiation areas (HBRAs). It is important to highlight that the levels of natural background radiation vary around the world.

16. Another source of public exposure to natural ionizing radiation is the industrial application of various materials containing sources of natural radiation, such as the mining, milling, and processing of ores and the use of fossil fuels containing natural radionuclides [U24]. In cases where natural sources of ionizing radiation are modified by industrial practices, the term naturally occurring radioactive materials (NORM) is used in this annex to refer to these materials.

2. Human-made sources of ionizing radiation

17. The world population is also exposed to environmental releases of ionizing radiation from human-made sources, such as those related to nuclear weapons production/testing, operating nuclear power production facilities, and other applications of human-made radionuclides used for various peaceful purposes (e.g., in medicine, some industries and in some consumer products). Other sources of exposure include the transport of radioactive material and radioactive waste management at the end of these technological chains. The evaluation of radiological consequences of those activities in terms of already received doses or dose commitments, individual and collective, constitutes the subject of chapter IV of the annex.

18. Currently, the largest-scale activity associated with continuous releases of human-made radionuclides into the environment is the generation of electrical energy in nuclear power plants (NPPs)[1] and related processes. Overall, nuclear power capacity has shown a gradual growth trend over the past decade [I41]. The availability of extensive monitoring and reporting of radionuclide discharges to the environment from nuclear facilities allows for a comprehensive evaluation of public exposures from this source. Estimates of doses and analysis of temporal trends are included in section IV.A of this annex.

19. Global fallout from atmospheric tests of nuclear weapons were the most significant sources of exposure of the world's population to human-made sources of ionizing radiation. Although atmospheric testing has ceased and the Committee's assessment of global doses based on measured deposition of ^{90}Sr remains an accurate evaluation of the resulting exposures, some new data on long-term exposure of the public were assessed and doses were re-evaluated by the Committee. Estimates of doses from long-lived radionuclides are presented in section IV.D of this annex.

20. Section IV.D also reviews new information on public exposure from sites contaminated with residual radionuclides associated with past military activities, commonly referred to as legacy sites. New data on radiation doses to the public residing in the vicinity of the Mayak Production Association facility, the first plutonium and tritium production facility in the former Soviet Union have been reconstructed from historical data and reviewed by the Committee for the purpose of this annex.

[1] The term nuclear power station (NPS) is also generally accepted as a synonym for NPP. For example it was used in UNSCEAR publications on the Fukushima NPS accident [U29].

21. Section IV.E includes an assessment of new data on public exposure from radiological accidents and other past practices. The Committee last evaluated radiological consequences of the accident at the Chornobyl NPP in its 2008 Report, annex D [U20]. Information collected since then has been reviewed in this annex. The Committee recently reviewed the radiological consequences of the Fukushima Daiichi NPS accident in its UNSCEAR 2020/2021 Report, annex B [U29]. A short summary is included in this annex since there has been no substantial new information published. Section IV.F summarizes the latest information related to transport of nuclear and radioactive material.

II. DOSE ASSESSMENT METHODOLOGY

22. The most recent reports describing the methodology for the assessment of public doses are the UNSCEAR 2000 Report, annex A [U15, U19, U24], the UNSCEAR 2008 Report, annex B [U15, U19, U24] and the UNSCEAR 2016 Report, annex A [U15, U19, U24]. The methodology was reviewed and updated as appropriate in this annex to take account of improvements in the models used and new data found in the literature, such as:

(a) Advances in the model used to calculate dose rate from cosmic rays outdoors to account for geomagnetic latitude, altitude and the 11-year solar activity cycle;

(b) Expanding the dose assessment methodology used to evaluate radioactive discharges from nuclear power production and related nuclear fuel cycle facilities to account for liquid discharges from uranium mining and milling.

Consistent values were also established for model parameters that are common to the dose assessment methodologies used for different topic areas and are provided in appendix A.

23. The methodology aimed to provide best estimates of the dose to a characteristic individual unless otherwise stated in contrast to other established methodologies which aim to ensure that doses are not underestimated and thus adopt cautious parameter values and assumptions. The Committee first defined a characteristic individual in its UNSCEAR 2016 Report, annex A [U24] and noted that this is not to be confused with the representative person (previously termed by the ICRP as the critical group) used for radiation protection purposes [I70]. The dose to the characteristic individual is indicative of most people living in an area and exposed to a particular source of ionizing radiation. The dose to the characteristic individual is assessed by means of dosimetric models that quantify external and internal exposure, as appropriate. The values of the parameters related to human habits (e.g., breathing rate, ingestion rates of food and drinking water, time spent indoors) of the characteristic individual were based on established generic data from published literature.

24. Doses to the public were either calculated based on environmental measurements or model predictions of radiological quantities, such as ambient dose equivalent rate or radionuclide activity concentrations in various media, or taken from scientific papers and official national and international reports. Models used in the assessment of doses varied in their complexity: very simple models were used to calculate doses from inhalation of radon while compartment models were used to calculate doses associated with global fallout or discharges from nuclear facilities. In some cases (e.g., non-nuclear source applications), the only available information is dose estimates published in the literature or official reports.

A. Dose quantities and units

25. The basic dosimetric quantity used in the Committee's evaluation of public exposure is the effective dose as this is the quantity that is better suited for comparison of public exposure from different sources and more widely used and reported by many regulatory authorities. The effective dose is a quantity defined by the ICRP for the purpose of radiological protection [I70] as:

$$E = \sum_t w_t \sum_r w_r D_{t,r} \quad (1)$$

where w_r and w_t are the radiation weighting factors and the tissue weighting factors respectively and $D_{t,r}$ is the mean absorbed dose received by the organ or tissue *t* due to radiation *r*. The effective dose is a conventional quantity defined by ICRP for a reference person based on the averaging of individual-related characteristics of the human body. The SI unit for the effective dose is J/kg, and its special name is sievert (Sv) [I70].

26. Another radiation protection quantity is the committed effective dose from radionuclides incorporated into the human body as defined by the ICRP as the effective dose expected to be delivered during the time when these radionuclides are expected to irradiate organs and tissues, called the commitment time. The commitment time is assumed to be 50 years for adults, and to age 70 years for other age groups [I70].

27. For consistency, this annex adopts the same approach used in the UNSCEAR 2000 Report, annex A [U15]. The total annual effective dose to members of the public (E_{total}) is the sum of the effective dose from external exposure (E_{ext}) received over one year, and the committed effective dose from internal exposure due intake of radionuclides over the same year (E_{int}) [U15]:

$$E_{total} = E_{ext} + E_{int} \quad (2)$$

28. The effective dose from external exposure can be derived from the operational quantity ambient dose equivalent or approximated by personal dose equivalent, provided by radiation monitoring equipment or can also be calculated from activity concentrations of radionuclides in the environment and appropriate dose coefficients for external exposure [I77].

29. The committed effective dose from internal exposure from intakes of radionuclides (E_{int}) is the sum of the committed effective dose due to inhalation (E_{inh}) and the committed effective dose due to ingestion of radioactive material (E_{ing}):

$$E_{int} = E_{inh} + E_{ing} \quad (3)$$

30. The latter method was commonly used to estimate effective doses from external exposure in this annex. The individual committed effective dose from exposure to internal radiation can be estimated from the activity concentration and physico-chemical forms of radioactive material in air foods, drinking water and dose coefficients for internal exposure contained in relevant ICRP publications [I69, I73, I75].

31. Since its 1993 Report, annexes A and B [U13], the Committee has also used the age-weighted effective dose, E_{a-w}, to assess doses to the public. This conventional quantity is the sum of the effective doses for three age groups (infants, children and adults), weighted using the fractions of these age groups in the overall population:

$$E_{a-w} = 0.05\, E_{infant} + 0.30\, E_{child} + 0.65\, E_{adult} \quad (4)$$

E_{infant}, E_{child} and E_{adult} are the doses to a 1-year-old infant, a 10-year-old child and an adult, respectively.

32. To obtain a global estimate of the exposure of members of the public to natural radiation sources, worldwide averages of the relevant doses were calculated using estimates for each country weighted according to the population of the country. It should be noted that worldwide average doses are in fact representative only of the countries for which information was available.

33. The collective effective dose S (in unit of person-Sv) is calculated from the average effective dose in a particular subgroup (E_i) and the number of people in that subgroup ($N(E_i)$ as:

$$S = \sum_i N(E_i)E_i \quad (5)$$

34. Extensive quantities, such as the collective dose, reflect the size of the system it describes and generally provide limited useful information unless they are related to another relevant extensive quantity. For instance, the Committee reported collective doses per unit of an attributable practice (e.g., the collective dose per unit of generated electrical energy) in previous reports [U24].

35. In this annex, collective effective doses were calculated mostly for radiation sources for which the Committee has developed specific dose assessment methodologies, such as radon and thoron, natural radionuclides, and radioactive discharges, and were used to compare the radiation exposures of populations from different sources of ionizing radiation locally and in different regions globally. The Committee does not consider it appropriate to extrapolate incremental doses equivalent to, or less than, normal natural background levels to estimate absolute numbers of radiation-induced health effects within a population.

B. Data sources

36. The evaluation of public exposure to ionizing radiation in this annex was based on input data obtained in the same manner as for previous UNSCEAR reports [U15, U19] from the following sources:

(a) UNSCEAR Global Survey on Public Exposure;

(b) Review of the published peer-reviewed literature and official reports;

(c) International organizations.

37. The timeframe of the information collected for this annex was the period between 2007 and 2020. The start year of 2007 was selected to capture data published in the year prior to the publication of UNSCEAR 2008 Report, annex B [U19]. Since public exposure from naturally occurring sources of ionizing radiation are generally considered to be well understood and relatively constant over time, the evaluation focused on identifying new data and improved understanding of these sources. For other sources of ionizing radiation, data and information were evaluated to quantify their magnitude, to determine if understanding of these sources has improved, and to identify any temporal trends. For completeness, information for the period 2005−2006 was also collected from the published literature that was not referenced in the UNSCEAR 2008 Report, annex B [U19].

1. Global Survey on Public Exposure

38. The UNSCEAR Global Survey on Public Exposure was conducted by means of a series of questionnaires distributed to all United Nations Member States through National Contact Persons

(NCPs), which were designed to elicit essential data on a national or regional scale from the Member States that are necessary to evaluate public exposures.

39. The questionnaire covered five topic areas: *(a)* radon and thoron; (*b)* natural sources other than radon; *(c)* discharges from nuclear fuel cycle facilities; *(d)* applications other than nuclear power; and *(e)* sites and areas contaminated with radionuclides due to past activities or accidents.

40. For exposure to radon and thoron, measurements of activity concentrations in indoor and outdoor air were identified as essential data. Activity concentrations of radon in drinking water were also considered essential.

41. For natural sources of ionizing radiation excluding radon and thoron, essential data included measurements of air kerma rates,[2] ambient dose equivalent rates both indoors and outdoors, and measurements of activity concentrations of radionuclides of natural origin in soils and building materials, such as concrete, bricks and rocks. Data for areas identified as HBRA were requested separately. For NORM industries, the number of facilities, annual production, and annual waste produced were identified as essential data. References were also requested to official publications containing more specific data, such as measurements of activity concentrations or dose evaluations.

42. The essential data requested for nuclear power production and related facilities were annual atmospheric and liquid discharges. The radionuclide composition of discharges, and if applicable, the body of water into which liquid discharges occurred (i.e., river, lake, marine) were also requested.

43. Preliminary research indicated that obtaining data for applications other than nuclear power production might be a challenge. Therefore, the questionnaire focused on identifying the prevalence of these sources in Member States, pathways of exposure, characteristics of exposed individuals, and estimated annual doses. The requested data were separated into three categories: *(a)* medical applications; *(b)* industrial, agricultural and research applications; *(c)* consumer products.

44. The essential data requested for sites and areas where radionuclides are present due to past civil or military activities or accidents. included the location of settlements, the spatial extent of residual radioactivity, a brief description of the affected area along with the inventory of the main radionuclides, including activity concentrations in the media of concern (e.g., soil, water). The time when these data were collected was also requested to account for radioactive decay and ingrowth. Data were requested only for those remediated sites that require continued management of any residual radioactivity.

2. Literature review

45. The approach to identify and evaluate peer reviewed literature on public exposure to ionizing radiation built on the experience gained in the preparation of the White Papers on the Fukushima Daiichi NPS accident following the UNSCEAR 2013 Report, annex A [U22], and subsequent reports, such as UNSCEAR 2017 Report, annex A, [U25] and UNSCEAR 2020/2021 Report, annex B [U29].

46. The objective of the literature review was to identify new data since the UNSCEAR 2008 Report, annex B [U19] to complement obtained from the UNSCEAR Global Survey on Public Exposure. The review also provided evidence to support assumptions and parameters used in the dose assessments performed for this annex.

[2] For external dose from terrestrial gamma radiation this may be assumed to be equivalent to absorbed dose rate in air.

47. A search and selection process was used to identify the publications with the potential to provide information for the Committee's evaluation. The publications compiled from the search and selection process were screened further using three key criteria:

(a) Absence of conflicts of interest among authors;

(b) Inclusion of only original publications, governmental, or international reports (editorials, commentaries and correspondence were excluded); and

(c) Inclusion of publications that contained quantitative measurement or assessment data of acceptable quality, in terms of completeness and ability to extract the data, information on quality control procedures and use of appropriate statistical methods.

48. Preference was given to scientific articles published in peer-reviewed journals and reports from international organizations, as they are subject to a rigorous review process prior to publication. Reports published by government departments and national organizations were also considered reliable sources as they also undergo a review and approval process before their publication.

49. Data on public exposure were used as originally reported. Where necessary, quantities and units were converted to those adopted in this annex.

3. Data from international organizations

50. In addition to the UNSCEAR Global Survey on Public Exposure and the literature review, international organizations were key sources of data to evaluate public exposure to ionizing radiation. Relevant international organizations included the Comprehensive Nuclear-Test-Ban Treaty Organization (CTBTO), Food and Agriculture Organization (FAO), European Commission (EC) and its Joint Research Centre (JRC), International Atomic Energy Agency (IAEA), International Civil Aviation Organization (ICAO), Nuclear Energy Agency of the OECD (OECD/NEA), United Nations Environment Programme (UNEP), and the World Health Organization (WHO).

51. Information provided by the international organizations is generally compiled in a consistent format and often on a global scale. Some datasets overlapped with those from other sources or lacked information on quality criteria, limiting their usefulness, but were nevertheless valuable to verify independently other information and, in some cases, to identify gaps. For example, the IAEA Power Reactor Information System (PRIS) database[3] [I56] was used to support data on nuclear power generation provided by Member States through the UNSCEAR Global Survey on Public Exposure. Similarly national radon survey data compiled by WHO were used to confirm whether results from these surveys were reported in the literature or provided through the UNSCEAR Global Survey on Public Exposure.

[3] The Power Reactor Information System (PRIS) is a comprehensive database developed and maintained by the IAEA that contains information on nuclear power reactors in operation, under construction, or those being decommissioned.

C. Review of data collected for the evaluation of public exposure

52. The data of interest for the evaluation of public exposure included:

(a) Dose rate measurements;

(b) Radionuclide activity concentrations in environmental media;

(c) Discharges of radionuclides to the environment;

(d) Doses to the public reported in published literature and official reports provided by Member States.

53. Activity concentrations of radionuclides in environmental media, such as air (indoor and outdoor), soil, rocks, building materials, drinking water, and food, are essential input data for assessing public radiation doses. Table 1 presents an inventory of environmental and source measurements compiled from the UNSCEAR Global Survey on Public Exposure, supplemented by published literature and other sources. These data were used to estimate public doses across different regions and globally.

54. Table 1 summarizes the number of measurement points for radon and its decay products in air and drinking water, as well as measurements of activity concentrations of other natural radionuclides in soil and building materials, categorized by region collated for this annex. European Member States contributed the majority of radon measurements, with significant input also from Member States in Asia and the Pacific, and North America. Indoor and outdoor activity concentrations of radon and thoron in air are typically derived from national or regional surveys. Table 1 also gives the number of measurements of natural radionuclides other than radon in soil and building materials, broken down by region. Most of these measurements were submitted by Member States in Africa, Asia and the Pacific, and Europe.

55. The most commonly measured quantities for external exposure are the air kerma rate and the ambient dose equivalent rate. These measurements are typically taken at a standard height of 1 metre above ground in locations where individuals spend a significant portion of their time or floor. In this annex, dose rates from terrestrial radiation were primarily estimated based on the activity concentrations of naturally occurring radionuclides in soil and rock. For human-made sources, radiation dose rates are measured through environmental monitoring programmes designed to verify that public exposure levels comply with national safety standards. Generally, the contribution of human-made sources to public exposure is lower than that of natural sources.

56. This annex uses data on activity concentrations in drinking water (tap water) obtained from literature surveys, along with IAEA analysis of other foods and mineral water up to 2017 [I44, I48], to evaluate internal exposure doses from naturally occurring radionuclides (excluding radon and thoron). These datasets have been supplemented with relevant information available through 2022 to ensure a more comprehensive assessment.

57. The volume of data on radioactive discharges from nuclear power production facilities reported by Member States reflects the geographic distribution of operational nuclear power plants, particularly in Asia and the Pacific, Europe, and North America (see Table 1). These datasets are generally comprehensive, as nuclear facilities are subject to strict regulatory oversight and are required to submit annual discharge reports to national authorities.

58. However, variations in analytical detection limits and reporting thresholds across nuclear facilities may introduce some uncertainty. These limits can also change over time. As emission controls and fuel performance have improved, resulting in reduced discharges, radionuclides that were previously excluded

from assessments—due to their minimal contribution to radiation dose—have increasingly been included in monitoring and reporting.

59. The same approach was applied to other situations where radiation conditions in the environment are non-uniform, such as areas impacted by the nuclear accidents at the Chornobyl Nuclear Power Plant (NPP) and the Fukushima Daiichi Nuclear Power Station (NPS). In these situations, a single assessment methodology is not feasible and, therefore, doses reported in the literature were used. Additionally, the radioecological conditions in areas affected by nuclear accidents evolve significantly over time and are typically monitored in the long term with less detail than during the initial years following the emergencies. Since this annex primarily focuses on the long-term consequences of major events involving large-scale radionuclide releases to the environment, the available information was often insufficient for the Committee to conduct a dose assessment. This limitation also extends to certain inhabited legacy sites or industrial areas, where detailed monitoring data is either scarce or not readily accessible.

60. Unlike occupationally exposed individuals, members of the public are generally not subject to routine radiation monitoring, except under exceptional circumstances. Nonetheless, analyses of natural and human-made radionuclides in human tissues, such as natural radionuclides in human tissues, ^{137}Cs in the whole body and ^{90}Sr in bones and teeth, have been carried out in the past, notably following global fallout from nuclear weapons testing, and summarized in the UNSCEAR 1962 Report [U9] and subsequent reports.

61. In more recent decades, numerous whole body measurements of activities of certain radionuclides (e.g., ^{137}Cs and ^{134}Cs), as well as assessments of external dose, were conducted in response to major nuclear accidents, such as those at Chornobyl NPP [U20] and Fukushima Daiichi NPS [U29]. Extensive individual monitoring of the public has also been conducted in the Urals for ^{90}Sr, ^{137}Cs, plutonium and primordial ^{40}K to evaluate exposures resulting from radioactive discharges to the Techa River and associated with the Kyshtym accident at the Mayak Production Association facility [D13, T15].

Table 1. Inventory of some activity concentration measurements, and operational NPPs that provided discharge data used to evaluate doses to the public from external and internal exposures

Region	*Activity concentration measurements*					*Radioactive discharges from nuclear facilities to the environment (Number of operational NPPs with discharge data [d])*	
	Radon in air and drinking water (Number of measurement points [a])			*Natural radionuclides [b] in environmental samples (Number of measurements [c])*			
	Indoor air	*Outdoor air*	*Drinking water*	*Soil*	*Building materials*	*Atmospheric*	*Liquid*
Africa	1 519	32	317	1 631	217	1	1
Asia and the Pacific	46 151	1 246	2 001	2 380	229	29	30
Europe	1 074 438	8 742	18 730	1 845	625	83	83
Latin America and the Caribbean	3 603	6	90	83	33	3	3
North America	27 512	82	175	40	5	71	65
West Asia	1 435	110	112	43	34	1	1
Worldwide	**1 154 658**	**10 218**	**21 425**	**6 022**	**1 143**	**188**	**183**

[a] Measurement points are dwellings, outdoor locations, and water sampling points, respectively.

[b] Other than radon.

[c] Radionuclides typically measured in soil and building materials are ^{40}K, ^{238}U, ^{226}Ra, and ^{232}Th.

[d] Number of facilities for which data were submitted via the UNSCEAR Global Survey on Public Exposure, for any year during the period 2007–2020.

D. Analysis of uncertainties and variabilities

62. The Committee evaluated uncertainties in risk estimates for radiation-induced cancer and identified uncertainties in the assessment of exposure and dose as a source of uncertainty in the epidemiological studies used to derive these risk estimates [U23]. In this annex, a Bayesian approach is used for the analysis of uncertainties and variabilities. For measurement uncertainties, the approach is in line with the internationally accepted methodologies formulated in the guides of the Joint Committee for Guides in Metrology (JCGM) [J11, J12, J13]. The Bayesian approach allows uncertainties which are derived from counting and repeated measurements—type A or aleatory uncertainties—and uncertainties originating from other sources—type B or epistemological uncertainties to be considered.

63. Whether it is feasible to quantify uncertainties and variabilities of input data depends on the type of data. The types of analysis that can be performed range from a full analysis of the uncertainty to merely descriptive statistics of the available data. Descriptions of the uncertainty analyses carried out for the dose assessments for different sources are given in the relevant sections of chapters III and IV of this annex.

64. The uncertainties arising from dose rate measurements include the spatial and temporal variabilities of the dose rate which depend on the area monitored. Factors, such as climate, time and season, can contribute to the uncertainties of the dose assessment based on this measurements [I91]. Uncertainties also arise from the different measurement devices used, the calibration and counting procedures, and the statistical calculation methods.

65. When doses from reports are used directly in the annex, the opportunity for independent dose validation is limited. The annex provides an overview of original dose estimates with an indication of their specific features. Uncertainty and variability in the collected data have been assessed and presented in the relevant sections of this annex with a discussion of how they have been considered.

66. Both variability and measurement uncertainty are described by probability density functions (PDFs) quantifying the probability that a quantity has a certain true value given all available information. The PDFs of the final quantities are obtained by propagating the PDFs associated with the input quantities. The mean values and the variances of the final PDF are the best estimates of the true values of the output quantities and quantify their associated uncertainty. The final PDFs also allow coverage intervals and any desired quantiles of the output quantities to be calculated. If temporal trends are investigated or comparisons between two data sets are required, the final PDFs also need to be taken into consideration. More information on how uncertainties and variabilities are dealt with, particularly with reference to this annex, is given in appendix B and in electronic attachment A-6.

III. PUBLIC EXPOSURE FROM NATURAL SOURCES OF IONIZING RADIATION

67. There are two main natural sources of ionizing radiation contributing to public exposures: high-energy cosmic ray particles incident on the atmosphere, and radionuclides that originated in the Earth's crust. Naturally occurring radionuclides are also released to the environment as a result of industrial activities associated with the processing of minerals, such as the production of phosphate fertilizer and oil and gas extraction.

A. Radon and thoron

68. Radon is a chemically inert noble gas. Its most common radioactive isotope, also commonly referred to as radon, is ^{222}Rn and has a half-life of 3.82 days. Radon is generated as an intermediate product in the radioactive decay chain of ^{238}U present in rocks and soils in varying concentrations across all geological formations. A portion migrates through pore spaces and fractures, eventually emanating into the atmosphere, leading to human exposure via inhalation of both radon and its short-lived radioactive progeny. Because of its solubility in water, radon is also present in groundwater that passes through uranium-bearing soils and rocks. Consequently, exposure may also occur through ingestion of water and inhalation of radon released from water into the air.

69. Thoron (^{220}Rn), a radioactive isotope of radon with a half-life of 55.6 seconds, is also an inert noble gas and arises from the decay chain of ^{232}Th. Thorium is a common element in the Earth's crust and therefore, similarly to radon, thoron is universally present in air at varying concentration levels. The radioactive half-lives of radon and thoron and their respective decay products are important in determining the exposures from these radionuclides. Since thoron has a much shorter half-life than radon, the distance it can travel before undergoing radioactive decay is much shorter than the distance radon can travel in the same medium. Factors affecting exposure from radon and thoron are discussed in more detail in sections III.A.2. and III.A.3, respectively.

70. Radon and its short-lived decay products are the most important radionuclides contributing to human exposure from natural sources. While the health risks associated with exposures to high environmental levels of radon in underground mines have been known for a long time, relatively little attention was paid to radon exposure in dwellings and workplaces until the 1970s, when scientists began to realize that exposures to indoor radon could be significant. Since then, there have been many studies and publications on this topic.

71. The Committee previously considered sources and effects of exposure to radon and thoron in three comprehensive reports [U15, U18, U19]. The Committee concluded that radon, thoron and their decay products are established carcinogens for the lung while doses to other organs and tissues were at least an order of magnitude smaller than doses to the lung. The Committee also recognized that the mean annual individual dose from inhalation of radon and its decay products was typically about half of the dose received on average by members of the public from all natural sources of ionizing radiation.

1. Outline of the dose assessment methodology

72. The methodology for the assessment of doses from inhalation of radon and thoron and ingestion of radon in drinking water used in this annex is based on the methodology adopted in previous UNSCEAR reports [U15, U21, U27].

73. Dose to the lungs from inhalation of radon and thoron decay products were based on the equilibrium equivalent concentrations (EEC) of radon and thoron which are obtained by measuring the decay products. For radon an alternative approach is to use activity concentration of radon in air only together with an equilibrium factor. This approach was not used for thoron because of the large variability in the values of the equilibrium factor for this radionuclide [U15]. The equilibrium factors for radon adopted in previous UNSCEAR reports [U15, U19] of 0.4 and 0.6 for indoor and outdoor concentrations were also used in this annex. More information on the equilibrium factors is given in appendix A.

74. This annex adopted the same dose coefficients of 9 and 40 nSv/(Bq h/m^3) for the EEC of radon and thoron respectively as used in previous UNSCEAR reports [U15, U19]. The Committee's review of recent dosimetric and epidemiological studies on lung cancer from inhalation of radon and its decay products, along with dosimetric models developed since 2006, supported the use of these dose coefficients [U28]. More information on the dose coefficients is given in appendix A.

75. For completeness, the annual doses from two other relatively minor exposure pathways were also estimated, namely the dissolution of radon and thoron in blood with distribution throughout the body following inhalation [U15] and ingestion of radon in drinking water.

76. In this annex average radon and thoron concentrations in air, both outdoors and indoors, and drinking water in various countries were estimated based on information provided by Member States through the UNSCEAR Global Survey on Public Exposure and supplemented by data collated from the literature review. The data include both activity concentrations of radon and thoron, and radon or thoron equivalent equilibrium activity concentrations. To ensure that the data were of the quality required and representative of population exposure, specific selection criteria and qualifiers were applied, including measurement duration, population size, number of measurements, sampling design and method (e.g., random or selective), and other factors (e.g., season, and detector location). The method used to determine the distribution of activity concentrations of radon in air (population- vs. non population-weighted) was also considered. Worldwide average concentrations of radon and thoron in air and radon in drinking water and doses to the public were estimated based on statistical parameters from national surveys—arithmetic mean, (AM) geometric mean (GM), geometric standard deviation (GSD).

77. A formal and comprehensive analysis of uncertainty in indoor radon concentrations was not possible because of the complex factors that affect indoor radon concentrations and exposure to radon. Nevertheless, information on sources of uncertainty were used to provide a qualitative evaluation of the uncertainty and variability in radon and thoron concentrations.

78. A more detailed description of the methodology to estimate doses to the public from inhalation of radon and thoron and ingestion of radon in water is given in appendix A. Additional detailed assessment data are presented in electronic attachment A-1.

2. Radon and its decay products

(a) *Factors affecting radon exposure*

79. This section describes the main factors affecting indoor radon concentrations and discusses the main determinants of spatial and temporal variability of these concentrations, as well as the factors affecting radon exposure. A comprehensive overview of the processes governing the generation of radon in the subsurface environment, its transport, and its exhalation is provided in the UNSCEAR 2000 and 2006 Reports [U15, U18] A description of the interdependent factors affecting radon exposure is given in electronic attachment A-1.

Sources of radon

80. The main source of radon is the Earth's subsurface. The concentration of the progenitors of radon, ^{238}U and ^{226}Ra in rock and soil and, consequently, the concentration of radon in the subsurface, varies greatly, mainly because of the geology of the subsurface. Some types of rock are frequently highly enriched in ^{238}U and ^{226}Ra. Typical examples of such rock types are acidic igneous rocks, such as granites

or rhyolites, but organic-rich metamorphic rocks, such as black shales or organic-rich sedimentary rocks, and some varieties of sandstone can also be highly enriched in uranium and radium [B41, K13, S24]. In recent years, numerous studies confirmed the dependence of indoor radon concentration on geogenic controls [A34, B6, B41, B43, C11, D16, L22, P19].

81. In addition to geological characteristics, which are the main controls of the radon potential in the geogenic compartment, the physical characteristics of the soil and weather conditions (e.g., precipitation, air pressure, air temperature) modify the radon potential [B43, P10, P20] by affecting the radon emanation, transport in the soil compartment, and exhalation from the ground. Relevant soil physical characteristics include grain-size distribution, pore-size distribution, bulk density or water saturation, and gas permeability. Weather conditions can modify soil physical characteristics or boundary conditions, which can affect radon emanation, transport, and exhalation. Emanation, transport and exhalation of soil radon differ significantly between open ground and ground under buildings, which shield the soil from the influence of the atmosphere, especially when covering a large area.

82. Emanation is the process by which radon is released in the connected pore space of a porous material, which can also be described as the process of radon generation in the pore space by radioactive decay of its parent radionuclide ^{226}Ra in the soil grains. Radon emanation depends on the concentration of ^{226}Ra and its distribution within the grains, the size and shape of the grains as well as water saturation of the porous material (see UNSCEAR 2000 Report, annex B [U15]). The dependence of radon emanation on soil moisture in unsaturated media has been the subject of several studies [A5, C35, H27, K31, S7]. Results for different clay samples suggest that this general pattern of dependence of radon emanation on soil moisture does not always apply [M26].

83. Radon transport in the ground and radon exhalation from the ground are governed by advective and diffusive processes. Similar to radon emanation, radon transport and exhalation depend on the physical characteristics of the soil and weather conditions [C14, H28, L8, P34, T4], the interplay of which, in turn, governs the soil gas permeability. The advective flux and exhalation of radon also depend on the pressure and temperature gradients between soil air and atmospheric air [S77].

84. A continental-scale map of radon exhalation was produced for Australia [G18] and Europe [K5] using physical-based models. A study by Seco et al. [S24] found a dependence of radon exhalation on the depositional environment of sedimentary rocks with highest values for sandstones and fine-grained siliciclastic rocks for Jurassic rocks. Another study described a large variation of radon exhalation from lithologically different granitic rocks in the Central Iberian Zone with highest values for syn- to late-tectonic mica granites [D21].

85. Radon concentrations in the outdoor environment depend primarily on the exhalation rate from the ground—measured as the activity released per unit time through a unit surface—and the dilution processes in the outdoor environment. The dilution of radon in the outdoor air is driven by weather conditions, since mixing and dilution of outdoor air largely depends on wind speed: higher wind speeds cause rapid mixing and, consequently, a larger dilution of outdoor radon. Certain meteorological conditions, such as inversion weather, can cause limited air exchange between near ground and upper air masses. Another important criterion is the radon concentration in air masses which varies according to its provenance and generally results in lower outdoor radon concentrations in areas near the coast and in higher outdoor radon concentrations in continental regions.

86. Building materials are another source of radon indoors. Recent studies emphasized the role of building materials in contributing to indoor radon concentrations [D16, G24, S2]. Although soil is the main contributor to the indoor radon concentration [C46], building materials may provide the larger fraction of the indoor radon levels in air in regions and countries in which the contribution from soil is small, such as

the Netherlands (Kingdom of the), where on average, approximately two thirds of indoor radon comes from building materials [S56], or in specific situations [S1], especially at higher floor levels [Y7], from very thick walls [F16] or reduced ventilation rates after energy retrofitting interventions [M15].

87. Some studies focused on measurements of radon exhalation rates from building materials which were used in the building structure [C14, F15, H14, K30, R2] and in decorative elements [C23, K24]. Others indicated that the radon exhalation rate depended either on physical characteristics of the material itself, mainly the activity concentration of ^{226}Ra [M36, V7] and the porosity [K48, Z6], or environmental conditions that affected the moisture content [H16]. The use of by-products from NORM industries in building materials should be carefully considered due to the enhanced content of natural radionuclides including ^{226}Ra [C53, K32, N31].

88. The contribution of radon in water to radon in indoor air depends on its activity concentration in the water serving the indoor environment. Different water usages (e.g., showering, laundry) have been investigated for different typologies of water supply in houses [B31] and specific workplaces [S59]. Radon levels at the distribution point depend on the origin of the water, with water from private wells having typically the highest concentrations, and the various processes prior to delivery to the consumer (e.g., storage, transport and treatment) [J19]. Dwellings using water from private wells have been found to have, on average, higher indoor radon concentrations [C11, C28].

Factors affecting indoor radon concentrations

89. Concentrations of radon indoors can be influenced by various factors, such as:

(a) Building characteristics, including tightness of the building shell, age of the building, wall coverings and floor coverings;

(b) Location of sites, including nearby environments, geological materials of the area, and the elevation of the sites;

(c) Meteorological parameters, including rainfall, relative humidity, pressure, temperature, and wind speeds [K38].

90. Entry of radon into buildings is caused by two processes: advective and diffusive flux [C18]. Advective flux results from pressure gradients triggering air flow from the subsurface into the building, while diffusive flux depends on the gradient of concentration and the diffusion coefficient. In instances of increased radon entry into buildings, advection typically emerges as the governing process [E2, M18, R22]. This process is driven by the pressure gradient between the building shell and the surrounding ground near the foundation. It is mainly caused by higher temperatures in the building envelope, leading to what is commonly known as stack effect, and by mechanical ventilation. Wind can also have an impact on the pressure gradients across the building shell and, as a consequence, on radon entry and dilution in a building. The efficacy of this pressure variance in drawing radon-laden soil gas through the foundation hinges on the effective permeabilities of both the building's foundation and the adjacent soil. Notably, wind can reduce the concentrations of radon entering a building due to its diluting effect on radon in the soil surrounding the building [R20].

91. Anomalous subterranean air flows have been observed in certain areas, such as hilly karst terrain, permeable glacial sediments, and rock-avalanche deposit [A37, G3, S77]. In the United States, it was observed that subterranean networks of cavities and fissures can facilitate advective transport of radon-bearing air and that in eskers, which are long, narrow, raised lines of earth, small stones, and sand left on the Earth's surface where melted ice once flowed under a glacier, the coarse sand facilitated underground air flows. In both cases, differences between underground and outdoor air temperatures and

the accompanying differences in air density caused subterranean air to move between the upper and lower parts of the area. Wind may also strongly affect the soil air and indoor radon concentrations in these areas. These air flows increase levels of indoor radon in winter or summer, depending on the location of the house, eventually leading to extreme reverse seasonal variation [D19]. Air flows due to thermal differences and seasonal patterns of radon concentrations, which are comparable with the observations described earlier, have been observed in caves and in mining regions close to the tunnels and air shafts [C67, K44, L25, M27, S87].

92. The indoor radon concentration is increased by showering and the transfer coefficient inside the bathroom was found to be about one order of magnitude higher than the transfer coefficient for the whole house [V18]. The ratio of the radon activity concentration in air to water was reported to be 1×10^{-4} [U13], a value also supported in a national review carried out in the United States based on experimental and model study results [N28]. These values are consistent with recent findings by Di Carlo et al. [D19] which have shown that an average radon concentration of 10 kBq/m³ in water implies a contribution of 1 Bq/m³ to radon in the air.

93. The outdoor radon concentration is generally much lower than the corresponding indoor radon concentration. Consequently, ventilating indoor environments usually decreases the radon concentration indoors due to the influx of outdoor air with lower radon concentration. The efficiency of this process depends on the indoor to outdoor concentration gradient. In addition, the outdoor radon concentration defines the minimum possible indoor radon concentration. However, in some situations, the outdoor radon can be a non-negligible source for the indoor radon, either permanently (e.g., former mining areas [K44, M27] or high background radiation areas [H31]), or temporarily, due, for example, to specific weather conditions [H19]. An area with significantly elevated levels of outdoor radon and thoron is the igneous Fen complex in Norway with elevated bedrock and levels of ^{238}U and ^{232}Th in soil. Parts of the area were mined extensively, and local natural ventilation of the mines has resulted in elevated outdoor levels of radon and thoron [H1, H2, M40]. In general, the outdoor radon concentration depends on the radon exhalation from the ground and atmospheric mixing processes.

Spatial and temporal variability of radon concentrations

94. The spatial variability of soil and outdoor radon concentrations is a result of the interplay of largely interdependent processes in the different compartments of the natural environment: lithosphere, pedosphere, atmosphere, hydrosphere, and biosphere [B43, C38]. A key determinant of large-scale variability of radon are differences in geogenic radon potential resulting from spatially varying geological characteristics, which affect concentrations of ^{226}Ra, soil physical properties, climatic conditions, and terrain attributes due to their combined effect on radon generation, transport and exhalation as described earlier.

95. In several studies, the geogenic radon potential has been mapped using natural conditions as covariables [C39, P10, P20]. The variability of geogenic factors is also a major factor for governing spatial variability of indoor radon concentration as shown in various studies in Austria [A16], Germany [P20], Republic of Korea [R18], Switzerland [V17], the United Kingdom [F5], and Europe [E24]. Small-scale spatial variability can be caused by changes in lithology [L22], the presence of tectonic faults [B21, P14], and volcanic activity.

96. Radon concentrations in soil, outdoors and indoors can vary on different temporal scales: hourly, diurnal, seasonal and even interannual. Short-term fluctuations on hourly or diurnal scales can be caused by daily changes in meteorological conditions [S23] (e.g., cyclic changes of land-sea breezes [H19]). Irregular, abrupt changes have been linked with tectonic and seismic activity [L1, L24], but also with the onset of heavy precipitation events [T17]. Seasonal variations in soil air radon concentrations [P18, T19, W14] and indoor radon concentrations [B40, K33, S71] are caused by cyclic changes of weather leading

to fluctuations in soil moisture, and groundwater level reversal of pressure and temperature gradients between indoors and soil, and indoors and outdoors, respectively [P18]. Indoor radon concentrations often reveal a diurnal variation with higher concentrations during night and lower concentrations during daytime [H31, X2], due to a diurnal change of meteorological conditions [S23] or a higher ventilation intensity by the residents during daytime [Y2].

97. The characteristics of the settlement and housing conditions can affect indoor radon concentrations due to their influence on the distribution of the population across floor levels and radon entry rates into buildings. While indoor radon concentrations can vary significantly from region to region, the variability from home to home is usually greater, even within relatively homogeneous regions, and can reach several orders of magnitude mainly due to differences in building characteristics (e.g., design of the building foundation).

98. Daily fluctuations in indoor radon concentrations can be an order of magnitude or more [F14, H31, V14]. Regarding seasonal variations, indoor radon concentrations vary by up to a factor of two or more between months depending on the floor level and environmental conditions [K33], as well as by a factor of up to three or more between seasons depending on construction type, environmental conditions, and cultural factors [S71]. Most buildings show higher radon levels in winter than in summer but sometimes the opposite pattern or the absence of a seasonal pattern can be observed. Indoor radon concentrations also vary on an annual basis [A32, H42, S55, S65] because of interannual variability of environmental and residential factors. Antignani et al. [A32] found considerable year-to-year variability (coefficient of variation of 17%) for a study with 84 dwellings in Italy from 1996 to 2006. Steck [S64] reported on median year-to-year variation of 26% (range: 3–110%) for a study comprising 98 residential houses in Minnesota (United States) from 1983 to 2000.

(b) *Indoor radon exposure*

99. Radon exposures were assessed in this annex based on a review of studies published between 2006 and 2022. A long-term perspective is required to evaluate the effects of radon preventive measures on exposures because time horizons measured in decades are typically necessary for these measures and other building characteristics to become prevalent in the building stock and to affect radon exposures [M5].

100. Variations in indoor radon concentrations have been associated with changes that have occurred for new and existing buildings, such as:

(a) Introduction of radon preventive measures for new housing;

(b) Improved ventilation;

(c) Retrofit radon mitigation programmes for existing housing;

(d) Energy efficiency retrofits for existing housing;

(e) Energy efficient designs for new housing;

(f) Changes in construction materials.

101. As given in more detail below, updated estimates reporting an increase in national radon exposure have been published for Canada and China. Reductions in national indoor radon exposures have been reported for Ireland and Japan, and reduced radon exposures in new construction housing have also been

reported for Finland, Norway, and the United Kingdom. These reductions have all been attributed to the implementation of building code changes for housing at a national level or in designated high radon regions.

102. Chen et al. [C26] reported a substantial increase in the population-weighted mean indoor radon concentration for low-rise housing in Canada, representing the majority of dwellings in the 2016 housing stock [G7]. However, the increase in radon exposure from the value reported in the UNSCEAR 2006 Report, annex E [U18] was attributed to be mainly due to the use of more accurate alpha track detectors for long-term measurement in residential homes, in comparison to the grab sampling employed in earlier surveys. An updated analysis that incorporated more recent regional radon survey data showed a much smaller increase [C28]. A trend of increasing indoor radon concentration by year of construction was noted nationally and in the Western Prairies region in Canada [C28, K14, S63].

103. A trend of increasing indoor radon concentrations was reported in a secondary analysis of residential radon surveys conducted in China since 1980. The average indoor radon concentration over 28 cities was estimated to be 0.8 Bq/(m^3 a) [Y1]. This secondary analysis of residential radon surveys focused on the trend by decade in cities that had at least five surveys conducted over the last four decades to minimize bias resulting from comparing studies based on different study designs. The increase was attributed to several factors: the construction of new buildings using natural materials, economic development leading to increased use of air conditioning with better sealed buildings and new measurement procedures based on longer measurement periods.

104. In Ireland, the country-wide population-weighted mean indoor radon concentration estimated from geographically based radon surveys of homes was reported to have decreased by 13% in 2015 [D22]. This decrease was attributed primarily to the 1998 change in building code regulations that mandated the installation of a radon membrane in new buildings in designated high radon areas, with a lower population-weighted mean indoor radon concentration reported for homes built after 1998 than those built before 1998. A 55% reduction in the AM of the indoor radon concentration was reported from a regional study of homes built before and after 1998 in County Cork (Ireland) [L27]. A new protocol was recently developed to estimate the population-weighted mean indoor radon concentration and will be used to characterize any future changes [M45].

105. The population-weighted mean indoor radon concentration in homes was reported to have decreased in Japan following changes to the building code in 2003, with a statistically significant decrease for modern wooden homes [S80]. The change in the building code, introduced to prevent sick building syndrome, required the installation of mechanical ventilation, which also reduced the indoor radon concentration.

106. The radon preventive measures in the building code and the associated practical guidelines were revised in Finland in 2004, requiring homes to be designed so that the indoor radon concentration would be lower than 200 Bq/m^3 [A38]. The mean reduction in indoor radon concentrations in low-rise housing following the implementation of these preventive measures was 33% overall, with measures adopted in 46% of new homes across the country. A mean reduction in indoor radon concentration of 47% was reported for housing in the higher radon zone where 83% of new homes adopted radon preventive measures. An ongoing trend of decreasing mean indoor radon was reported for apartments in contact with the ground constructed since the mid-1980s, while no trend was observed for apartments not in contact with the ground, which generally have lower radon concentrations [K45, V3].

107. In Norway, it was reported that the indoor radon concentration was significantly reduced in new dwellings, and almost halved in detached houses, after the building code was changed in 2010 to require the installation of a foundation radon barrier in combination with a passive radon depressurization system and a balanced ventilation system [F9, H3]. A 70% reduction in the number of new homes with radon concentration above 100 Bq/m^3 was also reported.

108. In designated radon affected areas in England and Wales, a building code change requiring a 10 mil[4] polyethylene radon membrane be installed in new homes as a basic radon preventive measure resulted in a 40% reduction in mean indoor radon concentration [H21]. This analysis included about 9,000 homes built between 1977 and 1992 and about 6,000 homes built from 2001 to 2011. Two studies in the county of Northamptonshire (United Kingdom) reported a reduction in the AM of indoor radon concentration following the installation of a 10 mil polyethylene radon barrier in new homes of 30–50% and 45%, respectively [D17, G23].

109. Improved ventilation following the widespread introduction of mechanical supply and exhaust ventilation systems decreased indoor radon concentrations in low-rise housing built after 1994 in Finland [V2]. A consistent trend of reduced mean indoor radon concentration by build year in Sweden has been attributed to the increased prevalence of mechanical supply and exhaust ventilation for new homes built after 1980 [K14] and improved ventilation in older houses [T18]. The use of mechanical supply and exhaust for indoor ventilation draws less soil gas through the foundations when compared to mechanical exhaust only ventilation. In Eastern Denmark, a lower median indoor radon concentration was reported for 200 newer homes having a balanced mechanical supply and exhaust ventilation system and an airtight foundation barrier [B51]. A trend of decreasing mean indoor radon concentration by build year was reported by the updated Austrian national radon survey [G25]. Similarly, a lower AM indoor radon concentration for dwellings built after the year 2000 than for those built between 1930 and 2000 was reported by a recent national radon survey in the Netherlands (Kingdom of the) [S56].

110. Retrofit mitigation of existing housing has been reported to be very effective in reducing the highest radon exposures in the population. Active radon depressurization is the most common and the most effective retrofit mitigation measure implemented [R19], with a reduction of indoor radon by a factor of 16 to 34 in schools [S85] and a reduction ranging from 61 to 95% in homes [B64, F17, G24, L27, S66]. The radon reduction tends to vary more in schools than homes because larger buildings have more complex structures and conditions can differ greatly between rooms in an individual school. The effectiveness of active sub-slab depressurization has been reported in these studies to depend on the radon emanation from the soil, the permeability of the granular fill placed under the structure and the airtightness of the building envelope. Active sub-slab depressurization was most effective when it was combined with a foundation radon barrier and when a homogeneous pressure field extension was maintained in the permeable aggregate layer beneath the slab by the fan. Higher radon reduction has also been reported for higher initial indoor radon concentrations, with sub-slab depressurization capable of reducing the contribution from the soil but not from the building materials. An average reduction in indoor radon of 65–75% in homes was reported after the installation of passive radon depressurization systems in Canada and Ireland [M38, Z7].

111. Increased indoor radon concentrations have been reported following retrofits to improve energy efficiency in existing housing [B1, D3, D29, F11, J15, M24, N15, P1, P24, P37, S84]. Common retrofit measures that increased airtightness of the above-ground sections of the building envelope included extra insulation of the walls above the ground level and the roof, replacement of old windows with double-glazed windows and improvement to the sealing around doors and windows. Nonetheless, several studies reported that energy efficiency retrofits completed in homes and apartments having adequate indoor ventilation did not result in any increase in mean indoor radon concentration [D29, F11, J16].

112. Indoor radon concentrations for new energy efficient housing designs have been reported to be lower than in conventional new housing in Austria [R21] and in Luxembourg according to data received through the UNSCEAR Global Survey on Public Exposure. Energy efficient designs for new

[4] 1 mil equals to one-thousandth of an inch.

housing may include insulation under the floor slab, which reduces radon ingress, and energy efficient ventilation, such as that provided by heat or energy recovery ventilation (HRV or ERV) systems, based on balanced mechanical supply and exhaust air to dilute radon and other indoor air contaminants [A39, M13]. Increased indoor radon concentrations were reported for housing having low average ventilation rates [B1, V8, V23, Y3, Y4, Y5, Z10].

113. Several studies have linked trends in indoor radon over time to changes in building materials. An increase in indoor radon concentrations in apartments built between 1990 and 2010 in Israel was partly attributed to the use of building materials containing higher concentrations of natural radionuclides [E30]. In the Chengdu and Shenzhen regions of China, a trend of increasing indoor radon in homes was reported following the widespread use of more porous bricks that incorporated industrial waste containing higher radionuclide concentrations, although a decrease was noted for homes built over the last 20 years that may reflect improved standards on radioactivity in building materials [W22, X3]. In the Russian Federation, lower indoor radon in residences built between 2005 and 2009 than in those built before 2000 was attributed to the implementation of regulations by 2000, limiting the radionuclide content of the aggregate used in the concrete in three cities [G16].

(c) *Concentrations of radon in indoor air*

114. Several new or updated methods designed to improve the evaluation of radon concentrations in indoor air have been introduced in this annex. These include:

(a) Use of defined criteria to select surveys, based on the evaluation of their representativeness;

(b) Identification of surveys that, on the basis of objective criteria, could have produced an over- or an underestimate of the radon concentration representative of population exposure;

(c) Evaluation of the differences between the data reported in this annex compared with previous ones, including the identification of some trends that are reported in more detail in section III.A.2.(b);

(d) Evaluation of the uncertainty in the world average radon concentration;

(e) Evaluation of the overall variability of radon levels;

(f) Attempt to estimate the radon concentration for those countries with no available data.

Indoor radon surveys

115. About 170 papers containing information on indoor radon concentrations identified through the literature review were included in this evaluation. Surveys were considered to provide a representative value of radon concentration in a specific country, they included at least 100 dwellings, with measurements lasting more than 30 days. Where a national survey was not available, regional surveys covering at least 1 million people were taken into consideration. Fifty countries submitted information through the UNSCEAR Global Survey on Public Exposure, reporting data on about 376 national and regional surveys, mostly in dwellings but also in other building types. Surveys from over half of these countries met the criteria for inclusion in the evaluation. Details on the surveys considered in the evaluation are given in electronic attachment A-1.

116. Findings from national surveys are summarized in table 2. Each survey was assessed to qualify in terms of representativeness—whether the indoor radon concentrations provided likely to be over- or underestimated—based on the IAEA report Nuclear Applications Series No. 33. [I31]. Table 2 gives the

values of the parameters that best describe the log-normal distribution for the indoor radon concentration: the arithmetic mean (AM), the geometric mean (GM) or median and the geometric standard deviation (GSD). The values reported in table 2 were primarily taken from surveys of radon in dwellings and are representative of annual exposures. Additional details are provided in electronic attachment A-1.

117. Many recent surveys have been carried out for mapping purposes and have focused on measurements taken mainly on the ground floor; therefore, data from less recent but more representative surveys were sometimes preferred for this evaluation. Values of the distribution parameters not reported in the original sources of information were estimated either by assuming that the data followed a log-normal distribution or by combining the available data using, for example, population or housing stock as weights. Details on these calculations are given in electronic attachment A-1. Figure I provides a global overview of available data on indoor radon concentrations globally.

Figure I. Mean indoor radon activity concentrations for countries with national surveys [a]

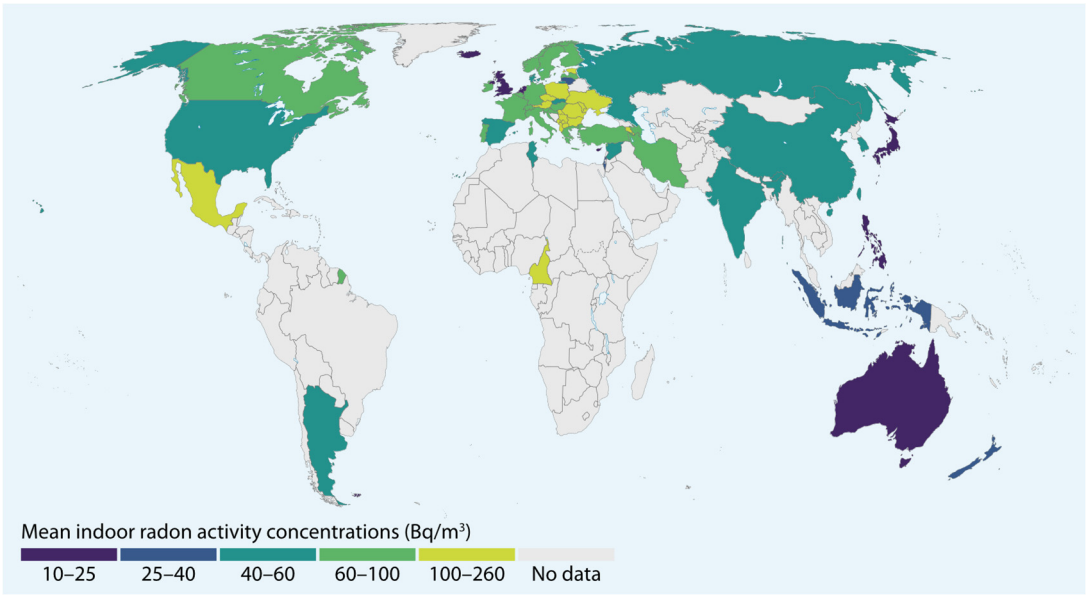

[a] The boundaries and names shown and the designations used in this map do not imply official endorsement or acceptance by the United Nations. Final boundary between the Republic of Sudan and the Republic of South Sudan has not yet been determined. Dotted line represents approximately the Line of Control in Jammu and Kashmir agreed upon by India and Pakistan. The final status of Jammu and Kashmir has not yet been agreed upon by the parties. A dispute exists between the Government of Argentina and the United Kingdom of Great Britain and Northern Ireland concerning sovereignty over the Falkland Islands (Malvinas).

118. The parameter values reported in national or regional surveys considered in this annex were not always population-weighted, since most surveys were not designed to evaluate exposures from radon. Typically, the only population-weighted parameter values reported in national surveys were the AMs of the indoor radon concentration. In table 2, underlined values are population-weighted, based on population distributions determined either using a sampling strategy or specific weights. Values for which information to verify whether they were population-weighted was insufficient are presented without being underlined.

Table 2. National surveys on indoor radon activity concentration

AM: Arithmetic mean; GM: Geometric mean; GSD: Geometric standard deviation. Underlined parameters are population-weighted

Country	*Population (millions)*	*Number of dwellings*	*Radon activity concentration parameters*		
			AM (Bq/m³)	*GM/Median [a] (Bq/m³)*	*GSD*
AFRICA					
Cameroon	26.5	1 400	107	83	2.0
Tunisia	12.1	119	50	40[c]	2.0
Total	**38.6**	**1 519**	**89**	**66 [b]**	**2.2 [b]**
ASIA AND THE PACIFIC					
Australia	25.7	3 416	12	9	2.1
China	1 424.9	20 450	55	40 [b]	2.4 [b]
India	1 396.4	1 500	40	23	2.6
Indonesia	271.9	2 144 [c]	38 [c]	34 [c]	1.2 [c]
Iran (Islamic Republic of)	87.3	4 414	75	71	1.5
Japan	125.2	3 900	14	11	2.1
New Zealand	5.1	241	31 [b,d]	23 [c]	2.1 [b]
Philippines	112.2	785	21	20	1.4 [b]
Republic of Korea	51.8	9 301	54	46	1.2
Total	**3 500.5**	**46 151**	**45**	**30 [b]**	**2.5 [b]**
EUROPE					
Albania	2.9	247	101 [d]	98 [c]	1.8
Armenia	2.8	217	177	114	2.6 [b]
Austria	8.9	27 630	112	79	2.6
Azerbaijan	10.3	2 404	84 [d]	58 [c]	2.4 [b]
Belgium	11.6	10 477	69	49	1.6
Bulgaria	7.0	2 778	111 [d]	81	2.2
Croatia	4.1	782	68	50	2.3
Cyprus	1.2	894	21	17 [b]	1.8 [b]
Czechia	10.5	3 582	119	94	1.9
Denmark	5.8	3 120 [c]	59 [c]	37 [c]	2.8 [c]
Estonia	1.3	440	103 [d]	57	2.8 [b]
Finland	5.5	2 882	96	62	2.5 [b]
France	64.5	10 843	90 [d]	53	2.5
Germany	83.3	7 000	63	41	2.0
Greece	10.5	1 577	72 [d]	40 [a]	1.8 [b]
Hungary	9.8	15 602	82 [b]	62	2.1
Iceland	0.4	250	13 [d]	9 [d]	2.6 [b]
Ireland	4.9	653	98	80 [a]	1.9 [b]
Israel	8.8	2 300	31	28 [b]	1.6

Country	*Population (millions)*	*Number of dwellings*	*Radon activity concentration parameters*		
			AM (Bq/m³)	*GM/Median [a] (Bq/m³)*	*GSD*
Italy	59.5	5 356	72	50	2.2
Latvia	1.9	447	74 [d]	54 [b]	2.2 [b]
Lithuania	2.8	1 009 [c]	32 [c]		
Luxemburg	0.6	3 738	72 [d]		
Montenegro	0.6	1 095	101	93	2.9
Netherlands (Kingdom of the)	17.4	2 567	16	12 [a]	1.9 [b]
North Macedonia	2.1	437	105	84	1.9
Norway	5.4	29 000	89	55 [b]	2.7 [b]
Poland	38.4	129	165 [d]	133	1.9
Portugal	10.3	1 706	66 [d]	37 [c]	3.1 [b]
Republic of Moldova	3.1	2 435	253 [d]	158	3.0
Romania	19.4	4 930	149 [d]	124 [b]	1.9
Russian Federation	145.6	797 363	53	41	2.0 [b]
Serbia	7.4	5 300	105 [e]	60	3.0
Slovakia	5.5	3 657	48 [d]	41	2.2
Slovenia	2.1	892	87	60	2.2
Spain	47.4	~3 000	53	25	3.4
Sweden	10.4	1 819	90	63 [b]	2.3 [b]
Switzerland	8.6	80 000	78	55	2.3 [b]
Türkiye	84.1	7 293	81	57	2.3
Ukraine	43.9	26 879	148 [d]	88	2.8 [b]
United Kingdom	67.1	2 093	22	15	2.2
Total	**837.7**	**1 074 438**	**77**	**46** [b]	**2.7** [b]
LATIN AMERICA AND THE CARIBBEAN					
Argentina	45.0	3 170	46	37 [b]	1.9 [b]
Mexico	126.0	433	112	63	2.9 [b]
Total	**171.0**	**3 603**	**95**	**55** [b]	**2.7** [b]
NORTH AMERICA					
Canada	37.9	21 818	82	55	2.5
United States of America	335.9	5 694	46	25 [b]	3.1
Total	**373.8**	**27 512**	**50**	**26** [b]	**3.1** [b]
WEST ASIA					
Syrian Arab Republic	20.8	1 435	44		

[a] Median, because GM was not reported.

[b] Calculated by assuming log-normality using different parameters reported in the references.

[c] Calculated by combining the distributions and weighting by population/housing stock.

[d] Potential overestimate.

[e] Potential underestimate.

119. The global population-weighted AM of the indoor radon concentration was estimated to be 53 Bq/m^3, based on data from 57 countries representing 63% of the world's population [U5] (see figure I). The inclusion of data from regional surveys does not significantly change this estimate, as they account for less than 1% of the global population (see electronic attachment A-1). For 17 countries, the reported AM of the radon concentration was qualified as overestimated, although the extent of the overestimation was not known. However, applying correction factors to adjust for the overestimation of the indoor radon concentration did not materially affect the estimate of the global average value.

120. A comparison of the average indoor radon concentration over 26 countries, covering about 35% of the world population, for which national average values were reported in the UNSCEAR 2006 Report, annex E [U18], shows that a population-weighted average of 55 Bq/m^3 was estimated for this annex, while a value of 46 Bq/m^3 was obtained for the UNSCEAR 2006 Report. The difference is not a reflection of a trend over time: 15 countries reported higher values than for the UNSCEAR 2006 Report, while 11 countries provided lower national or the same values. The population-weighted average indoor radon concentration for the other 31 countries included in this annex was estimated to be 51 Bq/m^3.

121. Given the uncertainty and variability in the data, as well as the lack of information from some major regions, such as Africa and South America, a rounded value of 50 Bq/m^3 was adopted as the reference value for the global mean indoor radon concentration.

Figure II. Worldwide radon activity concentration distribution

Comparison and Q-Q plot of worldwide radon activity concentration distribution versus theoretical log-normal distribution. GM: Geometric mean; GSD: Geometric standard deviation

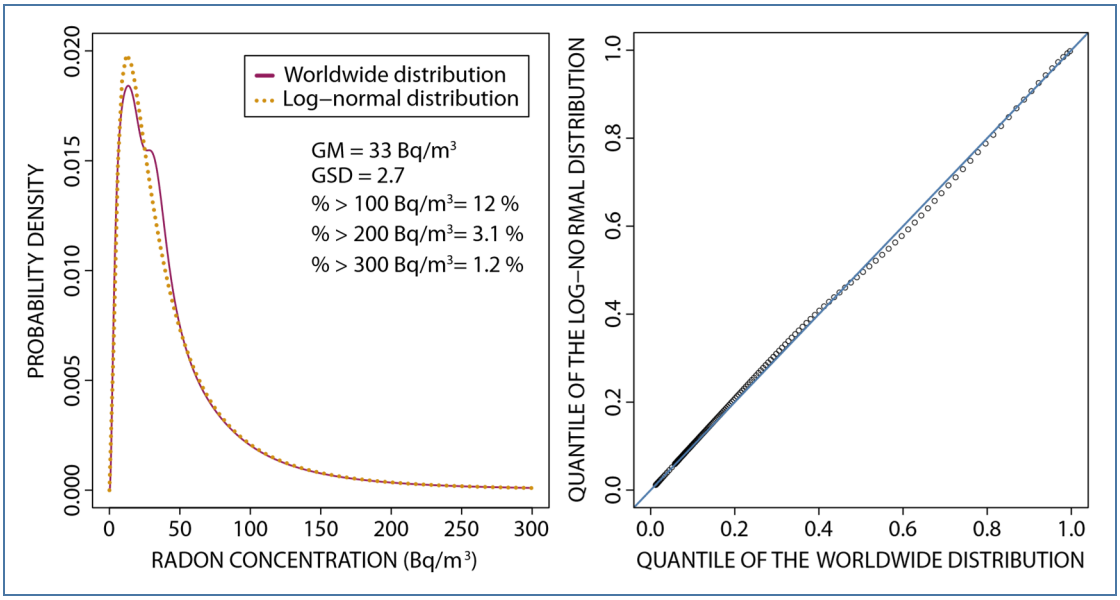

122. Indoor radon concentrations vary widely among dwellings within a country and typically follow a log-normal distribution. The distribution of the global indoor radon concentration was derived by combining national distributions, weighted by country population. The resulting distribution is log-normal, as illustrated in figure II. The methodology used for these calculations is detailed in electronic attachment A-1 and was also applied to estimate distribution parameters for major world regions: Africa, Asia and the Pacific, Europe, Latin America and the Caribbean, North America, and West Asia. Based on data from 54 countries for which values of the GM were provided, the global GM for indoor radon concentration was estimated at 33 Bq/m^3, with a GSD of 2.7 Bq/m^3.The proportions of the global population exposed to indoor radon concentrations exceeding the reference levels recommended by WHO of 100, 200, and 300 Bq/m^3 were estimated at approximately 12, 3.1 and 1.2%, respectively.

Correlation and regression analysis

123. Indoor radon concentrations were also analysed with respect to variables that are expected to act as proxies for factors governing radon concentration in indoor air on a larger scale. Potential correlations between the mean national indoor radon concentration and climate zones, geological (i.e., lithological) units, population density, and the Human Development Index (HDI) were evaluated. The HDI[5] is a summary measure of average achievement in key dimensions of human development: a long and healthy life, being knowledgeable, and having a decent standard of living. These variables were selected because they are expected to reflect geogenic radon potential in soil and rock (geology), building styles (climate, population density, HDI), airtightness of the building (climate, HDI), ventilation intensity/living habits (climate), and floor-level distribution of the people (population density).

124. Additionally, a model-based approach was developed to estimate the indoor radon concentration for those countries where no surveys were identified. The national AM of the indoor radon concentration was modelled as a function of those variables also used for correlation analysis (i.e., population distribution with respect to geology, climate, settlement typology and the HDI). A multivariate and non-linear regression model (quantile regression forest) was fitted to the available indoor radon data and used to predict the indoor radon concentration for those countries without data. However, the modelling approach did not provide reliable estimates, probably because of the lack of training data (i.e., representative national radon data, especially from tropical and arid climate regions), uncertainty in the national indoor radon data and coarse resolution of geological data. It was not possible, therefore, to establish meaningful predictor-response relationships for all relevant predictors and countries with missing data were not included in this evaluation. Details on the correlation analysis as well as the modelling approach are given in electronic attachment A-1.

High radon areas

125. High radon areas are regions where radon concentrations in air, soil air or water are significantly elevated due to local geological and environmental conditions. For example, elevated radon concentrations can be detected in locations within an HBRA, characterized by high levels of uranium in soil or rock or in areas with extremely high permeability of the soil, the existence of specific building styles, building materials or living habits. The relationship between geogenic conditions and radon concentration in outdoor air, soil air and water is often strong; however, the relationship between geogenic conditions and radon concentrations in indoor air is weaker because it is also influenced by anthropogenic factors.

126. In the UNSCEAR 2008 Report, annex B [U19], radon data were presented for HBRAs in Austria, Brazil, China, Czechia, Hungary, India, Indonesia, Iran (Islamic Republic of), Italy, Kyrgyzstan, Slovenia, Spain, and the United Kingdom. Data presented in this section are based on new information from studies conducted in areas described as HBRA in the literature; information presented in previous UNSCEAR reports is not summarized. Further details are given in electronic attachment A-1.

127. A new HBRA was identified in Mamuju on Sulawesi Island (Indonesia) by the National Nuclear Energy Agency of Indonesia.[6] It is characterized by very high outdoor radon concentrations, ranging from 22 Bq/m³ to 760 Bq/m³ with an AM of approximately 290 Bq/m³, which are similar to indoor radon concentrations. The style of local buildings and living habits prevent further accumulation of radon indoors. A comprehensive assessment of exposures from natural sources of radiation for this area estimated an annual effective dose of 27 mSv to the local population [H31]. The highest mean indoor radon concentrations were

[5] https://hdr.undp.org/data-center/human-development-index#/indices/HDI

[6] The National Nuclear Energy Agency of Indonesia has been replaced by the National Research and Innovation Agency, which was officially established as a standalone body in April 2021.

reported for Kinsarvik, Municipality of Ullensvang (Norway) [S76], Villar de la Yegua, Salamanca (Spain) [S4, S5], and Niška Banja, Nišavski (Serbia), the location of a radon spa [Z14]. The AMs of the indoor radon concentrations measured at these three locations were 4,340 Bq/m³ (n=104); 1,851 Bq/m³ (n=56); and 1,163 Bq/m³ (n=102), respectively.

128. It should be noted that HBRAs are not necessarily high radon areas. The HBRAs in Kerala and Odisha (India) are characterized by the presence of monazite sands and although external gamma doses are 5 to 10 times higher than in areas with typical levels of background radiation, indoor radon concentrations are not elevated, as indicated by several studies [B29, M32, N2, O8, R6]. The annual effective dose from inhalation of radon and thoron was estimated to range from 0.5 to 1 mSv [M32], due to the geological characteristics of the area, as well as other specific factors, such as building properties, high ventilation rates, and use of building materials from other locations.

Radon levels in dwellings and workplaces

129. Public doses from exposure to radon estimated by the Committee are based on a worldwide average radon concentration derived from residential surveys (i.e., surveys performed in dwellings). This approach implicitly assumes that radon concentrations in dwellings are similar, on average, to those in workplaces. A review of studies comparing radon concentration in dwellings and in workplaces, performed for this annex, found no systematic differences between them. Indoor radon levels in workplaces vary greatly depending on the type of workplace, and exposures depend on the distribution of workers across different activities, as noted in the UNSCEAR 2020/2021 Report, annex D [U30]. These factors introduce significant uncertainty in the estimation of radon exposure in workplaces. Therefore, the Committee considered it appropriate to continue using indoor radon concentrations measured in residential settings to estimate the exposure for the general population, recognizing that people spend most of their time indoors when at home, including night hours when radon levels are generally the highest, whereas workplaces are occupied during daylight hours when radon concentrations tend to be lower, likely due to the presence of ventilation systems. Information on the comparison between radon levels at workplaces and in dwellings is given in electronic attachment A-1.

Uncertainty

130. Estimating the overall uncertainty in assessments of the exposure in residential radon surveys remains a challenge and therefore it is rarely reported. Numerous sources contribute to this uncertainty, many of which are difficult to quantify. These include: *(a)* sampling-related factors (e.g., sampling design, selection or exclusion of specific building types, floor levels, or room types); *(b)* handling of non-responders, which often represent a substantial proportion of the sample; *(c)* measurement duration, particularly when detectors are deployed for less than a full year; *(d)* detector-related issues (e.g., calibration accuracy, sensitivity to thoron); and *(e)* analytical adjustments (e.g., application of seasonal correction factors, and corrections for sampling bias and non-response). A brief discussion of these uncertainty sources, along with a Monte Carlo-based estimate of the overall uncertainty in the population-weighted global mean indoor radon concentration, is provided in electronic attachment A-1.

(d) *Concentrations of radon and its decay products in outdoor air*

131. Studies on outdoor radon levels are limited, primarily because radon in outdoor air poses only a minor health risk to the general population, due to its low levels, resulting from rapid atmospheric dilution after exhalation from the ground, and to the relatively low occupancy of the outdoor environment. Consequently, doses from exposure to radon outdoors are considerably lower than those

from exposure to radon indoors. The lack of specific regulations or guidance for outdoor radon also contributes to the scarcity of measurements.

132. Data on outdoor radon concentrations from the UNSCEAR Global Survey on Public Exposure are provided in electronic attachment A-1. Global coverage of surveys assessing radon in outdoor air is only approximately 10%. To estimate the worldwide average concentration, the median of the outdoor radon concentrations was selected as the representative value because it is more robust than the AM, given the limited amount of data, since it is not skewed by extreme values and does not rely on representing data through a standard distribution curve.

133. The median of the AMs from 9 national and 35 regional surveys selected from both the literature review and the UNSCEAR Global Survey on Public Exposure was estimated to be 11 Bq/m^3, close to the typical radon concentrations value of 10 Bq/m^3 (with a range between approximately 1 and more than 100 Bq/m^3) reported in previous UNSCEAR reports [U15, U18].

134. Some studies included in the review indicated that exposures from radon in outdoor air cannot be overlooked in some specific locations where concentrations may reach hazardous levels, such as the sites of facilities in the NORM industry. For example, a German survey investigating the impact of mining and milling activities on outdoor radon levels, reported outdoor radon concentrations ranging from 5 to 1,700 Bq/m^3, with most values exceeding 50 Bq/m^3 [K44]. In the Nowa Ruda region, a former coal mining area in Poland, the mean outdoor radon concentration from 70 monitoring sites was 70 Bq/m^3, with the highest recorded value being 131 Bq/m^3 [T3]. Higher outdoor radon concentrations than the worldwide average have also been measured in some regions characterized by high levels of natural radiation, such as Niška Banja, Nišavski (Serbia), where an average annual outdoor radon concentration of 57 Bq/m^3 was recorded, with a maximum value of 168 Bq/m^3, and Kinsarvik, Municipality of Ullensvang (Norway), where a maximum radon concentration of 114 Bq/m^3 was measured [C38, Z15].

135. A limited number of surveys have been undertaken to measure the EEC of radon in outdoor air. Table 3 reports the descriptive statistical values derived from 10 surveys conducted in 6 countries and shows that the AMs of the EEC of radon ranged from 1.5 to 23 Bq/m^3. The observed variations in the values of the EEC of radon underscore the influence of local geological, environmental, and possibly anthropogenic factors on the distribution of radon decay products. The lack of information on standard deviations or range in some studies limits a comprehensive comparative analysis. Further research and standardized monitoring across regions are essential to interpret the factors contributing to these variations and their potential implications for public health.

136. The measurement of outdoor radon concentration poses distinct challenges compared to indoor measurements, primarily due to the significantly lower concentrations outdoors and the exposure of detectors to harsh environmental conditions, such as precipitation, humidity, sunlight, and wind. A review of outdoor radon surveys highlighted the use of various detector types, deployed at different heights and with varying shelter configurations, requiring the development of a standardized measurement protocol to harmonize and compare data [C14]. To optimize outdoor measurement protocols, techniques commonly used for indoor measurements may need to be adapted. Celikovic et al. [C14] explored specific treatments for Solid State Nuclear Track Detectors to enhance the sensitivity and reduce the background interference from other alpha emitters in environment [C14]. Notably, outdoor radon surveys have been conducted on a much smaller scale compared to indoor surveys. Details on survey design, quality control, and production of outdoor radon concentration maps are limited. Because of the smaller coverage of outdoor radon surveys and uncertainty regarding the representativeness of the measurements, the use of the results of these surveys to estimate a global mean radon concentration outdoors warrants caution.

Table 3. Compilation of descriptive statistics derived from surveys reporting radon equilibrium equivalent activity concentration in outdoor air

Country	*Number of locations*	*Radon EEC in outdoor air (Bq/m³)*			*Reference*
		Range	*Arithmetic mean*	*Standard deviation*	
China	8		7.1	2.7	[Z3]
China	1		4.9	2.7	[Z4]
India	1		4.7	0.73	[M2]
India	60	6.8–24.2	13.0		[M19]
Ireland	18		5.6	0.7	[G29]
Malaysia	234	0.4–4.6	1.5		[N33]
Romania	1		8.1	7.3	[F10]
Romania	24	15–28	23.1		[Z13]
Spain	25	1.2–15.8			[A35]
Spain	1		13.2	10.8	[G4]

137. Several studies which attempted to establish correlation factors between indoor and outdoor radon concentrations indicated that diverse parameters influence the concentrations [B8, H4, V13]. This suggests that relying solely on outdoor radon concentrations to predict indoor levels may be inadequate and that a simultaneous consideration of other influential factors is required.

(e) *Concentrations of radon in water*

138. Water can be enriched with radon following radon emanation into water-filled porous or interstitial spaces of rock matrixes or by radioactive decay of ^{226}Ra dissolved in water. Radon is soluble in water (0.01 mol/(kg·bar) at 293 K [L15]) and its solubility decreases with increasing temperature. Radon is removed slowly from still water by molecular diffusion, but agitation and heating cause it to de-emanate rapidly to the surrounding air. As a result, dissolved radon may escape during every step of the distribution chain to final consumption (i.e., extraction, treatment and pumping, transport, and normal household activities). The concentration of radon in drinking water, therefore, depends on the radon concentration in the source, the amount of dissolved ^{226}Ra, the time between extraction and use, and its treatment during extraction, transport, and distribution.

139. An average value of 8 kBq/m^3 resulting from a single survey carried out in China was given in the UNSCEAR 2000 Report [U15]. Reference values for radon concentrations in well-water, groundwater and surface water were derived in the UNSCEAR 1993 Report, annex A [U13] as 100, 10 and 1 kBq/m^3, respectively. According to the main classification for drinking water based on the accumulation site [W7] two different freshwater typologies are identified:

(a) Groundwater accumulated in underground water-bearing permeable rocks (from near-surface to a depth of more than 9,000 m);

(b) Surface water in different water bodies above the ground (e.g., streams, rivers, lakes, and reservoirs).

140. Higher radon concentrations are much more likely to be detected in groundwater than in surface water, since groundwater is in contact with larger radon emanating surfaces and is generally isolated from the atmosphere where radon can easily escape to. Groundwater can be further classified according to the uptake process in spring water and water drawn via private wells and boreholes. Spring and borehole waters are distributed in bottles or fed into the water supply network, whereas well water is often drawn for private use. The short time elapsing and the short path travelled from extraction to consumption are the main reasons why, at the time of consumption, radon concentrations in water from private wells are generally higher than in both surface water and other types of groundwater [D19, J19].

141. Data on radon concentrations in drinking water from 23 national surveys (22 in Europe and 1 in Asia) submitted through the UNSCEAR Global Survey on Public Exposure are reported in table 4. Further data from 28 regional surveys in 11 countries (11 in Europe and 17 in Asia) are provided in electronic attachment A-1. For each country, table 4 gives the AM, which was used to derive the reference value for calculating the dose, the SD, the GM, the GSD and the median, where available. Data on radon in drinking water were also taken from 25 papers identified through a review of the published literature. These papers provided data from two national surveys in two countries (Jordan and Luxemburg), included in table 4, and 23 regional surveys in 12 countries (3 in Africa, 1 in America, 6 in Asia, 2 in Europe) further discussed in electronic attachment A-1.

142. The surveys that were considered in the derivation of a representative value for a country had to refer to a population of at least 1 million people, with at least five measurements sites per 1 million people. The surveys were selected only if there was a clear indication that data related to drinking water. In countries where a national survey was available, regional surveys were not taken into consideration for this assessment. It should be noted that the original source of the water was not always specified or made clear. The very few data for surface water only indicated a concentration of radon below 1 Bq/L. In general, the data reported show a large variability, with the AM ranging from below 1 to 390 Bq/L, due to the influence of various parameters like the origin of the source, the sampling location (e.g., well, borehole, tap outlet or water network for groundwater, or lake, river or pond for surface water or water with a mixed origin) and the uptake process (e.g., borehole, well, spring or water network) on the radon concentration in drinking water.

Table 4. National surveys of radon activity concentrations in drinking water (as provided in the UNSCEAR Global Survey on Public Exposure and published literature, the values are rounded)

AM: Arithmetic mean; SD: Standard deviation; GM: Geometric mean; GSD: Geometric standard deviation

Country	*Population (millions)*	*Number of measurement sites*	*Radon activity concentration in water (Bq/L)*					*Reference*
			AM	*SD*	*GM*	*GSD*	*Median*	
ASIA AND THE PACIFIC								
Republic of Korea	51.8	501	91				70	Global Survey
EUROPE								
Belgium	11.6	214	37	57	21	0.9	13	Global Survey
Cyprus	4.1	200	<1	<1	<1	2.5	<1	Global Survey
Czechia	10.5	878	28	37	17	2.8	16	Global Survey
Denmark	5.8	70	<1					Global Survey
Finland	5.5	1 247			31			Global Survey
France	64.5	2 000	68	207	25		19	Global Survey

Country	Population (millions)	Number of measurement sites	Radon activity concentration in water (Bq/L)					Reference
			AM	SD	GM	GSD	Median	
Georgia	3.8	396	10	18	4	3	6	Global Survey
Georgia	3.8	113	6	8	2	3	2	Global Survey
Georgia	3.8	92	8	14	3	3	3	Global Survey
Germany	83.3	510	8	20	5	2.6	7.3	Global Survey
Italy	59.5	1 256	9.9	10.4	7.9	2.0	7.8	Global Survey
Latvia	1.9	154	7.2	5.1	5.8	2.1	6.0	Global Survey
Lithuania	2.8	117	3.4	3.9	2.0		2.0	Global Survey
Luxemburg	0.6	316	17					[T20]
Norway	5.4	33	31	23	22		25	Global Survey
Portugal	10.3	5 874	78	195			11	Global Survey
Slovakia	5.5	168	8.5	19.1				Global Survey
Slovenia	2.1	108	7.3	6.9			<1	Global Survey
Spain	47.4	1 801	48	147	7	5.7	5	Global Survey
Sweden	10.4	874	38					Global Survey
Switzerland	8.6	1 454					7	Global Survey
Ukraine	43.9	355	32	74	8.7	4.4	6	Global Survey
WEST ASIA								
Jordan	10.9	87	59	9				[A22]

143. To estimate the worldwide average concentration of radon in drinking water, the median was selected as the representative value because it is more robust than the AM, given the limited number of data and the different methodologies employed in the reported studies, it is not biased by extreme values and does not rely on representing the study measurements using a standard distribution curve. The results for national, regional surveys, and for both national and regional surveys are given in table 5. The median of the AMs was estimated at 11 Bq/L, taking account of data from both national and regional surveys. Given the high uncertainty (e.g., unclear origin of sources) and the high variability of the data and considering their low coverage, a reference value of 10 Bq/L was adopted in this annex.

Table 5. Worldwide radon concentrations in drinking water

Sources of data	Number of countries	Population (millions)	Worldwide population (%)	Median of arithmetic means (Bq/L)	Arithmetic mean ranges (Bq/L)
National surveys	20	433	5.5	14	<1–91
Regional surveys	21	147	2.0	11	1–390
National and regional surveys	41	580	7.5	11	<1–390

(f) *Dose estimates from exposure to radon and its decay products*

144. The annual dose to the lungs from inhalation of radon in air was derived from the equation A.1 in appendix A. Using an indoor radon concentration ($C_{222Rn,in}$) of 50 Bq/m^3, an annual occupancy rate indoors (O_{in}) of 0.8, an equilibrium factor for indoor radon ($F_{222Rn,in}$)[7] of 0.4 and a dose coefficient for EEC of radon ($DC_{EEC,222Rn}$) of 9 nSv/(Bq h/m^3) [U28] the annual dose was estimated to be 1.3 mSv. The annual dose to other organs from indoor radon dissolved in blood and soft tissue was estimated from equation A.7 in appendix A. Using a dose coefficient for radon in blood ($DC_{b,222Rn}$) of 0.18 nSv/(Bq h/m^3) [I75], the annual dose to other organs from radon dissolved in blood was estimated to be 0.06 mSv. The annual dose associated with inhalation of radon in indoor air was therefore estimated at 1.3 mSv.

145. Equations A.2 and A.10 in appendix A were used to estimate doses to the lungs and other organs from inhalation of outdoor radon. In this case using an outdoor radon concentration ($C_{222Rn,out}$) of 10 Bq/m^3, an annual occupancy rate outdoors (O_{out}) of 0.2 and an equilibrium factor for radon outdoors of 0.6 ($F_{222Rn,out}$) the annual dose to the lungs and to other organs were estimated at 0.095 mSv and 0.0032 mSv, respectively. The annual dose attributed to inhalation of radon in outdoor air was therefore estimated at 0.10 mSv.

146. The annual dose from ingestion of radon in drinking water was derived from equation A.11 in appendix A. Using a radon concentration drinking water ($C_{222Rn,dw}$) of 10 Bq/L, an annual ingestion rate of drinking water ($I_{ing,dw}$) of 0.5 m^3/a, and a dose coefficient for ingestion of radon ($e_{ing,222Rn}$) of 0.69 nSv/Bq [I75], the annual dose was estimated to be 0.0035 mSv. The total annual dose from inhalation and ingestion of radon and its decay products was therefore estimated at 1.4 mSv.

3. Thoron and its decay products

(a) *Factors affecting thoron exposure*

147. Thoron (^{220}Rn) is released into the environment through the natural decay of ^{232}Th in the Earth's crust. Notably, monazite and zircon sands are characterized by particularly high concentrations of thorium [V15]. Granite, black shale, and mylonitic rocks, are more likely to have an elevated thorium content [A1, S8], while basalt, limestone, and sandstone generally are characterized by below-average concentrations of thorium [R5]. The migration of thoron from the soil into buildings is limited by the short distance it can travel before it decays and therefore the main source of thoron in indoor air is thoron released through exhalation from the internal surfaces of building materials [C37, C66, D8, D9, H15, M21, N16, N34, R6, S53, T22, U1, Z9]. The indoor thoron concentrations are generally unaffected by floor levels [C66, R6, S72].

148. Data from the UNSCEAR 2006 Report, annex E [U18] and the open literature [C37, G12, M21] indicate that thoron concentrations in dwellings decrease with distance from the wall surface, resulting in a heterogeneous distribution within a room. In experiments conducted under controlled conditions in a facility built with unfired clay stones and clay plaster at the Helmholtz Zentrum Munich (Germany) thoron decay products were found to be uniformly distributed spatially, while thoron remained unevenly distributed [T23]. Since the dose from thoron exposure comes primarily from its decay products, thoron

[7] The equilibrium factor and the dose coefficient (equilibrium equivalent exposure) are correlated [I75] and therefore, it is not appropriate to use a value for the equilibrium factor different from 0.4.

measurements pose challenges because, without information about the location of the detectors, it is difficult to assess the representativeness of the measured concentrations. Consequently, dose assessments based on concentration of thoron decay products are more reliable than those based on the highly heterogeneous thoron concentrations [M33].

149. Significant efforts have been devoted to developing numerical models to understand the behaviour of thoron and its decay products within buildings, as well as their spatial distribution [A7, A8, D7, H37, U33, Z11]. However, understanding this behaviour is complex and depends on numerous factors, including airflow patterns, geometric configuration of the room, ventilation rates, locations of the thoron source, positions of inflow and outflow points, gas kinematics, aerosol behaviour, and other relevant parameters. Model results confirmed that the distribution of thoron within an enclosed space is highly non-uniform, decreasing exponentially from the source. In contrast, the concentration of thoron decay products is generally evenly distributed throughout the room due to their long half-lives.

150. Passive type measurement methods require careful calibration with respect to the deposition velocity. Deposition velocities depend on several environmental parameters, such as ventilation rate, turbulence, unattached fraction, and aerosol size distribution. These dependencies make the passive type of thoron decay product monitor site-specific meaning that the decay product deposition velocities must be determined for each location before deployment [M34].

151. Experimental results consistently show that thoron concentration depends on environmental parameters, particularly humidity. The thoron exhalation rate tends to increase with rising humidity until reaching a specific level beyond which it either saturates or decreases, as reported by Janik et al. [J6] and Syuryavin et al. [S86]. Consequently, inhabitants of dwellings with elevated humidity levels may receive higher doses from thoron and its decay products.

152. Tests investigating the effect of different wall paints on thoron exhalation indicate that, when applied without a primer, many paints fail to act as effective barriers. Conversely, other paints demonstrated their ability to reduce thoron exhalation by 70% or more with the application of a single just one coat. Furthermore, a simulation study to assess the average performance of commonly used paints and wallpapers, estimated an approximate 40% reduction in thoron concentration from the source [D9].

153. The concentration of indoor thoron may be affected by seasonal variation, often higher in winter and spring than in autumn and summer, likely because of poor ventilation [R6, S12, S14, S49, S72]. Regional surveys conducted in India, based on a year-long measurements, reported that the EEC of thoron was two to four times higher in winter than in other seasons, due to poor ventilation [G14, J4, J5, K9, K41, P8, P35, P36, P39, R12, R13, S6, S25, S31, S47, S48, S50]. Similar seasonal trends were reported for regional surveys carried out in China and Japan [H37]. In contrast, a study in India reported higher values of EEC of thoron during the rainy season than in other seasons [K42], while another one reported no seasonal variation based on long-term measurements [K10, O7]. These discrepancies highlight the need for more long-term studies across diverse regions and climates to better understand the mechanisms driving seasonal variation in the EEC of thoron.

154. The AMs of the EEC of thoron measured in dwellings in India made of mud or slate were reported as 0.94 and 0.89 Bq/m^3, respectively [G14]. These values were higher than those obtained in dwellings made of concrete or mud-tin (0.29 and 0.49 Bq/m^3). Measurements of the EEC of thoron taken over a three-month period of 12 ± 2, 3 ± 1, and 7 ± 1 Bq/m^3 were reported for mud-walled, metallic or iron sheet-walled, and stone-walled modern houses in the Kilimambogo region (Kenya) [N34]. Visnuprasad et al. analysed long-term passive measurements of EEC of thoron in the Chavara and Neendakara hamlets (Kollam district) across 58 houses categorized into four types: mud houses, brick houses with concrete roofs, houses with asbestos roofs and brick walls and houses with tiled floors [V19]. The highest average values of the EEC of

thoron were measured in mud houses and the lowest were in houses with tiled floors. Measurements in 93 Swedish dwellings grouped by construction material and location showed no significant difference in the EEC of thoron between houses built with uranium-rich blue concrete and other materials [S53].

(b) *Concentrations of thoron and thoron decay products in indoor air*

155. Indoor concentrations of thoron and its decay products were derived from data obtained from the UNSCEAR Global Survey on Public Exposure and the literature survey. National and regional studies conducted both in dwellings and in highly occupied public buildings (schools, kindergarten, hospitals) were considered. Only studies containing clear information on the detectors and their calibration, as well as measurements taken in more than five households and over a period of at least seven days were considered.

156. The distribution of thoron concentrations inside a room are fairly uniform up to 50 cm from the walls [H30, M21, S72, T23]; therefore, one of the criteria to select publications for the literature review was that the detector should be positioned at least 50 cm from the walls was. However, in the case of thoron decay products, the position of the detector does not need to be taken into account due to their relatively uniform concentration across the whole room. As a result, the use of direct measurements of the EEC of thoron is preferred as a more effective approach to assess exposures [T12].

157. Results from five studies on indoor thoron concentrations from Canada, India, Japan, North Macedonia, and Slovenia included in this evaluation are summarized in table 6. The thoron concentrations ranged from below detection limit to a few hundred Bq/m³. The GMs from three national surveys ranged from 7.5 to 28 Bq/m³. Further details of the surveys are provided in electronic attachment A-1.

Table 6. Compilation of descriptive statistics from national surveys reporting thoron activity concentrations in indoor air

AM: Arithmetic mean; SD: Standard deviation; GM: Geometric mean; GSD: Geometric standard deviation; Min: Minimum; Max: Maximum

Country	*Note*	*Number of locations*	*Thoron concentration in indoor air (Bq/m³)*							*Reference*
			AM	*SD*	*GM*	*GSD*	*Median*	*Min*	*Max*	
Canada	Whole country	3 534			13	1.9				[C29]
India	Summer	20	43	24	39		51	10	82	[K40]
	Autumn	20	75	59	69		75	16	149	
	Winter	20	79	36	75		39	24	104	
	Spring	20	119	33	108		86	29	171	
Japan	Whole country	24	11.1	12.7	7.5	2.5		<7.4	52.4	Global Survey
North Macedonia	Whole country	300			28	2.1		3	272	[S72]
Slovenia	Kindergartens	5	75					11	215	[V12]
	Elementary schools	35	87					21	368	

158. Results from five national surveys of EEC of thoron in indoor air conducted in five countries are presented in table 7. Details on the national surveys and of 61 regional surveys conducted in 12 countries are reported in electronic attachment A-1. It should be noted that more than 70% of these regional surveys were carried out in India. All surveys were conducted using a passive type, deposition based, thoron

decay product detector. The statistical analysis in this annex were based on data from both the national and regional surveys. The AMs of the EECs of thoron in indoor air varied between 0.47 and 11.4 Bq/m^3, with an estimated median of 1.2 Bq/m^3. This is higher than the value of 0.3 Bq/m^3 reported in the UNSCEAR 2008 Report, annex B [U19]. It should be noted that the results of this literature review and the UNSCEAR Global Survey on Public Exposure cover only 4% of the world population.

Table 7. Compilation of descriptive statistics from national surveys reporting thoron equilibrium equivalent concentration in indoor air

AM: Arithmetic mean; GM: Geometric mean; Min: Minimum; Max: Maximum

Country	*Measurement duration*	*Total sample size*	*Thoron EEC in indoor air (Bq/m^3)*					*Reference*
			AM	*GM*	*Median*	*Min*	*Max*	
Cameroon [a]	2 months (rainy or dry season)	350	6.8			0.4	36	[S3]
Canada	3 months (winter season)	138	0.55	0.37		0.07	8.03	[C25]
Ireland	At least 3 months	205	0.47	0.38	0.39	<0.1	3.69	[M16]
Netherlands (Kingdom of the)	1 year	2 780	0.64		0.53			Global Survey
Republic of Korea	1 year	450	0.89	0.60	0.70		5.82	[K19]

[a] The data from Cameroon is based on measurements in 4 out of 10 regions; surveys in other regions were ongoing at the time this annex was compiled.

Thoron in High Background Radiation Areas

159. This annex summarizes new findings since the UNSCEAR 2017 Report, annex B [U25], while detailed information on the surveys is given in electronic attachment A-1.

160. Nugraha et al. [N32] conducted a survey of indoor thoron decay products in 208 dwellings in the HBRA of Mamuju on Sulawesi Island (Indonesia) using passive-type thoron decay product detectors to take one year-long measurement over the period between November 2018 and March 2020. Most of the dwellings in the area have wooden walls and coated cement floors. The AM of the EEC of thoron was reported to be 13.6 ± 5.6 Bq/m^3. The maximum value of 39.8 Bq/m^3 was measured at Northern Botteng Village. The main source of Thoron in Mamuju is the soil which contains high levels of natural radioactivity. The concentrations of ^{238}U and ^{232}Th in the soil of this area were found to be 23–30 times and 27–60 times higher than the world average reported in the UNSCEAR 2008 Report, annex B [U19], respectively.

161. Kudo et al. [K39] determined the EEC of thoron at Yangjiang (China), based on long-term measurements from July 2013 to January 2014 using passive-type thoron decay product detectors. The AM was reported to be 7.8 ± 9.1 Bq/m^3 with a maximum value of 36.2 Bq/m^3. The study concluded that thoron exposure was not negligible. Ishikawa et al. [I88] reported that the AM and the maximum value of the EEC of thoron measured in 29 dwellings in Gejiu City, Yunnan Province (China) were 10.2 and 23.9 Bq/m^3, respectively.

162. Omori et al. [O7] performed long-term measurements of the EEC of thoron in Odisha (India) from October 2010 to November 2021 using passive type thoron decay product detectors. The measurements was almost constant throughout the year. The AMs measured in autumn-winter, summer, and during the rainy seasons were 3.3 ± 2.8, 3.2 ± 2.4 and 3.3 ± 3.1 Bq/m^3, respectively. The GMs in each season were also reported as 2.4 ± 2.2, 2.6 ± 1.9 and 2.4 ± 2,1 Bq/m^3, respectively.

163. In Norway, thoron decay products were measured in 11 municipal buildings, including kindergartens and schools around a NORM area with high bedrock thorium and old mines. Measurements were made during the cold season from December to April (112 days); and during the warm season from April to August (133 days). High indoor radon concentrations were measured during the winter season in some buildings, while in others high indoor radon and thoron concentrations, and very low associated EEC of thoron were measured in summer. The AMs of the EEC of thoron measured in summer and winter were 0.7 ± 0.5 Bq/m^3 and 0.8 ± 0.6 Bq/m^3, respectively, while the maximum values in the same seasons were 2.1 Bq/m^3 and 2.5 Bq/m^3, respectively.

Ratio of radon EEC to thoron EEC and indoor radon concentrations

164. Ratios of EEC of radon to EEC of thoron in indoor air and to radon concentrations measured in the same survey are given in electronic attachment A-1. The ratios were calculated using the AMs of the EECs measured in each survey. Ratios estimated for HBRAs were also included as they did not differ significantly from other values. The median of the ratio of the EEC of radon to the EEC of thoron was estimated at 0.07 (range: 0.01–1.13), while the median of the of EEC of radon to radon concentration was estimated at 0.03 (range: 0.002–0.28). Applying the equilibrium factor of 0.4 to indoor radon concentration to estimate the ECC of radon in indoor air yields a very similar ratio of the EEC of radon to EEC of thoron of 0.08 (range: 0.01–0.7). It should be noted that it is not feasible to deduce the EECs of thoron from radon concentrations or from the EEC of radon because of the wide range in the ratio of the EEC of radon to the EEC of thoron (a factor of about 100 between minimum and maximum values).

(c) *Thoron concentrations in outdoor air*

165. Similarly to radon, studies on thoron in outdoor air are limited because outdoor thoron does not represent a significant health risk to the general population, due to its low concentrations, associated with its short half-life, and the low occupancy factor for the outdoor environment. Outdoor thoron concentrations depend primarily on the concentration of thoron precursors in the ^{232}Th decay series in the subsurface and the properties of ground and the rocks, such as the size of mineral grains, porosity, permeability, moisture content, which affect thoron emanation from the soil and its transport through the soil towards the atmosphere. Other important factors are the type of soil cover that influences the thoron exhalation rate and meteorological conditions [P25, R5]. Hosoda et al. reported measurements taken at 191 sites in Japan showing that atmospheric parameters can affect significantly thoron exhalation rates, depending on the geology [H29]. The authors suggested that the influence of moisture saturation is greater than that of soil-surface temperature [H29].

166. Table 8 gives the range and average values of the outdoor EEC of thoron in outdoor air measured in various regions in ten countries. More detailed information on the surveys are given in electronic attachment A-1.

167. Due to the limited coverage of the collected data, the same approach used for outdoor radon was applied in the calculation of a global average of the outdoor thoron concentration, based on using median estimates. The use of median values mitigates biases caused by extreme measurements and avoids assumptions based on a log-normal distribution. Based on the results from 10 regional surveys obtained from the literature review and the UNSCEAR Global Survey on Public Exposure, the median of the EEC of thoron in outdoor air was estimated at 0.3 Bq/m³. For comparison the value reported in UNSCEAR 2000 Report [U15] was 0.1 Bq/m^3.

Table 8. Compilation of descriptive statistics from surveys reporting EEC of thoron in outdoor air

Country	*Number of locations*	*Range (Bq/m³)*	*Arithmetic mean (Bq/m³)*	*Standard deviation (Bq/m³)*	*Reference*
AFRICA					
Morocco	21	0.07–2.7			[M31]
Morocco	1	0.3–1.71	0.6		[A25]
ASIA AND THE PACIFIC					
China	8	0.08–0.97	0.29	0.28	[Z2]
India	60	0.98–3.27	1.65		Global Survey, [M19]
Japan	42		0.22		[I89]
Malaysia	234	0.1-1	0.3		[S74]
EUROPE					
Romania	1	0.02–0.97	0.2		[C64]
Romania	6	0.001–0.5			[S37]
Romania	1		0.42		[F10]
NORTH AMERICA					
United States	1	0.03–0.13	0.08	0.05	[H9]

168. Studies indicate that high outdoor thoron concentrations are potentially confined to specific locations with monazite deposits, such as the HBRAs of Kerala and Odisha in India, and affected by human activities involving NORM, such as thorium mining, milling, thermal power plants, or industries generating waste containing elevated activity concentration of ^{232}Th or ^{232}U [K3, R5].

169. The CTBTO has established a network of 80 radionuclide monitoring stations for the continuous global observation of aerosol samples containing radionuclides. The network reports activity concentrations outdoor air for 16 radionuclides, including thoron decay products (^{212}Pb, ^{212}Bi, ^{208}Tl), which are collectively referred to as '^{212}Pb Family', or '^{212F}Pb' [C63]. Concentrations of ^{212F}Pb in outdoor air collected at 1-day intervals from 52 stations between 2007 and 2021 were analysed to assess temporal trend and seasonal variations. A summary of the concentrations is shown in figure III. Concentrations of ^{212F}Pb in outdoor air ranged from 3 μBq/m^3 to 0.985 Bq/m^3 with an overall median of 0.013 Bq/m^3. Monthly data show that the median ^{212F}Pb concentration gradually increased from 0.009 Bq/m^3 in January to 0.017 Bq/m^3 in August, followed by a gradual decrease to 0.009 Bq/m^3 in December, indicating a marginal seasonal variation. Annual variations do not reveal systematic long-term changes in the concentrations of ^{212F}Pb in outdoor air.[8]

[8] The views expressed in this study are those of the authors and do not necessarily represent the views of the CTBTO Preparatory Commission.

Figure III. Monthly and yearly variations of ^{212F}Pb (^{212}Pb, ^{212}Bi, ^{208}Tl) concentration resulting from 15 years continuous data (1-day interval) during 2007–2021 at 52 CTBTO radionuclide monitoring stations [C63]

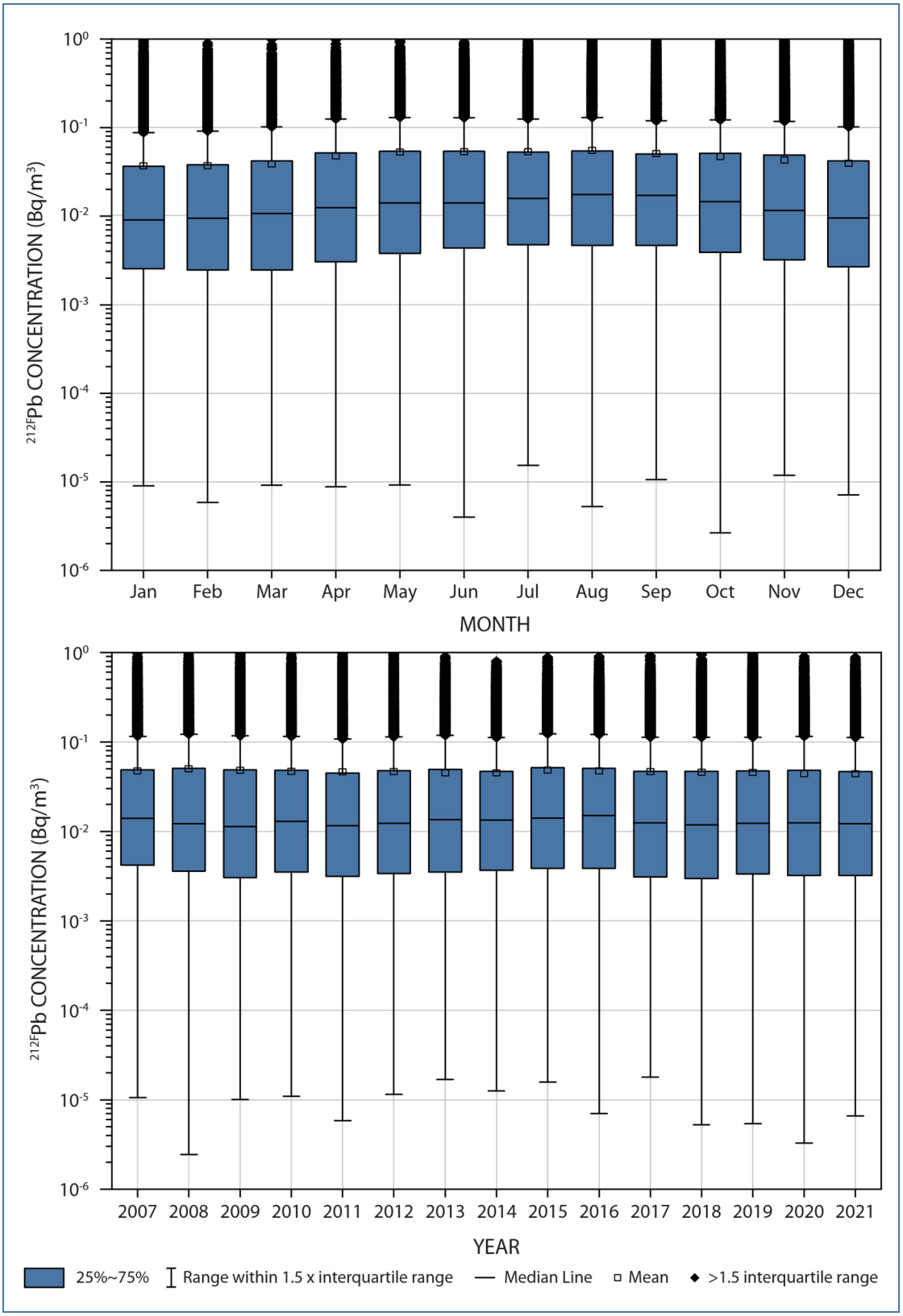

(d) *Doses from exposure to thoron and its decay products*

170. Since it was not possible to estimate updated values for the thoron concentrations air based on the information collected for this annex, due to the limitations of the studies investigated, a value of 10 Bq/m^3 for both the indoor and outdoor concentration of thoron, as reported in the UNSCEAR 2000 Report [U15] was used in the calculation of doses from inhalation of thoron.

171. The annual dose to the lungs from inhalation of thoron in air was estimated using equation A.2 in appendix A. Using an EEC of thoron in indoor air ($EEC_{220Rn,in}$) of 1.2 Bq/m^3, an annual occupancy rate indoors (O_{in}) of 0.8, and a dose coefficient for EEC of thoron ($DC_{EEC,220Rn}$) of 40 nSv/(Bq h/m^3) [U19] the annual dose was estimated at 0.34 mSv.

172. The annual dose to other organs from thoron dissolved in blood and soft tissue was estimated using equation A.8 in appendix A. Using an indoor thoron concentration ($C_{220Rn,in}$) of 10 Bq/m^3 and a dose coefficient for thoron in blood ($DC_{b,220Rn}$) of 0.11 nSv/(Bq h/m^3) [U13], the annual dose to other organs from thoron dissolved in blood was estimated at 0.008 mSv.

173. Equations A.5 and A.10 in appendix A were also used to calculate doses from inhalation of thoron outdoors. In this case using an EEC of thoron in outdoor air ($EEC_{220Rn,out}$) of 0.3 Bq/m^3, a thoron concentration in outdoor air ($C_{220Rn,out}$) of 10 Bq/m^3, and an annual occupancy rate outdoors (O_{out}) of 0.2 yields an annual dose to the lungs and to other organs from inhalation of thoron of 0.02 and 0.002 mSv, respectively. The annual dose from inhalation of radon in outdoor air was therefore estimated to be 0.02 mSv, while the total dose from inhalation of thoron was estimated at 0.36 mSv.

B. Natural sources of ionizing radiation other than radon and thoron

174. This section provides an overview of the natural sources of ionizing radiation excluding radon and thoron and associated exposures. Two sources are considered: cosmic radiation and terrestrial radionuclides—also called primordial radionuclides. More specifically this section provides estimates of doses to the public from external exposure to cosmic radiation and terrestrial radionuclides as well as internal exposure from ingestion and inhalation of terrestrial radionuclides other than radon and thoron.

1. Outline of the dose assessment methodology

175. The methodology to calculate doses from sources of natural radiation other than radon and thoron follows the approach used in previous UNSCEAR reports [U11, U12, U15, U21]. More detailed information on the methodology is given in appendix A.

176. The methodology for exposure to cosmic rays at ground level has been updated since previous UNSCEAR reports [U15, U19] to account for improvements in the Particle and Heavy Ion Transport code System (PHITS)-based Analytical Radiation Model in the Atmosphere (PARMA) version 4 [S15, S17]. PHITS is a general purpose Monte Carlo radiation transport code, also available as Excel-based program for calculating Atmospheric Cosmic-ray Spectrum (EXPACS) 4.10 [J1]. For exposure during air travel, the methodology described in previous UNSCEAR reports has been used and incorporates more detailed flight and passenger statistics. For cosmogenic radionuclides, the methodology relies on measurements of activity

concentrations in air at exposure locations provided by Member States through the UNSCEAR Global Survey on Public Exposure combined with data from the literature review and the CTBTO [C63].

177. External exposures to terrestrial radionuclides of natural origin in soil vary according to the underlying geology. The dose assessment methodology for outdoor external exposure to terrestrial radionuclides relies mainly on the measured activity concentrations in soil reported in the literature. Worldwide estimates of external dose are presented in this annex and were extrapolated to areas lacking data using geological data as a surrogate for activity concentrations or dose rates outdoors. High background radiation areas were identified based on statistical evaluations of the extracted literature data. External exposure also results from terrestrial radionuclides present in building materials, which serve both as a shield and source of exposure. The shielding factor for terrestrial radiation previously used by the Committee was applied to estimate doses from exposures indoors.

178. The methodology from the UNSCEAR 2008 Report, annex B [U19] was used to estimate the ingestion doses from ^{40}K. The methodology accounts for the natural abundance of ^{40}K in natural potassium and the homeostatic control of the concentration of potassium in the body. For other natural radionuclides—excluding radon but including its long-lived decay products—the ingestion dose was calculated based on activity concentrations measured in foods and drinking water.

179. The available data to quantify public exposures from the wide range of NORM industries are often limited, preventing the calculation of worldwide average doses. Due to the lack of discharge data and detailed information on exposure pathways, it was not possible to develop a consistent methodology for all NORM industries. Consequently, the evaluation relied primarily on dose estimates reported in the literature or provided by Member States through the UNSCEAR Global Survey on Public Exposure. Given the diversity of NORM industries and the challenges in characterizing sources and exposure scenarios, the assessment focused on specific case studies to estimate doses for particular situations rather than deriving global averages.

2. Cosmic radiation and cosmogenic radionuclides

(a) *Origin, composition and variability*

180. Cosmic rays of high-energy particles entering the Earth's atmosphere interact with atoms in the atmosphere, producing a cascade of secondary interactions. The flux of resulting secondary particles, which contribute to cosmic ray exposures, decreases with depth in the atmosphere. The cosmic ray interactions also produce radioactive nuclei known as cosmogenic radionuclides. The best known of these are ^{3}H, ^{14}C, ^{7}Be and ^{22}Na.

181. Most primary cosmic rays are galactic cosmic rays that arise outside the solar system. Galactic cosmic rays incident on the upper atmosphere consist of a nucleonic component, which accounts for 98% of the total flux, and electrons, which account for the remaining 2%. The nucleonic component consists primarily of protons (~85% of the total flux) and alpha particles (~12%), with the remainder being heavier nuclei (~1%) [U19]. The primary cosmic particles have an energy spectrum that ranges from 10^{8} eV to more than 10^{20} eV. The flux of particles decreases with increasing energy and corresponds to approximately 1 particle per m^{2}/s at 10^{11} eV; 1 particle per m^{2}/a at 10^{16} eV; and 1 particle per km^{2}/a at 10^{19} eV [S83, U15].

182. Solar cosmic rays are another form of cosmic rays. Solar cosmic rays originate from solar flares when the particles produced are directed towards the Earth. These events are of short duration, typically a few hours, and are highly variable in their strength. They have a negligible impact on long-term doses to the public.

Latitude effects

183. The Earth's magnetic field reduces the intensity of cosmic rays reaching the upper atmosphere. The shape of the Earth's magnetic field is such that only particles of higher energies can penetrate at lower geomagnetic latitudes. This produces the geomagnetic latitude effect, with intensities and dose rates minimal at the equator and maximal near the geomagnetic poles. The latitude effect is illustrated in figure IV, which shows the dose rate from neutrons only and the total cosmic ray dose rate—including directly ionizing components and photons—as a function of geomagnetic latitude at sea level and at an altitude of 12 km, respectively, for the northern hemisphere (N). For the southern hemisphere (S) the curves are not strictly symmetric as illustrated by the total dose at an altitude of 12 km.

Figure IV. Variation in dose rate of cosmic radiation as a function of geomagnetic latitude

Note the different vertical scales for the dose rate at sea level (right axis) and 12 km (left axis), respectively. Calculated using the PARMA model [S15] for a geographic longitude of 0°

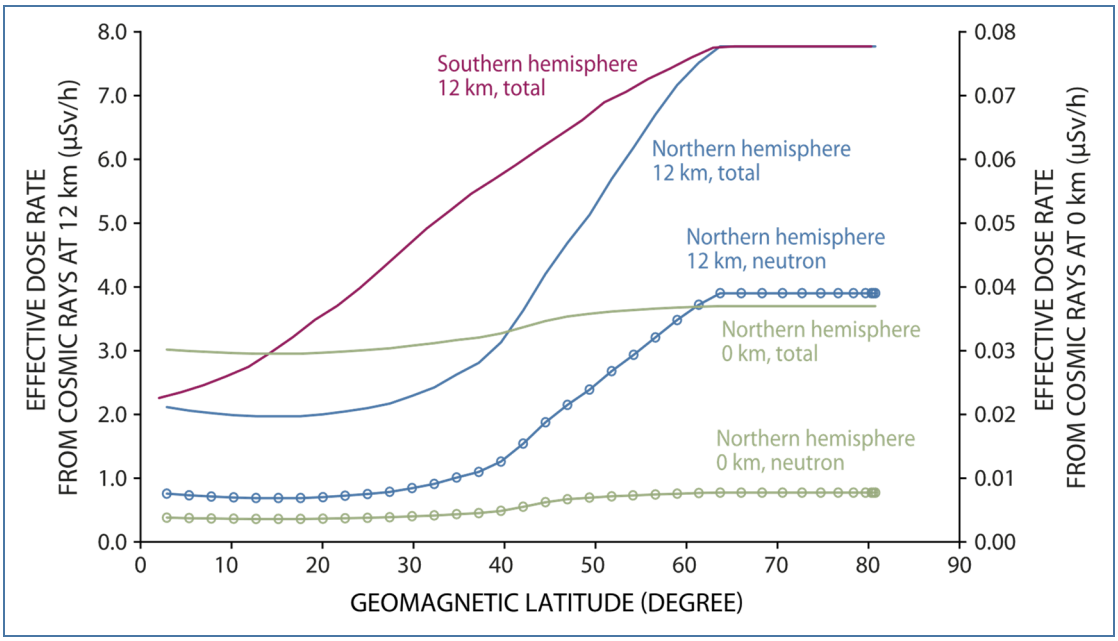

Altitude effects

184. An additional shielding to cosmic rays, besides the Earth's magnetic field, is provided by an air layer of approximately 10,000 kg/m^2, which is comparable to a 10 m thick layer of water. As a result, at sea level, cosmic radiation contributes about 10% of the total dose rate from natural radiation to which the public is generally exposed. However, at high altitudes in the atmosphere or in space, cosmic rays constitute the predominant source of ionizing radiation.

185. The complex set of secondary-charged and uncharged particles produced by cosmic rays incident on the atmosphere includes protons, neutrons, pions, muons and lower-Z nuclei. The relative contributions to the dose caused by secondary cosmic ray constituents at various depths in the atmosphere are illustrated in figure V.

186. Because of their longer mean free path, neutrons are the predominant nucleonic component at altitudes below approximately 20 km and their relative contribution to dose is highest at altitudes of around 5 km. Neutrally charged pions decay into high-energy photons, which in turn generate high-energy electrons. These electrons produce additional photons, initiating a chain reaction known as

the electromagnetic or photon/electron cascade. Photons, electrons, and positrons—alongside protons and neutrons—are the primary contributors to the cosmic ray dose at aircraft cruising altitudes (~12 km). Charged pions decay into muons, which, due to their long mean free path in the atmosphere, become the predominant component of the charged particle flux at ground level. Below an altitude of 1 km, muons can account for up to 70% of the total radiation dose.

Figure V. Effective dose rate as a function of altitude at a geomagnetic latitude of 45°N and relative contributions of the components of cosmic rays

The dashed line shows the total dose rate calculated using EXPACS 4.10 [S15]

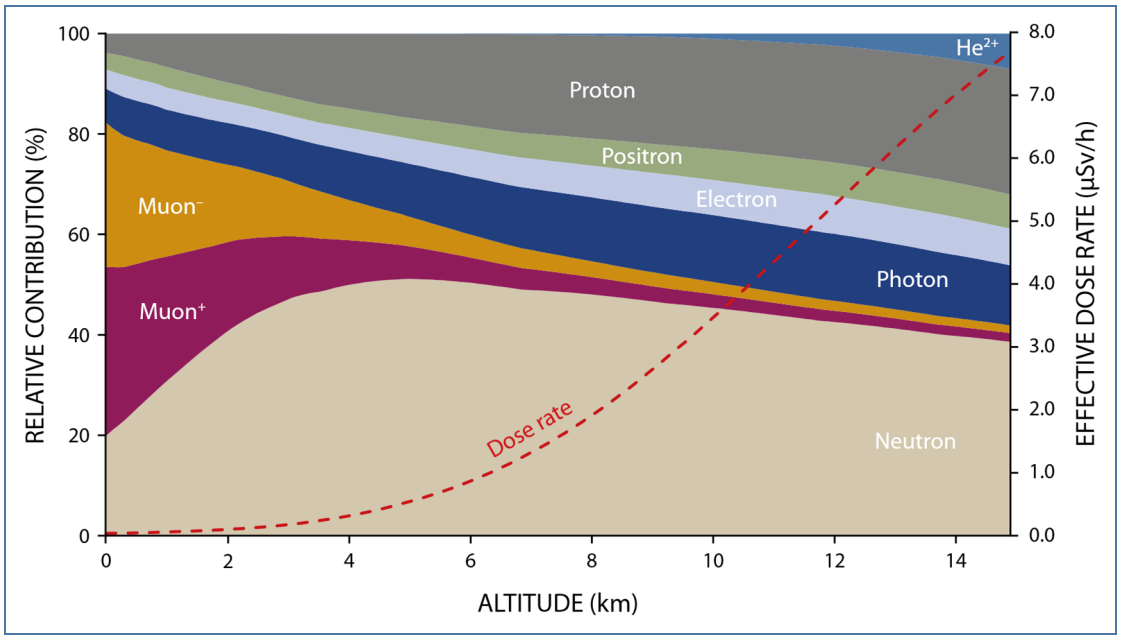

(b) *Exposure at ground level*

187. External exposure to cosmic rays at ground level varies according to the latitude and altitude of the exposure location and the 11-year solar activity cycle. The shielding offered by buildings reduces exposure at indoor locations.

188. Muons, with energies mainly of between 1 and 20 GeV, constitute the prevalent component of the cosmic ray field at ground level. At low latitudes, their relative contribution to the total dose rate from cosmic rays is at its highest (70%), although it should be noted that the increase of the absolute dose from muons with increasing latitude is very small. The absolute dose from muons increases with altitude, and at 4 km is approximately double that at sea level.

189. Neutrons arise from collisions of high-energy protons in the upper atmosphere. Incoming protons that initiate the cosmic ray neutron field are strongly affected by the Earth's magnetic field, resulting in a lower neutron fluence rate in equatorial regions than in polar regions. At altitudes below 2 km, their contribution to the total dose from cosmic rays is roughly between 20% and 40%.

190. The PARMA model [S15] was used to calculate outdoor dose rates for each populated area of 1 km^2 (see appendix A). This approach allowed the different contributing factors to the doses and their variability as a function of altitude and latitude to be accounted for, without requiring any simplifying

assumptions. The map of the resulting unshielded dose rate is shown in figure VI. More detailed maps for each country are available in electronic attachment A-2.

Figure VI. Map of the unshielded dose rate of cosmic radiation in populated areas at the altitude of Earth's surface[a]

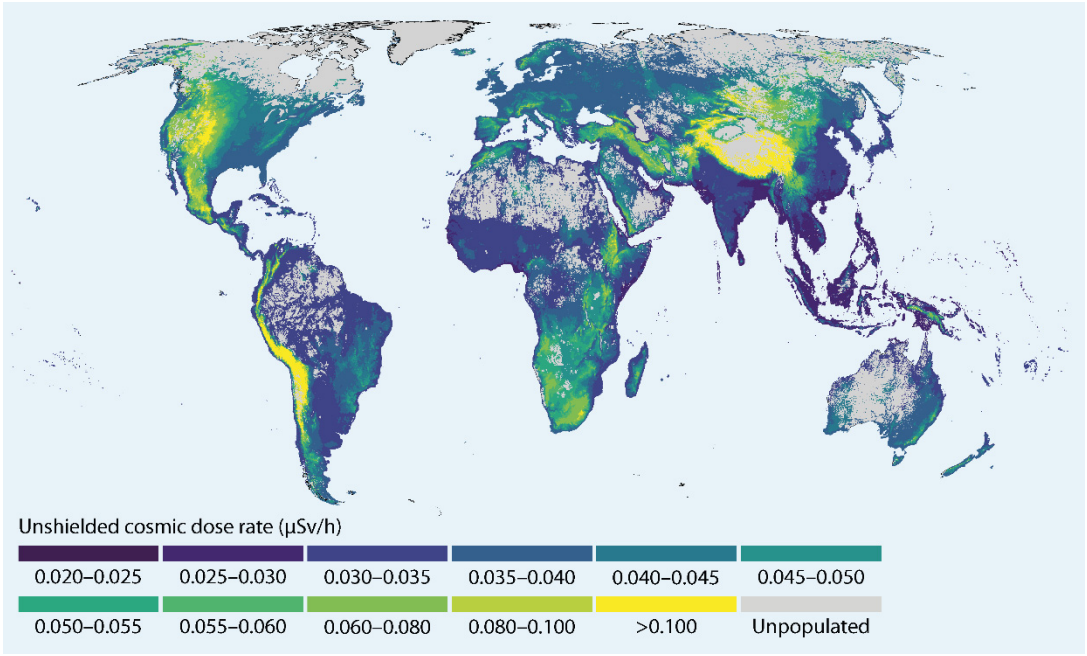

[a] The boundaries and names shown and the designations used in this map do not imply official endorsement or acceptance by the United Nations. Final boundary between the Republic of Sudan and the Republic of South Sudan has not yet been determined. Dotted line represents approximately the Line of Control in Jammu and Kashmir agreed upon by India and Pakistan. The final status of Jammu and Kashmir has not yet been agreed upon by the parties. A dispute exists between the Government of Argentina and the United Kingdom of Great Britain and Northern Ireland concerning sovereignty over the Falkland Islands (Malvinas).

191. To estimate the global population-weighted average dose rate from cosmic rays, calculated dose rates for each 1 × 1 km grid cell were combined with high-resolution population data [S20], which removed the need for simplifying assumptions about the population distribution. Using this approach the world population-weighted average dose rate was estimated to be 0.037 μSv/h; the uncertainty of the PARMA-based cosmic ray dose rates is estimated to be around a few percent [S16]. Ignoring the effect of building shielding, the world population-weighted annual dose was estimated to be 0.33 mSv. Applying a shielding factor (SF_C) of 0.9 and an indoor occupancy factor (O_{in}) of 0.8, the adjusted worldwide average annual dose from cosmic rays was estimated to be 0.30 mSv.

192. This estimate of the global average population-weighted annual dose due to cosmic rays is 21% lower than its previous estimate, which assumed a higher average annual dose before shielding of 0.46 mSv [U15]. In the UNSCEAR 1988 Report [U12], a representative absorbed dose rate in air at sea level was given as 30 nGy/h, similar to the value obtained from the PARMA model applied in this annex. However, at higher altitudes, the previous model predicted higher dose rates than the PARMA model resulting in a higher average dose before shielding. Another factor affecting the dose from cosmic rays was the relatively coarse population distribution model used in previous UNSCEAR reports based on a paper by Bouville and Lowder [B45], which had a spatial resolution of one degree and therefore tended to overestimate the altitude at which people reside, thereby overestimating the average dose.

193. The world population-weighted average dose rate from neutron component of cosmic rays was estimated to be 6.9 nSv/h. Neglecting the building shielding effect, the world population-weighted annual dose due to this component was estimated at 62 μSv. Using a shielding factor of 0.9 and an indoor occupancy fraction of 0.8, the world average annual dose from the neutron component of cosmic rays was estimated to be 56 μSv. In the UNSCEAR 2000 Report, annex B [U15], the average value for the neutron component of the annual cosmic-ray dose was estimated at 100 μSv.

194. The population-weighted annual effective dose due to cosmic rays by country is illustrated in figure VII. The highest value was estimated for Bolivia (0.81 mSv), primarily due to its high population-weighted elevation, despite its relatively low latitude in the southern hemisphere. In contrast, the annual dose for countries with similar geomagnetic latitude but lower altitude, such as Singapore, was estimated to be around 0.20 mSv. The total dose rate from cosmic rays at La Paz, Bolivia (3,625 m above sea level) was estimated to be 0.16 μSv/h, five times higher than the one in Singapore (0.03 μSv/h). The neutron component contributes significantly more at higher altitudes; for example, it contributes 38% of the total dose in La Paz as opposed to 13% in Singapore (5 m above sea level). Similarly, at higher latitudes, the contribution of the neutron component increases even at similar altitudes. For example, the dose rate in Oslo (94 m above sea level) is 0.038 μSv/h, with neutrons contributing 22%.

Figure VII. Average annual effective dose of cosmic radiation to the public by country (indoor occupancy factor is 0.8 and shielding factor is 0.9)[a]

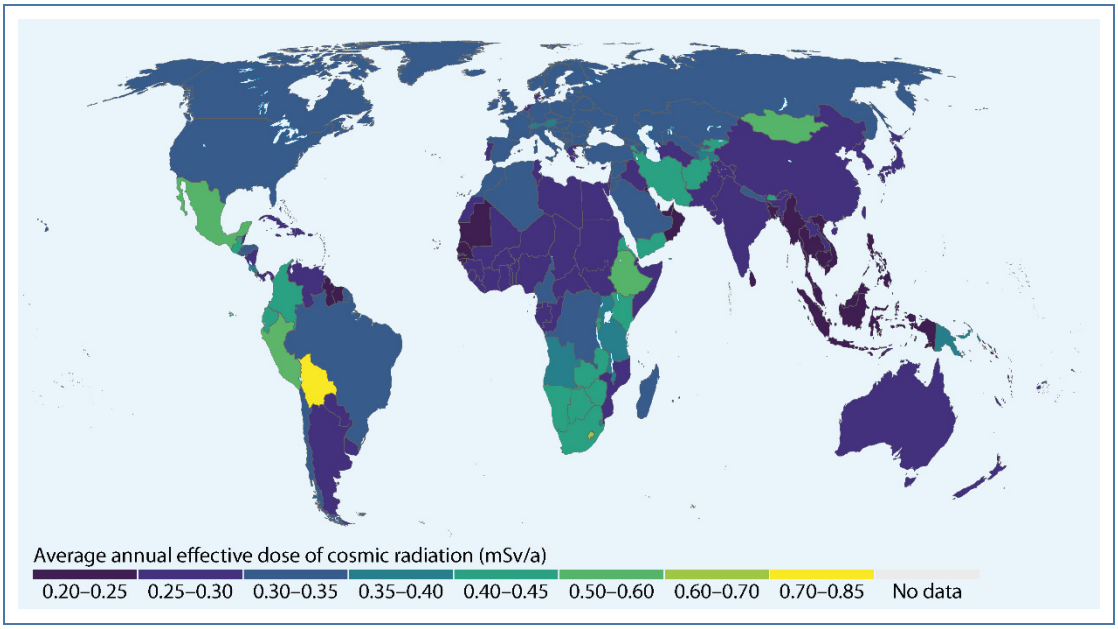

[a] The boundaries and names shown and the designations used in this map do not imply official endorsement or acceptance by the United Nations. Final boundary between the Republic of Sudan and the Republic of South Sudan has not yet been determined. Dotted line represents approximately the Line of Control in Jammu and Kashmir agreed upon by India and Pakistan. The final status of Jammu and Kashmir has not yet been agreed upon by the parties. A dispute exists between the Government of Argentina and the United Kingdom of Great Britain and Northern Ireland concerning sovereignty over the Falkland Islands (Malvinas).

195. Figure VIII shows a histogram of the distribution of the annual doses from cosmic rays for the world's population. It is estimated that 3 billion people receive an annual dose from cosmic rays in the range 0.25–0.3 mSv and about 2.5 billion people receive an annual dose in the range 0.2–0.25 mSv. About 19 million people living in regions at higher altitudes and latitudes receive an annual dose of more than 1 mSv from cosmic rays.

Figure VIII. Distribution of annual effective dose from cosmic rays for the world's population accounting for shielding by buildings (reference date 27 December 2015)

Note the change in the bin widths for doses above 1 mSv

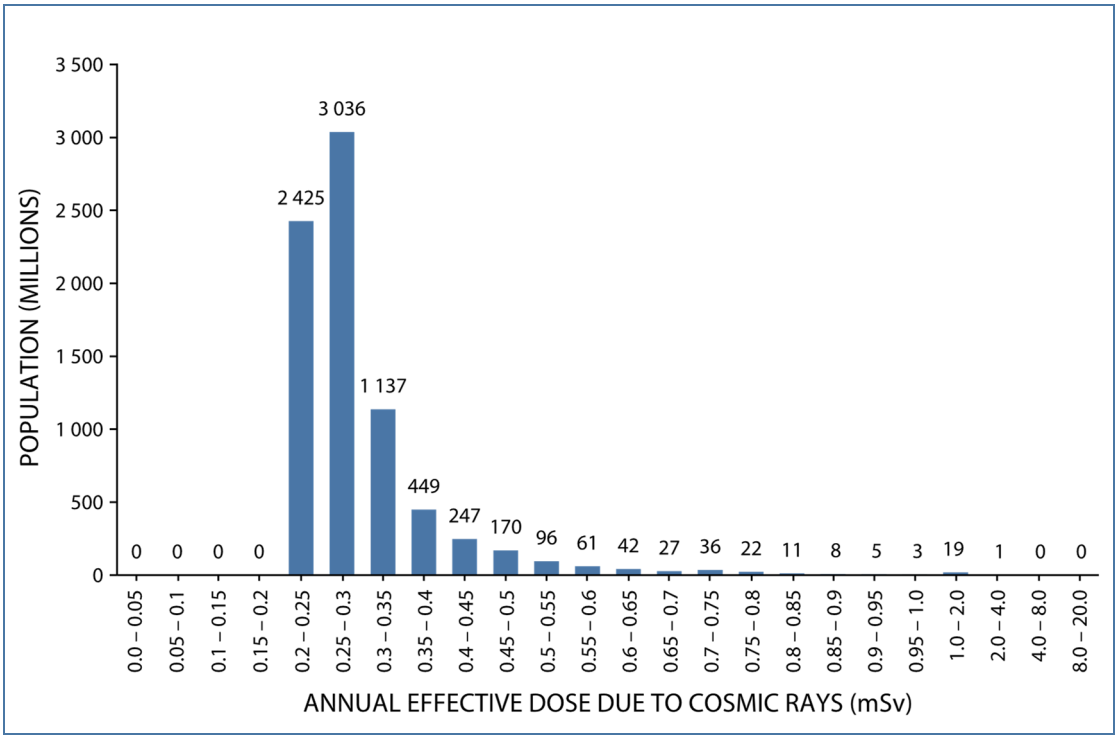

196. Cosmic ray fluxes at ground level also vary with the temporal variation in solar activity and other factors (see electronic attachment A-2. The temporal variations of the outdoor dose rates between 2000 and 2020 evaluated for Sydney (Australia), Vienna (Austria), and Jakarta (Indonesia) are shown in figure IX. For each location the dose rates shown were normalized to the dose rate obtained for a reference date (27 December 2015) on which the solar modulation index was close to its mean value of 50. The absolute values of the effective dose rates at the reference date for Sydney, Vienna, and Jakarta were 0.036, 0.039 and 0.029 μSv/h, respectively.

197. The most significant long-term solar effect is the 11-year cycle of the solar activity, which generates a corresponding cycle in total cosmic radiation intensity (figure IX). The periodic variation in solar activity produces a similar variation in the solar wind—a highly ionized plasma with associated magnetic field. The strength of this magnetic field modulates the intensity of galactic cosmic radiation. During periods of peak solar activity, the magnetic field reaches its highest level while the galactic cosmic radiation intensity is at its lowest due to the shielding effect of the magnetic field [B20].

198. The intensity of cosmic rays is also affected by short term events, such as ground level enhancements, which are sudden increases in the cosmic ray intensity near the ground, and Forbush decreases. Ground level enhancements are caused by the acceleration of charged particles, mostly protons, from the sun to energies above 500 MeV within the solar atmosphere or in interplanetary space [B20]. These enhancements cannot be reproduced by the PARMA model due to their short duration—typically a few hours or less. Forbush decreases are rapid reductions in the observed intensity of galactic cosmic rays, which are often associated with coronal mass ejection events during periods of high solar activity [K2] and last for several days. A coronal mass ejection is a phenomenon in which a large amount of plasma is ejected from the sun. This plasma cloud covers the near-Earth interplanetary space, blocking the penetration of low-energy

cosmic rays from the galaxy or the sun, resulting in a decrease in the observed cosmic ray intensity near Earth. The PARMA model accounts for these sudden drops in cosmic ray intensity using daily observations from neutron monitors. Various Forbush events are visible as negative spikes in figure IX, with the event that occurred between the end of October and beginning of November 2003 being the most pronounced.

Figure IX. Temporal variation of the effective dose rate due to cosmic rays for Sydney, Vienna, and Jakarta, normalized to the respective values determined for 27 December 2015

Note: Calculated using PARMA model [S15]

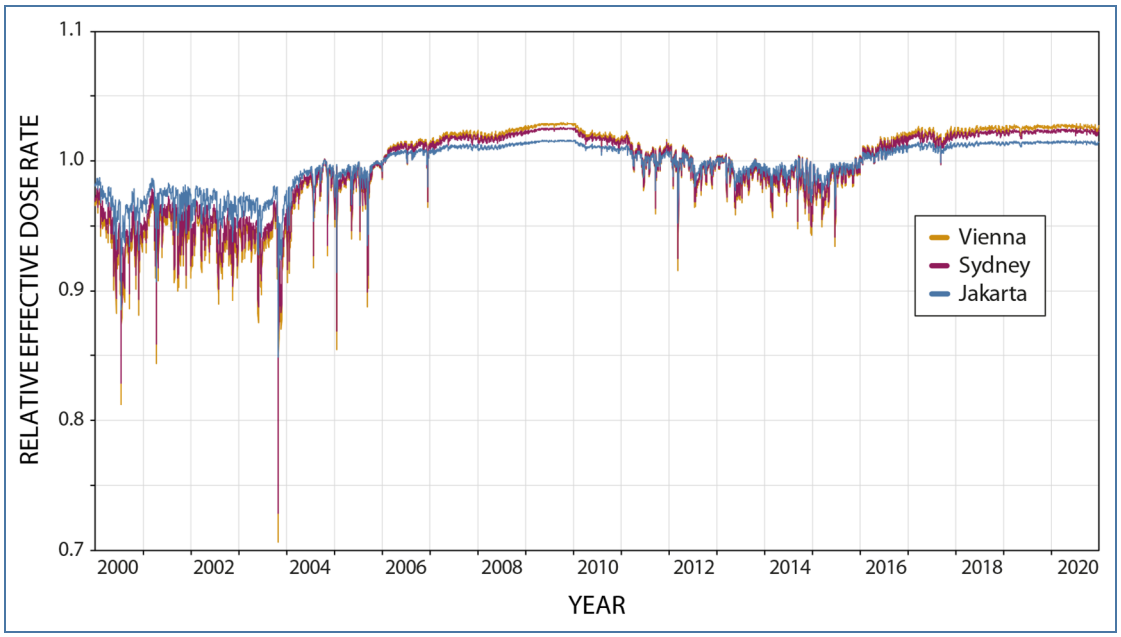

199. Chen [C22] investigated the annual effective dose from cosmic rays across Canada, using the PARMA model to estimate doses for over 1,500 communities, representing more than 85% of the Canadian population. Their estimate of a population-weighted average annual effective dose at ground level was 0.31 mSv, which is lower than the 0.37 mSv reported in this annex. This difference can be primarily attributed to two factors: the lower overall cosmic radiation intensity during the study period (2000–2006; see figure IX), and the higher spatial resolution of the population distribution model used in this annex.

200. The EXPACS 4.10 software was used to evaluate variations in dose rates due to cosmic rays, accounting for factors, such as the solar activity and water content of the ground. The neutron component of dose rate from cosmic rays was found to vary by 5–7% between periods of maximum and minimum solar activity, depending on the geomagnetic latitude, while the ionizing component was found to vary by 8–19%.

201. Variations in dose rates from cosmic ray due to different water contents in soil were specifically evaluated for Vienna (Austria). The investigation showed that the ionizing component remained unchanged across different moisture levels, while the neutron component was reduced by 10 and 14% at a moisture content of 5 and 10%, respectively, compared to that for dry soil. This reduction was attributed to the albedo effect, whereby increased hydrogen content in moist soil lowers neutron reflectivity. The rate of decrease the neutron component of the effective dose rate due to cosmic rays slows at very high moisture levels in the soil. The decrease of the dose rate at a moisture content of 100% (i.e., above a water surface) was estimated to be 28% compared to dry soil.

202. The latitudinal variation in the neutron component of the dose from cosmic rays at low latitudes was clarified through comprehensive measurements by Nagaoka et al. [N1] conducted in Japan. The effective dose rates due to the neutron component of cosmic rays between 14 and 36° of geomagnetic latitude varied by about a factor of two, from 4.8 to 8.3 nSv/h. The average effective dose rate across Japan due to the neutron component of the dose from cosmic rays was estimated to be 4.8 nSv/h.

(c) *Exposures on aircraft*

203. Aircraft passengers are exposed to significant higher levels of cosmic rays than people at ground level. The radiation field at cruising altitudes consists of neutrons, protons, and photons. Neutrons contribute between 40 and 80% of the dose rate, depending on altitude, latitude, and the phase in the solar cycle. The exposure on a flight depends on its altitude and geomagnetic latitude, as well as the flight duration. Dose rates vary from 1 μSv/h for a flight at low latitudes, to 6 μSv/h for a trans-Atlantic flight assuming that the cosmic rays are of intermediate strength (see electronic attachment A-2). For example, a flight from Mumbai to Delhi (duration: 1.8 hours) results in a dose of 2 μSv, while one from Los Angeles to London (duration: 10.9 hours) results in a dose of 61 μSv.

204. Frasch et al. [F13] analysed the variation doses to aircraft passengers during the solar cycle. Comparison of doses between the middle of the decreasing phase of solar cycle 23 (January 2004) and its minimum (January 2009) showed an increase from 25 to 30 μSv on the trans-equatorial route from Frankfurt to Johannesburg, and from 50 to 78 μSv on the polar route from Frankfurt to New York [F13]. In-flight measurements during solar storms have shown an increase of up to about 80% in the total dose for flights crossing the polar region [B9], though this increase could not be evaluated for this annex due to lack of available data.

205. Annual average effective doses from cosmic radiation during air travel for different regions of the world based on data for 2012, are given in table 9. These doses were calculated using the code SIEVERT [C40] and air traffic data from ICAO. For flights before July 2021, SIEVERT used tissue and radiation weighting factors taken from ICRP Publication 60 [I65]. Therefore, doses calculated using SIEVERT were multiplied by a factor of 0.8 to take account of the new factors included in ICRP Publication 103 [I70]. Details on how calculations were performed are given in appendix A and in electronic attachment A-2. Data provided by ICAO were revenue passenger kilometres (RPKs) for 50 region pairings, called route groups, for 10 long-term traffic forecasts regions in the year 2012 [I61]. Since no detailed data were available on the proportion of non-flyers, occasional flyers, and frequent flyers, the doses given in table 9 represent the average contribution of dose during air travel to the total dose from cosmic rays rather than the dose to a specific individual.

206. The worldwide average annual dose from exposure to cosmic rays during air travel for the year 2012 was estimated at around 3 μSv (see table 9). The average doses for the different ICAO Long-Term Traffic Forecasts regions [I61] range from 0.1 μSv for Sub-Saharan Africa to 25 μSv for North America. The high dose estimated for North America is a reflection of both the high number of flights per person and the higher dose per flight for countries at these high latitudes. The uncertainty in these annual doses is estimated to be around 10% (see electronic attachment A-2 for more information).

Table 9. Average annual doses (μSv) from cosmic radiation during air travel for major ICAO regions in 2012

Region	*Population (thousands)*	*Average annual dose (μSv)*
Central America/Caribbean	215 970	1.6
Central and Southwest Asia	3 251 598	0.5
Europe	834 928	8.7
Middle East	235 068	3.0
North Africa	183 085	0.8
North America	357 714	25.1
North Asia	202 021	6.1
Pacific Southeast Asia	619 219	1.6
South America	418 446	1.1
Sub-Saharan Africa	1 002 516	0.1
Worldwide average		**3.0**

207. It should be noted that an estimated 60% of the world population receive no dose from flying, while the annual dose to frequent flyers can exceed 1 mSv. The annual dose passengers flying an average of 100 h/a on domestic flights in North America was estimated at 0.63 mSv [U15]. The maximum dose for frequent flyers is close to the annual dose of crew members for whom the average dose was estimated to be 2.7 mSv (range: 1.5–4.5 mSv) [U30].

208. Air travel both in terms of passengers and RPKs have been steadily increasing by approximately 6% per year from 2001 to 2019 as presented in figure X. Due to the coronavirus pandemic, traffic was less than half in 2020 and 2021 compared to 2019 but started rising again from 2022 onwards. Between 2003 and 2019, the RPKs nearly tripled and thus, the global average annual per capita dose from cosmic rays during air travel increased from approximately 1.5 μSv to around 4.5 μSv over this period.

Figure X. Steady increase of air travel and pandemic effect between 2001 and 2022 [I63]

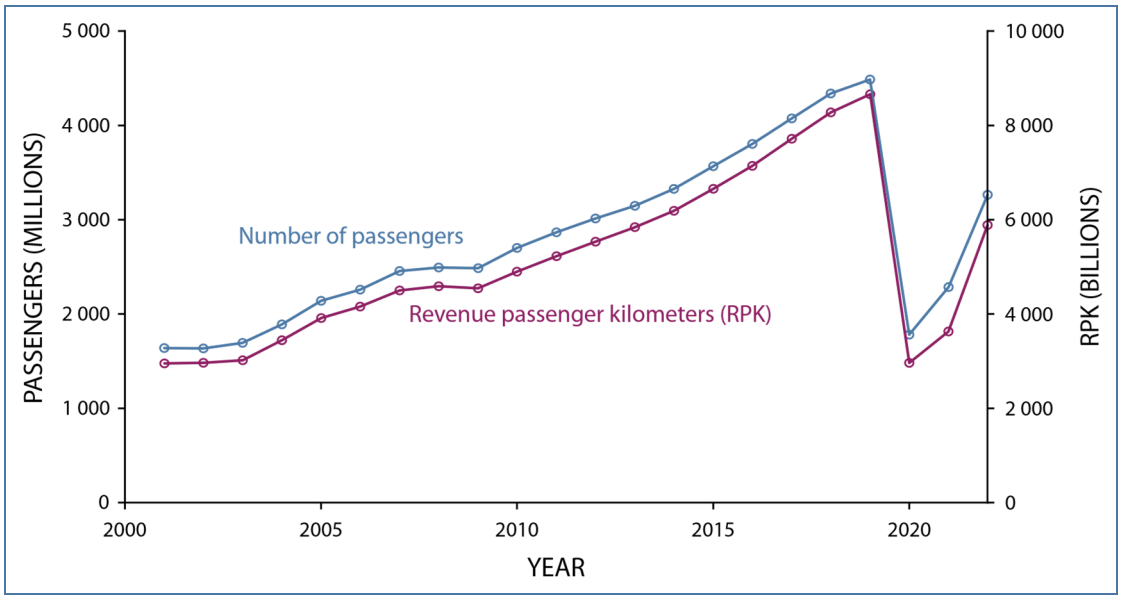

209. Chen and Mares estimated the fetal dose from cosmic rays for pregnant aircrew and frequent flyers on commercial flights [C21]. Doses were calculated for long-distance Canadian domestic flights and international flights between Canada and European countries using the Fluka Monte Carlo code. The study estimated an average dose rate to a fetus of 5.3 μSv/h which is about half the dose rate to the mother (10 μSv/h) during the commercial flight.

210. No significant differences in radiation doses have been observed when crossing the region of the South Atlantic Anomaly at an aircraft altitude of 13 km [M20]. The South Atlantic Anomaly is an area of anomalously low magnetic field strength in the South Atlantic region along the Brazilian coast. The anomaly affects the position of the Van Allen radiation belts, which are zones with high dose rates due to protons and electrons trapped in the Earth's magnetic field. While the inner radiation belt typically is situated at an altitude of a few thousand kilometres, it descends to a distance of a few hundred kilometres from the Earth's surface in the region of the South Atlantic Anomaly [U19].

(d) *Cosmogenic radionuclides*

211. Cosmic rays entering the Earth's atmosphere interact with atmospheric nuclei to produce cosmogenic radionuclides, such as ^{3}H, ^{7}Be, ^{14}C and ^{22}Na. In principle, all isotopes lighter than the target nuclei—mainly nitrogen, oxygen and argon—are produced by high-energy spallation reactions. Production rate of cosmogenic radionuclides is greatest in the upper stratosphere, but some energetic cosmic ray protons and neutrons reach the lower atmosphere, where they also produce cosmogenic radionuclides. A comprehensive list of cosmogenic radionuclides, with their properties, production rates and average tropospheric concentrations, is provided in the UNSCEAR 2000 Report [U15].

212. Cosmogenic radionuclides are produced continuously by nuclear reactions with cosmic rays, resulting in a steady state distribution in the environment. As described in the previous section, the intensity of cosmic rays in the atmosphere varies due to the influence of the magnetic field and attenuation due to air height distribution. This variability in cosmic ray intensity corresponds to a variability in the production rate of cosmogenic radionuclides. The production rate of cosmogenic radionuclides is also affected by the 11-year solar activity cycle, which modulates the penetration of cosmic rays through the Earth's magnetic field. Four of the cosmogenic radionuclides, ^{3}H, ^{7}Be, ^{10}Be and ^{14}C, are produced from nitrogen and oxygen and have a higher atmospheric production rate than other radionuclides, such as ^{22}Na, which are produced from argon, the fraction by volume of which in the Earth's atmosphere is only about 1%. Carbon-14 arises from the interaction of the slow neutron component of cosmic rays with ^{14}N. Annual global production rate due to cosmic rays is estimated to be $2.2 \pm 0.6 \times 10^{26}$ atoms ^{14}C, corresponding to 8.43×10^{14} Bq [K4]. This value is smaller than the past estimate of 1.54×10^{15} Bq for the annual quantity produced (see table 4 in UNSCEAR 2000 Report, annex B [U15]). The specific activity of cosmogenic ^{14}C before the atmospheric nuclear weapons tests is estimated at 222 Bq/kg C [U19]. The nuclear test explosions from the late 1950s and early 1960s introduced an estimated activity of 0.35×10^{18} Bq into the atmosphere. This resulted in a peak specific activity of ^{14}C in the northern hemisphere in the mid-1960s of around 400 Bq/kg C, corresponding to approximately 770 Δ^{14}C (‰) [H39]. Since then, ^{14}C in the atmosphere has been continuously absorbed into the marine environment. Releases from NPSs are small in comparison and mostly of local importance. The burning of fossil fuels dilutes the naturally produced ^{14}C and this so-called Suess-effect now dominates over the ^{14}C traces left in the atmosphere by the bomb tests. The decrease in atmospheric ^{14}C is illustrated by measurements of ^{14}C in tree leaves from remote stations in Switzerland as shown in figure XI. Today, the specific activity of ^{14}C in atmospheric CO_2 and fresh terrestrial organic matter is similar to, or even lower than, the level before the atmospheric nuclear weapons tests.

213. Tritium results from the interaction of cosmic rays with nitrogen and oxygen nuclei. Its production rate was estimated to be 0.20 ± 0.05 atoms/(s cm^2) [T5] (range: 0.14–0.37 atoms/(s cm^2)). More recent estimates are somewhat higher with an average of 0.32 atoms/s per cm^2 column [M10]. Multiplying this rate by the surface area of the Earth (5.1×10^8 km^2), the annual global production rate of cosmogenic tritium was estimated to be 9.2×10^{16} Bq [I57]. Tritium concentration in the atmosphere increased significantly due to the atmospheric nuclear tests in the early 1960s. Activity concentration of tritium in rainwater in the northern hemisphere was up to 1,000 Bq/L in 1963 [J9]. By the 2020s, atmospheric tritium was back to the levels before the atmospheric nuclear bomb tests with activity concentrations in rainwater being 1 Bq/L or less. For example, activity concentrations of tritium measured in rainwater collected in Japan from 2016 to 2017 were between 0.6 and 1 Bq/L [G30], while those in French river waters between 2014 and 2016 ranged from 0.1 to 0.9 Bq/L [D30]. In the Southern hemisphere, maximum concentrations of ^3H in the atmosphere in the 1960s were lower (less than 100 Bq/L) and the return to levels before the atmospheric nuclear weapons tests occurred earlier [L5].

Figure XI. Decrease of ^{14}C activity concentration in the atmosphere

The pre-bomb-level (early 1950s) corresponds to a ^{14}C activity concentration of 222 Bq/kg C. Data from Climate and Environmental Physics (CEP) and Laboratory for the Analysis of Radiocarbon with AMS (LARA), University of Bern, Switzerland [S70]

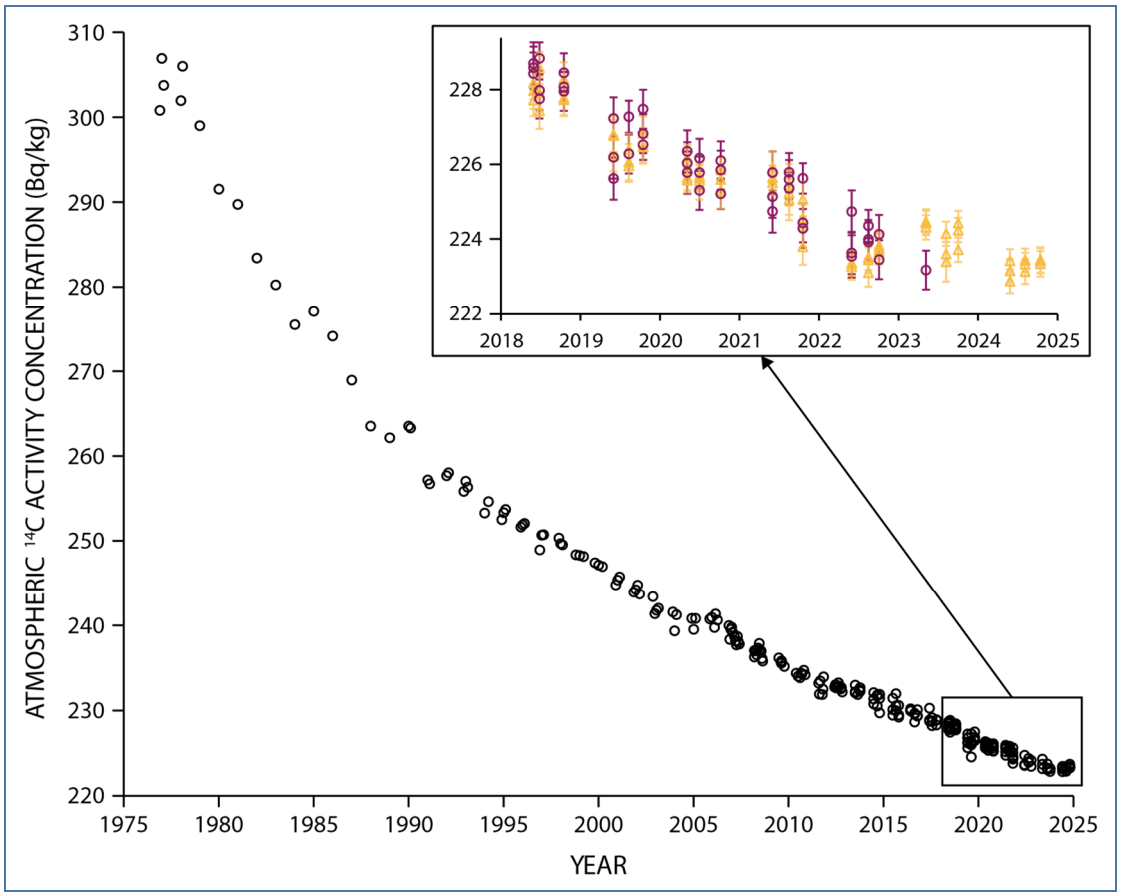

214. Beryllium-7 is a cosmogenic radionuclide produced by the interaction between nitrogen and oxygen atoms and energetic cosmic rays in the upper atmosphere, through reactions including $^{14}N(p,2\alpha)^7Be$, $^{16}O(p,^{10}B)^7Be$, $^{14}N(n,^8Li)^7Be$, and $^{16}O(n,^{10}Be)^7Be$. The production rate of ^7Be in the atmosphere has also been assessed in three-dimensional models of the atmosphere [U57]. The production rate varies with

cosmic ray intensity and depends on geomagnetic latitude, altitude, and solar activity. The production rate of ^{7}Be in the Earth's atmosphere range between 0.00578 and 0.081 atoms/(s cm^{2}) [H23]. Worldwide activity concentrations of ^{7}Be in the atmosphere are continuously monitored by the International Monitoring System of the CTBTO [H23]. Figure XII shows the ^{7}Be activity concentration in air measured by the CTBTO radionuclide monitoring network [C63]. The mean, median, 5th and 95th percentile activity concentrations of ^{7}Be in air were measured at 3.7, 3.1, 0.6, and 8.5 mBq/m^{3}, respectively.

Figure XII. Activity concentration of ^{7}Be and ^{22}Na in air obtained from the CTBTO radionuclide monitoring network [C63]

Data for ^{7}Be cover the full solar cycle 24 (2009 to 2019). Data for ^{22}Na were only available from 2005 to 2011, a period with low solar activity

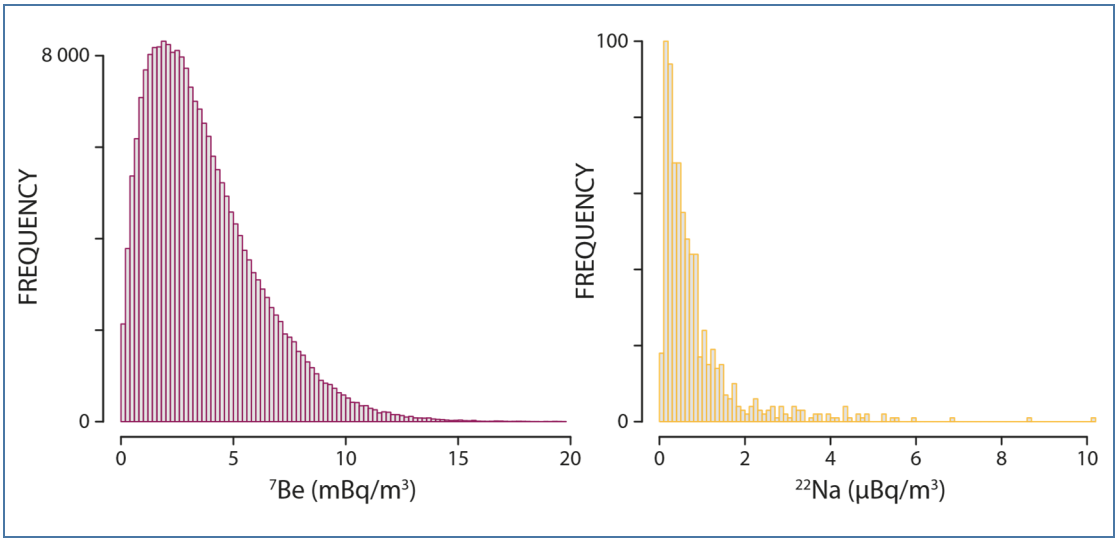

215. Sodium-22 is produced by nuclear reactions with atmospheric argon. Activity concentrations in air of ^{22}Na from 2005 to 2011 are available for selected radionuclide monitoring sites operated by CTBTO [H22]. The mean, median, 5th and 95th percentile activity concentrations of ^{22}Na in air were measured at 0.88, 0.55, 0.13, and 3.10 µBq/m^{3}, respectively (see figure XII).

216. The annual average intake of ^{14}C was estimated at approximately 2×10^{4} Bq by assuming an ingestion rate of carbon of 250 g/d [I64], and using the specific activity of cosmogenic ^{14}C before the atmospheric nuclear weapons tests of 222 Bq/kg. It should be noted that ICRP Publication 23 [I64] gives a value of 300 g/d for the ingestion rate of carbon; however, the Committee's view was that the daily ingestion rate adopted in this annex was more realistic based on the data given in the same publication. The average annual worldwide intakes through ingestion of cosmogenic ^{3}H, ^{7}Be and ^{22}Na were estimated at approximately 500, 1,000 and 50 Bq [U19]. Based on these intakes and using the dose coefficients for ingestion for adults from ICRP Publication 119 [I73] the worldwide average annual doses from ingestion of cosmogenic ^{14}C, ^{3}H, ^{7}Be and ^{22}Na were estimated to be 12, 0.009, 0.028 and 0.16 µSv, respectively.

217. The average annual worldwide doses to the public from external exposure to ^{7}Be and ^{22}Na in air were estimated to be much lower. Using the mean activity concentrations in air from the International Monitoring System of the CTBTO and the dose coefficients from ICRP Publication 144 [I77] the annual doses due to external exposure were estimated to be 2.4×10^{-4} and 2.7×10^{-6} µSv, respectively. On the basis of these estimates, the worldwide average annual dose to the public from exposure to cosmogenic radionuclides was estimated to be approximately 12 µSv, predominantly due to ^{14}C. This dose is the same as the value estimated in the UNSCEAR 2008 Report, annex B [U19].

3. Terrestrial radionuclides

(a) *Outdoor external exposure*

218. Naturally occurring radionuclides of terrestrial origin are present to various degrees in all media in the environment. Exposure is mainly due to gamma radiation from external sources and beta and alpha radiation from internal sources from radionuclides of the ^{238}U and ^{232}Th decay series and ^{40}K. Other terrestrial radionuclides, such as those in the ^{235}U decay series, ^{87}Rb, ^{138}La, ^{147}Sm, and ^{176}Lu, are present in the environment at such low levels that their contribution to public doses are negligible.

219. The radionuclides of the uranium and thorium decay series in rocks are typically in secular equilibrium, achieved when the activities of all members of a decay series are equal. In the surface environment of the Earth, this equilibrium can be disrupted since the elements in the decay series show a wide range of geochemical behaviour.

220. The distribution and mobility of the longer-lived isotopes of the decay chains of natural radionuclides in the environment is summarized in figure XIII. The isotopes ^{238}U and ^{234}U are in approximate secular equilibrium, as they are separated by two much shorter-lived radionuclides, ^{234}Th and ^{234}Pa. However, the recoil of the decay product facilitates the environmental transfer of ^{234}U. Therefore, ^{234}U may be slightly enriched relative to ^{238}U in groundwater [I53]. The activity concentrations of ^{226}Ra may differ from ^{238}U in certain soils. The half-life of radon is sufficiently long for it to be absorbed from the soil into the groundwater or emanate into the atmosphere. Its longer-lived decay products, ^{210}Pb and ^{210}Po, contribute significantly to the dose from inhalation or ingestion. Similar considerations apply to the ^{232}Th decay series. Radium-228 has a sufficiently long half-life to be separated from its parent, ^{232}Th.

Figure XIII. Illustration of the environmental behaviour of natural radionuclides

The dashed arrows indicate radioactive decay; the vertical arrows show environmental redistribution: 'red.' refers to reducing environment; 'ox.' to oxic conditions. The top row represents more mobile forms of the radionuclides; the bottom row shows less mobile forms

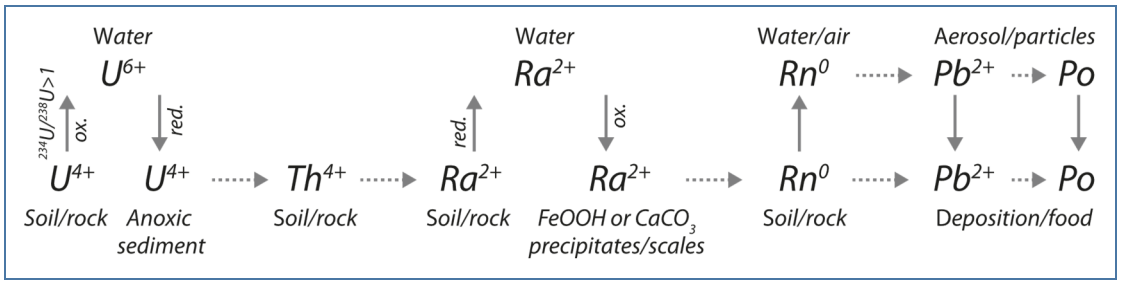

221. External exposures outdoors arise from terrestrial radionuclides present in soils. The specific levels are related to the types of rock from which the soils originate. Activity concentrations of natural radionuclides are in general higher in igneous rocks, such as granite, and lower in sedimentary rocks, although radionuclide levels in some shales and phosphate rocks are relatively high. Spectrometric measurements indicate that, with a typical composition of soil or building material, the gamma-emitting radionuclides in the ^{238}U and ^{232}Th decay series and ^{40}K, make similar contributions to the external exposure in typical situations both outdoors and indoors. The absorbed dose rate in air can also be measured directly. However, a reliable estimate of doses from these measurements is complicated by methodological issues, such as the correction for cosmic rays, the positioning of the probes, or temporal variations due to washout of radon decay products from the atmosphere.

222. The evaluation of doses from external radiation due to natural radionuclides in this annex was based on three sources of data:

(a) An extensive compilation of results of spectrometric measurements of radionuclides activity concentrations in soil, sands, and rocks, published in peer-reviewed journals. The focus was on laboratory measurements obtained using high purity germanium (HPGe) detectors or sodium iodide (NaI) detectors with sufficiently long counting times to ensure good data quality;

(b) Data on radionuclide concentrations in soil obtained from the UNSCEAR Global Survey on Public Exposure;

(c) Measurements of uranium, thorium and potassium in rocks and soils available from the EarthChem database [E1].

223. These three sources were complemented by direct measurements of dose rates obtained from the UNSCEAR Global Survey on Public Exposure. Where feasible the collected data on terrestrial radionuclides in rocks and soil were used to predict concentrations for areas lacking data to allow for a more detailed evaluation of terrestrial dose rate, on both a country level and a global scale.

224. A substantial amount of information on radionuclide concentrations in soils is available in the recent literature as there has been expanded interest in mapping exposures in many countries, especially in those where technical capabilities have increased significantly in recent years. However, surveys may focus on areas potentially posing problems in terms of radiation safety, leading to an uneven coverage of territory. To minimize possible bias towards higher activity concentrations in the present evaluation, data from areas with enhanced levels of natural radiation were treated separately from data from areas with typical levels of background radiation as discussed in section III.B.3(c).

225. Activity concentrations in this annex are given in Bq/kg dry weight. Earlier UNSCEAR reports accounted for soil activity concentrations under in situ conditions (i.e., Bq/kg wet weight). Although it is standard in almost all publications to report activity concentrations in Bq/kg dry weight, values are required in Bq/kg wet weight (i.e., in situ soil conditions) to calculate dose rates. In this annex a dry-to-wet conversion factor of 0.81 was used, as recommended in the UNSCEAR 2000 Report [U15] (see appendix A for more detail).

226. Table 10 summarizes average activity concentrations of the key terrestrial radionuclides for the 80 countries where information is available. Priority was given to results from the literature review. The worldwide population-weighted average activity concentrations of ^{238}U, ^{226}Ra, ^{232}Th and ^{40}K in soils, dry weight, are 30, 33, 42 and 512 Bq/kg. Compared to the activity concentrations published in the UNSCEAR 2000 Report, annex B [U15] and 2008 Report, annex B [U19], the new estimates for ^{238}U and ^{232}Th are approximately 25% lower. However, the new values are in good agreement with the average concentrations of natural radionuclides in the upper continental crust of the Earth [G19]. There is a large variation in activity concentrations, with reported maximum levels being between 6 to 11 times higher than the average values. More detailed information is provided in electronic attachment A-2.

227. Using equation A.15 in appendix A, the global average of the population-weighted absorbed dose rate in air from terrestrial gamma ray outdoors was estimated at 49 nGy/h, with an estimated uncertainty of around 10%. This value is 18% lower than the previous estimate by the Committee, due to the lower activity concentrations used for the radionuclides in the U and Th decay series in soil. Based on this dose rate in air and using equation A.13 the annual worldwide average outdoor dose due to external exposure to terrestrial radionuclides was estimated to be 0.06 mSv.

228. The range of absorbed dose rate in air from terrestrial radiation outdoors was evaluated based on the data extracted from the literature review after removing values from areas with high gamma background radiation. The 5th and 95th percentiles were calculated to be 10 and 100 nGy/h, respectively. Taking into account both the outdoor and the indoor exposures, the total annual dose from terrestrial radiation was estimated to be in the range of 0.1 to 0.8 mSv, which is lower than the Committee's previous estimate (range: 0.3–1.0 mSv) [U15, U19].

229. Lithology was used as a predictor for radionuclide concentrations in soil and rock to estimate population-weighted gamma dose rates from terrestrial radionuclides at country level. To predict concentrations in areas where measurements were not available, proxy data, such as geological information were evaluated using the global lithological map of OneGeology [O9] and Geographic Information System (GIS). Significant differences in average radionuclide concentrations across lithologies were identified. By considering the proportion of each lithology within a country and its associated activity concentrations, estimates the average activity concentrations of ^{238}U, ^{232}Th and ^{40}K were derived for every country. These estimates were used to calculate gamma dose rates from terrestrial radionuclides for each country (see electronic attachment A-2). The resulting population-weighted worldwide average absorbed dose rate in air was the same as the one presented in table 10. Consequently, the Committee has concluded that it would be reasonable to estimate the terrestrial gamma dose rate using the approach based on lithology, when country specific data are not available.

Table 10. Summary of country-average activity concentrations of natural radionuclides in soils and rocks and relevant absorbed dose rate in the air

L: Literature review; E: EarthChem portal; G: UNSCEAR Global Survey on Public Exposure; AM: Arithmetic mean

Country	*Data source*	*Soil/rock activity concentration, dry weight (AM in Bq/kg)*				*Absorbed dose rate in air (AM in nGy/h)* [a]
		^{238}U	*^{226}Ra*	*^{232}Th*	*^{40}K*	
Algeria	L+E	32	50	42	320	43
Argentina	L+E	27	32	35	638	48
Armenia	L	77	30	37	438	62
Australia	L	26	104	29	219	31
Austria	L	32		42	474	48
Bangladesh	L	37	27	48	452	53
Belarus	L+G	11	24	15	387	24
Bosnia and Herzegovina	L	44	33	34	377	45
Botswana	L+E	10	35	42	433	39
Brazil	L	79	40	67	796	89
Bulgaria	G	40	42	48	602	59
Cameroon	L		14	30	103	23
Canada	L	21	26	30	641	44
China	L	27	22	38	663	51
China, Taiwan Province	L	17	36	31	423	36
Congo	E	28		33	546	45
Croatia	L	36	37	29	388	41
Cuba	L	20		15	657	37

Country	*Data source*	*Soil/rock activity concentration, dry weight (AM in Bq/kg)*				*Absorbed dose rate in air (AM in nGy/h)* [a]
		^{238}U	^{226}Ra	^{232}Th	^{40}K	
Cyprus	L+G	7	23	19	628	39
Egypt	L	17	23	16	237	22
Finland	G	41		46	640	59
France	G	38	38	38	568	52
Georgia	L	39		53	880	70
Ghana	L	12	31	22	242	23
Greece	L	35	63	72	789	75
Hungary	L	35	32	34	422	44
India	L	27	37	54	471	52
Indonesia	E	27	41	33	569	46
Iran (Islamic Republic of)	L	50	35	38	488	54
Iraq	L	27	18	15	255	26
Ireland	E	52		67	471	68
Israel	L+E	13	31	15	151	17
Italy	L	56	48	39	723	64
Japan	L+G	34	52	40	421	47
Jordan	L	30	38	20	258	30
Kazakhstan	G	40	37	70	300	59
Kenya	L	52	28	63	897	81
Kuwait	L	15	15	12	342	23
Lebanon	L+G	27	62	24	246	30
Libya	E	11		28	675	41
Lithuania	G		34	20	525	40
Luxembourg	G				773	
Madagascar	E+L	25	29	29	588	43
Malawi	L	59		43	656	65
Malaysia	L	21	48	49	282	41
Mexico	L+E	24	31	37	618	48
Montenegro	L+E	104	18	26	283	61
Namibia	L	57		48	371	57
Nigeria	L	31	27	33	193	34
North Macedonia	L		39	48	569	57
Norway	E	25		38	776	54
Oman	L		19	13	45	15
Pakistan	L+E	8	39	50	554	46
Philippines	G	68		69	282	68
Poland	E	31		34	865	57
Portugal	G+E	34	20	19	401	36
Qatar	L		17	10	201	18

Country	*Data source*	*Soil/rock activity concentration, dry weight (AM in Bq/kg)*				*Absorbed dose rate in air (AM in nGy/h)* [a]
		^{238}U	*^{226}Ra*	*^{232}Th*	*^{40}K*	
Republic of Korea	L+E	26	65	83	1 015	85
Russian Federation	L	27	21	23	422	36
Saudi Arabia	L+E	19	30	23	221	26
Serbia	L	43	30	42	490	53
Slovakia	G		29	33	689	50
Slovenia	L	32	56	77	724	74
South Africa	L+E	24	24	28	254	31
Spain	L	30	21	22	493	39
Sri Lanka	E	4		4	219	11
Sudan	L	19	10	25	145	24
Sweden	G	28		29	566	44
Syrian Arab Republic	L+E	17	20	26	174	25
Tajikistan	L+E	23	34	80	578	67
Thailand	L	49	43	44	330	50
Türkiye	L	28	42	32	484	43
United Republic of Tanzania	L	52		36	564	56
United Arab Emirates	L	15		6	231	17
United Kingdom	G	31	31	33	411	42
United States of America	G	23	41	26	363	34
Vietnam	L+E	41	39	56	396	56
Yemen	L		29	39	1 042	65
Kosovo (under UNSC res. 1244)	L		17	27	340	31
State of Palestine	L	41		28	262	38
Population-weighted average		**30**	**33**	**42**	**512**	**49**

[a] Activity concentration of ^{226}Ra was used when activity concentration of ^{238}U was unavailable, assuming secular equilibrium in the ^{238}U decay chain.

(b) *Exposure indoors and building materials*

230. A summary of new data on radionuclide activity concentrations in building materials complementing the information provided in the UNSCEAR 2000 and 2008 Reports [U15, U19], is given in table 11. The new values are slightly lower than those reported in the UNSCEAR 2008 Report, annex B and in an extensive review of building materials from Europe [T21]. The table shows a high variability of activity concentrations of the three natural radionuclides ^{226}Ra, ^{232}Th and ^{40}K. Higher activity concentrations were measured in some natural stones and in materials containing residues from NORM industries. For example, the maximum value for ^{226}Ra for the brick and tiles category in table 11 is five times higher than the AM, while the ^{232}Th activity concentration in siliceous rocks can be 15 times the average value. Trevisi et al. [T21] reported maximum values of 906 Bq/kg for ^{232}Th in igneous plutonic rocks used as superficial building materials. For phosphogypsum, a NORM residue

which may be used in the cement industry, the authors report activity concentrations of ^{226}Ra up to 1,406 Bq/kg. However, average activity concentrations of natural radionuclides in the majority of building materials or their constituents, are comparable (e.g., concrete and cement) or lower (e.g., wood and natural gypsum) than those measured in soils.

231. Building materials are sources of radiation and simultaneously provide shielding against outdoor radiation. In wooden and lightweight houses, both the contribution of the walls as a source of radiation and their shielding effect against the outdoor radiation are negligible and the absorbed dose rate in air indoors can be lower than outdoors. Accordingly, the shielding factor provided by the walls is close to unity or lower. In contrast, in houses made of brick, concrete or stone, the gamma rays emitted outdoors are efficiently absorbed by the walls, and the indoor absorbed dose rate depends mainly on the activity concentration of natural radionuclides in the building materials. Indoor absorbed dose rates in this type of dwellings tend to be higher, with shielding factors typically close to two or higher.

Table 11. Worldwide average activity concentrations of natural radionuclides in materials used in the construction industry

Concrete includes aggregate, sand, and gravel. Cement includes all types of cement. Brick and tiles include clay and ceramics. NORM residues are phosphogypsum, fly ash and slag.
Data are from the literature and the UNSCEAR Global Survey on Public Exposure (for more details refer to electronic attachment A-2)

Group	*n* [a]	*Activity concentration (Bq/kg)*								
		^{226}Ra			*^{232}Th*			*^{40}K*		
		AM [b]	*GM* [c]	*GSD* [c]	*AM* [b]	*GM* [c]	*GSD* [c]	*AM* [b]	*GM* [c]	*GSD* [c]
Concrete	156	30	17	2.4	20	15	3.0	300	158	6.7
Cement	284	40	30	1.8	20	20	2.0	200	173	2.2
Brick and tiles	246	50	27	2.2	60	38	1.7	500	391	1.9
Marble	116	20	12	3.2	10	3	5.8	100	47	6.2
NORM residues	84	170	91	2.9	90	66	3.1	300	122	3.2
Siliceous rock	198	80	44	3.2	90	51	3.6	900	640	3.2
Natural gypsum	59	30	15	2.5	20	8	7.7	100	59	2.5
Wood [d]		20			10			200		

[a] The number of data (n) includes single values as well as averages.

[b] AM: Average of the arithmetic mean from literature review and the arithmetic mean from the UNSCEAR Global Survey on Public Exposure; the values are rounded to the next 10 Bq/kg (100 Bq/kg in the case of ^{40}K).

[c] GM/GSD: Geometric mean and geometric standard deviation calculated based on the results from the literature review.

[d] Average values taken from [B26].

232. Information on distributions of indoor exposures derived from direct measurements is not extensive, but doses can be estimated using information on soil, shielding, and building materials. One approach is to evaluate the indoor dose rate using models based on radionuclide activity concentrations in building materials and standard room geometries. However, detailed information on composition and market shares of building materials and building styles is often not available. Therefore, the Committee continues to use the approach from previous UNSCEAR reports, which estimates the indoor dose rate by multiplying the corresponding outdoor dose rate by a globally averaged shielding factor.

233. Although detailed statistics on the types of dwellings were not available for this annex, wooden houses and other relatively light constructions make up an important part of dwellings in many countries. Thus, the shielding factor that should be applied to estimate worldwide average indoor doses from building material would be lower than the one for concrete buildings. Based on outdoor and indoor dose rates reported by several countries through the UNSCEAR Global Survey on Public Exposure, the average ratio of the indoor to outdoor terrestrial dose rate, after correction for the contribution from cosmic rays was estimated at 1.2 (see electronic attachment A-2). Considering previous information provided in its previous evaluations, the Committee has recommended that the previous value for the shielding factor of 1.4 should be retained to estimate the worldwide average dose from indoor exposure to terrestrial radionuclides.

234. Based on average outdoor dose rate of 49 nGy/h, a shielding factor (SF_{terr}) of 1.4 and an indoor occupancy (O_{in}) of 0.8 and applying equation A.16 in appendix A, the annual worldwide average indoor dose from external exposure to terrestrial radionuclides was estimated at 0.34 mSv. Adding the contribution from the outdoor external exposure gives a total annual worldwide average dose due to external exposure from terrestrial radionuclides of 0.4 mSv. This new estimate is lower than the Committee's previous estimate of 0.48 mSv, due to the lower estimates of the activity concentrations of ^{238}U and ^{232}Th in soil adopted in this annex. The range of total annual dose from terrestrial radiation was estimated at 0.1–0.8 mSv.

(c) *High gamma background radiation areas*

235. In this annex, a statistical approach is used to identify areas with high gamma radiation from soils and rocks. Such areas are referred to as 'high gamma background radiation areas' rather than 'high background radiation areas' since the latter often includes areas with high indoor radon concentrations. Areas with high indoor radon concentrations are treated separately in sections III.A.2 and III.A.3.

236. The complete dataset of activity concentrations of ^{238}U, ^{226}Ra, ^{232}Th, and ^{40}K in soil compiled from the literature review was analysed by country and region to identify the extreme high values (EHVs), defined statistically as values above a threshold equal to the third quartile plus three times the inter-quartile range [T24]. The process was repeated by recalculating the threshold after the EHVs were removed until no EHVs were left in the dataset. All the activity concentrations identified as EHVs were verified against their sources, taking into consideration the geological setting. If a set of values was found to be representative of a specific area, this region was classified as a high gamma background radiation area. Data for these areas were evaluated separately, while single outliers were returned to the original dataset for further standard statistical analysis. By applying this purely statistical approach, which excluded subjective expert judgment, absorbed dose rates in air were found to vary by about two orders of magnitude, across different high gamma background radiation areas. However, it should be noted that these areas are country-specific, and their identification depends on the level of background radiation in that country. The analysis was also limited by the amount of information collected, since a larger dataset related to background radiation and better coverage of a country's territory would allow high gamma background radiation areas to be identified more accurately.

237. More than 50 new high gamma background radiation areas around the world were identified through the review of publications in the open literature performed for this annex, mainly in Africa and Asia. For each type of area, some examples are provided in table 12. More detailed information on the high gamma background radiation areas identified for this annex, are given in electronic attachment A-2.

238. About half of the identified high gamma background radiation areas are associated with igneous intrusive rocks, such as granites, granodiorites and thorium-rich carbonatites. These areas include the regions of Paraíba in north-eastern Brazil and the newly identified Mamuju area in West Sulawesi

(Indonesia). The second largest group consists of monazite and zircon coastal areas, characterized by beach sands or placer deposits which have high levels of thorium; the Kerala region in India is a notable example. Another type occurs where fault fluids enriched in radium, deposited from the waters when they emerge to the surface as springs, create thermal water areas; examples of this type have been identified in Africa, East Asia, and West Asia. Finally, uranium deposit areas include sedimentary uranium deposits hosted in sandstone and conglomerate, such as those in Türkiye, which are characterized by high concentrations of uranium and associated ^{226}Ra.

Table 12. Activity concentration in soil and rock and absorbed dose rates in air measured in some areas with different types of geology around the world with high gamma background

AM: Arithmetic mean; GM: Geometric mean; Min: Minimum; Max: Maximum

Country	*Area*	*Soil/rock activity concentration, dry basis (Bq/kg)* [a]												*Absorbed dose rate in air (nGy/h)* [b]
		^{238}U			*^{226}Ra*			*^{232}Th*			*^{40}K*			
		AM	*GM*	*Min–max*	*AM*	*GM*	*Min–max*	*AM*	*GM*	*Min–max*	*AM*	*GM*	*Min–max*	*AM*
MONAZITE AND ZIRCON COASTAL AREAS														
India	Kerala	936	282	3–6 023	60		33–98	4 952	820	7–41 280	530	258	22–2 531	2 774
Malaysia	Penang Island				1 023	354	24–2 641	2 086	626	37–5 622	381	373	296–495	1 408
Sri Lanka	Western Province (Kaluthara)	450		7–3 150				2 100		11–19 600	220		14–1 210	1 196
URANIUM DEPOSIT AREAS														
Jordan	Amman Governorate (Khan Al Zabib)	2 262	1 133	70–3 927	339		62–661	21		18–25	228		179–308	861
Norway	Troms og Finnmark (Orrefjell, Salangen)	433	138	10–2 000	873	281	33–6 800	13	8	1–29	374	275	41–630	181
Türkiye	Manisa Province (Köprübaşi)				2 911	514	24–9 800	55	53	29–80	801	774	410–1 215	1 139
RARE EARTH ELEMENT DEPOSITS (PLACERS)														
Russian Federation	Republic of Sakha (Yakutia)–Aldan Highlands (placer Vasilievka)	47	34	15–102				563	253	49–1 403	970	923	635–1 375	324
Vietnam	Northwest Region (Lào Cai Province, Bát Xát District)	213	117	23–1 635	250	119	21–3 633	866	280	41–15 160	876	611	124–3 788	530

Country	*Area*	*Soil/rock activity concentration, dry basis (Bq/kg)* [a]												*Absorbed dose rate in air (nGy/h)* [b]
		^{238}U			*^{226}Ra*			*^{232}Th*			*^{40}K*			
		AM	*GM*	*Min–max*	*AM*	*GM*	*Min–max*	*AM*	*GM*	*Min–max*	*AM*	*GM*	*Min–max*	*AM*
URANIUM AND THORIUM AREAS (IGNEOUS INTRUSION)														
Brazil	Paraíba (São Mamede)	27 994	10 282	1 847–199 384	18 265	8 514	1 979–85 049	3 137	1 559	381–26 458	14 191	13 724	10 268–24 229	12 438
Indonesia	West Sulawesi (Mamuju)	9 660	1 437	41–65 455	1 019	907	320–2 195	7 286	1 117	58–195 296	665	403	116–5 710	7 163
Yemen	Dhale Governorate (Juban District)				1 319	647	42–3 089	4 929	2 203	370–12 513	1 427	1 255	702–2 954	2 936
THERMAL WATERS														
Egypt	South Sinai (Ras Sedr)–Abu Sweera				849	510	157–2 082	29	16	6–120	51	49	30–67	332
Iran (Islamic Republic of)	Mazandaran (West, including Ramsar)				1 189		12–57 500	65		1–1 150	545		259–847	493
Thailand	Surat Thani Province–Khao-Than hot spring				3 057	1 527	151–10 201	126	83	12–408	198	109	24–571	1 207
OTHERS														
Indonesia	Kei Islands				2 162	863	8–6 326	70	45	1–157	31	23	3–99	840
Jordan	Zarqa Governorate (Zarqa)	258		12–943	214		13–1 040	22		11–37	249		120–483	115
Malaysia	Johor				138	114	38–300	217	172	56–513	199	143	6–363	164

[a] The values shown are AM; GM; min–max. GM and min–max may not be available for certain areas. Other parameters of distributions are available in electronic attachment A-2.

[b] The conversion factor for soil (dry to wet basis) of 0.81 was applied.

4. Internal exposures

(a) *Internal exposures from ingestion*

239. Doses from ingestion are mainly due to ^{40}K and the radionuclides in the ^{238}U and ^{232}Th series present in foods and drinking water. Potassium is uniformly distributed within the body, mainly associated with muscle tissue, and its concentration is homeostatically controlled. This means that the amount of ^{40}K in the human body is controlled by physiological processes and largely independent of the intake of ^{40}K and any residual intake is rapidly eliminated from the body. As potassium is mainly found in muscles, the average whole-body concentration of ^{40}K for females is lower than for males and results in a corresponding difference in the internal dose. For example, whole-body measurements on young adults from Switzerland showed average concentration of 57 Bq/kg for females and 70 Bq/kg for males [Y9]. A further difference exists between the dose to adults and the dose to children. Since these effects are biologically controlled, the estimates of annual doses for ^{40}K given in the earlier UNSCEAR reports [U15, U19] remain unchanged: 0.165 and 0.185 mSv for adults and children, respectively.

240. Exposures from ingestion of other natural radionuclides depend on the ingestion rates of foods and drinking water and on their radionuclide activity concentrations. Doses were estimated in this annex for nine radionuclides; results are given in this section for the four radionuclides that contribute the most to the dose from ingestion: ^{210}Po, ^{210}Pb, ^{228}Ra, and ^{226}Ra. The complete results of the dose assessment are given in electronic attachment A-2.

241. Table 13 gives median activity concentrations of the four most relevant radionuclides. The concentrations were taken from IAEA Safety Reports Series No. 114 [I48] which also provides a detailed statistical analysis (see electronic attachment A-2). It should be noted that some of the activity concentrations in the report are likely to be cautious estimates, due to several potential biases, such as preference given to areas where high activity levels were expected, even though no significant discrepancies were observed between information in published papers and data collected as part of national monitoring programmes [I48]. Also, the activity concentrations in the report do not take account of the decay during storage or losses due to cooking. Since radioactive decay of ^{210}Po in seafood during storage is known to be significant, a correction factor of 0.81 [J20] was used in this annex and replaces the correction factor of 0.6 used in the UNSCEAR 2000 Report [U15].

242. Another potential source of overestimation is the assumptions made to derive the ingestion rates for some food subcategories. For example, the ingestion rate for the food category ‘meat and offal’, is the combination of three different subcategories: eggs, meat and offal. Ingestion rates are given in appendix A; electronic attachment A-2 provides details of how these ingestion rates were derived.

243. Worldwide average annual doses from ingestion of ^{210}Po, ^{210}Pb, ^{228}Ra and ^{226}Ra in food were estimated using equation A.17 and are presented in the bottom row of table 13. The assessment of doses from ingestion of other natural radionuclides (^{238}U, ^{234}U, ^{235}U, ^{228}Th, ^{230}Th and ^{232}Th) was based on the methodology described in the UNSCEAR 2000 Report [U15] since the data provided for those isotopes in IAEA Safety Reports Series No. 114 [I48] are less comprehensive. The total annual dose from ingestion of radionuclides of natural origin in food was estimated at 0.25 mSv. Detailed information on how the doses were calculated is given in electronic attachment A-2.

Table 13. Worldwide average annual effective dose for adults from ingestion of terrestrial radionuclides other than ^{40}K

Food category	*Median activity concentration (Bq/kg)* [a]					*Annual dose (mSv)*
	^{210}Po [b]	*^{210}Pb*	*^{228}Ra*	*^{226}Ra*	*Other*	
Cereals	0.14	0.15	0.12	0.12		0.05
Vegetables and fruit	0.09	0.11	0.18	0.10		0.08
Milk and dairy products	0.04	0.04	0.02	0.03		0.007
Meat and offal	0.16	0.18	0.08	0.04		0.02
Freshwater fish	0.99	0.23	0.84	0.48		0.01
Marine fish	2.4	0.20	1.75	0.27		0.03
Crustaceans	9.38	0.14	0.40	0.06		0.01
Molluscs	25.1	2.00	0.19	0.20		0.04
Annual dose (mSv)	**0.13**	**0.04**	**0.06**	**0.01**	**<0.005**	**0.25**

[a] Primary source is IAEA Safety Reports Series No. 114 [I48] concentrations, or the average of medians for several food subcategories, if applicable. For details, refer to electronic attachment A-2.

[b] Activities of ^{210}Po in seafood are shown in this table as given by the IAEA at the time of analysis, but dose calculations are carried out after application of a 0.81 correction factor for ^{210}Po in seafood.

244. The total dose from ingestion of natural radionuclides other than ^{40}K calculated in this annex is compared with other estimates in table 14. The dose estimated in this annex is a factor of approximately 2 higher than the one in previous UNSCEAR reports [U15, U19], due in large part to the higher activity concentrations in food, particularly of ^{210}Po, in the IAEA Safety Reports Series No. 114 [I48]. This increase in the dose does not reflect a temporal upward trend in the activity concentrations, but rather the fact that more data on activity concentrations in food are available. Additionally, doses from ingestion given in IAEA Safety Reports Series No. 114 [I48], were based on dietary studies which tend to be lower than estimates based on radionuclide concentrations in single foods, due to fact that they use activity concentrations in food measured in food when consumed. It should be noted that the relative contributions of the different radionuclides to the total are similar.

245. Doses from ingestion of drinking water were not included in the estimate presented in table 13. IAEA Safety Reports Series No. 114 [I48] assessed the GMs of various radionuclides in natural mineral water. Based on these values and assuming an annual consumption rate of 0.5 m^3/a, the worldwide average annual dose would be 0.04 mSv if all water consumed was mineral water. In practice, drinking water typically includes both mineral and tap water, and an analysis of data from the literature review indicated that activity concentrations in tap water are generally lower than in mineral water. Taking these differences into account, and assuming a combined annual consumption of 0.5 m^3/a of both mineral and tap water, the worldwide average annual dose was estimated at about 0.02 mSv. More information on how this dose was calculated is provided in appendix A; complete results are provided in electronic attachment A-2. For consumption of tap water, there is an additional dose due to ingestion of radon of 0.003 mSv (see section III.A).

246. The total worldwide average annual dose to adults from ingestion of terrestrial radionuclides (e.g., ^{40}K, and radionuclides in the ^{232}Th and ^{238}U decay series) was estimated at 0.5 mSv.

Table 14. Reported worldwide average annual effective dose due to ingestion of natural radionuclides other than ^{40}K in foods (excluding water) from various international studies

Reference	*Approach*	*Ingestion dose (mSv)*
UNSCEAR reports [U15, U19]	Dose calculated from radionuclide concentrations in food and annual consumption of food according to equation 9	0.12
IAEA Safety Reports Series No. 114 [I48]	Dietary studies (all radionuclides)	0.19
This annex	UNSCEAR 2000 Report [U15] approach with updated concentration data from IAEA Safety Reports Series No. 114 [I48] combined with regional ingestion rates from the UNSCEAR 2016 Report [U24], with a correction factor for ^{210}Po	0.25

(b) *Internal exposure from inhalation*

247. Inhalation of natural radionuclides other than radon makes only a minor contribution to internal exposure. These radionuclides are present in air because of the suspension of soil particles. Assuming a dust loading of 50 μg/m^3 and activity concentrations of ^{238}U and ^{232}Th in soil of 25–50 Bq/kg, the activity concentrations in air would be 1–2 μBq/m^3. These values are consistent with direct measurements, although they are affected by a large variability, due to factors such as climate and type of soil. Another factor affecting the variability of activity concentrations of terrestrial radionuclides in air is the contribution to the dust loading of air from burning fuels, because fly ash contains significant concentrations of uranium, although its organic content is usually deficient in uranium compared with soil. In addition, at coastal locations, concentrations of uranium in air may be an order of magnitude lower than in continental or industrialized areas inland.

248. The UNSCEAR 1993 Report, annex A [U13] provides representative values of the activity concentrations of terrestrial radionuclides in air which were also adopted in this annex, because of the lack of new information. The activity concentrations ranged from 0.05 μBq/m^3 for ^{235}U to 500 μBq/m^3 for ^{210}Pb. The concentrations of the other radionuclides were: 50 μBq/m^3 for ^{210}Po; 1 μBq/m^3 for ^{238}U, ^{226}Ra, ^{228}Ra and ^{228}Th; 0.5 μBq/m^3 for ^{232}Th and ^{230}Th. The age-weighted annual dose due to inhalation of radionuclides from the uranium and thorium series in air was estimated to be 0.006 mSv [U15].

249. Smokers may receive additional doses due to intake of ^{210}Pb and ^{210}Po present in tobacco. Based on data from the literature on activities of ^{210}Pb and ^{210}Po in cigarettes, the average activity of both radionuclides in one cigarette was estimated to be 16 mBq. According to Desorgher et al. [D18], the annual dose to people smoking 20 cigarettes a day for similar activity concentrations is 0.3 mSv (see electronic attachment A-2).

C. Enhanced sources of NORM

250. Activities related to the extraction and processing of ores can lead to enhanced levels of natural radionuclides in raw materials, products, residues, and wastes. Following the approach of the UNSCEAR 2008 Report, annex B [U19], NORM industries are grouped into eight categories: *(a)* uranium mining and milling; *(b)* metal mining and smelting; *(c)* phosphate industry; *(d)* coal mines and power generation from coal; *(e)* oil and gas drilling; *(f)* rare earth and titanium oxide industries; *(g)* zirconium and ceramic

industries; and *(h)* groundwater treatment. Exposures from discharges operating uranium mines and mills are discussed in section IV.A.2.

251. Pathways of public exposure associated with NORM industries are site-specific and depend on local scenarios. Recent work under the EU project RadoNORM [M41], summarized typical public exposure scenarios for the different categories of NORM industries: *(a)* exposure in the vicinity of smaller water bodies (e.g., streams or small lakes), which receive discharges of liquid effluent containing NORM; *(b)* exposure in the vicinity of disposal sites for NORM waste; and *(c)* exposure during recreational time spent in the vicinity of old NORM-affected legacy sites. External exposure generally occurs when accessing residual tailings or processed materials, which in some cases may have been transported offsite. Exposure from inhalation of radon and radon decay products is most significant on site but may also contribute to the dose received by people who reside nearby. Internal exposure from ingestion of water, crops or animal products from affected areas can further contribute to the doses. Overall, the number of locations with potential for public exposure from NORM industries is very limited, and resulting doses are usually low.

1. Metal mining and smelting

252. The concentrations of uranium and thorium in metalliferous ores vary with geological formation and region. NORM in the metal mining and smelting industry include the ores themselves, intermediate streams, metal concentrates, tailings, and smelter slags. For some metals (e.g., copper, aluminium, iron, steel), large bulk waste streams can create potential public exposure scenarios, as some processes concentrate specific radionuclides. Depending on their geochemical affinities, radionuclides tend to accumulate in different materials: actinium associates with lanthanum; radium with barium and calcium; and polonium with tellurium and selenium [R4].

253. Activity concentrations of natural radionuclides in feed material for smelting of metals, such as aluminium, copper, iron, lead, niobium, tin, zinc, and gold as well as in most slags and other wastes are generally low, when considering. Activity concentrations of natural radionuclides in intermediary products and wastes, however, depend on the initial content of the ore and on the type of process used to extract the metal. In the case of thermal processes, a large part of the radionuclide content is concentrated in metallic slags, such as those produced in the tin industry [V6].

254. Activity concentrations of natural radionuclides in the niobium industry may be high; for example activity concentrations of ^{232}Th in pyrochlore are between 10 and 80 Bq/g [V6]. Activity concentrations of ^{228}Ra in barium sulphate waste in one niobium facility in Brazil were as high as 200 Bq/g, while those of ^{232}Th in the slag reached 117 Bq/g. The main exposure pathways for public exposure are contamination of groundwater with radium isotopes and external exposure to slag with high thorium content [I12, P27].

255. Exposures due to inhalation of suspended material from tin and niobium slag used as landfill have also been reported [V6]. In South Africa, the gold deposits from deep underground mines have low-grade uranium associated with them. Since 1952, 170,000 tonnes of U_3O_8 have been recovered as a by-product of gold mining. Some six billion tonnes of mining tailings, containing about 500,000 tonnes of uranium and 200 kg of ^{226}Ra, have been generated. New tailings are being generated at an annual rate of 86 million tonnes. Elevated activity concentrations of ^{226}Ra up to 1.7 Bq/L were measured in the discharges. Annual doses to nearby populations were estimated to be up to 0.04 mSv due to ingestion of water and up to 0.086 mSv due to ingestion of fish. Annual doses due to ingestion of terrestrial foods were much lower, ranging up to about 0.002 mSv. Annual doses to the public due to inhalation of radon and of dust from the tailings were estimated to be about 0.04 and 0.02 mSv, respectively [W24].

2. Phosphate industry

256. Global phosphate deposits are estimated to be 163 billion tonnes. Most of these deposits are of sedimentary origin, with as little as 4% being of igneous origin. More than 75% of the known reserves of phosphate rock in the world are found in Morocco and Western Sahara [I29]. Phosphate ores of sedimentary origin typically contain about 1.5 Bq/g of uranium and radium, (range: 0.2–2 Bq/g), although uranium concentrations in some phosphate rocks can be as high as 20 Bq/g [I29]. Ore is processed to produce fertilizer, and the resulting waste is calcium sulphate dihydrate, known as phosphogypsum. The fertilizer is enriched in uranium (up to 150% relative to the ore), while 80% of the ^{226}Ra, 30% of the ^{232}Th and 14% of the uranium are left in the phosphogypsum [V6]. In general, phosphate ores of sedimentary origin have higher concentrations of radionuclides of the uranium family. Phosphate minerals in magmatic rocks, such as those from Kola (Russian Federation), and Phalaborwa (South Africa), contain lower concentrations of radioisotopes of uranium and higher concentrations of radioisotopes of thorium, although the total activity concentration is lower than that from sedimentary minerals [V6].

257. Activity concentrations of ^{238}U and ^{232}Th in phosphate rock originating from sedimentary and igneous deposits in Europe are generally in the range 0.01–1.85 and 0.04–0.65 Bq/g, respectively; activity concentrations of ^{226}Ra, ^{210}Po, and ^{210}Pb are similar to that of ^{238}U indicating that they are in secular equilibrium. Data collected through the UNSCEAR Global Survey on Public Exposure are consistent those given in IAEA Safety Reports Series No. 78 [I29].

258. Activity concentrations of natural radionuclides in phosphate-based products may vary significantly depending on the raw material used, as well as on the different technological processes employed. From the available data, radionuclides of natural origin in the mineral fertilizers, detergents, and lime nitrates are found to be below 1 Bq/g. Activity concentrations of ^{238}U up to 1.3 Bq/g were only found in phosphoric acid, similar to values previously reported for the Netherlands (Kingdom of the) [M43] and Spain [B34]. Higher concentrations of ^{210}Pb and ^{210}Po in comparison to other natural radionuclides were measured in furnace dust and insoluble acid-residue minerals—up to 0.9 and 1.7 Bq/g, respectively. However, the majority of the information provided through the UNSCEAR Global Survey on Public Exposure reported the accumulation of radium salts in the form of scale in metal parts, pipes, vessels, filters and tubes of facilities in the phosphate, with activity concentrations of ^{226}Ra and ^{228}Ra up to 4,200 and 53 Bq/g, respectively. Similar findings were previously reported by the IAEA [I29].

259. During the initial on-site processing of the raw material to separate the valuable minerals from waste rock and impurities, three main fractions are obtained in similar proportions by mass. The first fraction is composed of muds containing approximately 45% of the total activity. The second fraction consists mainly of silica sands and contains low levels of radionuclides (<10% of the total activity). Finally, the third fraction (approximately 45% of the total activity) is the commercial phosphate rock and contains radionuclides in the ^{238}U decay series in secular equilibrium with activity concentrations of the order of 1 Bq/g [B34, D32, G9, M9, O13, Q1, S18].

260. Phosphogypsum is still present in large quantities worldwide; it was used widely in the past, for example, in agriculture and the construction industry, but was also considered waste and discharged to water bodies for permanent disposal. Following the introduction of more stringent environmental protection regulations, the disposal of phosphogypsum to water bodies ended while public concern also led to a significant reduction in the use of phosphogypsum. Information provided for European countries through the UNSCEAR Global Survey on Public Exposure included activity concentrations in phosphogypsum of ^{226}Ra up to 4 Bq/g, ^{210}Pb up to 0.71 Bq/g and ^{210}Po up to 0.95 Bq/g. The low solubility of ^{210}Pb and ^{210}Po in phosphogypsum prevents their migration through the environment (e.g., adjacent aquifers), while its low resuspension rate makes their radiological impact rather limited [G5].

261. Public exposure related to mining and processing of phosphate rock are very low regardless of the pathway, because these operations tend to be undertaken in remote areas and involve materials with low activity concentrations [D1, L29, Q1, S26, U32]. Most rock processing operations are conducted under wet conditions. Under unfavourable wind conditions, exposure to radionuclides in airborne dust generated by the crushing, milling, and drying of rock is possible. The migration of radionuclides from mining and waste management facilities into water bodies could result in the contamination of drinking water and foods but doses from this exposure pathway are not expected to be significant, particularly because process water is usually recycled within the facility [A15, A18, D1, Q1].

262. Dust created during the ore crushing carried out in phosphoric acid plants tends to become rapidly deposited in the vicinity of the source and is unlikely to be transported to nearby residential areas [A33, I29, O12]. Public exposure from contamination of surface water bodies is considered negligible because process water is generally recycled from the phosphogypsum tailings back into the acidulation process. Standard environmental protection requirements generally ensure that water discharged from the facility is treated to reduce radionuclide concentrations to acceptable levels.

263. Public exposure associated with the production or use of fertilizers containing phosphate is not regarded as a significant concern [M9]. Activity concentrations of ^{226}Ra, ^{238}U, ^{210}Pb, ^{210}Po and ^{230}Th in phosphogypsum used as a soil amendment in the south of Spain reported in a study by Enamorado et al. [E26] were about 600, 100, 500, 500 and 400 Bq/kg, respectively. The study estimated maximum annual external doses of about 0.02 mSv, with doses from all other exposure pathways being negligible. Some studies indicated that the application of fertilizers containing phosphogypsum to soil, generally at a rate of the order of 1 t/ha, increases the activity concentrations of natural radionuclides in foods by less than 1% above background concentrations [E25, E26, H18].

264. Some studies have measured the activity concentration of natural radionuclides in different materials containing calcium phosphates for animal feed, and in the tissues of animals (e.g., muscle and bone). A maximum annual dose from ingestion of chicken meat was estimated to be of the order of 0.01 mSv [C9, C10].

265. Phosphate tailings, known as phosphogypsum stacks, are, in many cases, not adequately confined and the migration of radionuclides through water is the main route of exposure. Despite this, exposures of members of the public, irrespective the pathway involved, are likely to be very low because mining operations tend to be conducted at considerable distances from residential areas and involve materials with relatively low activity concentrations [G27, G28, H17]. Studies in Spain and Florida (United States) have concluded that the annual doses received by the public from exposure to airborne aerosols generated by the phosphate tailings are lower than 1 μSv [B35]. A hard crust on the surface of inactive stacks essentially prevents resuspension and subsequent inhalation of phosphogypsum particles. Several studies have determined the doses received by workers and the public when actively working on phosphogypsum stacks. The annual doses from external exposure to gamma radiation received from stacks containing phosphogypsum from Morocco were estimated at about 0.3 mSv, assuming a cautious occupancy of 2,000 h/a [M9]. Public exposure may also result from releases of radon and particulate matter to the atmosphere. The ^{222}Rn exhalation rate from dry surfaces of inactive phosphogypsum stacks can be relatively high, with values one to two orders of magnitude higher than the typical values for soils of around 40 Bq/m^2 h [D32]. The exhaled radon is quickly diluted in the atmosphere and the increase in radon concentration decreases with distance and is generally less than a few Bq/m^3 at 1 km from the pile. The fresh radon coming from the piles has a low equilibrium factor; therefore, the increase in annual dose for the most exposed members of the public was estimated to be less than 1 mSv.

3. Coal industry and power generation from coal

266. The typical average activity concentration of both ^{238}U and ^{232}Th in coal is around 20 Bq/kg (range: 5-300 Bq/kg), with a U/Th ratio generally greater than one [I12, L6, U15, U24]. During the burning of coal, the organic compounds are converted into gases, while the naturally occurring radionuclides are concentrated in the coal combustion residuals that include fly ash, bottom ash and slag [L6, V6]. In general, the radionuclide enhancement factor in ash is about 10 (range: 3–20). Due to their volatility, ^{210}Pb and ^{210}Po are particularly enriched in the fly ash. As stated in the UNSCEAR 2000 Report, annex B [U15], a small amount of fly ash can be emitted into air. Typical annual emissions by a 600 MW coal fired power station are 0.4 GBq for ^{210}Pb and 0.8 GBq for ^{210}Po. Aerial discharges of NORM from modern plants is lower because they have more efficient filter systems [U24].

267. The UNSCEAR 2016 Report, annex B [U24] applied a comprehensive methodology to assess public exposure due to atmospheric discharges from electricity generation coal-fired power plants, from coal ash disposed in landfills and discharges from coal mining. Annual doses due to atmospheric discharges from a coal-fired 1 GW power plant running for one year received by a typical person living in the area around the discharge point were estimated to be in the range of 0.03–0.4 μSv [U24]. Global average dose for the year 2010 was estimated to be of the order of 0.1 μSv, mainly due to the emission of radionuclides bound to fly ash and of radon. Doses associated with coal mine tailings were not included in the dose assessment because the radioactive content of coal mine tailings does not differ significantly from background concentrations of natural radionuclides in soil [U24].

268. There are few restrictions on the use of fly ash in landfill and road construction because leaching from this material is low. The use of fly ash for building construction, however, results in exposure from external radiation. Disposal of fly ash to surface facilities may increase the radiation level around the disposal site. The most significant exposure pathways are ingestion and inhalation of ^{210}Pb and ^{210}Po [Z1].

269. There are about 50 underground coal mines in the Upper Silesian Coal Basin in the southern part of Poland. Activity concentrations of radium up to 390,000 Bq/m^3 have been measured in the water flowing from these mines mainly in the southern and central parts of the basin, where a thick layer of impermeable clay overlies the coal seams. Water from coal mining is discharged into surface settling ponds and into rivers from there. In some cases, radium isotopes are coprecipitated with barium in these ponds or are absorbed on bottom sediments [C19, W25]. Slags derived from coal mined in the vicinity of the town of Tatabánya in Hungary have elevated concentrations of ^{226}Ra (range: 0.85–2.4 Bq/g). The slag is used as filling and insulating material for the construction industry and as fill for playgrounds and roads [N14].

4. Oil and gas production

270. During the extraction process for oil and natural gas, radionuclides of natural origin from underground formations are mobilized and brought to the surface. Activity concentrations of ^{226}Ra and ^{228}Ra and their decay products in NORM released by oil and gas industries are often elevated, particularly in production waters. During extraction, radium and lead are coprecipitated along with barium and strontium and deposited in scales in tubing or discharged with effluents. Mean concentrations in wastewater of ^{226}Ra and ^{228}Ra of 4 and 2 Bq/L, respectively, have been reported, but can be higher by a factor of 50 [I11, I12]. The most radiologically significant radionuclides in the scales and other precipitates from the oil industry are the isotopes of radium, with activity concentrations ranging from 10 to 100 Bq/g. Activity concentrations in sludges are typically a factor of 10 lower. Some NORM wastes, however, contain ^{226}Ra and ^{228}Ra with activity concentrations up to several hundreds of Bq/g or more [A19, A20, I11]. The decay of radon in natural gas can result in high activity concentrations of ^{210}Po and ^{210}Pb deposited inside pipes [V6].

271. Waterborne pathways provide the most significant contribution to the dose to people living near oil and gas extraction facilities, mainly from external exposure to gamma radiation and inhalation of radon [R3]. However, no information on public exposures associated with the extraction of oil and natural gas was found in the literature review or provided through the UNSCEAR Global Survey on Public Exposure.

5. Rare earth and titanium oxide industries

272. The rare earth elements (REE) comprise the 15 lanthanide elements, yttrium and scandium. Compounds containing REE have many applications in electrical and electronic components, lasers, glass, magnetic materials, and general industrial processes [F3]. Bastnaesite and monazite are the most important minerals containing REE. Typical activity concentrations in bastnaesite range from 0.9 to 1.2 Bq/g for radionuclides in the ^{238}U decay series, and from 0.7 to 7 Bq/g for radionuclides in the ^{232}Th decay series. Conversely, typical activity concentrations in monazite vary between 10 and 50 Bq/g for radionuclides in the ^{238}U series and between 5 and 350 Bq/g for radionuclides in the ^{232}Th series. Activity concentrations of ^{232}Th in REE ores are typically in the range of 1–5 Bq/g with somewhat higher concentrations in heavy mineral sand, up to 16 Bq/g [I26]. The activity concentrations of ^{238}U in these ores may also be higher than natural background but typically remain below 1 Bq/g.

273. The ores are processed to obtain a heavy mineral fraction containing rare Earth minerals by chemical treatment for extraction and isolation of the REE of interest. The radionuclide activity concentrations in some specific solid residues obtained during this process can be high. For example, activity concentrations of ^{232}Th measured in barium-sulphate residues and of ^{238}U in lead-iron residues from the Bayan Obo REE mine in China were 89 and 57 Bq/g, respectively [I26].

274. Public exposure during the mining and processing of REE may occur from the storage and disposal of solid residues and liquid effluents. The annual dose received by people residing near the Bayan Obo City area in China was reported to be 0.044 mSv. The annual dose from exposure to gamma radiation attributable to bricks containing slag from the same area was estimated to be about 0.2 mSv [I26]. The same report concludes that public exposure in the REE mining area at Mount Weld (Australia) was not of concern, with gamma dose rates being at background levels.

275. In areas with deposits of heavy mineral sand, annual public doses from exposure to external gamma radiation can be up to several millisieverts. Studies from mining areas in India showed that the external dose rate was substantially lower after completion of mining activities and site remediation compared to the dose rate before mining started [I26]. Annual doses received by members of the public from the shallow land burial of waste from monazite processing plants can reach 0.25–0.3 mSv [I26].

276. For titanium production, activity concentrations of radionuclides in the ^{238}U and ^{232}Th decay series in amang, the mineral concentrate left after mining of tin ores, in Southeast Asia were reported to be in the range of 1 to 3.2 and 0.6 to 1 Bq/g, respectively. Activity concentrations in concentrates of single minerals, such as monazite or xenotime can reach several hundred Bq/g for radionuclides in both the ^{238}U and ^{232}Th decay series [I26]. Activity concentrations of the radionuclides in the ^{232}Th decay series in ilmenite sands are typically higher (range: 10–500 Bq/g) than those of the radionuclides in the ^{238}U series (range: 1–30 Bq/g) [I27]. Higher activity concentrations of up to 1,000 Bq/g or more were reported in scales generated during production of titanium dioxide pigment. However, activity concentrations of radionuclides in pigments are generally very low [I12].

277. Members of the public may be exposed to natural radionuclides in the vicinity of industries handling titaniferous feedstocks due to external gamma radiation from bulk quantities of material or from inhalation of dust, but the doses are negligible [G8]. Further potential exposure pathways arise from the

management of solid residues and the discharge of effluents from the feedstock upgrading process. These pathways may include external exposure to gamma radiation, inhalation of dust and ingestion of contaminated food and water. However, measures consistent with good environmental practice should be sufficient to ensure that exposures do not become significant [I27].

278. An environmental assessment for a facility producing titanium by the sulphate process, with full neutralization of acid effluent to produce red gypsum, concluded that members of the public did not receive any additional doses associated with the operation of the facility [I27]. The same conclusion was reached about the production of titanium by chloride process, as long as residues with higher activity concentrations are handled and disposed of correctly.

6. Zirconium and ceramic industries

279. Zircon, also referred to as zirconium silicate ($ZiSO_4$), is recovered during the processing of heavy mineral sands. In general, zircon sand has elevated activity concentrations of radionuclides in the ^{238}U and ^{232}Th decay series. Typical activity concentrations of ^{238}U and ^{232}Th are 3 and 0.6 Bq/g [U19], respectively; higher values can be detected in other materials which are not widely exploited on a commercial scale [K47]. Most zircon sand is used for the manufacture of zirconia, also known as zirconium dioxide (ZiO_2), ceramic pigments, glazed tiles, sanitary ware, and abrasives. It is also used for foundry sands and mould washes and in the production of refractory materials. For many of these applications, zircon sand is milled into smaller particles, in some cases down to particle sizes of less than 5 µm. Modern zircon milling operations maintain a high standard of dust control. Zirconia may be manufactured by melting zircon sand in a very high temperature furnace. Most of the ^{210}Pb and ^{210}Po in the feed material end up in the silica fume, which is removed by a fume collection system. Activity concentrations of ^{210}Pb and ^{210}Po in particulate matter in silica fumes are reported to be up to 200 and 600 Bq/g, respectively [B2].

280. Activity concentrations in baddeleyite or zirconia are more variable with typical activity concentrations between 3,000 and 13,000 Bq/kg for radionuclides in the ^{238}U series, and between 100 and 26,000 Bq/kg for those in the ^{232}Th series [I19]. Assessments performed in several countries indicate that the maximum annual dose received by an individual outside the facility would be less than 1 µSv from discharges to water and 56 µSv from emissions to atmosphere; doses to people living nearby were estimated to be negligible [I19].

7. Groundwater treatment

281. Some drinking water supply systems treat groundwater to remove impurities or contaminants, such as iron, manganese or arsenic. The filter gravels and filter sands used for this purpose often also remove the naturally occurring radionuclides contained in the drinking water. Iron hydroxides or manganese oxides which precipitate on the filters efficiently sorb radium isotopes. Uranium is sometimes removed using ion-exchange resins. Depending on the service life of such filters, relatively high concentrations of radionuclides can build up even with low-radionuclide concentrations in the water. An investigation of filter sands and gravels from Germany reported maximum activity concentrations of ^{238}U, ^{226}Ra, ^{228}Ra and ^{210}Pb of 2.5, 42, 13 and 2 Bq/g, whereas, maximum activity concentrations of ^{238}U and ^{234}U in uranium-adsorbing resins were 670 and 830 Bq/g, respectively [D33]. The same study found activity concentrations of ^{238}U, ^{226}Ra, and ^{228}Ra between 0.01 and 10 Bq/g in activated charcoal filters. Filter sludges, which are continuously removed, show lower levels of radioactivity.

282. Kleinschmidt and Akber [K25] calculated the dose to a suburban resident in southeast Queensland (Australia) assumed to have acquired 40 m^3 of groundwater treatment sludge for use as soil conditioner in a residential vegetable garden. The source term was based on the maximum sludge activity concentration (100 Bq/kg). The dose assessment also assumed that 10% of leafy vegetables consumed by the residents were produced from the garden. An annual dose of 0.21 mSv was estimated, with 89% being associated with external gamma dose, 9% with ingestion of food and the remainder with inhalation of dust and radon and ingestion of soil. The study also concluded that in a conventional water treatment plant, liquid waste with enhanced concentrations of radioactivity would generally be recycled within the treatment plant and therefore the public exposure would be negligible.

283. Hot, anoxic, and saline geothermal groundwater readily dissolves radium and radon. When this water is pumped as a heat source for geothermal plants, these radionuclides may be released or form deposits in the plants. Residues with an enhanced content of natural radionuclides result primarily from the use of deep water with high salinity. Regenspurg et al. [R15] reported the activity concentrations of naturally occurring radionuclides in filter residues at a geothermal site in the North German Basin. The highest activity concentrations were measured for ^{226}Ra (range: 1–102 Bq/g), ^{228}Ra (range: 1–75 Bq/g) and ^{210}Pb (range: 0.7–24 Bq/g).

D. Summary on public exposure from natural sources

284. Worldwide average annual effective doses from natural sources of ionizing radiation are summarized in table 15. The total worldwide average annual dose was estimated at 3.0 mSv, about 25% higher than the previous estimate of 2.4 mSv [U15, U19]. This increase mainly reflects more comprehensive datasets and higher-quality data, particularly for inhalation of radon and thoron and dietary intake of radionuclides. Table 15 also presents the ranges of the main dose components.

285. The doses in table 15 represent global averages intended as reference values or benchmarks for comparison purposes rather than actual doses received by people at specific locations. While doses from individual exposure pathways typically follow a log-normal distribution, correlations among pathways can lead to significant variations in the distributions at regional levels [U19]. These reference values can support assessments of population exposure to natural radiation and comparisons with doses from human-made sources.

Table 15. Summary on global public exposure from natural radiation sources

Source and pathway of exposure	*Characteristic average annual effective dose*[a, b] *(mSv)*	*Dose range*[b] *(mSv)*
INHALATION EXPOSURE		
Radon (^{222}Rn) and decay products	1.4 (1.15)	0.3–7.5
Radon (^{222}Rn) and decay products (indoors)	1.3 (1.05)	0.3–7 [c]
Radon (^{222}Rn) and decay products (outdoors)	0.10 (0.10)	0.01–0.5 [d]
Thoron (^{220}Rn) and decay products	0.36 (0.10)	0.15–3.2
Thoron (^{220}Rn) and decay products (indoors)	0.34 (0.09)	0.15–3 [d]
Thoron (^{220}Rn) and decay products (outdoors)	0.02 (0.01)	0.01–0.15 [d]
Terrestrial radionuclides	0.006 (0.006)	
Total inhalation exposure	**1.8 (1.3)**	**0.3–11 (0.2–10)**
COSMIC RADIATION EXPOSURE		
Indoors	0.23	
Outdoors	0.07	
Total cosmic radiation exposure	**0.3 (0.38)**	**0.2–0.8 [c] (0.3–1.0)**
EXTERNAL TERRESTRIAL RADIATION EXPOSURE		
Indoors	0.34 (0.41)	
Outdoors	0.06 (0.07)	
Total external terrestrial radiation exposure	**0.4 (0.48)**	**0.1–0.7 [c] (0.3–1.0)**
INGESTION EXPOSURE		
^{40}K	0.17 (0.17)	
Uranium and thorium series in food	0.25 (0.12)	
Drinking water (radon)	0.003 (0.002)	0.001–0.03 [c]
Drinking water (other radionuclides) [e]	0.02	
Cosmogenic radionuclides	0.01 (0.01)	
Total ingestion exposure	**0.5 (0.29)**	**0.2–1.0 (0.2–1.0)**
TOTAL		
Total exposure	**3.0 (2.4)**	**1–14 (1–13)**

[a] Refer to table A1 in appendix A for occupancy, shielding, equilibrium factors, inhalation rate, food and water ingestion rates, and dose coefficients.

[b] Result of previous evaluation [U19].

[c] Range of country averages.

[d] Range of regional averages.

[e] Natural radionuclides other than radon and its short-lived decay products.

1. Radon and thoron

286. The methodology for assessing public exposures from radon and thoron [U15, U18, U19, U27] was expanded to improve consistency and evaluate the representativeness of concentrations measured in national and regional surveys. Criteria were applied to survey design (e.g., population- versus geography-based), measurement parameters (e.g., duration, number of measurements, detector placement), and population coverage to improve the quality of the data. This approach will make the results of future UNSCEAR evaluations more comparable and improve the analysis of trends.

287. As in previous reports [U15, U18, U19, U27], inhalation of radon, thoron, and their decay products remains the predominant contributor to public exposures to natural radiation, accounting for about 60% of the total annual dose (1.8 mSv). The worldwide reference value for indoor radon concentration in this annex reflects broader coverage—63% of the global population compared with 37% in the UNSCEAR 2006 Report [U15, U18, U19, U27]. The population-weighted AM was estimated at 50 Bq/m³, higher than the previous estimate of 40 Bq/m³.

288. Data from regional surveys showed that radon concentrations indoors vary widely due to geological and environmental factors, with some areas exceeding 1,000 Bq/m³. Globally, concentrations follow a log-normal distribution, with a GM of 33 Bq/m³ and a GSD of 2.7 Bq/m³. National averages can change over time, due to the introduction of novel building practices and technologies which help reduce radon levels indoors, although thermal retrofitting and reduced ventilation can increase concentrations.

289. Coverage of data on radon outdoors, thoron indoors and outdoors, and radon in water remains limited, making dose estimates for these pathways less reliable than for indoor radon. Furthermore, about 37% of the world's population—mainly in Africa and Latin America—lacks representative national indoor radon surveys. The Committee recommends that countries conduct and periodically repeat such surveys using comparable methodologies to track trends.

2. Cosmic radiation and terrestrial radionuclides

290. The worldwide average annual effective dose from cosmic radiation was estimated at 0.3 mSv, lower than the Committee's previous estimate of 0.38 mSv [U19]. This estimate was derived using a comprehensive model with a higher resolution for the population distribution by altitude and latitude, enabling a more detailed assessment of the exposure from cosmic rays to be performed.

291. For public exposure during aircraft flights, doses received by passengers on individual flights were estimated to be low, ranging from a few to several tens of microsieverts. However, frequent flyers may receive doses comparable to those from natural radiation. Annual collective doses have tripled between 2003 and 2019, driven by the global increase in air travel.

292. Measurements of radionuclide concentrations in soils, drawn from the literature and supplied through the UNSCEAR Global Survey on Public Exposure and a geochemical database [E1], were analysed after excluding areas with high gamma background radiation. The resulting worldwide average annual external dose from terrestrial radiation was estimated at 0.4 mSv, a slightly lower value than the previous estimate of 0.48 mSv [U19].

293. Doses due internal exposure from ^{40}K in the body and ingestion of natural radionuclides were evaluated using the established UNSCEAR methodology [U15]. Analysis of recent data indicated that activity concentrations of ^{210}Po, ^{210}Pb and ^{228}Ra in food were higher than previously reported, increasing the estimated worldwide average annual ingestion dose to about 0.5 mSv.

294. Areas with high gamma background radiation were categorized through a statistical screening of radionuclide concentrations in soil. Several new potential high gamma background radiation areas were identified through this process. Because the variability of indoor radon concentrations depends on a number of factors unrelated to activity concentrations of ^{226}Ra in soil, the correlation between high gamma background areas and indoor radon levels is weak.

295. NORM industries worldwide can lead to public exposure from enhanced concentrations of naturally occurring radionuclides in products, by-products, and wastes, as well as through the disposal of residues to landfill or their use as building materials. Significant efforts are underway at national and international levels to assess exposure associated with NORM and develop strategies for managing such situations [D10, I18, I76, M42]. Annual doses to the public associated with the NORM industry are generally very low, typically only up to a few microsieverts.

IV. PUBLIC EXPOSURE FROM HUMAN-MADE RADIATION SOURCES

296. This chapter evaluates sources of human-made ionizing radiation and exposures of the public associated with these sources. In this annex sources of human-made ionizing radiation have been divided into the following categories:

(a) Exposure associated with nuclear power production and related nuclear fuel cycle facilities;

(b) Applications other than nuclear power production;

(c) Military use of nuclear and radioactive materials;

(d) Exposure associated with radiological accidents and past peaceful practices;

(e) Radioactive waste management;

(f) Transport of nuclear and radioactive material.

A. Nuclear power production and related nuclear fuel cycle facilities

297. The Committee has routinely collected data on radionuclide discharges from the operation of NPPs and related facilities and evaluated the associated public exposure. The UNSCEAR 1993 Report [U13] provided an overview of annual routine discharges of radionuclides from the main types of NPPs and other facilities in the nuclear power production cycle since the practice of commercial nuclear power generation began. Data for uranium mines and mills, NPPs, and reprocessing plants were provided for the years 1985–1989 [U13]. Data for the period 1990–1997 were presented in the UNSCEAR 2000 Report [U15], while operational data for NPPs and uranium mining for the periods 1998–2002 and 1998-2003, respectively, were provided in the UNSCEAR 2008 Report, annex B [U19]. Exposures from electricity generation, including nuclear power production, were also presented in the UNSCEAR 2016 Report [U24]. This annex provides data for the period between 2007 and 2020 and an assessment of

associated public exposure. As illustrated in figure XIV, the net generation of electricity was relatively stable over the period between the previous and this annex (2002–2007), such that the discharges in the intervening period are unlikely to have been significantly different from those presented in this annex, and broadly consistent with data for the representative year of 2009.

298. The generation of electrical energy by nuclear means grew steadily since the world's first commercial NPP, Calder Hall at Windscale (United Kingdom) started operating in 1956 until the early years of the current century, when capacity and electricity generation reached a plateau. The relatively rapid expansion in energy generation that occurred from 1970 to 1985, at an average annual rate of over 20%, slowed to a rate averaging around 3% per year from 1990 to 2000, as illustrated in figure XIV. Between 2003 and 2010, net generation continued at a steady level of around 300 GW a. There was a significant reduction of around 6% between 2011 and 2012, following the accident at the Fukushima Daiichi NPS; since then, net generation has increased steadily to reach the previous level of around 300 GW a. Since 2005, more than 80 reactors closed; 5 were shut down because of the accident at the Fukushima Daiichi NPS; 27 were closed prematurely, while the remaining 50 reactors were closed having fulfilled their purpose or being no longer economical to run [W19]. In 2020, there were 442 operating NPPs in 32 countries, representing a total capacity of 393 GWe and a net generation of 291 GW a, 5 connections to the grid and 52 NPPs under construction. Conversely, 172 NPPs were at various stages of the decommissioning process with 20 having been fully decommissioned [I56].

Figure XIV. Trends in the capacity of operational and suspended nuclear reactors and net generation worldwide [I56]

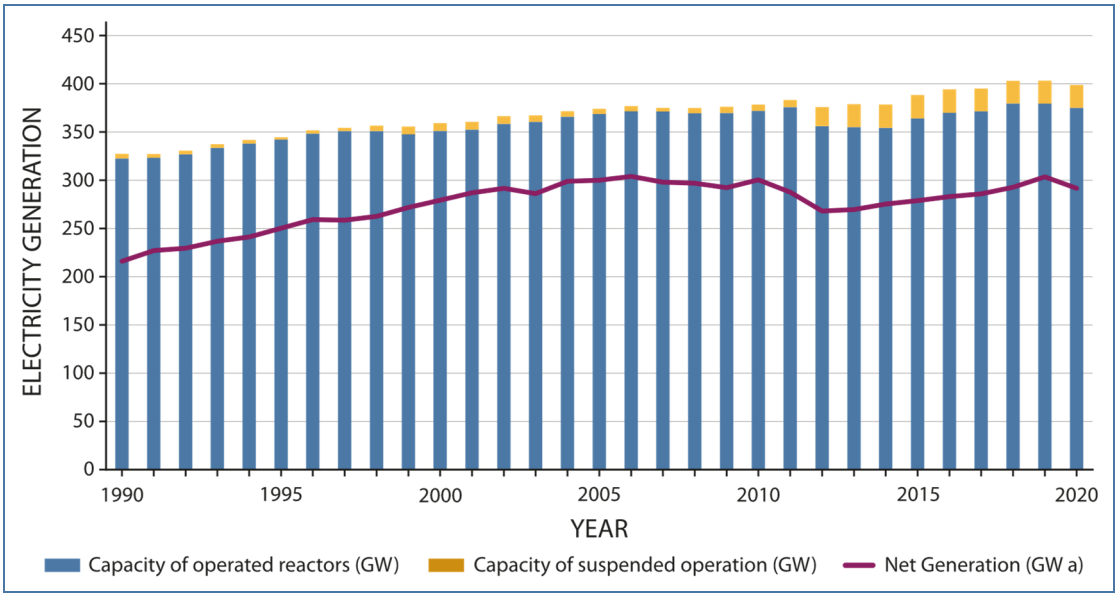

299. The nuclear power production cycle includes the mining and milling of uranium ore and its conversion to nuclear fuel; the fabrication of nuclear fuel elements; the production of energy at nuclear power plants (NPPs); disposal of spent nuclear fuel or its reprocessing, with the recycling of the fissile and fertile materials recovered; and the storage, discharge, treatment, and disposal of radioactive waste. For some types of NPPs, enrichment of the isotopic content of ^{235}U in the nuclear fuel is an additional step in the nuclear fuel cycle. The nuclear power production cycle also includes the transport of radioactive materials between various facilities. Public exposures associated with discharges from radioactive waste facilities are considered in section IV.B, while those related to the transport of radioactive materials are dealt with in section IV.F.

300. Public exposure resulting from radioactive discharges from facilities in the nuclear power production cycle were assessed in previous UNSCEAR reports [U15, U19, U24]. Given that the electricity generation profile does not generally vary significantly year-to-year on a regional or global scale, trends in normalized releases and the resultant doses from discharges from NPPs and associated processes are presented for two representative years in the period 2007–2020. The first representative year, 2009, was chosen to represent the period before the accident at the Fukushima Daiichi NPS, while the second, 2016, was chosen to represent the period after the accident when manufacturing had settled into a more normal pattern.

301. Doses to the public from exposure to effluents discharged by nuclear installations vary widely from one facility to another, between different locations and with time. To evaluate the total impact of radionuclides released at each stage of nuclear power production, the exposures have been evaluated in terms of collective dose per unit electrical energy generated, expressed as person–Sv/(GW a) The UNSCEAR 2016 Report [U24] also included an assessment of the public exposure from other forms of electricity generation, such as coal, natural gas, oil, and geothermal energy. This assessment indicated that the normalized collective dose from electricity generation from coal was between two to over three times greater than that from nuclear power production facilities, depending on the age of the coal plants involved. The normalized collective dose from geothermal technologies was also greater than nuclear power production, while the corresponding values for natural gas and oil were lower [U24].

1. Outline of dose assessment methodology

302. Doses to the public from radioactive discharges of operating nuclear fuel cycle facilities, including uranium mines and mills, in this annex have been estimated using the dose assessment methodology described in UNSCEAR 2016 Report [U24]. A review of the methodology was performed as part of this evaluation to ensure that model parameter values and habit and dosimetric data were up to date. Details of the review and of the changes made to the methodology are provided in this section, in appendix A and in electronic attachment A-3.

303. The dose to a characteristic individual was calculated in the 100th year following a continuous discharge at the rate for the year under consideration, which is equivalent to the integrated dose to 100 years from a single year's discharge [U24]. Collective doses were also calculated for discharges in a single year integrated to 100 years. When developing the methodology, the Committee considered that 100 years was a reasonable basis for the calculation as it covers the lifetime of individual NPPs and the possibility that additional NPPs may be constructed on the same site. The environmental models in the methodology take account of the accumulation of radionuclides in the environment over the integration period.

304. For atmospheric discharges, a Gaussian model was used to simulate the dispersion and deposition of radionuclides released to the atmosphere. Estimates of doses for discharges to atmosphere were based on the population distributions around coastal or inland NPPs, using updated population distributions generated for the different regions adopted by UNEP [U24]. The inland or coastal location of NPPs was determined from information provided in the PRIS database [I56].

305. The model for dispersion of radionuclides to freshwater is a simple dilution model which considers two generic types of rivers, small and large. The model used for the dispersion of radionuclides in the marine environment is a simple two-compartment model (e.g., a local compartment and a regional one). Further information on these models is provided in appendix A.

306. Collective doses to the world population for four globally circulating radionuclides (^{3}H, ^{14}C, ^{85}Kr and ^{129}I) were integrated to 500 and 10,000 years in addition to 100 years to evaluate the long-term

component of exposures arising from the discharge of these radionuclides. The Committee adopted these integration times using the approach described in the UNSCEAR 2016 Report [U24]. The longer integration periods are included for globally circulating radionuclides to take account of the fact that these radionuclides continue to contribute to the collective dose beyond 100 years. However, it should be noted that the collective doses calculated for longer time periods have increasing uncertainties associated with them and are not intended to be used for risk estimations.

307. The Committee updated its methodology to include aquatic discharges from uranium mines and mills to the freshwater environment [U24]. The updated methodology also takes account of the effect of different tailings management practices, on atmospheric releases related to different water coverage in arid and non-arid areas. Further information is provided in appendix A and in electronic attachment A-3.

2. Uranium mining and milling

308. Uranium ore can be extracted by physically removing it through conventional surface or underground mining methods or by chemically dissolving the uranium out of the rock ore through either heap leaching or in-situ leaching (ISL) [U48]. Surface mining techniques—also referred to as opencast, open pit or strip mining—are applied to ores that are close to the surface. Underground mining involves extracting rock through a tunnel or opening on the side of a hill or mountain and is generally applied for the extraction of higher-grade ores. In-situ leaching is generally applied to shallow deposits that exist in non-porous shale or mudstone, or in situations where uranium can be recovered from otherwise inaccessible or uneconomical formations [U48].

309. Uranium ores typically contain from about 0.05 to 0.3% of uranium oxide (U_3O_8) [U48], although some higher-grade ores exist (e.g., some ores in Canada contain from 4 to 11% of U_3O_8 [O3]). The mined uranium ore is sent to a mill for its processing, usually located close to the mine. Milling involves the extraction and purification of uranium from the uranium ore. After an initial purification process, uranium is precipitated in a partially refined form of uranium oxide concentrate, known as yellowcake. The uranium concentrate, typically containing 75–95% of uranium, is shipped to a chemical plant for further purification and chemical conversion [E27].

310. In-situ leaching is an alternative method to extract uranium through an ion-exchange process, and the yellowcake is then precipitated, dried and packed. After recovery of the uranium, wastewater containing various dissolved ions, such as chloride, sulphate, sodium, radium, arsenic and iron, is re-injected into approved disposal wells in a depleted portion of the ore body [U24].

311. In the past, open pit and underground mining were the main methods used to extract uranium. However, over the last 20 years, ISL has become the dominant method. In 2020, around 58% of the world production of uranium was from ISL, while around 19 and 16% was derived from open-pit and underground mining, respectively [O3]. The remaining 7% was recovered as a by-product of other mineral processing. According to the 2022 edition of the Joint NEA/IAEA Report on Uranium Resources, Production and Demand [O3], 17 countries produced uranium in 2020 with a total production of 47,342 tonnes of uranium. A summary of global production of uranium in 2020 is presented in table 16.

312. Since 2018, there has been a general reduction in uranium production in major producing countries as shown in figure XV, with the exception of Niger, largely due to depressed market prices and reduced activity resulting from work restrictions following the COVID-19 pandemic [O3]. Data from the World Nuclear Association indicate that, in 2022, over half of the world's uranium production was derived from 10 mines distributed among 5 countries: Australia, Canada, Kazakhstan, Namibia and Niger [W17].

Table 16. Uranium production in 2020 [O3]

Country (UNEP Region)	*Uranium production in 2020 (tonnes U)*
Australia (Asia and the Pacific)	6 195
Canada (North America)	3 878
China (Asia and the Pacific)	1 600 [a]
Czechia (Europe)	34
India (Asia and the Pacific)	540 [a]
Iran, Islamic Republic of (Asia and the Pacific)	21 [a]
Kazakhstan (Asia and the Pacific)	19 477
Namibia (Africa)	5 412
Niger (Africa)	2 991
Pakistan (Asia and the Pacific)	45 [a]
Russian Federation (Europe)	2 846
South Africa (Africa)	62 [a]
Ukraine (Europe)	711
United States (North America)	8 [a]
Uzbekistan (Asia and the Pacific)	3 512 [a]
Total	**47 342** [b]

[a] NEA/IAEA estimates.

[b] Small production from mine rehabilitation in Germany and Hungary included in the total, although not listed separately.

Figure XV. Trends in world uranium production [b] [O3]

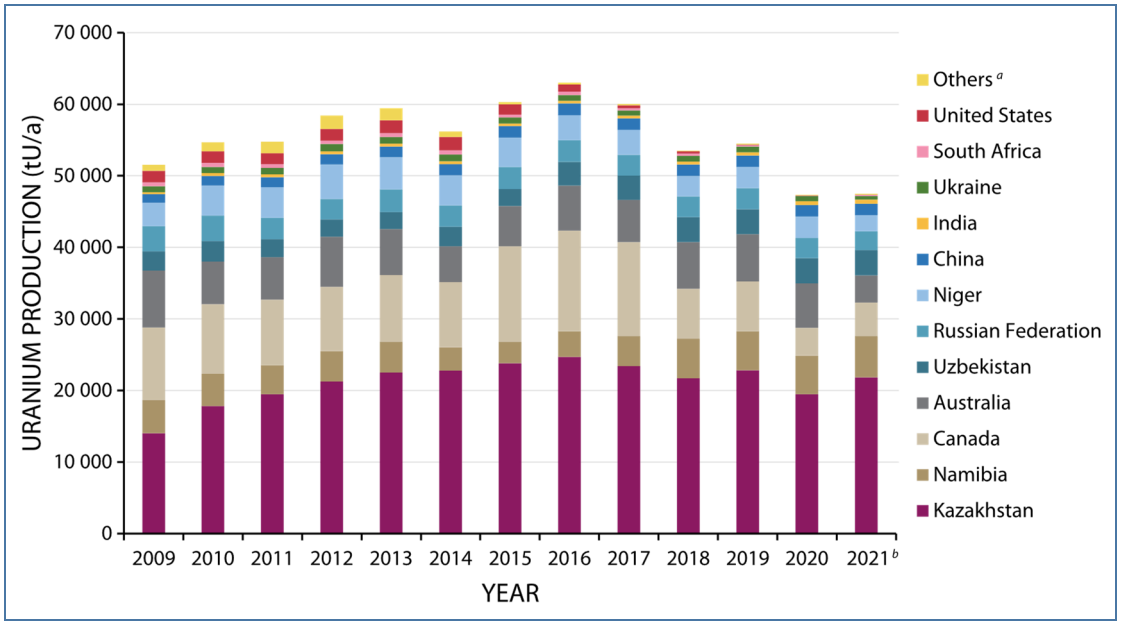

[a] "Others" include the remaining producers.

[b] NEA/IAEA estimate.

(a) *Effluents and solid waste*

313. The mining and milling processes create waste residues in addition to the uranium product, such as waste rock piles and tailings accumulated as a result of the mining operations carried out in open pits and underground mines. It has been estimated that uranium mill tailings are generated at a rate of about 1 tonne per tonne of ore extracted, and they generally retain 5–10% of the uranium and 85% of the total activity [U19]. The long-lived precursors of radon present in the mill tailings, namely ^{226}Ra and ^{230}Th, provide a long-term source of radon release to the atmosphere.

314. In-situ leaching facilities generate no surface tailings and limited radon emissions after closure [U10]. Radon is, however, released during the ISL process [B4, B5] and waste slurries and wastewater arise during recovery of the uranium. In non-arid environments, discharges of radon to the atmosphere are not expected due to the presence of water covering uranium tailings, but discharges to the aquatic environment may occur.

315. In previous assessments [U15, U19, U22], the average normalized radon releases were derived from the limited data available. For the purposes of the UNSCEAR 2016 Report, the radon release rate from non-ISL mines was estimated at 66 TBq/(GW a), while the corresponding values for other mines, milling and operational milling operations were each estimated at 3 TBq/(GW a) and 0.1 TBq/(GW a) for mill tailings from non-ISL processes [U24]. Data for releases of other radionuclides from milling activities, normalized to electricity generation, were also presented [U24].

316. In this evaluation, doses arising from discharges from mines and mills have been calculated based on information supplied by Australia, Canada, Czechia, and the Russian Federation through from the UNSCEAR Global Survey on Public Exposure and the data from OECD/NEA [O3]. The Committee's previous assessments did not explicitly address exposures from aquatic effluents from mines and mills and the management of tailings by water cover. However, the UNSCEAR Global Survey on Public Exposure provided estimates not only of emissions of radon and decay products resulting from current tailings management practices, such as saturation and water coverage, but also from discharges of radionuclides in the uranium decay series to the aquatic environment. Typical annual discharges are summarized in table 17. These discharges are averages over a five-year period between 2007 and 2020 chosen to represent typical operational discharges from the facility; consequently, the five-year period varied between facilities. It should be, however, noted that the data submitted through the UNSCEAR Global Survey on Public Exposure are only representative of non-ISL facilities (e.g., open pit, underground and by product production). No information was available for ISL facilities, which is the dominant production method. As a consequence, discharge data for ISL facilities to estimate worldwide average values were derived from information available in the UNSCEAR 2016 Report [U24].

Table 17. Typical annual discharges from uranium mines and mills averaged over a five-year period between 2007 and 2020

Radionuclide	*Average annual discharges from uranium mines and mills (GBq/a)*									
	Australia		*Canada*					*Czechia*		*Russian Federation*
	Olympic Dam	*Ranger*	*Cigar Lake*	*Key Lake*	*McArthur River*	*McClean Lake*	*Rabbit Lake*	*o. z. TÚU*	*o. z. GEAM*	*PPGHO*
ATMOSPHERIC DISCHARGES										
^{210}Pb				1.0×10^{-1}		3.0×10^{-2}			2.5×10^{-1}	
^{210}Po										
^{222}Rn	3.1×10^{5}								2.1×10^{5}	3.8×10^{5}
^{226}Ra				3.1×10^{-2}		4.4×10^{-3}			1.4×10^{-3}	
^{230}Th				3.5×10^{-3}		5.0×10^{-3}				
^{232}Th										4.1×10^{0}
^{234}U	4.1×10^{0}	1.3×10^{-1}		2.1×10^{0}		2.2×10^{0}				
^{238}U	4.1×10^{0}	1.2×10^{-1}		2.0×10^{0}		2.1×10^{0}		4.4×10^{-4}	2.3×10^{-2}	
LIQUID DISCHARGES										
^{210}Pb			7.9×10^{-3}	6.9×10^{-2}	5.0×10^{-2}	7.3×10^{-2}	2.7×10^{-1}			1.9×10^{0}
^{210}Po			1.9×10^{-3}	3.1×10^{-2}	1.2×10^{-1}	3.8×10^{-2}	1.1×10^{-1}		3.5×10^{-3}	1.1×10^{0}
^{222}Rn										
^{226}Ra			2.7×10^{-3}	7.9×10^{-2}	1.6×10^{-1}	1.3×10^{-2}	3.1×10^{-2}	3.5×10^{-1}	6.3×10^{-2}	3.0×10^{-1}
^{230}Th			3.5×10^{-3}	6.9×10^{-2}	2.5×10^{-2}	1.9×10^{-2}	8.5×10^{-2}			3.8×10^{0}
^{232}Th										
^{234}U			9.1×10^{-3}	2.4×10^{-1}	2.4×10^{-1}	8.2×10^{-2}	3.5×10^{0}			
^{238}U			8.8×10^{-3}	2.3×10^{-1}	2.4×10^{-1}	8.2×10^{-2}	3.5×10^{0}	1.2×10^{0}	1.7×10^{0}	1.6×10^{1}

(b) *Dose estimates*

317. Annual doses to the characteristic individual associated with the uranium mining and milling facilities for which discharge data were available are presented in table 18. The highest annual characteristic individual dose was 9.5 μSv, for the Priargunsky Mining and Chemical Production Association (PPGHO) facility in the Russian Federation. The corresponding annual doses estimated for the other facilities ranged from 0.001 to 0.7 μSv.

Table 18. Annual doses to characteristic individual from discharges from mines and mills

Country	*Site*	*Annual dose to characteristic individual (mSv)*		
		Atmospheric discharges	*Liquid discharges*	*All discharges*
Australia	Olympic Dam	4.2×10^{-4}		4.2×10^{-4}
	Ranger	1.3×10^{-5}		1.3×10^{-5}
Canada	Cigar Lake		2.0×10^{-5}	2.0×10^{-5}
	Key Lake	2.3×10^{-4}	1.8×10^{-4}	4.1×10^{-4}
	McArthur River		3.4×10^{-4}	3.4×10^{-4}
	McClean Lake	2.3×10^{-4}	1.5×10^{-4}	3.8×10^{-4}
	Rabbit Lake		7.0×10^{-4}	7.0×10^{-4}
Czechia	o. z. TÚU	2.2×10^{-8}	1.8×10^{-4}	1.8×10^{-4}
	o. z. GEAM	1.7×10^{-5}	8.6×10^{-5}	1.0×10^{-4}
Russian Federation	PPGHO	4.6×10^{-3}	4.9×10^{-3}	9.5×10^{-3}

318. Collective doses integrated to 100 years for uranium mines and mills for which discharges were provided through the UNSCEAR Global Survey on Public Exposure are presented in table 19. Collective doses from atmospheric discharges were calculated assuming that the facilities are located in areas with very low population density, while those from liquid discharges were based on the model for discharges into a small river. All the facilities in the table are non-ISL facilities which accounted for around 42% of the global uranium production in 2020 [O3]. The table shows that the total collective dose to the world population integrated to 100 years from a single year's discharges from these non-ISL facilities was estimated to be around 0.6 person–Sv. The collective dose was scaled up using the global uranium production for 2020 to estimate a collective dose for all non-ISL facilities of 1.3 person–Sv. No discharge data were made available to calculate a total collective dose to the world population for ISL facilities, which were therefore calculated based on the normalized collective dose per unit energy production of 0.22 person–Sv/(GW a), given in the UNSCEAR 2016 Report [U24], and the proportion of annual uranium production from ISL facilities for 2020. The collective dose to the world population from ISL was estimated at 29 person–Sv, while the overall collective dose to the world population due to discharges from uranium mines and mills was estimated at 31 person–Sv.

319. Using the nuclear power generation for 2020 of 291 GW a [I56], the normalized collective dose from a single year's discharges per unit energy production was estimated to be around 0.11 person–Sv/(GW a). This is a factor of two lower than that given in the UNSCEAR 2016 Report [U24], which was based on more limited data and past management practices. Nevertheless, significant uncertainties remain due to the limited data on discharges provided through the UNSCEAR Global Survey on Public Exposure, most notably the lack of information for ISL facilities, which represent the dominant production method for uranium.

Table 19. Collective doses integrated to 100 years due to a single year's discharges from uranium mines and mills

Country	*Site*	*Collective dose from uranium mines and mills (person–Sv)*				
		Atmospheric discharges			*Liquid discharges*	*All discharges*
		Local	*Regional*	*Total*		
Australia	Olympic Dam	2.9×10^{-3}	1.4×10^{-2}	1.7×10^{-2}		1.7×10^{-2}
	Ranger	9.1×10^{-5}	4.3×10^{-4}	5.2×10^{-4}		5.2×10^{-4}
Canada	Cigar Lake				1.3×10^{-3}	1.3×10^{-3}
	Key Lake	1.7×10^{-3}	7.9×10^{-3}	9.5×10^{-3}	1.1×10^{-2}	2.1×10^{-2}
	McArthur River				2.1×10^{-2}	2.1×10^{-2}
	McClean Lake	1.6×10^{-3}	7.7×10^{-3}	9.3×10^{-3}	9.6×10^{-3}	1.9×10^{-2}
	Rabbit Lake				4.4×10^{-2}	4.4×10^{-2}
Czechia	o. z. TÚU	1.5×10^{-7}	7.4×10^{-7}	8.9×10^{-7}	1.1×10^{-2}	1.1×10^{-2}
	o. z. GEAM	2.7×10^{-4}	1.3×10^{-3}	1.6×10^{-3}	5.1×10^{-3}	6.7×10^{-3}
Russian Federation	PPGHO	3.3×10^{-2}	1.6×10^{-1}	1.9×10^{-1}	3.1×10^{-1}	5.0×10^{-1}
Worldwide		4.0×10^{-2}	1.9×10^{-1}	2.3×10^{-1}	4.1×10^{-1}	6.4×10^{-1}

3. Nuclear fuel manufacturing

320. Nuclear fuel manufacturing include uranium conversion and enrichment and nuclear fuel fabrication. As of 2023, there were 12 commercial facilities for the conversion of uranium oxide, of which 9 were operational, and 21 for the conversion of UF_4 and UF_6, of which 11 were operational. These facilities are located in Canada, China, France, and Russian Federation. There were also 23 facilities for uranium enrichment, of which 14 were operational, located in France, Germany, Netherlands (Kingdom of the), Russian Federation, the United Kingdom, and the United States, and 84 nuclear fuel fabrication facilities existed, of which 41 were operational, 10 being decommissioned within one year, and 2 fully decommissioned [I49].

321. Radioactive discharges from nuclear fuel manufacturing facilities are generally low and consist mainly of radioisotopes in the uranium decay series. Discharges for nine uranium conversion facilities, three uranium enrichment installations and seven nuclear fuel fabrication plants, located in various countries, were provided through the UNSCEAR Global Survey on Public Exposure and were used to calculate doses to the characteristic individual and collective doses for the representative years 2009 and 2016. The annual doses to the characteristic individual for conversion and fuel fabrication facilities were estimated to be a small fraction of 1 μSv (further information is given in electronic attachment A-3).

322. Collective doses integrated to 100 years due to a single year's discharges in 2009 and 2016 from fuel manufacturing facilities were at around 0.9 and 0.5 person–Sv, respectively (see table 20). The largest contributions are from installations in Europe and North America. These values are similar to the collective dose from a single year's discharges of 0.8 person–Sv estimated for the period 1998–2002 in the UNSCEAR 2008 Report, annex B [U19]. The annual doses to characteristic individual were estimated to be negligible, typically of the order of less than 1 μSv. The highest doses were estimated for

Springfields (United Kingdom), for which annual doses to the characteristic individual were 1.4 and 0.7 μSv for the representative years of 2009 and 2016, respectively.

323. Normalized worldwide collective doses for nuclear fuel manufacturing facilities were calculated by dividing the worldwide collective dose by the average global electricity generation values for 2009 and 2016 of 292 and 282 GW a, respectively. The values of 0.003 and 0.002 person–Sv/(GW a) are consistent with the value of 0.003 person–Sv/(GW a), given in the UNSCEAR 2008 Report, annex B [U19], although uncertainties associated with this estimate are significant, mainly due to the discharge data being incomplete. Information on UF_6 global capacity for conversion, enrichment and fabrication of nuclear fuel for 2020 [W18], suggests that the sites for which discharge data were provided represent around 70% of the world conversion and enrichment capacities and around 30% of the fabrication capacity, although this latter value is based on data for fuel rods alone.

Table 20. Collective doses integrated to 100 years due to a single year's discharges from nuclear fuel manufacturing for representative years 2009 and 2016

Region	*Year*	*Collective dose for nuclear fuel manucaturing facilities (person–Sv)*				
		Atmospheric discharges			*Liquid discharges*	*All discharges*
		Local	*Regional*	*Total*		
Asia and the Pacific	2009	6.8×10^{-6}	1.3×10^{-5}	2.0×10^{-5}	5.0×10^{-5}	7.0×10^{-5}
	2016	8.9×10^{-6}	1.7×10^{-5}	2.6×10^{-5}	2.1×10^{-5}	4.7×10^{-5}
Europe	2009	7.6×10^{-2}	2.2×10^{-1}	3.0×10^{-1}	5.2×10^{-3}	3.1×10^{-1}
	2016	5.5×10^{-2}	1.7×10^{-1}	2.2×10^{-1}	1.0×10^{-2}	2.3×10^{-1}
Latin America and the Caribbean	2009	8.6×10^{-5}	4.2×10^{-5}	1.3×10^{-4}	2.4×10^{-3}	2.5×10^{-3}
	2016	7.2×10^{-7}	3.5×10^{-7}	1.1×10^{-6}	9.6×10^{-5}	9.7×10^{-5}
North America	2009	1.8×10^{-1}	3.1×10^{-1}	5.0×10^{-1}	1.1×10^{-2}	5.1×10^{-1}
	2016	9.0×10^{-2}	1.5×10^{-1}	2.4×10^{-1}	2.8×10^{-3}	2.5×10^{-1}
Worldwide	2009	2.7×10^{-1}	6.2×10^{-1}	9.0×10^{-1}	2.7×10^{-2}	9.2×10^{-1}
	2016	1.5×10^{-1}	3.4×10^{-1}	4.9×10^{-1}	1.8×10^{-2}	5.1×10^{-1}

4. Nuclear power plants

324. Nuclear reactors used for the generation of electrical energy in NPPs are for the most part classified according to their coolant systems and moderators: *(a)* light-water-moderated and -cooled pressurized- or boiling-water reactors (PWRs or BWRs); *(b)* heavy-water-cooled and -moderated reactors (HWRs); *(c)* gas-cooled, graphite-moderated reactors (GCRs); and *(d)* light-water-cooled, graphite-moderated reactors (LWGRs). These are all thermal reactors, in which the moderator material is used to slow down the fast fission neutrons to thermal energies. In fast-breeder reactors (FBRs), where there is no moderator, fission is induced by fast neutrons, and the coolant is a liquid metal. Fast-breeder reactors make only a minor contribution to global energy production. The distribution of types of operational NPPs by UNEP region is presented in table 21 based on data from the IAEA PRIS database [I56]. Pressurized water reactors are the most numerous nuclear reactors worldwide. The highest number of operational NPPs is in Europe, but it has decreased during the period of the assessment while the number of reactors in Asia and the Pacific region has increased.

Table 21. Number of operational NPPs by reactor type, location and UNEP region

All operational reactors are included, regardless of whether electricity was generated in the reference year. The last GCR was permanently shut down in 2015

Reactor type	*Africa*		*Asia and the Pacific*		*Europe*		*Latin America and the Caribbean*		*North America*		*Total*	
	2009	*2016*	*2009*	*2016*	*2009*	*2016*	*2009*	*2016*	*2009*	*2016*	*2009*	*2016*
PWR total	**2**	**2**	**52**	**83**	**140**	**139**	**2**	**2**	**69**	**66**	**265**	**292**
Coastal	2	2	51	80	34	34	2	2	16	13	105	131
Inland	0	0	1	3	106	105	0	0	53	53	160	161
BWR total	**0**	**0**	**38**	**28**	**19**	**14**	**2**	**2**	**35**	**34**	**94**	**78**
Coastal	0	0	38	28	9	9	2	2	2	2	51	41
Inland	0	0	0	0	10	5	0	0	33	32	43	37
HWR total	**0**	**0**	**23**	**25**	**2**	**2**	**2**	**3**	**18**	**19**	**45**	**49**
Coastal	0	0	11	11	0	0	0	0	1	1	12	12
Inland	0	0	12	14	2	2	2	3	17	18	33	37
LWGR total	**0**	**0**	**0**	**0**	**16**	**15**	**0**	**0**	**0**	**0**	**16**	**15**
Coastal	0	0	0	0	4	4	0	0	0	0	4	4
Inland	0	0	0	0	12	11	0	0	0	0	12	11
AGR (all coastal)	**0**	**0**	**0**	**0**	**14**	**14**	**0**	**0**	**0**	**0**	**14**	**14**
GCR total	**0**	**0**	**0**	**0**	**4**	**0**	**0**	**0**	**0**	**0**	**4**	**0**
Coastal	0	0	0	0	2	0	0	0	0	0	2	0
Inland	0	0	0	0	2	0	0	0	0	0	2	0
FBR (all inland)	**0**	**0**	**0**	**1**	**2**	**2**	**0**	**0**	**0**	**0**	**2**	**3**
All types total	**2**	**2**	**113**	**137**	**197**	**186**	**6**	**7**	**122**	**119**	**440**	**451**

325. Table 22 provides an overview of the electricity generated in the representative years 2009 and 2016 by type of nuclear reactor and UNEP region derived from the PRIS database [I56]. Data on the electrical energy generated by various types of NPPs for the period 1998–2002 and 2010 were presented in the UNSCEAR 2008 Report, annex B [U19] and the UNSCEAR 2016 Report [U24], respectively. The total energy generated in one year by NPPs in the reporting period was close to 300 GW, around 70% of which was generated by PWRs followed by BWRs. The contribution of BWRs to the global nuclear energy production decreased during this period from around 20 to 16%, due to reduced generation in the Asia and the Pacific region, following shutdowns and testing in the aftermath of accident at the Fukushima Daiichi NPS accident. Trends in nuclear electricity generation for the UNEP regions are shown in figure XVI. Data for 2009 are generally consistent with, albeit a little lower than, the value presented in the UNSCEAR 2016 Report for the year 2010 [U24].

Table 22. Electricity generation of NPPs (GW a) by reactor type and UNEP region

All operational reactors are included, regardless of whether electricity was generated in the reference year

Region	*Year*	*Electricity generation of NPPs (GW a)*							
		PWR	*BWR*	*HWR*	*LWGR*	*AGR*	*GCR*[a]	*FBR*	*Total*
Africa	2009	1.32	0	0	0	0	0	0	1.32
	2016	1.74	0	0	0	0	0	0	1.74
Asia and the Pacific	2009	38.08	17.26	4.83	0	0	0	0	60.18
	2016	42.99	1.95	6.03	0	0	0	0	50.97
Europe	2009	97.66	11.83	1.24	9.1	5.26	0.88	0.45	126.41
	2016	95.74	10.86	1.19	8.28	6.45	0	0.89	123.41
Latin America and the Caribbean	2009	1.4	1.15	0.87	0	0	0	0	3.42
	2016	1.71	1.17	0.88	0	0	0	0	3.76
North America	2009	60.42	30.55	9.72	0	0	0	0	100.69
	2016	60.54	31.46	10.92	0	0	0	0	102.92
West Asia	2009	0	0	0	0	0	0	0	0
	2016	0	0	0	0	0	0	0	0
Total	**2009**	**198.87**	**60.8**	**16.65**	**9.1**	**5.26**	**0.88**	**0.45**	**292.02**
	2016	**202.72**	**45.45**	**19.01**	**8.28**	**6.45**	**0**	**0.89**	**282.8**

[a] The last GCR was permanently shut down in 2015.

Figure XVI. Illustration of trends in nuclear electricity generation by region [I56, W19]

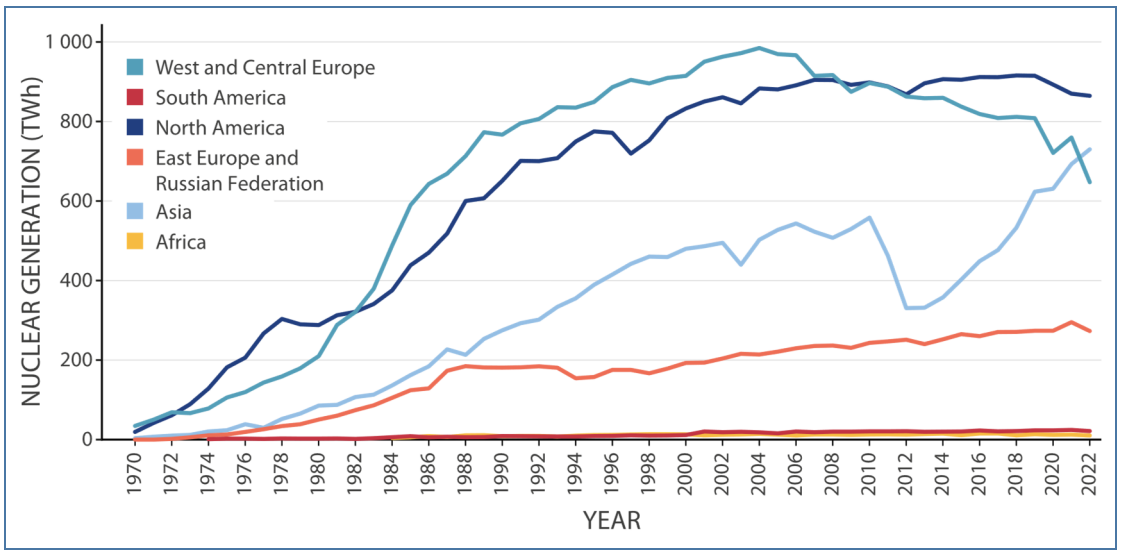

(a) *Effluents*

326. Annual radioactive discharges from operating NPPs were provided by 28 United Nations Member States through the UNSCEAR Global Survey on Public Exposure and were supplemented by information obtained from national and international organizations where necessary. Most of the available data were related to PWRs, BWRs, and HWRs. Only limited information was available for AGRs, GCRs, LWGRs, and FBRs. A full compilation of the discharges provided, for each NPP and each year in the period 2007–2020 is provided in electronic attachment A-3.

327. Normalized discharges have traditionally been compiled separately for each reactor type because of the different composition in the discharges, notably for noble gases and tritium. Discharges are often only available for groups radionuclides; however, to be able to estimate doses using the UNSCEAR methodology, it is necessary to apportion these groups to one or more particular radionuclides. The assumptions made in this assessment to derive the radionuclide composition of different groups of discharges are summarized in table 23, while the approach is described in detail in annex B of the UNSCEAR 2016 Report [U24]. It should be noted that these assumptions are intended only for use in estimating doses from discharges from operating NPPs for the purpose of this annex.

Table 23. Composition of radionuclide groups reported in discharges

Radionuclide groups	*Radionuclides*
ATMOSPHERIC DISCHARGES	
Noble gases	^{41}Ar, ^{85}Kr, ^{133}Xe, ^{135}Xe, ^{138}Xe, 'Noble gases'
Tritium	^{3}H
^{131}I	^{131}I
^{14}C	^{14}C
Particulates	^{54}Mn, ^{58}Co, ^{60}Co, ^{65}Zn, ^{90}Sr, ^{106}Ru, ^{129}I, ^{134}Cs, ^{137}Cs, ^{210}Pb, ^{210}Po, ^{226}Ra, ^{230}Th, ^{232}Th, ^{234}U, ^{238}U, ^{239}Pu, ^{240}Pu, ^{241}Am, 'Gross alpha', 'Gross beta' and 'Other'
AQUATIC DISCHARGES	
Tritium (liquid)	^{3}H
Other	^{14}C, ^{35}S, ^{54}Mn, ^{58}Co, ^{60}Co, ^{65}Zn, ^{90}Sr, ^{99}Tc, ^{106}Ru, ^{129}I, ^{131}I, ^{134}Cs, ^{137}Cs, ^{210}Pb, ^{210}Po, ^{226}Ra, ^{230}Th, ^{232}Th, ^{234}U, ^{238}U, ^{239}Pu, ^{240}Pu, ^{241}Am, 'Gross alpha', 'Gross beta', 'Particulates' and 'Other'

328. Normalized annual discharges per unit energy generated from NPPs in different UNEP regions for the representative years of 2009 and 2016 are presented in table 24. Tritium and noble gases provide the highest contributions. Discharges of noble gases are higher for LWGRs than for other reactor types. Normalized discharges of ^{3}H in both atmospheric and liquid effluents are higher for HWRs than for other reactor types.

Table 24. Normalized discharges from NPPs in the representative years of 2009 and 2016 by reactor type

Radionuclide	*Year*	*Normalized discharges per unit electricity generated (TBq/(GW a))*						
		PWR	*BWR*	*HWR*	*LWGR*	*AGR*	*GCR*	*FBR*
DISCHARGES TO ATMOSPHERE								
Noble gases	2009	3.6×10^{0}	1.1×10^{1}	6.4×10^{1}	1.1×10^{2}	1.5×10^{1}	5.3×10^{1}	1.0×10^{1}
	2016	2.2×10^{0}	6.6×10^{0}	3.6×10^{1}	1.6×10^{2}	1.0×10^{1}		1.2×10^{1}
^{3}H	2009	1.8×10^{0}	1.2×10^{0}	2.9×10^{2}	2.6×10^{1}	3.6×10^{0}	5.6×10^{0}	4.9×10^{1}
	2016	2.0×10^{0}	1.9×10^{0}	2.3×10^{2}	2.6×10^{1}	1.5×10^{0}		4.9×10^{1}
^{131}I	2009	4.7×10^{-5}	1.0×10^{-4}	3.1×10^{-5}	2.4×10^{-4}	9.6×10^{-5}		2.0×10^{-4}
	2016	2.2×10^{-5}	9.0×10^{-5}	6.0×10^{-4}	2.2×10^{-4}	5.1×10^{-5}		1.8×10^{-3}
^{14}C	2009	1.9×10^{-1}	4.3×10^{-1}	6.2×10^{-1}	1.3×10^{0}	1.5×10^{0}	3.2×10^{0}	1.2×10^{-1}
	2016	2.6×10^{-1}	5.2×10^{-1}	6.0×10^{-1}	1.3×10^{0}	1.6×10^{0}		1.2×10^{-1}
Particulates[a]	2009	2.1×10^{-5}	4.3×10^{-5}	2.1×10^{-5}	1.0×10^{-4}	3.0×10^{-5}		1.8×10^{-5}
	2016	9.1×10^{-6}	6.7×10^{-3}	3.0×10^{-4}	7.4×10^{-5}	2.1×10^{-5}		8.0×10^{-6}
^{35}S	2009					6.3×10^{-2}	2.9×10^{-1}	
	2016					5.7×10^{-2}		
AQUATIC DISCHARGES								
^{3}H	2009	2.0×10^{1}	1.0×10^{0}	2.4×10^{2}	2.7×10^{-1}	3.3×10^{2}	2.3×10^{0}	2.1×10^{0}
	2016	1.9×10^{1}	1.1×10^{0}	2.5×10^{2}	3.0×10^{-2}	3.0×10^{2}		5.5×10^{-1}
Other[a]	2009	5.8×10^{-3}	4.4×10^{-4}	3.0×10^{-2}	9.1×10^{-5}	3.3×10^{-1}	3.4×10^{-1}	1.7×10^{-4}
	2016	6.2×10^{-3}	1.1×10^{-3}	2.0×10^{-2}	2.1×10^{-5}	7.1×10^{-1}		1.7×10^{-4}

[a] Refer to table 23.

(b) *Dose estimates*

329. Doses to the characteristic individual from all discharges, normalized to electricity generation, were estimated to be in the range 0.1–0.8 μSv/(GW a). These data are presented in table 25 by discharge mode and region. Typical individual doses associated with electricity generation in 2009 estimated for NPPs in Europe, which was the only region to include all types of reactors, ranged between around 0.003 and 6 μSv across reactor type and location (see electronic attachment A-3).

330. Collective doses to the local and regional populations for atmospheric and liquid discharges, to coastal and inland sites for an integration period of 100 years, are presented in table 26 as a function of region for the representative years of 2009 and 2016. The total worldwide collective doses from a single year's discharges to the local and regional populations for all reactor types are of the order of 120 person–Sv for both representative years.

Table 25. Annual doses to the characteristic individual, normalized to electricity generation due to discharges from NPPs in the representative years of 2009 and 2016

Region	*Year*	*Normalized annual dose to characteristic individual (mSv/(GW a))*		
		Atmospheric discharges	*Liquid discharges*	*All discharges*
Africa	2009	2.8×10^{-5}	7.5×10^{-5}	1.0×10^{-4}
	2016	3.7×10^{-5}	8.0×10^{-5}	1.2×10^{-4}
Asia and the Pacific	2009	9.7×10^{-5}	7.5×10^{-5}	1.7×10^{-4}
	2016	1.0×10^{-4}	1.1×10^{-4}	2.1×10^{-4}
Europe	2009	7.6×10^{-5}	2.6×10^{-4}	3.4×10^{-4}
	2016	8.6×10^{-5}	6.7×10^{-4}	7.6×10^{-4}
Latin America and the Caribbean	2009	2.1×10^{-4}	9.7×10^{-5}	3.1×10^{-4}
	2016	1.8×10^{-4}	1.1×10^{-4}	2.9×10^{-4}
North America	2009	1.1×10^{-4}	5.3×10^{-5}	1.6×10^{-4}
	2016	1.3×10^{-4}	5.5×10^{-5}	1.8×10^{-4}

Table 26. Collective doses due to a single year's discharges from NPPs for the representative years 2009 and 2016

Region	*Year*	*Collective dose for NPPs (person–Sv)* [a]						
		Atmospheric discharges				*Liquid discharges*		*All discharges*
		Local population		*Regional population*				
		Inland	*Coastal*	*Inland*	*Coastal*	*Inland*	*Coastal*	
Africa	2009	0	2.7×10^{-2}	0	3.8×10^{-3}	0	2.1×10^{-4}	3.1×10^{-2}
	2016	0	4.7×10^{-2}	0	6.6×10^{-3}	0	2.9×10^{-4}	5.4×10^{-2}
Asia and the Pacific	2009	1.0×10^{0}	8.3×10^{0}	3.2×10^{0}	1.8×10^{1}	1.1×10^{0}	3.8×10^{-2}	3.2×10^{1}
	2016	2.2×10^{0}	6.0×10^{0}	6.7×10^{0}	1.3×10^{1}	2.9×10^{0}	4.0×10^{-2}	3.1×10^{1}
Europe	2009	3.6×10^{0}	2.6×10^{0}	1.3×10^{1}	6.7×10^{0}	1.6×10^{1}	5.8×10^{-2}	4.2×10^{1}
	2016	3.7×10^{0}	3.1×10^{0}	1.3×10^{1}	7.8×10^{0}	1.5×10^{1}	1.5×10^{-1}	4.3×10^{1}
Latin America and the Caribbean	2009	3.5×10^{-1}	4.5×10^{-2}	2.7×10^{-1}	9.3×10^{-2}	1.3×10^{0}	5.5×10^{-4}	2.0×10^{0}
	2016	2.9×10^{-1}	7.6×10^{-2}	2.3×10^{-1}	1.6×10^{-1}	1.3×10^{0}	8.2×10^{-4}	2.1×10^{0}
North America	2009	5.1×10^{0}	2.3×10^{-1}	1.2×10^{1}	3.5×10^{-1}	2.4×10^{1}	2.9×10^{-3}	4.2×10^{1}
	2016	5.8×10^{0}	4.6×10^{-1}	1.3×10^{1}	7.8×10^{-1}	2.5×10^{1}	3.0×10^{-3}	4.5×10^{1}
Worldwide	2009	1.0×10^{1}	1.1×10^{1}	3.3×10^{1}	2.2×10^{1}	4.2×10^{1}	3.6×10^{-1}	1.2×10^{2}
	2016	1.1×10^{1}	1.0×10^{1}	3.5×10^{1}	2.1×10^{1}	4.4×10^{1}	8.6×10^{-1}	1.2×10^{2}

[a] Excluding the contribution from globally circulating radionuclides.

331. Figure XVII shows that HWRs in North America and Asia and the Pacific regions, provide the greatest contribution to the worldwide collective dose. Pressurized water reactors are the second highest contributors to the collective doses, primarily in Europe, North America and, to a lesser extent, in Asia and the Pacific regions.

Figure XVII. Collective doses integrated to 100 years, due to discharges from NPPs by UNEP region and reactor type, excluding globally circulating radionuclides

(a) 2009

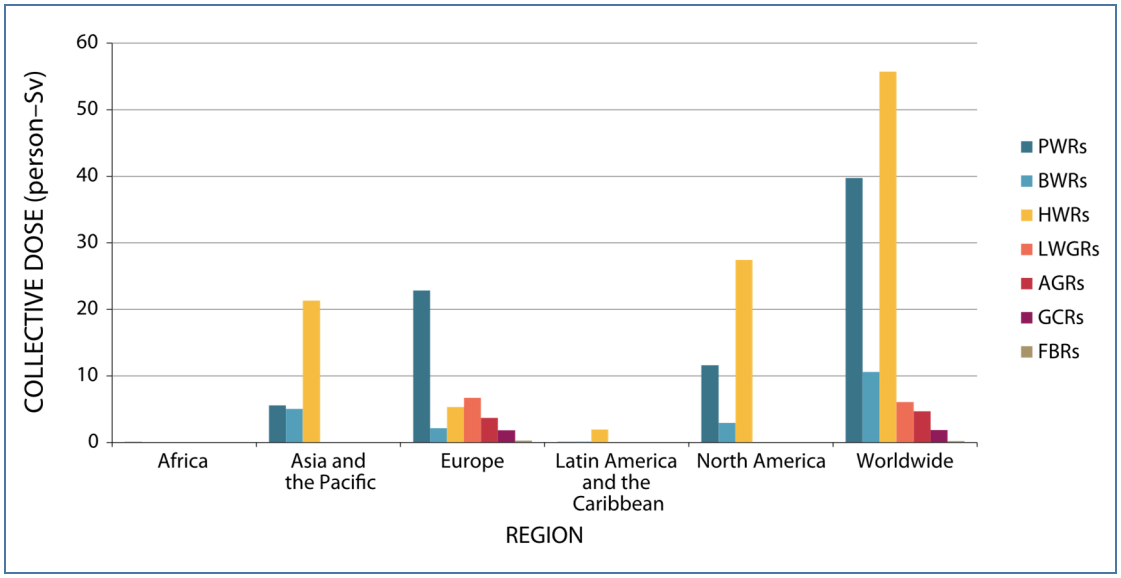

(b) 2016

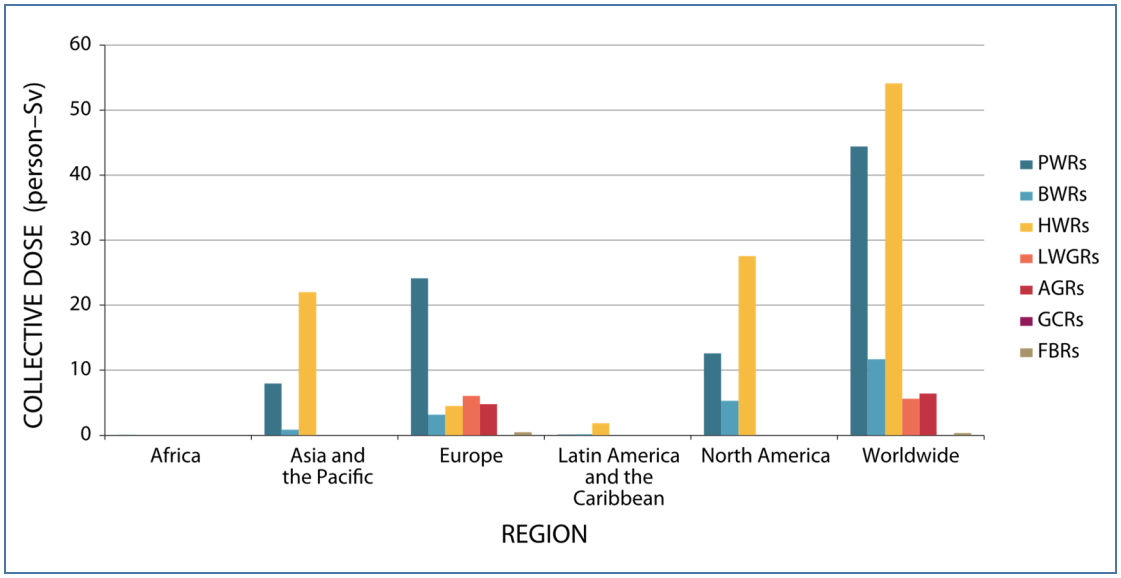

332. Collective doses integrated to 100 years due to a single year's discharges from NPPs normalized to electricity generation for the representative years of 2009 and 2016 are presented in table 27. The worldwide annual collective doses for the representative years 2009 and 2016 were estimated at 0.41 and 0.44 person–Sv/(GW a), respectively. These values are higher than that given in the UNSCEAR 2016 Report, annex B, mainly due to increases in the discharges and to a lesser extent to the use of revised age-related dose coefficients, but are consistent with the normalized collective doses evaluated for the period 1985–1997 [U19].

Table 27. Collective doses integrated to 100 years due to a single year's discharges from NPPs normalized to electricity generation for the representative years of 2009 and 2016

Region	*Year*	*Collective dose per unit electricity generated for NPPs (person–Sv/GW a)* [a]						
		Atmospheric discharges				*Liquid discharges*		*All discharges*
		Local		*Regional*				
		Inland	*Coastal*	*Inland*	*Coastal*	*Inland*	*Coastal*	
Africa	*2009*	0	2.0×10^{-2}	0	2.9×10^{-3}	0	1.6×10^{-4}	2.3×10^{-2}
	2016	0	2.7×10^{-2}	0	3.8×10^{-3}	0	1.7×10^{-4}	3.1×10^{-2}
Asia and the Pacific	*2009*	1.1×10^{0}	1.4×10^{-1}	3.3×10^{0}	3.1×10^{-1}	1.2×10^{0}	6.5×10^{-4}	5.3×10^{-1}
	2016	9.3×10^{-1}	1.3×10^{-1}	2.8×10^{0}	2.8×10^{-1}	1.2×10^{0}	8.9×10^{-4}	6.5×10^{-1}
Europe	*2009*	4.0×10^{-2}	7.2×10^{-2}	1.5×10^{-1}	1.8×10^{-1}	1.8×10^{-1}	1.6×10^{-3}	3.4×10^{-1}
	2016	4.4×10^{-2}	8.2×10^{-2}	1.6×10^{-1}	2.1×10^{-1}	1.8×10^{-1}	3.9×10^{-3}	3.6×10^{-1}
Latin America and the Caribbean	*2009*	4.1×10^{-1}	1.8×10^{-2}	3.1×10^{-1}	3.7×10^{-2}	1.5×10^{0}	2.1×10^{-4}	6.0×10^{-1}
	2016	3.4×10^{-1}	2.6×10^{-2}	2.6×10^{-1}	5.4×10^{-2}	1.5×10^{0}	2.8×10^{-4}	5.5×10^{-1}
North America	*2009*	5.9×10^{-2}	1.6×10^{-2}	1.4×10^{-1}	2.5×10^{-2}	2.8×10^{-1}	2.1×10^{-4}	4.2×10^{-1}
	2016	6.5×10^{-2}	3.3×10^{-2}	1.5×10^{-1}	5.7×10^{-2}	2.8×10^{-1}	2.2×10^{-4}	4.4×10^{-1}
Worldwide	*2009*	5.8×10^{-2}	9.2×10^{-2}	1.8×10^{-1}	2.0×10^{-1}	2.4×10^{-1}	3.1×10^{-3}	4.1×10^{-1}
	2016	6.5×10^{-2}	1.0×10^{-1}	2.0×10^{-1}	2.1×10^{-1}	2.5×10^{-1}	8.5×10^{-3}	4.4×10^{-1}

[a] Excluding the contribution from globally circulating radionuclides.

333. Figure XVIII shows the collective doses integrated to 100 years from a single year's discharges per unit of electricity generation, to the population of different regions of the world for different reactor types for the representative years of 2009 and 2016, excluding the contribution from globally circulating radionuclides. Discharges from HWRs provide the highest contribution to the collective dose per unit electricity generation, followed by GCRs in 2009, and by AGRs in 2016.

334. Table 28 presents the collective doses the world population integrated to 100 years due to a single year's discharges from NPPs normalized to electricity generation for the representative years 2009 and 2016 by radionuclide and reactor type, excluding the contribution from globally circulating radionuclides. The table shows that the most significant contribution to the collective doses comes from discharges of ^{3}H from HWRs, and ^{14}C from GCRs in 2009.

Figure XVIII. Collective doses integrated to 100 years due to a single year's discharges from NPPs normalized to electricity generation for the representative years of 2009 and 2016 by UNEP region and reactor type

(a) 2009

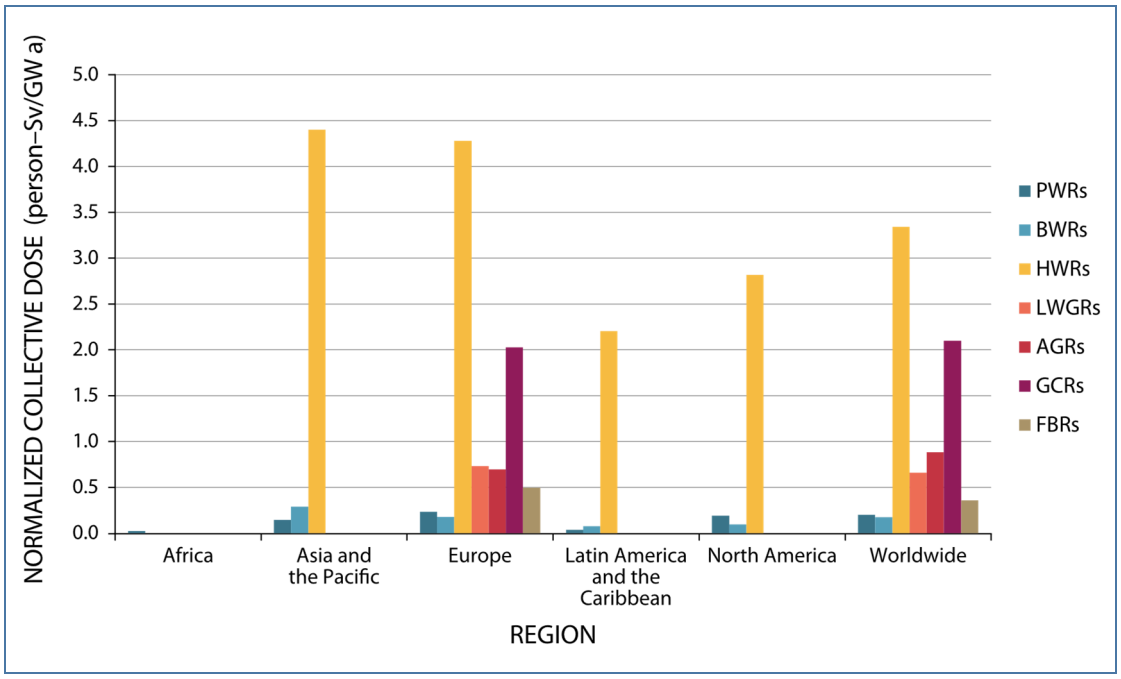

(b) 2016

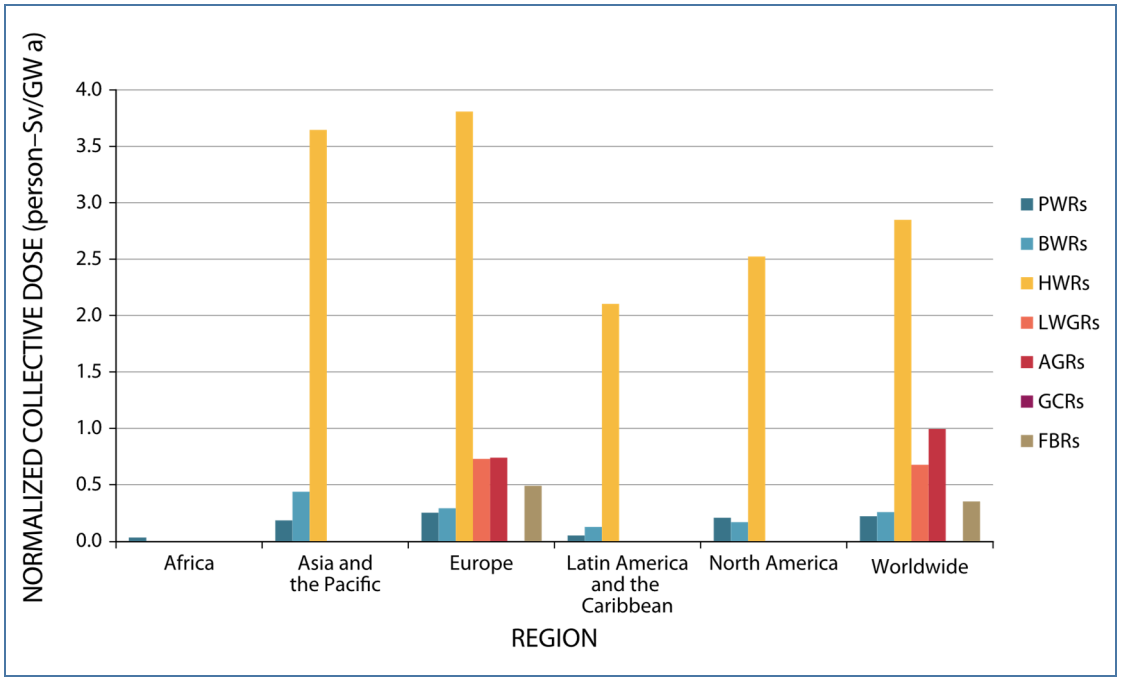

Table 28. Collective doses to the world population integrated to 100 years due to a single year's discharges from NPPs normalized to electricity generation for the representative years 2009 and 2016 by radionuclide (excluding contribution from globally circulating radionuclides)

Radionuclide	*Collective dose to the world population for NPPs per unit electricity generated (person–Sv/(GW a))*													
	PWR		*BWR*		*HWR*		*LWGR*		*AGR*		*GCR*		*FBR*	
	2009	2016	2009	2016	2009	2016	2009	2016	2009	2016	2009	2016	2009	2016
^{3}H	8.9×10^{-2}	8.5×10^{-2}	1.2×10^{-2}	1.4×10^{-2}	3.1×10^{0}	3.0×10^{0}	1.9×10^{-1}	1.7×10^{-1}	3.2×10^{-2}	1.6×10^{-2}	5.0×10^{-2}	-	3.2×10^{-1}	6.1×10^{-1}
^{14}C	1.1×10^{-1}	1.4×10^{-1}	1.6×10^{-1}	1.4×10^{-1}	2.2×10^{-1}	2.2×10^{-1}	4.7×10^{-1}	4.3×10^{-1}	6.8×10^{-1}	9.3×10^{-1}	1.4×10^{0}	-	3.8×10^{-2}	7.4×10^{-2}
^{35}S	0	0	0	0	0	0	0	0	1.1×10^{-1}	1.2×10^{-1}	4.5×10^{-1}	-	0	0
^{41}Ar	3.7×10^{-5}	2.3×10^{-5}	4.0×10^{-5}	1.6×10^{-5}	3.0×10^{-3}	1.8×10^{-3}	1.0×10^{-3}	1.4×10^{-3}	1.1×10^{-3}	9.0×10^{-4}	3.3×10^{-3}	-	0	0
^{54}Mn	4.7×10^{-5}	4.6×10^{-5}	1.8×10^{-5}	1.2×10^{-3}	0	0	8.8×10^{-6}	5.8×10^{-6}	0	0	0	-	1.4×10^{-6}	2.6×10^{-6}
^{58}Co	6.9×10^{-5}	7.4×10^{-5}	6.0×10^{-6}	1.0×10^{-4}	0	0	3.9×10^{-7}	2.6×10^{-7}	0	0	0	-	1.3×10^{-6}	2.4×10^{-6}
^{60}Co	3.4×10^{-4}	3.1×10^{-4}	3.2×10^{-4}	3.1×10^{-2}	3.7×10^{-4}	5.5×10^{-3}	6.8×10^{-4}	4.5×10^{-4}	5.7×10^{-2}	1.5×10^{-1}	1.4×10^{-3}	-	2.8×10^{-4}	2.6×10^{-4}
^{65}Zn	0	0	5.4×10^{-5}	1.6×10^{-3}	0	0	1.0×10^{-5}	7.0×10^{-6}	2.0×10^{-4}	1.7×10^{-4}	0	-	0	0
^{85}Kr	4.0×10^{-6}	2.4×10^{-6}	2.6×10^{-5}	1.1×10^{-5}	0	0	0	0	0	0	0	-	9.6×10^{-5}	2.2×10^{-4}
^{90}Sr	7.5×10^{-5}	3.2×10^{-5}	6.7×10^{-5}	5.5×10^{-3}	0	0	8.2×10^{-4}	5.2×10^{-4}	2.0×10^{-5}	5.3×10^{-5}	9.3×10^{-2}	-	0	0
^{106}Ru	5.7×10^{-5}	5.9×10^{-5}	5.4×10^{-8}	5.8×10^{-6}	0	0	0	0	0	0	0	-	0	0
^{129}I	0	0	0	0	0	0	0	0	0	0	0	-	0	0
^{131}I	8.2×10^{-5}	3.8×10^{-5}	1.8×10^{-4}	1.1×10^{-4}	5.1×10^{-5}	1.0×10^{-3}	4.1×10^{-4}	3.4×10^{-4}	2.1×10^{-4}	1.4×10^{-4}	0	-	2.9×10^{-4}	5.3×10^{-3}
^{133}Xe	9.2×10^{-5}	5.5×10^{-5}	1.2×10^{-4}	4.9×10^{-5}	0	0	3.2×10^{-3}	4.4×10^{-3}	0	0	0	-	0	0
^{135}Xe	2.8×10^{-5}	1.7×10^{-5}	2.9×10^{-4}	1.2×10^{-4}	0	0	7.4×10^{-4}	1.0×10^{-3}	0	0	0	-	0	0
^{138}Xe	1.8×10^{-9}	1.1×10^{-9}	3.8×10^{-7}	1.5×10^{-7}	0	0	4.7×10^{-7}	6.5×10^{-7}	0	0	0	-	0	0
^{134}Cs	4.8×10^{-4}	5.0×10^{-4}	3.2×10^{-5}	4.9×10^{-4}	0	0	1.6×10^{-5}	7.1×10^{-6}	2.7×10^{-4}	7.3×10^{-4}	7.6×10^{-3}	-	8.0×10^{-5}	1.5×10^{-4}
^{137}Cs	6.3×10^{-4}	6.5×10^{-4}	6.5×10^{-5}	2.8×10^{-3}	4.4×10^{-2}	3.3×10^{-2}	3.1×10^{-4}	1.7×10^{-4}	2.5×10^{-4}	6.6×10^{-4}	1.2×10^{-1}	-	5.7×10^{-5}	1.1×10^{-4}
Total	$\mathbf{2.0 \times 10^{-1}}$	$\mathbf{2.2 \times 10^{-1}}$	$\mathbf{1.7 \times 10^{-1}}$	$\mathbf{1.9 \times 10^{-1}}$	$\mathbf{3.3 \times 10^{0}}$	$\mathbf{3.2 \times 10^{0}}$	$\mathbf{6.6 \times 10^{-1}}$	$\mathbf{6.2 \times 10^{-1}}$	$\mathbf{8.8 \times 10^{-1}}$	$\mathbf{1.2 \times 10^{0}}$	$\mathbf{2.1 \times 10^{0}}$	**-**	$\mathbf{3.6 \times 10^{-1}}$	$\mathbf{6.9 \times 10^{-1}}$

5. Spent nuclear fuel reprocessing

335. Reprocessing of spent nuclear fuel has been carried out in a number of countries to separate out and recover reusable uranium and plutonium from spent nuclear fuel from nuclear reactors which is currently mostly retained on site in interim storage. As of December 2016, there were operational commercial scale reprocessing facilities at La Hague (France), Mayak Production Association (Russian Federation), and Sellafield (United Kingdom). The THORP and Magnox Reprocessing facilities at Sellafield ceased operation in 2018 and 2021, respectively. Decommissioning of the UP1 reprocessing facility at Marcoule (France), which was shut down in September 1997, and of La Hague's first reprocessing facility, UP2-400, which was shut down in January 2004, is still ongoing. The Rokkasho-Mura facility (Japan) is in the commissioning phase due to be completed in early 2027, while the RT-2 Zheleznogorsk (Russian Federation) is under development [I42]. According to the IAEA, between the start of nuclear power electricity production in 1954 and the end of 2016, a total of about 390,000 tonnes of heavy metal (t HM) of spent nuclear fuel was generated from all nuclear power plants worldwide. About one third of all spent nuclear fuel generated in nuclear power plants (127,000 t HM) has been reprocessed [I34].

(a) *Effluents*

336. Annual discharges from reprocessing facilities of spent nuclear fuel were provided through the UNSCEAR Global Survey on Public Exposure and supplemented by information from other sources. The full dataset of the discharges for each facility and each year in the period 2007–2020 is provided in electronic attachment A-3. Annual discharges for the representative years of 2009 and 2016 are presented in table 29.

Table 29. Annual discharges from spent nuclear fuel reprocessing facilities for the representative years 2009 and 2016

GKhK–Mining and Chemical Combine; JAEA–Japan Atomic Energy Agency; JNFL–Japan Nuclear Fuel Limited

(a) 2009

Radionuclide	Annual discharges *from spent nuclear fuel reprocessing facilities (Bq/s)*													
	Atmospheric							*Liquid*						
	JAEA-Tokai	*JNFL*	*Sellafield*	*La Hague*	*Marcoule*	*Mayak*	*GKhK*	*JAEA-Tokai*	*JNFL*	*Sellafield*	*La Hague*	*Marcoule*	*Mayak*	*GKhK*
^{3}H	7.0×10^{2}	3.4×10^{2}	1.9×10^{5}	4.7×10^{4}				1.0×10^{3}	4.1×10^{3}	1.5×10^{6}	9.1×10^{6}		1.7×10^{4}	
^{14}C			3.8×10^{2}	1.5×10^{4}						8.2×10^{3}	6.1×10^{3}			
^{54}Mn							1.1×10^{2}				1.8×10^{0}			2.2×10^{0}
^{58}Co							1.4×10^{-1}				6.9×10^{-2}			5.5×10^{0}
^{60}Co						8.9×10^{-3}	9.1×10^{-2}			8.3×10^{1}	8.9×10^{1}			3.2×10^{1}
^{65}Zn						8.9×10^{-3}	3.4×10^{-3}							1.8×10^{1}
^{85}Kr	7.2×10^{0}		4.2×10^{7}	2.0×10^{8}		5.4×10^{4}	1.6×10^{6}							
^{90}Sr			3.9×10^{-2}							2.9×10^{3}			8.5×10^{2}	
^{106}Ru			9.7×10^{-1}							3.2×10^{3}				
^{129}I	8.4×10^{-3}	1.8×10^{-3}	7.6×10^{0}	4.5×10^{0}				6.5×10^{-3}	1.2×10^{-2}	2.5×10^{2}	1.1×10^{3}			
^{131}I			6.9×10^{-1}	1.6×10^{-1}							1.1×10^{1}			
^{134}Cs						1.5×10^{-2}	1.1×10^{-2}			1.4×10^{2}	6.9×10^{1}			4.9×10^{-1}
^{137}Cs			1.3×10^{1}			1.4×10^{0}	2.8×10^{-1}			2.6×10^{4}	1.0×10^{3}		4.0×10^{1}	7.9×10^{0}
^{239}Pu			1.3×10^{-1}			5.4×10^{-1}		2.0×10^{-5}		2.7×10^{2}				
^{241}Am			1.9×10^{-2}							4.6×10^{1}				

(b) 2016 [a]

Radionuclide	Annual discharges from spent nuclear fuel reprocessing facilities in 2016 (GBq/a)													
	Atmosphere							Aquatic						
	JAEA-Tokai	JNFL	Sellafield	La Hague	Marcoule	Mayak	GKhK	JAEA-tokai	JNFL	Sellafield	La Hague	Marcoule	Mayak	GKhK
^{3}H	2.3×10^{2}	1.2×10^{2}	1.2×10^{5}	7.5×10^{4}	1.8×10^{1}	1.0×10^{1}		1.9×10^{2}	4.9×10^{1}	2.1×10^{6}	1.2×10^{7}	3.8×10^{4}		
^{14}C	7.1×10^{0}		4.4×10^{2}	1.9×10^{4}						4.8×10^{3}	7.6×10^{3}	4.6×10^{0}		
^{54}Mn											2.4×10^{0}			
^{58}Co											5.0×10^{-1}			
^{60}Co						4.6×10^{-3}	2.4×10^{-2}			3.5×10^{1}	5.8×10^{1}			4.1×10^{-1}
^{85}Kr	2.4×10^{-1}		8.8×10^{7}	3.2×10^{8}		4.1×10^{7}								
^{90}Sr			3.0×10^{-2}				1.4×10^{-1}			2.0×10^{3}			3.0×10^{2}	5.9×10^{0}
^{106}Ru			7.0×10^{-1}				2.2×10^{-3}			1.1×10^{3}				
^{129}I			1.3×10^{1}	5.9×10^{0}				3.7×10^{-3}	8.2×10^{-3}	5.2×10^{2}	1.4×10^{3}			
^{131}I			4.2×10^{-1}	3.7×10^{-1}		2.6×10^{-1}					1.5×10^{1}			
^{134}Cs						3.2×10^{-1}				6.6×10^{1}	5.0×10^{1}			
^{137}Cs			1.2×10^{1}			3.7×10^{0}	1.8×10^{-2}			2.0×10^{4}	6.6×10^{2}			4.4×10^{0}
^{222}Rn			4.3×10^{1}											
^{234}U										7.9×10^{4}				
^{239}Pu			1.3×10^{-1}			1.0×10^{0}	2.8×10^{-2}			4.3×10^{2}		1.7×10^{0}		1.2×10^{-1}
^{241}Am			1.4×10^{-2}							2.6×10^{1}				

[a] By 2016, JAEA-Tokai and GKhK had shut down, while JNFL was in the process of active testing. Discharges from these sites are therefore unlikely to be direct result of reprocessing operations.

(b) *Dose estimates*

337. Annual doses to the characteristic individual were calculated for each of the nuclear fuel reprocessing facilities for which discharge information was available: La Hague and Marcoule in France, JAEA-Tokai and JNFL facilities in Japan, Ozersk (Mayak) and GKhK in the Russian Federation, and Sellafield in the United Kingdom. Doses for the representative years of 2009 and 2016 range from nanosieverts for JNFL, to 40 and 60 μSv at La Hague and Sellafield, respectively (see table 30), mostly from liquid discharges. The worldwide collective dose integrated to 100 years due to a single year's discharges was estimated to be around 20 person–Sv (see table 31), with the main contribution coming from European facilities which are responsible for the largest production of reprocessed uranium and mixed oxide nuclear fuel [I56].

338. Table 32 summarizes the contribution of different exposure pathways and radionuclides to the collective doses integrated to 100 years due to a single year's discharges from spent nuclear fuel reprocessing facilities. This table shows that the predominant contribution to the collective doses is due to discharges to atmosphere (around 70% in 2009 and over 80% in 2016). Carbon-14 provided the greatest radionuclide contribution to collective dose in both years. Other notable contributing radionuclides are ^{85}Kr, ^{90}Sr and ^{3}H.

339. In the UNSCEAR 2000 Report, annex A [U15], discharges and collective doses from spent nuclear fuel reprocessing facilities were normalized to electricity generation. However, in the UNSCEAR 2008 Report, annex B [U19], information on the amount of nuclear fuel reprocessed was not available and therefore normalized values were not provided. For the UNSCEAR 2016 Report, annex B [U24], it was only possible to derive normalized values for La Hague, although it was acknowledged that discharges from that and other installations (e.g., Sellafield) would include contributions from operations other than reprocessing, such as decommissioning. Although facilities in France continue to operate, no assemblies containing reprocessed nuclear fuel have been used in the country since 2013 [I56]. Furthermore, NPPs in Japan have not used reprocessed nuclear fuel in recent years [I56]. Consequently, reprocessing cannot be directly linked with energy generation for the period under consideration and the Committee did not consider it appropriate to estimate collective doses normalized to electricity generation for the representative years of 2009 and 2016 for this annex.

Table 30. Annual doses to the characteristic individual due to discharges from spent nuclear fuel reprocessing plants in the representative years 2009 and 2016

Facility	*Year*	*Annual dose to the characteristic individual (mSv)*		
		Atmospheric discharges	*Liquid discharges*	*All discharges*
JAEA-Tokai	2009	1.5×10^{-6}	9.8×10^{-9}	1.5×10^{-6}
	2016	1.4×10^{-6}	2.2×10^{-9}	1.4×10^{-6}
JNFL	2009	6.9×10^{-7}	2.7×10^{-8}	7.1×10^{-7}
	2016	2.3×10^{-7}	2.8×10^{-9}	2.3×10^{-7}
Sellafield	2009	1.1×10^{-3}	5.8×10^{-2}	5.9×10^{-2}
	2016	1.3×10^{-3}	5.7×10^{-2}	5.9×10^{-2}
La Hague	2009	3.5×10^{-3}	2.6×10^{-2}	2.9×10^{-2}
	2016	4.9×10^{-3}	3.0×10^{-2}	3.5×10^{-2}
Marcoule	2009			
	2016	3.7×10^{-8}	6.5×10^{-5}	6.5×10^{-5}
Mayak	2009	3.6×10^{-4}	1.1×10^{-3}	1.4×10^{-3}
	2016	9.1×10^{-4}	3.6×10^{-4}	1.3×10^{-3}
GKhK	2009	7.8×10^{-5}	1.5×10^{-5}	9.3×10^{-5}
	2016	2.1×10^{-5}	9.1×10^{-6}	3.0×10^{-5}

Table 31. Collective doses integrated to 100 years due to single year's discharges from spent nuclear fuel reprocessing facilities for the representative years 2009 and 2016

Region	*Year*	*Collective dose for spent nuclear fuel reprocessing facilities (person–Sv)*				
		Atmospheric discharges			*Liquid discharges*	*All discharges*
		Local	*Regional*	*Total*		
Asia and the Pacific	2009	3.8×10^{-3}	9.9×10^{-3}	1.4×10^{-2}	8.2×10^{-7}	1.4×10^{-2}
	2016	2.9×10^{-3}	6.0×10^{-3}	8.8×10^{-3}	1.1×10^{-7}	8.8×10^{-3}
Europe	2009	2.8×10^{0}	8.2×10^{0}	1.1×10^{1}	4.7×10^{0}	1.6×10^{1}
	2016	3.9×10^{0}	1.1×10^{1}	1.5×10^{1}	2.3×10^{0}	1.8×10^{1}
Worldwide	2009	4.3×10^{0}	9.3×10^{0}	1.4×10^{1}	6.3×10^{0}	2.0×10^{1}
	2016	5.9×10^{0}	1.3×10^{1}	1.9×10^{1}	4.0×10^{0}	2.3×10^{1}

Table 32. Collective doses to the world population integrated to 100 years due to a single year's discharges from spent nuclear fuel reprocessing facilities for the representative years 2009 and 2016 by radionuclide (excluding contribution from globally circulating radionuclides)

Radionuclide	*Collective dose for spent nuclear fuel reprocessing facilities (person–Sv)*					
	Atmospheric discharges		*Liquid discharges*		*All discharges*	
	2009	*2016*	*2009*	*2016*	*2009*	*2016*
^{3}H	2.1×10^{0}	1.8×10^{0}	1.2×10^{-1}	2.7×10^{-1}	2.3×10^{0}	2.1×10^{0}
^{14}C	6.9×10^{0}	9.0×10^{0}	7.9×10^{-1}	7.9×10^{-1}	7.7×10^{0}	9.8×10^{0}
^{54}Mn	5.0×10^{-2}		3.0×10^{-4}	2.8×10^{-4}	5.1×10^{-2}	2.8×10^{-4}
^{58}Co	4.5×10^{-5}		4.0×10^{-4}	2.8×10^{-5}	4.4×10^{-4}	2.8×10^{-5}
^{60}Co	1.6×10^{-3}	4.5×10^{-4}	7.8×10^{-2}	3.5×10^{-2}	7.9×10^{-2}	3.6×10^{-2}
^{65}Zn	5.5×10^{-5}		7.1×10^{-3}		7.2×10^{-3}	
^{85}Kr	3.2×10^{0}	5.9×10^{0}			3.2×10^{0}	5.9×10^{0}
^{90}Sr	1.8×10^{-3}	5.9×10^{-3}	4.5×10^{0}	1.6×10^{0}	4.5×10^{0}	1.6×10^{0}
^{106}Ru	3.0×10^{-3}	2.2×10^{-3}	4.4×10^{-2}	1.5×10^{-2}	4.7×10^{-2}	1.7×10^{-2}
^{129}I	8.7×10^{-1}	1.3×10^{0}	5.4×10^{-3}	8.0×10^{-3}	8.7×10^{-1}	1.4×10^{0}
^{131}I	1.8×10^{-3}	2.1×10^{-3}	4.9×10^{-6}	6.6×10^{-6}	1.8×10^{-3}	2.1×10^{-3}
^{134}Cs	1.9×10^{-4}	2.4×10^{-3}	2.2×10^{-3}	4.6×10^{-4}	2.4×10^{-3}	2.8×10^{-3}
^{137}Cs	1.8×10^{-1}	1.8×10^{-1}	1.8×10^{-1}	7.3×10^{-2}	3.6×10^{-1}	2.5×10^{-1}
^{222}Rn		2.8×10^{-8}				2.8×10^{-8}
^{234}U				3.9×10^{-1}		3.9×10^{-1}
^{239}Pu	3.1×10^{-1}	5.1×10^{-1}	5.1×10^{-1}	8.2×10^{-1}	8.2×10^{-1}	1.3×10^{0}
^{241}Am	9.6×10^{-3}	7.1×10^{-3}	2.8×10^{-2}	1.6×10^{-2}	3.8×10^{-2}	2.3×10^{-2}
Total	$\mathbf{1.4 \times 10^{1}}$	$\mathbf{1.9 \times 10^{1}}$	$\mathbf{6.3 \times 10^{0}}$	$\mathbf{4.0 \times 10^{0}}$	$\mathbf{2.0 \times 10^{1}}$	$\mathbf{2.3 \times 10^{1}}$

6. Globally dispersed radionuclides

340. Long-lived radionuclides that are easily dispersed in the environment can give rise to doses to people across the world. The radionuclides of specific interest are ^{3}H, ^{14}C, ^{85}Kr and ^{129}I. Large uncertainties are associated with estimating doses over prolonged time periods due to the difficulty in predicting environmental pathways, population distributions, dietary habits, the effect of climate change and other factors. The uncertainties in dose calculations increase when the integration of the dose is carried out for very long periods of time—hundreds or thousands of years or even longer.

341. The methodology presented in the UNSCEAR 2016 Report, annex A [U24] was applied to the calculation of doses from these radionuclides. The collective doses to the world population from a single year's discharges from facilities in the nuclear fuel cycle integrated to 100, 500, and 10,000 years for 2009 and 2016 are presented in table 33. The predominant contribution to the collective doses from a single year's discharges integrated to 100 years are discharges from NPPs, which is of the order of 1,000 person-Sv. The corresponding values for the collective doses from a single year's discharges from nuclear fuel manufacturing and spent nuclear fuel reprocessing installations were estimated to be lower, at around 0.01 and 300 person-Sv, respectively.

Table 33. Collective and worldwide annual average individual doses to the public due to globally circulating radionuclides from fuel manufacturing, electricity generation from NPPs and spent nuclear fuel reprocessing in the representative years of 2009 and 2016

Integration time (years)	*Collective dose to the world population (person–Sv)*		*Worldwide annual average individual dose (Sv)* [a]	
	2009	*2016*	*2009*	*2016*
NUCLEAR FUEL MANUFACTURING				
100		1.4×10^{-2}		1.4×10^{-12}
500		2.9×10^{-2}		
10 000		1.5×10^{-1}		
NUCLEAR POWER PRODUCTION				
100	8.6×10^{2}	9.6×10^{2}	8.6×10^{-8}	9.6×10^{-8}
500	1.7×10^{3}	1.9×10^{3}		
10 000	8.3×10^{3}	9.2×10^{3}		
SPENT NUCLEAR FUEL REPROCESSING				
100	2.5×10^{2}	3.3×10^{2}	2.5×10^{-8}	3.3×10^{-8}
500	4.8×10^{2}	6.0×10^{2}		
10 000	2.5×10^{3}	2.8×10^{3}		

[a] Worldwide annual average individual doses are presented for the integration period of 100 years only.

342. Collective doses per unit energy generation from globally dispersed radionuclides were also estimated for NPPs and are presented in table 34. The annual collective dose integrated to 100 years was estimated to be of the order of 3 person–Sv/(GW a), while the worldwide annual average individual dose was estimated at 3×10^{-10} Sv/(GW a).

Table 34. Collective and worldwide annual average individual doses due to a single year's discharges of globally dispersed radionuclides per unit electricity generated from NPPs for the representative years 2009 and 2016

Integration time (years)	*Collective dose to the world population (person–Sv/(GW a))*		*Worldwide annual average individual dose* [a] *(Sv/(GW a))*	
	2009	*2016*	*2009*	*2016*
100	3.0×10^{0}	3.5×10^{0}	3.0×10^{-10}	3.5×10^{-10}
500	5.8×10^{0}	6.8×10^{0}		
10 000	2.8×10^{1}	3.3×10^{1}		

[a] Worldwide annual average individual doses are presented for the integration period of 100 years only.

343. Figure XIX illustrates the collective doses per unit of electricity generated due to the globally circulating radionuclides (^{3}H, ^{14}C and ^{85}Kr) integrated to 100, 500, and 10,000 years, for each type of NPP considered for the representative year of 2016. The figures illustrate the predominant contribution of ^{14}C to the doses, which increases with integration time. Doses from global circulation for ^{129}I are not included, since this radionuclide is only discharged from spent nuclear fuel reprocessing installations.

Figure XIX. Collective doses from globally circulating radionuclides per unit electricity generated from discharges in 2016

(a) Tritium

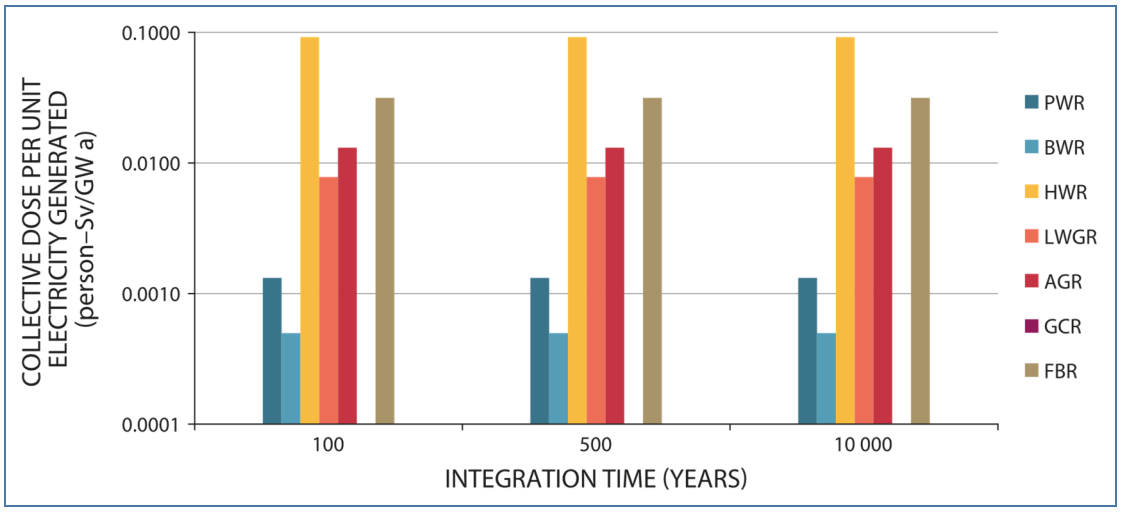

(b) Carbon-14

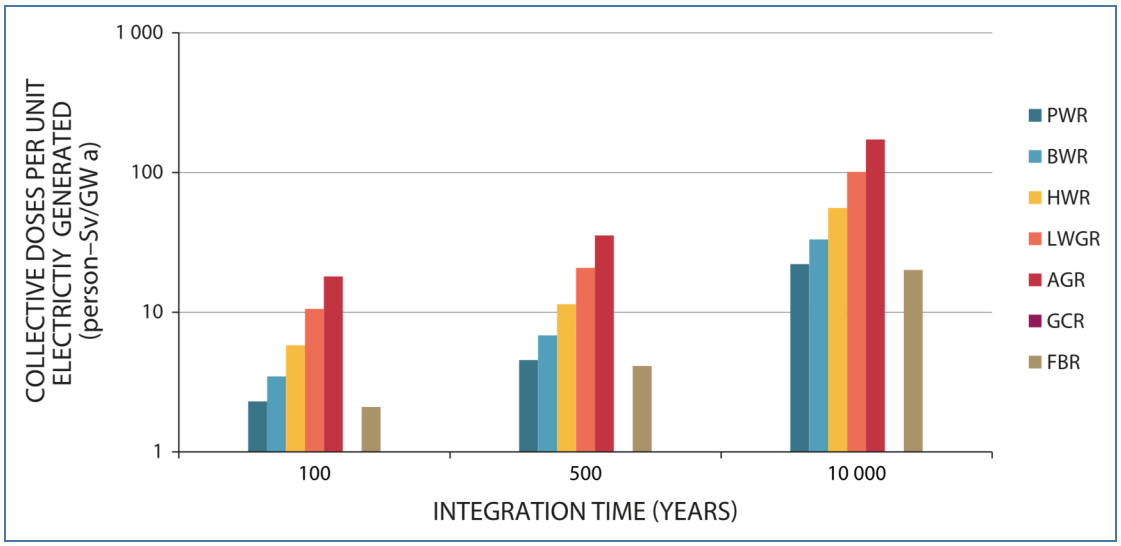

(c) Krypton-85

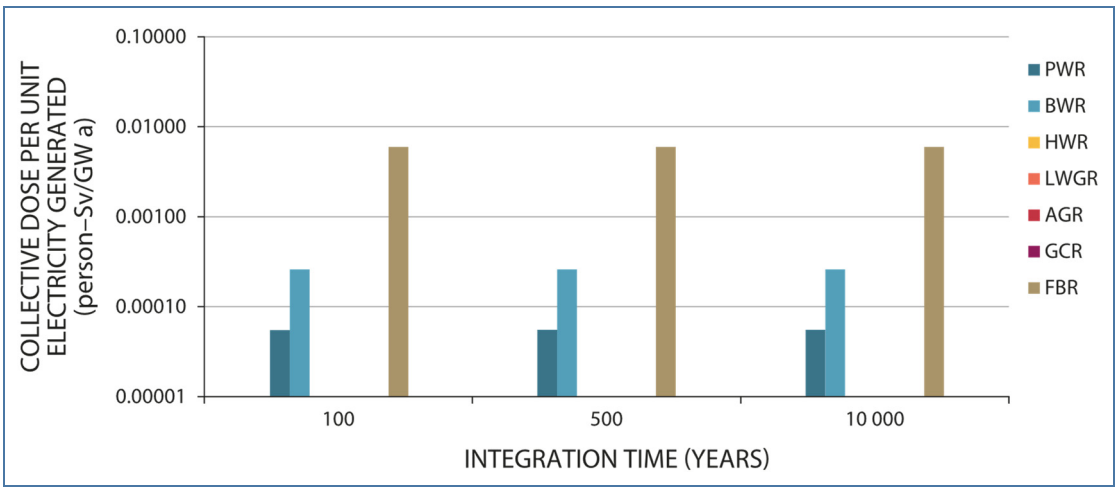

7. Annual doses to members of the public around nuclear facilities reported in monitoring programmes

344. Monitoring surveys of the environment around nuclear facilities are regularly performed by either the facility operators or the national organizations regulating the nuclear industry, to determine whether the operators are compliant with the terms of their authorizations. The data collected generally include measurements of dose rates and activity concentrations in various environmental media, which are combined with appropriate habit data to estimate doses received by people living in the vicinity of the nuclear facilities. The objective of these assessments is to ensure that doses to people living near nuclear facilities are below the criteria established in national regulations and the methodologies used differ substantially from those adopted in this annex. Dose assessments for regulatory purposes focus on people who are likely to receive the highest dose from a given facility, and therefore, are generally based on cautious assumptions. It should also be noted that monitoring data may include contributions from different nuclear facilities located on the same site and past discharges, as well as other sources, such as global fallout from nuclear weapons tests and major nuclear accidents. Therefore, a direct comparison between doses estimated in this annex and those evaluated through monitoring surveys of nuclear facilities cannot be made. Nevertheless, the latter provides a useful indication of the upper level of the doses received by members of the public in the vicinity of nuclear facilities. Some examples of doses estimated in Canada, China, France and the United Kingdom are provided in this section.

(a) *Canada*

345. In Canada results of environmental monitoring programmes around nuclear facilities are submitted annually to Canada's regulatory authority to verify compliance with applicable guidelines and limits. An element of the reports submitted is the calculation of doses to people living around the nuclear facilities who are likely to receive the highest dose. The methods to calculate these doses differ between NPPs and are based on a mixture of monitoring data and model predictions: annual doses have been estimated to be in the order of a few microsieverts [C44]. For example, the highest annual doses to the public living around the Bruce NPP were estimated to be around 2 μSv [C44]. The annual doses to people representative of the most highly exposed individuals residing around Point Lepreau NPP for the period 2018–2022 were estimated to be between 0.64 and 1.29 μSv for atmospheric discharges and between

0.03 and 0.08 μSv for liquid discharges, while the corresponding values for people representative of the most highly exposed individuals residing near the Darlington NPP (farmer) and Pickering NPP (urban resident) for the period 2019–2022 were estimated to be in the range 0.4–0.6 and 1.2–2.0 μSv, respectively. Finally, annual doses to people representative of the most highly exposed individuals living near the Gentilly NPP for the period 2016-2022 were estimated to be between 1 and 9 μSv.

(b) *China*

346. In China, measurements of radioactive effluents from NPPs and radioactivity in the surrounding environment are reported to the Ministry of Ecology and Environment monthly and annually. Strontium-90 and ^{137}Cs can be detected in some environmental samples around some NPPs, which are mainly due to the fallout from nuclear weapons tests and are not related to the normal operation of NPPs. In general, activity concentrations of radionuclides except for tritium and ^{14}C in various environmental media are far below the detection limits.

347. The annual dose received by people representative of the most highly exposed individuals and the collective dose to the public due to normal operation of NPPs and nuclear fuel cycle facilities between 2006 and 2013 were evaluated using the effluent release data and the site-specific environmental and habit data [P5]. Annual doses to people representative of the most highly exposed individuals around NPPs in China were estimated to be between 0.2 and 2.6 μSv, mainly due to ingestion of agriculture produce or marine produce and seashore activities. The most radiologically significant radionuclides vary across the NPPs, being ^{14}C for Qinshan NPP, ^{110m}Ag for Daya Bay NPP, and ^{59}Fe for Tianwan NPP, respectively. For nuclear fuel cycle facilities in China, the doses to people representative of the most highly exposed individuals were estimated to be between 0.6 nSv and 1.8 μSv, mainly due to internal exposure from ingestion of agriculture produce and inhalation.

(c) *France*

348. In France, measurements of radioactivity in the environment carried out by the Institut de Radioprotection et de Sûreté Nucléaire (IRSN)[9] close to nuclear facilities allow the assessment of doses to people living in the surrounding area for different radionuclides and various exposure pathways. Tritium and ^{14}C are measured in the atmospheric and terrestrial environment mainly within 5 km of PWR NPPs. Tritium, ^{14}C and gamma emitters (mainly ^{58}Co, ^{60}Co and ^{137}Cs) can be found in the river or marine environment, notably fish. Annual doses due to discharges were estimated to be below 1 μSv for people living close to NPPs. The main exposure pathways were ingestion of terrestrial foods and freshwater fish for ^{14}C, and ingestion of water for ^{3}H [I83].

349. In the environment around the reprocessing plant at La Hague, ^{85}Kr is regularly measured in the atmosphere. Tritium and ^{14}C are measured in both the terrestrial environment and in the marine environment, as are ^{129}I and gamma emitters. Annual doses estimated for different groups of people (fishermen and farmers) living in the vicinity of this facility were estimated to be below 10 μSv, mainly due to external exposure to ^{85}Kr and ingestion of terrestrial or marine foods containing ^{14}C [I83].

[9] The Institut de Radioprotection et de Sûreté Nucléaire (IRSN) was merged with the Autorité de Sûreté Nucléaire (ASN) to form the Autorité de Sûreté Nucléaire et de Radioprotection (ASNR) on 1 January 2025.

(d) *United Kingdom*

350. In the United Kingdom, an independent monitoring programme of radioactivity in food and the environment around nuclear sites is undertaken annually by different government agencies. This programme supplements surveys carried out by operators of nuclear sites and includes measurements of activity concentrations in food generally consumed around the sites and other environmental media and gamma doses rates. An assessment of doses to people living near the facilities who are likely to receive the highest dose is also carried out based on the results of the monitoring programme. The report published in 2022 included an analysis of trends in doses evaluated for the period 2009 to 2020 [C13]. Annual doses received by people living near operating NPPs in the United Kingdom were estimated to be between less than 5 and 67 μSv, while doses calculated for NPPs which were closed down in this period were estimated to be in the range of less than 5 to 320 μSv. It should be noted that the main contribution to the higher doses in these ranges was from direct radiation rather than from discharges to the environment. Similar annual doses were calculated for facilities involved in fuel enrichment and fabrication (range: 28-260 μSv); again, the higher doses in the range were delivered through direct radiation from the facility. Finally, doses to people living near the nuclear fuel reprocessing plant at Sellafield in the period 2009 to 2020 were estimated to range from 76 to 420 μSv, mostly due to liquid discharges not only from the site but also from other nuclear and non-nuclear facilities in the area.

B. Radioactive waste management

351. Solid radioactive wastes arise from the use of radioactive substances in industry and research and at various stages in nuclear power production. They include low- and intermediate-level radioactive waste from the operation of NPPs and other industrial processes; high-level waste from spent nuclear fuel reprocessing; and spent nuclear fuel for direct disposal. Low- and intermediate-level wastes are generally disposed of in engineered near surface facilities. Intermediate-level waste, containing long-lived radionuclides, are subject to greater isolation during storage and disposal at depths of the order of tens to a few hundred of metres is recommended [I20]. High-level waste and spent nuclear fuel are currently retained in interim storage pending the development of appropriate disposal facilities recommended to be within deep geological formations at a depth of several hundred of metres [I20].

1. Amounts of radioactive waste

352. Information on the amounts of radioactive waste and spent nuclear fuel can be obtained from the national reports of countries that are parties to the Joint Convention on the Safety of Spent Nuclear Fuel Management and on the Safety of Radioactive Waste Management [I45]. The UNSCEAR 2008 Report, annex B [U19] summarized the amounts of spent nuclear fuel that had been generated and in storage and reprocessed up until the end of 2002. In addition, information on the amounts of long-lived and high-activity radioactive waste produced in a cross-section of countries was used to estimate the annual amount of radioactive waste generated by different types of reactors per unit installed capacity. However, there are two difficulties associated with this approach: radioactive waste disposed of in dedicated facilities does not originate solely from nuclear energy production; and more recent information on solid radioactive waste does not generally include data on its radionuclide composition. It should be noted that an increasing number of nuclear facilities are being decommissioned, giving rise to an additional source of radioactive waste.

353. The IAEA report on status and trends in spent nuclear fuel and radioactive waste management provides an overview of the volumes of different forms of radioactive waste in storage and disposal facilities, as of December 2016 [I42], derived from information in national profiles and reports under the Joint Convention on the Safety of Spent Nuclear Fuel Management and on the Safety of Radioactive Waste Management. This information is summarized in table 35, which shows that the highest volumes of radioactive waste for disposal are in the very low and low-level waste categories and that the highest waste arisings are in the Americas.

Table 35. Volumes of different forms of radioactive waste by region [I42]

Regions and radioactive waste categories are specified in [I42]

Region	*Volume of radioactive waste in storage and disposal, 31 December 2016 (m^3)*			
	Very low-level waste	*Low-level waste*	*Intermediate-level waste*	*High-level waste*
STORAGE				
Africa	14 000	25 000	1 000	0
Americas	2 309 000	303 000	85 000	6 000
Asia	350 000	249 000	69 000	600
Europe	245 000	890 000	2 583 000	22 000
Oceania	0	4000	0	0
Global total	**2 918 000**	**1 471 000**	**2 740 000**	**29 000**
DISPOSAL				
Africa	0	14 000	0	0
Americas	11 041 000	15 392 000	91 000	0
Asia	800	67 000	0	0
Europe	369 000	3 002 000	43 000	0
Oceania	432 000	24 000	0	0
Global total	**11 842 000**	**18 499 000**	**134 000**	**0**

354. Some national reports for the Joint Convention on the Safety of Spent Fuel Management and on the Safety of Radioactive Waste Management, provide information on the relative volumes of radioactive waste at some radioactive waste facilities that are associated with nuclear energy production, and the volumes of wastes within specific categories derived from, for example, decommissioning and research activities. Some examples are provided in the remainder of this section.

355. Finland [F8] reported that 6,541 m^3 of low-level waste and 2,117 m^3 of intermediate-level waste are disposed in rock caverns at intermediate depth near the Olkiluoto NPP. In total, 2,261 tonnes heavy metal (t HM) of spent nuclear fuel will be disposed of in a deep geological repository, for which a construction license was granted in 2015. The predominant radionuclides in the waste are reported to be ^{137}Cs, ^{241}Pu and ^{90}Sr [A36].

356. France reported that the closed radioactive waste repository at Manche—known as the Centre de stockage de la Manche (CSM)—received 527,000 m^3 of low- and intermediate-level waste. The waste disposed of at the Manche repository mainly contains radionuclides with a half-life of less than 30 years, but also long-lived radionuclides, such as radium, uranium, thorium and plutonium [A26].

357. Germany [G11] reported that 124,736 m^3 of radioactive waste with negligible heat generation were in storage at the Konrad site. The volume of waste from NPPs in operation in 2019 was relatively small (7% of the total volume) compared with waste from research institutions (36%) and from the decommissioning of NPPs (32%). Approximatively 37,000 m^3 of low- and intermediate-level waste were emplaced at the Morsleben repository for radioactive waste [G11], containing mainly ^{137}Cs, ^{63}Ni, ^{90}Sr, ^{14}C and ^{60}Co and low concentrations of alpha emitters. About 80% of the emplaced waste originated from the operation and decommissioning of NPPs; the remaining 20% came from research, industry, the medical sector, and other waste producers.

358. Japan reported that low-level waste was classified into four categories (L1, L2, L3, and TRU waste) each of which is disposed at different types of facilities ranging from surface facility to disposal in geological formation. For example, L2 type waste is disposed of in a concrete pit at the depth of 10 metres or more at the JNFL site, with a total capacity of 124,672 m^3.

359. Sweden [S82] reported that approximately 36,000 spent nuclear fuel assemblies were stored in pools located at NPPs or in the central interim storage facility before placement in a disposal facility. The repository for short-lived low- and intermediate-level waste (SFR) situated beneath the Baltic Sea, had received approximatively 40,000 m^3 of radioactive waste in 2019. The main radionuclides in the waste were ^{63}Ni, ^{60}Co, ^{137}Cs and ^{55}Fe [S52]. The shallow land disposal facilities situated near the NPPs as well as the Studsvik site had received approximately 28,000 m^3 of very low-level radioactive waste in 2019. In general, the predominant radionuclides were ^{60}Co, ^{137}Cs and ^{63}Ni.

360. The United Kingdom [O10] reported that the volumes of high-, intermediate-, low-level and very low-level radioactive waste reported in April 2019 were 2,150 m^3, 102,000 m^3, 27,400 m^3, and 1,040 m^3, respectively. However, the United Kingdom Office for Nuclear Regulation estimated that the volume of low- and very low-level radioactive waste that would arise in the future could be equal to 1,480,000 m^3 and 2,830,000 m^3, respectively, because of decommissioning of nuclear facilities. It also estimated that up to 6,000 tonnes of spent nuclear fuel were in reactor core or in storage.

2. Discharges and exposures from radioactive waste facilities

361. Information on discharges from radioactive waste facilities was provided through the UNSCEAR Global Survey on Public Exposure and other sources, mainly for sites in Europe, specifically in Belgium, France, Spain, Sweden and the United Kingdom. Doses in this annex were calculated using the average annual discharges for the period between 2016 and 2020 (see table 36).

362. The characteristic individual, regional and global collective doses associated with these discharges estimated using the UNSCEAR methodology for assessment of doses from discharges [U24] are presented in table 37. The table shows that the characteristic annual individual doses in the vicinity of these waste disposal facilities range from a small fraction of a microsievert in most cases, to around 10 μSv for the Low Level Waste Repository (LLWR) in the United Kingdom.

363. For general context, these values may be compared with those included in national reports. In France, for example, the national operator assessed individual doses from radioactive discharges from the Centre de stockage de l'Aube (CSA) and the Centre de stockage de la Manche (CSM). The annual dose to an adult for CSA was estimated to be 0.19 nSv [A27], while the estimated annual dose to an adult using the Saint Hélène River near CSM was 0.11 μSv [A28].

Table 36. Average annual discharges from radioactive waste disposal facilities during 2016–2020

Radionuclide	*Average annual discharge from radioactive waste disposal facilities (GBq/a)*							
	Belgium		*France*		*Spain*	*Sweden*		*UK*
	Belgoprocess site 1	*Belgoprocess site 2*	*CSA*	*CSM*	*El Cabril*	*Clab*	*Studsvik*	*LLWR*
ATMOSPHERIC								
^{3}H	4.8×10^{0}	1.9×10^{0}	9.0×10^{-2}		9.1×10^{-1}		5.8×10^{1}	
^{14}C			6.1×10^{-2}		1.4×10^{-1}			
^{54}Mn							1.5×10^{-5}	
^{60}Co						3.3×10^{-3}	1.0×10^{-3}	
^{85}Kr						4.6×10^{0}	4.0×10^{2}	
^{106}Ru							6.7×10^{-6}	
^{131}I							1.1×10^{-5}	
^{134}Cs							3.6×10^{-3}	
^{137}Cs							1.5×10^{-2}	
^{240}Pu						1.2×10^{-5}		
^{241}Am						3.9×10^{-5}	6.0×10^{1}	
Gross Alpha	2.5×10^{-4}	2.7×10^{-5}	9.1×10^{-7}		1.7×10^{-5}		4.6×10^{-4}	6.6×10^{-6}
Other	3.4×10^{-4}	1.3×10^{-4}	2.1×10^{-5}		7.4×10^{-5}	5.4×10^{-5}	9.0×10^{-5}	5.1×10^{-5}
LIQUID								
^{3}H		1.2×10^{3}	7.8×10^{-4}	2.0		5.9×10^{-1}	3.4×10^{2}	5.5×10^{1}
^{14}C			2.1×10^{-4}					
^{60}Co		1.9×10^{-2}				1.3×10^{-2}	2.2×10^{0}	
^{90}Sr		1.1×10^{-1}					8.0×10^{-2}	
^{134}Cs		9.6×10^{-3}					4.9×10^{-4}	
^{137}Cs		1.8×10^{-1}				5.3×10^{-3}	1.8×10^{-1}	
^{226}Ra		2.7×10^{-2}						
^{234}U							3.4×10^{-4}	
^{238}U							7.1×10^{-5}	
^{239}Pu							2.7×10^{-5}	
^{240}Pu						3.6×10^{-7}		
^{241}Am		1.2×10^{-2}				2.8×10^{-6}	1.2×10^{-4}	
Gross Alpha		3.7×10^{-2}	3.9×10^{-6}	3.0×10^{-3}			1.1×10^{-3}	5.1×10^{-2}
Gross Beta		3.8×10^{-1}	1.1×10^{-4}	1.0×10^{-2}			1.7×10^{-1}	8.7×10^{-1}
Other						9.1×10^{-2}	2.9×10^{-4}	

Table 37. Annual doses to characteristic individual from average discharges from waste disposal facilities for the period 2016–2020

Country	*Site*	*Annual dose to the characteristic individual (mSv)*		
		Atmospheric discharges	*Liquid discharges*	*All discharges*
Belgium	Belgoprocess site 1	6.8×10^{-7}		6.8×10^{-7}
	Belgoprocess site 2	1.8×10^{-7}	6.5×10^{-4}	6.5×10^{-4}
France	CSA	3.3×10^{-8}	2.8×10^{-7}	3.1×10^{-7}
	CSM		1.6×10^{-4}	1.6×10^{-4}
Spain	El Cabril	1.2×10^{-7}		1.2×10^{-7}
Sweden	Clab	1.3×10^{-7}	1.1×10^{-3}	1.1×10^{-3}
	Studsvik	9.2×10^{-7}	2.1×10^{-3}	2.1×10^{-3}
UK	LLWR	6.4×10^{-8}	1.1×10^{-2}	1.1×10^{-2}

364. Table 38 presents the collective doses associated with discharges from radioactive waste facilities. The total collective doses due to a single year's discharges integrated to 100 years to the European and world populations were estimated to be around 0.1 and 0.6 person–Sv, respectively. The additional contribution from globally dispersed radionuclides was estimated of 0.003 person–Sv. It is recognized that there are many more radioactive waste disposal facilities in the world than those on which the evaluation in this annex was based and that these results are therefore incomplete.

Table 38. Collective doses to the world population integrated to 100 years from a single year's discharges from radioactive waste disposal facilities for the period 2016–2020

Country	*Site*	*Collective dose for waste disposal facilities (person–Sv)*				
		Atmospheric discharges			*Liquid discharges*	*All discharges*
		Local	*Regional*	*Total*		
Belgium	Belgoprocess site 1	1.7×10^{-4}	5.3×10^{-4}	6.9×10^{-4}		6.9×10^{-4}
	Belgoprocess site 2	4.5×10^{-5}	1.4×10^{-4}	1.9×10^{-4}	4.1×10^{-2}	4.1×10^{-2}
France	CSA	1.2×10^{-5}	3.7×10^{-5}	4.8×10^{-5}	2.6×10^{-5}	7.4×10^{-5}
	CSM				9.9×10^{-4}	9.9×10^{-4}
Spain	El Cabril	3.9×10^{-5}	1.2×10^{-4}	1.6×10^{-4}		1.6×10^{-4}
Sweden	Clab	4.6×10^{-5}	1.1×10^{-4}	1.5×10^{-4}	6.9×10^{-3}	7.1×10^{-3}
	Studsvik	3.6×10^{-4}	9.9×10^{-4}	1.4×10^{-3}	1.3×10^{-2}	1.4×10^{-2}
UK	LLWR	1.7×10^{-5}	4.0×10^{-5}	5.7×10^{-5}	6.9×10^{-2}	6.9×10^{-2}
Europe		6.9×10^{-4}	2.0×10^{-3}	2.7×10^{-3}	1.3×10^{-1}	1.3×10^{-1}
Worldwide		$\mathbf{8.7 \times 10^{-4}}$	$\mathbf{1.8 \times 10^{-3}}$	$\mathbf{2.7 \times 10^{-3}}$	$\mathbf{5.6 \times 10^{-1}}$	$\mathbf{5.6 \times 10^{-1}}$

3. Long-term (post-closure) exposures

365. In addition to the assessment of doses from discharges from radioactive waste disposal facilities, previous UNSCEAR reports [U15, U21] included an evaluation of long-term (post-closure) doses from leaching of radionuclides to groundwater from waste disposed of at these facilities. The approach used was based on parameter values that are now outdated and depend on assumptions about the containment of the solid waste and the site characteristics. Furthermore, a representative radionuclide specific inventory of low- and intermediate-level waste that is directly associated with electricity generation is difficult to determine. A fraction of the waste inventories is associated with, for example, decommissioning activities or waste from other sectors. In addition, the timescales for estimating post-closure exposures differ from other forms of public exposure and are difficult to present in a consistent manner. Therefore, the Committee decided that an update of long term (post closure) doses associated with radioactive waste disposal facilities was beyond the scope of the current evaluation.

366. As an alternative, this annex provides relevant information from case studies on long-term safety assessments for low- and intermediate-level waste carried out by some Member States and reported in official publications:

(a) In Sweden, for the SFR 1 disposal facility for low-level waste and intermediate-level waste located at an intermediate depth of 60 m of rock, the highest individual annual dose for the reference scenario was estimated at 12 μSv with organic ^{14}C as the predominant radionuclide [S51];

(b) In France, the highest individual annual dose for the reference scenario for the disposal facility at CSM, was estimated around 0.1 mSv [A26];

(c) In Canada, the Canadian National Laboratories proposed to construct and operate the Near Surface Disposal Facility for the disposal of solid low-level waste at Canadian National Laboratories in Chalk River. The maximum annual dose to the critical receptor in the Normal Evolution Scenario was estimated at 0.015 mSv [C43].

C. Applications other than nuclear power production

367. Applications other than nuclear power production include a broad range of human activities that can cause public exposure. These applications can be divided into three categories:

(a) Medical applications for both human and veterinary medicine;

(b) Industrial and research applications;

(c) Production, use and disposal of consumer products.

It should be noted that these applications can also result in occupational and medical exposures, but only public exposures are assessed in this annex.

368. Doses to the public resulting from these applications are typically very low; however, the improper use of radioactive sources, as well as incidents, accidents and malevolent acts involving radioactive sources may result in elevated levels of public exposure. Public exposure caused by such events where there is no long-term contamination of the environment with radioactive materials is covered in this

section, while public exposure due to long-term contamination of the environment caused by past civilian and military applications, and past accidents is described in sections IV.D and IV.E.

369. In previous UNSCEAR reports dealing with public exposure to ionizing radiation [U15, U19] the Committee did not develop specific dose assessment methodologies for this topic area, due to the wide variety of sources, the numerous exposure scenarios, and the sparse nature and inhomogeneity of relevant information. Estimates of doses to the public from applications other than nuclear power production available in the literature, are generally performed using a variety of methodologies. Consequently, a single, robust methodology to assess public exposure on a global scale could not be developed by the Committee and dose estimates in earlier UNSCEAR reports were taken from national reports and publications in the open literature. The Committee adopted the same approach for this annex and updated and expanded its evaluation of public exposure from applications other than nuclear power production to the extent possible based on the information provided through the UNSCEAR Global Survey on Public Exposure, information from the open literature, and reports of national and international organizations.

1. Medical applications: human and veterinary medicine

370. Technologies that make use of ionizing radiation are widely employed in medicine, for example, in the detection, diagnosis and treatment of cancer. Medical applications of ionizing radiation also play an important role in different areas, such as the treatment of injuries, cardiovascular diseases and the management of noncommunicable and infectious diseases.

371. Public exposure can occur before, during, and after medical procedures as an unintended consequence. Sources of public exposure in medicine include radiopharmaceuticals, sealed radionuclide sources and radiation generators. Members of the public can be exposed to sources of ionizing radiation in a variety of medical applications, such as radiopharmaceuticals and sealed radioactive sources for medical applications; nuclear medicine; radiation therapy; diagnostic and interventional radiology and veterinary medicine. Medical and occupational exposures related to medical applications were evaluated by the Committee most recently in UNSCEAR 2020/2021 Report, annex A [U31] and annex D [U30], respectively.

(a) *Production and supply of radiopharmaceuticals*

372. Radiopharmaceuticals can be bound to vehicle molecules or used in an ionic or inert form for the in vivo and in vitro diagnosis of diseases and therapy. The use of radiopharmaceuticals in clinical applications and biomedical research is rapidly growing. The most common radionuclides used for medical diagnostic imaging and therapy are ^{99m}Tc, ^{131}I and ^{133}Xe. Due to their short half-lives, these radionuclides cannot be stockpiled and must be constantly produced and delivered to medical facilities. Technetium-99m is the decay product of ^{99}Mo, which is produced in research reactors as a fission product of ^{235}U, or can be obtained by the neutron activation of ^{98}Mo in a high neutron flux reactor. As of 2016, about 95% of the global production of ^{99}Mo for medical use was carried out in seven research reactors in Australia, Canada, Europe, and South Africa and supplied from five target processing facilities. Companies in Australia, Canada, Europe, South Africa, and the United States participate in this global supply chain for ^{99}Mo and ^{99m}Tc, while Argentina, Brazil, China, Republic of Korea, and the Russian Federation provide regional supplies of ^{99}Mo. About 10,000 targets are used annually to produce ^{99}Mo for medical application. Production of ^{99}Mo is frequently expressed in a quantity called six-day curie (Ci), which is the residual activity of ^{99}Mo six days after it leaves the production facility. In 2016, the estimated annual production capacity of ^{99}Mo was approximately 1.5 six-day MCi corresponding to roughly 5.5 10^4 six-day TBq [N5].

373. Other medical radionuclides, such as ^{59}Fe, ^{123}I and ^{201}Tl, can also be produced in research reactors and cyclotrons. Radiopharmaceuticals containing ^{18}F, ^{13}N, ^{11}C and ^{15}O for positron emission tomography (PET) are generally produced using cyclotrons. In 2012, at least 150 cyclotrons were producing PET radiopharmaceuticals in the United States [O6]. A study on the use of cyclotrons for nuclear medicine and radiopharmacy in Austria, Germany, and Switzerland [Z12] indicated that the total number of cyclotrons used for production of radiopharmaceuticals in these countries increased from 23 in 1998 to 28 in 2006 and 42 in 2022.

374. Reliable estimates of doses to the public resulting from the production and distribution of medical radionuclides are unavailable owing to the complexity of the global production and supply chains, and the limited availability of data. Facilities involved in the production of radiopharmaceuticals comply with national regulations to control their radioactive discharges which typically result in negligible levels of public exposure. The UNSCEAR 2008 Report, annex B [U19] estimated that the annual collective dose due to the production and use of radioisotopes in medicine was of the order of 100 person–Sv.

(b) *Nuclear medicine*

375. The UNSCEAR 2020/2021 Report, annex A [U31] estimated that the global annual number of diagnostic procedures and radionuclide treatments of nuclear medicine were 40 million and 1.4 million, respectively, an increase of 22% and 63%, respectively, compared to the data presented in the UNSCEAR 2008 Report, annex B [U19]. The most common radionuclide used in nuclear medicine diagnostic procedures is ^{99m}Tc, which is employed in 30 million examinations worldwide [O5].

376. Nuclear medicine facilities can cause exposure of members of the public via discharges of radioactive material to the environment or to the sewer systems. Decay tanks and other abatement technologies substantially reduce the activity of these discharges from hospitals. In a hospital, exposure of other patients, visitors, and staff not classified as radiation workers may occur due to their proximity to a treated patient. A patient released from the hospital can expose family members, other members of the public and bystanders. The exposure pathways are direct radiation from the body, excreta, vomit masses, and exhalation of residual amounts of the administered radionuclide or its decay products.

377. The impact of hospital discharges into sewage system in Denmark, Finland, Iceland, Norway and Sweden was investigated by Sundell-Bergman et al. [S78]. The study focused on selected sewage treatment plants that serve various hospitals handling radionuclides for medical purposes and carried out assessments of doses to members of the public. The annual discharges were between 1.4 and 7.5 TBq for ^{99m}Tc and between 0.1 and 0.9 TBq for ^{131}I. The study estimated that the doses to workers at the sewage treatment plant from inhalation and external exposures were higher than those to farmers who consume crops fertilized with sludges from the plant. All predicted annual doses were below 10 μSv. A study in Spain [J14] analysed the levels of ^{131}I in sludge from a sewage treatment plant and estimated an annual dose of 800 μSv to workers at the plant due to external exposure from sludges [J14].

378. Most recent studies focused on family members or caregivers who come in contact with therapeutically treated patients. Doses from external exposure to caregivers of 31 outpatients and 33 inpatients treated with 1.11 GBq and 3.7–7.4 GBq of ^{131}I after thyroidectomy, respectively, were estimated using thermoluminescence dosimeters. The average dose was estimated to be 0.61 ± 0.56 mSv (median: 0.50 mSv) for outpatients who were isolated for two hours after treatment, and 0.16 ± 0.34 mSv (median: 0.06 mSv) for inpatients who were quarantined in the hospital for 2–3 days after treatment, over seven days after discharge [L10]. A study by Gründel et al. [G26] estimated that the dose from inhalation of radioiodine exhaled by patients treated with 0.2–10 GBq of ^{131}I was 0.77 mSv to children and less than 0.1 mSv to adult relatives. A study of internal doses to family

members of patients treated with radioactive iodine indicated that the highest observed equivalent dose to thyroid based on measurements using whole body counter was 2.4 mSv [B55].

379. Studies of exposures of children, other household members and relatives of patients treated with radioiodine demonstrated that typical doses were of the order of 1 mSv or less [D6, G1, G2, G21, L10, L19, M6]. However, a study by Barrington et al. [B7] reported that in the case of outpatients, many young children received more than 1 mSv at home, while an investigation by Mathieu et al. [M12] found that if children of outpatients stayed away from home for the first eight days after therapy, median doses over the two weeks following treatments for thyroid cancer and hyperthyroidism were 0.08 and 0.13 mSv, respectively. It also indicated that providing relevant safety information to patients and their relatives when patients were released allowed exposure of household members and other members of the public to be reduced to small fractions of one millisievert. In contrast to these findings, a study of 22 caregivers in India reported that doses to caregivers in the week following discharge of the patients after radioiodine therapy ranged from 9.7 to 24.2 mSv [K15].

380. Targeted alpha therapy with ^{223}Ra, ^{227}Th and ^{225}Ac is widely used for the treatment of metastasis in patients with prostate cancer [F12], while ^{225}Ac labelled antibodies and peptides have been used to target various types of cancer [S33]. Public exposure is caused by decay products of ^{223}Ra and ^{227}Th, such as ^{219}Rn exhaled by patients and ^{219}Rn decay products (^{215}Po, ^{211}Pb, ^{211}Bi and^{207}Tl). Hosono et al. [H32] estimated that the dose to a member of the public or caregiver was about 3.5 μSv following an injection of 3.0 MBq of ^{223}Ra. Public exposure is also associated with the production of alpha-emitting radiopharmaceuticals containing alpha-emitting radionuclides, such as ^{225}Ac, which is produced by radiochemical extraction from ^{229}Th sources or by accelerator driven processes. Actinium-227 is also a by-product of the accelerator-based production of ^{225}Ac.

381. Positron emission tomography uses various radiopharmaceutical tracers for the functional imaging of biokinetic processes, such as blood flow, regional chemical composition, and absorption. The most common radionuclides used as PET tracers are ^{18}F, ^{15}O, and ^{11}C, ^{68}Ga, ^{89}Zr, and ^{124}I. Single-photon emission computed tomography (SPECT) uses gamma-emitting radionuclides, such as ^{123}I, ^{99m}Tc, ^{133}Xe, ^{201}Tl and ^{111}In, for imaging of the blood distribution within tissues. An overview of public exposure from mobile PET and SPECT systems by Studenski [S73] reported that, following a 555 MBq injection, the dose rate at 30 cm from a patient was 0.8 mSv/h for ^{18}F and 0.13 mSv/h for ^{99m}Tc.

382. In a study by Lee and Park [L11] to determine the appropriate isolation time for patients with differentiated thyroid carcinoma treated with ^{131}I, ambient dose equivalent rates were measured at 1 m from 71 patients who had been administered between 3.7 and 7.4 GBq of ^{131}I. Upper estimates of doses to other members of the public ranged from 0.2 mSv to 2.14 mSv. A similar study conducted in Germany to estimate the exposure of members of the public from patients with prostate cancer undergoing treatment with ^{177}Lu-PSMA-617 [K46] reported ambient dose equivalent rates measured at a distance of 2 m from the patients. The average dose to members of the public was estimated at 70 μSv, with a maximum value of around 260 μSv when patients were discharged 48 hours after treatment.

(c) *Radiation therapy*

383. The UNSCEAR 2020/2021 Report, annex A [U31] estimated that the global annual number of radiation therapy treatment courses was 6.2 million, an increase of 22% from the 5.1 million treatments reported in the UNSCEAR 2008 Report, annex B [U19]. Of these, 5.8 million were delivered using external beam therapy, and 0.4 million were brachytherapy.

384. Public exposure from external beam therapy and radiosurgery is restricted by the design criteria of the facility. Members of the public receive high doses only following unauthorized access to the therapeutic units or events associated with the loss of control over radioisotope units. An example of such an event is the accident that occurred at Goiânia (Brazil) in 1987, which is illustrated in the UNSCEAR 1993 Report, annex B [U13] and in the UNSCEAR 2008 Report, annex C [U20] and described in detail in a dedicated IAEA report [I1].

385. Public exposure in case of interstitial or intracavitary brachytherapy is predominantly associated with external exposure from sealed radioactive sources in the form of seeds, wires and tubes containing such radionuclides as ^{60}Co, ^{131}Cs, ^{137}Cs, ^{125}I, ^{192}Ir, ^{103}Pa, ^{106}Ru or ^{226}Ra, which are temporarily or permanently placed into or next to the tumour or with external exposure from a sealed radioactive source in the form of a container temporarily placed in a body cavity, such as the rectum, uterus, or vagina.

386. In intra-arterial microbrachytherapy, which involves injecting insoluble microspheres with embedded ^{90}Y or ^{166}Ho into the bloodstream, some fraction of microspheres can be eliminated from the patient with excreta, blood or vomit masses and cause exposure to people in close contact. Pathways of public exposure are similar to those following treatment with soluble radiopharmaceuticals. Prince et al. [P38] estimated that external doses to people in close contact with patients treated with ^{166}Ho microspheres with an activity of up to 7 GBq would not exceed 5 mSv and that for microsphere with higher activities, restricting contact during the first six hours after treatment would keep doses to people in close contact below this level.

387. Exposure of members of the public in close contact with 108 prostate cancer patients who underwent brachytherapy with low dose-rate implants of ^{125}I and a prescribed absorbed dose to target areas of 145 Gy was reported by Licciardello et al. [L19]. In the study the air kerma rates were measured at different distances from the patients (e.g., in contact with the skin, at 0.5 m and 1 m). The estimated doses to these individuals were estimated to be in the range of 0.1–1.2 mSv with a median value of 0.5 mSv at 1 m from the patient, assuming an occupancy factor of 0.25. In a different study [D5] the exposure rates at 30 cm from the anterior skin surface were measured in 1,127 colleagues of patients with prostate cancer who underwent ^{125}I seed implantation. The upper estimate of the dose to colleagues of patients with ^{125}I seed implantation was 0.041 mSv [D5].

388. Radiopharmaceuticals and brachytherapy sources are typically used for patients with a sufficiently long-life expectancy. Nevertheless, death can occur shortly after administration of radioactive material. Improper management of a body containing radioactive material can result in public exposure, especially in the case of cremation [A6, I30].

(d) *Diagnostic and interventional radiology*

389. Radiological imaging procedures, such as mammography, computer tomography and interventional radiology, are the most extensively used medical applications of ionizing radiation. More than one billion procedures are carried out in the European Union and United States annually [E21, S60]. Computed tomography accounts for about 10% of Europe's radiological imaging procedures [E16]. In general, public exposure from a stationary imaging facility is negligible. However, mobile scanners used in emergencies, in remote locations or field conditions, may cause elevated exposure to members of the public, if appropriate protective equipment and procedures are not utilized [K21].

(e) *Veterinary medicine*

390. Veterinary medicine includes most of the procedures described in previous sections. However, in veterinary medicine, such procedures can be less optimized, as they are often applied outside dedicated facilities and generally require the presence of additional people, such as animal handlers. These factors potentially increase the magnitude of public exposure associated with veterinary medicine [I40]. Information on public exposure are not available, but a survey by Epp and Waldner [E29] indicated that the annual doses to individuals manually restraining animals for veterinary radiological procedures exceeded 20 mSv and that, among individuals who manually restrained animals, 39% experienced unintended exposure.

2. Industrial, research and other applications

391. Applications of ionizing radiation in industrial, research, and other sectors include research reactors, accelerators and other research and industrial facilities, nuclear propulsion and autonomous power sources, non-medical human body imaging, imaging of objects with ionizing radiation for security screening, non-destructive testing and ensuring product quality (e.g., industrial gauges, moisture and density gauges, industrial radiography).

(a) *Research reactors and research facilities*

392. Nuclear fission reactors have been used for research, development, education, and training for over 80 years. Nowadays, research reactors serve as a neutron source for research, medicine, various industrial applications, non-destructive testing, analysis of materials, and production of radioisotopes for medical, industrial, and research use. Many research reactors were built in the 1960s and 1970s. In 1975, the number of operational research reactors in 55 countries was 373. As of April 2023, the total number of research reactors in 70 countries exceeded 800, with 222 operational in 50 countries, 573 shut down or decommissioned, and 23 reactors planned or under construction in 16 countries [I50]. Research reactors require less nuclear fuel to operate and generate fewer fission products than nuclear power reactors but use uranium typically enriched to up to 20% in ^{235}U, and to as much as 90% in ^{235}U in some cases. The thermal power output of research reactors ranges from zero (e.g., for critical assemblies), to a few hundred megawatts.

393. Memon et al. [M23] reported radiation levels in and around research reactors at the Pakistan Institute of Nuclear Science and Technology. Measurements of ambient dose equivalent were made with thermoluminescent dosimeters between 1998 and 2002. The mean ambient dose equivalent rates for individual locations ranged from 0.14 ± 0.01 to 0.19 ± 0.03 μSv/h, with a mean value of 0.16 ± 0.03 μSv/h. Khomich et al. [K16] reported on a WWR-M heterogeneous water moderated pool type research reactor operating with thermal neutrons at a power level of 10 MWth. The primary radionuclides released into the atmosphere were noble radioactive gases and radioisotopes of iodine. During the period between 1979 and 2011, measurements of activities of noble gases discharged from the reactor showed that the predominant radionuclide was ^{41}Ar—contributing about 95% of the discharges—with minor contributions from ^{85}Kr, ^{88}Kr and ^{135}Xe. Among radioisotopes of iodine, ^{131}I was the primary contributor. Atmospheric discharges ranged from 10^{12} Bq/d for the noble gases to 9.4×10^{6} Bq/d for ^{131}I, and 1.3×10^{4} kBq/d for long-lived radionuclides, such as ^{110m}Ag, ^{58}Co, ^{60}Co, ^{51}Cr, ^{134}Cs, ^{137}Cs, ^{59}Fe, ^{54}Mn, ^{90}Sr, ^{95}Nb, and ^{95}Zr. The activity concentrations of the radionuclides discharged to the environment were generally below detection limits.

394. Fernandez et al. [F4] reported on the environmental monitoring of terrestrial ecosystems in the Obninsk region (Russian Federation), where the WWR-c research reactor is used mainly for the production of medical radioisotopes as well as gamma and electron irradiation facilities. Upper-level estimates of doses to members of the public due to ^{131}I arising from the production of radiopharmaceuticals were several orders of magnitude below the dose limit. The activity concentrations of ^{137}Cs in environmental samples were slightly higher than the levels from global fallout; however, there was no clear evidence that such slight elevation was due to the operation of the research reactor.

395. Amekudzie et al. [A24] reported ambient equivalent dose rates around the nuclear research reactor on the publicly accessible premises of the Ghana Atomic Energy Commission in the range of 0.14–0.27 μSv/h with an average value of 0.2 μSv/h. The survey also showed that measured dose rates are primarily due to natural background and no estimates of associated public exposure were performed. Hoq et al. [H26] reported on the activity concentration of radionuclides discharged from the TRIGA Research Reactor at the Bangladesh Atomic Energy Commission reactor. The primary activation product released from the reactor was ^{41}Ar and its activity concentrations in the air were well below the permissible level. No estimates of public exposure were carried out. Adelikhah et.al. [A4], performed dose assessments for liquid discharges into the sewage system from the Tehran Research Reactor in Iran. The assessment showed that the annual dose to members of the public was below 10 μSv.

396. In Canada, research reactor and high energy accelerator facilities are required to provide the Canadian Nuclear Safety Commission with estimates of annual releases and associated estimates of dose to members of the public. Annual doses to members of the public from Canadian research reactors are below 10 μSv. Data for 18 research reactors in Canada were also provided to the Committee through the UNSCEAR Global Survey on Public Exposure. The SLOWPOKE-2 reactors are designed to operate at low power and are fuelled with either highly enriched uranium, (e.g., research reactors at University of Alberta and the Saskatchewan Research Council), or low-enriched uranium (e.g., research reactors at the Royal Military College of Canada and École Polytechnique de Montréal). The SLOWPOKE-2 facilities discharge negligible quantities of noble gases, mainly ^{133}Xe and ^{135}Xe, from the weekly purge of reactor head space, and ^{41}Ar from irradiation activities. The McMaster Nuclear Reactor, which first became operational in 1959, generally operates at a thermal power of 3 MW. Iodine-125 and ^{41}Ar are the only radionuclides routinely discharged to the environment in measurable quantities. According to data provided to the UNSCEAR Global Survey on Public Exposure, the maximum annual doses to members of the public due to discharges from research reactors in Canada, were of order of a few μSv or less.

397. Cyclotrons are widely used in basic research, production of radiopharmaceuticals, and for particle therapy, where a particle beam is applied directly to pathological tissues of the patient. According to the IAEA Database of Cyclotrons for Radionuclide Production there were over 1,500 cyclotron facilities around the world as of 2020 [I51]. Additionally there were more than 50 synchrotron radiation facilities in the world in 2023 [L20], which have various research, industrial, and medical applications.

398. During routine operation, a cyclotron can produce high intensity neutrons and gamma radiation. The neutrons undergo multiple scattering events with nitrogen and oxygen in air and public exposure may result from the skyshine. Kaur et al. [K8] reported that the highest ambient dose equivalent rate of 0.93 μSv/h were measured at the back wall of the radiochemistry laboratory facing the cyclotron vault during the bombardment period of 40 minutes. The radiochemistry laboratory was accessible to non-occupationally exposed individuals. Typically, public exposure from a cyclotron is limited by licensing conditions and applicable dose constraints. For example, regulations in the United States require ensuring that air emissions of radioactive material should not result in an annual dose above 0.1 mSv and the total dose received in any 1 hour in any unrestricted area should not exceed 0.02 mSv [U53].

399. The synchrotron is a component of the highest energy Large Hadron Collider of the European Organization for Nuclear Research (CERN), which is the world's leading international laboratory for particle physics, with nuclear facilities at two main campuses in Meyrin, Switzerland on the French-Swiss border, and in Prévessin (France). In 2011, CERN generated 398 m^3 of solid radioactive waste and processed 342 m^3 of radioactive effluents and its activities resulted in an annual dose to members of the public living in the immediate vicinity below 0.02 mSv in a typical year assuming that all the CERN facilities are operational [C16, C17]; for the major part this dose was due to stray radiation. For example, in 2011, atmospheric releases from CERN accelerator facilities resulted in a dose to members of the public of less than 6.6 μSv, mostly from external exposure to photon radiation of short-lived radioactive gases. Releases of radionuclides to the aquatic environment (HTO, ^{22}Na) resulted in an annual dose below 0.05 μSv. Except for trace amounts of ^{54}Mn in sediments and moss from the Le Lion and L'Allondon Rivers, no radionuclides originating from CERN could be clearly identified [C15].

400. The TRIUMF facility, located in Vancouver, British Columbia (Canada), is a major producer of radioisotopes for medical diagnosis and operates one 520 MeV cyclotron accelerator facility, four smaller cyclotrons, and three linear accelerators. Annual doses to members of the public from TRIUMF were estimated to range from 7 to 16 μSv [M28]. The Canadian Light Source Inc. operates a synchrotron facility at the University of Saskatchewan campus in Saskatoon, Saskatchewan (Canada). Data from its 2016 monitoring programme showed that doses to members of the public were not distinguishable from natural background [C45].

401. Thermonuclear fusion devices used in research have been in operation for many decades. Currently there are more than 140 fusion facilities operating, in construction, or planned in 28 countries [I55]. ITER is a global thermonuclear fusion project of 35 nations. Its thermonuclear reactor in Cadarache (France) is scheduled to begin its research operations in 2034. An overview of exposure pathways and projected levels of public exposures associated with ITER is presented in safety reports by Taylor et al. [T1, T2].

(b) *Nuclear propulsion and autonomous power sources*

402. Nuclear reactors generating thermal and electrical energy are used on surface ships and submarines operated by several nations, including China, France, Russian Federation, United Kingdom and the United States. The main sources of radioactivity in liquid effluents from operating naval nuclear propulsion systems are activated corrosion and wear products from metal components in contact with cooling water of the reactor, namely ^{51}Cr, ^{59}Fe, ^{55}Fe, ^{58}Co, ^{60}Co, ^{63}Ni, ^{95}Nb, ^{95}Zr, ^{54}Mn, ^{65}Zn, ^{125}Sb, ^{181}Hf, ^{182}Ta, and ^{187}W. Cobalt-60 is the most radiologically important among these radionuclides [M44].

403. As of 2022, the United States Navy operated 11 aircraft carriers and 64 submarines powered by nuclear reactors [N30, U47]. In 2019, the total activity of long-lived gamma emitters in liquid discharges to the environment from all United States nuclear-powered ships and supporting tenders, naval bases, and shipyards was less than 74 MBq [M44]. These discharges would give rise to doses to the public of a few microsieverts or less. Reliable information about discharges and public exposure associated with marine nuclear propulsion in other countries is not available.

Power sources in space and terrestrial autonomous instruments

404. Radionuclide power systems are important sources of energy for spacecraft and satellites. A Radioisotope Thermoelectric Generator (RTG) converts the heat released by radioactive decay into electricity without a chain reaction. Most RTGs use ^{238}Pu due to its high energy yield of 0.56 kW/kg, short-range alpha radiation, low gamma radiation, and minimal requirements for shielding. Radioisotope Thermoelectric Generators with the yield of 0.15 kW/kg are also used by the European Space Agency.

To date, the major users of nuclear power systems in space are China, the European Space Agency, the Russian Federation, and the United States. As of 2021, over 45 RTGs powered more than 25 United States space vehicles, including Apollo, Pioneer, Viking, Voyager, Galileo, Ulysses, Cassini, and New Horizons space missions. The latest design RTG with 4.8 kg of ^{238}Pu dioxide and a thermal power of 2 kW is being used in the Mars rover Curiosity, which was launched by the United States National Aeronautics and Space Administration (NASA) in 2011 and landed on Mars the following year. As well as RTGs, ^{238}Pu heaters with a power of typically 1 W and a mass of less than 3 g are used in outer space equipment. Both RTGs and heaters are designed to withstand major launch and re-entry accidents. Radionuclides have also been used in various onboard instruments [W16].

405. The former Soviet Union and the United States also used radionuclide power systems in autonomous ground and sea-based navigation beacons, uncrewed lighthouses, meteorological stations, and similar facilities in remote areas. Over a thousand RTGs were deployed at unmanned, remote facilities along the northern coast of the Russian Federation [P31], primarily as energy sources for lighthouses, each containing high-activity sources of ^{90}Sr. Following the collapse of the Soviet Union in 1991, an international programme was launched to decommission these sources and bring them into safe and secure storage due to the significant threat they posed [S57, S58]. By 2015, 751 RTGs had been recovered [P31] and by 2019 all initially manufactured RTGs were decommissioned [R32]. Terrestrial radionuclide power systems have since been phased out because of environmental and safety concerns.

406. Miniature diamond semiconductor batteries, as low as 3 × 3 × 0.03 mm in size, are used as a DC or pulse power source with a high lifespan. These batteries contain up to 2 TBq of ^{63}Ni [B24]. No estimates of public exposure are available for such batteries.

407. Nuclear fission reactors were used on satellites by the former Soviet Union and the United States. Between 1967 and 1988, the former Soviet Union launched 34 Radar Ocean Reconnaissance Satellites (RORSATs), within the Cosmos series, equipped with low-powered fission reactors with thermoelectric converters. These reactors included fast spectrum graphite reactors with 90% enriched uranium, which produced 3 kW for up to four months. The United States flew one system for nuclear auxiliary power, the SNAP-10A (System for Nuclear Auxiliary Power), in 1965. This reactor operated for 43 days at 590 W but remains in orbit as of 2023 [W16].

(c) *Non-medical imaging of a human body with ionizing radiation*

408. Non-medical human imaging with ionizing radiation is the intentional exposure to ionizing radiation for purposes other than medical diagnosis, treatment, or biomedical research. Such applications are used for security screening at airports, sport venues and other public facilities, customs checkpoints, diamond mines, detention facilities, for evaluating the age of children for legal purposes, identifying the physical potential and development of young individuals and to underpin professional contracts, insurance, and compensation claims in sport, performing arts and other areas.

409. X-ray transmission and backscatter imaging are the two leading security full-body scanning technologies that use ionizing radiation. Security X-ray full-body scanning can expose a subject for imaging and other bystanders, who may receive a dose because of their proximity to the inspection area. Bystanders include passengers, operators, security and airline personnel [I39, N5]. In X-ray transmission imaging a subject stands between the X-ray tube and the detector array and is scanned by an X-ray beam about 2 mm wide. The X-ray peak voltage is usually in the range of 140–220 kV, the current is 0.1–4 mA, and the duration of the exposure is between 5 and 15 seconds. The transmission imaging typically results in a dose of 0.1–5 μSv per screening [E16].

410. X-ray backscatter imaging is based on the Compton scattering effect. A detector array is placed on the same side of the body as the X-ray tube. A typical system uses a peak voltage of about 50 kV and a current of 5 mA. The duration of a single scan can be up to eight seconds. Backscatter body imaging results in a typical dose of 0.01–0.1 μSv per screening; for example, the Rapiscan Secure 1000 SP system delivers a dose in the range of 11–33 nSv per screening. The dose to bystanders can be up to 10% of the doses to screened individuals [N4].

411. A report by the National Academies of Sciences, Engineering, Medicine of the United States [N5] indicated that for two backscatter systems, a dose of 250 nSv per screen would not be exceeded regardless of the age and weight of the screened individual. The absorbed dose to the skin's epithelial layer of radiosensitive cells is 1.6% higher than the average absorbed dose to the skin as defined by the ICRP [I70]. The report confirmed that the tissue absorbed doses received by the lens of the eye, skin, or female breast are at least two orders of magnitude below the thresholds of harmful tissue reactions [I72].

412. X-ray security body scanners can be classified as 'general use systems', which deliver a dose under 250 nSv per screening and 'limited use systems' which deliver higher doses. Annual doses due to systems in both categories are usually expected to be less than 250 μSv for a single source or set of sources under the control of an operator [N11].

413. A report by IRSN [I82] indicates that potential malfunctions of intensively used security body scanners may result in abnormally high exposures to a large number of people. X-ray body scanners for security screening have not been allowed in European airports since 2012 [E18] nor used in United States airports since 2013. Nowadays, many other countries have also switched to security scanners without ionizing radiation. X-ray body scanners can be used for other purposes, such as customs control at national borders and security screening in prisons. In 2021, 52 prisons in the United Kingdom used specialized X-ray body scanners developed for the Prison Service [M29]. Norway reported through the UNSCEAR Global Survey on Public Exposure that its custom authorities had used four X-ray body scanners for control of suspected smugglers between 2007 and 2021. These systems produced about 2,000 body images and each image resulted in a dose of up to 5 μSv.

(d) *Imaging of objects with ionizing radiation*

414. Imaging of objects is widely used for security and customs screening both in industry for quality control and production optimization, and in research. The range of applications of such imaging devices is constantly growing. Members of the public might be exposed to radiation due to their proximity to the imaging area, human errors, and malfunction of the equipment or access barriers.

415. Scanning of letters, parcels, baggage, cargo containers, and vehicles is usually performed with X-rays generated by a vacuum tube with a peak voltage of up to 450 kV. Trace quantities of explosives and narcotics can be detected with a ^{63}Ni source, which emits beta particles with a maximum energy of 67 keV. A typical activity of the source in such devices is about 600 MBq [I30, I39]. Photons produced by ^{137}Cs and ^{60}Co sources are also used for inspection, although devices using X-ray tubes and linear accelerators are preferred in many applications. The typical activity of a ^{60}Co source is around 50–100 GBq, but sources with activities in the order of 10 TBq are also common [I39]. The design criteria for such equipment usually stipulate that in normal circumstances, radiation doses to operators and people in the vicinity should be less than 10 μSv [I30, I39].

416. The use of ionizing radiation to screen cargo containers is increasing. Vehicle scanners typically use X-rays tubes with a peak voltage above 160 kV. Systems with radionuclide sources and neutron generators are also in operation. Interlocks in the scanner and controlled area ensure that doses to

bystanders are low, typically less than a few microsieverts. In some drive-through systems, drivers are present in scanning vehicles and exposed to the scattered beam only. Safety systems prevent drivers from being exposed to the primary beam. Individuals may be concealed in a cargo container and inadvertently exposed to the primary beam. In typical conditions, estimates of whole-body dose to a driver in drive-through systems range from 250 nGy, for a beam energy of 4.5 MeV, to 600 nGy, for a beam energy of 6–9 MeV, per scanning. In accident conditions with exposure to the primary beam, the estimated whole body absorbed dose is about 0.1 mGy [G15].

417. Mobile scanning accelerator-driven devices typically use photons with an energy of 3–6 MeV. Mobile scanning devices usually operate with a photon energy of about 6 MeV, and stationary cargo scanning facilities use photon beams of up to 9 MeV [I39]. Most portable X-ray security screening devices produce an open beam and consist of an X-ray generator with a 250–300 kV peak voltage placed at the front the object to be inspected, and an imaging system placed behind. Exposure of bystanders is minimized by a controlled area around the object being examined. Handheld backscatter X-ray devices typically use peak voltage in the 50–120 kV range and produce an open beam. A controlled area of around 3 m in the direction of the beam is usually required to minimize the exposure of bystanders. There is a growing trend in using handheld backscatter X-ray devices due to the rising demand for various applications. Annual doses to the operator and bystanders of security scanners—typically of a few microsieverts—are restricted by the design criteria. The actual dose depends primarily on the scanners' frequency and mode of operation. In the UNSCEAR Global Survey on Public Exposure, Norway reported the use of 434 X-ray scanners with peak voltage in the 75–270 kV range for customs and security control. Norway indicated that these scanners are designed to comply with national and international radiation protection standards, and the annual dose to members of the public is much less than 1 mSv.

3. Consumer products and other goods

418. Radionuclides can be added to a consumer product for functional reasons because of their physical or chemical properties. Examples of consumer products containing radionuclides are radioluminous products, smoke detectors, thoriated tungsten welding electrodes, high-intensity discharge lamps and lamp starters, gemstones with colour intensified or altered by irradiation, and high-voltage radiation generators or electronic tubes capable of producing ionizing radiation [I36, U55].

419. Products containing radioluminous paint or tritium light sources include timepieces, navigational instruments, such as compasses, torches, fishing floats, exit signs, dials and switches on boats and aircraft. weapon sights and key fobs. Historically, the predominant radionuclide used in radioluminous consumer products was ^{226}Ra, but its use has been discontinued because of safety concerns, as this radionuclide presents a significant hazard due to its gamma emission and it has been replaced by less radiotoxic radionuclides, such as ^{147}Pm and ^{3}H [E4].

420. A gaseous tritium light source (GTLS) consists of a sealed glass container filled with gaseous tritium and coated internally with phosphor. A gaseous tritium light device (GTLD) contains one or more GTLS. International standards [O2] require that members of the public be exposed to GTLDs as little as practicable, and the annual dose received by a member of the public is constrained to a small fraction of 1 mSv. A GTLS is not allowed for use unless it is contained in a GTLD. Only ^{3}H in the form of $^{3}H_2$ or $H^{3}H$ is allowed in a GTLS except for small amounts of tritiated water, provided that, during the lifetime of the GTLS, the activity in the form of tritiated water does not exceed 2% of the total tritium activity.

421. Ionization chambers, smoke, gas, and aerosol detectors and alarm systems usually contain ^{241}Am but other radionuclides, such as ^{63}Ni, ^{85}Kr, ^{226}Ra, ^{238}Pu and ^{239}Pu have also been used. A smoke detector

with 40 kBq of ^{241}Am results in an ambient dose equivalent rate below 2.4×10^{-5} μSv/h at 2 m from the detector. The estimated maximum annual dose is less than 0.07 μSv assuming a daily exposure of eight hours [U19]. An environmental assessment of ionization chamber smoke detectors was also undertaken in the United States [U54]. The report concluded that radiation doses associated with these detectors were far below that from natural background.

422. Thorium, ^{85}Kr and tritium are all used by the lamp industry to improve the metallurgical properties of electrodes, optimize the light spectrum, or provide a starter aid in high-intensity or fluorescent lamps. Example applications of high-intensity lamps include Xe car lighting and low-wattage specialist lamps.

423. The United States Nuclear Regulatory Commission [U55] estimated public exposure caused by selected goods during their normal life cycle, including distribution and transport, expected routine use, and disposal. Estimated annual individual doses for two products—thoriated gas mantles and tungsten inert gas arc welding electrodes—were equal to or greater than 0.1 mSv:

(a) Thoriated gas mantles generate bright luminescent light when heated by a flame. The estimated annual dose for incandescent gas mantles was estimated to be 2 mSv for a person using lighting gas lanterns only, while the dose to an individual using portable camping lanterns was estimated at 0.1 mSv [U55]. A study by Hassan et al. [H13] analysed five different types of thoriated mantles. The highest activity of ^{232}Th in the mantle was 1.25×10^4 Bq. The ambient dose equivalent rate on the surface of a single mantle was 0.68 μSv/h, and 1.9 μSv/h on the surface of a package of six mantles. It was estimated that the annual dose to a member of the public handling such mantles could be up to several millisieverts. Previously, the Committee indicated that the collective dose associated with portable camping lanterns might exceed 100 person–Sv [U19];

(b) Thorium added to tungsten inert gas arc welding electrodes improves the welding characteristics and prolongs the lifetime of the electrodes. Some members of the public use these consumer products. The estimated annual dose to welders is usually well below 1 mSv [H35]. The annual dose to a dedicated grinder of welding rods representing an atypical exposure scenario was estimated to be 8 mSv [U55]. The estimated collective dose to members of the public who are welders was about 300 person–Sv [U19].

424. The colour of gemstones can be enhanced by irradiation with neutrons generated by research reactors, electron beams from linear accelerators, or photons emitted by radionuclides. Some levels of public exposure can be associated with gemstones, such as topaz, that contain activation products after irradiation in research reactors [I36]. Studies carried out in the United States [N12, S21] estimated that the annual equivalent dose to the skin of a member of the public, continuously wearing an irradiated 6 g topaz, can be up to 15 mSv. A European study of 5,000 gemstones [E4] sold directly to the public did not identify any residual activation products in these items.

425. Some members of the public collect fossils, rocks, or minerals, which might contain significant concentrations of natural radionuclides. The overall dose from such specimens under normal handling and display conditions is only a very small fraction of the overall dose from natural radiation [U55].

426. Photographic lenses used to have ^{232}Th added to them to increase the refractive index. Photographers carrying a camera with such lenses around the neck for several hours a day on many days of the year could receive an annual dose of a few hundred microsieverts [U55]. However, in many countries the use of such lenses has been discontinued.

427. Glass, to which uranium is added to produce a yellow or green colour, was popular for over a hundred years and is still made in Czechia and the United States. The dose rate from gamma radiation close to the surface of the glass item is less than 0.1 μSv/h. A typical surface dose rate due to beta radiation

is 15 μSv/h, while dose rates measured a few centimetres from the surface are negligible. Individual doses to owners of some collections of uranium glass could be up to 0.5 mSv annually.

428. Uranium salts have also been used for glazing ceramic products, such as tableware and tiles. They were also used as a colourant in the United States in ceramic tableware produced in the 1930s and 1940s. Nowadays, these items may be found in collectors' markets. Handling such items may give rise to low-level radioactivity on the skin, while using this tableware for eating could lead to very low ingestion doses [W2].

(a) *Depleted uranium*

429. The term depleted uranium (DU) refers to uranium containing lower fractions of ^{234}U and ^{235}U than natural uranium. Depleted uranium is usually a by-product of the processing of natural uranium to produce enriched uranium. The mass fractions of ^{235}U and ^{234}U in DU are typically 0.2–0.3% and 0.001–0.002%, respectively, and therefore the specific activity of DU is about 60% that of natural uranium [U24]. The properties and biological effects of uranium were reviewed in the UNSCEAR 2016 Report, annex D [U24] and in other publications by international organizations [E8, W5].

430. Because of its availability, high density—DU is 1.67 times denser than lead—and chemical properties, DU has a variety of civilian and military applications. Military applications of depleted uranium are described in section IV.D.6. Depleted uranium is used as ballast and counterweights in forklifts, sailboat keels, aircraft, and missiles and is also a valuable material for radiation shielding and collimation in medicine, industry and research. A list of devices that contain DU is provided in the IAEA report Services Series 22 [I33]. Depleted uranium is used as shielding and collimators of medical radiation instruments, such as teletherapy, brachytherapy, and scanner units. The typical DU mass in such equipment can be up to about 600 kg. Similarly, DU shingling masses are used in industrial radiography, measurement gauges, well-logging devices, research, and academic equipment [I33].

431. Under normal conditions, most such devices can result in low-level external exposure to members of the public of the order of microsieverts. For example, the IAEA recommends a procedure to determine whether the shielding or collimator in the device contains DU by using a dose rate meter held close to the suspected DU material. A dose rate reading more than 2 μSv/h above the background level indicates the potential presence of DU [I46].

D. Military use of nuclear and radioactive materials

432. The most significant impact on public exposure associated with the military use of nuclear and radioactive materials is due to global fallout from the testing of nuclear weapons. All types of tests—atmospheric, underground, and underwater—have created legacy sites that have had an impact on the surrounding environment, but only atmospheric tests have contributed significantly to global fallout and exposures at local and regional levels.

433. Nuclear weapons tests were carried out at various locations by eight countries—China, Democratic People's Republic of Korea (DPRK), France, India, Pakistan, United Kingdom, United States, and the former Soviet Union. In all, 530 atmospheric tests were conducted between 1945 and 1980—although testing was most active between 1952 and 1958 and between 1961 and 1962—with a total fission and fusion yield of 440 Mt [U19] (see electronic attachment 4-A). After the Treaty Banning Nuclear Weapons Tests in the Atmosphere in Outer Space and Under Water was signed in 1963, tests of nuclear weapons

were mainly conducted underground. It has been estimated that there have been 1,882 underground nuclear weapons tests in total. This figure is a slight increase to the number of 1,877 reported in a UNSCEAR 2008 Report, annex B [U19], as it includes an additional five tests performed by the DPRK since 2008 [D15]. Some radionuclides were unintentionally vented during a few underground tests, although data remains insufficient to assess their radiological impact. Excluding the tests performed by the DPRK, India, and Pakistan, the total yield of the underground tests was estimated to be 90 Mt [U19]. The debris from these tests remains underground but is a potential source of human exposure.

434. This section primarily addresses public exposures associated with global fallout from nuclear weapons tests and legacy sites from the production and testing of nuclear weapons. Public exposure resulting from nuclear weapons programmes and other military uses including the use of depleted uranium in ammunition are also considered in this section.

435. The radiological consequences of the explosion of atomic bombings over the cities of Hiroshima and Nagasaki (Japan) in August 1945 was not included in this annex since this topic has not been discussed in previous UNSCEAR reports; however, a short summary of the public exposure has been included for completeness.

1. Outline of dose assessment methodology

436. Detailed data on the deposition of radionuclides on the Earth's surface as a function of time and geographical latitude due to global fallout from nuclear weapons tests are available and the Committee has developed a robust methodology to assess public exposure, which allows doses to be updated and refined when new environmental and dosimetric models become available. The methodology adopted in this annex to estimate public doses due to global fallout is largely the same as the one used in the UNSCEAR 2000 Report, annex A [U15]. Minor changes were made to the methodology to estimate doses from external exposure to account for updated dose coefficients from ICRP Publication 144 [I77].

437. For the calculation of doses to the public from external exposure, the only radionuclide currently of interest is ^{137}Cs, and its decay product ^{137m}Ba, in soil, given that more than 40 years have elapsed since the last atmospheric test. Based on recent information for soil depths reported for ^{137}Cs, the Committee adopted for this annex the same approach described in the UNSCEAR 2020/2021 Report, annex B [U29], as a more realistic exponential distribution of ^{137}Cs in soil rather than using a planar source (0.5 g/cm^2) [B15] and an attenuation function. Relaxation mass depths of 10 g/cm^2 or 20 g/cm^2 correspond reasonably well to the reported soil depths for ^{137}Cs in global fallout, for a range of soil bulk of ^{137}Cs+^{137m}Ba densities. Updated, age-dependent dose coefficients from ICRP Publication 144 [I77] for ^{137}Cs+^{137m}Ba and for ^{125}Sb were used in this annex (see appendix A and electronic attachment A-4). These coefficients are based on exponential distributions of the radionuclide for various relaxation mass depths, which were selected to allow for increased migration of the radionuclides into soil over time.

438. Updates to the methodology for evaluating doses from ingestion due to radioactive discharges [U24] have not been implemented to estimate doses from global fallout because doses for this exposure pathway were expected to be very low. The dose estimates for ^{3}H and ^{14}C are based on global specific-activity models as described in the UNSCEAR 2000 Report, annex A [U15]. Doses from inhalation were assessed as only occurring when tests took place and used dose coefficients compiled in ICRP Publication 119 [I73]. These are the same dose coefficients for inhalation for members of the public that were used for the UNSCEAR 2008 Report, annex B [U19].

439. For other military sources of radiation, information on the radiological conditions usually does not contain complete datasets needed to enable the Committee to perform an independent assessment of public

doses. Due to the many types and sources of public exposure associated with legacy sites from testing and production of nuclear weapons and the numerous exposure scenarios, previous UNSCEAR reports [U15, U19] did not include specific assessment methodologies on this topic but relied on data on public exposure published in literature, information compiled by international organizations or submitted through the UNSCEAR Global Survey on Public Exposure. This approach was retained for this annex.

2. Exposures from global fallout

440. The UNSCEAR 2000 Report, annex C [U15] estimated worldwide annual average doses by radionuclide and exposure pathway (external exposure, inhalation, and ingestion) for various periods from 1945 onwards. Except for ^{3}H and ^{14}C, these dose estimates were based on the time-integrated cumulative deposition densities provided in the UNSCEAR 2000 Report, annex C [U15]. Table 39 gives worldwide annual average doses to adults for the period 1945–1999 and 2000–2099. Doses for the period 1945–1999 are the same as those in the UNSCEAR 2000 Report, annex A [U15]. The worldwide annual average dose to adults from ingestion for the period 2000–2099 was estimated at 139 μSv; ^{14}C was the predominant radionuclide (120 μSv), with lower contributions from ^{137}Cs (10 μSv) and ^{90}Sr (8.6 μSv). As a result of changes to the dose coefficients for external exposure and other parameters, the revised worldwide annual average dose to adults from external exposure has been estimated at 78 μSv, almost entirely due to ^{137}Cs. The total worldwide annual average doses due to global fallout for the period 2000-2099 previously reported as 253 μSv [U19] has been revised to a value of 217 μSv. Age-dependent estimates of the doses are provided in electronic attachment A-4.

Table 39. Estimated individual average doses due to global fallout received by the world population [B46, U13, U15][a]

Radionuclide	*Adult dose received in 1945–1999 (μSv)*				*Adult dose to be received in 2000–2099 (μSv)*
	External exposure	*Inhalation*	*Ingestion*	*All pathways*	*All pathways*
^{3}H			24	24	0.10 (ingestion)
^{14}C			144	144	120 (ingestion)
^{54}Mn	19	0.1		19	
^{55}Fe		0.01	6.6	6.6	
^{89}Sr		2.6	1.9	4.5	
^{90}Sr		9.2	97	106	8.6 (ingestion)
^{91}Y		4.1		4.1	
^{95}Zr	81	2.9		84	
^{103}Ru	12	0.9		13	
^{106}Ru	25	35		60	
^{125}Sb	12	0.1		12	0.003 (external)
^{131}I	1.6	2.6	64	68	
^{140}Ba	27	0.4	0.5	28	
^{141}Ce	1.1	0.8		1.9	
^{144}Ce	7.9	52		60	

Radionuclide	*Adult dose received in 1945–1999 (μSv)*				*Adult dose to be received in 2000–2099 (μSv)*
	External exposure	*Inhalation*	*Ingestion*	*All pathways*	*All pathways*
^{137}Cs	166	0.3	154	320	88 (external and ingestion)[b]
^{239}Pu		20		20	
^{240}Pu		13		13	
^{241}Pu		5		5	
Total	**353**	**149**	**492**	**994**	**217**

[a] Adapted from UNSCEAR 2008 Report, annex B, table 36 [U19].

[b] 78 μSv from external irradiation and 10 μSv from ingestion.

441. Figure XX is a revision of figure XXVII of the UNSCEAR 2008 Report, annex B [U19] showing updated doses for the period 2000–2024. The average annual individual effective dose to the global population for the period 2020–2024 was estimated at 3 μSv.

Figure XX. Global fallout doses for the period 1945–2024

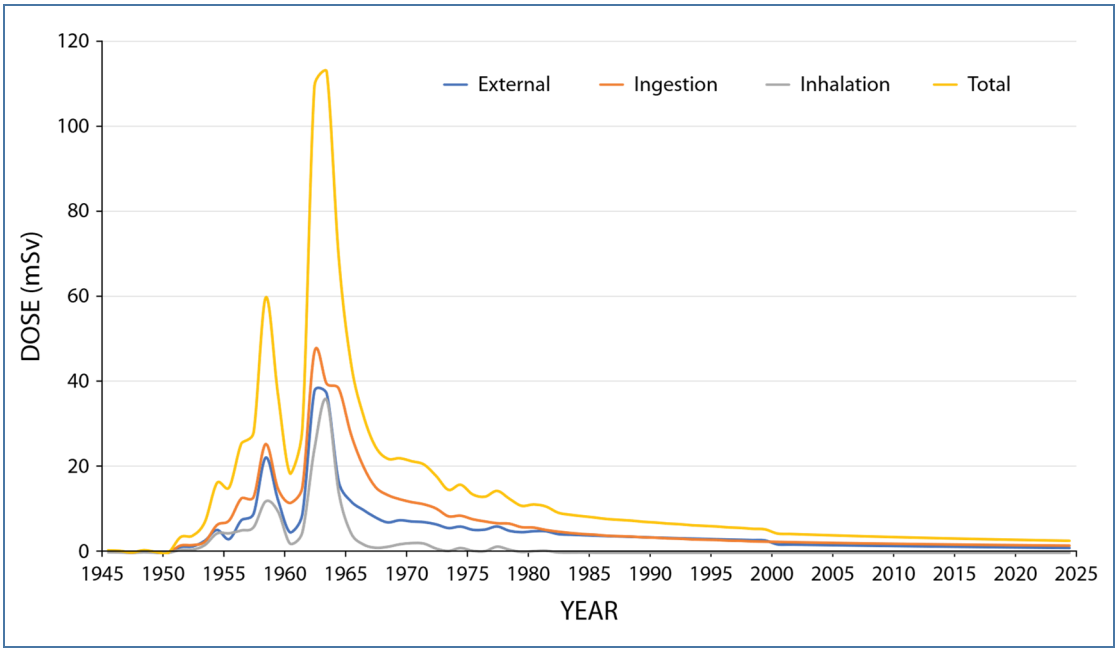

442. In response to concerns about the extent and impact of global fallout, the island of Guam was included in aerial surveys from 1952 [N29], while a monitoring station was operated on the island from 1954 [E28, H8], as part of the global fallout monitoring system. Guam is part of the Northern Mariana Islands in the South Pacific and a United States territory. It was not used as a site for any nuclear weapons testing and it is located approximately 1,900–2,200 km west of Enewetak and Bikini Atolls in the Marshall Islands, where major nuclear weapons testing occurred between 1946 and 1958. Radionuclide activity concentrations in samples of fish, plants, and soil collected in Guam in 1975 were similar to those measured in comparable samples from other Pacific Islands (Palau, Ponape, and Truk) and lower than those measured in the Marshall Islands [N13]. Hamilton [H6] concluded that deposition of fallout in Guam was consistent with worldwide values and that the annual external dose

in Guam in 2001 was about 0.017 mSv. The United States National Research Council [N29] estimated that fallout in Guam during the period of nuclear weapons testing in the Pacific was similar to that in other parts of the United States and its territories and concluded that the estimated annual dose to residents of Guam from nuclear weapons testing was a small fraction of the dose received by these residents from natural sources of radiation [N29].

3. Public exposure after military uses of nuclear devices

443. In August 1945, at the end of World War II, two atomic bombings were detonated over the Japanese cities of Hiroshima and Nagasaki. The atomic bombing deployed over Hiroshima used enriched ^{235}U as its fissile material and had an energy yield equivalent to 16 kt of 2,4,6-trinitrotoluene (TNT), while the atomic bombing deployed over Nagasaki used ^{239}Pu, and had an energy yield equivalent to 21 kt of TNT [J21]. The explosions were followed by localized radioactive fallout of fission products, including some settling on the ground described as 'black rain'. The death tolls from the detonations of the nuclear weapons up to the end of 1945 were estimated to be between 130,000 and 150,000 in Hiroshima and between 60,000 and 80,000 in Nagasaki [J8]. The causes of death included burns, mechanical injury, and radiation sickness from exposure to gamma radiation, although the contribution of these causes to the deaths varied significantly between the two detonations [J8].

444. The Radiation Effects Research Foundation (RERF) has published two reports on radiation dosimetry related to the atomic bombings in Japan. The reports estimated the radiation exposure to organs resulting from the explosions and residual radioactivity in the environment using a methodology known as Dosimetry System 2002 (DS02) [J21, R16]. Dose estimates received by the civilian population as a function of distance from the epicenter are shown in electronic attachment A-4; doses received by the public up to 1 km away from the epicenter of the explosions were more than 4 Gy for Hiroshima and 8 Gy for Nagasaki. Some more recent work by RERF has revised its estimates of organ doses based on corrections to the locations of the survivors [C65]. Exposure from the initial blast was due to gamma radiation and neutrons; the impact of residual radionuclides on individuals varied based on their habits, making it a challenge to provide general assessments.

445. According to the calculations performed with DS02, doses from external exposure to gamma ray to an individual near the epicenter of the Hiroshima blast ranged from 120 Gy immediately after the blast to 130 mGy for an individual accessing the area one day after the explosion and staying for a full day. The dose would decrease to 2 mGy for an individual accessing the area one week later and staying for one week. However, the accuracy of these calculations is difficult to determine as their uncertainty can be significant depending on conditions. Consideration was given to the internal exposure through inhalation or ingestion of radioactive materials on individuals visiting the city shortly after the explosion or engaging in activities, such as searching for survivors or disposing of corpses [H20].

446. The RERF has also responsibility for conducting the Life Span Study, a cohort study consisting of about 120,000 survivors who have been followed since 1950. Cohorts of in utero survivors and survivors' children, which include about 3,600 and 77,000 subjects respectively, have been followed since 1945. Radiation doses were estimated based on bombing location and shielding conditions. Exposures received by the Life Span Study participants, estimated using a recent revision of the DS02 dosimetry system (DS02R1), are provided in electronic attachment A-4. Approximately 2,200 people in the cohort received doses greater than 1 Gy while 45% of the people in the cohort received doses of less than 5 mGy [C65]. More detailed information can be found on the RERF website [R17].

4. Nuclear legacy sites (tests and residues)

447. Nuclear weapons tests produce short-term local, regional and global exposures as well as long-term exposures due to residual radionuclides that are still present in the environment [U15, U19]; nuclear weapons test legacy sites remain a potential source of public exposure. Areas within a few hundred kilometres of the test site are generally designated as local, while those within a few thousand kilometres are defined as regional. Local fallout may include as much as 50% of the total radioactive material produced by a surface test and includes large radioactive aerosol particles. Atmospheric nuclear weapons tests were conducted in relatively remote areas; therefore, in general, exposure of local populations did not contribute significantly to the global collective dose. However, individuals living downwind of the test sites received significant doses.

448. Six papers published in 2022 described an internally consistent method for the estimation of deposition of fallout radionuclides and both external and internal doses to humans from the deposited fallout, within a few hundred kilometres of the site of an atmospheric nuclear fission event [A31, B19, B49, M22, S46, T9]. The method emphasizes that doses received during the first year following an event constitute 90% of the lifetime dose from that event [B49]. This method is based on experience gained in estimating the deposition and doses from atmospheric weapons testing, including several nuclear legacy sites described in this annex, such as the Trinity Test in New Mexico (USA) and the Nevada National Security Site (NNSS) in the United States; Marshall Islands; French Polynesia and Semipalatinsk (Kazakhstan). Locations of all nuclear weapons test sites are provided in figure XXI.

Figure XXI. Sites of nuclear weapons tests [U19]

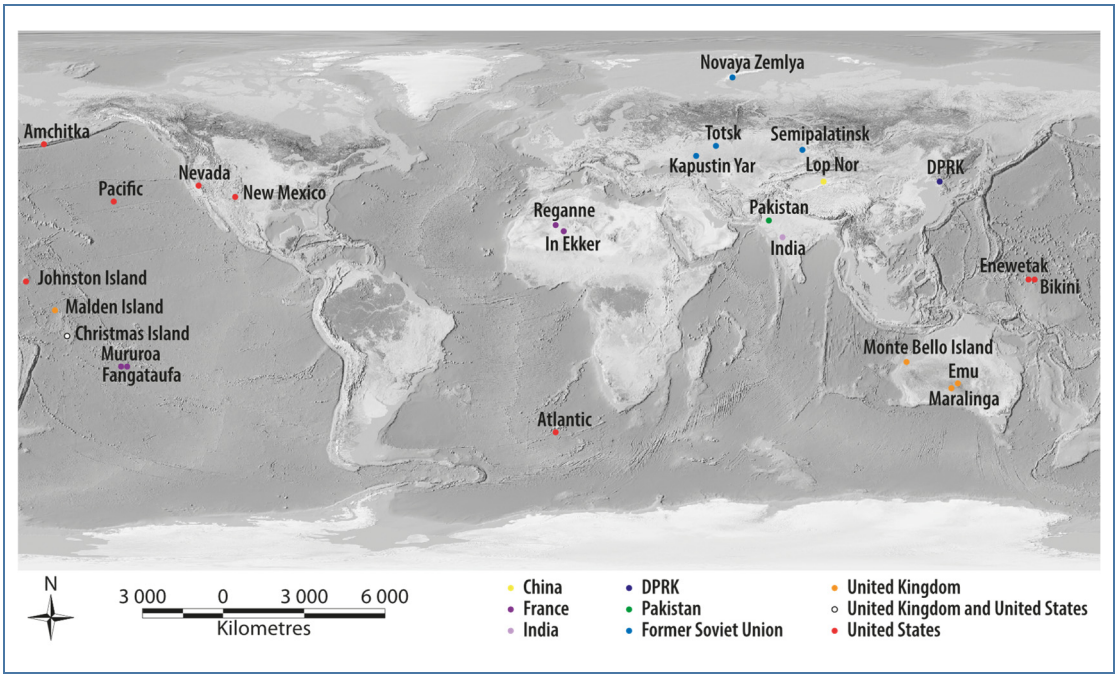

(a) *United States*

Nevada

449. The Nevada National Security Site (NNSS), formerly known as the Nevada Test Site, in the United States was the location of 86 atmospheric nuclear tests carried out between 1951 and 1962 [S41, U39]. In addition, 38 of the approximately 800 underground tests at the site involved releases of radioactive material that were detectable offsite but did not contribute significantly to public exposure in comparison with the atmospheric test releases [S41, U39]. A comprehensive review of the radiological effluents released from these tests between 1961 and 1992 was performed by the United States Department of Energy [S22]; however this review did not include an assessment of doses relating to leakage from underground tests.

450. Estimates of doses from external exposure due to atmospheric tests at the NNSS were derived from survey meter and film badge measurements of approximately 180,000 people living in 300 communities in an area within 300 km of the test site, including locations in the states of Nevada, southwestern Utah, and parts of Arizona and California [A29, A30, S41]. Most individual doses, accounting for shielding, were estimated to be less than 5 mSv [S41]. The population-weighted average was 2.8 mSv, with the highest doses being in the range of 60–90 mSv. Exposures resulted primarily from short-lived gamma emitters, with half-lives of less than 100 days. Collective doses to the population within 300 km and 800 km of the test area due to external exposure were estimated at about 500 person Gy and 12,000 person Gy, the latter value arising primarily from exposure in areas with large populations [A29, S41].

451. Doses from internal exposure resulting from atmospheric testing at the NNSS were estimated from deposition measurements using an environmental transfer model [S41]. Absorbed doses to organs and tissues from internal exposure were substantially lower than those from external exposure, except for the dose to the thyroid, for which ingestion of ^{131}I in milk contributed relatively higher doses. Estimates of absorbed doses to the thyroid in 3,545 individuals living in the vicinity of the site ranged from 0 to 4.6 Gy, with an average of 98 mGy [S41, T10].

452. Current annual dose from all exposure pathways to the maximally exposed individual[10] was estimated to be 6 μSv [U42], mostly due to ingestion of 20 kg of game meat (5.4 μSv), with contribution from inhalation being 0.61 μSv.

New Mexico, Trinity Test

453. The first nuclear weapons test ever carried out was the Trinity Test, which took place on 16 July 1945 in New Mexico [S45, W9]. Until recently, no assessment of public exposure from this event [C1, S44, S45, W9] had been undertaken, and the Trinity Test was not included in previous UNSCEAR reports on public exposure.

454. The Trinity Test involved a plutonium implosion device of the type dropped on 9 August 1945 over Nagasaki (Japan) [W9]. The device was placed atop a 30.5 m (100 ft) shot tower located at ground zero on the Alamogordo Bombing and Gunnery Range in New Mexico. Several ranches were located in an area within 48 km of ground zero, the nearest being 19 km away, while 14 small towns were also in the area within 48 km of ground zero, five of which were at a distance of 32 km or less. Two towns

[10] Maximally exposed individual is a concept used in the United States defined as a hypothetical member of the public at a fixed location who, over an entire year, receives the maximum effective dose equivalent (summed over all pathways) from a given source of radionuclide release.

with populations of at least 1,000 people were located at a distance of just over 48 km from ground zero, The United States Army operated a monitoring programme during and after the test, which provided some information on dose rates at various times and locations following the test, albeit with early instrumentation and limited capabilities.

455. The device that detonated during the Trinity Test contained approximately 6 kg of ^{239}Pu as its sole fissile material, with an often cited yield of 21 kt of TNT equivalent [B18, W9]. Following the explosion, the highest deposition of fallout was detected in a region approximately 160 km long and 48 km wide, extending to the northeast from ground zero [W9]. Field measurements of exposure rates recorded on the day of the test "ranged as high as 15 R/h (0.14 Sv/h)", "vicinity of 20 R/h (0.19 Sv/h)", and "off scale". Estimates of total accumulated external exposures over 14 days were as high as 139 R (1.3 Sv), uncorrected for height or shielding, in an area that came to be known as Hot Canyon. Isopleths of the measurements taken after the test are presented in figure XXII. No measurements to determine internal exposures were made following the test, although members of the public were certainly exposed through inhalation and ingestion of contaminated water and food products [W9].

456. The heaviest fallout was toward the area northeast and north of ground zero, but the whole area to the east, north, and some distance to the west was affected (see figure XXII) [B48, C12, Q3]. For each geographic area in the state of New Mexico (31 counties in 1945) the exposure rates and times of arrival of fallout were assessed [B48]. These data were used to estimate the external doses in each precinct and the deposited activity for each of 63 radionuclides (activation and fission products and $^{239+240}$Pu). Normalized time-integrated activity concentrations in air, foods, and drinking water were calculated and used to estimate internal doses. Six population types living in New Mexico in 1945 were categorized in terms of location and ethnicity to characterize their diet and other habits [P32, S45].

457. Simon et al. [S45] estimated absorbed doses during the first year after the Trinity Test to five organs or tissues—thyroid, red bone marrow, colon, stomach, and lungs—from external and internal irradiation from 63 radionuclides as a function of diet, age, and location. Dose estimates for the 721 precincts were summarized in terms of population-weighted average doses by county, ethnicity, and age group. Doses from external exposure from the Trinity Test ranged up to 100 mGy immediately downwind of ground zero, but in most areas were considerably lower; and most organ doses were also low. Individuals living in locations not on the centre line of the deposition pattern generally received doses at least a factor of 1,000 lower than those along the centre line. Thyroid doses were larger than the doses from external exposure, reaching values up to 250–350 mGy for 1 to 2-year-olds in some counties. The most important exposure pathway contributing to internal doses to the thyroid was ingestion of cow's milk, followed by consumption of drinking water, leafy vegetables, fruits and berries predominantly from ^{131}I and ^{133}I, with smaller contributions from ^{131m}Te, ^{132}Te and ^{135}I. Cahoon et al. [C1] provided a summary of the population-weighted average organ doses by age group for the state, the five counties most affected by fallout from the Trinity Test, and the remaining counties.

458. Currently, the site remains within the boundaries of the White Sands Missile Range under the control of the United States Air Force. Public access to the site is limited to open visits twice a year, and doses to visitors were estimated to be less than 10 μSv per visit [H7]. Based on available data from soil sampling and modelling, Beck et al. [B18] estimated that approximately 60% of the non-fissioned plutonium had been deposited within 100 km of the detonation site, and 80% deposited within the state of New Mexico. Most of the fallout plutonium was expected to be fixed on large, non-respirable particles, limiting exposure from inhalation. Given the time elapsed since the test, plutonium has migrated through the soil and is no longer available for resuspension and inhalation; therefore, the remaining plutonium from the Trinity Test is not considered to pose a radiological hazard to members of the public.

Figure XXII. Isopleths of exposure rates at 12 hours after the Trinity test (adapted from [B48])

Note: The isopleths are derived from measurements of exposure rate (mR/h) conducted during the first days following the test. Fuzzy spots show the locations of the eight cities with 1945 populations greater than 10,000. The approximate centre line of the fallout is represented by two segments [C12]

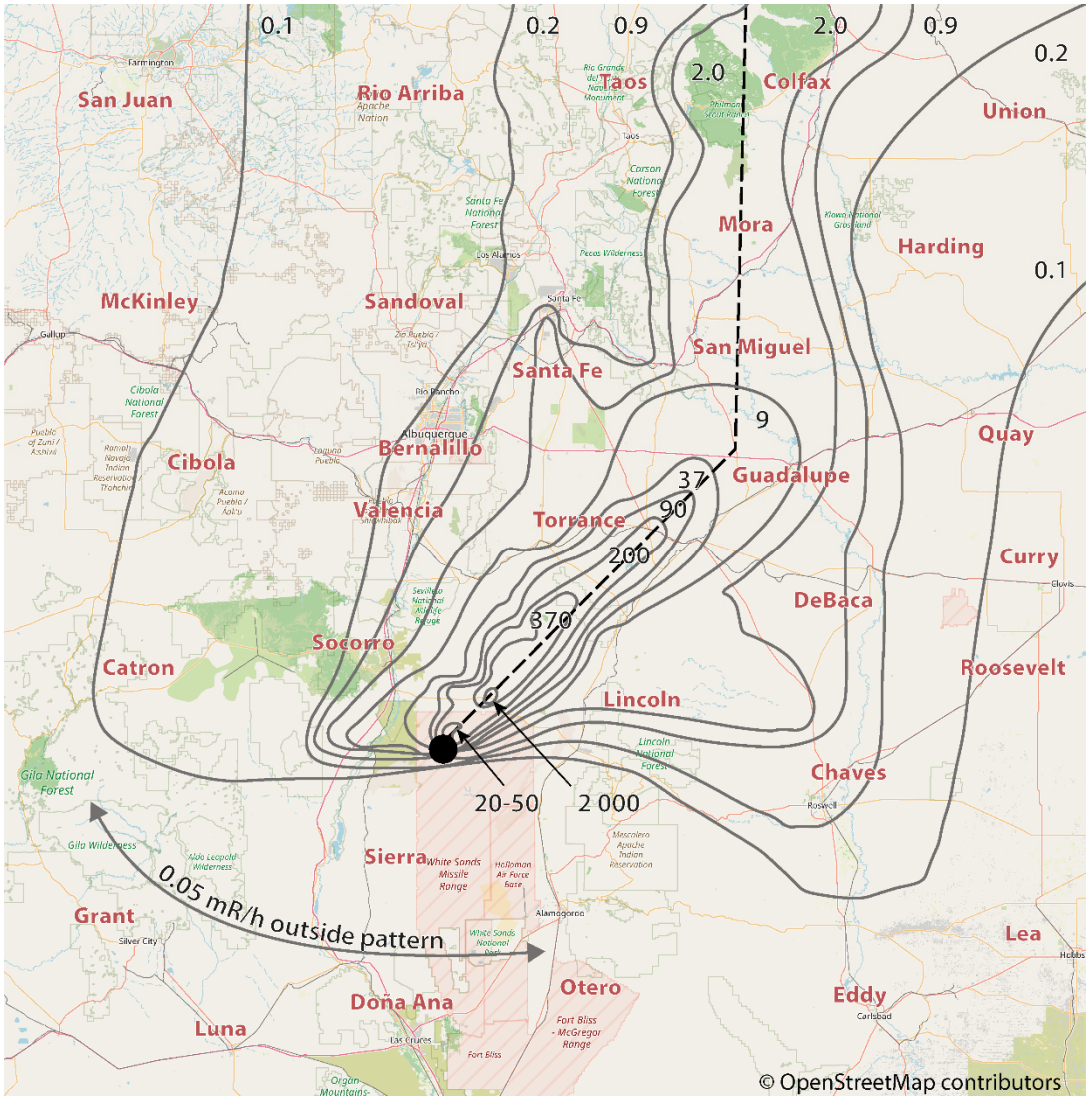

Bikini and Enewetak Atolls, Marshall Islands

459. Bikini and Enewetak Atolls in the north-western end of the Marshall Islands, were the sites of 66 nuclear weapons tests carried out by the United States between 1946 and 1958. Twenty of these tests resulted in measurable fallout over the Marshall Islands in areas away from the test sites [S40, S42]. A substantial body of literature describes the history of nuclear weapons testing in the Marshall Islands and its aftermath [N17, S38], assessments of the ground deposition and continued presence of radioactivity in the environment [A2, B17, B58, C51, H40, R24, S39, W4], estimates of external and internal doses to members of the public [B47, L18, M46, R23, S42, S43, S75], resulting health effects or health risks to members of the public [C55, H33, L2, S42], and the prospects for resettling evacuated areas [I4, R25]. The Committee has previously provided summaries of public exposure due to nuclear

weapons testing in the Marshall Islands [U15, U19], and a map of the test sites and evacuation locations is provided in electronic attachment A-4.

460. Bikini Atoll was the site of 23 underwater, ground level, and above ground nuclear weapons tests [U39]. An additional test was carried out about 100 km west of Bikini Atoll in 1958 [S40]. Enewetak Atoll was the site of 43 tests [U39]. The total explosive yield for the 66 tests was 108 Mt TNT equivalent, of which 76.8 Mt was from tests at Bikini Atoll and 31.6 Mt was from tests at Enewetak Atoll [S40, U39]. A summary of the 20 tests presumed to have contaminated parts of the Marshall Islands beyond the immediate test locations is provided in electronic attachment A-4 [S42]. These tests included several thermonuclear devices, with fusion yields ranging from 0.04 to 6 Mt TNT [S42].

461. The largest thermonuclear device ever exploded at Marshall Islands was Castle Bravo, which was detonated on 1 March 1954 at Bikini Atoll, yielding 15 Mt TNT equivalent, including a fusion yield of 6 Mt TNT equivalent [S40, S42, U39]. The total explosive yield of Castle Bravo was three times the expected yield and twice the expected upper limit [S38]. At the time of the test, winds above 17,000 feet caused heavy fallout east of Bikini Atoll at Rongelap, Ailinginae, Rongerik, and Utrik Atolls [B17], while lower levels of fallout were detected at more distant atolls southeast of Bikini Atoll, including two of the most populated atolls, Kwajalein Atoll and Majuro Atoll [B17, S38]. This test resulted in the exposure of the population of Rongelap and Utirik, United States service personnel and the crew of the Japanese fishing vessel Daigo Fukuryu Maru (Lucky Dragon). Estimates of doses to these groups have been previously reported by the Committee in the UNSCEAR 2008 Report, annex B [U19].

462. Beck et al. [B17] estimated the total deposition of 63 radionuclides on all inhabited islands from each of the 20 tests that were presumed to have contaminated inhabited islands. Several radionuclides contributed to external and internal doses immediately after each test; however, in the long-term, ^{137}Cs+^{137m}Ba were the most radiologically significant. The dose assessment took account of the transfer of ^{137}Cs through the environment over time and, whenever relevant, of the relocation of various groups of people; in all, doses were calculated for 26 population groups as shown in electronic attachment A-4 [B47, S43].

463. Simon et al. [S42] estimated the total internal doses to four organs—red bone marrow, thyroid, stomach wall, and colon—and external whole-body dose, for acute and chronic exposures, for four representative population groups living on the islands of Majuro, Kwajalein, Utrik, and Rongelap. Table 40 presents the population-weighted average total organ doses to adults of these four population groups from all tests. Doses to the population of Rongelap Island were the highest, several times greater than those to the population of Utrik Island.

464. The average uptake of ^{239}Pu by adult residents of Enewetak Atoll has been estimated at 4.7 Bq, with an average committed dose of 0.2 mSv to age 70 years [S75]. This estimate was based on urine samples collected in 1989 and 1991, following repatriation of the people of Enewetak Atoll in 1980 and assumed constant intake from 1980 to 1990. The assessment is supported by more recent assessments of exposure to the inhabitants of the Marshall Islands [I60].

465. Ambient dose equivalents were measured in 2015 at Enewetak, Rongelap, and Bikini Islands. Enewetak Atoll was remediated prior to resettlement and measurements of annual dose ranged from 0.0048 to 0.166 mSv, with a mean value of 0.076 mSv. The average ambient annual dose equivalents on Rongelap and Bikini Islands were estimated to be 0.198 and 1.84 mSv, respectively (range for Bikini Island: 0.10–6.48 mSv). These measurements do not account for shielding or time spent in various locations [B39].

Table 40. Population-weighted average total dose to adults of four groups of atolls and/or communities [S42]

Grouping is based on similar levels of deposition of total ^{137}Cs. Range in parentheses represents the minimum and maximum total dose within the group of atolls or communities. All values are rounded to two significant digits

Atoll or population group	*Total dose to red bone marrow–mGy (range)*	*Total dose to thyroid–mGy (range)*	*Total dose to stomach wall–mGy (range)*	*Total dose to colon mGy (range)*
Southern latitude [a]	10 (6.1–43)	30 (17–75)	10 (6.0–39)	14 (8.0–49)
Mid-latitude [b]	37 (24–65)	130 (89–220)	38 (24–66)	56 (36–100)
Utrik community [c]	160	890	170	340
Rongelap Atoll/ Ailinginae/ Rongerik evacuees [d]	1 000 (500–1 600)	5 900 (3 000–9 200)	1 400 (700–2 100)	2 800 (1 400–4 400)
All	**29 (6.1–1 600)**	**124 (17–9 200)**	**32 (6.0–2 100)**	**56 (8.0–4 400)**

[a] Ailinglaplap, Arno, Aur, Ebon, Jaluit, Kili Island, Lae, Lib Island, Majuro, Maloelap, Mili, Namorik, Namu, Ujae and Kili Islands were the primary residence locations of the Bikini Atoll community during the testing years. Majuro includes Majuro permanent residents and Rongelap control group.

[b] Ailuk, Kwajalein, Likiep, Mejit Island, Ujelang, Wotho, Wotje and Ujelang were the primary residence locations of the Enewetak community during the testing years.

[c] Utrik and atoll of relocation.

[d] Rongelap, Ailinginae, Rongerik, and atolls of relocation.

Johnston Island

466. Johnston Atoll is located about 1,330 km southwest of Honolulu, Hawaii (United States). The largest island in the atoll, Johnston Island, was used by the United States as the launch site for 12 high-altitude nuclear weapons tests: two in 1958 and ten in 1962 [S40, S41, U39]. An additional four tests launched from Johnston Island in 1962 were aborted before detonation of the nuclear devices and are not included in the list of nuclear weapons tests conducted by the United States [B22, N24, U36, U39]. Three of the aborted tests resulted in radioactive contamination on or near the atoll; in particular, extensive residual contamination of alpha-emitting radionuclides occurred in the aftermath of a launch pad fire [B22, D28, J2, N24, R1, S41, V16]. The radionuclide contamination was primarily in the form of particulate debris from the rockets or weapons [B22, J2, R1, S41, W21]. The 12 successful tests contributed to global fallout; local fallout did not occur [B22, S41]. The island has been extensively surveyed and remediated [B22, D28, J2, R1, V16, W12, W13].

467. There is no evidence of native populations ever having lived on Johnston Atoll [S41], and the closest populated islands are those of Hawaii. Non-essential personnel were evacuated from the atoll during every test [B22, R1] and it is believed that no members of the public were within the immediate area to be exposed to the radioactive debris from the aborted tests. Johnston Atoll is not accessible to the public [U50, U51]; access is generally limited to personnel and volunteers with the United States Fish and Wildlife Service. Therefore, exposures to members of the public are currently limited to a very small number of people, generally for no more than about six months at a time.

Amchitka Island

468. Amchitka Island is part of the Aleutian Island chain of Alaska and was the site of three underground nuclear tests carried out by the United States: Long Shot in 1965; Milrow in 1969; and Cannikin in 1971. With a yield of approximately 5 Mt TNT, Cannikin was the largest United States underground test [D4, S27, U39]. The island is uninhabited, but it is part of the large area used for subsistence fishing and hunting by the Aleuts, the indigenous people living on Aleutian Islands. The Bering Sea to the north and the North Pacific Ocean to the south of Amchitka Island are important commercial fishing areas [B57, B61, B62, B63, D4, U35] and, therefore, any radionuclides released from the test locations could potentially lead to exposure of members of the public through consumption of seafood and wildlife.

469. Following the 1965 Long Shot test, trace quantities of ^{3}H, ^{85}Kr and ^{131}I were detected in samples of water and soil gas taken from the immediate area of the detonation site [D4, S27], but only ^{3}H was detectable one year after the test [S27], and its concentrations declined significantly in the following years [D4, S27, S35]. The peak activity concentrations of ^{3}H in water samples measured in 1966 near the Long Shot test site were of similar levels to those measured throughout the 1960s in rainfall at Adak Island, 300 km east of Amchitka; and at continental locations in the United States and Europe [S27]. No migration of radionuclides was observed following either the 1969 Milrow or 1971 Cannikin tests [S27], although there was some venting of ^{85}Kr, ^{3}H, and ^{14}C from a Cannikin post-shot drill pipe in 1972 [D4]. Plutonium concentrations measured in various terrestrial and marine biota have always been very low [B57, D4, U35, U42]. The ratios of ^{240}Pu to ^{239}Pu are consistent with plutonium originating from atmospheric deposition from global fallout, and a secondary marine source, likely to be the nuclear weapons tests in the South Pacific [B57].

470. Potential releases of radionuclides from the test locations on the Amchitka Island raised public concern, and the monitoring programme implemented in 2000 reflected a high level of public involvement, including the assistance of the Aleuts with the sampling of fish and wildlife using their traditional methods [B62, B63, P33, U42]. In general, radionuclide concentrations in environmental samples on and near Amchitka Island are comparable to those on the islands selected as measurement controls, Adak and Kiska [B57, B59, B60, B61, U42], and reflect primarily the contributions from global fallout, nuclear weapons testing undertaken by China, and the accidents at the Chornobyl NPP and Fukushima Daiichi NPS [B57, P33, S27, U42]. Currently, releases of radionuclides to the biosphere due to leakage from the test sites on Amchitka Island are considered unlikely [B57, U35, U42].

(b) *United Kingdom*

Montebello Islands, Australia

471. The Montebello Islands are a chain of remote uninhabited islands approximately 130 km off the Northwest Coast of Australia. In 1952 and 1956, the United Kingdom detonated a total of three nuclear devices in atmospheric tests at different locations across the islands (see electronic attachment A-4). The 1952 test, known as Operation Hurricane, took place on board the naval ship HMS Plym harboured 700 m off Trimouille Island, while the two tests conducted in 1956, known as Operation Mosaic, were based on 31 m tall towers located on Timouille and Alpha Islands.

472. Public exposure resulting from the tests was assessed as part of the exposure of the Australian population to all nuclear testing [W15]. The total collective dose to the Australian population from the Montebello tests was estimated to be 172 person–Sv. Population centres across Northwestern Australia —Broome, Onslow, Port Headland—received the highest doses from the tests followed by population centres located in the same latitudinal band across Australia (i.e., Cloncurry, Townsville, Fitzroy Crossing). Doses are provided in electronic attachment A-4 [W15].

473. An assessment of possible exposure to visitors to the islands, now a marine park, was published by the Australian Radiation Laboratory [C49]. It indicated that inhalation of dust was the most significant pathway contributing to the exposure at specific sites, with a cautious estimate that an occupancy of three days at one site would result in a dose of 1 mSv. External exposure to gamma radiation was the next highest contributor with a minimum of eight days required at one site to receive a dose of 1 mSv. Doses from ingestion were assessed to be negligible and consumption of seafood in the region is not restricted. However, this assessment is more than 30 years old and exposures at the site are likely to have significantly changed since then. The site has been the subject of a recent investigation of radionuclide activity concentrations and re-evaluation of doses, the findings of which are yet to be published.

Emu and Maralinga sites, Australia

474. Emu and Maralinga are remote locations in the northwest of the state of South Australia (Australia) (see figure XXIII). Two nuclear weapons tests were performed as part of Operation Totem at the Emu site in 1953, while seven tests were carried out at the Maralinga site, with four being conducted under Operation Buffalo in 1956, and three as part of Operation Antler in 1957 [U15]. The United Kingdom also conducted hundreds of minor trials involving chemically generated explosions of radioactive material at Maralinga. These minor trials resulted in the dispersion of ^{239}Pu over some hundreds of square kilometres around Maralinga.

475. Estimates of collective doses to the Australian population for each test were published along with those for the tests that occurred in the Montebello Islands [W15]. Collective doses were estimated at 70 person–Sv and 60 person–Sv, respectively for the Totem tests 1 and 2 performed at Emu; 83 person–Sv, 11 person–Sv, 56 person–Sv and 101 person–Sv for the Buffalo tests 1–4; and 3 person–Sv, 28 person–Sv and 118 person–Sv for the Antler tests 1–3 all performed near Maralinga. The total collective dose to the Australian population from the Emu and Maralinga tests was estimated at 528 person–Sv.

476. More recently, estimates of the exposure to a group of Aboriginal people camped 170 km downwind from Emu Field during the Totem 1 test have been revised [W11]. This work included skin dose estimates and determined that an upper estimate of the effective doses received was of the order of 4 mSv during the time the Aboriginal group were located there.

477. The Emu and Maralinga sites underwent three rehabilitation programmes run by the United Kingdom in 1963, 1964 and 1967 and were finally rehabilitated by the Australian government between 1995 and 2000 [M8]. The subsequent dose assessment considered the use of the test sites for visitors as well as permanent occupancy and traditional use by the Tjarutja Aboriginal people. The report provided a maximum potential annual exposure of 3.6 mSv to 10-year-old children permanently residing in the worst affected 3 km^2 area; other annual doses estimated for permanent occupants were generally below or around 1 mSv. The report noted that the estimates were very cautious.

Figure XXIII. Maralinga and Emu sites

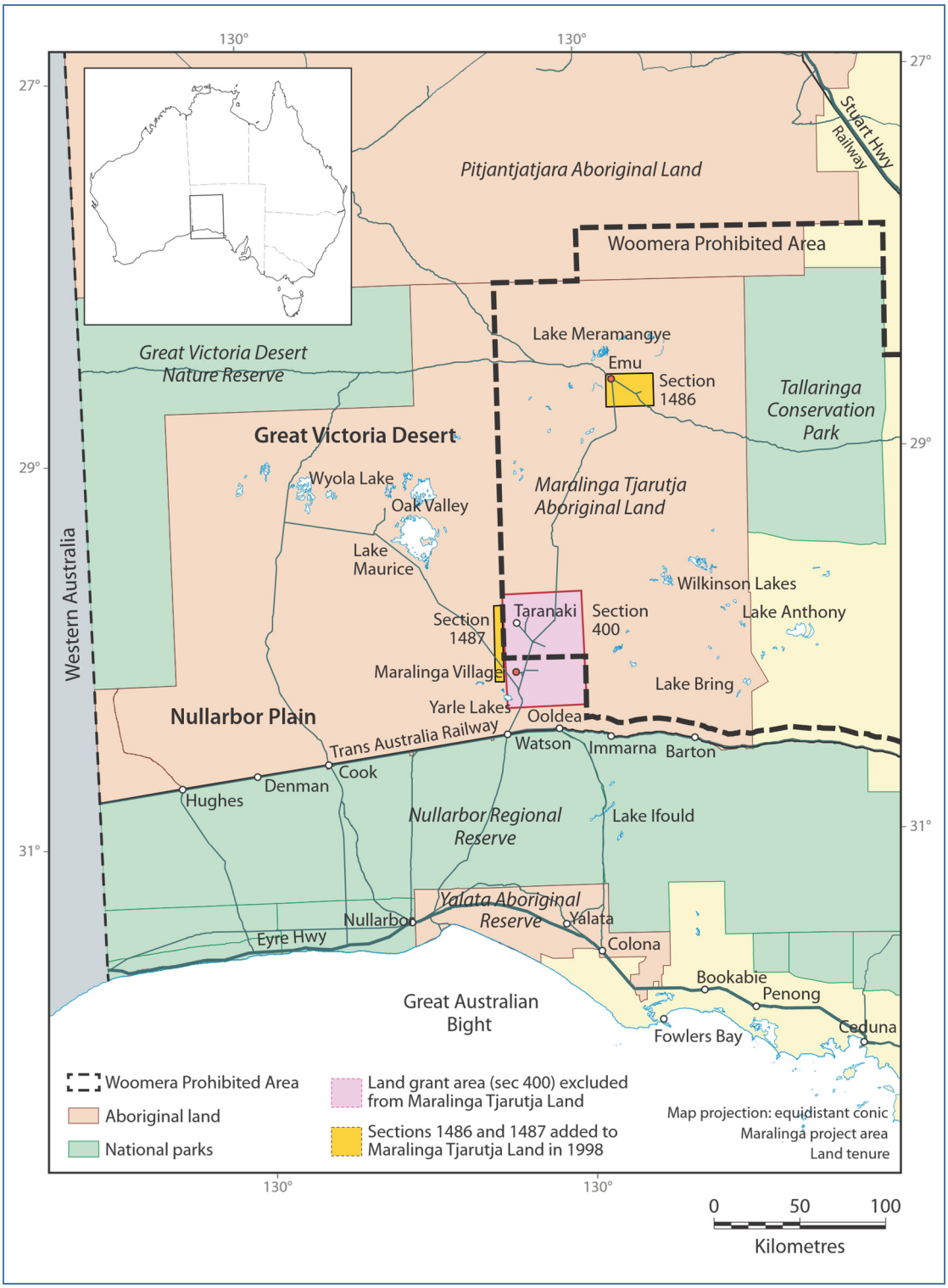

(c) *Joint test sites (United Kingdom and United States)*

Kiritimati (Christmas) and Malden Islands, Kiribati

478. Kiritimati (Christmas) and Malden Islands in Oceania were used by both the United Kingdom and United States to test nuclear military devices from 1957 to 1958 (Operation Grapple), and in 1962 (as part of Operation Dominic), respectively. Malden Island is uninhabited, while Kiritimati Island had a population of approximately 500 at the time of the tests.

479. The United Kingdom tested three devices on Malden Island in 1957, and another six tests were conducted at the southeast end of Kiritimati Island. In 1962, the United States, in an agreement with the United Kingdom, used Kiritimati Island for a series of 24 tests that took place in the vicinity of the island. All the tests that occurred on Kiritimati and Malden Islands were airburst over the ocean or explosion of devices suspended from balloons at 300–450 m above land. Local fallout is believed to have been minimal from this testing, and no reliable information has been found relating to exposures of public or civilian personnel involved in the tests [S41, U19].

480. Following clean-up operations at the sites, an environmental radiological survey was conducted and found that while traces of residual radionuclides from the tests were detectable in a few localized areas, the radiological conditions on Kiritimati Island did not present a risk to health or required any restriction on use; the annual dose from consumption of locally produced foods and water was estimated to be 0.01 mSv [M14].

(d) *Former Soviet Union*

Semipalatinsk

481. The Semipalatinsk Test Site (STS) was the largest site in the former Soviet Union used for the testing of nuclear weapons. It is located in the north-eastern territory of modern Kazakhstan. In total, 456 nuclear tests with 616 nuclear devices were carried out at the test site between 1949 and 1989, of which 340 were underground, 86 atmospheric, and 30 surface tests. The largest number of tests occurred in the early 1960s, when the transition from atmospheric tests to underground tests occurred [I5, L30, N7]. A map of the STS is provided in figure XXIV.

482. The experimental field site was the first area of the STS which was intended for near ground and high altitude atmospheric nuclear tests between 1949 and 1962. The site is characterized as a flat landscape typical of the plains of the dry Eurasian steppe, with a diameter of about 20 km and surrounded on three sides by low hills. The site is located about 50 km from the city of Kurchatov. The first test of a nuclear device at the experimental field was conducted on 29 August 1949; the site was also used for the first test of a neutron enhanced nuclear device on 12 August 1953. In total, 116 nuclear tests were conducted at the experimental field site, 86 of which were atmospheric and 30 were ground-based.

483. The Sary-Uzen and Balapan sites were used to conduct underground nuclear explosions in drill shafts. From 1965 to 1989, 105 tests were carried out in 106 wells and 167 nuclear charges were detonated, while 13 wells remained unused. A small difference between the sites was the depths of the charges and their yield: the average depth for Balapan was 650 m, while for Sary-Uzen it was about 250 m.

484. The Degelen Test Site was used to conduct tests of medium and low power nuclear weapons. The site is in the mountain range of the same name, which is a dome-shaped uplift measuring 17–18 km in diameter [L30, N7, P7]. The total area of the site is about 300 km^2. A total of 209 nuclear tests were conducted in 181 tunnels between 1961 and 1989. Of the underground tests, 13 resulted in the release of

radioactive gases to the atmosphere [U19]. A radioecological survey of the Degelen site showed that most of its territory had no residual fissile radioactive materials, since more than 90% of the radionuclides generated during past nuclear weapons tests was concentrated in the cavities of the tunnels. However, there are areas with increased concentrations of radionuclides in soil, water and vegetation [K37, L3, L30, P7, P30].

Figure XXIV. Map of Semipalatinsk Test Site [L31]

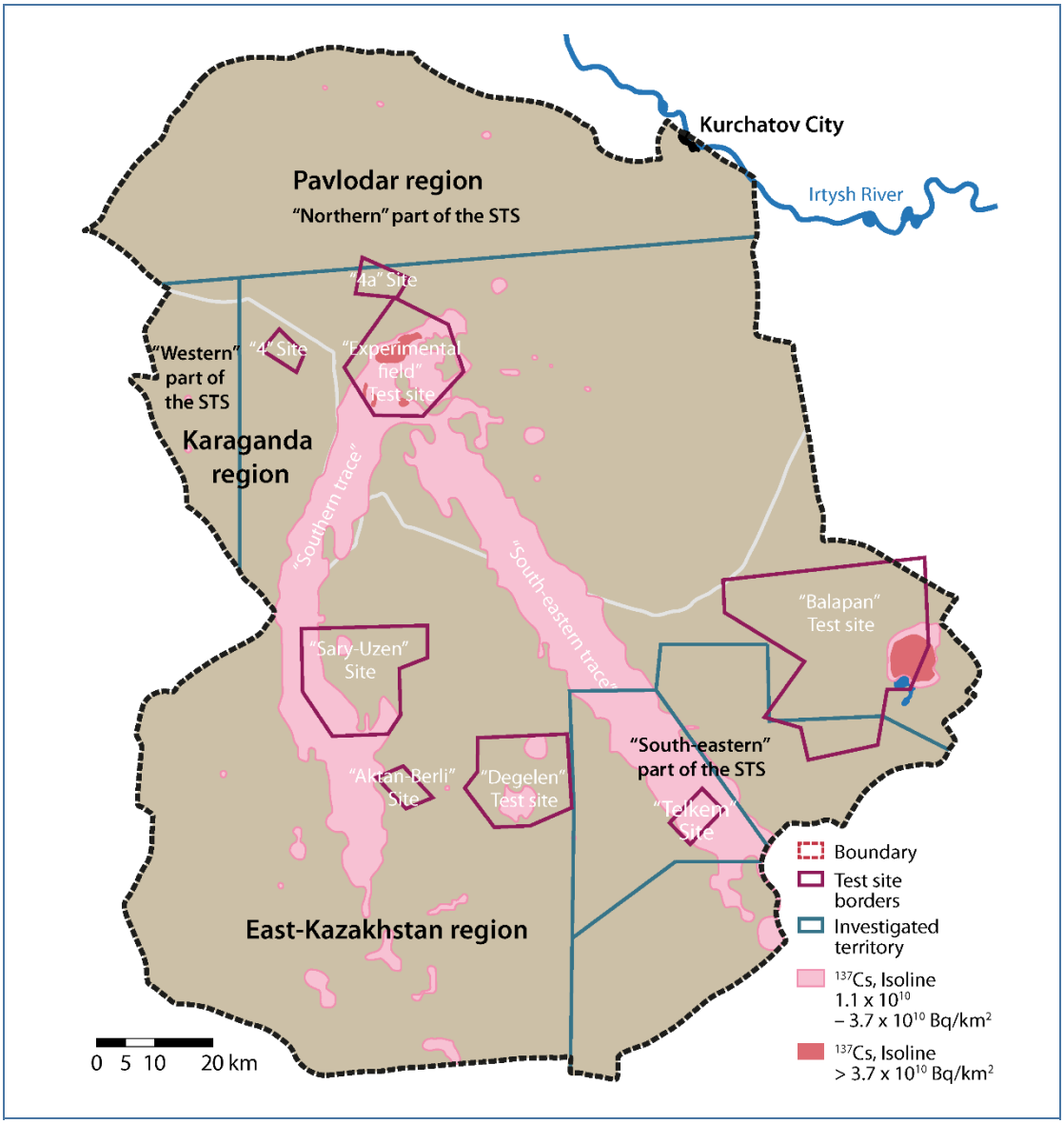

485. Radioactive clouds generated by the nuclear weapons tests at the STS went beyond the boundaries of the site, leading to the deposition of radioactive material on the adjacent areas. The main footprints of the fallout—known locally as traces—were directed in northeast, southeast and south directions. Radionuclides spread for hundreds of kilometres forming traces tens of kilometres wide. The only settlements within the STS in period when tests were carried out were the town of Kurchatov, north of technical area Š, built for servicing the test site, and the small settlements of Akzhar and Moldari along its northern edge. Two tests led to the most significant exposures of the population of Kazakhstan: the first test on 29 August 1949; and the first thermonuclear test on 12 August 1953. These and two

additional tests on 24 September 1951 and 24 August 1956, are considered to have contributed 85% of the total collective dose from all tests combined [U19].

486. Doses estimated by the Committee in the range of 0.2–0.9 Gy [U19] were revised using a more detailed methodology [B19, B49]. Updated whole-body doses to the residents in the Semipalatinsk area were estimated to range from 0.02 to 0.63 Gy [G22].

487. Following two missions to the site in 1993 and 1994, the IAEA concluded that residual radioactivity over most of the test site was low. The missions detected localized radioactivity at the ground zero of technical area Š and Lake Balapan areas which were described as heavily contaminated. The dose assessments carried out by the IAEA indicated that annual effective doses of 10 mSv could be received by individuals making daily visits to these sites and annual effective doses of the order of 100 mSv could be received if these sites became permanently inhabited. The estimates of annual effective doses to the nearby settlement of Dolon and other settlements were 0.14 mSv and 0.06 mSv, respectively [I5].

488. Surveys performed between 2012 and 2016 showed the presence of traces of radioactive fallout far beyond the test sites. The traces from the ground-based nuclear weapons tests extended from the experimental field almost to the borders of the STS with the width of traces being up to 15 km, and a length of over 100 km. Several radionuclides (^{60}Co, ^{90}Sr, ^{137}Cs, $^{239+240}$Pu, ^{241}Am, and Eu isotopes) were detected in soils withing these traces. The maximum activity concentrations in soils due to radioactive fallout were detected about 40 km from the epicentre of the tests [L4, L30].

489. Currently, the average activity concentrations of radionuclides from the tests in the soil of the most affected settlements—Dolon, Sarzhal, and Bodene—do not exceed the national reference levels [N8]. The water bodies of this territory and groundwater are used by the local population for drinking and household needs; activity concentrations of radionuclide levels in water do not exceed the WHO guidance levels [L30].

490. Measurements of activity concentrations of human-made radionuclides—^{137}Cs, ^{90}Sr, $^{239+240}$Pu and ^{241}Am—in food products of animal and agricultural origin were below 1 Bq/kg. However, activity concentrations of ^{137}Cs up to 260 Bq/kg were detected in mushrooms. Whole body monitoring of residents in settlements adjacent to the borders of the STS did not detect ^{137}Cs activity. It was estimated that the projected annual dose to the public, under the worst-case scenario, did not exceed 0.3 mSv. Special measures aimed at reducing the dose to the public by recultivating affected areas, limiting access and optimizing economic activities are not currently required [L30].

Novaya Zemlya

491. Novaya Zemlya is an island located at the most northerly edge of Europe. Testing of nuclear weapons by the former Soviet Union on Novaya Zemlya began in 1955. Novaya Zemlya was the site of the world's largest nuclear weapons test, a 50 Mt detonation at an altitude of about 3.5 km. In total, 91 atmospheric nuclear tests took place on Novaya Zemlya, and tests performed on the island account for about one half of the total energy yield of all nuclear tests carried out in the entire world. Only one test, in 1957, was conducted on the ground surface. In addition, there were two tests on the water surface and three underwater tests. There were also 17 underground tests that vented radioactivity, resulting, in most cases, in onsite contamination only.

492. Testing at Novaya Zemlya was conducted in three distinct areas, and residual radionuclides were reported in all the testing areas. The most affected areas are the site of one of the surface test sites and the sediments where underwater testing occurred [E23]. The native population was relocated to mainland Russian Federation before tests took place, and the current population consists of military personnel, families, and construction workers located in two towns. No information relating to public exposure from the testing or from the current condition of the sites is publicly available.

Kapustin Yar

493. Kapustin Yar is the site of a missile testing range located 250 km northwest of the Caspian Sea. Ten atmospheric nuclear tests took place at Kapustin Yar over a period of six years from 1957. All the tests were conducted at high altitude (10.4–300 km) and no residual radioactive material was reported on the ground [E23, U19]. The high-altitude explosions contributed predominantly to global fallout and did not cause significant exposure to the population residing in the local area or in the wider region.

Totsk

494. In September 1954, a 40 kt atmospheric test was conducted at a military range near the village of Totsk in the Orenburg Oblast. This test was part of a nuclear exercise involving more than 40,000 troops who were close to the explosion and advanced through areas impacted by the blast towards ground zero within an hour of the explosion. Nearby villages within 7 km from the test site were evacuated, while villages further away were partially evacuated or sheltered during the test [H25].

495. No doses were reported to local inhabitants of the region that were affected by the fallout from this exercise. Two studies performed to investigate the health status of children living in the region and the long-term consequences [B33, K28, L9] provide some details on the radioecological conditions in local villages that were affected by the exercise, noting that the activity concentrations of ^{137}Cs, ^{239}Pu and ^{240}Pu were all elevated above background levels for the region by up to 2.5 times for ^{137}Cs and up to 5 times for ^{239}Pu and ^{240}Pu [B33, K28]. Surveys of ambient gamma dose rate performed at five affected villages, ground zero, and a non-affected village 255 km away reported no increased dose rates in the affected villages [K28].

(e) *China*

Lop Nor, China

496. The Chinese nuclear weapons test site of Lop Nor is located in a desert region of the Xinjiang Autonomous Region in northwest China. A total of 22 atmospheric and 12 underground tests were performed at the site between 1964 and 1988. The total yield of the atmospheric tests was 20.72 Mt [P4, S41, U19]. It was previously reported [U19] that the average dose from external exposures to the population of cities and towns 400–800 km downwind of the test site was estimated to be 0.044 mSv. Thyroid doses to people living in the region due to ^{131}I ranged from 0.06 mGy to 2.5 mGy while the average thyroid dose to the population of China was 0.14 mGy.

497. Studies which evaluated doses from external exposure to the population in the Jiuquan district, as well as exposure resulting from the deposition of fallout radionuclides in the Xinjiang area, were summarized in a report on the radiation levels in China [P4]. An average dose commitment of 4.86 mSv (range: 1.52–18.9 mSv), and a collective dose of 374 person–Sv were reported. The assessment of exposure resulting from measurements of ^{90}Sr and ^{137}Cs in water, vegetation and soil was also reported for the Xinjiang area, which was separated into a control area and a survey area. The report estimated average annual individual doses of 0.79 mSv for the population in the control area and 0.98 mSv for the survey area, while collective doses were estimated to be 237 person–Sv for the control area (based on a population of 300,000 people) and 196 person–Sv, for the survey area (based on a population of 200,000 people). These doses include a contribution from fallout from the tests conducted at the Semipalatinsk site [P4].

(f) *France*

Reggane and In Ekker, Algeria

498. Between 1960 and 1966, France conducted four atmospheric tests, 13 underground tests and 40 minor experiments at remote locations near Reganne and In Ekker, in southern Algeria. The Reggane Test Sites are in the Sahara Desert approximately 50 km south-southwest of the village of Reggane, which had an estimated population of a few thousand inhabitants at the time of the tests. The tests conducted at Reganne are known as the Gerboise series of tests (Gerboise Bleue, Gerboise Blanche, Gerboise Rouge, and Gerboise Verte); the total yield was previously reported as 73 kt but has more recently been estimated to be between 70 kt and 120 kt [S41, U19].

499. For the atmospheric tests that occurred at the Reggane Test Sites, film badge monitoring was performed on members of the local population including nomads in the region. A total of 125 civilians located in Reggane were monitored for the first test, Gerboise Bleue, while 70 nomads located around Tamanrasset, approximately 700 km southeast of the test site, were monitored for the third test, Gerboise Rouge. A report published by the Parliamentary Evaluation Office of Scientific Technologies noted that no activity was detected from the monitoring of civilians. Meteorological monitoring was a key safety measure to ensure that the conditions were suited to a test, particularly that the wind direction carried emissions away from populated areas [B11].

500. The second main Algerian site used by France was the Taourirt Tan Afella massif located near In Ekker in southern Algeria, which was used for 13 underground tests. The area is reported to have had no more than 2,000 people living within 100 km of the site at the time of the tests. Four of the 13 tests were not fully contained, and two of these resulted in a significant release of radionuclides to the atmosphere. The impact to local populations was assessed for each of the unplanned releases and described in a parliamentary report which indicated that committed doses to 280 people following the Amethyst test were less than 1 mSv from external irradiation; the dose from radionuclides detected 150 km from the test sites at Tamanrasset following the Rubis test was 0.01 mSv and that no public exposures were estimated following the Beryl and Jade tests [B11]. Thirty-five subsidiary experiments were performed at the Reggane Test Sites and another five in the region of Adrar Tikertine, 30 km southwest of Taourirt Tan Afella. These tests resulted in localized dispersion of plutonium in the environment with no potential for public exposures.

501. The Algerian test sites were the subject of an IAEA radiological assessment conducted in 1999 [I16]. The study estimated that daily doses to visitors of the Reggane Test Sites would be of the order of a few microsieverts and estimated annual doses to residents of the town of Reggane at less than 1 μSv. The assessment also concluded that the annual doses received by nomadic herders or their families at the subsidiary trial site of Adrar Tikertine would be unlikely to exceed 1 μSv. The report noted that it was possible for nomadic camel and goat herders to receive annual doses of up to 50 μSv around two of the galleries at In Ekker where the Beryl and Amethyst tests took place, and that scavenging activities could result in exposures of 0.5 mSv in eight hours.

Mururoa and Fangataufa, French Polynesia

502. France conducted 193 nuclear experiments at the atolls of Mururoa and Fangataufa between July 1966 and January 1996. Of these, 178 were nuclear tests, in which nuclear devices were exploded with large releases of fission energy, and 15 were safety trials. Forty-one atmospheric tests (37 at Mururoa Atoll and 4 at Fangataufa Atoll) were completed between July 1966 and September 1974; and 137 underground nuclear tests (127 at Mururoa Atoll and 10 at Fangataufa Atoll) were carried out between June 1975 and January 1996. Of the 15 safety trials, all of which were carried out at Mururoa Atoll, 5 were atmospheric and 10 were underground [U19].

503. Most atmospheric tests were conducted at an altitude designed to minimize surface interaction and thereby reduce local fallout. Four atmospheric tests, three at Mururoa and one at Fangataufa, were conducted with the devices mounted on barges floating in the lagoons and produced the majority of residual radioactive material present in the environment. The underground nuclear tests were conducted in the basalt basement at depths of between about 500 and 1,100 m in shafts drilled vertically beneath the rims of the lagoons. Much of the residual radioactive material associated with the underground nuclear tests was trapped in molten basalt rock that solidified as glass-like lava, but some radionuclides were deposited on fractured basalt rock that collapsed into the cavity-chimney and remained available for exchange with water [I3].

504. Since 2013, studies have been performed to review the doses received by populations of French Polynesia and other countries [D24, D26, D27]. One of these assessments reviewed the monitoring data from several nations and provided whole-body doses for the populations of Australia and French Polynesia (Tahiti) and thyroid doses for Australia, Bolivia, Chile, Colombia Ecuador, French Polynesia (Tahiti), Madagascar, New Zealand, and Peru for the years 1966 to 1974 [D27]. As noted in previous UNSCEAR reports [U15, U19], the highest whole-body dose (average: 0.34 mSv) and thyroid dose (average: 3.2 mSv) to the inhabitants of Tahiti were calculated for 1974 mainly due to a rain-out that occurred after the test of 17 July 1974 [D27]. The Committee previously reported that maximally exposed individuals received doses between 1 and 5 mSv during 1974 [U19]. Average whole-body doses to the population of Tahiti between 1966 and 1973 were less than 0.1 mSv (range: 0.0036–0.032 mSv), while average thyroid doses were less than 1 mSv (range: 0.053–0.87 mSv) [D27].

505. The IAEA performed a series of studies on the radiological conditions at Mururoa and Fangataufa Atolls between 1996 and 1998 [I3]. These studies estimated the doses that people living in the South Pacific would receive due to the residual radioactive material present in the accessible environment of Mururoa and Fangataufa Atolls and their surrounding waters. The main exposure scenario included in the assessment was the release of residual radioactive material underground into the lagoons or directly into the surrounding ocean through migration across the geosphere, modified by the hydrogeological effects of the nuclear testing. Particular attention was paid to three radionuclides of potential radiological significance, ^{90}Sr, ^{137}Cs and ^{239}Pu, in addition to ^{3}H, which is a useful tracer for model validation. Doses were calculated to hypothetical dwellers of the atolls who were presumed to eat mostly local seafood and other locally grown food. Using cautious assumptions about diet and other habits, the study estimated an upper limit of the annual dose of 0.01 mSv. A cautious estimate of the annual dose received by the present population of Tureia Atoll, the nearest inhabited island to Mururoa and Fangataufa Atolls, located at a distance of about 130 km, was less than 0.1 μSv [I3].

506. French authorities have monitored the radiological conditions in French Polynesia since 1962, specifically outside of the testing sites of Mururoa and Fangataufa Atolls to assess possible exposures to the public. Annual reports on the monitoring programme are readily available, and since 2020 the monitoring programme has been incorporated into the French National Monitoring Network to widen its accessibility. The annual report for 2021 and 2022 calculated that annual individual dose to the population of Tahiti from exposure to human-made radionuclides from nuclear weapons testing was 2.3 μSv, with 1 μSv due to external exposure and 1.3 μSv to ingestion [I85].

(g) *India*

507. India has conducted six underground nuclear weapons tests at the Pokhran site located in the Indian state of Rajasthan. The first test, carried out in 1974, was named Smiling Buddha, also referred to as Pokhran-I. The device used in the test was a plutonium fission bomb with an estimated yield of approximately 12 kt. On 11 and 13 May 1998, India also conducted five tests at the site, under Operation

Shakti, which are commonly referred to as the Pokhran-II tests. The largest device detonated during these tests was a 45 kt thermonuclear device; the total yield of all the devices was reported to be 60 kt [S36].

508. The official statement provided after the 1998 tests was that there was no release of radioactive material into the atmosphere [I80]. There have been four Bhabha Atomic Research Centre publications relating to fission signatures, yield estimates, and radioactivity measurements from borehole samples [A42, M3, S36]. No publications have been identified with information on any monitoring performed or possible exposures to the public.

(h) *Pakistan*

509. Pakistan conducted six nuclear weapons tests at two locations in the Chagai district of the Province of Balochistan in 1998. All tests were underground, with five of the six tests conducted simultaneously on 28 May 1998, and the sixth test on 30 May 1998. These tests are referred to as Chagai-I and Chagai-II. The first of them was announced to have a total yield of between 30 and 45 kt, while the yield of the second was 18 kt. Other estimates based on seismic data have concluded that these tests had lower yields [S30]. No publications have been identified with information on any monitoring performed or possible exposures to the public.

(i) *Democratic People's Republic of Korea*

510. The Democratic People's Republic of Korea (DPRK) conducted six underground nuclear weapons tests between 9 October 2006 and 3 September 2017. Assessment of the seismic data shows that they occurred at the Punggye-ri Test Site in the North Hamgyong Province. Due to the secrecy applied by the DPRK, the yield of these tests could only be estimated from seismic data applied to modelling tools [D15]. There is no publicly available information to confirm the site's current state or possible exposures to the public. Higher concentrations of ^{133}Xe detected in Yellowknife (Canada) in October 2006 were consistent with leakage from the test that occurred on 9 October 2006; ^{133}Xe was also detected in Takasaki (Japan) in February 2013, consistently with leakage from the test that occurred on 12 February 2013. No detections of noble gas have been reported related to leakages from the other tests [C58, C59, C60, C61, C62].

5. Nuclear weapons production, maintenance and decommissioning

511. In addition to nuclear weapons testing, facilities at which nuclear material was produced, and weapons that were fabricated or are decommissioned have been sources of radionuclides released to the environment. Information relating to significant releases, including accidents and the resulting public exposure, has been provided in previous UNSCEAR reports [U13, U15, U20]. This section summarizes information relating to public exposure from these facilities since the UNSCEAR 2008 Report [U20]. Information on public exposures due to accidents at weapons production facilities is provided in section IV.E.

512. Nuclear weapons require a combination of industrial processes for the production, management, and decommissioning of nuclear warheads. These include uranium mining, milling and enrichment facilities to supply and produce weapons grade uranium; reactors to produce plutonium; tritium production facilities, required to boost yields; assembly, decommissioning, and associated fabrication facilities; waste disposal sites; and supporting institutions for research and development. These processes are performed across a range of sites within countries that have nuclear weapons capability. As nuclear weapons have been available for almost 80 years, several sites used for their production, maintenance

and decommissioning have themselves been decommissioned and are managed as legacy sites with the potential for public exposure. France, Russian Federation, the United Kingdom, and the United States no longer produce fissile material for nuclear weapons programmes [I81]. Only France and the United States have reported a reduction in their warhead stockpiles [U6].

(a) *United States*

513. The United States Department of Energy (USDOE) has overall responsibility for all weapons related research and development activities, the management of legacy sites that have been decommissioned, the decommissioning of sites that have ceased activities, and reporting of releases and public exposures relating to current nuclear weapons activities. Public exposures are provided in two main reports produced by the USDOE, for both active sites and those currently undergoing decommissioning. The latest iteration of these reports, published in 2022, summarize results for the period 2015–2018 [U40, U41] and provide the results of monitoring from 43 sites that have the potential for radionuclide releases to the environment. Eight of these sites are involved with the United States nuclear weapons programme. The Office of Environmental Management is currently performing decommissioning activities at seven sites, four of which have been involved in the nuclear weapons programme at some stage. Individual Annual Site Environmental Reports for the sites are summarized in the multi-year summary report that is also available [U46].

514. Public exposure from sites relating to decommissioning, current activities and research, and development associated with nuclear weapons are provided in electronic attachment A-4. The total annual dose to the maximally exposed individual estimated for all USDOE nuclear weapons programme related sites between 2015 and 2018 ranged from less than 0.001 mSv to 0.129 mSv. Three of these sites have reported exposures greater than 0.01 mSv were possible in 2018. These are the Paducah Gaseous Diffusion Plant decommissioning works (0.051 mSv); Nevada National Security Site (0.129 mSv); and Sandia National Laboratories in California (0.04 mSv) [U41]. Exposures reported from USDOE legacy sites are provided in electronic attachment A-5.

(b) *Russian Federation*

515. The main sites where weapons material was produced in the former Soviet Union are Chelyabinsk-40 (now Ozersk) and Chelyabinsk-70 (now Snezhinsk), Krasnoyarsk-26 (now Zheleznogorsk), and Tomsk-7 (now Seversk). Public exposure relating to accidents and releases from the Mayak Production Association facility in Chelyabinsk has been analysed in detail in previous UNSCEAR report [U20], as well as the 1993 accident that occurred at the Seversk facility of the Siberian Chemical Plant (see section IV.E.2).

516. The Russian Federation's nuclear weapons programme provides limited information on public exposure from its facilities. A summary of public exposure is provided in their annual reports with doses only mentioned for the area in the Chelyabinsk region that has the highest exposure due to the Mayak Production Association facility [R29]. The nuclear weapons production sites, are included in an automated radiation monitoring system programme [I59], which provides real-time dose rate monitoring at stations located around the facilities; historical data dating back to the start of monitoring at each station can be viewed through the interface.

517. Krasnoyarsk-26, also known as the Mining and Chemical Combine, was the site of a nuclear power plant and a reprocessing facility located approximately 50 km north from the city of Krasnoyarsk in Siberia. Operations at three industrial graphite reactors for the production of weapon-grade plutonium from irradiated natural uranium at Krasnoyarsk-26 began in late 1958. Two of the reactors were designed to extract cooling water directly from the Yenisei River and subsequently discharge it back to the river.

The water discharged into the river contained both activation and fission products causing significant radionuclide contamination for hundreds of kilometres downstream [I10, U20].

518. The contaminated floodplains provide the most significant pathways for public exposure in the coastal settlements downstream from Krasnoyarsk-26. Current doses to the public from the plant's present and past activities are significantly lower than the levels of exposure from natural background radiation. Average annual public doses due to human-made radionuclides range from 0.06 to 0.11 mSv. Annual doses from external exposure vary between 0.011 to 0.053 mSv, while annual doses from internal exposure range from 0.045 to 0.058 mSv. The most important exposure pathway contributing to internal dose is consumption of fish [P6] (see electronic attachment A-4).

(c) *United Kingdom*

519. The United Kingdom began its nuclear weapons programme in the 1950s with a range of sites dedicated to their development (Springfields, Capenhurst, Sellafield, Aldermaston, Harwell, and Chapelcross). In the early years, these sites were exclusively dedicated to nuclear weapons activities, However, some of them became subsequently involved with the United Kingdom's civilian nuclear power programme. An accident that occurred at the Windscale reactor (Sellafield) in 1957 is described in section IV.E.2 of this annex. The current United Kingdom nuclear weapons programme operates two major sites: Aldermaston, for research and development, and Burghfield, for assembly, maintenance and decommissioning, both located in Berkshire. Results of their monitoring programmes including an assessment of public exposure are reported annually [C13]. The latest available report published for 2022 shows that doses to the public from the two sites are less than 0.005 mSv [C13]. Public exposure from United Kingdom legacy sites, including those used for the production, maintenance and decommissioning of nuclear weapons are provided in electronic attachment A-5.

(d) *France*

520. Three main sites are part of France's nuclear weapons programme: Bruyères-le-Châtel (design and simulation), established in 1957; CEA Valduc Centre (production, maintenance, and decommissioning) created in 1957; and Centre d'Études Scientifiques et Techniques d'Aquitaine (research and development), founded in 1965. Comprehensive monitoring programmes are in place for the three facilities [C3] with information available online via an interactive map including data from a real-time radiation monitoring network [I86]. Public exposure estimates for the sites of Bruyères-le-Châtel and CEA Valduc Centre are provided in an annual report of environmental monitoring [I84]. The results of the monitoring programme at Bruyères-le-Châtel are too low to estimate public exposure from the operation, while the annual effective dose from CEA Valduc Centre is estimated to be 1 μSv for a person spending significant time near the site, with ingestion of ^{3}H being the most significant exposure pathway. Information on exposures from legacy sites associated with the French nuclear weapons programme are provided in the electronic attachment A-5.

(e) *China*

521. China has a range of sites dedicated to the production and maintenance of nuclear weapons. Monitoring programmes have been established at each site and provide adequate information to assess possible exposures [N20]. The monitoring programmes are also supported by automated radiation monitoring stations, and an assessment of the data provided by these stations, with a note regarding public

exposures, is provided in annual reports [N22]. Public doses from specific facilities are not readily available; the latest available annual report of the National Nuclear Safety Administration notes that "the assessment results indicate that the radiation doses exposure to the public caused by the operation of the above-mentioned nuclear facilities were far lower than the national limits, without any impact on environmental safety and public health" [N21].

522. Public exposure estimates from the Chinese nuclear weapons programme were noted in UNSCEAR 2000 Report [U15], which indicated that an assessment of exposures to populations living in the vicinity of nuclear installations had been reported by Pan et al. [P2, P3]. Since China did not develop a civilian nuclear programme until the 1990s, the nuclear installations considered in these papers were taken to be part of China's nuclear weapons programmes.

6. Residual radioactive material in the environment due to other military applications

523. In military applications, depleted uranium (DU) is used as ammunition for its exceptional armour-piercing capabilities, due to its high density, kinetic energy, and pyrophoric properties, making it very effective against armoured targets [B32]. DU is also used in heavy tank armour plates. DU ammunition was first deployed during the 1991 Gulf War and continued to be used in other conflicts, such as the war in the Balkan region in the late 1990s, the 2003 Gulf War, and it has been recently used in the conflict in Ukraine.

524. When DU ammunition, commonly known as penetrators, strike a target, part of the material is released into the environment as metal fragments, and dust containing uranium oxides is deposited on the soil surface. DU penetrators that do not hit any target may remain intact and penetrate soft soil for several metres underground, where they slowly oxidize and dissolve over a long period of time, depending on soil conditions. It has been estimated that DU penetrators deposited near the ground surface completely dissolve within 35 years [M17, U7]. The main radiological risk from DU residues in the environment is inhalation of resuspended dust, but annual public doses from this exposure pathway were estimated to be low—typically a few microsieverts per year [U7]. Direct dermal contact with DU metal is another potential exposure pathway of radiological significance, usually through handling of DU fragments [I13]. Dissolved depleted uranium may add to the levels of natural uranium in the soil, but this increase would be minimal, due to the comparatively high levels of natural uranium already in the soil and would not significantly affect public exposure. For example, ingestion of food is not considered a radiologically significant exposure pathway due to the low mobility of depleted uranium through the environment.

525. A few studies have examined public exposure due to the military use of depleted uranium [B23, C6, M7, R11, S9]. Of these, an assessment based on a worst-case scenario estimated that children assumed to play for 500 hours in abandoned or destroyed vehicles would receive a dose of 49 mSv; while they would receive a dose of 1.5 mSv if they played 50 hours [M7]. The general conclusion of these studies was that radiation exposure from DU after military use poses a low radiological risk and is confined to areas where residues are present.

526. Nuclear propulsion systems developed for naval vessels are designed to allow the vessels to remain at sea for very long periods of time. Except for accidents relating to these vessels or the transport of the decommissioned units, as described in section IV.E, public exposure associated with these reactors during operation and storage is considered negligible. A study of the site used for the temporary storage of spent nuclear fuel and radioactive waste, established by the Russian Federation as part of its programme of decommissioning and remediation of its Navy's bases in the Russian Far East, located at Sysoeva Bay, indicated that the annual dose to the public from the remediated site was less than 0.04 mSv [K23].

E. Exposure from radiological accidents and past peaceful practices

527. Public exposure from nuclear and radiological accidents were addressed in previous UNSCEAR reports. In particular, the Committee has published scientific reports and White Papers that have specifically addressed the two most severe accidents in the history of the nuclear industry, at the Chornobyl NPP (Ukraine) in 1986 and the Fukushima Daiichi NPS (Japan) in 2011 [U12, U13, U14, U16, U20, U26, U29]. These comprehensive reports remain the primary sources of information on public exposure associated with the accidents at these nuclear facilities.

528. Exposures related to accidents described in this section include not only nuclear accidents, but also other radiological incidents which resulted in releases of radionuclides, such as those involving industrial and orphan sources and the peaceful use of underground nuclear explosions. The focus of this annex is on the current radiological consequences of these activities, with a summary of past events. Due to the diversity of the events and the radiological conditions, the Committee has not developed a specific methodology for the assessment of doses from radiological incidents other than major accidents. Estimates of doses were instead compiled from various sources, including reports from national and international organizations, publications in the open literature and information submitted through the UNSCEAR Global Survey on Public Exposure.

529. Past peaceful practices considered in this section include public exposure from legacy sites and disposal at sea. Previous UNSCEAR reports [U13, U15, U19] have provided details on public exposure from legacy sites resulting from past peaceful practices. The evaluation of public exposure from legacy sites presents a challenge since the radiological conditions at these sites can vary significantly and the assessment methodologies are not standardized. This annex therefore relied on information on assessments of public exposure from legacy sites provided through the UNSCEAR Global Survey on Public Exposure, or available in the open literature or in publications from national and international organizations.

1. Radiological accidents

530. This section summarizes previous evaluations carried out by the Committee on public exposures associated with the accidents at the Chornobyl NPP and Fukushima Daiichi NPS and provides an updated assessment of current exposures to the public. Other accidents, such as those involving industrial and orphan sources, spacecraft and satellites, the loss of radioactive material at sea or other accidents reported in this section either occurred since the publication of the UNSCEAR 2008 Report, annex C [U20], had not been previously reported, or have had exposure assessments updated. This section is limited to a description and analysis of public exposures related to these events. Further information on these accidents is provided in electronic attachment A-5.

531. Relevant IAEA reports on radiological accidents [11] were the main source of information for accidents that have resulted in public exposures included in this annex. The IAEA also maintains the Unified System for Information Exchange in Incidents and Emergencies (USIE) website for the exchange of details during emergencies relating to radiological accidents. Information from the USIE website was reviewed to obtain data about accidents with an International Nuclear and Radiological Event Scale (INES) rating of 3 or higher that resulted in public exposures.

[11] www.iaea.org/publications/search/topics/accident-reports.

(a) *Accidents at nuclear facilities*

USSR: Southern Urals, Techa River (1949–1956) and Kyshtym accident (1957)

532. The first facility in the former Soviet Union dedicated to the production of plutonium was built in 1948 in an area east of the southern Ural Mountains, about halfway between the major cities of Ekaterinburg and Chelyabinsk. The facility, now known as the Mayak Production Association, was designed to irradiate uranium in reactors, separate the resulting plutonium in reprocessing plants, and prepare plutonium metal in the metallurgical plant. Several operational and accidental releases of radionuclides led to radioactive contamination of large territories of the Urals region in the 1950s and 1960s as shown in figure XXV. Information on these releases was provided in previous UNSCEAR reports [U13, U15, U19, U20].

533. Discharges of a total of approximately 115 PBq of uranium fission products in operational low-level liquid radioactive waste into the Techa River started in January 1949 followed by major releases in September 1950 [A12, D11, D12]. In 1951, liquid wastes were diverted to Lake Karachay, which still holds over 4 EBq of radioactive waste. In the spring of 1951, accidental releases periodically occurred because of damage to tanks storing high activity waste; the largest releases occurred in September and October 1951. The liquid radioactive waste contained a large array of radionuclides, such as ^{89,90}Sr, ^{137}Cs, ^{103,106}Ru, ^{95}Zr, ^{95}Nb, ^{141,144}Ce, ^{91}Y and ^{140}Ba, with ^{137}Cs and ^{90}Sr contributing to the largest portion of activity released. Radionuclides were transported downriver and deposited in sediments and adjacent floodplain soils [A14, S28].

534. The Techa River served as the main supply of drinking water for 41 villages, and its floodplains were used to produce cattle pasture and hay. The primary exposure pathway for internal irradiation was ingestion of radionuclides in water and milk. Between 1953 and 1956, authorities implemented measures to prohibit the use of river water for drinking and domestic purposes [A17, P28]. Additional measures to control public exposures included the creation of a system of dams in the upper reaches of the Techa River, known as the Techa Cascade of Reservoirs, and the resettlement of residents of villages that had been affected. Between 1955 and 1960, 19 settlements comprising approximately 7,500 people were evacuated from the upper reaches of the Techa River. However, these protective actions were implemented several years after the initial releases, resulting in prolonged exposure of the local population [D14]. The estimated intakes of ^{90}Sr for a typical adult resident in the villages of Metlino and Muslyumovo [T13, T14], located 7 km and 78 km downstream from the release site, respectively, are provided in electronic attachment A-5.

Figure XXV. Relationship of the areas impacted by releases from the Mayak Production Association facility: Techa River, East Urals Radioactive Trace, and Karachay Trace (adapted from [K29])

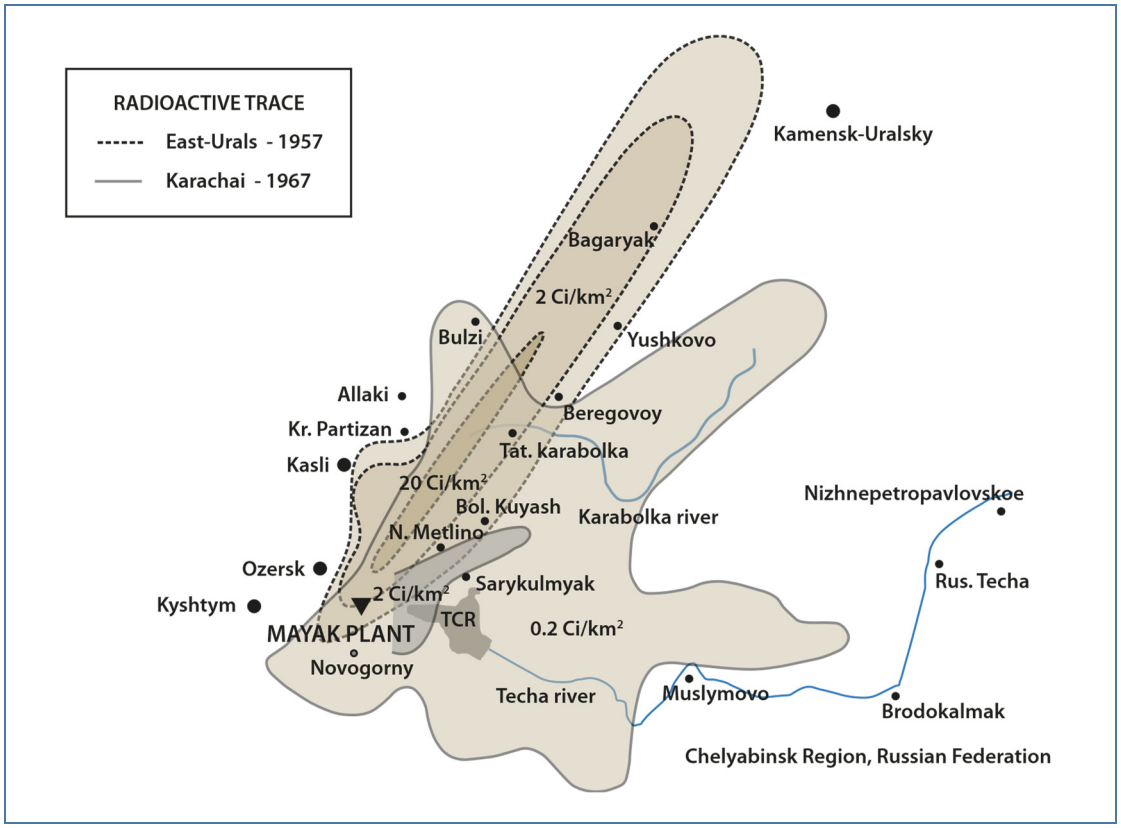

535. On 29 September 1957, a major radiation accident occurred at the Mayak Production Association when a storage tank containing liquid radioactive waste exploded due to a disruption in the operation of the cooling system. Approximately 90% of the total activity released by the explosion was deposited within a 5 km radius of the epicentre. The remaining activity was carried into the upper atmosphere forming a radioactive cloud that led to widespread deposition [I94, R28]. This event resulted in the formation of the East Urals Radioactive Trace (EURT), characterized by a total deposition of 74 PBq of radionuclides [A11, A12]. The area where deposition levels were above 3.7 kBq/m^2 extended to 23,000 km^2 and included 217 settlements with a combined population of 270,000 people [A11]. Three of the most heavily contaminated settlements with deposition levels ranging from 59 to 122 MBq/m^2 and a population of approximately 1,100 people were evacuated within two weeks. An additional 2,280 residents were evacuated within 250 days from areas with an initial ^{90}Sr deposition of exceeding 150 kBq/m^2. Over the next 110 to 420 days, approximately 7,300 people were also relocated from settlements with deposition levels of ^{90}Sr above 74 kBq/m^2.

536. Between October 1957 and April 1958, external exposure was the predominant exposure pathway; later, internal exposure from ingestion of ^{90}Sr in local food became significant [T16]. Data on daily intake of ^{90}Sr and the contribution of various food products to the daily intake in different time periods are presented in electronic attachment A-5 for populations in non-evacuated areas with an initial deposition of 37 kBq/m^2. After the year 2000, vegetables were identified as the most contaminated foods [K34].

537. A second radiological accident occurred in 1967 at the Mayak Production Association facility, when approximately five hectares of Lake Karachay dried out. Windstorms dispersed the exposed lake sediments resulting in the deposition of radioactive material with a total activity of 22 TBq over an area

of 2,700 km^2 [P17] forming the Karachay Radioactive Trace. The radionuclide composition of the trace included ^{90}Sr (34%), ^{137}Cs (48%), and ^{144}Ce (18%). The most highly contaminated areas were uninhabited; the average deposition of ^{90}Sr in villages and on agricultural land was 7.4 kBq/m^2 with peak values reaching 40 kBq/m^2 [I94]. In Bolshoy Kuyash, the most affected village, deposition levels of ^{90}Sr and ^{137}Cs between 2009 and 2011 varied between 5.7 and 20 kBq/m^2 and between 10.6 and 69 kBq/m^2, respectively [K11].

538. Radionuclide deposition in the Karachay Radioactive Trace was approximately two orders of magnitude lower than that measured in Muslyumovo on the Techa River. No follow-up health studies were conducted for the populations residing in the areas covered by the Karachay Radioactive Trace. Notably the Karachay Radioactive Trace partially overlapped with the EURT resulting in an additional source of exposure for residents of those areas (see figure XXV). Lake Karachay was successfully remediated in 2015 by covering the water surface and the surrounding areas, thereby minimizing the risk of further radionuclide transfer. After the remediation was completed the lake was designated as a storage facility for special radioactive waste [M37].

539. Residents of the Urals Region were exposed to environmental releases of radionuclides through similar pathways. The accidents occurred over a relatively short period of time and affected rural populations with similar lifestyles. Intakes of ^{90}Sr resulted in very heterogeneous dose distributions within the body. Estimated doses to bone marrow and bone surfaces were at least an order of magnitude higher than doses to other tissues [D14, S29, S34]. Internal exposure was the predominant pathway for the populations of both EURT and the Techa River [S34]. Trends in ^{90}Sr body burdens among various groups of residents of the Urals region from 1950 to 1996 are presented in electronic attachment A-5.

540. Historical exposures of residents of the Urals region to releases from the Mayak Production Association have been extensively analysed in several epidemiological studies [A13, A14, D14, N3, S34, U25]. Average doses to extra-skeletal tissues of people living near the Techa River and in the EURT region were estimated to be 60 and 10 mGy, respectively, with maximum values not exceeding 1,500 and 200 mGy, respectively. Doses to active marrow were significantly higher, averaging 350 and 30 mGy, with maximum estimates of 8,000 and 400 mGy [S34].

541. Villages along the Techa River that were not evacuated continue to be now routinely monitored and current exposures are regularly reported [B3, K35, Y6]. The Techa River's broad floodplains in its upper reaches and narrower channels downstream influence the key exposure pathways: external irradiation, consumption of river water and, in the upper portion, consumption of milk from cows grazing in the contaminated floodplains [K35]. In 2010, cautious estimates of the annual doses to the most exposed groups of residents in the Chelyabinsk and Kurgan regions ranged from 0.12 mSv (Zatechenskoe village, lower river) to 1.1 mSv (Muslyumovo village) [K35]. Residents of Muslyumovo were relocated between 2007 and 2012 to a nearby uncontaminated area. Since 2011, a management system of the Techa Cascade of Reservoirs has been implemented to minimize risks and accelerate the natural purification of the river system [U58]. The remediation of 82% of approximately 90,000 hectares of previously restricted EURT territories was completed by 1981 [K34]. Current annual doses in the affected areas due to human-made radionuclides are below 1 mSv [A12, K35]. Annual effective doses ranged from 0.02 to 0.2 mSv; higher estimates are for teenagers because of their higher milk consumption rates and time spent outdoors [U13, U20]. A summary of estimates of annual exposures for the most highly exposed groups of Urals residents is given in electronic attachment A-5.

United Kingdom: Windscale accident (1957)

542. In 1957, a fire in the Windscale graphite reactor that lasted three days resulted in a major release of radioiodine and other radionuclides into the environment in Cumbria. Several estimates of the activity

released during the fire have been made. The most recent estimate indicated that the release of ^{131}I was 1,800 TBq (range: 900–3,700 TBq) [G6]. It was accompanied by an estimated 180 TBq of ^{137}Cs, 3 TBq of ^{106}Ru, 26 PBq (range: 8–80 PBq) of ^{133}Xe, and 42 TBq (range: 14–110 TBq) of ^{210}Po, plus several other radionuclides [G6]. While estimates of the source term have changed, the doses estimated from the release were based on measurements at the time and have not changed [G6, U20]. The maximum doses to the thyroid for local individuals were estimated to be 0.01 Gy for adults and 0.1 Gy for children. Measurements in Leeds and London indicated thyroid doses of 1 and 0.4 mGy. The collective effective dose estimated for the United Kingdom and Europe was 2,000 person–Sv [U20].

United States: Three Mile Island (1979)

543. In March 1979, an accident occurred at Three Mile Island NPP near Harrisburg, Pennsylvania. The sequence of events leading to the accident began with the closure of a valve that fed water to the boiler. A series of events thereafter led to fuel melting within the reactor core and the release of fission products through a relief valve in the primary water make-up system. Most fission products were retained in the water, but about 370 PBq of noble gases, mainly ^{133}Xe, and about 550 GBq of ^{131}I were released into the atmosphere. The resulting effective dose to the public averaged 15 μSv within 80 km of the plant with a maximum dose of 0.85 mSv. The collective effective dose was estimated to be 40 person–Sv [U13].

Ukraine, USSR: Chornobyl (1986)

544. The accident that occurred at the Chornobyl NPP in April 1986 was the most severe accident to have occurred in the history of the civilian nuclear industry. Two workers died in the immediate aftermath, and high doses of radiation to 134 plant staff and many emergency personnel resulted in acute radiation syndrome which proved fatal for 28 of them. The accident caused the largest uncontrolled radionuclide release into the environment ever recorded for any civilian nuclear facility, including 1,760 PBq of ^{131}I, 86 PBq of ^{137}Cs, 10 PBq of ^{90}Sr, and 3 PBq of plutonium radioisotopes. The most affected countries were Belarus, the Russian Federation and Ukraine [I17].

545. In the aftermath of the accident, radioactive material was deposited over large areas of the former Soviet Union and other countries in Europe, contaminating land, water, and biota, and causing serious social and economic disruption for about 6 million people living in areas of Belarus, the Russian Federation, and Ukraine where the deposition density of ^{137}Cs exceeded 37 kBq/m^2. Of these, about 400,000 people lived in areas classified by Soviet authorities at the time as ‘areas of strict radiation control’ with the deposition density of ^{137}Cs exceeding 555 kBq/m^2. Of this group, 116,000 people were evacuated to uncontaminated areas in the spring and summer of 1986 and another 220,000 people were relocated in subsequent years [I17, I79, U20]. The deposition density of ^{137}Cs in an area of more than 200,000 km^2 across Europe exceeded 37 kBq/m^2 [C52]. Over 70% of this area was in Belarus, the Russian Federation, and Ukraine as presented in figure XXVI; the full deposition distribution across Europe is shown in electronic attachment A-5. Most of the strontium and plutonium radioisotopes were deposited locally within 100 km of the Chornobyl NPP, due to these radioisotopes being associated with larger particles.

546. Radioactive fallout was deposited over urban, agricultural, semi-natural, and aquatic environments leading to significant exposures to humans and other organisms [C52]. For the public, external exposure to radionuclides deposited on soil and other surfaces and ingestion of contaminated food were the two most important exposure pathways. Fallout of radioisotopes of iodine caused raised public concern in the first two months following the accident. In this early period, the most significant contribution to the dose was from the short-lived radionuclides ^{131}I, ^{132}Te/^{132}I and ^{106}Ru. After the decay of ^{131}I, ^{137}Cs and ^{134}Cs were of greatest radiological importance for the first decade. Caesium-137 remained of radiological significance over the longer term due to its longer half-life [I17, I79, U20].

Figure XXVI. Calculated plume formation according to the meteorological conditions for instantaneous releases on the following dates and times (GMT) [I17]

(1) 26 April 1986, 00:00; (2) 27 April 1986, 00:00; (3) 27 April 1986, 12:00; (4) 29 April 1986, 00:00; (5) 2 May 1986, 00:00; and (6) 4 May 1986, 12:00

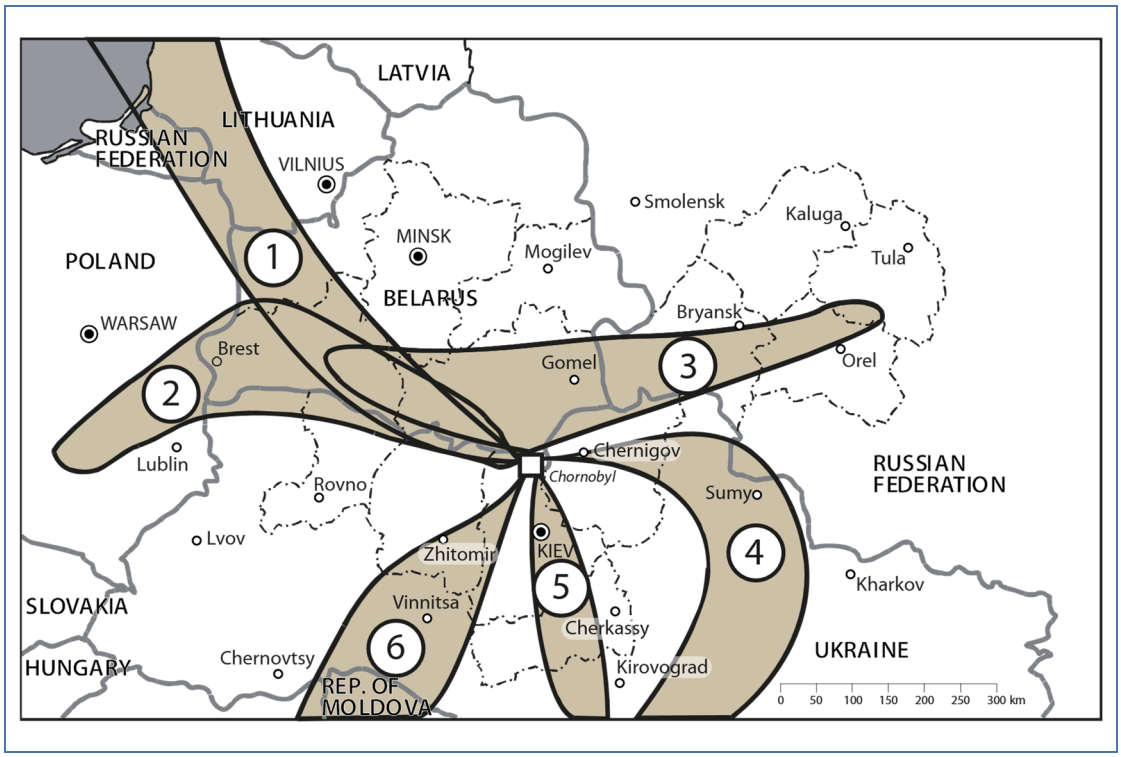

547. Thyroid doses to the populations of Belarus, the Russian Federation and Ukraine from the consumption of fresh milk contaminated with ^{131}I in the first weeks after the accident were estimated between 0.05 Gy and 5 Gy [U20]. As far as whole-body doses are concerned, the residents of the areas of the former Soviet Union considered to be significantly affected received annual average doses for the period 1986–2005 of about 9 mSv, which is equivalent to an integrated dose over this period of 180 mSv. The average dose to 98 million people who were affected in the three republics was 1.3 mSv, while the integrated dose from 1986 to 2005 was estimated at 26 mSv, with about three-quarters of it due to external exposure. The dose due to natural background radiation over the same period was approximately 50 mSv [U20].

548. As of 2020, residual radioactive material in the Russian Federation due to the Chornobyl NPP accident was still detected in 11,164 settlements [I58, V1]. The Bryansk region is the most affected area; additionally, deposition densities of ^{137}Cs measured in 183 settlements of the Kaluga region, 326 settlements in the Orel region and 798 settlements in the Tula region exceeded 37 GBq/km^2. Compared to 1987, the area of agricultural land affected in these four regions has more than halved; in the Bryansk region, the area of land belonging to the exclusion zone has decreased by an order of magnitude. The spatial distribution of ^{137}Cs in soil in the affected territories of the Russian Federation is highly variable, with the deposition density of ^{90}Sr in soil being one or two orders of magnitude lower compared to ^{137}Cs. The estimated annual doses to inhabitants of these settlements varied from 0.01 to 5.6 mSv. More information on current levels of deposition in the affected areas is provided in electronic attachment A-5.

549. Predicted estimates for the year 2056 indicate that average annual effective dose to 90% of the population should remain above 1 mSv in only four settlements of the Bryansk region, with a predicted

maximum annual dose of 1.4 mSv [B56]. In the 13 regions remaining under control, the predicted annual average effective doses from Chornobyl fallout in 2056 are predicted to vary between 0.02 and 0.08 mSv.

550. According to a long-term study on the reconstruction of absorbed doses to the thyroid from exposure to ^{131}I received within the first couple of months after the accident, the absorbed doses to pre-school children in the affected areas of the Bryansk region were above 0.05 Gy. Estimates were carried out for children residing in 1,106 settlements where soil deposition of ^{137}Cs exceeded the legislative criterion of 37 GBq/km^2. Children under 3 years of age received the maximum individual absorbed doses to the thyroid, up to about 10 Gy in 17 settlements [K27].

551. For 374,416 residents in the Bryansk, Kaluga, Orel, and Tula regions listed in the Russian radiation epidemiological register, the average integrated dose received from 1986 to 2020 was 0.03 Sv. The absorbed dose to the thyroid received by adults, due to iodine radioisotopes, averaged 0.084 Gy, while that to children reached a peak of 4 Gy in the aftermath of the accident [I58].

552. Epidemiological cohort studies were established in Belarus and Ukraine to examine the prevalence of thyroid cancer and other thyroid pathologies in people exposed as children or adolescents to radioactive fallout from the Chornobyl NPP accident. These cohorts initially consisted of people who had direct thyroid radioactivity measurements taken in May to June 1986 and have been the subject of regular thyroid screening examinations since 1998 [S69]. Estimates of doses have been reported previously [D23, O11] but the most recent review of the cohorts and thyroid doses received revised the cohort sizes to 11,732 individuals in Belarus and 13,204 in Ukraine with average thyroid doses of 0.68 Gy and 0.65 Gy, respectively [D25].

553. Currently, deposition densities of ^{137}Cs are greater than 37 kBq/m^2 in 2,193 settlements in Belarus. As of 2020, it was estimated the annual doses to the population in 34 settlements were equal to or exceeded 1 mSv. The average annual dose in the period 2021–2025 to people living in the settlements in Belarus where deposition densities of ^{137}Cs exceeded 37 kBq/m^2, was 0.25 mSv. According to estimates from measurements of activity concentrations in soil and whole-body counting, this dose will be reduced to 0.17 mSv in the period 2026–2030 and to 0.14 mSv in the period 2031-2035 [V21]. The distribution of doses to the population of the affected in Belarus between 2011 and 2025 is provided in electronic attachment A-5.

554. Similarly to the Russian Federation, the spatial distribution of ^{137}Cs in soil in the affected territories of Belarus is highly variable and the deposition density of ^{90}Sr is one or two orders of magnitude lower than ^{137}Cs (see electronic attachment A-5). The area of affected agricultural land in the six regions of Belarus impacted by the Chornobyl accident continues to decline. Belarus maintains a State Register of persons affected by radioactive contamination from the Chornobyl NPP accident; this register includes 276,154 people. The average cumulative dose to this people since the accident to 2020 was estimated to be 24 mSv, with 17 mSv due to external exposure [V20].

555. A comprehensive monitoring programme in the affected territories of Ukraine ran from 1991 to 2013 as part of the programme of dosimetric passportization for settlements within the radioactive contaminated territories. A Ukrainian State Register of persons affected by the Chornobyl NPP accident was also established. The passportization monitoring programme included the measurement of radionuclides in food and in humans using whole body counting. The settlements where the average annual dose exceeds 1 mSv in at least one of the years between 2011 and 2013 is shown in electronic attachment A-5 [N6].

556. Assessment of public exposures in Ukraine due radionuclide deposition from the accident at Chornobyl NPP estimated that the annual effective doses did not exceed *(a)* 1.24 mSv for adults and 0.65 mSv for children in the Rivne Region in 2020; *(b)* 1.8 mSv for adults and 0.5 mSv for children in

the Zhytomyr Region in 2021; and *(c)* 0.5 mSv in the Kyiv Region in 2019 [V9, V10, V11]. Significant changes have recently been made to the monitoring and dose assessment methodology used to determine exposures in the affected regions [B13].

Russian Federation: Tomsk (1993)

557. In April 1993, a serious accident occurred at the Siberian Chemical Enterprises facility at Tomsk-7. The accident caused damage to both the reprocessing line and the building, resulting in the release of about 30 TBq of beta- and gamma-emitting radionuclides and about 6 GBq of ^{239}Pu. Radiological monitoring of plant personnel demonstrated that only six individuals received doses above the 0.2 mGy detection thresholds of the dosimeters used. Dosimetry on 14 of the 20 firefighters indicated individual doses between 1 and 7 mGy [I6]. The IAEA performed a thorough investigation of the accident, including an assessment of the possible exposure of the local population. The total predicted doses were between 0.14 and 0.37 mSv in the absence of protective measures and between 0.13 and 0.35 mSv with measures in place. The maximum dose received by any resident was less than 0.4 mSv [I6].

Japan: Tokaimura Fuel Conversion Plant (1999)

558. In September 1999, a criticality accident occurred in a fuel conversion plant in Tokaimura during the processing of highly enriched fuel for an experimental fast reactor, when workers, following unauthorized procedures, poured 16.6 kg of uranium enriched to 18.8% into a precipitation tank, resulting in a criticality excursion. Two workers died because of the accident, which also resulted in the exposure of nearby population from direct neutron and gamma irradiation. One hundred and sixty-one residents living within a 350 m radius of the plant were evacuated and another 310,000 were advised to stay indoors. Dose assessments were performed for 666 people and the dose equivalent for most of the neighbouring residents was estimated at less than 5 mSv while the highest dose was estimated to be 21 mSv. Fission products were detected in environmental samples, but the levels were well below the intervention level prescribed for foods [A10, I7].

Japan: Fukushima Daiichi (2011)

559. On 11 March 2011, a 9.0 magnitude earthquake along the Japan Trench produced a devastating tsunami, which affected the coast of the Tohoku area, including the Fukushima prefecture and caused widespread devastation. As a result of the tsunami, the Fukushima Daiichi NPS lost its emergency power supply. Throughout the next four days, hydrogen explosions occurred at three of the six reactor units resulting in the release of significant amounts of radionuclides into the environment. The releases of ^{131}I and ^{137}Cs were crucial contributors to the doses received by the local and regional populations.

560. According to the UNSCEAR 2020/2021 Report, annex B [U29], the highest average doses where estimated to individuals who were not evacuated residing in the municipalities with high ground deposition density within Fukushima Prefecture. The average doses to infants for the first year in each municipality were estimated to be between 3.6 and 5.3 mSv; average doses to adults were estimated to be about 70% of those for infants. For the municipalities of neighbouring prefectures (Ibaraki, Miyagi, Tochigi, and Yamagata), the estimated average doses to adults in the first year ranged from 0.1 to 0.9 mSv, while the average doses to adults in the remaining prefectures of Japan were estimated to be in the range of 0.004 to 0.4 mSv. External exposure to deposited radionuclides was the predominant pathway of exposure in all the regions.

561. The estimated average doses to adults in the first year for the different evacuation groups varied from less than 0.05 to about 6 mSv. The corresponding average absorbed doses to the thyroid in the first year ranged from less than 1 to about 15 mGy for adults and between about 2 to about 30 mGy for infants. The absorbed dose to the thyroid up to age 80 years was estimated to be about twice that received in the

first year, largely due to continued external exposure to irradiation and to ingestion of the longer-lived radioisotopes of caesium. However, it should be noted that these dose estimates do not take account of the effects of remediation work carried out in the most affected area [U29].

562. The Fukushima prefectural government has undertaken the Fukushima Health Management Survey since June 2011. It includes a basic survey, sent to 2 million residents, which was used to estimate external radiation exposure during the immediate post-accident months [F6]. External doses of residents in Fukushima prefecture have been continuously estimated based on monitoring results and responses to the basic survey. According to the reported data as of 31 March 2022, excluding those occupationally exposed, 99.8% of the 467,256 people living in the prefecture received a dose of less than 5 mSv with a maximum of 25 mSv and an average of 0.8 mSv [F6].

563. In the months following the accident, following a request from the Nuclear Safety Commissions Technical Advisory Organisation in an Emergency, external measurements of dose rates from children's thyroids were taken to determine potential internal exposures due to radioiodine. The study reported that absorbed doses to the thyroid in the subjects were estimated to be less than 30 mGy [K20]. The external counting survey also conducted whole body exposure measurements on 346,394 people by 30 November 2021. For over 99.9% of them, the committed doses due to internal exposure from ^{134}Cs and ^{137}Cs was estimated to be below 1 mSv with a maximum of 3 mSv [M35].

564. The onsite monitoring programme at the Fukushima Daiichi NPS includes the monitoring of radioactivity in groundwater, surface water, seawater, dust, and soils as well dose rates in air. Various Japanese government organizations carry out offsite monitoring programmes for dose rates in air, and radioactivity in dust, fallout, soils, foods, surface water, groundwater, seawater, sediments, drinking water, sewage, and flora and fauna. Regular reports on the results of the monitoring programmes are publicly available [N25, N26, T8].

565. Data submitted to the UNSCEAR Global Survey on Public Exposure gave average annual ambient dose equivalents for the cities of Fukushima, Shirakawa and Nihonmatsu of 0.068, 0.16 and 0.28 mSv, respectively. There were no significant changes in the recent monitoring results for ambient dose equivalent rates in air, and activity concentrations in dust, soil, seawater, sediment, and marine biota during the period from October to December 2022 [J7]. Monitoring data on the major food products in the fiscal year 2021 in Japan show that all activity concentrations were below the national safety standards. According to the Total Diet Study for Japanese food, the annual dose in 2022 was estimated at between 0.5 and 0.8 μSv [M25].

566. Since late 2023, operations have began to discharge treated water from the Fukushima Daiichi NPS site to sea. Although these releases commenced after the data submission period for consideration in this current evaluation had closed, some general information is provided for completeness. Treatment of site water to remove radionuclides is carried out via the Advanced Liquid Processing System (ALPS). The treated water is then released to sea at a rate that ensures that the activity discharged meets regulatory requirements. Japan provides regular analysis of the water discharged and reporting of discharges from the site and seawater monitoring [I47]. In 2023, the IAEA released a comprehensive report on the safety review of the ALPS treated water [I52]. This report reviewed the assessment made by the operator of the Fukushima Daiichi NPS [T7] and agreed with the conclusion that the release of the water would result in doses to representative persons between 0.02 and 0.04 μSv, predominantly from ingestion of seafood.

(b) *Industrial accidents*

567. Only one accident involving radionuclide sources which occurred over the period 2007–2022 was identified as having the potential for public exposure. In 2008, the waste division of the Institute for Radioelements in Fleurus (Belgium) accidentally released 45 GBq of ^{131}I into the environment. An assessment of individual doses, calculated based on very cautious assumptions, indicated that there was a potential for an effective dose of 160 μSv and an equivalent dose of 3 mSv to the thyroid of young children. Restrictions on local food and milk consumption were enforced and measurements of 1,320 individual's thyroids indicated no measurable exposure [V4].

(c) *Accidents involving orphan sources*

568. In April 2009, in Nouakchott, Mauritania, a construction worker collected and kept on his person for an extended period a lost Category III radiography source containing 600 GBq (16 Ci) of ^{192}Ir. The prolonged exposure caused severe injury to his left leg. The worker was transported to France for treatment and was discharged in September 2009 after recovery [I21].

569. In April 2010, a patient in a hospital in New Delhi (India) showed suspected radiation-induced symptoms. The patient was a scrap metal dealer and radioactive material was detected in his shop and in two other shops nearby. The source of this material was traced to a ^{60}Co source from an old gamma cell irradiator purchased by the Delhi University in 1969. Doses received by seven exposed individuals, assuming protracted exposure of 1–2 days, were estimated to range from 0.6 to 6.8 Gy. One individual who received a protracted dose of 3.1 Gy did not survive [K43, S32].

570. A radiation accident occurred in Turmero, Aragua State (Venezuela) on 3 June 2010 when workers handled an unshielded Category II ^{192}Ir industrial radiography source with an activity of 2.4 TBq (65 Ci). The IAEA assessed the medical condition of the most exposed individuals and provided advice for their medical treatment. Following highly specialized and effective medical treatment in France, the most exposed person recovered entirely after receiving surgery and adjuvant administration of mesenchymal stem cells [I24].

571. In October 2010, in Honduras, elevated dose rates up to 14 mGy/h were detected from a shallow buried source in a courtyard of a medical facility. Initial actions were taken to shield the area and install appropriate cordons and signs. A subsequent source inventory revealed that a ^{137}Cs brachytherapy source with an activity of 555 MBq (15 mCi) was missing. The source was recovered from a depth of approximately 2 cm below the surface. Dose reconstruction determined that overexposure of any individual was extremely unlikely [I24].

572. In December 2013, a vehicle transporting a teletherapy unit head with a ^{60}Co source from a medical facility in Tijuana to a disposal facility in Santa Maria Maquixco (Mexico) was stolen by a group of armed individuals. Twenty-seven members of the public received doses above regulatory limits: ten received doses of 0–5 mSv, six doses of 30–50 mSv, four doses of 50–100 mSv, five doses of 100–500 mSv, one a dose of 1–2 Sv, and one a dose of 2–3 Sv. Nineteen emergency workers received doses of less than 1 mSv, twenty-seven doses of 1–5 mSv, two doses of 5–10 mSv and two doses of 15–20 mSv [I43].

573. On 7 May 2014, a ^{192}Ir source of 960 TBq (26 Ci) in Nanjing city (China), was not returned to its shielded housing and was misplaced by industrial radiographers. The source was found and taken home by a temporary worker, exposing his relatives and three lodgers. Two days later he also took it to his parents' house, exposing other relatives and several lodgers. On 10 May, the source was discarded on a grassy area near the worker's house, where 30 people were working. The source was successfully recovered on the

same day. The worker was estimated to have been exposed directly for 3 hours and 15 minutes and to have received a whole-body dose of approximately 1.5 Gy and a local skin dose of 4,100 Gy. He survived but suffered significant complications from the exposure and died in December 2020 due to complications relating to wound infection [Z8].

574. On 17 October 2016, a ^{192}Ir radiography source was left unsecured at a worksite, near Adana, Türkiye, and collected by a 16-year-old member of the public, who placed the source in his back pocket and showed it to household members and other people. The source was reported lost to the Turkish Atomic Energy Authority Disaster and Emergency Management Center by its owner on 20 October 2016 and was recovered on the same day. Twenty people were referred to hospital because of suspected irradiation. The individual who collected the source received the highest whole-body dose of 1 Gy [I35].

(d) *Accidents involving spacecraft and satellites*

575. Out of the 74 space missions that have involved radioactive sources in reactors, radioactive heating units or RTGs, there have been eight recorded cases of failures with the potential to cause public exposure. Two of these accidents resulted in environmental contamination from the uncontrolled release of radioactive material: *(a)* to the United States Transit-5BN-3 satellite in 1964, which released an estimated 600 TBq of ^{238}Pu from a SNAP-9A RTG into the stratosphere, and *(b)* to the Soviet Union's Cosmos-954 satellite in 1978, which dispersed about 15 kg of enriched uranium from its U-Mo reactor over parts of Canada. Collective doses to the world population for the Transit-5BN-3 accident were estimated at 2,100 person–Sv from inhalation and 2.4 person–Sv from ingestion, while the total collective dose to the world population for the Cosmos-954 accident was estimated at 16 person–Sv [U13, U19, U20]. Other recorded cases include the re-entry of the nuclear reactor section of the Soviet Union's military satellite Cosmos-1402 into the Earth's atmosphere near Ascension Island in 1983. The Committee previously reported on these events and the resulting public exposure in the UNSCEAR 1993 Report [U13]. Detailed information regarding all eight accidents is provided in electronic attachment A-5. Some information on the accidents involving the Transit-5BN-3 and the Cosmos-1402 satellite is also provided in the inventory of accidents and losses at sea involving radioactive material published by the IAEA in 2015 [I32].

(e) *Accidental loss of radioactive material at sea*

576. There have been eight cases of nuclear submarines which have sunk as the result of accidents, with two from the United States (USS Thresher in 1963 and USS Scorpion in 1968), and three from the former Soviet Union (K-8 in 1970, K-219 in 1986, and K-278/Komsomolets in 1989) lost in the Atlantic Ocean. A further submarine from the former Soviet Union (K-429 in 1983 and 1985), sank in the Pacific Ocean near the Kamchatka Peninsula, was recovered and sank again at its base port. The Russian Federation has also lost two submarines in the Barents Sea near the coast of Kola Peninsula (K-141/Kursk in 2000 and K-159 in 2003).

577. Radiological surveys at the wreck site of USS Thresher and USS Scorpion concluded that there was no detectable levels of human-made radionuclide released by the two submarines [M44], while the Joint Norwegian-Russian Expert Group concluded that there was no evidence of any releases from the reactors onboard K-159 [J17]. Environmental investigations around the Komsomolets nuclear submarine reported that releases from the reactor were likely to have occurred since it sank [H24, J18]. In 2019, elevated levels of ^{137}Cs, ^{90}Sr, ^{236}U and ^{239,240} Pu were detected in seawater sampled directly from the ventilation pipe where releases from the reactor were occurring, but sampling of seawater and sediments around the Komsomolets have shown that these releases had no impact on the area around the submarine [G31, J18].

There has been no evidence of any releases of ^{239,240}Pu to the marine environment from the two nuclear warheads in the submarine's torpedo compartment [G31, J18].

578. There have been seven recorded accidents that have resulted in the confirmed loss of one or more nuclear weapons carried by submarines, surface ships, aircrafts, and rockets [U21]; two of these, the accident at Palomares (Spain) in 1966 and at Thule (Greenland) in 1968, have had an impact on the surrounding environment and are covered in detail in section IV.E.1.g.

579. There have been two recorded incidents involving emergency disposal of RTGs during transport by helicopter, both occurring over the eastern coast of Sakhalin Island in the Sea of Okhotsk. In the first incident in 1987, an RTG containing 1.2×10^4 TBq of ^{90}Sr was disposed of at sea. The second incident in 1997 involved an RTG containing 1.3×10^4 TBq of ^{90}Sr, which was recovered in 2007 [G20, I32]. No public exposure linked to either of these incidents has been reported.

(f) *Polonium-210 poisoning*

580. In 2006, Alexander Litvinenko died after being poisoned in London with ^{210}Po [O14]. His intake by ingestion was estimated to be around 4 GBq, and the resulting organ doses ranged from about 20 Gy to over 100 Gy [H10, O14]. The potential radiological risk to other individuals exposed to ^{210}Po associated with the poisoning was also assessed. In total, 1,029 UK residents were identified as individuals who could have been potentially exposed, associated with the 11 locations where the highest activity concentrations were detected. Of these, 974 were interviewed, and 787 were offered urine tests for ^{210}Po excretion. Doses to 53 people were estimated to be above 1 mSv with the highest radiation dose estimated at approximately 100 mSv, while 139 individuals showed evidence of probable intakes associated with the incident [H11, M1].

(g) *Other radiological accidents*

Spain (1966)

581. On 17 January 1966, a United States Air Force B-52 bomber crashed near the village of Palomares (Spain) after colliding in mid-air with a KC-135 refueling tanker. Of the four thermonuclear weapons carried by the aircraft, one fell into the ocean and was retrieved on 7 April 1966; another was recovered intact from the fields where it had landed, while the remaining two were destroyed on impact. The pyrophoric plutonium metal was ignited, creating a cloud of oxide fumes that contaminated an area of 2.26 km^2. The top 10 cm layer of soil was removed immediately after the accident, but residual plutonium and americium remained present in some areas [I9, U20].

582. Immediately after the initial clean-up, an environmental monitoring programme was initiated due to the risk of plutonium and americium entering the food chain. The transfer to meat and other foods of transuranic radionuclides present in the environment as isolated refractory particles was found to be limited despite the presence of biological fertilizers and microorganisms. Plutonium present in the Palomares soils appeared highly insoluble in water and not readily available, therefore hindering its transfer through the food chain [S11].

583. From 2007 to 2009, a detailed 3D map of the distribution of the remaining transuranic radionuclides (^{238}Pu, ^{239}Pu, ^{240}Pu, ^{241}Pu, ^{241}Am, and ^{235}U) in the area affected by the accident was developed [E7]. The total inventory of ^{239,240}Pu was estimated to be 485 g. Particle sizes ranged from submicron to fragments exceeding 1 mm. The average particle size immediately after the accident was around 100 μm, but it

decreased with time due to weathering, indicating that resuspension of particles remained possible in the arid conditions of the region around Palomares [S11]. A collective dose of 3 person–Sv to the local and regional population was previously reported [U20]. Current estimate of the collective dose based on the updated inventory and distribution map is lower by approximately 25% [E7].

Greenland (1968)

584. On 21 January 1968, a United States Air Force B-52 bomber crashed near the Thule airbase—now called Pituffik Space Base—in northern Greenland. The bomber carried four nuclear weapons which were destroyed, spreading plutonium over a large area. Monitoring surveys carried out during four expeditions between 1968 and 1979 showed that most of the radioactivity released, including ^{241}Am, was confined to the sediments and the benthic environment within 50 km of the crash site [I9]. An assessment of radiation doses from the remaining radioactivity in the environment was performed by the Danish government in 2011 [N9]. The report on the assessment concluded that annual radiation doses to representative persons in the Thule area would be lower than 1 mSv even under very cautious assumptions.

Europe (2017)

585. From the end of September until early October 2017, elevated levels of ^{106}Ru were recorded by air monitoring stations across Europe. Although to date the source of the release has not been confirmed, studies have indicated that the release most likely originated from the Ural region of the Russian Federation with potential source locations extending between Northern Kazakhstan and Novaya Zemlya [B42] and that the Mayak Production Association was the most likely source, based on atmospheric models. The total activity of ^{106}Ru in the release was estimated at approximately 250 TBq [M11, S19]. Individual doses across various cities in Europe were estimated at between less than 0.01 and 0.33 μSv, while the collective doses to the European population, excluding the Russian Federation and Türkiye, was estimated to be approximately 23 person–Sv [B42, J3, S79]. Doses from the release of ^{106}Ru estimated for various age groups at four cities in Croatia for the period 29 September to 5 October 2017 are provided in electronic attachment A-5.

China (1992)

586. Between 1982 and 1984, recycled steel contaminated with discarded ^{60}Co sources was used to manufacture reinforcing bars at the Hsin Jong Iron and Steel Company in Taoyuan, province of Taiwan (China). These bars were incorporated into more than 180 buildings, including approximately 1,600 apartments, schools, and businesses, notably the Minsheng Villas complex in Taipei [C33]. The contamination was first detected in 1992, prompting an investigation by the Taiwanese Atomic Energy Council to identify the number of buildings that had been affected and assess exposures [B52, C4, C31, C32, C33, H36, H44, L12, L13, T25]. Estimates of annual effective doses received by residents of the affected apartments ranged from 1 to 140 mSv. This broad range reflected the different exposure scenarios and source terms for each of the affected apartments [L12]. Dose rates varied significantly within rooms and apartments and estimates of the occupancy of residents were affected by large uncertainties [H36, T25]. Personal and phantom measurements were also performed in some studies to validate dose reconstructions [C31, L12, L13].

587. The remediation plan was broadly based on the exposure of the residents, with the apartments divided into four categories according to the annual dose received. Remedial measures included the provision of regular free physical examinations for residents who received annual doses above 5 mSv, shielding or rebar replacement, demolition, evacuation, or leaving buildings in place to allow for radioactive decay [C32]. Residents who received annual doses exceeding 15 mSv were given the option to sell the residence to the government. Follow-up studies indicated that more than 10,000 people received a total average dose of 600 mSv (range: 120-4,000 mSv) over the 20 year period between 1983 and 2003 [C20].

2. Nuclear explosions for peaceful purposes

588. Both the United States and the former Soviet Union tested nuclear explosions for non-military peaceful purposes from the late 1950s into the 1980s. These tests involved investigating the use of nuclear explosions for civil excavation work, fracking, extinguishing burning gas fountains, and a range of other mining and research applications. By 1976, these tests were controlled under the Treaty on Underground Nuclear Explosions for Peaceful Purposes [U3], and today such tests are banned under the Comprehensive Nuclear-Test-Ban Treaty adopted in 1996 [U4]. Information on the peaceful nuclear explosion tests carried out by the United States and the former Soviet Union are provided in electronic attachment A.5.

(a) *United States*

589. The United States carried out numerous peaceful nuclear explosions as part of the Plowshare Program and the Vela Uniform Program. The Plowshare Program was intended to explore non-military uses for nuclear explosions, including the production of isotopes and heavy elements, natural gas stimulation, and various types of civil excavation (i.e., canals, harbours, or dams) [G10, H5, T6, U39]. Under the Plowshare Program, the United States carried out 36 individual nuclear detonations between December 1961 and May 1973 as well as experiments involving non-nuclear detonations [B14, U39]. Most tests took place at the NNSS, with two tests occurring in New Mexico and another two in Colorado. All the detonations occurred underground, with releases of radionuclides of some tests being detectable offsite. Yields of the Plowshare detonations ranged from 35 tons to 378 kt [U39].

590. The first Plowshare test, Project Gnome, was carried out in New Mexico in 1961 and resulted in offsite releases [F2]. A tracer test using ^{137}Cs, ^{90}Sr, ^{131}I and ^{3}H was conducted at the Gnome site in 1963 to evaluate potential movement of radionuclides in groundwater [P29, U43]. Materials from the subsequent surface clean-up activities were stored onsite or removed to the NNSS [F2]. The area is remote and under institutional controls including monitoring of groundwater [U43]; public exposure from the tests was negligible and future exposures are unlikely.

591. Project Rulison was a proof-of-concept experiment in natural gas stimulation performed under the Plowshare Program in Colorado in 1969 [D2, U45]. Most of the radionuclides produced by the detonation remain onsite, solidified in the melted rock [D2]. Gas from a test well was flared to the atmosphere and tritiated methane was removed along with ^{14}C and ^{85}Kr [D2]. Releases were monitored by State and federal authorities to protect public health [U45]. The well was shut in 1971 and plugged in 1976 [U45]. Drilling is currently prohibited in the immediate area of the detonation site and monitoring of groundwater and nearby gas wells indicated no offsite movement of any remaining ^{3}H [D2, U45]. An assessment of public exposure from released ^{3}H was based on activity concentrations in the range between 2.2×10^{-6} and 20.7 Bq/m^3 measured during atmospheric monitoring of the production testing in 1970. The assessment estimated that the highest lifetime excess cancer risk was less than 1×10^{-6} which was considered negligible, but did not provide any dose estimates [D2].

592. Field assessments prior to two proposed tests of the Plowshare Program included use of radioactive tracers [B14]. Project Pinot in Colorado in 1960 used a small amount of ^{85}Kr in conjunction with conventional explosives to study gas migration following an underground explosion [B14]. As part of Project Chariot, a radiotracer experiment was carried out in 1962 at Cape Thompson, Alaska, to evaluate the mobility of fission products in soils and surface water [U44]. The experiment used soil from the NNSS contaminated with ^{137}Cs, ^{85}Sr, ^{131}I, and other radionuclides [U44]. Following the experiment, the contaminated soil was removed and stored locally and in the 1990s it was permanently removed to the NNSS [B14, U44]. The Chariot site was remediated in 1993. Doses prior to remediation were estimated to be lower than 0.01 mSv for an exposure time of 10 hours standing on the mound of waste material,

while post remediation exposures were at background level [U37]. The Project Pinot test site is inaccessible and therefore public exposure was not assessed [B14].

593. The seven nuclear explosions carried out under the Vela Uniform Program were research experiments in nuclear test detection [U39]. The intent of the programme was "to develop the technological capability to detect and identify underground and underwater nuclear detonations" to verify compliance with nuclear testing moratoriums related to treaties [B14]. All detonations performed as part of the Vela Uniform Program occurred underground, including three at the NNSS, one at another location in Nevada, two in Mississippi and one at Amchitka, Alaska [B14, U39]. Yields ranged from 380 t to 80 kt [U39] and since no offsite releases of radioactivity occurred [U39] public exposure were unlikely.

(b) *Former Soviet Union*

594. In the period between 1965 and 1988, 122 underground nuclear explosions with 128 explosives for peaceful purposes were conducted at 115 sites in the former Soviet Union (Kazakhstan, Russian Federation, Turkmenistan, Ukraine and Uzbekistan) [L26, N23]. The detonations were conducted for experimental, industrial and scientific research purposes. The explosion sites are shown in figure XXVII.

Figure XXVII. Sites of peaceful underground nuclear explosions in the territory of the former Soviet Union [N23]

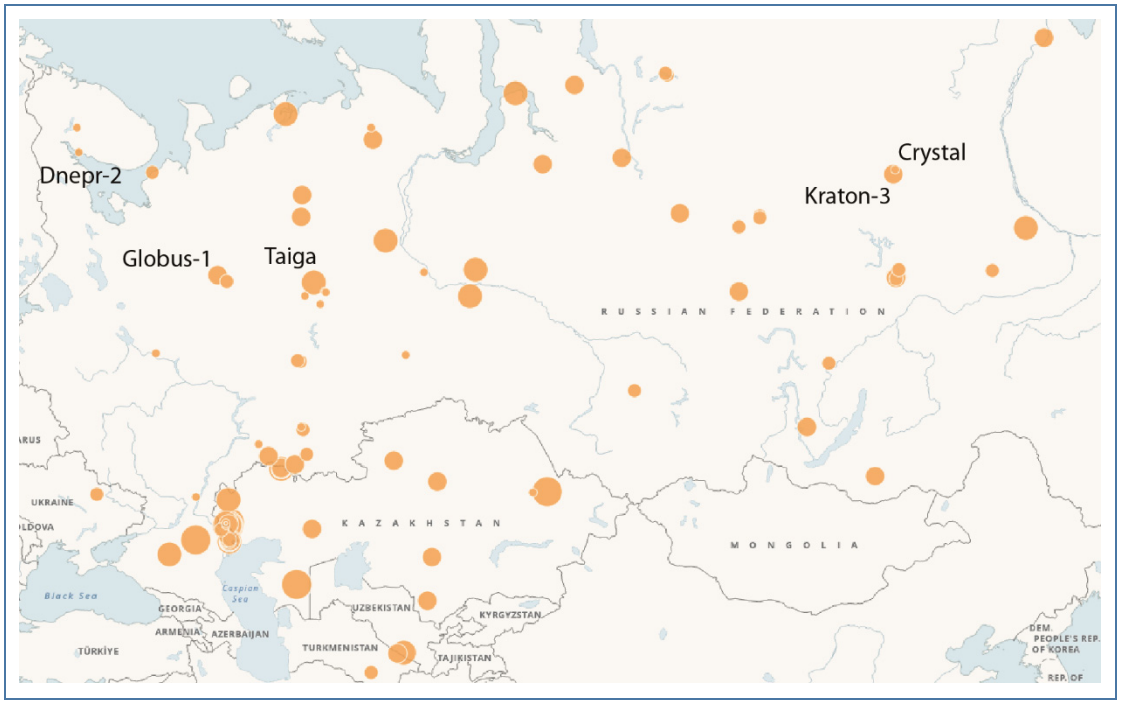

595. In total, 84 charges were detonated with energy yields between 0.3 kt and 38 kt. The total energy yield of peaceful nuclear explosions (PNE) reached 0.75 Mt or 2% of the value for all underground nuclear explosions carried out in the former Soviet Union. Solid and liquid radioactive waste generated by these detonations are stored in various hydrogeological environments located in central locations. The waste is currently classified as non-recoverable radioactive waste [R31], and contains mainly ^{90}Sr, ^{137}Cs, ^{3}H and alpha-emitting radionuclides [L26].

596. The radioactive contamination at each PNE site is unique. Most explosions were underground, leaving residual radioactive materials buried; solid waste is generally stable and contained. However, radionuclides that dissolve in water can be transported through hydrogeological processes which may be enhanced since the explosion creates an area of fractured and crushed rock [K6]. At most sites—excluding emergency and excavation explosions—the radiological situation is characterized by external gamma dose rates of 0.1-0.15 μSv/h and activity concentrations of ^{90}Sr, ^{137}Cs in soil at levels comparable with those from global fallout [B30, K17, K18, L26, T11]. A release of tritiated water to the surface occurred following the Dnepr-2 test. Specific activities of ^{3}H in water from a mountain audit measured in 2008 and 2019 were 7,500 and 1,200 Bq/kg, respectively [R10]. The release of radionuclides following the Globus-1 and Kraton-3 emergency explosions generated substantial contamination in the surrounding area [K7, R7].

597. Remediation work is being carried out in the Russian Federation to address the nuclear legacy of PNE sites. This activities have significantly improved the radiological situation in the territory of the Globus-1 site [K7, K17, K18], where ambient dose equivalent rates have decreased from 1.5 μSv/h to natural background levels of 0.05–0.1 μSv/h [K17]. In contrast, the fallout footprint at the Kraton-3 facility has become the largest and most contaminated among all PNE sites. A notable feature of the residual radioactive material in soil at the Kraton-3 site is the predominance of ^{90}Sr over ^{137}Cs [R8]. The integrated gamma-ray doses in the air attributed to the explosions varied from 1.2 to 10 Gy, with the maximum value estimated 70 m from the Kraton-3 borehole [R8].

598. Excavation explosions, such as Taiga and Crystal, resulted in release of radioactive material and its dispersion to the surrounding environment. At the Taiga underground nuclear explosion site, contamination was confined to an area of approximately 1 km^2, now covered with a newly grown mixed forest surrounding the artificial lake created by the explosion. Dose rates exceed the levels of natural background radiation by up to 10–20 times and are mainly attributable to ^{60}Co and ^{137}Cs released during the explosion [R9].

599. Given that areas surrounding PNE sites are characterized by low population density, radiation doses were generally estimated for recreational scenarios, such as tourism [H43]. These scenarios assumed that people spent two weeks a year visiting the areas near the PNE sites. The main exposure pathways considered in the assessment included external exposure from surface deposition, inhalation of resuspended soil, ingestion of wild berries, fish, mushrooms and drinking water from both surface and ground sources. The annual external dose from the human-made source at the Taiga site was estimated at 70 μSv for tourists and 8.7 μSv for investigators [R9]. The contribution to the internal dose from ingestion of ^{137}Cs, ^{90}Sr and ^{3}H in natural water and wild food products (mushrooms, berries, fish) was estimated at 2–4 μSv. Doses via inhalation of resuspended particles containing ^{137}Cs, ^{90}Sr, ^{238}Pu, ^{239,240}Pu, ^{241}Am and ^{60}Co were estimated to be 1–2 μSv assuming a one-week stay at the site. The estimated annual doses due to residual radioactivity at other PNE sites were in the range 4.5 to 18 μSv.

3. Other past practices

(a) *NORM legacy sites*

600. The term ‘NORM legacy sites’ refers to several types, such as mining sites, waste rock sites, processing facilities and tailings storage sites. Exposure pathways and radiological impact of mining and waste rock sites vary significantly, depending on the extraction method. Both open-cut and underground mining generate large volumes of waste material, such as waste rock, overburden, and tailings. Acid rock drainage and other chemical leaching processes may also occur and pose environmental challenges. Processing plants typically

have a small footprint and can be remediated more easily than tailings facilities, which require considerable engineering controls with ongoing management. Specifically for uranium mining, ISL operations leave a smaller environmental footprint with limited waste material but may affect groundwater pathways. Equipment used in mining and processing can be decontaminated for reuse or recycling or may simply be disposed of with other waste products. The radiological risk associated with equipment at legacy sites arises from ore, ore concentrates, and waste products.

601. The predominant exposure pathways are specific to the legacy site and, therefore, specific exposure scenarios are required when assessing doses. External exposure is generally related to residual tailings or exposed mineralized material present on site, although in some cases this material might have been transported offsite to local residential areas. Exposure from inhalation of radon and its decay products is highest on the sites but also contributes to the overall exposure of people residing in nearby locations. Internal exposure from ingestion of water and food produced on legacy sites or adjacent areas can result in significant exposure.

Uranium

602. The United States, which has over 4,000 uranium legacy sites, has developed a radiological human health risk conceptual site model which can be applied to legacy mines of all sizes, based on a range of site use scenarios to determine the potential radiological risk [U38]. The United States also has a uranium location database that provides an overview of their uranium legacy sites [U49]. Similarly, France has also established a database of their uranium legacy sites and information on dose assessments performed for the sites included in the database is provided by the IRSN [I87].

603. Canada requires the companies or organizations responsible for uranium legacy sites to provide relevant assessments that are updated if site conditions change. Due to their remote locations, the radiological impact on the public from several Canadian legacy sites are monitored from a watershed location further downstream. All Canadian legacy sites require a licence to decommission through the Canadian Nuclear Safety Commission. These legacy sites, which have been or are being remediated, have a goal of reducing the annual dose at or below 1 mSv. Sites that have completed remediation and are open to the public are inspected every three years.

604. In Australia, the assessment of potential environmental and public exposure from uranium legacy sites has informed the remediation of sites in the Northern Territory [B36, B37]. In the South Alligator Valley area, the annual dose to local indigenous people accessing the area was estimated to be 0.3 mSv [B38]. Furthermore, the annual effective dose to indigenous people for a realistic scenario for the Rum Jungle site was estimated to be 0.5 mSv above background level but could be as high as 2–3 mSv if the site was occupied for five months a year [B37].

605. All major uranium mining activities in Western Europe closed at the end of the twentieth century, and remedial work has been completed at most sites, although with varying levels of effectiveness. France, Portugal and Spain were the main European uranium producers; uranium was also produced in Eastern European countries—Bulgaria, Czechia, Estonia, East Germany, Hungary, Poland, Romania, Slovenia and Ukraine. Limited uranium mining activities still occur in Czechia and Romania. The Wismut mining region in the former German Democratic Republic was the predominant uranium production area in Europe. Estonia, Finland and Sweden also produced some minor quantities of uranium; sites in these countries have been fully remediated [E11].

606. Portugal has over 60 legacy uranium mines and mills mainly located in the central eastern part of the country. Some of these operations were active prior to 1944 when the focus was on the extraction of radium. Ore from a range of minor sites was processed at a central facility in Urgeirica which resulted in

the production of significant tailings [E10]. Several environmental studies were undertaken in the regions on and around uranium legacy sites indicating that annual doses varied from 2 to 20 mSv or higher [C5, C7, C8, K12, P15]. One of the control measures in place is the requirement that water released from the Urgeirica site should undergo treatment [P26].

607. In Spain, more than 20 mines and some mills in the west and south of the country were decommissioned by the end of the twentieth century and subsequently remediated [E14]. Some studies performed in and around the legacy sites reported increased exposures, but these areas are either not populated, or the exposures are related to natural sources rather than uranium residues from the legacy sites. Potential annual average doses were estimated to be 2.5 mSv at an abandoned site in Salamanca, western Spain [G13]. Other assessments estimated annual doses ranging from 3.2 to 5.1 mSv in populated areas near six uranium legacy sites in western Spain, based on measurements taken in 2000 and 2001 [Q2].

608. Czechia has approximately 66 uranium legacy sites and currently produces uranium from one site. Most legacy sites have been remediated recently; annual doses to the public from ingestion of water runoff from the sites were reported to range from less than 0.01 to 0.05 mSv [E9, J24]. Poland operated approximately 15 uranium mines. Of these only one site—a tailing facility—has been remediated, while the remaining mines have been abandoned and are accessible to the public [E15, W1]. Significant environmental contamination has been detected at many of these sites. For one of them, which is now a tourist attraction, estimated radiation doses could exceed 1 mSv within a single hour of exposure [F7].

609. One underground uranium mine in the Mecsek region in Hungary has been closed and partially remediated. The mine was flooded and the remediation work focused on the management of contaminated groundwater; however, no dose assessment is readily available [C57, J23, O4, S68]. The only uranium legacy site in Slovenia has also been completely remediated with some parts under public use; a monitoring programme is in place [E12, P12]. Bulgaria had a significant number of mines for the extraction of uranium by various methods, such as ISL and heap leaching. The majority of the 39 identified deposits have been exhausted and uranium mining operations ceased in 1992 [I2]. All sites have undergone some level of remediation to reduce significant contamination from the operation of the mines. However, remediation work has been insufficient in many cases and water contamination issues have emerged at some sites [D20, E6, E13, I93]. No information on assessments of doses for the public was readily available for inclusion in this annex.

610. Romania also maintains some uranium production and has many legacy sites. Approximately 23 sites have been closed but only two have been remediated. Abandonment of sites and a lack of funding for remediation resulted in significant environmental issues. Little information on the current state of the sites, plans for remediation, or public exposure is available [E5, F1]. During the early periods of operation, materials sourced from the uranium mines were used in the construction of houses nearby, resulting in high radon concentrations that required remediation [C54, P22].

611. Ukraine has uranium legacy sites from historical operations at several mines, including some ISL facilities, and one mill. [D31]. Historical management of the sites resulted in environmental issues, mainly due to groundwater contamination, that are still ongoing at sites that have not been fully remediated [D31, L7, R30, V22]. Public exposure was assessed to be negligible, with doses of less than 0.1 μSv [U2]. One assessment noted that dose to individual living on the banks of a river affected by the contamination could be as high as 0.1–0.15 mSv [V22].

612. In Germany, the company Wismut GmbH was established to manage the remediation of the uranium legacy sites in the former German Democratic Republic, where uranium mining and processing took place at many sites in the Saxony and Thuringia regions. Uranium mining operations, led by the demand for uranium in the former Soviet Union, resulted in significant environmental contamination and

public exposure [E3, I2, I15]. A remediation has been put in place at more than 60 sites across Germany [L16], with the aim to reduce annual doses received by members of the public to below 1 mSv [B28, E3]. An extensive monitoring programme has been established and is in place to assess the relevant discharges from the remediated sites. Annual doses due to discharges of radon and long-lived alpha emitters at the Schlema/Alberoda site to the local waters were estimated to be up to 0.33 mSv for some individuals in the affected populations under realistic exposure scenarios [B27].

613. Several uranium legacy sites are present in the territory of the Russian Federation, across the two districts of Zabaikalsky Krai and Stavropol Krai. Historical public exposures associated with uranium legacy sites have been significant. For example, the annual dose associated with the construction of houses from materials sourced from uranium mines in the village of Oktyabrsky, Zabaikalsky region prior to the relocation of the population, was estimated to be 14 mSv (range: 1.3–85 mSv) [K22]. In the Stavropol region, doses to adults and children associated with legacy sites around the town of Lermontov were estimated to range from 0.1 to 5.8 mSv and 0.1 to 7.9 mSv, respectively [I25]. The uranium legacy sites at Lermontov have since been remediated.

614. Many uranium legacy sites are present in Central Asia (Kazakhstan, Kyrgyzstan, Tajikistan, and Uzbekistan) [I23, I37, M30, S67] from mining operations carried out by the former Soviet Union. Several studies about these sites reported that annual doses to the public typically exceeded 1 mSv [L17, S10, S54, S67] and were estimated to be as high as 21.4 mSv for adults and 39.2 mSv for children [V5].

615. Several uranium mines and mills are still operating in China and there are several uranium legacy sites from the early stage of its nuclear programme. All uranium mining and milling legacy sites have been fully remediated and maximum individual and collective doses are reported to meet national radiation safety standards [C34]. China had almost 20 uranium processing plants served by small mines prior to the 1980s and 13 of them were closed down or put on standby [P11]. One study indicated that herders using areas around remediated tailings sites would receive an annual dose of 0.035 mSv from external exposure [Z5]. Generally, no comprehensive assessment of public exposure at individual sites is available, although some information on the uptake of radionuclides by uranium mill tailings and public exposure from ingestion was found in the open literature [C30, H38, W23, X1].

616. An assessment of uranium legacy sites was undertaken in Argentina in 2006. Public exposure was assessed at several uranium legacy sites as one of the criteria used to prioritize their remediation [C41, C42]. To date only the site containing the tailings from the closure of a uranium mill in Malargüe has been remediated. Brazil has one uranium legacy site in a high precipitation region on the Poços de Caldas plateau, in the state of Minas Gerais. There have been no reports of public exposure exceeding the regulatory dose constraint of 0.3 mSv/a [P16, R26].

617. African nations historically involved in the production of uranium that have legacy sites include the Democratic Republic of the Congo, Gabon, Madagascar, Niger, South Africa, and Zambia. The Shinkolobwe uranium mine in the Democratic Republic of the Congo, which was the source of uranium for the atomic bombings used on Hiroshima and Nagasaki, was closed in 1960 but has been accessed by artisanal miners for the extraction of non-uranium minerals. The Kitwe region in Zambia was the location of minor uranium production in the early 1950s and has left some legacy tailings that required management. The most affected population was resettled not because of their exposure to radiation but because of other safety issues [K26]. More recently, the Akouta mine in Niger ceased operations in 2021 and is undergoing remediation, which is expected to take 20 years.

618. The Gabon region of Mounana was the site of several uranium mines from 1962 to 1999. Restoration work in the late 1990s saw annual doses to two groups of public decrease from 2.9 and 2.3 mSv to 0.97 and 1.23 mSv, respectively [L28]. One facility in Madagascar that operated from 1946

to 1952 has had little remediation and has become a populated rural environment. The village of Vatovory is the most heavily affected with annual doses exceeding 20 mSv for gamma and radon only; annual doses in other villages in the area also exceed 1 mSv [K1, R14].

619. Most uranium production in South Africa has taken place as a by-product of gold mining in the Witwatersrand Basin. Due to the uranium association with gold in this region, there are many mining legacy sites that have issues associated with management of NORM. It is estimated that there are more than 400 gold tailings sites that can be exploited for uranium and many others that remain in-situ. This legacy has resulted in exposure to radiation and other hazards to the population living in the vicinity. One example is the Tudor shaft tailings site where an informal settlement has been established on tailings material. Assessments of exposure for people living in this area estimated that annual doses from external exposure ranged from 0.17 to 0.25 mSv [N18], while the maximum total dose from all pathways was 1.6 mSv [N19]. Assessments at other sites affected by gold mine tailings estimated a total annual dose of 6.9 mSv; the dose from external exposure was estimated at 2.4 mSv, while that from internal exposure was estimated at 4.5 mSv [K1].

Metal industry

620. Activity concentrations of radionuclides in the waste streams generated by metal production, tailings, and slag, are normally low. Pyrometallurgy involves operations where furnace treatments at high temperatures are used to obtain metals of interest from concentrate; the waste from furnaces, slag, and dusts may contain elevated activity concentrations depending on the geology of the ore body.

621. Tin slag is relatively resistant to environmental weathering and can contain activity concentrations of radium in the range 1 to 10 Bq/g. Since tin mining has been in existence for thousands of years, unknown legacy sites can cause public exposure [I12]. Uranium and thorium can also be present in significant concentrations within other metal ores, such as copper and gold. In these situations, exposure to NORM in the resulting waste materials can be non-trivial [A21, B53, E31]. During the production of alumina from bauxite, large volumes of residue—commonly known as red mud—are generated and stored in extensive piles. Despite the large quantities of waste stored at legacy sites, radiological assessments indicate that the public exposure is potentially low [O1].

Phosphate industry

622. Residues created during the production of phosphate (phosphogypsum) contain elevated concentrations of natural radionuclides, particularly isotopes of radium, compared to the feed or product. Due to the high global demand for phosphate in agriculture, large quantities of phosphate tailings (phosphogypsum stacks) exist worldwide. Some of the legacy sites containing phosphogypsum stacks have been remediated, but many others have been abandoned, posing a radiological risk to populations living nearby. In many cases, since these tailings are not adequately confined, migration of radionuclides through water represents the primary exposure pathway. Depending on site-specific exposure scenarios, annual public doses could exceed 1 mSv [I29].

623. Few studies have assessed public exposures associated with legacy sites in the phosphate industry. One study conducted in a phosphate region of central Florida in the United States, investigated several unrestored pit lakes formed when mining cuts filled with water containing relatively high levels of natural radionuclides. The main conclusion of the study was that there was no significant radiological risk associated with former mining activities in the phosphate industry [L29, M39, R27]. Other studies in Florida and South Africa concluded that annual doses to people representative of the most highly exposed individuals from consumption of food could reach 0.2 mSv [B25, L29, M39].

624. For more than half a century, phosphate ores of marine origin containing ^{226}Ra have been processed in Belgium to produce calcium phosphate for use in cattle fodder. Hydrochloric acid was used to acidulate the phosphate ore, producing large quantities of wastewater that retained most of the radium. The wastewaters were discharged into two small rivers, one of which is the Laak. Elevated concentrations of ^{226}Ra were observed along the riverbank, mostly within a 10 m strip along both sides of the river, including flooding zones. As of 1999, no dwellings or crops for direct human consumption were located in these areas, resulting in no immediate risk to the population [P9].

625. The residual solids generated when phosphate rock is melted in a furnace at high temperature with sand, iron oxide and coal to produce elemental phosphorus typically contain ^{226}Ra concentrations ranging from 0.75 to 1,100 Bq/kg [I12]. This material, commonly known as slag, has been used as construction material in the United States. Surveys conducted in 1,472 residences in three communities found that fewer than 12% of the dwellings in Soda Spring in south-eastern Idaho contained slag, while in Pocatello and Fort Hall, no houses were found containing the slag, although slag was found in between 20 and 27% of the public roads. The highest individual annual dose was estimated to be 1.3 mSv, and only nine individuals were identified as receiving more than 1 mSv [A23].

Coal industry

626. Potential radiological risk to the public from legacy sites of the coal industry are associated with the inadequate remediation of disposal sites for the fly ash generated during coal combustion. Activity concentrations of uranium have been measured in fly ash from the United States were low—of the order of 10–30 parts per million [U52]—while worldwide activity concentrations of ^{238}U between 6.3 and 480 Bq/kg have been reported [U24]. No information on public exposure from legacy fly ash deposits were found in the literature or provided through the UNSCEAR Global Survey on Public Exposure. Inhalation of radon and its progeny is the only exposure pathway that would pose a radiological risk to the public, but doses are not expected to be significant, given the low radionuclide concentrations and the low emanation rate of radon from fly ash.

Oil and gas industry

627. Radioactive waste generated during oil and gas extraction includes large volumes of produced water and small amounts of sludges and scales. Activity concentrations of natural radionuclides in produced water are generally low, while those in sludges and scales are much higher. Appropriate decommissioning of the oil and gas facilities and disposal of the waste are essential to prevent exposure of members of the public, particularly given the long half-life of the radionuclides in the waste, such as ^{226}Ra [I11]. Potential exposure pathways for the public near legacy sites of the oil and gas industry include ingestion of seafood, external exposure to gamma radiation, and inhalation of radon and its decay products. However, no information on public exposure associated with these sites were identified in the literature or provided through the UNSCEAR Global Survey on Public Exposure.

Rare earths, titanium oxide, and zirconium industries

628. Public exposure from legacy sites in the rare earth industry depends on the type of mining used at the site. Rare earth can be extracted from mineral sands deposits, such as those containing monazite and xenotime, which also produce other mineral concentrates including titanium and zirconium, or from hard rock.

629. Residues generated by extraction from mineral sands typically contain low activity concentrations of natural radionuclides, although activity concentrations of thorium and uranium isotopes in monazite can be as high as 50–70 and 1–10 Bq/g, respectively. Historically these residues have been disposed of in mining voids or disposal pits, used in other reclamation areas or exploited as a separate resource. Global monazite wastes up to 2003 were estimated to be approximately 23,000 tonnes [I12]. Exposures of members of the

public, who may visits the mines after closure, are generally below background levels [I26]. A review of exposures from various NORM industries concluded that the annual doses received by members of the public from shallow land burial of waste from monazite processing were less than 0.25 mSv [I26].

630. Rare earth elements are also mined from hard rock, tin, and clay deposits with most of the world's production occurring in China. Activity concentrations of uranium and thorium in these ores are typically in the range of 1–10 Bq/g and monazite may also be present [I12, I26]. In South Africa, radionuclides released from a monazite processing plant that operated from 1950 to 1965 contaminated local water courses, and an informal settlement was later established on site. In Brazil, significant contamination was detected at a monazite processing site which was due for decommissioning and restoration as a residential site [I26].

631. Processing of titanium minerals generates residues that are used in agriculture, construction, and cement production, with only small amounts of residues requiring disposal to landfill [I27]. Given the relatively low activity concentrations of the material, public exposure from these residues is not of significant concern. Residues from zircon production do not generally pose a radiological risk, unless volatized during smelting in which case exposures to radionuclides in dust may be non-trivial. Assessments performed for various uses of legacy sites show that annual doses received to members of the public would be low, even under full occupancy scenarios and in most cases negligible [I12, I19].

(b) *Other legacy sites*

632. Legacy sites unrelated to NORM activities include radioactive waste disposal and storage facilities, former nuclear reactors, radiological laboratories, and areas affected by accidents involving radioactive materials. Except for locations impacted by accidents, information on public exposure from other legacy sites is limited. Information provided through the UNSCEAR Global Survey on Public Exposure is summarized in electronic attachment A-5, along with additional data collated from national reports on Joint Convention on the Safety of Spent Fuel Management and on the Safety of Radioactive Waste Management. This list is not comprehensive; therefore, case-by-case examples are also provided to illustrate potential exposures to the public from such sites.

(c) *Disposal at sea*

633. Between 1946 and 1993 radioactive waste was disposed of in the Arctic Ocean, the North Atlantic, the North Pacific, and the West Pacific. Disposal of radioactive material was banned in 1994 when the Convention on the Prevention of Marine Pollution by Dumping of Wastes and Other Matter (London Convention) was amended. In 1989, the IAEA was requested to collate information on the global inventory of radioactive material that had entered the marine environment from all sources. The inventory was updated in 2006 resulting in the publication of IAEA-TECDOC-1776 [I32], which provides the most comprehensive overview of radioactive material in the marine environment from historical disposal, accidents, and losses at sea. Data provided in the IAEA report and in supplementary files were the primary source of information for this annex; relevant tables are presented in electronic attachment A-5.

634. The total activity disposed of in the Arctic Ocean, the North Atlantic, the North Pacific, and the West Pacific at the time of dumping between 1946 until 1993, was estimated to be 85 PBq; at present it is estimated to be 17 PBq and it will be further reduced to less than 10 PBq by 2050 or around 11% of the total activity that was disposed of at sea [I32]. The waste disposed of at sea includes reactors with and without spent nuclear fuel and low-level waste—both solid and liquid. A detailed breakdown of the activities of different types of waste dumped in the Atlantic and Pacific Oceans and in the Arctic Ocean

is given in the report IAEA-TECDOC-1776 [I32]; 43% of the total activity is associated to reactors with spent nuclear fuel dumped in the Arctic Ocean, while 52% is associated to the low-level solid waste dumped in the Atlantic.

635. Since 1977, the disposal locations of the Atlantic Ocean have been periodically surveyed since radioactive waste disposed of at sea constitutes a potential source of future exposures. Generally, these surveys have not detected any radionuclide associated with the disposal operations. From the 1990s, monitoring of sediments showed elevated activity concentrations of ^{14}C, ^{137}Cs, $^{239,240}Pu$ and ^{241}Am at some locations. Elevated activity concentrations of ^{60}Co, ^{137}Cs and $^{239,240}Pu$ were detected between 1992 and 1994 in sediment samples from the fjords in Novaya Zelmya located near the waste disposal locations. However, there was no clear indication of leakage from the reactors disposed at the site and the elevated concentrations were not radiologically significant. There was no measurable increase of radionuclide activity concentrations in the other parts of the fjord [I32].

636. Measurements of activity concentrations in environmental materials suggest that the annual individual doses due to artificial radionuclides in the Kara Sea and the Barents Sea are in the range of 1–20 μSv [U19]. An IAEA report assessed doses to critical population groups in coastal areas of the Arctic, North Atlantic, and Far East regions of the Russian Federation due to consumption of seafood containing human-made radionuclides; the assessment showed that doses would be less than 1% of those from exposure to natural background radiation [I10].

F. Transport of nuclear and radioactive material

637. Materials containing radionuclides from both natural and human-made sources are widely transported around the world, such as radiopharmaceuticals for medical purposes, sources used in industry, spent nuclear fuel, and radioactive waste. All modes of transport (road, rail, air, and sea) are commonly used to carry radioactive material used in medicine, industry and research, and radioactive waste, although transport of nuclear material by air is carried out only to a limited extent [W10].

638. In broad terms, in the evaluation of radiation doses associated with the transport of radioactive material, the term ‘public’ is often taken to also include *(a)* workers that are involved in the transport operations but are not classified as radiation workers; and *(b)* workers that are operating at transport hubs or are present on means of transport but are not necessarily aware that radioactive material is being carried (e.g., operatives working at ports, crew members of commercial airplanes transporting radiopharmaceutical in the hold). Whenever possible, exposures of these groups of workers are considered separately from the exposures of other members of the public, such as pedestrians, airplane or ferry passengers, drivers of vehicles, and bystanders.

639. Exposures included in this section are those that occur during transport of radioactive material under normal conditions, that is, during operations that occur without loss or damage to the package and without an accident involving the means of transport. Exposure which may have occurred during transport accidents or incidents, in which the package or conveyance is damaged, or the contents are lost or destroyed, are not considered in this section. Over the years, radiological consequences due to accidents and incidents during transport have been generally limited by built-in safety features of the package together with the controls required for transport, including emergency response procedures [I28].

640. Data on numbers, types and contents of packages containing radioactive material transported vary widely between countries and are generally recorded with a very good degree of accuracy for shipments in the nuclear industry, as the transport operations of nuclear material are strictly regulated, but less so

for other radioactive material and waste in the medical, industrial and research sectors. Additionally, in recent years there has been a marked decrease in publicly available information on both the volume of radioactive material transported and on the evaluation of the radiological impact associated with the transport of radioactive material and radioactive waste. The available data indicate that exposures under normal conditions of transport are low, and that, at least in Europe, the transport of material from the nuclear fuel cycle contributes significantly less to the exposure of transport workers than radioactive material from other sectors [W10].

641. The IAEA has estimated that 20 million shipments of radioactive material are carried out annually [I54]. It has been estimated that only 5% of these shipments are related to the nuclear industry [W20]. In the recent past, the EC has published information on shipments of spent nuclear fuel and radioactive waste from and to its Member States for three-yearly periods, the most recent of which was for the period 2018 to 2020 [E20, E22]. It reported that in this period, 195 authorizations were issued by 21 Member States corresponding to a total of 1,770 shipments. Of these shipments, 1,732 (98%) were of radioactive waste and only 38 (2%) were related to spent nuclear fuel. The number of shipments between European Union Member States amounted to 1,639, of which 1,618 were of radioactive waste. There were 83 shipments of material imported from countries outside the European Union, 70 of which were shipments of radioactive waste, while the other 13 were shipments of spent nuclear fuel. Exports from the European Union to third countries included 44 shipments of radioactive waste and four of spent nuclear fuel. The report indicates that in 79% of the shipments of radioactive waste, the waste was from the nuclear industry while 21% was from non-nuclear activities (e.g., medicine, research). Processing of radioactive waste, reprocessing of spent nuclear fuel, or return of radioactive waste or spent nuclear fuel to the country of origin were the main purposes of the shipments. Total numbers of shipments for the period 2015–2017 were similar with 1,791 involving radioactive waste and 43 spent nuclear fuel [E20, E22]. Reports for earlier periods (2008–2011 and 2012–2014) only include information on authorizations rather than actual shipments [E17, E19].

642. A review carried out in the United States of publicly available information on transport of spent nuclear fuel worldwide showed that at least 25,400 shipments were made between 1962 and 2016, but it is likely that the actual figure is significantly higher if all forms of spent nuclear fuel are considered. The shipments within and into the United States accounted for approximately 10–17% of the total. The review also found that 130 shipments containing 2,350 canisters of high-level waste were reprocessed at the reprocessing plant in La Hague, France before being shipped back to the originating country [C47].

643. Data from the Federal Office for the Safety of Nuclear Waste Management in Germany indicate that the number of transport operations involving spent nuclear fuel and large sources in Germany remained relatively steady throughout the period between 2009 and 2018. The number of shipments of nuclear fuel varied from 310 in 2011 to 478 in 2012, while the number of shipments of large sources of ionizing radiation was much lower and ranged from six in 2014 to 22 in 2011. These shipments were carried out by road, rail, and sea, but not by air [B10].

1. Transport by road and rail

644. In Canada, the radiological impact of the used fuel transportation programme (UFTP) was evaluated by the Nuclear Waste Management Organization in 2012. Transport of spent nuclear fuel occurs in the public domain; therefore, members of the public and transport workers may be in the proximity of passing UFTP shipments. A study was carried out to estimate doses for three road transport scenarios to a range of different members of the public, such as persons living along the transport route; drivers or passengers in vehicles sharing transport routes; individuals at rest stops; cyclists; UFTP transport crew; transport inspectors; and

roadside workers. Annual radiation doses calculated in the study ranged from 1.3×10^{-6} mSv for a hitchhiker along the transport route, to 0.35 mSv for the transport crew [B12, S61, S62].

645. Acena et al. [A3] reported that the number of annual shipments by the main transport operators of excepted type A packages containing medical and industrial sources carried out in Spain was around 100,000. They also estimated that around 10,000 shipments of type B packages from the industrial gamma radiography sources sector were performed annually, with less than 10 of them containing high-activity radioactive sources. They also reported that around 70 shipments of unirradiated nuclear fuel per year, mostly by road, but also by sea and road, while the transport volume of irradiated nuclear fuel was found to be negligible. In addition, there are around 250 shipments of radioactive waste per year by road from nuclear and other facilities, mainly in industrial packages. The highest annual doses were estimated for workers involved in transport by road of radiopharmaceuticals within the medical sector. Doses were calculated for three scenarios: transport of radioisotopes used nuclear medicine, radioactive waste, and mobile gamma radiography sources. Annual estimated doses for members of the public ranged from 0.01 to 0.1 mSv; the annual dose to a member of the hospital staff was estimated at 0.1 mSv [A3].

646. Also in Spain, owing to a renewed interest in 2011 in the risk associated with the transport of medium and high activity radioactive wastes, a study was carried out to evaluate the radiological impact of the transport of these wastes [C2]. Doses received by workers while loading or driving the vehicle, and by people living near the main road routes were computed using a software code which took account of relevant information, such as the transport route, the travelling time and populations affected, and the characteristics of the wastes and the containers. The highest annual dose received by a driver or passenger of a vehicle travelling on the same route as the radioactive material and at the same time was estimated to be 0.97 μSv, while the dose to a member of the public who resides in the areas through which the shipment passed was estimated at 0.00192 μSv.

647. A study carried out by the Korea Institute of Nuclear Safety in 2010 [C36] estimated the individual and collective doses to the public due to transport by road of high activity sources of ^{192}Ir, ^{131}I and ^{99}Mo for industrial or medical application in the Republic of Korea. The maximum individual dose associated with transport by road of these sources was calculated to be 0.00482 μSv, while the collective dose was calculated to be 3.31×10^{-6} person–Sv.

648. In France, it was estimated that 980,000 packages containing radioactive material are transported annually in about 770,000 consignments [A41]. Most of the packages are transported by road and are intended for the non-nuclear industry or for non-nuclear research. These packages mainly contain radioactive sources which are used in multiple locations and need to be transported with considerable frequency. About one third of the packages transported are for the medical sector, most of which contain radioactive material with low activity or short half-life. Only about 114,000 packages in 19,000 shipments were found to contain radioactive material used for the nuclear industry. The total number of shipments of nuclear material included the following categories:

(a) 200 shipments transporting spent nuclear fuel from the nuclear power plants to the La Hague reprocessing plant;

(b) About 100 shipments of plutonium in oxide form between the La Hague reprocessing plant and the nuclear fuel production plant in the Gard department;

(c) 250 shipments of UF_6 used for nuclear fuel fabrication;

(d) About 450 shipments of fresh uranium-based and fresh mixed oxide nuclear fuel;

(e) 2,000 shipments of 58,000 packages from or to foreign countries or transiting via France.

649. In 2012, the United States Nuclear Regulatory Commission, which is responsible for issuing regulations for the packaging of spent nuclear fuel intended for transport, published a report presenting the results of the fourth investigation into the safety of transport of spent nuclear fuel [C48, U56]. In this study, the risk associated with transport of spent nuclear fuel was estimated by examining the behaviour of three different casks during transport under routine and accidental conditions. Potential doses received by transport workers and people sharing the highway or railway and at stops along the route from four facilities to four different destinations were calculated using the RADTRAN model [U56]. The highest collective dose to members of the public during routine transport by road and rail was estimated at 0.0037 person–Sv for the shipment from the Maine Yankee Nuclear Power Plant to Oak Ridge National Laboratory.

650. The number of packages containing radioactive material transported annually by road in the United Kingdom in the years 2014 to 2016 was estimated to be about 110,000, although this value should be considered only a broad estimate since the information is likely to be incomplete [J22]. Of these, about 83,800 were medical sources, about 22,300 in 3,000 consignments were packages transported for use by the nuclear industry, and the remaining 3,900 were industrial sources. The main radiopharmaceutical transported by road in the United Kingdom is ^{99m}Tc in the form of generators, which are manufactured in the United Kingdom from the processing of ^{99}Mo imported from other countries. Transport of radioactive material by rail is confined to the movement of material with high levels of radioactivity, such as irradiated nuclear fuel flasks. About 1,500 packages in 750 consignments were moved by rail to and from nuclear power stations and the United Kingdom nuclear reprocessing facility [J22].

651. Doses to members of the public arising from the transport of radioactive materials were found to be extremely low. The annual dose to a person living in a building 5 m from a set of traffic lights by which a lorry carrying technetium generators passed each week was estimated to be of the order of 1 μSv. Annual doses to office staff, security guards, and members of the public at a seaport around flasks containing high-level radioactive waste arriving by rail from a reprocessing plant for onward shipment by sea were estimated to be in the range of 0.1 to 13 μSv [J22]. Annual doses to operatives involved in the road transport of radioactive materials in the United Kingdom vary according to the sector. The lowest annual doses were estimated for operatives involved in the transport by both road and rail in the nuclear industry (0.1 to 20 μSv), although doses to personnel involved in the transport of radioactive waste for metal recycling can be as high as 0.5 mSv. Annual doses for transport workers in the medical sector were estimated to be between 0.1 and 0.2 mSv. Annual doses received by personnel in the transport of industrial sources were similar, although, in one case, the estimated dose was 2 mSv [J22].

2. Transport by sea and air

652. In the United Kingdom, a study carried out in 2009 to determine the radiological consequences from the transport of radioactive material by sea estimated that 1,000 consignments of radioactive material were made annually, involving some 30,000 packages. The radiological impact on operatives involved in the transport of radioactive material by sea and members of the public was assessed using measurements of dose rates taken at ports, onboard ships and at other locations. Annual doses received by the majority of crew members of ships transporting radioactive material and operatives at ports were estimated to be of the order of a few microsieverts or less, although the highest individual annual dose was estimated at about 0.2 mSv. The annual collective dose from all these shipments was estimated to be about 0.002 person–Sv, approximately two thirds of which was from a single shipment of cylinders containing depleted UF_6 [H41].

653. A survey of the radiological impact of the transport of radioactive material by air undertaken in 2012 reported that about 46,500 packages were transported annually by air from the United Kingdom on over 4,400 flights. The majority of these were medical sources sent by cargo or passenger flights, while

radioactive material from the nuclear industry is exclusively transported by road and rail or ship. The highest annual dose was estimated to a member of staff of a cargo handling company (~7.0 mSv). Doses to air crew and passengers from exposure to radioactive material transported on aircraft were generally very low. The highest average annual doses to the flight and cabin crew were estimated to be 25 μSv and 73 μSv, respectively, while the highest average annual dose to passengers was estimated at 73 μSv on long-haul flights. The total collective doses received by the flight and cabin crew were 0.0075 person-Sv and 0.058 person–Sv, respectively, while the collective dose to the passengers from all flights was estimated to be about 4.4 person–Sv [H12].

654. Krembel [K36] reported that about 50,000 packages containing radioactive material are consigned annually by air in France. Most of these packages contain limited quantities of radioactive material for medical use although a few tens of shipments of high activity sources for medical use, or fissile material for research reactors onboard cargo aircrafts also occur. Few data were available concerning transport flow from abroad to France, in transit, or overflying French territory.

G. Summary on public exposure from human-made radiation sources

1. Nuclear power production

655. Public exposure from discharges from NPPs and related facilities were assessed using the methodology developed for the UNSCEAR 2016 Report, annex A [U24]. The methodology has also been expanded to evaluate doses from aquatic discharges from uranium mines and mills, the management of mill tailings by water coverage in non-arid regions. Some of the parameters were also updated, notably the dose coefficients for external exposure and the distribution coefficients for freshwater to be consistent with more recent data.

656. Annual doses to characteristic individuals in the vicinity of uranium mines and mills were estimated to be between 0.001 and 0.7 μSv. The contribution of doses from radon and associated with the aquatic discharges depend upon the nature of the facility and on the environment. The collective dose associated with the production of uranium was estimated to be around 31 person–Sv, which corresponds to a normalized value of about 0.1 person–Sv/(GW a). This value is a factor of around two lower than value given in the UNSCEAR 2016 Report, annex B [U24]. This reduction reflects improvements in management practices and more comprehensive discharge data. However, uncertainties remain significant due to gaps that still remain in the availability of discharge data.

657. The normalized effective doses to the characteristic individual due to discharge of radionuclides from operating nuclear reactors were estimated to be 0.1–0.8 μSv/(GW a), depending on region and reactor type, while the total collective dose integrated to 100 years was 120 person–Sv or 0.4 person-Sv/(GW a). These values are about a factor of two higher than those given in the UNSCEAR 2016 Report, annex B [U24] due to the application of revised age-related dose coefficients and updated discharge data. The value of 0.4 person–Sv/(GW a) is consistent with the values calculated for the period between 1985 and 1997 [U19]. Generally, HWRs provide the greatest contributions to collective dose due to discharges of ^{3}H. Carbon-14 is the predominant radionuclide contribution to collective doses from other reactor types. The contribution from globally dispersed radionuclides to the collective dose was also estimated to have increased from 530 person–Sv [U24] to around 900 person–Sv.

658. Public exposure from nuclear fuel manufacturing are low with annual doses to the characteristic individual generally estimated at a fraction of 1 μSv, and annual collective doses at less than 1 person–Sv. An indicative collective dose per unit nuclear energy generation of around 0.003 person–Sv/(GW a) was estimated, consistent with the value included in previous reports [U17]. Public exposure from discharges from the spent nuclear fuel reprocessing plants vary among the various facilities. Annual doses to the characteristic individual were estimated to vary from less than 1 nSv to tens of μSv for the facilities at La Hague and Sellafield. The worldwide annual collective dose from discharges from spent nuclear fuel reprocessing plants was estimated at about 20 person–Sv.

659. Doses from discharges from radioactive waste disposal facilities were calculated for those installations for which discharge data were available. The highest annual dose to the characteristic individual was estimated at about 10 μSv. The total annual collective dose from these facilities to the European and world population were estimated to be around 0.1 person–Sv and 0.6 person–Sv, respectively. However, this value is likely to be underestimated and highly uncertain because it was calculated based on incomplete data for a subset of the worldwide disposal facilities.

660. The UNSCEAR 2016 Report, annex B included an assessment of the public exposure from other forms of electricity generation, including coal, natural gas, oil and geothermal energy. The assessment indicated that the normalized collective dose from electricity generation from coal and geothermal technologies were greater than that from nuclear technologies, while the corresponding values for natural gas and oil were lower [U24]. These general conclusions were not affected by the updated estimates for nuclear power production, presented in this annex.

2. Applications other than nuclear power

661. Public exposure from a wider range of applications other than nuclear power production, such as human and veterinary medicine, research reactors, sources used in industrial and research sectors and consumer goods, were assessed in this annex as compared to previous reports [U15, U19]. While global doses cannot be estimated due to limited information available, doses to members of the public reported in the literature are general very low, with typical annual doses from applications other than nuclear power production being of the order of microsieverts, although in exceptional cases, doses to some population groups may reach a few millisieverts in specific scenarios involving particular sources.

3. Military use of nuclear and radioactive materials

662. The model used to estimate doses due to global fallout from atmospheric nuclear weapons tests was essentially the same as the one published in previous reports [U13, U15], although dose coefficients were updated with revised values from ICRP publication 144. Current annual doses to the public from global fallout were estimated to be very low, typically a few microsieverts, and are expected to decrease further in the future.

663. Estimates of past and current public exposures at nuclear weapons test sites in New Mexico, Marshall Islands, Mururoa and Fangataufa, and Semipalatinsk have been updated based on scientific assessment of exposures at these sites published since the UNSCEAR 2008 Report, annex C [U20]. While exposures at many of these sites were significant in the immediate aftermath of the tests, present-day doses are generally much lower than natural background levels although the potential for significant exposures in certain circumstances remains. Public exposures relating to other military applications of nuclear and radioactive

material, such as nuclear weapons production, propulsion systems, radioluminous and depleted uranium ammunition are low, excluding the radiological impact of potential significant accidents.

4. Accidents, and past peaceful practices

664. This annex summarizes the evaluations of public exposure related to the nuclear accidents at Chornobyl NPP (1986) and Fukushima Daiichi NPS (2011), published in previous UNSCEAR reports and provides an update on these exposures based on new information in the literature. Current estimates of annual doses to residents in areas of Belarus, the Russian Federation, and Ukraine affected by the accident at the Chornobyl NPP range between tens of microsieverts and a few millisieverts, while doses to residents of non-evacuated municipalities near the Fukushima Daiichi NPS, vary from a few microsieverts to about 0.3 mSv. Multiple historical events at the Mayak Production Association in the Russian Federation have also contributed to public exposure; however, current annual doses in the East Urals region related to these events are below 1 mSv.

665. Accidents involving orphan sources have occasionally resulted in high exposure to small numbers of individuals, causing, in some cases, health effects or fatalities. Exposures relating to notable accidents were updated when new information emerged. These include: *(a)* the loss of nuclear weapons at Palomares, Spain in 1966 and Thule, Greenland in 1968; *(b)* the contamination of rebar with ^{60}Co in the Taiwan Province of China rebar between 1982 and 1984, resulting in cumulative average exposures over a 20 years period of 600 mSv; and *(c)* the detection of ^{106}Ru across Europe in 2017, resulting in doses between less than 0.01 and 0.33 μSv.

666. Other past practices, such as the peaceful use of nuclear explosions, have left residual radionuclides in the environments of the United States and former Soviet Union, similar to those found at weapons test sites. As these tests were underground and subject to institutional controls, public exposures are minimal, with annual doses to local populations from test carried out by the former Soviet Union ranging from around 3 to 18 μSv.

667. Apart from uranium legacy sites, data on public exposure from the NORM industries remain insufficient. Worldwide doses cannot be estimated because of a lack of a suitable methodology; exposures at these sites are assessed individually based on the requirements of national regulations.

V. IMPLICATIONS FOR FUTURE EVALUATIONS

668. Previous evaluations of public exposure to ionizing radiation and the one described in this annex have relied on data collected through global surveys during relatively short, designated periods that have coincided with reviews of the open literature. These time constraints made data collection a challenging procedure particularly for Member States that had to manage large volumes of data. Establishing a system for regular collection and submission of data to the Committee between evaluations would ensure that the collection of information would be a more structured, standardized and consistent process while reducing the pressure of gathering and extensive volume of data within limited project timelines. Making the information collected available for future use would also be beneficial since data on some sources, such as terrestrial radionuclides, do not change markedly over time.

669. Similarly to previous evaluations of public exposures to ionizing radiation, inconsistencies in the availability of essential input data have led to different approaches and methodologies being adopted for the assessment of doses. There is potential to further harmonize these methodologies.

670. The literature review carried out for this annex highlighted the urgent need for standardized international protocols for environmental radiation measurements—notably for measurements of activity concentrations of radon in outdoor air and thoron decay products indoors and outdoors. It is essential to align methodologies and establish international guidelines to ensure consistency and reliability across independent measurements campaigns, especially those focused on radon and thoron.

671. Greater participation by Member States in future evaluations is essential to improve the geographical representation of the evaluations and enable extrapolation of data for regions or countries in which such information is currently not available (e.g., exposure to radon).

672. Additional data on sources and levels of ionizing radiation in the environment should be collected under clearly defined quality criteria in the following areas:

(a) Population-weighted national surveys of radon and thoron;

(b) Discharges from facilities and activities of NORM industries;

(c) High background radiation areas;

(d) Discharges from and inventories of radioactive waste management facilities associated with both nuclear power production and non-nuclear applications;

(e) Levels of public exposure from legacy sites;

(f) Levels of public exposure during armed conflicts;

(g) Discharges and other relevant data for non-nuclear power applications, such as research facilities (e.g., research reactors);

(h) Global statistics for transport of radioactive material (class 7).

673. The Committee emphasizes the need for continued development of data inventories and methodologies for the evaluation of public exposure to ionizing radiation to provide a broader global and regional perspective. Future evaluations should include sensitivity analyses of all model input parameters to identify those with the greatest impacts on model predictions. Parameters contributing most to changes in public doses estimated by these models should be prioritized in future research to determine whether there is scientific merit in updating these values. Additionally, given the wide variation in exposures associated with natural background, more effort is required to determine the detailed population distributions of by dose intervals for these exposures; up-to-date demographic data are essential to perform such analysis.

674. The current evaluation of public exposure has focused on estimating worldwide average doses. A more accurate assessment of doses from exposure to natural sources on a regional or national scale would require more specific data from Member States, such as radionuclide activity concentrations in soil as well as information on the built environment (e.g., types of construction material and buildings) and on people's habits (e.g., occupancy times). Advanced data processing technologies may take account of the variability in human parameters (e.g., age of the exposed population and ingestion rates) and the variety of exposure scenarios. Comparison of doses across different technologies for power production

(nuclear versus non-nuclear) using updated radioecological and dosimetric models might be a topic of scientific interest in a future evaluation as a follow-up to the UNSCEAR 2016 Report, annex B [U24].

675. Because of the complexity and disparity in the exposure scenarios and the lack of discharge data and environmental measurements for NORM industries and applications other than nuclear power production, dose estimates presented in this annex for these sectors were taken directly from published sources of information. Comprehensive data on exposures from these sources are essential to improve the accuracy and reliability of future dose assessments.

676. Databases on a variety of datasets have been developed by various international organizations. The success of these efforts depends on the voluntary compliance of Member States submitting annual reports to organizations, such as UNSCEAR, IAEA, and OECD/NEA, and on worldwide interest in sustaining these programmes. Collaboration of the Committee with other international organizations should be strengthened. To provide access to Member States and the public to data on public exposure to ionizing radiation, a collaborative network of United Nations regional and worldwide data platforms related to public exposure could be created by the Committee and its secretariat.

VI. SUMMARY AND CONCLUSIONS

677. The main natural sources of ionizing radiation are radon and thoron and their decay products, cosmic rays and terrestrial radionuclides. The most significant exposure pathways are inhalation of radon and thoron and their decay products, ingestion of uranium and thorium series radionuclides and ^{40}K and external exposure arises from cosmic rays and terrestrial radionuclides. Global average annual doses from natural radionuclides were estimated based on measurements of radionuclide concentrations in soil, air, and foods provided through the UNSCEAR Global Survey on Public Exposure or taken from published papers and reports. Exposures from NORM industries were assessed from estimates of doses provided through the UNSCEAR Global Survey on Public Exposure, or from published papers and reports. Exposures from inhalation of radon and thoron and their decay products were calculated using the same dose coefficients provided in previous UNSCEAR reports [U15, U19] in accordance with the Committee's recent review [U27].

678. The range of average annual effective dose to the public from natural radiation sources was estimated at 1–14 mSv. This range remains consistent with previous estimates of 1–13 mSv [U15, U19]. In this annex, the worldwide average annual effective dose from natural sources was estimated to be around 3.0 mSv (see figure XXVIII), of which the major contribution (1.8 mSv) is from inhalation of radon, thoron and their decay products. Ingestion of uranium and thorium series radionuclides and ^{40}K represents a smaller contribution at around 0.5 mSv. External exposure to terrestrial radionuclides and cosmic radiation contribute 0.40 mSv and 0.30 mSv, respectively.

Figure XXVIII. Global average annual effective dose from natural sources

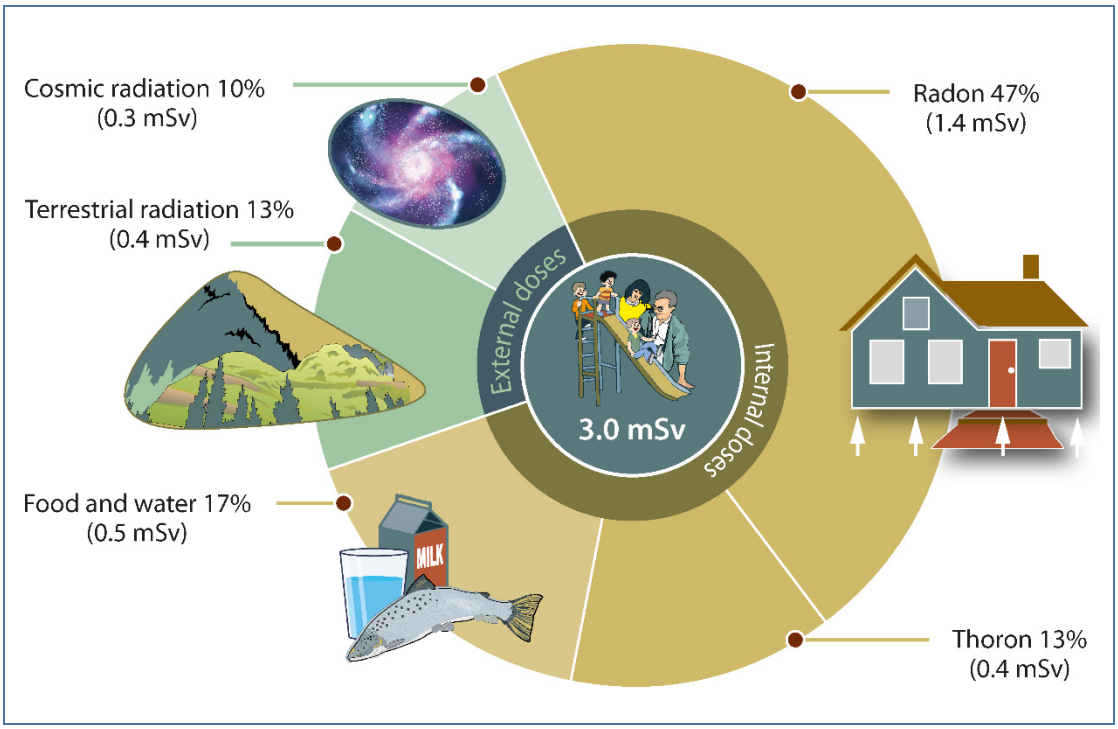

679. The worldwide average annual dose from natural sources of 3.0 mSv estimated in this annex represents an increase from the value of 2.4 mSv indicated in the UNSCEAR 2008 Report, annex B [U19]. This increase reflects methodological improvements and greater availability of data (i.e., data on EEC of thoron or on activity concentrations in terrestrial foods) compared to previous UNSCEAR reports rather than an actual rise in public exposure either globally or in a region of the world, associated with any specific source. For example, estimates of doses for radon and its decay products in this annex are based on data covering over 60% of the world's population, whereas the previous estimate reflected information relative to less than 40% of the world population. Account should also be taken that the estimate of doses from natural sources of ionizing radiation are affected by large uncertainties, and the increase in the worldwide dose may reflect statistical fluctuations in the mean values used in the calculations.

680. Compared to natural sources, exposure of the public from human-made sources is generally lower, except in the rare situation of major accidents. Figure XXIX shows a comparison of ranges of doses estimated for various human-made sources of ionizing radiation with the worldwide average annual effective dose, estimated in this annex.

Figure XXIX. Range of average annual effective doses to the public in early 2020s from major global and local/regional radiation sources

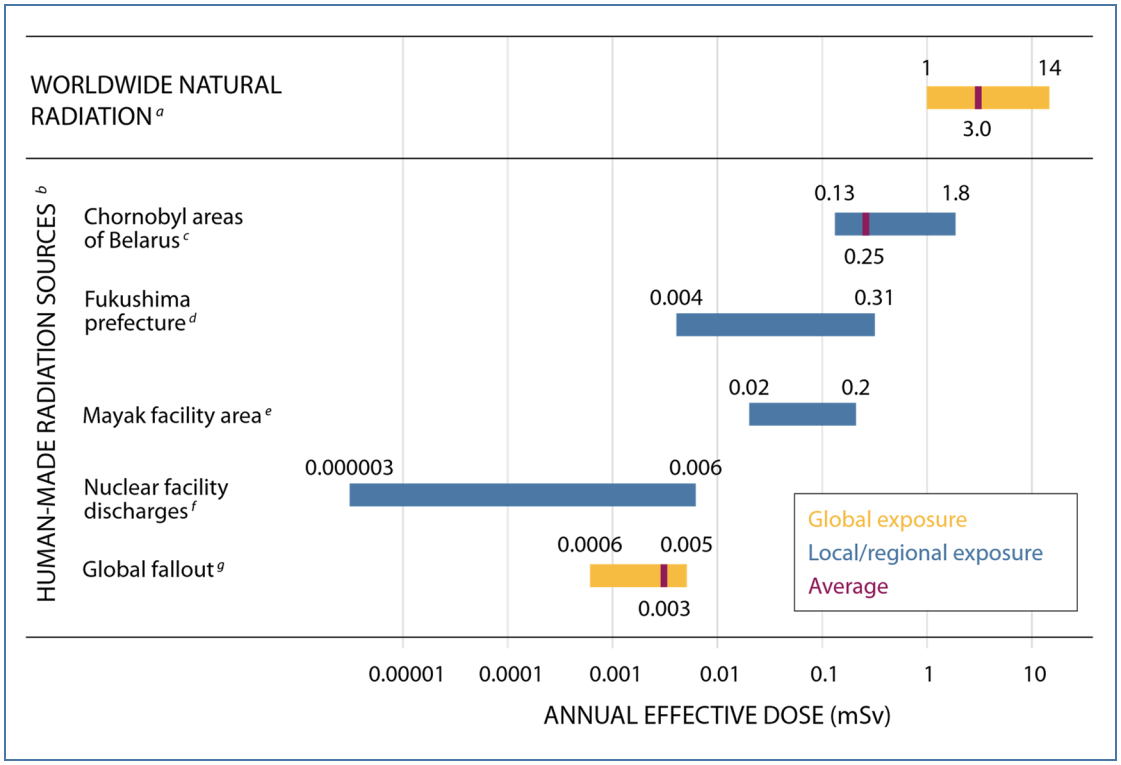

[a] This annex, table 15.

[b] Doses from human-made sources are additional to natural background doses.

[c] Electronic attachment A-5, table A-5.8.

[d] UNSCEAR 2020/2021 Report, annex B, table A16 [U29].

[e] Electronic attachment A-5, table A-5.3.

[f] This annex, section IV.A.

[g] This annex, section IV.D.2. The range is an estimate for mean doses in latitudinal bands in both hemispheres based on the data from table 8, UNSCEAR 2000 Report, annex C [U15].

681. Exposure to the public associated with nuclear power production has been evaluated by means of discharge information provided through UNSCEAR Global Survey on Public Exposure and the assessment methodology from the UNSCEAR 2016 Report, annex B [U24], with some minor modifications. It should be noted that this annex does not provide an update on its evaluation of exposure from other forms of electricity generation technologies, such as coal, natural gas, oil and biofuels and geothermal, wind and solar power provided in the UNSCEAR 2016 Report.

682. Estimated annual doses to members of the public from nuclear power production facilities generally do not exceed a few tens of microsieverts. The results are slightly higher than those presented in the UNSCEAR 2016 Report, annex B [U24] due to the use of updated discharge data and population distribution information, and the application of an approach that takes account of the different age groups in the population. The worldwide collective effective dose per unit electricity due to radioactive discharges from NPPs, has been estimated to be around 0.4 person–Sv/(GW a). This value is higher than the one estimated in the UNSCEAR 2016 Report, annex B [U24], mainly due increases in the discharges, but is consistent with the collective dose per unit electricity estimated for the period between 1985 and 1997 [U19].

683. Analysis of data on public exposure from other applications of sources of ionizing radiation, such as applications used in medicine, industry and research, and consumer products, concluded that doses for these applications of sources are generally very low, typically of the order of microsieverts, although in exceptional cases, doses to some population groups may be significantly higher.

684. Estimates of past and current public exposures at nuclear weapons test sites in New Mexico, Marshall Islands, Mururoa and Fangataufa, and Semipalatinsk have been updated since the publication of the UNSCEAR 2008 Report, annex C [U19]. While exposures at many of these sites were significant in the immediate aftermath of the tests, present-day doses are generally much lower than natural background levels. Public exposures relating to other military applications of nuclear and radioactive material, such as nuclear weapons production, propulsion systems, radioluminous products and depleted uranium ammunition are low, excluding the radiological impact of potential significant accidents.

685. The Committee has previously published detailed reports relating to the accidents that occurred at Chornobyl NPP in 1986 and Fukushima Daiichi NPS in 2011. There has been a continuous reduction of radionuclide levels in soil, air, water bodies, vegetation, and foodstuffs due to radionuclide decay and migration within ecosystems, and remedial measures in the affected areas. Doses to the public residing in those areas have decreased accordingly. Current annual doses to the public residing in the areas surrounding the Chornobyl NPP in areas of Belarus, the Russian Federation and Ukraine range from tens of microsieverts to a few millisieverts, while doses to residents of non-evacuated municipalities near the Fukushima Daiichi NPS, vary from a few microsieverts to 0.3 mSv. Since late 2023, treated water has been routinely discharged from the Fukushima Daiichi NPS site. These releases commenced after the data submission period for consideration in this current evaluation had closed. The Committee acknowledges that data from environmental monitoring and assessments are now available. This data and any subsequent publications in the scientific literature will be monitored through the Committee's ongoing programme of work and considered for inclusion in a future evaluation.

686. A comprehensive uncertainty analysis of public exposure could not be included due to the nature of the available data. Descriptive statistics have been used to quantify the distributions of the environmental activity concentrations and public exposure, where possible, and an updated methodology to quantify uncertainties and variability in dose assessments has been proposed to guide future evaluations.

ACKNOWLEDGEMENTS

The Committee acknowledges with gratitude the work of the experts involved in conducting the evaluation, all the support staff in their organizations who assisted them, as well as the critical reviewers for their valuable independent expertise. Further, the Committee would like to commend the spirit of collaboration with the Member States that contributed with data which greatly enhanced the outcome of this study. The views expressed in the annex remain those of the Committee and do not necessarily represent the views of the United Nations or its Member States.

A. Members of Expert Group

Coordinating lead writer: M. Balonov (Russian Federation); *Quality Assurance Lead Writer*: H. Grogan (United States), *Senior Technical Advisors:* H. Vanmarcke (Belgium) and B. Napier (United States).

Task group quality criteria for sources and exposures; uncertainty analysis

Lead Writer: H. Grogan (United States); *Members*: M. Simon-Cornu (France), R. Michel (Germany), K. Jang (Republic of Korea), M. Kim (Republic of Korea), H. Yu (Republic of Korea).

Task group natural radiation sources

Lead Writers: P. Steinmann (Switzerland), J. C. Mora (Spain); *Members*: M. Simon-Cornu (France), B. Hoffmann (Germany), G. Cinelli (Italy), M. Kowatari (Japan), D. Kononenko (Russian Federation), J. P. Bolivar (Spain), D. Perez Sanchez (Spain); *Observers*: G. Cinelli (EC), J. Brown (IAEA), E. van Deventer (WHO).

Task group radon exposure

Lead Writer: W. Ringer (Austria); *Members*: M. Ait-Ziane (Algeria), B. Tate (Australia), J. Gaskin (Canada), G. Ielsch (France), E. Petermann (Germany), B. Sahoo (India), M. Bahreyni Toossi (Iran, Islamic Republic of), S. Sina (Iran, Islamic Republic of), G. Cinelli (Italy), F. Bochicchio (Italy), S. Antignani (Italy), C. Carpentieri (Italy), C. Di Carlo (Italy), M. Hosoda (Japan), M. Janik (Japan), K. Kozak (Poland); *Observers*: G. Cinelli (EC), J. Brown (IAEA), O. German (IAEA), E. van Deventer (WHO).

Task group nuclear power production

Lead Writers: C. Robinson (Norway), T. Cabianca (United Kingdom); *Members*: A. Ethier (Canada), M. McKee (Canada), D. Yang (China), G. Mathieu (France), M. Kowatari (Japan), A. Haegg (Sweden), T. Anderson (United Kingdom), D. Hagemeyer (United States); *Observers*: H. Li (OECD/NEA), Y. Zhang (OECD/NEA).

Task group other applications of radioactive materials

Lead Writer: V. Berkovskyy (Ukraine); *Members*: D. Chambers (Canada), S. Liu (China), D. Yang (China), M. Budzanowski (Poland), K. Jang (Republic of Korea).

Task group: Past activities and accidents, legacy sites

Lead Writer: C. Lawrence (Australia); *Members*: K. Akahane (Japan), S. Kiselev (Russian Federation), S. Lukashenko (Russian Federation); R. Garcia-Tenorio (Spain), K. Thiessen (United States); *Observers*: S. Mundigl (EC), J. Brown (IAEA).

Critical reviewers

H. Vanmarcke (Belgium), J. Chen (Canada), G. Proehl (Germany), C. Murith (Switzerland), N. Harley (United States) and B. Napier (United States).

Other contributing experts

V. Gruber (Austria), C. Guo (China), H. Zhu (China), J. Park (Republic of Korea), M. Foster (United Kingdom).

B. National Contact Persons and national experts/contributors to UNSCEAR Global Survey on Public Exposure

Country code [a]	*Country*	*National Contact Persons*	*National experts*
DZA	Algeria	Z. Lounis-Mokrani	M. Ait-Ziane D. Maouche S. Sehad A. Seghour D. Taieb Errahmani A. Yennoune
ARG	Argentina	M.G. Ermacora	D. Alvarez J.P. Bonetto A. Canoba F. López
ARM	Armenia	K. Ohanyan	
AUS	Australia	B. Tate	C. Lawrence S. Long B. Orr B. Paritsky A. Yule
AT	Austria	M. Ditto	V. Gruber
BGD	Bangladesh	J. Ferdous	S. Banik
BLR	Belarus	L. Sheuchuk A. Stojarov	A. Avetisov G. Astashko A. Nikalayenka
BEL	Belgium	P. Willems	B. Dehandschutter D. Van Der Meersch
BRA	Brazil	P.R.R. Ferreira	V.V. de Oliveira
BGR	Bulgaria	J.N. Djounova-Velikova	K. Ivanova R. Kamenova-Totzeva S. Stoyanova
CMR	Cameroon	S. Saidou C. E. Bibi	K. Francois T.S.Y. Flore O.B. Modibo J.E. Ndjana Nkoulou II B.G. Samuel G.D. Soulfit
CAN	Canada	J. Chen	A. Gaw S. Hamlat J. Lam M. McKee R. Stainforth
CPV	Cape Verde	S.M.V. Semedo	M. dos Anjos Lopes

Country code [a]	*Country*	*National Contact Persons*	*National experts*
CHN	China	S. Liu	
COD	Congo	G.B. Dallou	G.B. Dallou J.S. Sondz R.R.C. Moubakou Diahou
CYP	Cyprus	M. Tzortzis	
CZE	Czechia	K. Petrova	M. Bercikova M. Cermak L. Dragounovas I. Fojtikova F. Houser M. Hort M. Jurda L. Neubauer J. Neuzil J. Nozickova J. Pospichal K.N. Rovenska P. Schmutzer O. Tomášek J. Váša I. Zenata
DEN	Denmark	K. Breddam	H.S. Thomsen
EST	Estonia		A. Polt
EGY	Egypt	M. Gomaa T. Morsi	
FIN	Finland	R. Bly	S. Hellstén K. Kojo P. Kurttio L. Togneri T. Turtiainen
FRA	France	M.S. Cornu	P. Blanchart H. Caplin A. Hoorelbeke G. Lelsch
DEU	Germany	U. Kulka	C. Ilgner E. Petermann
GHA	Ghana	F. Otoo	
IND	India	A.U. Sonawane M.M. Kulkarni	V. Anuradha S. Sinha
IDN	Indonesia	E.D. Nughraha	D. Iskandar H. Presetio U. Untara W. Wahyudi

Country code [a]	*Country*	*National Contact Persons*	*National experts*
IRN	Iran (Islamic Republic of)	A. Rahimi A.R. Khoshmakani	
ISR	Israel	G. Haquin	L. Epstein K. Kovler
ITA	Italy	F. Bochicchio	S. Antignani C. Carpentieri C. Di Carlo C. Nuccetelli S. Procopio F. Trotti
JPN	Japan	K. Akahane	M. Hosoda I. Kawaguchi S. Kinase M. Kowatari M. Nakano T. Sanada T. Takahashi K. Iwaoka
KAZ	Kazakhstan	N. Kozhakmetov	
KWT	Kuwait	E. Alfares	H. Yatim N. Alazemi M. Maarafi
LVA	Latvia	D. Satrovska	
LBN	Lebanon	O. El-Samad	R. Baydoun
LTU	Lithuania	J. Ziliukas	R. Aganauskaite K. Dacyte V. Grigoniene A. Juskaite A. Pasiskevicius L. Pilkyte A. Tankeviciūte
LUX	Luxembourg	N. Harpes	M. Lecomte K. Pier
MRT	Mauritania	I. Moussa	M.M. Mahmoud
MEX	Mexico	J.A. Gómez	D.A.M. Chable J.A. Gomez M.E.C. Juárez J.M. Lizardo R.F. Ortega
NLD	Netherlands (Kingdom of the)	B. Godhelp	F. Dekkers C.P. Tanzi

Country code [a]	*Country*	*National Contact Persons*	*National experts*
NGA	Nigeria	G.D. Ekong	T.C. Akpa C.A. Charles A.C. Chikwado Y.U. Idris I. Sambo
NOR	Norway	A.L. Rudjord	I. Finne T.N. Hevroy M. Komperød T. Mette Sjømoen J. Mrdakovic Popic H. Thørring Additional support: A. Andersen N. Bratteteig K. Gulliksrud B.V. Haland M.V. Holmstrand T.D. Jorgensen E. Ohlin H.A. Sollund
PER	Peru	N. Palomino Figueroa	
PHL	Philippines	K.M. Romallosa	A.T. Bautista VII C.M.T. Betos M.P. Catalig R.R. Encabo
POL	Poland	D. Kluszczyński	
PRT	Portugal	J. Martins	G. Cardoso C. Diamantino H. Fonseca M. Malta J. Pereira M. Pereira P. Rosário F. Batsita
KOR	Republic of Korea	K. Jang	
RUS	Russian Federation	D. Kononenko	S. Kiselev A. Marennyy A. Onishchenko A. Vasilyev I. Yarmoshenko
SMR	San Marino	C. Muccioli	
SVK	Slovakia	V. Drábová	M. Helej

Country code [a]	*Country*	*National Contact Persons*	*National experts*
SVN	Slovenia	N. Jug	P. Farkas M. Cindro T. Gregorčič
ZAF	South Africa	A. Muller	F. Beeslaar K. Ditlhake C. Kros B. Lechwety K. Madi T. Pather S. Pietersen W. Speelman W. van der Westhuizen
ESP	Spain	A. Hernandez	D. Belles J.P. Bolivar M. García-Talavera D. Pérez-Sánchez B. Robles M. Sánchez
SDN	Sudan	R.O.A. Alfaki	
SWE	Sweden	P. Eriksson	P. Andersson K. Aquilonius A. Hägg R. Holzwarth P. Sopher
CHE	Switzerland	P. Steinmann	F. Barazza M. Palacios
UKR	Ukraine	V. Chumak	A. Bendyk M. Buzynnyi O. Glavatsky V. Kostenko T. Pavlenko A. Stavenko
ARE	United Arab Emirates	A. Al Shehhi	A. S. Al Abdouli E. Bosc S. Al Mansoori D. Trifunovic A. Woodruffe
GBR	United Kingdom	A. Bexon	
USA	United States of America	T. Johnson	J. Major
VNM	Vietnam	H.Q. Ngyuen	T.M.H. Ngyuen K.T. Pham L. N. Sieu

[a] Note: The International Organization for Standardization Country Code 3166 was used in some tables and figures [I92].

APPENDIX A. METHODOLOGY FOR EVALUATING PUBLIC EXPOSURE TO IONIZING RADIATION

I. INTRODUCTION

A1. This appendix provides information on the methodologies used to evaluate doses to the public from exposure to ionizing radiation for the topic areas included in this annex along with common assumptions made and parameter values used. The methodologies are based on those used in previous UNSCEAR reports on public exposure to ionizing radiation and in other reports [U15, U18, U19, U27]. The methodologies were reviewed and updated for this annex to take account of recent scientific developments and new data. Further information can be found in electronic attachments A-1 to A-6.

A2. A key challenge when assessing public exposures is to ensure that doses from different sources are estimated using a consistent approach. This is not always straightforward because public exposures are associated with a broad range of sources with diverse characteristics. For example, public exposures due to discharges from NPPs are regularly estimated in detail using established methodology, whereas those from NORM industries receive less attention.0

A3. In this annex, the Committee used three different approaches to assess public exposure:

(a) Doses based on environmental measurements and model calculations. Environmental measurements include external dose rates and radionuclide activity concentrations in environmental media (air, soil, food and drinking water). In this annex equilibrium equations were used to convert environmental data into individual doses. An example of this approach is the calculation of dose to the public due to natural sources of ionizing radiation, such as radon and thoron, cosmic rays and terrestrial radionuclides and global fallout.

(b) Doses based on the source term with model calculations. In this case simple environmental models were used to estimate activity concentrations in environmental media from activities discharged by nuclear facilities (source term); these activity concentrations are in turn used to estimate doses in a similar way to approach *(a)*. An example of this method is the assessment of public exposure due to nuclear energy production.

(c) For some topic areas a suitable methodology to assess public exposures could not be developed, either because information on exposure scenarios and other input data was not available or because the exposure situation was too complex. For these cases, doses in this annex are based on direct estimates reported in the literature or provided by national and international organizations. Examples of this approach are the assessments of exposure associated with the NORM industry, applications other than nuclear power production and areas with residual radionuclides due to past activities or accidents.

II. OVERVIEW OF THE DOSE ASSESSMENT METHODOLOGY

A. Data for exposure assessment

1. Assumptions on parameter values

A4. In this annex a common set of parameter values was established to ensure consistency between the methodologies used to calculate public doses from different sources. The parameters can be divided into three categories, namely: dose coefficients; environmental parameters; and parameters describing human habits and their values are summarized in table A1. Other input parameters used to quantify radionuclide transfer in the environment for individual topic areas of this annex are described in the relevant sections in this appendix.

A5. The dose coefficients used in this annex were taken from the most recent available sources of the International Commission of Radiological Protection (ICRP). For internal exposure (ingestion and inhalation) dose coefficients for all radionuclides, except radon and thoron, were taken from ICRP Publications 119 [I67, I68]. Dose coefficients for inhalation were those calculated for 1-μm activity median aerodynamic diameter particulates except for gases and tritium, both in the form of tritiated water and organically bound tritium. Dose coefficients for radon and thoron are described in section III.A.2 of this appendix. The dose coefficients for external exposure used in previous UNSCEAR reports were replaced with values taken from ICRP Publication 144 [I77]. Although differences are relatively minor, the use of dose coefficients from ICRP publication ensure consistency of approach with the calculation of doses from internal exposure.

A6. Common environmental parameters comprise the shielding factors assumed for buildings and the dry-wet factor for soil density. Values for the shielding factor for radionuclides in air (SF_{air}) and deposited material (SF_{dep}) used in the UNSCEAR 2016 Report, annex A [U24] were adopted for this annex. The shielding factor for cosmic rays (SF_{cos}) of 0.9 used in this annex is higher than the factor of 0.8 adopted in previous UNSCEAR reports to reflect the fact that cosmic rays with high energy, in particular muons, more easily penetrate building materials than gamma rays from terrestrial radionuclides with energies less than 3 MeV. It was based on an assessment by Sato [S16] of the building shielding factors for cosmic rays, which gave a possible range of 0.8–0.98. The dry-wet factor for soil density (f_{dw}) of 0.81 was taken from UNSCEAR 2000 Report, annex B [U15] and is based on an assumed average soil moisture of 30% by volume and a density of 1.3 g/cm^2.

A7. The values of the common parameters describing the habits of characteristic individual (e.g., breathing and ingestion rates and occupancy factors) are based on established generic data from published literature and specific values used in previous UNSCEAR reports were updated to ensure consistency. For example. the ingestion rate of drinking water rate used in this annex for the calculation of doses from exposure to radon has been increased from the earlier value used in UNSCEAR 2000 Report, annex B [U15]. Values used to estimate doses for specific topic areas that differ from those in table A1 described in the respective sections dealing with the assessment methodologies for these sources.

Table A1. Common parameters

Parameter	*Symbol*	*Value*	*Reference*	*Units*
DOSE COEFFICIENTS				
Dose coefficient for external exposure from immersion in air from radionuclide *i*	$e_{ex\ air,i}$	Radionuclide dependent	[I77]	Sv/(Bq s/m^3)
Dose coefficient for external exposure from radionuclide *i* in surface deposition	$e_{ex,dep,i}$	Radionuclide dependent	[I77]	Sv/(Bq s/m^2)
Dose coefficient for inhalation of radionuclide *i*	$e_{inh,i}$	Radionuclide dependent	[I67, I68]	Sv/Bq
Dose coefficient for ingestion of radionuclide *i* except radon and thoron	$e_{ing,i}$	Radionuclide dependent	[I68]	Sv/Bq
ENVIRONMENTAL PARAMETERS				
Building shielding factor for radionuclides in air	SF_{air}	0.2	[U25]	unitless
Building shielding factor for deposited material	$SF_{deposit}$	0.1	[U25]	unitless
Building shielding factor for cosmic radiation	SF_{cos}	0.9	This annex	unitless
Building shielding factor for terrestrial radiation	SF_{terr}	1.4	[U15]	unitless
Dry-wet factor for soil density	f_{dw}	0.81	[U15]	unitless
HUMAN PARAMETERS				
Occupancy factor indoors	O_{in}	0.8	[U12, U13, U24]	unitless
Occupancy factor outdoors	O_{out}	0.2	[U12, U13, U24]	unitless
Inhalation rate	I_{inh}	20	[I67]	m^3/d
Ingestion rate for food type *f* and region *r*	$I_{f,r}$	Dependent on food type and region	[U24, W8]	kg/a
Drinking water ingestion rate	I_{dw}	0.5	[U15, U24]	m^3/a

(a) *Occupancy rates*

A8. In the UNSCEAR 1988 Report, annex A [U12], the annual indoor and outdoor occupancies were taken to be 7,000 and 1,760 h/a, respectively, corresponding to indoor and outdoor occupancy factors of 0.8 and 0.2. A comprehensive review of published literature related to occupancy factors was performed for this annex; findings of this review are summarized in electronic attachment A-1. Most of the papers reviewed referenced the values adopted in the UNSCEAR 1988 Report. A small number of papers used the indoor occupancy factor of 0.7 recommended by the United States Environmental Protection Agency, as suggested by the Committee on the Biological Effects of Ionizing Radiation (BEIR VI) [N27]. Most studies gave a single overall value for indoor occupancy factor, either indoor residential or total indoor hours including office hours, and some separated residential occupancy into multiple areas or rooms. Slightly lower estimates were reported for residential occupancy factors (between 0.6 and 0.7) than for total indoor occupancy that included working hours in office environments (between 0.8 and 0.9). Several papers centred

on the African region quoted occupancy factors ranging from 0.4 to 0.6, indicating markedly different indoor living habits in the regions. indicated that the indoor occupancy value of 0.8 is still valid. Based on this review the indoor and outdoor occupancy factors of 0.8 and 0.2 were retained.

2. Definition of spatial units and population density assumptions

A9. The data on natural radiation exposures are sufficiently extensive to enable the evaluation of spatial variations within, and between, countries. The broader geographic regions of the world beyond individual countries considered in this annex are those recommended by UNEP[12] (see figure A-I): Africa, Asia and the Pacific, Europe, Latin America and the Caribbean, North America, and West Asia.

Figure A-I. Population density of the world resampled at a 10 km resolution [a] [S20]

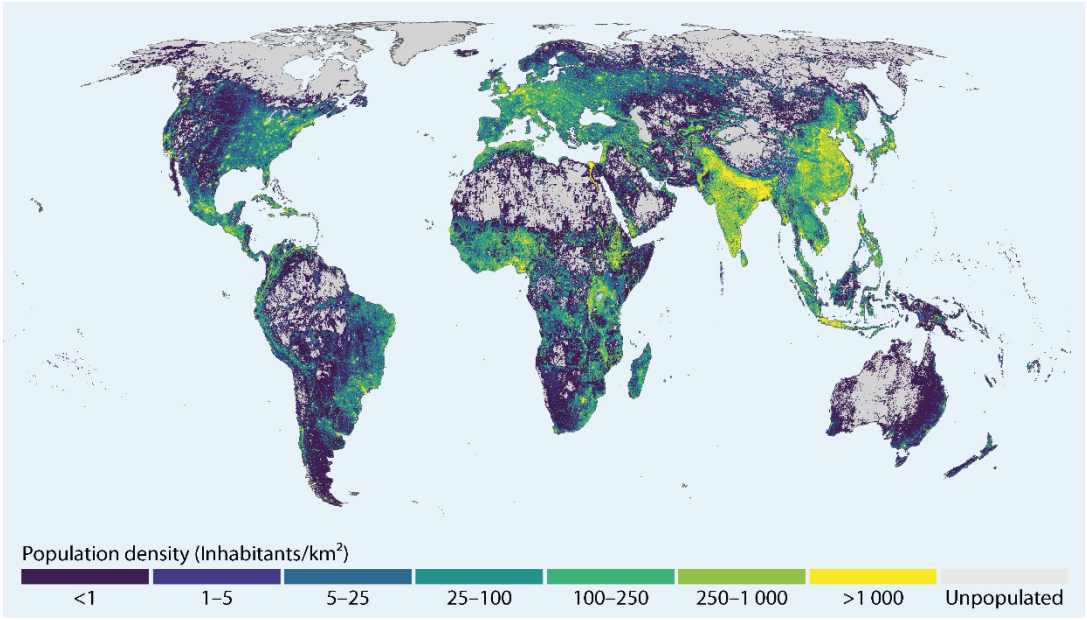

[a] The boundaries and names shown and the designations used in this map do not imply official endorsement or acceptance by the United Nations. Final boundary between the Republic of Sudan and the Republic of South Sudan has not yet been determined. Dotted line represents approximately the Line of Control in Jammu and Kashmir agreed upon by India and Pakistan. The final status of Jammu and Kashmir has not yet been agreed upon by the parties. A dispute exists between the Government of Argentina and the United Kingdom of Great Britain and Northern Ireland concerning sovereignty over the Falkland Islands (Malvinas).

A10. These regions were adopted by the Committee in its 2016 Report, annex A [U24] and vary slightly from those used in earlier evaluations of public exposures [U15, U19]. Using the UNEP regions allows the dose assessment methodology results to be integrated with population distribution data provided by the European Commission Joint Research Centre (JRC) in the data package Global Health Settlement (GHS) P2022. In this annex the GHS population grid (R2022) for 2020 with 1 km resolution was used [S20]. For consistency, the literature review adopted the same spatial units to identify data relevant to specific regions in the world.

[12] www.unep.org/UNEP-regions.

A11. The parameters that define the underlying data were examined to determine the spatial scale they represent and to establish consistency in the reported exposures. For public exposures that are ubiquitous, such as from cosmic rays and terrestrial radiation, the spatial scale of the exposure data were directly correlated with the population distributions at high spatial resolution. For public exposure associated with localized sources, such as discharges from nuclear power production and related nuclear fuel cycle facilities, simplifying assumptions were required to identify the population that is potentially exposed:

(a) To calculate the dose at the midpoint of distance bands or annuli (of 0–100, 100–500, 500–1,000 and 1,000–1,500 km) around the point of discharge; and

(b) To distinguish three spatial categories: local (0–100 km); regional (>100–1,500 km); and global (>1,500 km). The number of people within each annulus is aligned to the GHS population grid (R2022) [S20] as noted previously.

III. APPLICATION OF UNSCEAR DOSE ASSESSMENT METHODOLOGY TO SPECIFIC TOPIC AREAS

A. Dose assessment methodology for radon and thoron

1. Approach

A12. The assessment of doses to the public from exposure to radon and thoron and their short-lived decay products was based on the methodology used by the Committee in previous reports [U15, U18, U19, U27]. Two exposure pathways were considered: inhalation of indoor and outdoor air and ingestion of drinking water. Doses from exposure due to the dissolution of radon in blood were also included for completeness. Table A2 gives a summary of the parameters used in the calculation of doses from exposure to radon and thoron.

A13. The dose from inhalation of radon ($E_{inh,222Rn,in}$) and thoron ($E_{inh,220Rn,in}$) and their decay products indoors were estimated using the following equations derived from those in UNSCEAR 2000 Report, annex A [U15]:

$$E_{inh,220Rn,in} = EEC_{222Rn}\, T_{in}\, DC_{EEC,222Rn} = C_{222Rn,in}\, F_{222Rn,in}\, T_{in}\, DC_{EEC,222Rn} \quad \text{(A.1)}$$

$$E_{inh,220Rn,in} = EEC_{220Rn,in}\, T_{in}\, DC_{EEC,220Rn} \quad \text{(A.2)}$$

where $EEC_{222Rn,in}$ and $EEC_{220Rn,in}$ are the equilibrium equivalent concentrations of radon and thoron in air indoors (Bq/m^3); $C_{222Rn,in}$ is the concentrations of radon in air indoors (Bq/m^3); $F_{222Rn,in}$ is the indoor equilibrium factor for radon (unitless); and $DC_{EEC,222Rn}$ and $DC_{EEC,220Rn}$ are the dose coefficients for radon and thoron equilibrium equivalent concentrations (nSv/(Bq h/m^3). T_{in} is the occupancy time indoors (h/a), given by:

$$T_{in} = O_{in}\, 8760 \quad \text{(A.3)}$$

where O_{in} (0.8) is the indoor occupancy factors (see table A1) and 8760 is the number of hours in a year.

A14. Similar equations are used to calculate the doses from inhalation of radon and thoron and their decay products outdoors ($E_{inh,222Rn,out}$ and $E_{inh,220Rn,out}$ respectively):

$$E_{inh,222Rn,out} = EEC_{222Rn,out}\, T_{out}\, DC_{EEC,222Rn} = C_{222Rn,out}\, F_{222Rn,out}\, T_{out}\, DC_{EEC,222Rn} \quad (A.4)$$

$$E_{inh,220Rn,out} = EEC_{220Rn,out}\, T_{out}\, DC_{EEC,220Rn} \quad (A.5)$$

where $EEC_{222Rn,out}$ and $EEC_{220Rn,out}$ are the equilibrium equivalent concentrations of radon and thoron in air outdoors (Bq/m^3); $C_{222Rn,out}$ is the concentrations of radon in air outdoors (Bq/m^3); $F_{222Rn,out}$ is the outdoor equilibrium factor for radon (unitless) ($DC_{EEC,222Rn}$ and $DC_{EEC,220Rn}$ are the same as those used for doses indoors). T_{out} is the occupancy time outdoors (h/a), given by:

$$T_{out} = O_{out}\, 8760 \quad (A.6)$$

where O_{out} is the outdoor occupancy factors (see table A1) and 8760 is the number of hours in a year.

A15. The doses from dissolution of radon and thoron in blood both indoors ($E_{b,222Rn,in}$ and $E_{b,220Rn,in}$ respectively); and outdoors ($E_{b,222Rn,out}$ and $E_{b,220Rn,out}$ respectively), were estimated using the following equations:

$$E_{b,222Rn,in} = C_{222Rn,in}\, T_{in}\, DC_{b,222Rn} \quad (A.7)$$

$$E_{b,220Rn,in} = C_{220Rn,in}\, T_{in}\, DC_{b,220Rn} \quad (A.8)$$

$$E_{b,222Rn,out} = C_{222Rn,out}\, T_{out}\, DC_{b,222Rn} \quad (A.9)$$

$$E_{b,220Rn,out} = C_{220Rn,out}\, T_{out}\, DC_{b,220Rn} \quad (A.10)$$

where $DC_{b,222Rn}$ and $DC_{b,220Rn}$ are the dose coefficients for radon and thoron in blood, taken to be 0.18 nSv/(Bq h/m^3) [I75] and 0.11 nSv/(Bq h/m^3) [U13], respectively.

A16. The annual dose from ingestion of radon in drinking water ($E_{ing,222Rn}$) was calculated using uses the following equation [U15]:

$$E_{ing,222Rn} = C_{222Rn,\mathrm{w}}\, I_{dw}\, e_{ing,222Rn} \quad (A.11)$$

where $C_{222,Rn}$ is the radon concentration in water (Bq/m^3); I_{dw} is the ingestion rate of drinking water (see table A1) and $e_{ing,222Rn}$ is the dose coefficient for ingestion of radon (0.69 nSv/Bq), which was taken ICRP Publication 137 [I75].

Table A2. Parameter values for the calculation of doses from radon

Parameter	*Symbol*	*Value*	*Units*	*Reference*
DOSE COEFFICIENTS				
Dose coefficient for equilibrium equivalent concentration of radon exposure	$DC_{EEC,222Rn}$	9×10^{-9}	Sv/(Bq h/ m^3)	[U27]
Dose coefficient for equilibrium equivalent concentration of thoron exposure	$DC_{EEC,220Rn}$	4×10^{-8}	Sv/(Bq h m^{-3})	[U15]
Dose coefficient for radon in blood	$DC_{b,222Rn}$	1.8×10^{-10}	Sv/(Bq h/ m^3)	[I75]
Dose coefficient for thoron in blood	$DC_{b,220Rn}$	1.1×10^{-10}	Sv/(Bq h/ m^3)	[U13]

Parameter	*Symbol*	*Value*	*Units*	*Reference*
Dose coefficient for ingestion of ^{222}Rn in water	$e_{ing,222Rn}$	6.9×10^{-10}	Sv/Bq	[I75]
ENVIRONMENTAL PARAMETERS				
Indoor equilibrium factor for radon	$F_{222Rn,in}$	0.4	Unitless	[U15, U24]
Outdoor equilibrium factor for radon	$F_{222Rn,out}$	0.6	Unitless	[U15, U24]

2. Dose coefficients for inhalation of radon and thoron decay products

A17. The dose coefficients for inhalation of EEC of radon and thoron ($DC_{EEC,222Rn}$ and $DC_{EEC,220Rn}$) adopted in previous UNSCEAR reports [U27], where they are referred to as dose conversion factors, were calculated using: *(a)* epidemiological analysis of the risk of lung cancer from exposure to radon in miners, survivors of the atomic bombings, and cancer cases in residential houses and *(b)* dosimetric models that took into account various parameters, such as aerosol size distribution, unattached fraction, breathing characteristics, fractional deposition in the airways, mucous clearance rate, and location of the target cells in the airways.

A18. Different dose coefficients for inhalation of radon and decay products were published by the Committee in the 1980s [U11, U12] and ICRP in 1993 [I66], with the dose coefficient used by UNSCEAR being higher than the one recommended by ICRP. In 2018, the ICRP issued Publication 137 which provided a revised dose coefficient for exposures due to radon in workplaces [I75]. The revised dose coefficient was higher by about a factor of 2 than the previous value. Uniquely in the case of radon, in addition to dosimetric data, the ICRP took account of epidemiological data. A key epidemiological observation that lung cancer risk estimates based on miner studies were generally higher for lower levels of exposure resulted in an increase in the dose coefficient recommended by ICRP [I78]. In 2019, the Committee reviewed the most recent dosimetric and epidemiological studies of lung cancer resulting from inhalation of radon and decay products and also the results of dosimetric models since 2006 and concluded that, given that the ranges observed in these data since 2006 were similar to those observed in the Committee's previous assessments and recognizing the uncertainties, it was appropriate to continue to use the same dose coefficient as in previous assessments [U27]. Therefore, the dose coefficient of 9 nSv/(Bq h/m^3) for the EEC of radon recommended by the Committee was used in this annex. Similarly, the same dose coefficient of 40 nSv/(Bq h/m^3) for the EEC of thoron as recommended in previous reports was used in this annex [U15, U19].

3. Equilibrium factor for radon and thoron indoors and unattached fraction of radon and thoron decay products

A19. Previous UNSCEAR reports adopted a value of 0.4 for the equilibrium factor for indoor radon ($F_{222Rn,in}$) [U12, U13, U14]. UNSCEAR 2006 Report, annex E reported that most of the estimates were within 30% of the value of 0.4 previously assessed by the Committee [U18] and recommended caution on the use of an equilibrium factor for thoron because of the significant variation in indoor thoron concentration with the distance from the closest thoron source, generally the closest wall. Equilibrium factors for thoron were given as survey-specific single values because of the large variability of indoor thoron concentrations [U18].

A20. A literature review was performed for this annex to update the state of knowledge on the equilibrium factors for radon and thoron indoors and on the unattached fraction of their decay products. Ony studies based on measurements lasting more than 30 days and taken in a residential environment, involving at least 10 houses of a common type were considered. Regarding thoron measurements, the position of the detector had to be at least 50 cm away from the nearest thoron source.

A21. The results for radon were based on findings from 22 surveys, about 80% of which were conducted in Asia (see electronic attachment A-1 for more details). The AMs of the radon equilibrium factor of those surveys ranged from 0.24 to 0.80 with an AM of 0.45 and a median of 0.44. Using the number of monitored dwellings as weights increased the value of the radon equilibrium factor to 0.53. The most significant contribution came from a large study of more than 12,000 dwellings in Canada [C24], in which a mean radon equilibrium factor of 0.54 was reported. More than 90% of the estimates reported by the individual surveys fell within the range 0.27–0.63. Considering the variability in the radon equilibrium factor, it was considered appropriate to continue using the equilibrium factor of 0.4 adopted in previous UNSCEAR reports. Figure A-II shows the boxplot for the radon equilibrium factors.

A22. Twenty-six papers were used to derive the results for thoron. The estimates of the thoron equilibrium factor ($F_{220Rn,in}$) ranged from 0.01 to 0.12 with an AM of 0.05 and a median of 0.04. These results were based on the findings of 31 surveys, about 65% of which were performed in Asia (see details in attachment A-1). If only the measurements taken from four different surveys performed at exactly 50 cm from the closest likely thoron source were considered, the AM would increase slightly to 0.08. The AM weighted for the number of monitored dwellings was estimated at 0.05, if all the surveys were considered regardless of the detector position, and 0.09, if only those where the distance from the closest thoron source was 50 cm. The box plot of the equilibrium factor estimates for thoron as found in the selected papers is shown in figure A-II. The figure shows the larger variability of the thoron equilibrium factor in comparison to radon.

A23. A recent report on long-term measurements of thoron and its decay products concentrations found that the equilibrium factor has a very wide range between 0.0003 and 0.3 [H30]. Additionally, Chen and Harley [C27] reported a wide range in the values of the equilibrium factor for thoron from 0.003 to 0.14. These findings support the Committee's recommendation that the use of an equilibrium factor for thoron should be limited to situations where a large spatial variation of thoron concentrations is not observed [U18], to avoid the large uncertainty in the estimation of doses.

Figure A-II. Radon and thoron indoor equilibrium factors resulting from studies that meet the selection criteria

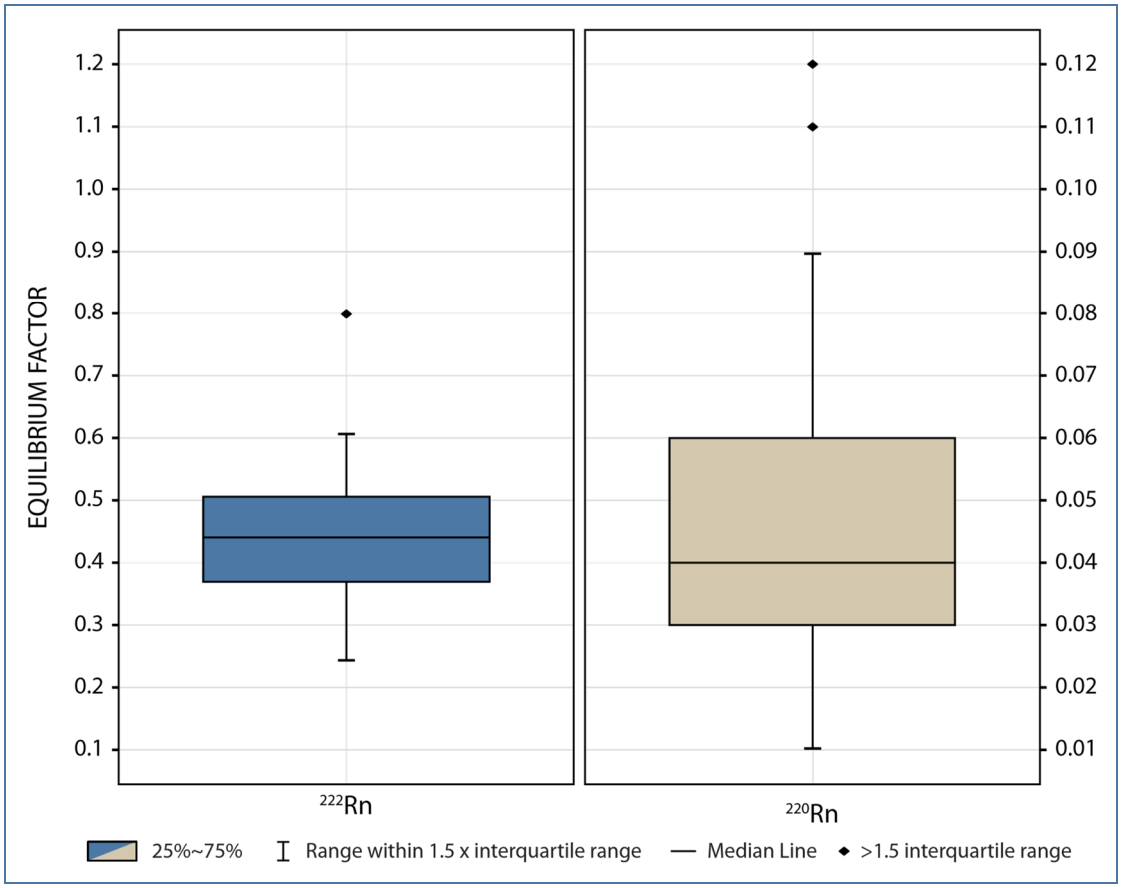

A24. The estimates of the unattached fraction of radon and thoron decay products were based on findings from six and five surveys, respectively (see electronic attachment A-1 for more details). The unattached fraction for radon ranged from 0.07 to 0.24 with an AM of 0.12 and a median of 0.10. This result agrees with the assumption underpinning the dose coefficient for EEC of radon used in this annex. The unattached fraction for thoron ranged from 0.07 to 0.26 with an AM of 0.14 and a median of 0.09. Although the unattached fraction for thoron decay products is theoretically expected to be lower than for radon, the values are similar, probably because the experimental determinations of unattached fractions radon and thoron are not always carried out within the same surveys.

B. Dose assessment methodology for exposure to cosmic rays, cosmogenic radionuclides and terrestrial radionuclides

1. Cosmic rays and cosmogenic radionuclides

A25. Public exposures to cosmic rays at ground level were assessed in previous UNSCEAR reports [U14, U15], [U19] based on dose rates calculated using the Particle and Heavy Ion Transport code System (PHITS)-based Analytical Radiation Model in the Atmosphere (PARMA) version 4 [S15, S17]. This

model is also available as an Excel-based Program for calculating Atmospheric Cosmic-ray Spectrum (EXPACS) 4.10. The fluence to dose coefficients for the isotropic irradiation geometry specified in ICRP Publication 116 [I71] and ICRP Publication 123 [I74] were employed in the model. The dose rates were combined with population data on the same spatial scale to calculate average dose rates by country, and to identify the population exposed to the highest dose rate.

A26. The annual dose from external exposure to cosmic rays ($E_{ext,cos}$) was calculated using the equation:

$$E_{ext,cos} = \dot{E}_{cos,out}(O_{out} + SF_{cos}\ O_{in})\ 8760 \quad \text{(A.12)}$$

where $\dot{E}_{cos,out}$ is the outdoor dose rate (mSv/h); O_{out} and O_{in} are the outdoor and indoor occupancy factors; SF_{cos} is the shielding factor for cosmic rays (see table A1) and 8760 is the number of hours in a year.

A27. Various codes have been developed to estimate doses to aircrew according to specific parameters related to the flight routes, for example: CARI [C50], EPCARD [M4], JISCARD [Y8], and PCAIRE [P13]. For this evaluation, it was convenient to use the well-established SIEVERT code [B44] that is publicly available. Using data from ICAO, collective doses were calculated for 46 ICAO route groups and average per capita doses to residents for the different regions. A route group refers to the traffic within or between the 10 ICAO long-term forecasts regions (ICAO LTF region).

A28. Market pairs (flight routes) were extracted together with the associated revenue passenger kilometres (RPK) for the year 2015 from ICAO [I62] where RPK is the number of passengers multiplied by the distance flown in kilometres. For each market pair, the corresponding ICAO route group as defined by ICAO [I61] was determined and the dose calculated using SIEVERT code [B44, C40]. The input parameters for the SIEVERT code included departure and destination airport, flight date and duration. The date of 27 December 2015 was chosen as the flight date for the calculations because it represented a day with cosmic rays of intermediate intensity. The flight duration was obtained using an online resource [A9]. For each route group, three to seven market pairs were selected and the average dose per km calculated. Multiplying a route group's average dose per km by its total RPK gave the total collective dose for each route group. The total RPK for the ICAO route groups had been extracted for the year 2012 from the figures in ICAO traffic forecasts for passenger and cargo [I61].

A29. The collective doses for the route groups were then apportioned to the respective regions by applying a weighting factor that described the likelihood of the region's population to travel by airplane. The total collective dose attributed to each region was divided by the corresponding population to obtain the average doses per capita given in table 9 of the annex. The adjustment for the likeliness to travel by airplane is based on the average income of the region. Weighting factors were selected such that the likelihood tripled between successive income classes: low, lower-middle, upper-middle and high income. This is roughly proportional to the flying population percentage for each income group estimated by Gössling and Humpe [G17]. Since 56% of the collective dose due to air travel (27,000 person–Sv) is attributed to flights within or between North America and Europe, it was determined that a different weighting would result in a minimal change to the overall result. All results and calculations are available as tables in electronic attachment A-2.

A30. The contribution made by cosmogenic radionuclides to the annual dose was calculated from their annual intake via ingestion and inhalation. Data for concentrations of ^{14}C and ^{3}H in the atmosphere were obtained from the UNSCEAR Global Survey on Public Exposure and the literature review. For ^{7}Be and ^{22}Na, additional monitoring data on concentrations in ground-level air were obtained from CTBTO's International Monitoring System [C63]. The isotopic composition of carbon (i.e., activity of ^{14}C per unit mass of C) in food and drinking water was assumed to be equal to that in the atmosphere [H39].

2. Terrestrial radionuclides

(a) *External exposure*

A31. External exposure outdoors from terrestrial radionuclides present in soils was treated extensively by the Committee in several reports [U11, U12, U13, U15, U19]. As in previous UNSCEAR reports, the annual dose from external exposure to terrestrial radiation ($E_{ext,terr}$) was the sum of the doses from external exposure outdoors ($E_{ext,terr,out}$) and indoors ($E_{ext,terr,in}$):

$$E_{ext,terr} = E_{ext,terr,out} + E_{ext,terr,in} \quad \text{(A.13)}$$

A32. Doses from external exposure outdoors ($E_{ext,terr,out}$) calculated using the equation:

$$E_{ext,terr} = \dot{E}_{terr,out}\ O_{out}\ e_D\ 8760 \quad \text{(A.14)}$$

where $\dot{E}_{terr,out}$ is the outdoor dose rate (nSv/h); O_{out} is the outdoor occupancy factor; e_D is the dose coefficient converting absorbed dose rate in air to dose rate (Sv/Gy) and 8760 is the number of hours in a year.

A33. Figure A-III shows a schematic for the conversion of measured quantities to dose for the natural decay series of ^{238}U and ^{232}Th as well as ^{40}K. A value of 0.7 Sv/Gy for the dose coefficient e_D (DC2 in figure A-III) was adopted in this annex. This value was taken from the UNSCEAR 2000 Report, annex A [U15] and is corroborated by the results of the calculation of these dose coefficients for the radionuclides in the ^{232}Th series and the ^{238}U series as well as ^{40}K carried out by Petoussi et al. [P21]. The average value for all natural radionuclides calculated by Petoussi et al. [P21] for the ICRP reference phantom was 0.7 Sv/Gy; dose coefficients calculated for children (0.8 Sv/Gy) and infants (0.9 Sv/Gy) were similar to those used in previous UNSCEAR reports [U13].

A34. The outdoor dose rate ($\dot{E}_{terr,out}$) was estimated from activity concentrations of radionuclides in the soil, using the equation:

$$\dot{E}_{terr,out} = f_{dw} \sum_i d_R\ C_{soil,i} \quad \text{(A.15)}$$

where $C_{soil,i}$ is the activity concentration of radionuclide i in soil (Bq/kg, dry weight); d_R is the dose coefficient converting the concentrations to absorbed dose rate in air ((nGy/h)(Bq/kg)); and f_{dw} is the factor that accounts for the water content in soil for samples dried prior to measurement (see table A1).

A35. In figure A-III DC1 indicates the dose coefficients d_R used for calculating the absorbed dose rate in air from the activity concentrations in soil (Bq/kg) assuming a homogeneous distribution in the soil. Table A3 gives the values of d_R given in various UNSCEAR reports as well as in papers published since the UNSCEAR 2008 Report. Given the general consistency shown by the values in table A3, the dose coefficients given in the UNSCEAR 2000 Report, annex A [U15] were used for this annex.

Figure A-III. Conversion of measured radionuclide concentrations in soils to dose rate

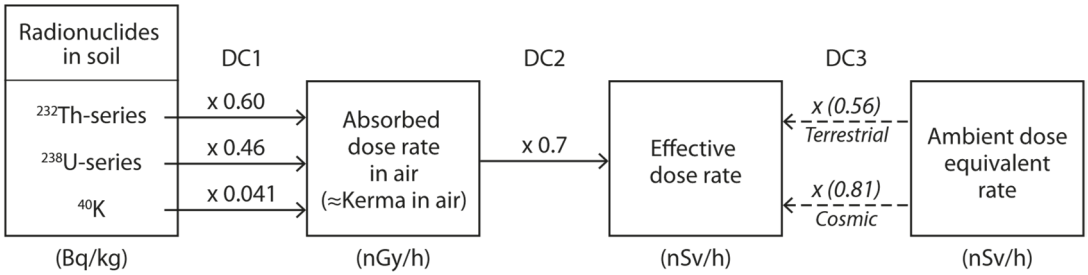

Table A3. Coefficients (d_R) to convert activity concentration of a radionuclide R in soil, to absorbed dose rate in air at a height of 1 m above the ground as used in different published sources

Publications	d_R *(nGy/h(Bq/kg))*		
	^{238}U	^{232}Th	^{40}K
UNSCEAR 1982 [U11], 1988 [U12]	0.427	0.662	0.043
UNSCEAR 1993 [U13]	0.461 (^{226}Ra)	0.623	0.0414
UNSCEAR 2000 [U15]	0.462	0.604	0.0417
Lemercier et al., 2008 [L14]	0.45	0.599	0.0427
Sanusi et al., 2021 [a] [S13]	0.46	0.66	0.042
Askri et al., 2023 [A40]	0.41/0.48	0.60/0.67	0.041/0.047

[a] Average of eight studies.

A36. The dose from external exposure indoors ($E_{ext,terr,in}$) was calculated using the equation:

$$E_{ext,terr,in} = \dot{E}_{terr,out}\, SF_{terr}\, O_{in}\, e_D\, 8760 \qquad \text{(A.16)}$$

where SF_{terr} is the shielding factor for terrestrial radiation, O_{in} is the indoor occupancy factor (see table A1) and 8760 is the number of hours in a year.

A37. The shielding factor SF_{terr} accounts for both the protection provided by buildings and the additional dose from radionuclides in building materials. Models for a standard room can be used to predict indoor dose rates from radionuclide activity concentrations in the building materials. The indoor dose rate for a room with dimensions of 400 × 500 × 280 cm, wall density of 2.35 g/cm^3 and wall thickness of 20 cm, built with material containing 40 Bq/kg ^{226}Ra, 30 Bq/kg ^{232}Th, and 400 Bq/kg ^{40}K predicted by a model developed by Croymans et al. [C56] would be about 100 nGy/h. The outdoor dose rate estimated from equation A.14, assuming that the soil has the same composition as the building material of the room would be be about 55 nGy/h, implying a value for SF_{terr} of about 1.8. However, direct measurements of the dose rates from the literature review suggest a lower value of about 1.2, closer the value of 1.4 adopted in previous UNSCEAR reports [U15, U19]. Since model-based estimates mainly apply to concrete buildings and do not represent other building types, the Committee retained its earlier value as more representative on a global scale.

A38. Although monitoring of ambient dose equivalent rates is widely used in nuclear or radiological emergency preparedness and response systems, doses from external exposures to terrestrial radionuclides were calculated in this annex using activity concentration in soil because estimating exposures to

terrestrial radiation using ambient dose rate data from monitoring networks is not a trivial task, since the monitoring station must be positioned correctly to avoid any influence from building materials, trees or similar structures, and at a consistent height above the ground. Such information is difficult to retrieve from studies in the open literature. Also, different instrument types are used in monitoring stations with different characteristics (e.g., photon energy responses, calibration methods) leading to different results in the measurement of ambient dose rates. In addition, it is essential to account for all variable components influencing the signal, such as the washout of radon progeny due to precipitation, the presence of snow cover, and other environmental factors, as well as the contribution from secondary cosmic rays and human-made radioisotopes which is not always included in measurements available in the open literature. Comprehensive monitoring using time series data is required, as single-measurement surveys are insufficient for a reliable analysis. Measurements of ambient dose equivalent rates carried out in different regions or countries available in literature are, in general, of limited duration and may not be representative of longer periods of exposure. A detailed assessment of the different contributions to the measurements of ambient dose equivalent rates can be found in a study by Liu et al. [L23].

(b) *Ingestion of food and drinking water*

A39. The dose from ingestion of ^{40}K in terrestrial food was calculated using the methodology described in the UNSCEAR 2008 Report, annex B [U19]. The methodology accounts for homeostatic control of the concentration of potassium in the body, the annual equivalent ^{40}K tissue doses which are calculated based on the natural abundance of ^{40}K in natural potassium, the specific activity for ^{40}K and the dose rate coefficient.

A40. The annual effective dose from ingestion of other radionuclides of natural origin in terrestrial foods ($E_{ing,terr}$) was calculated using the equation:

$$E_{ing,terr} = \sum_i e_{ing,i} \sum_f I_{f,world}\, C_{f,i} \quad \text{(A.17)}$$

where $C_{f,i}$ (Bq/kg) is the activity concentration of radionuclide i in food f; $I_{f,r}$ (kg/a) is the worldwide annual ingestion rate of food f and $e_{ing,i}$ (Sv/Bq) is the dose coefficient for ingestion of radionuclide i. The ingestion dose was calculated for ten radionuclides: ^{210}Po, ^{210}Pb, ^{228}Ra, ^{226}Ra, ^{228}Th, ^{230}Th, ^{232}Th, ^{238}U, ^{234}U, and ^{235}U. Population-weighted worldwide average ingestion rates of adults for eight food categories are given in table A4. They were taken from the UNSCEAR 2016 Report, annex A [U24] and are based on the World Health Organization (WHO) cluster diets [W6] and reorganized according to UNEP regions. Note that regional variations in radionuclide concentrations in foods were not considered in this annex. Activity concentrations in terrestrial foods ($C_{f,i}$) were updated based on data from IAEA Safety Reports Series No. 114 [I48] and are given in section III.B.4.

A41. The annual effective dose from ingestion of other radionuclides of natural origin in drinking water ($E_{ing,dw}$) was calculated using the equation:

$$E_{ing,dw} = \sum_i \left(e_{ing,i} I_{dw} C_{dw,i}\right) \quad \text{(A.18)}$$

where $C_{dw,i}$ (Bq/m^3) is the activity concentration of radionuclide i in drinking water; I_{dw} is the annual ingestion rate of drinking water (see table A1); and $e_{ing,i}$ (Sv/Bq) is the dose coefficient for ingestion of radionuclide i. Activity concentrations in drinking water ($C_{dw,i}$) were updated based on data from IAEA Safety Reports Series No. 114 [I48].

Table A4. Ingestion rates of terrestrial foods used in calculation of doses from ingestion of natural radiation

Food category	*Ingestion rate (kg/a)*
Cereals	130
Vegetables and fruit	230
Milk and dairy products	65
Meat and offal	44
Freshwater fish	5.7
Marine fish	7.5
Crustaceans	1.1
Molluscs	1.6

C. Dose assessment methodology for nuclear power production and related nuclear fuel cycle facilities

1. Approach

A42. The dose assessment methodology described in the UNSCEAR 2016 Report [U24] to evaluate the global radiological impact of different electricity generating technologies was used to estimate public doses from nuclear power production and related facilities in the nuclear fuel cycle. The methodology is designed to evaluate the activity concentrations of radionuclides in environmental media from radioactive discharges to the atmosphere, freshwater and marine environments. By necessity, the methodology uses simplifying assumptions because it is impractical to conduct a site-specific assessment for each facility in the world that discharges radionuclides to the environment. The methodology is robust, transparent, and builds on experience gained by the Committee in applying earlier versions to the assessment of public exposures [U15, U19]. The dose assessment methodology was updated for consistency with the input data used in the evaluation across the different sources of public exposure. For the first time, discharges to freshwater from uranium mines and mills were evaluated using the approach for discharges to small rivers described in the UNSCEAR 2016 Report, annex A [U24].

A43. The literature review in this topic area focused on model parameters used in the methodology (as presented in electronic attachments A-3.1 and A-3.2) with two objectives:

(a) To identify updated information related to key parameters impacting dose estimates, such as K_d values and globally representative flow rates for large rivers that receive discharges from nuclear power facilities.

(b) To identify updated information on parameters common to other topic areas and where appropriate, establish consistent values for the evaluation, such as population density data.

2. Input data

A44. The primary source of data for the dose assessment methodologies used by the Committee to evaluate public exposure from NPPs and related nuclear fuel cycle facilities is the information on discharges supplied by Member States in the UNSCEAR Global Survey on Public Exposure. Facility specific annual discharges were reported for individual radionuclides by mode of discharge (atmospheric and liquid) and the facility or reactor type identified. Discharges provided for groups of radionuclides (e.g., total alpha, particulates) were apportioned among the relevant radionuclides included in the methodology using an established procedure [U24]. For discharges reported as total gamma/beta or particulate, the facility type and supporting information was provided to determine how the radionuclides are apportioned.

A45. Atmospheric particulates discharged to the environment have a size distribution which depends on emission controls and facility type. The methodology assumed that atmospheric particulate discharges have a default size of 1 μm activity median aerodynamic diameter, except for gases and ^{3}H, both in the form of tritiated water and organically bound tritium (OBT). This is a reasonable assumption because nuclear facilities typically have high efficiency particulate air filtration systems to remove larger particulates.

3. Atmospheric and terrestrial environment

A46. The methodology for the calculation of doses from atmospheric discharges is based on a simple Gaussian model used to determine the dispersion of radioactivity released to atmosphere. Activity concentrations in air at distance x, $C_a(x)$ (Bq/m^3) are calculated using the equation:

$$C_a(x) = D_1 \, Q \, x^{-n} \tag{A.19}$$

where D_1 is the annual average dilution factor at 1 km (s/m^3); Q is the discharge rate (Bq/s); and n is an empirically determined index which depends on radionuclide (1.4 for ^{14}C, 1.2 for noble gases and 1.42 for all other radionuclides). A release height of 30 m was assumed for all facilities, and no account was taken of local topology. A simplified approach was used to account for deposition of radionuclides to the ground using an effective deposition velocity of 0.002 m/s to represent both dry and wet deposition for all radionuclides apart from noble gases, ^{3}H and ^{14}C. A value of zero was used for noble gases because their deposition is negligible. A specific-activity approach was used for ^{3}H and ^{14}C as theses radionuclides have a rapid exchange rate between the atmosphere and the ground.

A47. This approach was considered sufficiently robust when it was evaluated in some detail for the UNSCEAR 2000 Report, annex A [U15]. The use of Gaussian models for the dispersion of radioactivity in the atmosphere from routine discharges is a consolidated and well accepted approach for radiological assessments. The output from the UNSCEAR model was compared with that of the Gaussian model implemented in PC CREAM 08 [H34]. General agreement was found and no changes to any parameters were made. It is recognized that for site-specific evaluations more sophisticated atmospheric dispersion and transport modelling techniques are often required.

A48. The exposure pathways included in the methodology for discharges to atmosphere were:

(a) Internal exposure from inhalation of radionuclides in the plume;

(b) External exposure (beta and gamma emitters) from radionuclides in the plume;

(c) External exposure from radionuclides deposited from the plume; and

(d) Internal exposure from ingestion of radionuclides incorporated in food.

A49. Activity concentrations in terrestrial foods were calculated using transfer factors taken from the FARMLAND model [B54], a well-established compartment model specific to European conditions developed by the United Kingdom Health Security Agency and included in PC CREAM 08. The FARMLAND model has been subject to international verification and validation exercises and has not been updated since the UNSCEAR 2016 Report, annexes A [U24] was published. Individual doses were calculated assuming that the characteristic individual lived within a defined distance from the point of discharge and that 25% of their food is produced in the area.

A50. Activity concentrations of ^{3}H and ^{14}C in terrestrial foods were calculated using a specific activity approach:

(a) Activity concentrations of ^{3}H were derived on the basis of the water content in plants and a partition factor that accounts for the presence of exchangeable hydrogen in the dry weight of the plant;

(b) Activity concentrations of ^{14}C in plants were based on its concentration in air and the ratio of stable carbon to ^{14}C. Activity concentrations of ^{14}C in animal products were based on concentration in pasture and ratio of stable carbon in animal products to pasture.

4. Freshwater environment

A51. The model for the dispersion of radionuclides to freshwater is a simple dilution model which considers two generic types of rivers—small and large. The methodology assumes complete mixing of radioactivity following their discharge into freshwater and the activity concentration of radionuclide *i*, in unfiltered freshwater at the discharge point ($C_{uw,i}$) is given by:

$$C_{uw,i} = \frac{Q_i}{F} \quad \text{(A.20)}$$

where Q_i is the discharge rate of radionuclide *i* (Bq/s); and F is the volumetric flow rate of the river at the point of discharge (m^3/s).

A52. This is a cautious approach commonly used in dose assessment for discharges into rivers and considered adequate for the Committee's generic approach. The assumption of complete mixing provides a robust estimate of the activity concentrations in the river and ensures a reasonable and consistent approach. More complex models that account for characteristics of different rivers around the world would be difficult to implement for the Committee's assessment and require the collection of a considerable amount of information on local conditions.

A53. Two generic values were used for the flow of large (1,000 m^3/s) and small (10 m^3/s) rivers, based mainly on European rivers. The same approach was used to determine the dimensions of the rivers (depth, width and length). A comparison of these flow rates to non-European rivers is included in the UNSCEAR 2016 Report, annex A [U24]. A review of data for rivers that receive radioactive discharges from nuclear facilities outside Europe found that these flow rates are broadly consistent with those adopted in the methodology for the UNSCEAR 2016 Report, annex A.

A54. A review of data on the suspended sediment loads in large rivers in the open literature has found them to be in the range of 0.1 to 1 kg/m^3, and in general agreement with the value of 0.5 kg/m^3 adopted in the UNSCEAR 2016 Report, annex A [U24]. Data on suspended sediment loads for smaller rivers were not readily available in the open literature to suggest a value different from the value of 0.02 kg/m^3 adopted in the methodology.

A55. Values of the sediment distribution factors (K_d) and concentration factor (CF) for freshwater fish in the UNSCEAR 2016 Report, annex A [U24] were taken mainly from the IAEA Technical Report Series (TRS) No. 472 [I8, I22] supplemented in some cases by values from the National Council on Radiation Protection and Measurements Report No.123 [N10]. A review of K_d and CF values for the freshwater environment was carried out by the IAEA for the MODARIA programme.[13] The review also included consideration of regional variation with a comparison between data from arid regions and Fukushima (Japan). The data from the Fukushima Prefecture on K_d and CF values have been published in IAEA-TECDOC-1927 [I38] but are limited to a few radionuclides (^{137}Cs, ^{134}Cs and ^{131}I). K_d values reviewed during the IAEA MODARIA programme were published in the open literature [B50] and included in the ERICA tool;[14] and therefore, have been incorporated in the methodology.

A56. The exposure pathways included in the methodology for discharges to freshwater were:

(a) Internal exposure from ingestion of radionuclides in drinking water;

(b) External exposure (beta and gamma emitters) from radionuclides in sediments deposited on the riverbank;

(c) Internal exposure from ingestion of radionuclides incorporated into freshwater fish; and

(d) Internal exposure from ingestion of radionuclides incorporated into terrestrial foods irrigated with water abstracted from the river where discharges occurred.

A57. Treatment factors used in the calculation of doses from drinking water were based on those given in the UNSCEAR 2000 Report, annex A [U15], which was updated with information included in the fourth edition of the WHO Drinking Water Guidelines published in 2011. These treatment factors were compared to those given in the fourth edition of the WHO Drinking Water Guidelines published in 2017 and 2022 and no difference was found [W7].

A58. Doses to the public from ingestion of crops irrigated with water from rivers were included for the first time in the UNSCEAR 2016 Report, annex A [U24]. Doses for this exposure pathway were based on irrigation factors which were derived from the FAO data specific for different regions of the world. No updates to the irrigation factors were considered necessary by the Committee for this evaluation.

5. Marine environment

A59. The model used for the dispersion of radioactivity in the marine environment published in the UNSCEAR 2016 Report, annex A [U24] is a simple two-compartment model—a local compartment and a regional one—and includes transfer out of the regional compartment and to bottom sediments. The dimension of the compartments and the volumetric exchange rates between compartments, as well as sedimentation rates and suspended sediment loads are typical of European waters and there was no indication from the open literature that these values needed to be changed. Assumptions similar to those used for the freshwater environment regarding food ingestion rates and population sizes were used to account for regional differences.

A60. Sediment distribution factors (K_d) and bioaccumulation factors in seafood (B) were taken from IAEA TRS 422 [I14]. The IAEA MODARIA programme carried out a limited review of the values of marine K_d

[13] https://www-ns.iaea.org/projects/modaria/

[14] https://erica-tool.com/

and seafood bioaccumulation factors for the Fukushima Prefecture, which have been published in the IAEA-TECDOC-1927 [I38]. However, data were limited to a few radionuclides (^{137}Cs, ^{134}Cs and ^{131}I).

A61. The exposure pathways included in the methodology for discharges to marine environments are:

(a) External exposure (beta and gamma emitters) from radionuclides in sediments; and

(b) Internal exposure from ingestion of radionuclides incorporated into marine foods (fish, crustaceans and molluscs).

6. Methodology for uranium mines and mills

A62. The methodology in the UNSCEAR 2016 Report, annex A [U24] refers to the use of small rivers to assess doses associated with aquatic pathways for discharges to freshwater from uranium mines and mills, but no results are included for aquatic pathways. The current analysis has focused on integrating the assessment of doses from liquid discharges from uranium mines and mills to the freshwater environment with the methodology [U24] used for other nuclear facilities. The annex contains information needed to perform this integration, including the small river option, which had not been used before. The updated methodology also takes account of the effect of different tailings management practices. For example, in some areas, tailings are covered with water which reduces atmospheric releases. Water is unlikely to be available for such measures in arid regions, with the result that exposures from atmospheric releases may differ between arid and non-arid areas.

D. Dose assessment methodology for global fallout from nuclear weapons testing

A63. In this annex, public doses associated with global fallout from weapons testing were calculated using essentially the methodology described in the UNSCEAR 2000 Report, annex A [U15], although some of the parameter values (e.g., dose coefficient for external exposure) were updated to ensure consistency with other methodologies adopted in this annex. Figure A-IV reproduces figure I of the UNSCEAR 2000 Report and provides the general method of assessing doses resulting from global fallout of nuclear weapons tests [U15]. The impact of changes to the dose coefficients and the methodology on the doses estimated in previous annexes are described in electronic attachment A-4. Doses calculated for remaining exposure pathways from 2000–2024 using the updated dose coefficients only. Future doses were not estimated but data regarding estimated deposition densities are provided as per the information in the previous UNSCEAR 2008 report, annex B [U19].

Figure A-IV. Terrestrial pathways of transfer of radionuclides and dose to humans [U15]

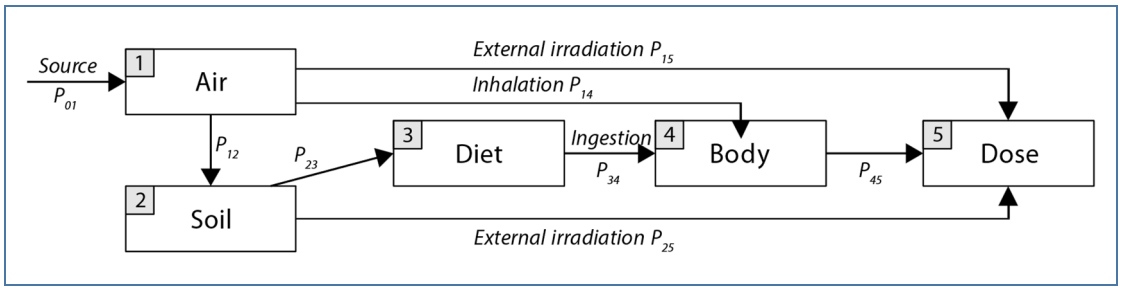

A64. The methodology for external exposure from deposited radionuclides as described in detail in the UNSCEAR 2000 Report, annex A [U15] derived the total yields for atmospheric releases for each year, applied a fusion to fission ratio that was yield dependent and modelled dispersion and deposition of the fallout for latitudinal bands. The yields originally published in the UNSCEAR 1993 Report, annex B [U13] were updated in the UNSCEAR 2000 Report, annex A [U15]; no updates were identified for this annex and values in the UNSCEAR 2000 Report, annex A were retained.

A65. The dose coefficients for external exposure provided in the UNSCEAR 2000 Report, annex A, which were taken from Beck [B16] were superseded for the current evaluation by those given in ICRP Publication 144 [I77]. The dose rate coefficients for exponentially distributed sources of ^{137}Cs+^{137m}Ba for different age groups are given in table A5. The table includes values for a planar source at relaxation mass depths of 0.5 g/cm^2 and for an exponentially distributed source at relaxation depths of 0.5, 10, 20 and 50 g/cm^2. The values for an exponential relaxation mass depth of 10 g/cm^2 were used to estimate doses from external exposure from global fallout. The dose coefficients for external dose from ^{137}Cs presented in table A5 are corrected by a factor of 0.944 to include contribution from ^{137m}Ba.

Table A5. Selected dose coefficients for external dose from ^{137}Cs in soil (nSv/h per Bq/m^2 from ICRP Publication 144 [I77]) for various vertical distributions and relaxation mass depth

Age group	*Dose coefficients for external dose for ^{137}Cs in soil (nSv/h per Bq/m^2)*				
	Planar (0.5 g/cm^2)	*Exponential*			
		0.5 g/cm^2	*10 g/cm^2*	*20 g/cm^2*	*50 g/cm^2*
Adult	1.26×10^{-3}	1.32×10^{-3}	4.87×10^{-4}	3.18×10^{-4}	1.81×10^{-4}
15-year-old children	1.29×10^{-3}	1.35×10^{-3}	5.01×10^{-4}	3.29×10^{-4}	1.87×10^{-4}
10-year-old children	1.38×10^{-3}	1.46×10^{-3}	5.34×10^{-4}	3.48×10^{-4}	1.99×10^{-4}
5-year-old children	1.51×10^{-3}	1.59×10^{-3}	5.78×10^{-4}	3.78×10^{-4}	2.15×10^{-4}
1-year-old children	1.63×10^{-3}	1.74×10^{-3}	6.11×10^{-4}	3.99×10^{-4}	2.28×10^{-4}
Newborn	1.83×10^{-3}	1.95×10^{-3}	6.69×10^{-4}	4.35×10^{-4}	2.47×10^{-4}

A66. The approach taken by the Committee to determine doses associated with internal exposure from ingestion in previous evaluation was significantly changed for the current one. The previous approach developed for the UNSCEAR 2000 Report, annex A [U15] in figure A-III. Transfer coefficients P_{23}, P_{34} and P_{45} were determined from regression analysis of models that related deposition to concentrations in diet and used dose coefficients taken from publication NRPB-M288 [P23]. The updated approach used for this annex is the same as that developed for the UNSCEAR 2016 Report, annex A [U24] which updated this aspect of the methodology based on substantial improvements in modelling the transfer of radionuclides through the terrestrial environment.

A67. It should be noted that the model for ingestion of terrestrial food in the UNSCEAR 2016 Report, annex A [U24], was designed to estimate doses from a long-term, continuous discharge of radionuclides; while the starting point for global fallout is a measured or estimated deposition density. Although the section of the model from deposition to ingestion dose could be applied to estimate present-day doses related to global fallout, this calculation was not considered justified given the amount of work required in comparison to the very small doses to the public due to this exposure pathway.

A68. In the calculation of doses from ingestion of ^{137}Cs and ^{90}Sr, root uptake is the only relevant pathway, since deposition no longer occurs. The dose estimates for adults in the UNSCEAR 2000 report, annex A were based on an ingestion rate of 500 kg/a of food [U15]. In this annex a total ingestion rate of 485 kg/a was used for adults and 15-year-olds for consistency with the dose assessment methodology for ingestion of terrestrial radionuclides. For 10-year-old children a total ingestion rate of 320 kg/a, corresponding to approximately two-thirds of the adult ingestion rate was used, while for 1-year-old children the ingestion rate adopted was 160 kg/a, corresponding to one-third of the adult ingestion rate [U15].

A69. Doses from inhalation were estimated only in the year that tests took place Using the methodology applied in the UNSCEAR 2008 Report, annex B [U19]. That methodology was based on the use of activity concentrations in air, an appropriate inhalation rate, and the relevant dose coefficients for intake by inhalation.

APPENDIX B. ANALYSIS OF UNCERTAINTIES AND VARIABILITIES

I. GENERAL APPROACH TO UNCERTAINTY AND VARIABILITY IN UNSCEAR EVALUATIONS

B1. The approach developed by the Committee to deal with uncertainty ad variability draws upon the experience gained in recent evaluations of medical exposure and occupational exposure [U30, U31], exposure due to radioactive discharges [U24] and uncertainties in reviewing epidemiological data [U23]. In its assessment of public exposure due to the accident at the Fukushima Daiichi NPS [U29] the Committee used an approach based on Bayesian statistics to deal with variabilities and uncertainties in dose assessment (see electronic attachment A-6 for a detailed description). This approach is consistent with the international methodology as described in the JCGM Guides [J11, J12, J13], which also contain the terminology of the International Vocabulary of Metrology (VIM) [J13]. A similar method was used in this annex wherever possible. Because the calculation of radiation doses involves the use of complex measurements and models, the approach follows ISO/IEC Guide 9-3:2008/Supplement 1 [J11]. Although the full JCGM method could not be applied to every type of public exposure considered in this annex, a summary of recent developments in metrology, including examples, that can be found in ISO 11929-4 [I90] is provided in electronic attachment A-6.

B2. The ISO/IEC Guide [J12] distinguishes two types of uncertainties, Type A and Type B, which reflect different ways to evaluate uncertainties. However, the Committee prefers to use the terms ‘aleatory’ and ‘epistemic’ to define these types of uncertainties. Aleatory uncertainty relates to outcomes that cannot be predicted and arises from repeated measurements, whereas epistemic uncertainty is related to incomplete information, such as information associated with published values, values of certified reference materials, or obtained from a calibration certificate, from the accuracy class of a measuring instrument or from limits deduced through expert judgment. Epistemic uncertainties cannot be assessed using frequentist methods and are often the most important uncertainties in the evaluation of public doses.

B3. Measurement uncertainty refers to estimating a fixed but unknown true value, such as the dose to an individual. It is described using probability density functions (PDF). Variability refers to the fact that there may be differing true values across a population or sample set. The actual true value is a random variable itself for which only a probability in the form of a PDF can be given, where each value itself is a random variable described by a PDF. Both types of PDFs must be propagated appropriately (e.g., using Monte Carlo methods) to fully characterize the uncertainty in the dose.

B4. Probability density functions for dose estimates reflect uncertainties in input quantities, including parameters in models used in the calculations, which may not have any defined uncertainties [U29]. These PDFs express the probability of the true dose value $\widetilde{D}$, based on the information about the input quantities. The goal of any measurement and evaluation is to obtain an estimate of the true value via a posterior PDF, representing Bayesian probabilities. These can be derived using Bayes’ Theorem or the Principle of Maximum Entropy [J10] as guided by GUM Supplement 1 [J11]. In a Bayesian approach [W3], the PDFs can be derived using Bayes’ Theorem or the Principle of Maximum Information Entropy [J10]. Guidance on methods to derive PDFs is provided in the Guide to the expression of Uncertainty in Measurement (GUM) Supplement 1 [J11].

B5. Before adopting a specific PDF with estimated parameters, a quantile-quantile plot should be used to validate the assumptions made and assess deviations. The PDF reflects both incomplete knowledge

about the dose and the distribution of doses across a population. In this context, measurement uncertainty and variability become synonyms and are difficult to distinguish.

B6. BFor any measured or estimated quantity *X*, the PDF $f_X(\tilde{x}|x)$ is the conditional probability density that the true value of the measurand is $\tilde{x}$, given the measured or estimated result *x*. A PDF can be represented by relevant moments of the distribution, such as the mean, median, and specified percentiles. The best estimate of the measurand and its associated standard uncertainty can be calculated as the expectation value $E\left(f_X(x)\right)$:

$$E\left(f_X(x)\right) = \int_{-\infty}^{+\infty} x\, f_X(x)\, dx \tag{B.1}$$

and the square root of the variance $u(x)$:

$$u(x) = \sqrt{Var\left(f_x(x)\right)} = \sqrt{\int_{-\infty}^{+\infty} \left(x - E\left(f_x(x)\right)^2\right) f_x(x)\, dx} \tag{B.2}$$

B7. Coverage interval is the interval where the true value of the measurand lies with a preselected probability. Coverage interval is used instead of confidence interval to emphasize that it applies to the true value of a measurand. A coverage interval is defined as:

$$\int_{\tilde{x}_l}^{\tilde{x}_u} f_x(\tilde{x}|x)\, d\tilde{x} = 1 - \gamma \tag{B.3}$$

where $1 - \gamma$ is the coverage probability and $\tilde{x}_l$ and $\tilde{x}_u$ are the lower and upper limit of the coverage interval, respectively. The true value $\tilde{x}$ is the variable and the measurement result *x* is a given constant. Limits of the coverage interval are defined in such a way that the coverage interval contains the true value of the measurand with the specified probability $1 - \gamma$.

B8. In contrast to the coverage interval, the confidence interval is defined as:

$$\int_{x_l}^{x_u} f_x(x|\tilde{x})\, dx = 1 - \gamma \tag{B.4}$$

where $1 - \gamma$ is the confidence probability and x_i and x_u. are the limits of the confidence interval. In this case the measurement result *x* is the variable and the true value $\tilde{x}$ is a given constant. Limits of the confidence interval are defined in such a way that the confidence interval contains expected future measurement results of the measurand with the specified probability $1 - \gamma$.

B9. BIt is frequently assumed that the posterior PDF of the dose $f_D\left(\widetilde{D}|x\right)$ can be represented by a log-normal distribution. This is because in the calculation of doses multiple input quantities generally combine multiplicatively. The log-normal distribution is the general solution for multifactorial quantities, such as the dose, according to the multiplicative limiting theorem of statistics. To check if the assumption of a log-normal distribution is valid a quantile-quantile-plot should be used for each case. There is also a theoretical basis for assuming a log-normal distribution: the logarithmic normal distribution is the maximum entropy PDF if the logarithms of the data are known.

B10. Another reason for assuming a log-normal distribution is that the dose is a non-negative quantity with large variability. If dose estimates alone were available to quantify the dose, the maximum entropy PDF would be a normal distribution. However, given the large variability in dose estimates, if the posterior function was assumed to be a normal distribution, a non-negligible part of the PDF would be represented by negative values of the dose which is physically impossible. Since the log-normal distribution only produces non-negative values, it naturally accounts for the non-negativity of the dose. At the same time, the log-normal distribution can account for asymmetric and tailed distributions and describe deviations from normal distributions [L21].

B11. While the normal distribution is characterized by the arithmetic mean (AM) and standard deviation (SD) as parameters, the log-normal distribution is characterized by the geometric mean (GM) and geometric standard deviation (GSD), although the best estimate of the value of the dose remains the expectation value of the PDF (i.e., the AM of the original data).

B12. A particular problem arises from the fact that the calculation of the total dose is the sum of doses from different exposure pathways, i.e., inhalation, ingestion and external radiation. The moments and the quantiles of the posterior PDF of the dose cannot be simply calculated from the moments and quantiles of the PDFs of the doses from different exposure pathways since the sum of log-normal distributions is not *a priori* log-normal. The posterior PDF of the total dose can be calculated appropriately using Monte Carlo techniques.

B13. It is often the case that some of the input parameters are assumed to have fixed values even though, in principle, all input quantities have inherent uncertainties and variabilities associated with their values. There are three categories of fixed parameters used in this annex:

(a) Parameters describing human habits (e.g., as occupancy factors, inhalation and ingestion rates;

(b) Parameters used in environmental models (e.g., shielding factors, equilibrium factors for radon, transfer factors in terrestrial and aquatic compartmental models; and

(c) Dose coefficients.

II. TREATMENT OF UNCERTAINTY FOR DIFFERENT TYPES OF DOSE ESTIMATES

B14. A mixed approach may be appropriate to address uncertainty of doses calculated using environmental measurements or source term, whereby data derived from model calculations are defined as parameters and the remaining data processed according to the JCGM Guides. The relevance of the different sources of uncertainties also needs to be analysed, for instance by a sensitivity analysis. In some cases, multi-model approaches may help to estimate the uncertainties. The sensitivity analysis used to treat the uncertainties for the methodology in the UNSCEAR 2016 Report, annex A [U24] is described in electronic attachment 4 of that report and the results compared with earlier methodologies in electronic attachment 1.

B15. For doses reported by governments or institutions only descriptive statistics are possible, such as a discussion of the type of distribution and its moments of the distribution (e.g., means, medians, and specified percentiles). For these estimates an uncertainty analysis and an evaluation of the probability of a possible underlying true value cannot be performed. An example of this type of assessment is the treatment of uncertainties in the UNSCEAR 2020/2021 Report, annex D [U30]. Another approach for this type of assessment was used in the UNSCEAR 2020/2021 Report, annex A [U31]. However, these two documents are not consistent in their approach regarding the assessment of uncertainties.

III. EXTRAPOLATION OF DATA

B16. In this annex it was generally assumed that the data reported by different countries (e.g., submitted through the UNSCEAR Global Survey on Public Exposure) were not accurate estimates of the true value but had uncertainty associated with them represented by a log-normal distribution. Moreover, it was assumed that the true values of the reported data were equally likely to be smaller or greater than the reported values, that is, the reported data and predicted values each represent a median (50th percentile) of an uncertainty distribution. The GM of the data was taken to be an estimate of the median of the log-normal uncertainty distribution.

B17. Given the assumption that the reported and extrapolated values for individual countries were GMs and the uncertainties were the GSDs, accepted statistical rules for log-normal distributions were used to determine sums of, for example, number of exposed individuals, averages of, for example, doses, as well as the overall uncertainty of each quantity. The total number of exposed people was estimated as the sum of the reported values and predicted values, both assumed as GMs of individual countries.

B18. The average dose per exposed person is estimated from the country-specific reported values by determining the average value and assuming it is a geometric mean (GM):

$$GM = e^{\left(\frac{1}{n}\sum_{i=1}^{n} ln(x_i)\right)} \quad \text{(B.5)}$$

where x_i are the reported or extrapolated data values and n is the total number of countries considered in the calculation. The standard uncertainty is then given by the GSD:

$$GSD = e^{\left(\sqrt{\frac{1}{n-1}\sum_{i=1}^{n}\left(ln(x_i)-\overline{ln(x_i)}\right)^2}\right)} \quad \text{(B.6)}$$

B19. The overall uncertainty on the number of exposed persons and average dose per exposed person for a region is determined by combining the estimated GSDs for the countries involved:

$$GSD_{combined} = e^{\left(\sqrt{\sum_{k=1}^{m} ln(GSD_k)^2}\right)} \quad \text{(B.7)}$$

B20. The approach described above is clearly an approximation used because of the lack of quality data on public exposure in all Member States for which uncertainties for individual countries can be assessed. Potential systematic biases, due to lack of information provided by countries for all topic areas constitute the most serious problem regarding the reliability of the extrapolation process and the accuracy of the extrapolated values.

IV. UNCERTAINTY IN ENVIRONMENTAL MODELS

B21. Public exposures are generally assessed using quantities that can be measured directly, such as absorbed dose rates, activity concentration in environmental media and deposition rates from global fallout of nuclear weapons testing. In some cases, the levels of radionuclides in the environment are below detection limits and therefore the assessment of public doses is based on data for the source term (e.g., discharges from nuclear facilities) combined with environmental models.

B22. The sources of uncertainty in environmental models have been studied intensively in recent years [U34]. The following sources of uncertainty can be distinguished:

(a) Uncertainty due to the choice and range of model parameters;

(b) Uncertainty due to the model structure and conceptualization (conceptual model uncertainty);

(c) Uncertainty due to sampling and monitoring of input variables;

(d) Uncertainty in the knowledge of the scenario to be modelled;

(e) Uncertainty in the subjective interpretation of the assessment problem (modeller's uncertainty);

(f) Uncertainty in the mathematical/numerical implementation of the model.

B23. Uncertainty due to the choice and range of model parameters is the most studied source of uncertainty and is linked to the parameter values, such as transfer coefficients of radioecological models, and their correlations. A key stage in these evaluations is to identify the most sensitive parameters and to determine the impact of likely variations in these parameters on the estimated doses.

B24. Conceptual uncertainty plays an important role in radioecology. An example is the assumption that the system is in equilibrium when this is not the case due to dynamic behaviour. For example, the use of distribution coefficients (K_d), which assumes reversible, equilibrium conditions, and neglects system dynamics and process kinetics, would be inappropriate for modelling rapidly varying conditions, but is considered acceptable in this case because discharges were provided on an annual basis.

B25. Scenario uncertainty includes uncertainties linked to missing information about the characteristics of the exposed person. This source of uncertainty is not relevant in this annex because the characteristics of the exposed person were defined in this annex based on generic data. In addition to discharges and human characteristics, other input information includes meteorological data (e.g., wind speed and direction, precipitation) for atmospheric discharges and hydrological data for liquid discharges.

V. DOUBLE COUNTING

B26. Double counting is another source of uncertainty, potentially leading to an overestimation of doses, if the same exposure situation is accounted for more than once in the evaluation. Indeed, a given source of radionuclide (e.g., a facility being dismantled, a former mine being remediated) might be understood by some experts (e.g., the NCPs completing the UNSCEAR Global Survey on Public Exposure or the Committee's experts) as falling in one category (e.g., impact of the operating facility, considering that operating continues until the end of the life cycle of the facility) and by others as falling in another category (e.g., legacy site). In addition, doses calculated from measurement data for naturally occurring radioactive materials in areas impacted by uranium mining or in high background radiation areas, for example, may differ depending on the assumptions made regarding background concentrations. Laying out the methodologies used to calculate doses provides transparency to identify and eliminate such eventuality.

VI. DATA GAPS

B27. Data gaps arise when Member States do not report data related to sources of public exposure, either across regions or over time. These gaps may be partially addressed through literature reviews or filled using extrapolation, interpolation, and model-fitting techniques. However, these methods require assumptions about the completeness of data sources and how to handle missing information, especially when extending findings to areas with no available data.

B28. A key challenge involves measurements that fall below detection thresholds due to limitations in the sensitivity of the measurement methods. These values—generally referred to as below detection limit or non-detects—are excluded by metrological or regulatory limits, such as detection limits, quantification thresholds, or minimum detectable activities. Terminological inconsistencies can lead to confusion, especially when distinguishing between technical detection capabilities and legal reporting requirements.

B29. More problematic is the use of reporting levels (RL) which quantify doses below which no results are reported as a censoring threshold because it is based on considerations about the radiological relevance of the data for legal purposes and may result in the loss of information about the data. A particular aspect of censoring thresholds is the problem of how to deal with non-detects in a data set. Seven different approaches on how to deal with non-detects have been described in the open literature: substitute '0' for non-detects, substitute 'RL/2' for non-detects, substitute 'RL' for non-detects, regression on order statistics, maximum likelihood estimation, Kaplan-Meier methodology, and Markov Chain Monte Carlo. A review and an assessment of the performance of the different methods and their associated biases was provided in a paper by Suzuki [S81]. Ultimately the Committee decided to adopt the RL/2 substitution approach for non-detects as a practical compromise, given the amount and the heterogeneity of the available data, although it recognized the tendency of this method to overestimate geometric means and to underestimate the variance. [S81].

GLOSSARY

Absorbed dose: Fundamental dosimetric quantity defined as the energy imparted by ionizing radiation in unit mass of matter; the SI unit of absorbed dose is joule per kilogramme (J kg^{-1}), and its special name is grey (Gy).

Activity: An amount of a radionuclide in a particular energy state at a given time, defined as $A(t) = \frac{dN}{dt}$, where *dN* is the expectation value of the number of spontaneous nuclear transformations from the given energy state in the time interval *dt.* The SI unit of activity is reciprocal second (s^{-1}). As the unit is so small, multiples are frequently used, such as megabecquerels (MBq) which is 10^6 or a million becquerels. (1 GBq is 10^9 Bq; 1 TBq is 10^{12} Bq; and 1 PBq is 10^{15} Bq) [U22, U28, U29].

Collective dose: The sum of individual effective doses incurred by members of a specified population. Its special name is person–Sv.

Committed effective dose, E(τ): The effective dose of internal exposure equal to time integral over time, τ, of effective dose rate. The integration time following the intake is taken to be 50 a for adults, and to age 70 a for children.

Dose: A measure of the energy deposited by radiation in a target. Dose can be used as a shorthand for absorbed dose, effective dose, and committed effective dose, when the context is clear.

Dose coefficient/dose per unit intake: The committed effective dose or committed absorbed or equivalent dose in a tissue or organ resulting from an intake, by a specified means (usually ingestion or inhalation), of unit activity of a specified radionuclide in a specified chemical form.

Dose rate: Dose delivered or received per unit time. Measurements are usually made in terms of the dosimetric quantity, ambient dose equivalent rate, H*(10), in units of µSv/h.

Effective dose, E: The sum over all tissues and organs of the equivalent doses weighted by the tissue weighting factor w_T, which represents the contribution of that organ or tissue to the total detriment resulting from uniform irradiation of the whole body. Effective dose has the unit joule per kilogram, which is given the special name sievert (Sv). The recommended values of w_T are given in the ICRP Publication 103.

Equilibrium equivalent concentration, EEC: The activity concentration of radon, in equilibrium with its short-lived decay products, that would have the same potential alpha energy concentration as the existing non-equilibrium mixture.

Equilibrium factor, F: The ratio of the equilibrium equivalent concentration to the radon concentration. In other words, the ratio of potential alpha energy concentration for the actual mixture of radon decay products to that which would apply at radioactive equilibrium.

Error: The difference between an observed or estimated value and the true (but unknown) value. Since the true value is unknowable, error cannot be quantified. Error can be contrasted with uncertainty, which can be estimated by repeated measurements or Bayesian inference.

Exposure: The act or condition of being subject to irradiation. External exposure is exposure to radiation from a source outside of the body. Internal exposure is exposure to radiation from a source within the body.

Model: An analytical or physical representation or quantification of a real system and the ways in which phenomena occur within that system, used to predict or assess the behaviour of the real system under specified (often hypothetical) conditions. This is in contrast to a relationship, which is simply the way two or more factors are connected or related (i.e., relationships include causal relationships, those based on models, and those that simply fit the observed data).

NORM (naturally occurring radioactive material): Radioactive material containing no significant amounts of radionuclides other than naturally occurring radionuclides. Material in which the activity concentrations of the naturally occurring radionuclides have been changed by some processes are included in NORM [I70]. The designation NORM is most typically used for materials associated with industrial activities.

Potential alpha energy concentration: The concentration of short-lived ^{222}Rn or ^{220}Rn decay products in air in terms of the alpha energy emitted during complete decay from ^{222}Rn decay products to ^{210}Pb or from ^{220}Rn decay products to ^{208}Pb of any mixture of short-lived ^{222}Rn or ^{220}Rn in a unit volume of air. The SI unit for potential alpha energy concentration is J/m^3.

Public exposure: Exposure incurred by members of the public from radiation sources, excluding any occupational or medical exposure.

Radionuclide: A radioactive isotope of an element. Different isotopes of an element have the same number of protons but different numbers of neutrons and hence different atomic masses [U22, U28, U29].

Uncertainty: Expression of having doubt, or being unsure about study results, hypotheses, model-based estimations or results of measurements, and specifically the true value of a quantity of interest. This may be due to lack of complete knowledge about true values for an individual or to a lack of complete knowledge of factors explaining the inter-individual variability of true values in a defined subgroup or population. Unlike error, uncertainties can be quantified. Estimates of uncertainty represent the amount or percentage by which an observed or calculated value might differ from its true value. For a quantity of interest that has a true fixed value, uncertainty is defined here as a degree of belief probability distribution comprising many realizations of possibly true values. For a quantity of interest that is a group or population of true values, uncertainty can be characterized as many alternative realizations as possible of sets of true values.

Variability: Heterogeneity, diversity or a range which characterizes variation in estimated, measured, or true values of a quantity of interest. The term "variability" is often used to describe differences in measured or true values among individuals in a population or cohort. Examples include inter-individual differences in body weight and/or dose or inter-cohort differences in exposure–response due to differences in sensitivity to a hazardous agent. Further study cannot reduce variability but may provide additional information to explain reasons why some of this variability occurs. This additional information can reduce the fraction of inter-individual variability initially treated as stochastic.

REFERENCES

A1 Abdul-Hadi, A., W. Al-Qadhi and E. El-Zeen. Determination of uranium, thorium and potassium contents of rock samples in Yemen. J Radioanal Nucl Chem 290(2): 261-266 (2011).

A2 Abella, M., M.R. Molina, I. Nikolić-Hughes et al. Background gamma radiation and soil activity measurements in the northern Marshall Islands. J Proc Natl Acad Sci USA 116(31): 15425-15434 (2019).

A3 Acena, V., F. Zamora and M. Garcia. Dose assessment to the members of the public resulting from the transport activity in Spain. Proceedings from the 20th International Symposium on the Packaging and Transportation of Radioactive Materials (PATRAM 22), Juan-les-Pins, France, 11–15 June 2023.

A4 Adelikhah, M.E., R. Ahangari and O. Noori. Calculation of liquid waste discharge limits for routine discharge of Tehran research reactor. Kerntechnik 83(2): 121-128 (2018).

A5 Adler, P.M. and F. Perrier. Radon emanation in partially saturated porous media. transport in porous media. Trans Porous Med 78(2): 149-159 (2009).

A6 AFCN. Dépouilles radioactives. Agence Fédérale de Contrôle Nucléaire. [Internet] Available from (https://afcn.fgov.be/fr/professionnels/professions-medicales/radiotherapie/depouilles-radioactives) on 08.12.2023. (French).

A7 Agarwal, T.K., B.K. Sahoo, J.J. Gaware et al. CFD based simulation of thoron (^{220}Rn) concentration in a delay chamber for mitigation application. J Environ Radioact 136: 16-21 (2014).

A8 Agarwal, T.K., B.K. Sahoo, M. Joshi et al. CFD simulations to study the effect of ventilation rate on ^{220}Rn concentration distribution in a test house. Radiat Phys Chem 162: 82-89 (2019).

A9 Air Miles Calculator. Air Miles Calculator. [Internet] Available from (https://www.airmilescalculator.com/) on 27.07.2023.

A10 Akashi, M., H. Aoki, A. Endo et al. Lessons learned from the JCO nuclear criticality accident in Japan in 1999. International Atomic Energy Agency, Vienna, 2009.

A11 Akleyev, A.V., L.Y. Krestinina, M.O. Degteva et al. Consequences of the radiation accident at the Mayak production association in 1957 (the 'Kyshtym Accident'). J Radiol Prot 37(3): R19-R42 (2017).

A12 Akleyev, A.V. and M.O. Degteva. Radioecological consequences of radioactive releases due to weapons-grade plutonium production at the 'Mayak' facility in the Russian Federation. J Radiol Prot 41(2): S67–S78 (2021).

A13 Akleyev, A.V., M.O. Degteva and L.Y. Krestinina. Medical consequences of the Urals radiation accidents: Comparative analysis. Environ Advan 9(3): 100253 (2022).

A14 Akleyev, A.V., M.O. Degteva and L.Y. Krestinina. Overall results and prospects of the cancer risk assessment in the Urals population affected by chronic low dose-rate exposure. Radiat Med Prot 3(4): 159-166 (2022).

A15 Al-Hwaiti, M.S., H.J. Brumsack and B. Schnetger. Heavy metal contamination and health risk assessment in waste mine water dewatering using phosphate beneficiation processes in Jordan. Environ Earth Sci 77(19): 661 (2018).

A16 Alber, O., C. Laubichler, S. Baumann et al. Modeling and predicting mean indoor radon concentrations in Austria by generalized additive mixed models. Stochastic Environ Res Risk Assess 37: 3435-3449 (2023).

A17 Aleksakhin, R.M., L.A. Buldakov, V.A. Gubanov et al. Large radiation accidents: Consequences and protective countermeasures. IzdAT, Moscow, Russian Federation, 2001. (Russian).

A18 Alhawsawi, A.M., E.I. Shababa, M.M.T. Qutub et al. Radiological characterization of the phosphate deposit in Al-Jalamid phosphate mining area, Saudi Arabia. Nukleonika 66(1): 35-44 (2021).

A19 Ali, M.M.M., H. Zhao, Z. Li et al. Concentrations of TENORMs in the petroleum industry and their environmental and health effects. RSC Adv 9(67): 39201-39229 (2019).

A20 Ali, M.M.M., Z. Li, H. Zhao et al. Characterization of the health and environmental radiological effects of TENORM and radiation hazard indicators in petroleum waste–Yemen. J Proc Safe Environ Protec 146: 451-463 (2021).

A21 Aliyu, A.S., T.A. Mousseau, A.T. Ramli et al. Radioecological impacts of tin mining. Ambio 44(8): 778-787 (2015).

A22 Alomari, A.H., M.A. Saleh, S. Hashim et al. Activity concentrations of ^{226}Ra, ^{228}Ra, ^{222}Rn and their health impact in the groundwater of Jordan. J Radioanal Nucl Chem 322(2): 305-318 (2019).

A23 Alvarez, J.L., R. Geddes, J.E. Rice et al. Elemental phosphorus slag exposure study in Southeastern Idaho, USA. Intl Congress Series 1225: 131-138 (2002).

A24 Amekudzie, A., G. Emi- Reynolds, D.O. Kpeglo et al. Determination of dose rate levels around nuclear installations in Ghana. Intl J Sci Technol 1(3): 144-147 (2011).

A25 Amrane, M., L. Oufni, B. Manaut et al. Measurements of ^{222}Rn, ^{220}Rn and their decay products in the environmental air of the Errachidia area (Morocco) using SSNTDs. Ener Environ Eng 1(2): 62-67 (2013).

A26 ANDRA. Mémoire de synthèse pour les générations futures (CSM). Agence nationale pour la gestion des déchets radioactifs, Chatenay-Malabry, 2008. (French).

A27 ANDRA. Rapport d'information 2020 sur la sûreté nucléaire et la radioprotection. Le Centre de stockage de l'Aube. Agence nationale pour la gestion des déchets radioactifs, Soulaines-Dhuys, 2020. (French).

A28 ANDRA. Rapport d'information 2021 sur la sûreté nucléaire et la radioprotection. DP/DICOM/22-0041. Le Centre de stockage de la Manche Agence nationale pour la gestion des déchets radioactifs, Soulaines-Dhuys, 2022. (French).

A29 Anspaugh, L.R. and B.W. Church. Historical estimates of external gamma exposure and collective external gamma exposure from testing at the Nevada Test Site I. Test series through Hardtack II, 1958. Health Phys 51(1): 35-51 (1986).

A30 Anspaugh, L.R., Y.E. Ricker, S.C. Black et al. Historical estimates of external gamma exposure and collective external gamma exposure from testing at the Nevada Test Site. II. Test series after Hardtack II, 1958, and summary. Health Phys 59(5): 525-532 (1990).

A31 Anspaugh, L.R., A. Bouville, K.M. Thiessen et al. A methodology for calculation of internal dose following exposure to radioactive fallout from the detonation of a nuclear fission device. Health Phys 122(1): 84-124 (2022).

A32 Antignani, S., G. Venoso, M. Ampollini et al. A 10-year follow-up study of yearly indoor radon measurements in homes, review of other studies and implications on lung cancer risk estimates. Sci Total Environ 762: 144-150 (2021).

A33 Aoun, M., A.G. El Samrani, B.S. Lartiges et al. Releases of phosphate fertilizer industry in the surrounding environment: investigation on heavy metals and polonium-210 in soil. J Environ Sci 22(9): 1387-1397 (2010).

A34 Appleton, J.D. and J.C. Miles. A statistical evaluation of the geogenic controls on indoor radon concentrations and radon risk. J Environ Radioact 101(10): 799-803 (2010).

A35 Arnold, D., A. Vargas and X. Ortega. Analysis of outdoor radon progeny concentration measured at the Spanish radioactive aerosol automatic monitoring network. J App Rad Iso 67(5): 833-838 (2009).

A36 Aro, L. Safety case for the operating license application: Description and data of the surface environment 3 - Forests and mires. Posiva working report 2019-13. Natural Resources Institute Finland (Luke), 2021.

A37 Arvela, H., A. Voutilainen, T. Honkamaa et al. High indoor radon variations and the thermal behavior of eskers. Health Phys 67(3): 254-260 (1994).

A38 Arvela, H., O. Holmgren and H. Reisbacka. Radon prevention in new construction in Finland: A nationwide sample survey in 2009. Radiat Prot Dosim 148(4): 465-474 (2012).

A39 Arvela, H., O. Holmgren, H. Reisbacka et al. Review of low-energy construction, air tightness, ventilation strategies and indoor radon: Results from Finnish houses and apartments. Radiat Prot Dosim 162(3): 351-363 (2014).

A40 Askri, B., K. Manai, A. Bouzouita et al. Estimation of the gamma-ray field in air from radioactive sources in the ground by numerical solution of the Boltzmann transport equation. Radiat Prot Dosim 199(7): 631-645 (2023).

A41 ASN. ASN Report on the state of nuclear safety and radiation protection in France in 2022. Autorité de sûreté nucléaire, ASN, Montrouge, 2022. (French).

A42 Attarde, R.B., V.K. Shukla, B.A.R. Babu et al. Fission signatures of tests on sub/kiloton devices. BARC Newsletter 188: 1-3 (1999).

B1 Baeza, A., J. Garcia-Paniagua, J. Guillen et al. Influence of architectural style on indoor radon concentration in a radon prone area: A case study. Sci Total Environ 610-611: 258-266 (2018).

B2 Ballesteros, L., I. Zarza, J. Ortiz et al. Occupational exposure to natural radioactivity in a zircon sand milling plant. J Environ Radioact 99(10): 1525-1529 (2008).

B3 Balonov, M.I., G.Y. Brook, V.Y. Golikov et al. Assessment of current exposure of the population living in the Techa River basin from radioactive releases of the Mayak facility. Health Phys 92(2): 134-147 (2007).

B4 Banzi, F.P., P. Msaki and I.N. Makundi. A survey of background radiation dose rates and radioactivity in Tanzania. Health Phys 82(1): 80-86 (2002).

B5 Baran, A. and E. Pollman. Radiation exposure due to railway transport of radioactive materials. Proceedings from the 7th International Symposium on the Packaging and Transportation of Radioactive Materials (PATRAM), New Orleans, USA, 15–20 May 1983. Oak Ridge National Laboratory.

B6 Barnet, I. and I. Fojtikova. Soil gas radon, indoor radon and gamma dose rate in CZ: Contribution to geostatistical methods for European atlas of natural radiations. Radiat Prot Dosim 130(1): 81-84 (2008).

B7 Barrington, S.F., M.J. O'Doherty, A.G. Kettle et al. Radiation exposure of the families of outpatients treated with radioiodine (iodine-131) for hyperthyroidism. Eur J Nucl Med 26(7): 686-692 (1999).

B8 Barros, N., D.W. Field, D.J. Steck et al. Comparative survey of outdoor, residential and workplace radon concentrations. Radiat Prot Dosim 163(3): 325-332 (2015).

B9 Barton, N., C. Wilson, R. Gelder et al. Sea transport of radioactive materials. Radiol Prot Bulletin (189): 7-8 (1997).

B10 BASE. Facts and figures on nuclear fuel transports. Federal Office for the Safety of Nuclear Waste Management. [Internet] Available from (https://www.base.bund.de/en/interim-storage-facilities/transports/transports_content.html) on 12.09.2023.

B11 Bataille, C. and H. Revol. Rapport sur les incidences environnementales et sanitaires des essais nucleaires effectues par la France entre 1960 et 1996 et elements de comparaison avec les essais des autres puissances nucleaires, Office parlementaire d'évaluation des choix scientifique et technologiques, Paris, 2001. (French).

B12 Batters, S., K. Tsang and U. Stahmer. Generic transportation dose assessment. NWMO TR-2012-06. Nuclear Waste Management Organization, Ontario, 2012.

B13 Bazyka, D.A., V.O. Sushko, O.M. Ivanova et al. On the methodology of passport doses calculation for Ukrainian settlements radioactively contaminated due to the Chornobyl NPP accident. Prob Radiat Med Radiobiol 28: 110-142 (2023). (Russian).

B14 Beck, C.M., S.R. Edwards and M.L. King. The off-site Plowshare and Vela uniform programs: Assessing potential environmental liabilities through and examination of proposed nuclear projects, high explosive experiments, and high explosive construction activities, Vol. 1 of 3. DOE/NV/26383-22. United States Department of Energy, Las Vegas, 2011.

B15 Beck, H.L. Environmental gamma radiation from deposited fission products, 1960-1964. Health Phys 12(3): 313-322 (1966).

B16 Beck, H.L. Exposure rate conversion factors for radionuclides deposited on the ground. EML-378. Environmental Measurements Laboratories. US Department of Energy, New York, 1980.
B17 Beck, H.L., A. Bouville, B.E. Moroz et al. Fallout deposition in the Marshall Islands from Bikini and Enewetak nuclear weapons tests. Health Phys 99(2): 124-142 (2010).
B18 Beck, H.L., S.L. Simon, A. Bouville et al. Accounting for unfissioned plutonium from the trinity atomic bomb test. Health Phys 119(4): 504-516 (2020).
B19 Beck, H.L., A. Bouville, S.L. Simon et al. A method for estimating the deposition density of fallout on the ground and on vegetation from a low-yield, low-altitude nuclear detonation. Health Phys 122(1): 21-53 (2022).
B20 Beer, J., K. McCracken and R. Steiger. Cosmogenic Radionuclides: Theory and Applications in the Terrestrial and Space Environments. Springer-Verlag Heidelberg, Berlin, 2012.
B21 Bena, E., G. Ciotoli, L. Ruggiero et al. Evaluation of tectonically enhanced radon in fault zones by quantification of the radon activity index. Sci Rep 12: 21586 (2022).
B22 Berkhouse, L., S.E. Davis, F.R. Gladeck et al. Operation DOMINIC I-1962: United States Atmospheric Nuclear Weapons Tests Nuclear Test Personnel Review. DNA 6040F. Kaman Tempo, Washington, DC, 1983.
B23 Besic, L., I. Muhovic, A. Asic et al. Meta-analysis of depleted uranium levels in the Balkan region. J Environ Radioact 172: 207-217 (2017).
B24 BETAVOLT. The atomic energy battery. Beijing Beta Volt New Energy Co. Ltd.,. [Internet] Available from (https://www.betavolt.tech/cp_531390.html) on 21.02.2024. (Chinese).
B25 Bezuidenhout, J. In situ gamma ray measurements of radionuclides at a disused phosphate mine on the West Coast of South Africa. J Environ Radioact 150: 1-8 (2015).
B26 BfS. Umweltradioaktivität und Strahlenbelastung: Jahresbericht 2015. Bundesministerium für Umwelt, Naturschutz, Bau und Reaktorsicherheit (BMUB), Bonn, 2016. (German).
B27 BfS. Umweltradioaktivität und Strahlenbelastung: Jahresbericht 2020. Bundesministerium für Umwelt, Naturschutz, Bau und Reaktorsicherheit (BMUB), Bonn, 2021. (German).
B28 BfS. Umweltradioaktivität und Strahlenbelastung: Jahresbericht. Bundesamt für Strahlenschutz (BfS). Bundesministerium für Umwelt, Naturschutz, Reaktorsicherheit und Verbraucherschutz (BMUV). [Internet] Available from (https://www.bfs.de/DE/mediathek/expertenwissen/umweltradioaktivitaet/umweltradioaktivitaet_node.html) on 05.03.2024. (German).
B29 Bhaskaran, R., R.C. Damodaran, V.A. Kumar et al. Inhalation dose and source term studies in a tribal area of Wayanad, Kerala, India. J Environ Public Health 2017: 1930787 (2017).
B30 Biblin, A.M., E.V. Khramtsov, V.S. Repin et al. Radiation situation at the "Pirit" peaceful underground nuclear explosion site. Radiat Hygiene 15(4): 149-161 (2022). (Russian).
B31 Binesh, A., S. Mohammadi, A.A. Mowlavi et al. Evaluation of the radiation dose from radon ingestion and inhalation in drinking water sources of Mashhad. Res J Appl Sci 5(3): 221-225 (2010).
B32 Bleise, A., P.R. Danesi and W. Burkart. Properties, use and health effects of depleted uranium (DU): A general overview. J Environ Radioact 64(2-3): 93-112 (2003).
B33 Boev, V.M., E.V. Popova, A.I. Smoliagin et al. Characteristics of the radio-ecologic situation in the area of Totsk nuclear explosion and the immune status of school children residing in the vicinity. Gigiena Sanitariia 1: 47-49 (1998). (Russian).
B34 Bolivar, J.P., J.E. Martin, R. Garcia-Tenorio et al. Behaviour and fluxes of natural radionuclides in the production process of a phosphoric acid plant. Appl Radiat Isot 67(2): 345-356 (2009).
B35 Bolivar, J.P., J.P. Perez-Moreno, J.L. Mas et al. External radiation assessment in a wet phosphoric acid production plant. Appl Radiat Isot 67(10): 1930-1938 (2009).
B36 Bollhöfer, A., B. Ryan, K. Pfitzner et al. A radiation dose estimate for visitors of the South Alligator River Valley, Australia, from remnants of uranium mining and milling activities. Proceedings of the International Conference on Uranium Mining and Hydrogeology III, Freiberg, Germany, 15–21 September 2002. Springer-Verlag Berlin Heidelberg
B37 Bollhöfer, A., K. Pfitzner, B. Ryan et al. Radiological assessment of Rum Jungle Mine, Northern Territory. Australian Government Department of the Environment and Water Resources Supervising Scientist, Darwin, 2007.

B38 Bollhöfer, A., C. Doering, P. Medley et al. Assessment of expected maximum doses from the El Sherana airstrip containment, South Alligator River Valley. Australian Government, Department of Sustainability, Environment, Water, Population and Communities, Darwin, 2013.

B39 Bordner, A.S., D.A. Crosswell, A.O. Katz et al. Measurement of background gamma radiation in the northern Marshall Islands. Proc Natl Acad Sci 113(25): 6833-6838 (2016).

B40 Bossew, P. and H. Lettner. Investigations on indoor radon in Austria, part 1: Seasonality of indoor radon concentration. J Environ Radioact 98(3): 329-345 (2007).

B41 Bossew, P., G. Dubois and T. Tollefsen. Investigations on indoor radon in Austria, part 2: Geological classes as categorical external drift for spatial modelling of the radon potential. J Environ Radioact 99(1): 81-97 (2008).

B42 Bossew, P., F. Gering, E. Petermann et al. An episode of Ru-106 in air over Europe, September-October 2017 - Geographical distribution of inhalation dose over Europe. J Environ Radioact 205-206: 79-92 (2019).

B43 Bossew, P., G. Cinelli, G. Ciotoli et al. Development of a geogenic radon hazard index-concept, history, experiences. Int J Environ Res Public Health 17(11): 4134 (2020).

B44 Bottollier-Depois, J.F., A. Biau, P. Blanchard et al. Assessing exposure to cosmic radiation aboard aircraft: The SIEVERT system. Radioprotection 38(3): 357-366 (2003).

B45 Bouville, A. and W.M. Lowder. Human population exposure to cosmic radiation. Radiat Prot Dosim 24(1-4): 293-299 (1988).

B46 Bouville, A., S.L. Simon, C.W. Miller et al. Estimates of doses from global fallout. Health Phys 82(5): 690-705 (2002).

B47 Bouville, A., H.L. Beck and S.L. Simon. Doses from external irradiation to Marshall Islanders from Bikini and Enewetak nuclear weapons tests. Health Phys 99(2): 143-156 (2010).

B48 Bouville, A., H.L. Beck, K.M. Thiessen et al. The methodology used to assess doses from the first nuclear weapons test (Trinity) to the populations of New Mexico. Health Phys 119(4): 400-427 (2020).

B49 Bouville, A., H.L. Beck, L.R. Anspaugh et al. A methodology for estimating external doses to individuals and populations exposed to radioactive fallout from nuclear detonations. Health Phys 122(1): 54-83 (2022).

B50 Boyer, P., C. Wells and B. Howard. Extended $K(_d)$ distributions for freshwater environment. J Environ Radioact 192: 128-142 (2018).

B51 Brauner, E.V., T.V. Rasmussen and L. Gunnarsen. Variation in residential radon levels in new Danish homes. Indoor Air 23(4): 311-317 (2013).

B52 Brock, K.M., C.M. Neumann, K.A. Higley et al. A dose reconstruction of ^{60}Co-contaminated window frames in a Taiwanese school. Health Phys 81(1): 3-7 (2001).

B53 Brown, A.C. Close linkage of copper (and uranium) transport to diagenetic reddening of "upstream" basin sediments for sediment-hosted stratiform copper (and roll-type uranium) mineralization. J Geochem Expl 89(1): 23-26 (2006).

B54 Brown, J. and J.R. Simmonds. FARMLAND: A dynamic model for the transfer of radionuclides through terrestrial food chains. NRPB-R-273. National Radiological Protection Board, Chilton, 1995.

B55 Brudecki, K., A. Kluczewska-Galka, P. Zagrodzki et al. ^{131}I thyroid activity and committed dose assessment among family members of patients treated with radioactive iodine. Radiat Environ Biophys 59(3): 559-564 (2020).

B56 Bruk, G.J., A.B. Bazykin, A.N. Barkovsky et al. The exposure for populations of the Russian Federation due to the Chernobyl accident and main directions of further work in the coming period. Radiat Hygiene 7(4): 72-83 (2014).

B57 Bu, K., J.V. Cizdziel and D. Dasher. Plutonium concentration and ^{240}Pu/^{239}Pu atom ratio in biota collected from Amchitka Island, Alaska: Recent measurements using ICP-SFMS. J Environ Radioact 124: 29-36 (2013).

B58 Buesseler, K.O., M.A. Charette, S.M. Pike et al. Lingering radioactivity at the Bikini and Enewetak Atolls. Sci Total Environ 621: 1185-1198 (2018).

B59 Burger, J., M. Gochfeld, D.S. Kosson et al. Radionuclides in marine macroalgae from Amchitka and Kiska Islands in the Aleutians: Establishing a baseline for future biomonitoring. J Environ Radioact 91(1-2): 27-40 (2006).

B60 Burger, J. and M. Gochfeld. Metals and radionuclides in birds and eggs from Amchitka and Kiska Islands in the Bering Sea/Pacific Ocean ecosystem. Environ Monit Assess 127(1-3): 105-117 (2007).

B61 Burger, J., M. Gochfeld, D. Kosson et al. Radionuclides in marine fishes and birds from Amchitka and Kiska Islands in the Aleutians: Establishing a baseline. Health Phys 92(3): 265-279 (2007).

B62 Burger, J., M. Gochfeld, C.W. Powers et al. Scientific research, stakeholders and policy: Continuing dialogue during research on radionuclides on Amchitka Island, Alaska. J Environ Manage 85(1): 232-244 (2007).

B63 Burger, J., M. Gochfeld and K. Pletnikoff. Collaboration versus communication: The Department of Energy's Amchitka Island and the Aleut community. J Environ Res 109(4): 503-510 (2009).

B64 Burghele, B.D., M. Botos, S. Beldean-Galea et al. Comprehensive survey on radon mitigation and indoor air quality in energy efficient buildings from Romania. Sci Total Environ 751: 141858 (2021).

C1 Cahoon, E.K., R. Zhang, S.L. Simon et al. Projected cancer risks to residents of New Mexico from exposure to Trinity radioactive fallout. Health Phys 119(4): 478-493 (2020).

C2 Calleja, J.A., F. Gutierrez and C. Colon. Impact from road transport of radioactive wastes in Spain. Proceedings from the 12th International Conference on Environmental Science and Technology, Rhodes, Greece, 8–10 September 2011.

C3 Calvez, M. and P. Fracas. Environmental radioactive monitoring of the CEA research centres in France: Overview and perspectives. Radioprotection 46(6): S723-S729 (2012).

C4 Cardarelli, J., 2nd, L. Elliott, R. Hornung et al. Proposed model for estimating dose to inhabitants of ^{60}Co contaminated buildings. Health Phys 72(3): 351-360 (1997).

C5 Carvalho, F.P., M.J. Madruga, M.C. Reis et al. Radioactivity in the environment around past radium and uranium mining sites of Portugal. J Environ Radioact 96(1-3): 39-46 (2007).

C6 Carvalho, F.P. and J.M. Oliveira. Uranium isotopes in the Balkan's environment and foods following the use of depleted uranium in the war. J Environ Int 36(4): 352-360 (2010).

C7 Carvalho, F.P. and A. Fajgelj. Radioactivity in drinking water: Routine monitoring and emergency response. Water Air Soil Pollut 224(6): 1597 (2013).

C8 Carvalho, F.P., J.M. Oliveira and M. Malta. Preliminary assessment of uranium mining legacy and environmental radioactivity levels in Sabugal region, Portugal. Intl J Ener Environ Eng 7(4): 399-408 (2016).

C9 Casacuberta, N., P. Masqué, J. Garcia-Orellana et al. Incorporation of ^{210}Pb and ^{210}Po to poultry through the addition of dicalcium phosphate (DCP) to the diet. Proceedings from The Natural Radiation Environment: 8th International Symposium (NRE VIII), Rio de Janeiro, Brazil, 7–12 October 2007. AIP Conference Proceedings.

C10 Casacuberta, N., P. Masque and J. Garcia-Orellana. Fluxes of ^{238}U decay series radionuclides in a dicalcium phosphate industrial plant. J Hazard Mater 190(1-3): 245-252 (2011).

C11 Casey, J.A., E.L. Ogburn, S.G. Rasmussen et al. Predictors of indoor radon concentrations in Pennsylvania, 1989-2013. Environ Health Perspect 123(11): 1130-1137 (2015).

C12 Cederwall, R.T. and K.R. Peterson. Meteorological modeling of arrival and deposition of fallout at intermediate distances downwind of the Nevada Test Site. Health Phys 59(5): 593-601 (1990).

C13 CEFAS, FSA, FSS et al. Radioactivity in food and the environment (RIFE) report 2022. Annual assessment report of radioactivity in food and the environment and the public's exposure to radiation. RIFE 28. Centre for Environment,, Fisheries and Aquaculture Science on behalf of the Environment Agency, Food Standards Agency, Food Standards Scotland, Natural Resources Wales, Northern Ireland Environment Agency, Scottish Environment Protection Agency, HMSO, London, 2023.

C14 Celikovic, I., G. Pantelic, I. Vukanac et al. Outdoor radon as a tool to estimate radon priority areas-A literature overview. Int J Environ Res Public Health 19(2): 662 (2022).

C15 CERN. Radiation protection and environment: Annual report 2011. EDMS No. 1269537. Organisation Européenne pour la Recherche Nucléaire, Geneva, 2012.
C16 CERN. Environment report 2019-2020. Organisation Européenne pour la Recherche Nucléaire, Geneva, 2021.
C17 CERN. Environment report 2021-2022. Organisation Européenne pour la Recherche Nucléaire, Geneva, 2023.
C18 Chakraverty, S., B.K. Sahoo, T.D. Rao et al. Modelling uncertainties in the diffusion-advection equation for radon transport in soil using interval arithmetic. J Environ Radioact 182: 165-171 (2018).
C19 Chalupnik, S., B. Michalik, M. Wysocka et al. Contamination of settling ponds and rivers as a result of discharge of radium-bearing waters from Polish coal mines. J Environ Radioact 54(1): 85-98 (2001).
C20 Chen, J., R. Falcomer and B.L. Tracy. Preliminary results of radon measurements in Ottawa homes. Canadian J RespTherapy 43(3): 27-28 (2007).
C21 Chen, J. and V. Mares. Estimate of doses to the fetus during commercial flights. Health Phys 95(4): 407-412 (2008).
C22 Chen, J. A preliminary design of a radon potential map for Canada: a multi-tier approach. Environmental Earth Sciences 59(4): 775-782 (2009).
C23 Chen, J., N.M. Rahman and I. Abu Atiya. Radon exhalation from building materials for decorative use. J Environ Radioact 101(4): 317-322 (2010).
C24 Chen, J. and L. Marro. Assessment of radon equilibrium factor from distribution parameters of simultaneous radon and radon progeny measurements. J Radiat Environ Biophys 50(4): 597-601 (2011).
C25 Chen, J., D. Moir, A. Sorimachi et al. Characteristics of thoron and thoron progeny in Canadian homes. J Radiat Environ Biophys 50(1): 85-89 (2011).
C26 Chen, J., D. Moir and J. Whyte. Canadian population risk of radon induced lung cancer: A re-assessment based on the recent cross-Canada radon survey. Radiat Prot Dosim 152(1-3): 9-13 (2012).
C27 Chen, J. and N.H. Harley. A review of indoor and outdoor radon equilibrium factors-part II: ^{220}Rn. Health Phys 115(4): 500-506 (2018).
C28 Chen, J. A summary of residential radon surveys and the influence of housing characteristics on indoor radon levels in Canada. Health Phys 121(6): 574-580 (2021).
C29 Chen, J. Assessment of thoron contribution to indoor radon exposure in Canada. J Radiat Environ Biophys 61(1): 161-167 (2022).
C30 Chen, S.B., Y.G. Zhu and Q.H. Hu. Soil to plant transfer of ^{238}U, ^{226}Ra and ^{232}Th on a uranium mining-impacted soil from southeastern China. J Environ Radioact 82(2): 223-236 (2005).
C31 Chen, W.L., C.C. Liao, M.T. Wang et al. Preliminary study of dose equivalent evaluation for residents in radioactivity contaminated rebar buildings. Appl Radiat Isot 49(12): 1641-1647 (1998).
C32 Chen, W.L. Radiation surveys and dose equivalent assessments for ^{60}Co-contaminated rebar buildings. Appl Radiat Isot 56(6): 901-906 (2002).
C33 Chen, W.L. and S.H. Yeh. The measurement of ^{60}Co contaminated rebar buildings with thermoluminescence dosemeters. Radiat Prot Dosim 103(3): 235-240 (2003).
C34 China. Fifth National Report for the Seventh review meeting of the Joint Convention on the Safety of Spent Fuel Management and on the Safety of Radioactive Waste Management. Beijing, 2020.
C35 Chitra, N., S. Bala Sundar, I. Inigo Valan et al. Modeling and experiments to estimate radon emanation factor in soil-grain size and moisture effect. Radiat Prot Dosim 194(2-3): 104-112 (2021).
C36 Cho, Y.H. and B.S. Kang. Analysis of the photoneutron activation effects generated by 9 MeV X-ray in a container cargo inspection facility. Radiat Prot Dosim 140(1): 1-8 (2010).
C37 Cinelli, G., B. Capaccioni, M.A. Hernández-Ceballos et al. Radiological risk from thoron, a case study: The particularly radon-prone area of Bolsena, and the lesson learned. Radiat Phys Chem 116: 381-385 (2015).

C38 Cinelli, G., T. Tollefsen, P. Bossew et al. Digital version of the European Atlas of natural radiation. J Environ Radioact 196: 240-252 (2019).
C39 Ciotoli, G., M. Voltaggio, P. Tuccimei et al. Geographically weighted regression and geostatistical techniques to construct the geogenic radon potential map of the Lazio region: A methodological proposal for the European Atlas of Natural Radiation. J Environ Radioact 166(2): 355-375 (2017).
C40 Clairand, I., N. Fuller, J.F. Bottollier-Depois et al. The SIEVERT system for aircrew dosimetry. Radiat Prot Dosim 136(4): 282-285 (2009).
C41 CNEA. Uranium Mining Environmental Restoration Project (PRAMU): Environmental assessment - Executive summary. National Nuclear Energy Commission, 2006.
C42 CNEA. Environmental restitution project: Environmental assessment of Malargüe. National Nuclear Energy Commission, 2008. (Spanish).
C43 CNL. Near surface disposal facility safety case. Safety Assessment Report. Canadian Nuclear Laboratories, Ontario, 2021.
C44 CNSC. Investigation of the environmental fate of tritium in the atmosphere. Tritium Studies Project, INFO-0792. Canadian Nuclear Safety Commission, Ottawa, 2009.
C45 CNSC. Regulatory oversight report for research reactors and Class IB accelerators: 2016–2017. CMD: 18-M32. Canadian Nuclear Safety Commission, Ottawa, 2018.
C46 Collignan, B., C. Lorkowski and R. Améon. Development of a methodology to characterize radon entry in dwellings. Build Environ 57: 176-183 (2012).
C47 Connolly, K.J. and R.B. Pope. A historical review of the safe transport of spent nuclear fuel. Fuel cycle research and development. Oak Ridge National Laboratory. Argonne National Laboratory, Springfield, 2016.
C48 Cook, J.R., D.J. Ammerman, R.F. Weiner et al. Spent fuel transportation risk assessment: Overview. Proceedings from the 17th International Symposium on the Packaging and Transportation of Radioactive Materials (PATRAM 2013), San Francisco, USA, 18–23 August 2013.
C49 Cooper, M.B., L.J. Martin, M.J. Wilks et al. Radiological hazard assessment at the Monte Bello Islands. Technical report ARL/TR096. Australian Radiation Laboratory, Yallambie, 1990.
C50 Copeland, K. CARI documentation: Radiation transport in the atmosphere. Federal Aviation Administration, Oklahoma, 2021.
C51 Corcho-Alvarado, J.A., C. Guavis, P. McGinnity et al. Assessment of residual radionuclide levels at the Bokak and Bikar Atolls in the Northern Marshall Islands. Sci Total Environ 801: 149541 (2021).
C52 Cort, M.D. Atlas of caesium deposition on Europe after the Chernobyl accident. EUR-19801-EN-RU: Office for Official Publications of the European Communities, Luxembourg, 1998.
C53 Cosma, C., A. Cucos-Dinu, B. Papp et al. Soil and building material as main sources of indoor radon in Baita-Stei radon prone area (Romania). J Environ Radioact 116: 174-179 (2013).
C54 Cosma, C., A. Cucoş, B. Papp et al. Radon and remediation measures near Băiţa-Ştei old uranium mine (Romania). Acta Geophysica 61(4): 859-875 (2013).
C55 Cronkite, E.P., R.A. Conard and V.P. Bond. Historical events associated with fallout from Bravo Shot–Operation Castle and 25 Y of medical findings. Health Phys 73(1): 176-186 (1997).
C56 Croymans, T., F. Leonardi, R. Trevisi et al. Gamma exposure from building materials – A dose model with expanded gamma lines from naturally occurring radionuclides applicable in non-standard rooms. Const Build Mater 159: 768-778 (2018).
C57 Csövári, M., Z. Berta, J. Csicsák et al. Remediation on the former uranium mining and processing site in Hungary: Case study. DIFPOLMINE Conference, Budapest, Hungary, 4–8 July 2005.
C58 CTBTO. Annual report 2006. CTBT/PC-28/INF.1, 2. Provisional Technical Secretariat of the Preparatory Commission for the Comprehensive Nuclear-Test-Ban Treaty Organization, Vienna, 2007.
C59 CTBTO. Annual report 2009. CTBT/ES/2009/7. Provisional Technical Secretariat of the Preparatory Commission for the Comprehensive Nuclear-Test-Ban Treaty Organization, Vienna, 2010.

C60 CTBTO. Annual report 2013. CTBT/ES/2013/5. Provisional Technical Secretariat of the Preparatory Commission for the Comprehensive Nuclear-Test-Ban Treaty Organization, Vienna, 2014.

C61 CTBTO. Annual report 2016. CTBT/ES/2016/5. Provisional Technical Secretariat of the Preparatory Commission for the Comprehensive Nuclear-Test-Ban Treaty Organization, Vienna, 2017.

C62 CTBTO. Annual report 2017. CTBT/ES/2017/5, Corr.1. Provisional Technical Secretariat of the Preparatory Commission for the Comprehensive Nuclear-Test-Ban Treaty Organization, Vienna, 2018.

C63 CTBTO. Radionuclide data from the International Monitoring System, Virtual data exploitation centre. Preparatory Commission for the Comprehensive Nuclear-Test-Ban Treaty Organization, Vienna, 2023.

C64 Cuculeanu, V., F. Simion, E. Simion et al. Dynamics, deterministic nature and correlations of outdoor ^{222}Rn and ^{220}Rn progeny concentrations measured at Bacau, Romania. J Environ Radioact 102(7): 703-712 (2011).

C65 Cullings, H.M., E.J. Grant, S.D. Egbert et al. DS02R1: Improvements to atomic bomb survivors' input data and implementation of dosimetry system 2002 (DS02) and resulting changes in estimated doses. Health Phys 112(1): 56-97 (2017).

C66 Curguz, Z., Z. Stojanovska, Z.S. Zunic et al. Long-term measurements of radon, thoron and their airborne progeny in 25 schools in Republic of Srpska. J Environ Radioact 148: 163-169 (2015).

C67 Czarwinski, R., R. Lehman and R. Rönsch. Radon in Eastern German houses - Surveys and outcomes. Radiat Prot Dosim 56(1-6): 281-286 (1994).

D1 Dabbebi, R., P. Perumal and S. Moukannaa. Management and valorization of phosphate beneficiation slime: A critical review. Intl J Environ Sci Technol 20(10): 11763-11776 (2023).

D2 Daniels, J.I. and J.B. Chapman. Determination and maintenance of DE minimize risk for migration of residual tritium (^{3}H) from the 1969 Project Rulison nuclear test to nearby hydraulically fractured natural gas wells. Health Phys 104(5): 517-531 (2013).

D3 Daraktchieva, Z., J.M. Wasikiewicz, C.B. Howarth et al. Study of baseline radon levels in the context of a shale gas development. Sci Total Environ 753: 141952 (2021).

D4 Dasher, D., W. Hanson, S. Read et al. An assessment of the reported leakage of anthropogenic radionuclides from the underground nuclear test sites at Amchitka Island, Alaska, USA to the surface environment. J Environ Radioact 60(1-2): 165-187 (2002).

D5 Dauer, L.T., M.A. Kollmeier, M.J. Williamson et al. Less-restrictive, patient-specific radiation safety precautions can be safely prescribed after permanent seed implantation. Brachytherapy 9(2): 101-111 (2010).

D6 De Carvalho, J.W., M. Sapienza, C. Ono et al. Could the treatment of differentiated thyroid carcinoma with 3.7 and 5.55 GBq of (^{131}I)NaI, on an outpatient basis, be safe? Nucl Med Commun 30(7): 533-541 (2009).

D7 De With, G. and P. de Jong. CFD modelling of thoron and thoron progeny in the indoor environment. Radiat Prot Dosim 145(2-3): 138-144 (2011).

D8 De With, G., P. de Jong and A. Rottger. Measurement of thoron exhalation rates from building materials. Health Phys 107(3): 206-212 (2014).

D9 De With, G., R. Smetsers, H. Slaper et al. Thoron exposure in Dutch dwellings - An overview. J Environ Radioact 183: 73-81 (2018).

D10 DECC, Welsh Government, DOE et al. Strategy for the management of Naturally Occurring Radioactive Material (NORM) waste in the United Kingdom. UK NORM Waste Strategy. Department of Energy & Climate Change, Welsh Government, Northern Ireland Department of the Environment, The Scottish Government, Edinburgh, 2014.

D11 Degteva, M.O., N.B. Shagina, M.I. Vorobiova et al. Re-evaluation of waterborne releases of radioactive materials from the Mayak Production Association into the Techa River in 1949-1951. Health Phys 102(1): 25-38 (2012).

D12 Degteva, M.O., N.B. Shagina, M.I. Vorobeva et al. Contemporary understanding of radioactive contamination of the Techa River in 1949-1956. Radiats Biol Radioecol 56(5): 523-534 (2016). (Russian).

D13 Degteva, M.O., E.I. Tolstykh, K.G. Suslova et al. Analysis of the results of long-lived radionuclide body burden monitoring in residents of the Urals Region. Radiat Hygiene 11(3): 30-39 (2018). (Russian).

D14 Degteva, M.O., B.A. Napier, E.I. Tolstykh et al. Enhancements in the Techa River Dosimetry System: TRDS-2016D code for reconstruction of deterministic estimates of dose from environmental exposures. Health Phys 117(4): 378-387 (2019).

D15 Delbridge, B.G., J.D. Carmichael, W.S. Phillips et al. Source characterization of the declared North Korean nuclear tests from regional distance coda wave spectral ratios. J Geophys Res Solid Earth 128(3): e2022JB024728 (2023).

D16 Demoury, C., G. Ielsch, D. Hemon et al. A statistical evaluation of the influence of housing characteristics and geogenic radon potential on indoor radon concentrations in France. J Environ Radioact 126: 216-225 (2013).

D17 Denman, A.R., R.G.M. Crockett and C.J. Groves-Kirkby. An assessment of the effectiveness of UK building regulations for new homes in radon affected areas. J Environ Radioact 192: 166-171 (2018).

D18 Desorgher, L., A. Berthet, J. Rossier et al. Dosimetry in the lungs of alpha-particles (^{210}Po) and beta-particles (^{210}Pb) present in the tobacco smoke of conventional cigarettes and heated tobacco products. J Environ Radioact 263: 107178 (2023).

D19 Di Carlo, C., M. Ampollini, S. Antignani et al. Extreme reverse seasonal variations of indoor radon concentration and possible implications on some measurement protocols and remedial strategies. Environ Pollut 327: 121480 (2023).

D20 Dolchinkov, N.T. and T.A. Paramonova. Overview and analysis of the development of uranium mining in the Republic of Bulgaria. Int Sci J Science Business Society 4(2): 69-72 (2019).

D21 Domingos, F.P., S.L.R. Sêco and A.J.S.C. Pereira. Thoron and radon exhalation and emanation from granitic rocks outcropping in the Central Iberian Zone (Portugal). Environ Earth Sci 80(22): 753 (2021).

D22 Dowdall, A., P. Murphy, D. Pollard et al. Update of Ireland's national average indoor radon concentration - Application of a new survey protocol. J Environ Radioact 169-170: 1-8 (2017).

D23 Drozdovitch, V., V. Minenko, V. Khrouch et al. Thyroid dose estimates for a cohort of Belarusian children exposed to radiation from the Chernobyl accident. Radiat Res 179(5): 597-609 (2013).

D24 Drozdovitch, V., A. Kesminiene, M. Moissonnier et al. Uncertainties in radiation doses for a case-control study of thyroid cancer among persons exposed in childhood to ^{131}I from Chernobyl fallout. Health Phys 119(2): 222-235 (2020).

D25 Drozdovitch, V. Radiation exposure to the thyroid after the Chernobyl accident. Front Endocrinol 11: 569041 (2021).

D26 Drozdovitch, V., A. Bouville, M. Taquet et al. Thyroid doses to French Polynesians resulting from atmospheric nuclear weapons tests: Estimates based on radiation measurements and population lifestyle data. Health Phys 120(1): 34-55 (2021).

D27 Drozdovitch, V., F. de Vathaire and A. Bouville. Radiological impact of atmospheric nuclear weapons tests at Mururoa and Fangataufa Atolls to populations in Oceania, South America and Africa: Comparison with French Polynesia. Asian Pac J Cancer Prev 22(3): 801-809 (2021).

D28 DTRA. Defense's Nuclear Agency 1947-1997. DTRA History Series. Defense Threat Reduction Agency, U.S. Department of Defense, Washington, DC, 2002.

D29 Du, L., V. Leivo, T. Prasauskas et al. Effects of energy retrofits on indoor air quality in multifamily buildings. Indoor Air 29(4): 686-697 (2019).

D30 Ducros, L., F. Eyrolle, C.D. Vedova et al. Tritium in river waters from French Mediterranean catchments: Background levels and variability. Sci Total Environ 612: 672-682 (2018).

D31 Dudar, T. Uranium mining and milling facilities legacy sites: Ukraine case-study. Environ Problems 4(4): 212-218 (2019).

D32 Dueñas, C., E. Liger, S. Canete et al. Exhalation of ^{222}Rn from phosphogypsum piles located at the Southwest of Spain. J Environ Radioact 95(2-3): 63-74 (2007).

D33 DVGW. Radionuklidhaltige Rückstände aus der Aufbereitung von Grundwasser - Bewertung und Entsorgung. Technische Regel - Arbeitsblatt. DVGW W 256 (A). Deutscher Verein des Gas- und Wasserfaches e.V. Technisch-wissenschaftlicher Verein, Bonn, 2020. (German).

E1 EarthChem. EarthChem Portal. Lamont-Doherty Earth Observatory, Columbia University. [Internet] Available from (http://portal.earthchem.org/) on 01.01.2024.

E2 EC. Review of CEC radon research. Doc. No. EUR-17628 European Commission, Luxembourg, 1997.

E3 EC. Verifications under the terms of article 35 of the EURATOM treaty, Germany. Technical Report DE-07/05. European Commission Directorate-General for Energy, Brussels, 2007.

E4 EC. Guidelines for the regulatory control of consumer products containing radioactive substances in the European Union. Report No. 147. Radiation Protection. Directorate-General for Energy and Transport, European Commission Publications Office, Luxembourg, 2007.

E5 EC. Uranium mining and processing and national monitoring networks, Romania. Verifications under the terms of article 35 of the EURATOM treaty. Technical Report RO-08/06. European Commission Directorate-General for Energy, Brussels, 2008.

E6 EC. Uranium sites: Environmental radioactivity and discharge monitoring, Bulgaria. Verifications under the terms of article 35 of the EURATOM treaty. Technical Report BG-09/07. European Commission Directorate-General for Energy, Brussels, 2009.

E7 EC. Plutonium contaminated sites in the Palomares region, Spain. . Verifications under the terms of article 35 of the EURATOM treaty. Technical Report ES-10/01. European Commission Directorate-General for Energy, Brussels, 2010.

E8 EC. Opinion on the environmental and health risks posed by depleted uranium. European Commission Directorate-General for Health and Consumers, European Commission Publications Office, Brussels, 2010.

E9 EC. Uranium sites: Environmental radioactivity and discharge monitoring and part of national monitoring system for environmental radioactivity, Czech Republic. Verifications under the terms of article 35 of the EURATOM treaty. Technical Report CZ-10/07. European Commission Directorate-General for Energy, Brussels, 2010.

E10 EC. Uranium sites: Environmental radioactivity and discharge monitoring and part of national monitoring system for environmental radioactivity, Portugal. Verifications under the terms of article 35 of the EURATOM treaty. Technical Report PT-11/01. European Commission Directorate-General for Energy, Brussels, 2011.

E11 EC. Commission Staff Working Paper–Situation concerning uranium mine and mill tailings in the European Union. Report No. ATO 13 7721/11. Council of the European Union, European Commission, Brussels, 2011.

E12 EC. Monitoring of environmental radioactivity of former uranium mining and milling sites and national monitoring network for environmental radioactivity, Slovenia. Verifications under the terms of article 35 of the EURATOM treaty. Technical Report SI-11/02. European Commission Directorate-General for Energy, Brussels, 2011.

E13 EC. Uranium sites: Environmental radioactivity and discharge monitoring, Bulgaria. Verifications under the terms of article 35 of the EURATOM treaty. Technical Report BG-11/04. European Commission Directorate-General for Energy, Brussels, 2011.

E14 EC. Southern and western Spain – former uranium installations and national monitoring, Spain. Verifications under the terms of article 35 of the EURATOM treaty. Technical Report ES-12/06. European Commission Directorate-General for Energy, Brussels, 2012.

E15 EC. Verifications under the terms of article 35 of the EURATOM treaty, Poland. Technical Report PL-12/03. European Commission Directorate-General for Energy, Brussels, 2012.

E16 EC. Health effects of security scanners for passenger screening (based on X-ray technology). Scientific Committee on Emerging and Newly Identified Health Risks. European Commission, Brussels, 2012.

E17 EC. Report from the Commission to the European Parliament, the Council and the European Economic and Social Committee on Member States implementation of the Council Directive 2006/117/EURATOM on the supervision and control of shipments of radioactive waste and spent fuels. COM(2013) 240 final. European Commission, Brussels, 2013.

E18 EC. Commission Implementing Regulation (EU) 2015/1998 of 5 November 2015 laying down detailed measures for the implementation of the common basic standards on aviation security. Official Journal of the European Union (L 299/1): 1-142 (2015).

E19 EC. Report from the Commission to the European Parliament, the Council and the European Economic and Social Committee on Member States implementation of the Council Directive 2006/117/EURATOM on the supervision and control of shipments of radioactive waste and spent fuel. Second report. COM(2018) 6 final. European Commission, Brussels, 2018.

E20 EC. Report from the Commission to the European Parliament, the Council and the European Economic and Social Committee on Member States implementation of the Council Directive 2006/117/EURATOM on the supervision and control of shipments of radioactive waste and spent fuel. Third report. SWD(2019) 437 final. European Commission, Brussels, 2019.

E21 EC. Strategic agenda for medical ionising radiation applications (SAMIRA). SWD(2021) 14 final. Commission staff working document. European Commission, Brussels, 2021.

E22 EC. Report from the Commission to the European Parliament, the Council and the European Economic and Social Committee on Member States implementation of the Council Directive 2006/117 EURATOM on the supervision and control of shipments of radioactive waste and spent fuel. Fourth report. COM(2023) 43 final. European Commission, Brussels, 2023.

E23 Egorov, N., V.M. Novikov, F.L. Parker et al. The Radiation Legacy of the Soviet Nuclear Complex: An Analytical Overview. 1st edition. Routledge, London, 2000.

E24 Elío, J., G. Cinelli, P. Bossew et al. The first version of the Pan-European indoor radon map. Nat Hazards Earth Syst Sci 19(11): 2451-2464 (2019).

E25 Enamorado, S., J.M. Abril, J.L. Mas et al. Transfer of Cd, Pb, Ra and U from phosphogypsum amended soils to tomato plants. Water Air Soil Pollut 203(1): 65-77 (2009).

E26 Enamorado, S., J.M. Abril, A. Delgado et al. Implications for food safety of the uptake by tomato of 25 trace-elements from a phosphogypsum amended soil from SW Spain. J Hazard Mater 266: 122-131 (2014).

E27 Encyclopaedia Britannica. Nuclear reactor. [Internet] Available from (https://www.britannica.com/technology/nuclear-reactor) on 01.12.2023.

E28 Energy Research and Development Administration. Final tabulation of monthly ^{90}Sr fallout data: 1954-1976. HASL-329. Health and Safety Laboratory, New York, 1977.

E29 Epp, T. and C. Waldner. Occupational health hazards in veterinary medicine: Physical, psychological, and chemical hazards. Can Vet J 53(2): 151-157 (2012).

E30 Epstein, L., J. Koch, T. Riemer et al. Radon concentrations in different types of dwellings in Israel. Radiat Prot Dosim 162(4): 605-608 (2014).

E31 Esdale, D., D.F. Pridmore, J. Coggon et al. The Olympic Dam copper-uranium-gold-silver-rare earth element deposit, South Australia: A geophysical case history. ASEG Exten Abst 2003(3): 147-168 (2003).

F1 Falck, W.E. The long-term safety of uranium mine and mill tailing legacies in an enlarged EU. Report No. 49047. JRC Scientific and Technical Reports. JRC European Commission, Petten, 2008.

F2 Faller, S.H. Residual soil radioactivity at the Gnome test site in Eddy County, New Mexico, Environmental Monitoring Systems Laboratory, Las Vegas, 1994.

F3 Favot, M. and A. Massarutto. Rare-earth elements in the circular economy: The case of yttrium. J Environ Manage 240: 504-510 (2019).

F4 Fernandez, S.Q., A.A. Oudalova, T.V. Melinkova et al. Environmental impact of the Research Institute of Physical Chemistry in Obninsk on soils of the nearby territory. J Phys Conf Ser 1701: 12-21 (2020).

F5 Ferreira, A., Z. Daraktchieva, D. Beamish et al. Indoor radon measurements in south-west England explained by top soil and stream sediment geochemistry, airborne gamma-ray spectroscopy and geology. J Environ Radioact 181: 152-171 (2018).

F6 FHMS. Report of the Fukushima Health Management Survey. Radiation Medical Science Center Fukushima Medical University, Fukushima, 2022. (Japanese).

F7 Fijalkowska-Lichwa, L. Extremely high radon activity concentration in two adits of the abandoned uranium mine 'Podgorze' in Kowary (Sudety Mts., Poland). J Environ Radioact 165: 13-23 (2016).

F8 Finland. 7th Finnish National Report as referred to in Article 32 of the Convention. STUK-B 259. Joint Convention on the Safety of Spent Fuel Management and on the Safety of Radioactive Waste Management. Radiation and Nuclear Safety Authority, Helsinki, 2020.

F9 Finne, I.E., T. Kolstad, M. Larsson et al. Significant reduction in indoor radon in newly built houses. J Environ Radioact 196: 259-263 (2019).

F10 Florea, N. and O.G. Duliu. Eighteen years of continuous observation of radon and thoron progenies atmospheric activity. J Environ Radioact 104: 14-23 (2012).

F11 Francisco, P.W., S. Gloss, J. Wilson et al. Radon and moisture impacts from interventions integrated with housing energy retrofits. Indoor Air 30(1): 147-155 (2020).

F12 Frantellizzi, V., L. Cosma, G. Brunotti et al. Targeted alpha therapy with thorium-227. Cancer Biother Radiopharm 35(6): 437-445 (2020).

F13 Frasch, G., L. Kammerer, R. Karofsky et al. Radiation exposure of German aircraft crews under the impact of solar cycle 23 and airline business factors. Health Phys 107(6): 542-554 (2014).

F14 Fronka, A. Indoor and soil gas radon simultaneous measurements for the purpose of detail analysis of radon entry pathways into houses. Radiat Prot Dosim 145(2-3): 117-122 (2011).

F15 Frutos-Puerto, S., E. Pinilla-Gil, E. Andrade et al. Radon and thoron exhalation rate, emanation factor and radioactivity risks of building materials of the Iberian Peninsula. Peer J 8: 10331 (2020).

F16 Frutos, B., F. Martín-Consuegra, C. Alonso et al. Inner wall filler as a singular and significant source of indoor radon pollution in heritage buildings: An exhalation method-based approach. Build Environ 201: 108005 (2021).

F17 Fuente, M., D. Rabago, J. Goggins et al. Radon mitigation by soil depressurisation case study: Radon concentration and pressure field extension monitoring in a pilot house in Spain. Sci Total Environ 695: 133746 (2019).

G1 Gabriel, S., B. Farman-Ara, M. Bourrelly et al. Radiation doses to co-habitants of patients undergoing radioiodine ablation for thyroid cancer: Poor compliance with radiation protection guidelines but low radiation exposure. Nucl Med Comm 32(9): 829-833 (2011).

G2 Gains, J.E., C. Walker, T.M. Sullivan et al. Radiation exposure to comforters and carers during paediatric molecular radiotherapy. Pediatr Blood Cancer 62(2): 235-239 (2015).

G3 Gammage, R.B., C.S. Dudney, D.L. Wilson et al. Sub-terranean transport of radon and elevated indoor radon in hilly karst terrains. Atmos Environ 26(12): 2237-2246 (1992).

G4 Garcia-Talavera, M., J.L. Matarranz, M. Martinez et al. Natural ionizing radiation exposure of the Spanish population. Radiat Prot Dosim 124(4): 353-359 (2007).

G5 García-Tenorio, R. ^{210}Po and ^{210}Pb in NORM mineral processing industries. EU-NORM 1st International Symposium Tallinn, Estonia, 5–8 June 2012.

G6 Garland, J.A. and R. Wakeford. Atmospheric emissions from the Windscale accident of October 1957. Atmos Environ 41(18): 3904-3920 (2007).

G7 Gaskin, J., J. Whyte, L.G. Zhou et al. Regional cost effectiveness analyses for increasing radon protection strategies in housing in Canada. J Environ Radioact 240: 106752 (2021).

G8 Gázquez, M., J. Bolívar, R. Garcia-Tenorio et al. A review of the production cycle of titanium dioxide pigment. Mater Sci Applications 5(7): 441-458 (2014).

G9 Gebrehiwet, R., D. Xiaohua, L. Zhonghua et al. Environmental impact of phosphate mining and beneficiation: review. Intl J Hydrol 2(4): 424-431 (2018).

G10 Gerber, C.R., R. Hamburger and E.W.S. Hull. Plowshare. Division of Technical Information, U.S. Atomic Energy Commission, 1967.

G11 Germany. Report of the Federal Government for the Seventh review meeting of the Joint Convention on the Safety of Spent Fuel Management and on the Safety of Radioactive Waste Management. Federal Ministry for the Environment, Nature Conservation and Nuclear Safety, Bonn, 2020.

G12 Gierl, S., O. Meisenberg, P. Feistenauer et al. Thoron and thoron progeny measurements in German clay houses. Radiat Prot Dosim 160(1-3): 160-163 (2014).

G13 Gil-Pacheco, E., J.A. Suárez-Navarro, S.M. Sánchez-González et al. A radiological index for evaluating the impact of an abandoned uranium mining area in Salamanca, Western Spain. Environ Pollut 258: 113825 (2020).
G14 Giri, A. and D. Pant. Inhalation dose due to Rn-222, Rn-220 and their progeny in indoor environments. Appl Radiat Isot 132: 116-121 (2018).
G15 Gomes, R.S., J.D.A. Gomes, M.L.L. Costa et al. Dose to drivers during drive-through cargo scanning using GEANT4 Monte Carlo simulation. Proceedings from the International Nuclear Atlantic Conference (INAC 2013), Recife, Brazil, 24–29 November 2013. Associacao Brasileira de Energia Nuclear (ABEN).
G16 Gorsky, G.A. On the necessity- of radiation survey of the buildings after the construction, repair, or reconstruction. Radiat Hygiene 3(1): 28–32 (2010).
G17 Gössling, S. and A. Humpe. The global scale, distribution and growth of aviation: Implications for climate change. Glob Environ Change 65: 102194 (2020).
G18 Griffiths, A.D., W. Zahorowski, A. Element et al. A map of radon flux at the Australian land surface. Atmos Chem Phys 10(18): 8969-8982 (2010).
G19 Grigor'ev, N.A. Average concentrations of chemical elements in rocks of the upper continental crust. Geochem Intl 41(7): 711-718 (2003).
G20 Grigoriev, A.G. and A. Katashev. RTG Disposal Program in Russia - Status of RTG decommissioning activities. Proceedings from the 26th IAEA Contact Expert Group Plenary Meeting, Paris, France, 18–19 October 2012.
G21 Grigsby, P.W., B.A. Siegel, S. Baker et al. Radiation exposure from outpatient radioactive iodine (^{131}I) therapy for thyroid carcinoma. J Am Med Assoc 283: 2272-2274 (2000).
G22 Grosche, B., D.T. Lackland, C.E. Land et al. Mortality from cardiovascular diseases in the Semipalatinsk historical cohort, 1960-1999, and its relationship to radiation exposure. Radiat Res 176(5): 660-669 (2011).
G23 Groves-Kirkby, C.J., A.R. Denman, P.S. Phillips et al. Radon mitigation in domestic properties and its health implications-a comparison between during-construction and post-construction radon reduction. Environ Int 32(4): 435-443 (2006).
G24 Groves-Kirkby, C.J., A.R. Denman, P.S. Phillips et al. Domestic radon remediation of UK dwellings by sub-slab depressurisation: Evidence for a baseline contribution from constructional materials. Environ Int 34(3): 428-436 (2008).
G25 Gruber, V., S. Baumann, G. Wurm et al. The new Austrian indoor radon survey (ONRAP 2, 2013-2019): Design, implementation, results. J Environ Radioact 233: 106618 (2021).
G26 Gründel, M., B. Kopka and R. Schulz. ^{131}I exhalation by patients undergoing therapy of thyroid diseases. Radiat Prot Dosim 129(4): 435-438 (2008).
G27 Guerrero, J.L., I. Gutiérrez-Álvarez, F. Mosqueda et al. Pollution evaluation on the salt-marshes under the phosphogypsum stacks of Huelva due to deep leachates. Chemosphere 230: 219-229 (2019).
G28 Guerrero, J.L., I. Gutiérrez-Álvarez, F. Mosqueda et al. Evaluation of the radioactive pollution in the salt-marshes under a phosphogypsum stack system. Environ Pollut 258: 113729 (2020).
G29 Gunning, G.A., D. Pollard and E.C. Finch. An outdoor radon survey and minimizing the uncertainties in low level measurements using CR-39 detectors. J Radiol Prot 34(2): 457-467 (2014).
G30 Gusyev, M.A., U. Morgenstern, T. Nishihara et al. Evaluating anthropogenic and environmental tritium effects using precipitation and Hokkaido snowpack at selected coastal locations in Asia. Sci Total Environ 659: 1307-1321 (2019).
G31 Gwynn, J.P., H.E. Heldal, J.K. Flo et al. Norwegian monitoring (1990-2015) of the marine environment around the sunken nuclear submarine Komsomolets. J Environ Radioact 182: 52-62 (2018).
H1 Haanes, H., I.E. Finne, T. Kolstad et al. Outdoor thoron and progeny in a thorium rich area with old decommissioned mines and waste rock. J Environ Radioact 162-163: 23-32 (2016).
H2 Haanes, H., I.E. Finne, H.K. Skjerdal et al. Indoor and outdoor exposure to radon, thoron and thoron decay products in a NORM area with highly elevated bedrock thorium and legacy mines. Radiat Res 192(4): 431-439 (2019).

H3 Haanes, H., T. Kolstad, I.E. Finne et al. The effect of new building regulations on indoor radon in radonprone municipalities. J Euro Radon Assoc 3: (2022).
H4 Habib, R.R., R.Y. Nuwayhid, Z. Hamdan et al. Indoor and outdoor radon concentration levels in Lebanon. Health Phys 115(3): 344-353 (2018).
H5 Hacker, B.C. Fallout from Plowshare: Peaceful nuclear explosions and the environment, 1956-1973. Conference Paper from the Annual Meeting of the Organization of American Historians, Washington, DC, 7–10 April 2010. Lawrence Livermore National Laboratory.
H6 Hamilton, T. Radiation Fallout-Guam. Report No. UCRL-TR-204361. University of California, Lawrence Livermore National Laboratory, Livermore, 2001.
H7 Hansen, W.R. and J.C. Rodgers. Radiological survey and evaluation of the fallout area from the Trinity test: Chupadera Mesa and White Sands Missile Range, New Mexico. Report No. LA-10256-MS. Los Alamos National Laboratory, Los Alamos, 1985.
H8 Harley, J.H., N.A. Hallden and L.D. Ong. Summary of gummed film results through December, 1959. HASL Report 93. U.S. Atomic Energy Commission, 1960.
H9 Harley, N., P. Chittaporn, R. Medora et al. Measurement of the indoor and outdoor ^{220}Rn (thoron) equilibrium factor: application to lung dose. Radiat Prot Dosim 141(4): 357-362 (2010).
H10 Harrison, J., T. Fell, R. Leggett et al. The polonium-210 poisoning of Mr Alexander Litvinenko. J Radiol Prot 37(1): 266-278 (2017).
H11 Harrison, J., T. Smith, T. Fell et al. Collateral contamination concomitant to the polonium-210 poisoning of Mr Alexander Litvinenko. J Radiol Prot 37(4): 837-851 (2017).
H12 Harvey, M.P., A.L. Jones, T. Cabianca et al. Survey into the radiological impact of the normal transport of radioactive material by air. Report No. PHE-CRCE-006. Public Health England, Chilton, 2014.
H13 Hassan, H.J., S. Hashim, M.S.M. Sanusi et al. The radioactivity of thorium incandescent gas lantern mantles. Appl Sci 11(3): 1311 (2021).
H14 Hassan, N.M., M. Hosoda, T. Ishikawa et al. ^{222}Rn exhalation rate from Egyptian building materials using active and passive methods. Jpn J Health Phys 44(1): 106-111 (2009).
H15 Hassan, N.M., M. Hosoda, K. Iwaoka et al. Simultaneous measurement of radon and thoron released from building materials used in Japan. Prog Nucl Sci Technol 1: 404-407 (2011).
H16 Hassan, N.M., T. Ishikawa, M. Hosoda et al. The effect of water content on the radon emanation coefficient for some building materials used in Japan. Radiat Meas 46(2): 232-237 (2011).
H17 Hazou, E. and T.E. Patchali. Assessment of radiological hazards in the phosphate mining area of Kpogamé, Togo. Case Studies Chem Environ Eng 3: 100077 (2021).
H18 Hentati, O., N. Abrantes, A.L. Caetano et al. Phosphogypsum as a soil fertilizer: Ecotoxicity of amended soil and elutriates to bacteria, invertebrates, algae and plants. J Hazard Mater 294: 80-89 (2015).
H19 Hernandez-Ceballos, M.A., A. Vargas, D. Arnold et al. The role of mesoscale meteorology in modulating the ^{222}Rn concentrations in Huelva (Spain)-impact of phosphogypsum piles. J Environ Radioact 145: 1-9 (2015).
H20 HICARE. Effects of A-bomb radiation on the human body Hiroshima International Council for the Health Care of the Radiation-Exposed, Hiroshima, 2012. (Japanese).
H21 Hodgson, S.A., H. Fonseca, D.M. Rees et al. Performance of basic radon protection in new homes. Report No. PHE-CRCE-046. Public Health England, Chilton, 2019.
H22 Hoffman, I., B. Lewis, P. Chan et al. Analysis of (22)Na using a spectral summation technique on high-volume aerosol samples. J Environ Radioact 169-170: 151-158 (2017).
H23 Hoffman, I., B. Lewis and P. Chan. Circulation of cosmogenic (22)Na using the global monitoring network of the Comprehensive Nuclear-Test-Ban Treaty Organization. J Environ Radioact 187: 8-15 (2018).
H24 Høibråten, S., P.E. Thoresen and A. Haugan. The sunken nuclear submarine Komsomolets and its effects on the environment. Sci Total Environ 202(1-3): 67-78 (1997).
H25 Holloway, D. Stalin and the Bomb: The Soviet Union and Atomic Energy 1939-1956. Yale University Press, Pennsylvania, 1994.
H26 Hoq, M.A., M.A.M. Soner, A. Rahman et al. Estimation of ^{41}Ar activity concentration and release rate from the TRIGA Mark-II research reactor. J Environ Radioact 153: 68-72 (2016).

H27 Hosoda, M., M. Shimo, M. Sugino et al. Effect of soil moisture content on radon and thoron exhalation. J Nucl Sci Technol 44(4): 664-672 (2007).
H28 Hosoda, M., A. Sorimachi, Y. Yasuoka et al. Simultaneous measurements of radon and thoron exhalation rates and comparison with values calculated by UNSCEAR equation. J Radiat Res 50(4): 333-343 (2009).
H29 Hosoda, M., S. Tokonami, A. Sorimachi et al. Influence of soil environmental parameters on thoron exhalation rate. Radiat Prot Dosim 141(4): 420-423 (2010).
H30 Hosoda, M., H. Kudo, K. Iwaoka et al. Characteristic of thoron ^{220}Rn in environment. Appl Radiat Isot 120: 7-10 (2017).
H31 Hosoda, M., E.D. Nugraha, N. Akata et al. A unique high natural background radiation area - Dose assessment and perspectives. Sci Total Environ 750: 142346 (2021).
H32 Hosono, M., H. Ikebuchi, Y. Nakamura et al. Introduction of the targeted alpha therapy (with Radium-223) into clinical practice in Japan: learnings and implementation. Annals Nucl Med 33(3): 211-221 (2019).
H33 Howard, J.E., A. Vaswani and P. Heotis. Thyroid disease among the Rongelap and Utirik population-An update. Health Phys 73(1): 190-198 (1997).
H34 HPA. The methodology for assessing the radiological consequences of routine releases of radionuclides to the environment used in PC-CREAM 08. Report No. HPA-RPD-058. Health Protection Agency, Chilton, 2009.
H35 HSS. Use of tungsten welding rods containing thorium, Safety Bulletin 2007-04. Office of Health, Safety and Security, Washington, D.C., 2007.
H36 Hsu, F.Y., H.Y. Tsai, C.Y. Hsu et al. Dose reconstruction for residents living in buildings with moderate and minor ^{60}Co contamination in rebar. Health Phys 85(3): 357-364 (2003).
H37 Hu, J., Y. Wu, M.A. Saputra et al. Radiation exposure due to ^{222}Rn, ^{220}Rn and their progenies in three metropolises in China and Japan with different air quality levels. J Environ Radioact 106830: 244-245 (2022).
H38 Hu, N., D. Ding, G. Li et al. Vegetation composition and ^{226}Ra uptake by native plant species at a uranium mill tailings impoundment in South China. J Environ Radioact 129: 100-106 (2014).
H39 Hua, Q., J.C. Turnbull, G.M. Santos et al. Atmospheric radiocarbon for the period 1950–2019. Radiocarbon 64(4): 723-745 (2022).
H40 Hughes, E.W., M.R. Molina, M. Abella et al. Radiation maps of ocean sediment from the Castle Bravo crater. PNAS 116(31): 15420-15424 (2019).
H41 Hughes, J.S. and M.P. Harvey. Survey into the radiological impact of the normal transport of radioactive material by sea. Report No. HPA-RPD-050. Health Protection Agency, Chilton, 2009.
H42 Hunter, N., C.B. Howarth, J.C.H. Miles et al. Year-to-year variations in radon levels in a sample of UK houses with the same occupants. Radioact Environ 7: 438-447 (2005).
H43 Hunter, N., C.R. Muirhead, J.C. Miles et al. Uncertainties in radon related to house-specific factors and proximity to geological boundaries in England. Radiat Prot Dosim 136(1): 17-22 (2009).
H44 Hwang, J.S., C.C. Chan, J.D. Wang et al. Radiation exposure modeling for apartment living spaces with multiple radioactive sources. Health Phys 74(3): 379-386 (1998).
I1 IAEA. The radiological accident in Goiânia. International Atomic Energy Agency, Vienna, 1988.
I2 IAEA. Planning for environmental restoration of uranium mining and milling sites in central and eastern Europe. IAEA-TECDOC-982. International Atomic Energy Agency, Vienna, 1997.
I3 IAEA. The radiological situation at the Atolls of Mururoa and Fangataufa. Main Report. Radiological Assessment Reports Series. International Atomic Energy Agency, Vienna, 1998.
I4 IAEA. Radiological conditions at Bikini Atoll: Prospects for resettlement. Radiological Assessment Reports Series. International Atomic Energy Agency, Vienna, 1998.
I5 IAEA. Radiological conditions at the Semipalatinsk test site, Kazakhstan: Preliminary assessment and recommendations for further study. Radiological Assessment Reports Series. International Atomic Energy Agency, Vienna, 1998.

I6 IAEA. Radiological accident in reprocessing plant at Tomsk. International Atomic Energy Agency, Vienna, 1998.
I7 IAEA. Report on the preliminary fact-finding mission following the accident at the nuclear fuel processing facility in Tokaimura, Japan. International Atomic Energy Agency, Vienna, 1999.
I8 IAEA. Generic models for use in assessing the impact of discharges of radioactive substances to the environment. IAEA Safety Reports Series No.19. International Atomic Energy Agency, Vienna, 2001.
I9 IAEA. Inventory of accidents and losses at sea involving radioactive material. IAEA-TECDOC-1242. International Atomic Energy Agency, Vienna, 2001.
I10 IAEA. Radiation legacy of the 20th century: Environmental restoration. IAEA-TECDOC-1280. International Atomic Energy Agency, Vienna, 2002.
I11 IAEA. Radiation protection and the management of radioactive waste in the oil and gas industry. IAEA Safety Reports Series No. 34. International Atomic Energy Agency, Vienna, 2003.
I12 IAEA. Extent of environmental contamination by Naturally Occurring Radioactive Material (NORM) and technological options for mitigation. IAEA Technical Reports Series No. 419. International Atomic Energy Agency, Vienna, 2003.
I13 IAEA. Radiological conditions in areas of Kuwait with residues of depleted uranium. Radiological Assessment Report Series. International Atomic Energy Agency, Vienna, 2003.
I14 IAEA. Sediment distribution coefficients and concentration factors for biota in the marine environment. IAEA Technical Reports Series No. 422. International Atomic Energy Agency, Vienna, 2004.
I15 IAEA. Environmental contamination from uranium production facilities and their remediation. Proceedings from the International Workshop on Environmental Contamination from Uranium Production Facilities and their Remediation, Lisbon, Portugal, 11–13 February 2004.
I16 IAEA. Radiological conditions at the former French nuclear test sites in Algeria: Preliminary assessment and recommendations. Radiological Assessment Reports Series. International Atomic Energy Agency, Vienna, 2005.
I17 IAEA. Environmental consequences of the Chernobyl accident and their remediation: Twenty years of experience. Radiological Assessment Reports Series. International Atomic Energy Agency, Vienna, 2006.
I18 IAEA. Assessing the need for radiation protection measures in work involving minerals and raw materials. IAEA Safety Reports Series No. 49. International Atomic Energy Agency, Vienna, 2006.
I19 IAEA. Radiation protection and NORM residue management in the zircon and zirconia industries. IAEA Safety Reports Series No. 51. International Atomic Energy Agency, Vienna, 2007.
I20 IAEA. Classification of radioactive waste. IAEA Safety Standards Series No. GSG-1. International Atomic Energy Agency, Vienna, 2009.
I21 IAEA. Nuclear safety review for the year 2009. GC(54)/INF/2. IAEA/NSR/2009. International Atomic Energy Agency, Vienna, 2010.
I22 IAEA. Handbook of parameter values for the prediction of radionuclide transfer in terrestrial and freshwater environments. IAEA Technical Reports Series No. 472. International Atomic Energy Agency, Vienna, 2010.
I23 IAEA. Assessment and way forward for legacy uranium production sites in Central Asia: An international approach. International Atomic Energy Agency, Vienna, 2010.
I24 IAEA. Nuclear safety review for the year 2010. GC(55)/INF/3. IAEA/NSR/2010. International Atomic Energy Agency, Vienna, 2011.
I25 IAEA. The Uranium Mining Remediation Exchange Group (UMREG): Selected papers 1995–2007. International Atomic Energy Agency, Vienna, 2011.
I26 IAEA. Radiation protection and NORM residue management in the production of rare earths from thorium containing minerals. IAEA Safety Reports Series No. 68. International Atomic Energy Agency, Vienna, 2011.

I27 IAEA. Radiation protection and NORM residue management in the titanium dioxide and related industries. IAEA Safety Reports Series No. 76. International Atomic Energy Agency, Vienna, 2012.
I28 IAEA. INES: The international nuclear and radiological event scale user's manual, 2008 edition. International Atomic Energy Agency, OECD Nuclear Energy Agency, Vienna, 2013.
I29 IAEA. Radiation protection and management of NORM residues in the phosphate industry. IAEA Safety Reports Series No. 78. International Atomic Energy Agency, Vienna, 2013.
I30 IAEA. Radiation protection and safety of radiation sources: International basic safety standards. IAEA Safety Standards Series GSR Part 3. International Atomic Energy Agency, Vienna, 2014.
I31 IAEA. National and regional surveys of radon concentration in dwellings. Analytical Quality in Nuclear Applications Series No. 33. International Atomic Energy Agency, Vienna, 2014.
I32 IAEA. Inventory of radioactive material resulting from historical dumping, accidents and losses at sea. IAEA-TECDOC-1776. International Atomic Energy Agency, Vienna, 2015.
I33 IAEA. Safeguards implementation guide for states with small quantities protocols. IAEA Services Series 22. International Atomic Energy Agency, Vienna, 2016.
I34 IAEA. Managing the unexpected in decommissioning. IAEA Nuclear Energy Series No. NW-T-2.8. International Atomic Energy Agency, Vienna, 2016.
I35 IAEA. Overexposure of a member. International Atomic Energy Agency. [Internet] Available from (https://iec.iaea.org/usie) on 04.03.2024.
I36 IAEA. Radiation safety for consumer products. IAEA Safety Standards No. SSG-36. International Atomic Energy Agency, Vienna, 2016.
I37 IAEA. Strategic master plan: Environmental remediation of uranium legacy sites in Central Asia. International Atomic Energy Agency, Vienna, 2018.
I38 IAEA. Environmental transfer of radionuclides in Japan following the accident at the Fukushima Daiichi Nuclear Power Plant. IAEA-TECDOC-1927. International Atomic Energy Agency, Vienna, 2020.
I39 IAEA. Radiation safety of Xray generators and other radiation sources used for inspection purposes and for non-medical human imaging. IAEA Safety Standards Series No. SSG-55. International Atomic Energy Agency, Vienna, 2020.
I40 IAEA. Radiation protection and safety in veterinary medicine. IAEA Safety Reports Series No. 104. International Atomic Energy Agency, Vienna, 2021.
I41 IAEA. Nuclear power reactors in the world, 2022 edition. Reference Data Series No. 2. International Atomic Energy Agency, Vienna, 2022.
I42 IAEA. Status and trends in spent fuel and radioactive waste management. IAEA Nuclear Energy Series NW-T-1.14 (Rev. 1). International Atomic Energy Agency, Vienna, 2022.
I43 IAEA. The radiological incident in Hueypoxtla. International Atomic Energy Agency, Vienna, 2022.
I44 IAEA. Exposure due to radionuclides in food other than during a nuclear or radiological emergency. IAEA-TECDOC-2011. International Atomic Energy Agency, Vienna, 2022.
I45 IAEA. Joint Convention on the Safety of Spent Fuel Management and on the Safety of Radioactive Waste Management. International Atomic Energy Agency. [Internet] Available from (https://www.iaea.org/topics/nuclear-safety-conventions/joint-convention-safety-spent-fuel-management-and-safety-radioactive-waste) on 01.05.2023.
I46 IAEA. Management of depleted uranium used as shielding in disused radiation devices. IAEA Nuclear Energy Series NW-T-1.30. International Atomic Energy Agency, Vienna, 2023.
I47 IAEA. Fukushima Daiichi status updates. International Atomic Energy Agency. [Internet] Available from (https://www.iaea.org/newscenter/focus/fukushima/status-update) on 12.02.2024.
I48 IAEA. Exposure due to radionuclides in food other than during a nuclear or radiological emergency. Part 1: Technical material. IAEA Safety Reports Series No. 114. International Atomic Energy Agency, Vienna, 2023.
I49 IAEA. Nuclear fuel cycle facilities database. [Internet] Available from (https://infcis.iaea.org/NFCFDB/) on 2.5.2023.

I50 IAEA. Research Reactor Database (RRDB). International Atomic Energy Agency. [Internet] Available from (https://nucleus.iaea.org/rrdb/#/home) on 2.5.2023.

I51 IAEA. Database of cyclotrons for radionuclide production. International Atomic Energy Agency. [Internet] Available from (https://nucleus.iaea.org/sites/accelerators/Pages/Cyclotron.aspx) on 08.12.2023.

I52 IAEA. IAEA comprehensive report on the safety review of the ALPS-treated water at the Fukushima Daiichi Nuclear Power Station. International Atomic Energy Agency, Vienna, 2023.

I53 IAEA. The environmental behaviour of uranium. IAEA Technical Reports Series No. 488. International Atomic Energy Agency, Vienna, 2023.

I54 IAEA. Transport security. International Atomic Energy Agency. [Internet] Available from (https://www.iaea.org/topics/transport-security) on 22.06.2023.

I55 IAEA. World survey of fusion devices 2022. International Atomic Energy Agency, Vienna, 2023.

I56 IAEA. PRIS–Power Reactor Information System. International Atomic Energy Agency. [Internet] Available from (http://www.iaea.org/pris/home.aspx) on 22.01.2024.

I57 IAEA. Tritium in the environment. IAEA Technical Reports Series No. 495. International Atomic Energy Agency, Vienna, 2025.

I58 IBRAE. 35 Years of the Chernobyl accident. Results and prospects of overcoming its consequences in Russia 1986-2021. Nuclear Safety Institute of the Russian Academy of Sciences, Moscow, 2021. (Russian).

I59 IBRAE. Radiation situation at Rosatom Enterprises. Institute for Safe Development of Nuclear Energy of the Russian Academy of Sciences. [Internet] Available from (https://www.russianatom.ru/) on 23.11.2023. (Russian).

I60 Ibrahim, S.A., S.L. Simon, A. Bouville et al. Alimentary tract absorption (f1 values) for radionuclides in local and regional fallout from nuclear tests. Health Phys 99(2): 233-251 (2010).

I61 ICAO. ICAO Long-term traffic forecasts: Passenger and cargo. International Civil Aviation Organization, 2016.

I62 ICAO. ICAO Traffic flow 2015. International Civil Aviation Organization. [Internet] Available from (https://gis.icao.int/portal/home/item.html?id=08d1fb09abef4168b382728703d20b9f) on 27.07.2023.

I63 ICAO. Annual reports of the council. International Civil Aviation Organization. [Internet] Available from (https://www.icao.int/about-icao/Pages/annual-reports.aspx) on 01.07.2023.

I64 ICRP. Report of the task group on reference man. ICRP Publication 23. International Commission on Radiological Protection, Pergamon Press, Oxford, 1975.

I65 ICRP. 1990 recommendations of the International Commission on Radiological Protection. ICRP Publication 60. Annals of the ICRP 21 (1-3). International Commission on Radiological Protection, Pergamon Press, 1991.

I66 ICRP. Protection against radon-222 at home and at work. ICRP Publication 65. Annals of the ICRP 23(2). International Commission on Radiological Protection, Pergamon Press, 1993.

I67 ICRP. Age-dependent doses to members of the public from intake of radionuclides: Part 4. Inhalation dose coefficients. ICRP Publication 71. Annals of the ICRP 25(3-4). International Commission on Radiological Protection, Pergamon Press, 1995.

I68 ICRP. Age-dependent doses to members of the public from intake of radionuclides: Part 5. Compilation of ingestion and inhalation dose coefficients. ICRP Publication 72. Annals of the ICRP 26(1). International Commission on Radiological Protection, Pergamon Press, 1995.

I69 ICRP. Doses to the embryo and fetus from intakes of radionuclides by the mother. Annals of the ICRP 31(1-3). International Commission on Radiological Protection, Pergamon Press, 2001.

I70 ICRP. The 2007 Recommendations of the International Commission on Radiological Protection. ICRP Publication 103. Annals of the ICRP 37(2-4). International Commission on Radiological Protection, Elsevier Ltd., 2007.

I71 ICRP. Conversion coefficients for radiological protection quantities for external radiation exposures. ICRP Publication 116. Annals of the ICRP 40(2–5). International Commission on Radiological Protection, Pergamon Press, 2010.

I72 ICRP. ICRP statement on tissue reactions / early and late effects of radiation in normal tissues and organs–threshold doses for tissue reactions in a radiation protection context. ICRP Publication 118. Annals of the ICRP 41(1-2). International Commission on Radiological Protection, Elsevier Ltd., 2012.

I73 ICRP. Compendium of dose coefficients based on ICRP Publication 60. ICRP Publication 119. Annals of the ICRP 41(Suppl. 1). International Commission on Radiological Protection, Elsevier Ltd., 2012.

I74 ICRP. Assessment of radiation exposure of astronauts in space. ICRP Publication 123. Annals of the ICRP 42(4). International Commission on Radiological Protection, Elsevier Ltd., 2013.

I75 ICRP. Occupational intakes of radionuclides: Part 3. ICRP Publication 137. Annals of the ICRP 46(3-4): International Commission on Radiological Protection, SAGE, 2017.

I76 ICRP. Radiological protection from naturally occurring radioactive material (NORM) in industrial processes. ICRP Publication 142. Annals of the ICRP 48(4). International Commission on Radiological Protection, SAGE, 2019.

I77 ICRP. Dose coefficients for external exposures to environmental sources. ICRP Publication 144. Annals of the ICRP 49(2). International Commission on Radiological Protection, SAGE, 2020.

I78 ICRP and UNSCEAR. Information note for participants at the IAEA technical meeting on the implications of the new dose conversion factors for radon, 1–4 Oct 2019. International Commission on Radiological Protection, Vienna, 2020.

I79 ICRU. Radiation monitoring for protection of the public after major releases of radionuclides to the environment. ICRU Report 92. International Commission on Radiation Units and Measurements, Bethesda, MD, 2015.

I80 India. Effects of Pokhran tests, Press Information Bureau, New Delhi, 2020.

I81 IPFM. Global fissile material report 2022. Fifty years of the nuclear non-proliferation treaty: Nuclear weapons, fissile materials, and nuclear energy. International Panel on Fissile Materials, Princeton, New Jersey, 2022.

I82 IRSN. Assessment of health risk of X-ray backscatter body scanners. Radiation Protection and Human Health Division. Institut de Radioprotection et de Sûreté Nucléaire, Fontenay-aux-Roses, France, 2010.

I83 IRSN. Radiological report of the French environment from 2015 to 2017. Institut de Radioprotection et de Sûreté Nucléaire, Fontenay-aux-Roses, France, 2018.

I84 IRSN. Bilan de l'état radiologique de l'environnement français de 2018 a 2020. Institut de Radioprotection et de Sûreté Nucléaire, Fontenay-aux-Roses, France, 2021. (French).

I85 IRSN. Bilan de la surveillance de la radioactivité en Polynésie française en 2021 et 2022. Synthesé des résultats du réseau de surveillance de l'IRSN. Institut de Radioprotection et de Sûreté Nucléaire, Fontenay-aux-Roses, France, 2023. (French).

I86 IRSN and ASN. Le réseau national de mesures de la radioactivité de l'environnement. Institut de Radioprotection et de Sûreté Nucléaire, Autorité de sûreté nucléaire. [Internet] Available from (https://www.mesure-radioactivite.fr/#/) on 24.02.2024. (French).

I87 IRSN. Programme MIMAUSA. Institut de Radioprotection et de Sûreté Nucléaire (IRSN). [Internet] Available from (https://mimausabdd.irsn.fr/) on 05.03.2024. (French).

I88 Ishikawa, T., S. Tokonami, Y. Kobayashi et al. Preliminary results of indoor radon/thoron concentrations and terrestrial gamma doses in Gejiu, Yunnan, China. Proceedings of the 8th International Symposium on the Natural Radiation Environment, Buzious, Brazil, 7–12 October 2007. AIP Conference Proceedings.

I89 Ishimori, Y. Time-integrated monitoring of thoron progeny concentration around closed uranium mine sites in Japan. Radiat Prot Dosim 141(4): 452-456 (2010).

I90 ISO. Determination of the characteristic limits (decision threshold, detection limit and limits of the coverage interval) for measurements of ionizing radiation — Fundamentals and application — Part 4: Guidelines to applications, ISO 11929-4. International Organization for Standardization, Geneva, 2020.

I91 ISO. Measurement of radioactivity in the environment–Guidelines for effective dose assessment using environmental monitoring data, Part 1: Planned and existing exposure situation. International Organization for Standardization, Geneva, 2021.

I92 ISO. Country codes: The International standard for country codes and codes for their subdivisions. ISO 3166 Maintenance Agency, International Organization for Standardization. [Internet] Available from (https://www.iso.org/obp/ui/) on 02.05.2023.

I93 Ivanova, K., Z. Stojanovska, V. Badulin et al. Radiological impact of surface water and sediment near uranium mining sites. J Radiol Prot 35(4): 819-834 (2015).

I94 Izrael, Y.A. Atlas of the East Ural and Karachay radioactive trace including forecast up to 2047. IGCE Roshydromet and RAS, Moscow, 2013.

J1 JAEA. Excel-based Program for calculating Atmospheric Cosmic-ray Spectrum (EXPACS). Japan Atomic Energy Agency. [Internet] Available from (https://phits.jaea.go.jp/expacs/) on 16.08.2021.

J2 Jaffe, R.S. and W.J. Tipton. A radiological survey of Johnston Atoll. Dates of survey: April-August 1980. Defense Nuclear Agency, Washington, D.C., 1981.

J3 Jakab, D., G. Endrodi, A. Kocsonya et al. Methods, results and dose consequences of ^{106}Ru detection in the environment in Budapest, Hungary. J Environ Radioact 192: 543-550 (2018).

J4 Jamir, S., B.K. Sahoo, R. Mishra et al. A study on indoor radon, thoron and their progeny level in Mokokchung district of Nagaland, India. J Radioanal Nucl Chem 331(1): 21-30 (2022).

J5 Jamir, S., B.K. Sahoo, R. Mishra et al. A comprehensive study on indoor radon, thoron and their progeny level in Dimapur district of Nagaland, India. Radiat Prot Dosim 198(12): 853-861 (2022).

J6 Janik, M., Y. Omori and H. Yonehara. Influence of humidity on radon and thoron exhalation rates from building materials. Appl Radiat Isot 95: 102-107 (2015).

J7 Japan, Government of. Events and highlights on the progress related to recovery operations at TEPCO's Fukushima Daiichi Nuclear Power Station, 2023.

J8 Japan National Preparatory Committee. A call from Hibakusha of Hiroshima and Nagasaki. Proceedings from the International Symposium on the Damage and After-Effects of the Atomic Bombing of Hiroshima and Nagasaki,(S. Kawasaki, ed.) Tokyo, Japan, 21 July–9 August 1977. Asahi Evening News.

J9 Jasechko, S. Global isotope hydrogeology - review. Reviews Geophys 57(3): 835-965 (2019).

J10 Jaynes, E.T. Probability Theory: The Logic of Science. Cambridge University Press, Cambridge, 2003.

J11 JCGM. Evaluation of measurement data – Supplement 1 to the "Guide to the expression of uncertainty in measurement" – Propagation of distributions using a Monte Carlo method. JCGM 101:2008. Joint Committee for Guides in Metrology, 2008.

J12 JCGM. Evaluation of measurement data – Guide to the expression of uncertainty in measurement. JCGM 100:2008. Joint Committee for Guides in Metrology, 2008.

J13 JCGM. International vocabulary of metrology – Basic and general concepts and associated terms (VIM). JCGM 200:2012. Joint Committee for Guides in Metrology, 2012.

J14 Jiménez, F., L. Debán, R. Pardo et al. Levels of ^{131}I and six natural radionuclides in sludge from the sewage treatment plant of Valladolid, Spain. Water Air Soil Pollut 217(1): 515-521 (2011).

J15 Jiranek, M. and V. Kacmarikova. Dealing with the increased radon concentration in thermally retrofitted buildings. Radiat Prot Dosim 160(1-3): 43-47 (2014).

J16 Jiranek, M. and V. Kacmarikova. Applicability of ventilation systems for reducing the indoor radon concentration. Radiat Prot Dosim 191(2): 202-208 (2020).

J17 JNREG. Investigation into the radioecological status of the site of the sunken nuclear submarine K-159 in the barents sea: Results from the 2014 research cruise. Joint Norwegian-Russian Expert Group for investigation of Radioactive Contamination in the Northern Areas, Oslo, 2014.

J18 JNREG. Investigation into the radioecological status of the sunken nuclear submarine Komsomolets in the Norwegian Sea. Results from the 2019 Norwegian research cruise. Joint Norwegian-Russian Expert Group for investigation of adioactive contamination in the Northern Areas, Oslo, 2023.

J19 Jobbágy, V., T. Altzitzoglou, P. Malo et al. A brief overview on radon measurements in drinking water. J Environ Radioact 173: 18-24 (2017).

J20 Johansen, M.P., J.G. Carpenter, S. Charmasson et al. Seafood dose parameters: Updating ^{210}Po retention factors for cooking, decay loss and mariculture. J Environ Radioact 268-269: 107243 (2023).
J21 Joint US-Japan Working Group, R.W. Young and G.D. Kerr. Reassessment of the atomic bomb radiation dosimetry for Hiroshima and Nagasaki. Volumes 1 and 2. Dosimetry system 2002. The Radiation Effects Research Foundation, Hiroshima, 2005.
J22 Jones, A.L. and T. Cabianca. Survey into the radiological impact of the normal transport of radioactive material in the UK by road and rail. PHE-CRCE-Series 035. Public Health England, Chilton, 2017.
J23 Juhász, L., P. Szerbin, Z. Lendvai et al. Results of pilot studies of environmental restoration of uranium mining tailings ponds in Hungary. Sci Total Environ 272(1): 251-252 (2001).
J24 Jurda, M. and M. Němec. Remediation of the uranium industry in the Czech Republic: Regulation aspects and main technologies. J Radiol Prot 42(1): 010504 (2022).
K1 Kamunda, C., M. Mathuthu and M. Madhuku. An assessment of radiological hazards from gold mine tailings in the province of Gauteng in South Africa. Int J Environ Res Public Health 13(1): 138 (2016).
K2 Kane, R.P. Severe geomagnetic storms and Forbush decreases: Interplanetary relationships reexamined. Ann Geophys 28(2): 479-489 (2010).
K3 Kanse, S.D., B.K. Sahoo, J.J. Gaware et al. A study of thoron exhalation from monazite-rich beach sands of high background radiation areas of Kerala and Odisha, India. Environ Earth Sci 75(23): 1465 (2016).
K4 Kanu, A.M., L.L. Comfort, T.P. Guilderson et al. Measurements and modeling of contemporary radiocarbon in the stratosphere. Geophys Res Letters 43(3): 1399-1406 (2016).
K5 Karstens, U., C. Schwingshackl, D. Schmithüsen et al. A process-based ^{222}radon flux map for Europe and its comparison to long-term observations. Atmos Chem Phys 15(22): 12845-12865 (2015).
K6 Kasatkin, V.V., V.A. Il'itchev, E.N. Kamnev et al. Geological and radioecological problems of the objects formed by peaceful nuclear explosions – special radwaste repositories. Atom Energy 113(5): 363-368 (2013).
K7 Kasatkin, V.V., A.V. Kasatkin, V.A. Il'ichev et al. Stages for reclassifying globus-1 Peaceful nuclear explosion object as a site for preserving special radwastes. Atom Energy 116(3): 201-205 (2014).
K8 Kaur, A., S. Sharma and B. Mittal. Radiation surveillance in and around cyclotron facility. Indian J Nucl Med 27(4): 243-245 (2012).
K9 Kaur, M., A. Kumar, R. Mehra et al. Assessment of radon, thoron, and their progeny concentrations in the dwellings of Shivalik hills of Jammu and Kashmir, India. Environ Geochem Health 45(8): 5685-5701 (2020).
K10 Kaushal, A., M. Joshi, A. Sarin et al. Dosimetry of indoor alpha flux belonging to seasonal radon, thoron and their EECs. Environ Monit Assess 194(2): 119 (2022).
K11 Kazachonok, N.N., V.A. Kostyuchenko, I.Y. Popova et al. Current status of the radioactive contamination of the Eurt and other territories in the Mayak PA effect zone. Radiat Safe Issues 73(1): 33 (2014). (Russian).
K12 Keatley, A.C., P.G. Martin, K.R. Hallam et al. Source identification of uranium-containing materials at mine legacy sites in Portugal. J Environ Radioact 183: 102-111 (2018).
K13 Kemski, J., R. Klingel, A. Siehl et al. From radon hazard to risk prediction-based on geological maps, soil gas and indoor measurements in Germany. Environ Geol 56(7): 1269-1279 (2008).
K14 Khan, S.M., D.D. Pearson, T. Ronnqvist et al. Rising Canadian and falling Swedish radon gas exposure as a consequence of 20th to 21st century residential build practices. Sci Rep 11(1): 17551 (2021).
K15 Kheruka, S.C., N. Shankar, M. Ora et al. Do current radiation safety guidelines allow the safe release of a thyroid cancer patient after high-dose radioiodine therapy? An Indian perspective. Indian J Nucl Med 36(2): 148-152 (2021).
K16 Khomich, I.V., Y.N. Lobach, Y.N. Nesteruk et al. Operational radiation protection at the Kiev´s research reactor WWR-M. Int Nucl Safety 1(1) (2012).

K17 Khramtsov, E.V. Radiation situation on the territory of the peaceful nuclear explosion «Globus-1» after performing the rehabilitation works. Radiat Hygiene 12(3): 58-68 (2019). (Russian).

K18 Khramtsov, E.V. Radiation situation on the territory of the peaceful nuclear explosion «Globus-1» before performing the rehabilitation works. Radiat Hygiene 12(2): 81-88 (2019). (Russian).

K19 Kim, C.-K., Y.-J. Kim, H.-Y. Lee et al. ^{220}Rn and its progeny in dwellings of Korea. Radiat Meas 42(8): 1409-1414 (2007).

K20 Kim, E., K. Yajima, S. Hashimoto et al. Reassessment of internal thyroid doses to 1,080 children examined in a screening survey after the 2011 Fukushima nuclear disaster. Health Phys 118(1): 36-52 (2020).

K21 Kim, E., Y. Choi, H. Park et al. Assessment of radiation dose of mobile computed tomography in intensive care units. Radiat Prot Dosim 196(1-2): 60-70 (2021).

K22 Kiselev, M., N. Shandala, G. Gneusheva et al. Radiation protection of workers from uranium mines and of the public living nearby uranium mining and milling facilities. Proceedings from the 12th International Congress of the International Radiation Protection Association (IRPA 12): Strengthening Radiation Protection Worldwide, Buenos Aires, Argentina, 19–24 October 2008.

K23 Kiselev, S., N. Shandala, T. Laschenova et al. Comprehensive environmental monitoring during remediation of a nuclear legacy site in the far east of Russia. J Radiol Prot 41(3): S216–S229 (2021).

K24 Kitto, M.E., D.K. Haines and H.D. Arauzo. Emanation of radon from household granite. Health Phys 96(4): 477-482 (2009).

K25 Kleinschmidt, R. and R. Akber. Naturally occurring radionuclides in materials derived from urban water treatment plants in southeast Queensland, Australia. J Environ Radioact 99(4): 607-620 (2008).

K26 Komex. Zambia - Copperbelt Environment Project : Environmental Impact Assessment (Vol. 2): Main report World Bank. Komex International Ltd., 2022.

K27 Konstantinov, Y.O., G.V. Arkhangel'skaya, K.G. Andersson et al. Radiological and hygienic issues of the mitigation of the Chernobyl NPP accident consequences. Federal Service for Supervision of Consumer Rights Protection and Human Welfare, St. Petersburg, 2016. (Russian).

K28 Korneev, A.G., V.S. Zhurkov, N.P. Kuleshov et al. Radio-ecological and genetic assessment of late consequences of Totsk nuclear explosion. Gigiena Sanitariia (6): 46-50 (1998). (Russian).

K29 Kostyuchenko, V.A., L.M. Peremyslova, I.Y. Popova et al. Main dependencies in reduction of radiation exposure to the population of the Southern Urals. Health Phys 103(1): 42-46 (2012).

K30 Kotrappa, P. and F. Stieff. Radon exhalation rates from building materials using electret ion chamber radon monitors in accumulators. Health Phys 97(2): 163-166 (2009).

K31 Kovacs, T., Z. Sas, J. Somlai et al. Radiological investigation of the effects of red mud disaster. Radiat Prot Dosim 152(1-3): 76-79 (2012).

K32 Kovler, K. Does the utilization of coal fly ash in concrete construction present a radiation hazard? Const Build Mater 29: 158-166 (2012).

K33 Kozak, K., J. Mazur, B. Kozlowska et al. Correction factors for determination of annual average radon concentration in dwellings of Poland resulting from seasonal variability of indoor radon. Appl Radiat Isot 69(10): 1459-1465 (2011).

K34 Kravtsova, E.M. Issues of radiation and social protection of the population living in the unevacuated territory of the EURT. Regional Ecological Almanac 2007 (2007). (Russian).

K35 Kravtsova, O.S., G.Y. Brook, V.Y. Golikov et al. Radiation situation in areas of the Urals federal district located in the Mayak impact zone. Pub Health Life Environ 5(230): 6-11 (2012). (Russian).

K36 Krembel, D. The control of the transport of radioactive material by air in France. Proceedings from the 13th International Symposium on the Packaging and Transportation of Radioactive Materials (PATRAM 2001), Chicago, USA, 3–7 September 2001. Institute of Nuclear Materials Management.

K37 Krivitskiy, P.Y., N.V. Larionova, Y.V. Baklanova et al. Characterization of area radioactive contamination of near-surface soil at the Sary-Uzen site in the Semipalatinsk test site. J Environ Radioact 249: 106893 (2022).

K38 Kropat, G., F. Bochud, M. Jaboyedoff et al. Major influencing factors of indoor radon concentrations in Switzerland. J Environ Radioact 129: 7-22 (2014).
K39 Kudo, H., S. Tokonami, Y. Omori et al. Comparative dosimetry for radon and thoron in high background radiation areas in China. Radiat Prot Dosim 167(1-3): 155-159 (2015).
K40 Kumar, A., R.P. Chauhan, M. Joshi et al. Implications of variability in indoor radon/thoron levels: A study of dwellings in Haryana, India. Environ Earth Sci 73(8): 4033-4042 (2014).
K41 Kumar, A., R. Vij, S. Sharma et al. Seasonal variation of indoor radon/thoron and their progeny levels in lesser-Himalayas of Jammu & Kashmir, India. J Radioanal Nucl Chem 323(1): 495-506 (2019).
K42 Kumar, M., P. Kumar, A. Agrawal et al. Measurements of ^{222}Rn, ^{220}Rn and their progeny concentrations indoors around a coal/gas-based power plant and estimation of annual inhalation dose to the public. J Radioanal Nucl Chem 326(1): 65-74 (2020).
K43 Kumar, R., G.K. Panda, B.K. Singh et al. Lessons learned from the radiological accident in Mayapuri, New Delhi. International Conference on Safety and Security of Radioactive Sources: Maintaining continuous global control of sources throughout their life cycle, Abu Dhabi, United Arab Emirates, 27–31 October 2013. International Atomic Energy Agency, Vienna (2015).
K44 Kümmel, M., C. Dushe, S. Muller et al. Outdoor ^{222}Rn-concentrations in Germany – part 2 – former mining areas. J Environ Radioact 132: 131-137 (2014).
K45 Kurkela, O., J. Nevalainen, S.M. Patsi et al. Lung cancer incidence attributable to residential radon exposure in Finland. Radiat Environ Biophys 62(1): 35-49 (2023).
K46 Kurth, J., B.J. Krause, S.M. Schwarzenbock et al. External radiation exposure, excretion, and effective half-life in ^{177}Lu-PSMA-targeted therapies. EJNMMI Res 8(1): 32 (2018).
K47 Kuzmanović, P., N. Todorović, D. Mrđa et al. Radiation exposure to zircon minerals in Serbian ceramic industries. J Radioanal Nucl Chem 322(2): 949-960 (2019).
K48 Kuzmanović, P., B. Miljević, N. Todorović et al. The influence of building material structure on radon emanation. J Radiol Prot 42(4): 041508 (2022).
L1 La Delfa, S., F. Vizzini and G. Patanè. Radon migration into different building types at medium and low south-eastern flank of Mt Etna (Sicily): Connection with the volcanic activity. Environ Earth Sci 66(3): 923-931 (2011).
L2 Land, C.E., A. Bouville, I. Apostoaei et al. Projected lifetime cancer risks from exposure to regional radioactive fallout in the Marshall Islands. Health Phys 99(2): 201-215 (2010).
L3 Larionova, N.V., S.N. Lukashenko, O.N. Lyakhova et al. Plants as indicators of tritium concentration in ground water at the Semipalatinsk test site. J Environ Radioact 177: 218-224 (2017).
L4 Larionova, N.V., S.N. Lukashenko, A.M. Kabdyrakova et al. Transfer of radionuclides to plants of natural ecosystems at the Semipalatinsk Test Site. J Environ Radioact 186: 63-70 (2018).
L5 László, E., L. Palcsu and Á. Leelőssy. Estimation of the solar-induced natural variability of the tritium concentration of precipitation in the northern and southern hemisphere. Atmos Environ 233: 117605 (2020).
L6 Lauer, N.E., J.C. Hower, H. Hsu-Kim et al. Naturally occurring radioactive materials in coals and coal combustion residuals in the United States. Environ Sci Technol 49(18): 11227-11233 (2015).
L7 Lavrova, T. and O. Voitsekhovych. Radioecological assessment and remediation planning at the former uranium milling facilities at the Pridnieprovsky Chemical plant in Ukraine. J Environ Radioact 115: 118-123 (2013).
L8 Lawrence, C.E., R.A. Akber, A. Bollhofer et al. Radon-222 exhalation from open ground on and around a uranium mine in the wet-dry tropics. J Environ Radioact 100(1): 1-8 (2009).
L9 Lebed'kova, S.E., V.V. Sumenko, G.B. Katsova et al. Health status of children living in rural localities in the area of Totsk nuclear explosion. Gigiena Sanitariia (6): 50-53 (1998). (Russian).
L10 Lee, H.K., S.J. Hong, K.H. Jeong et al. An engagement factor for caregiver radiation dose assessment with radioiodine treatment. Radiat Prot Dosim 163(4): 499-508 (2015).
L11 Lee, J.H. and S.G. Park. Estimation of the release time from isolation for patients with differentiated thyroid cancer treated with high-dose I-131. Nucl Med Mol Imaging 44(4): 241-245 (2010).

L12 Lee, J.S., S.L. Dong, W.P. Chang et al. Evaluation of external dose equivalent with thermoluminescent dosimeters from residents living in radiation-contaminated buildings. Appl Radiat Isot 48(9): 1237-1243 (1997).

L13 Lee, J.S., S.L. Dong and T.H. Wu. Estimation of organ dose equivalents from residents of radiation-contaminated buildings with rando phantom measurements. Appl Radiat Isot 50(5): 867-873 (1999).

L14 Lemercier, M., R. Gurriaran, P. Bouisset et al. Specific activity to H*(10) conversion coefficients for in situ gamma spectrometry. Radiat Prot Dosim 128(1): 83-89 (2008).

L15 Lerman, A. Geochemical Processes. Water and Sediment Environments. John Wiley and Sons, Inc., New York, USA, 1979.

L16 Lersow, M. and P. Schmidt. The Wismut remediation project. pp. 181-190 in: Mine Closure 2006. Australian Centre for Geomechanics, Perth, 2006.

L17 Lespukh, E., P. Stegnar, A. Usubalieva et al. Assessment of the radiological impact of gamma and radon dose rates at former U mining sites in Kyrgyzstan. J Environ Radioact 123: 28-36 (2013).

L18 Lessard, E.T., R.P. Miltenberger, S.H. Cohn et al. Protracted exposure to fallout: The Rongelap and Utirik experience. Health Phys 46(3): 511-527 (1984).

L19 Licciardello, T., G. Feliciani, G. Mazzotti et al. Radiation protection and dosimetry issues for patients with prostate cancer after I-125 low-dose-rate brachytherapy permanent implant. Brachytherapy 20(1): 272-278 (2021).

L20 Lightsources.org. Light sources of the world. [Internet] Available from (https://lightsources.org/lightsources-of-the-world/) on 08.12.2023.

L21 Limpert, E. and W.A. Stahel. Problems with using the normal distribution – and ways to improve quality and efficiency of data analysis. PLoS One 6(7): e21403 (2011).

L22 Lindsay, R., R.T. Newman and W.J. Speelman. A study of airborne radon levels in Paarl houses (South Africa) and associated source terms, using electret ion chambers and gamma-ray spectrometry. Appl Radiat Isot 66(11): 1611-1614 (2008).

L23 Liu, C., M. Benotto, K. Ungar et al. Environmental monitoring and external exposure to natural radiation in Canada. J Environ Radioact 243: 106811 (2022).

L24 Liu, L., Z. Chen, Y. Li et al. Emission of Rn and CO_2 from soil at fault zones caused by seismic waves. Earth Space Sci 10(6): e2023EA003012 (2023).

L25 Lively, R.S. and B.C. Krafthefer. ^{222}Rn variations in Mystery Cave, Minnesota. Health Phys 68(4): 590-594 (1995).

L26 Logachev, V.A. Current Radioecological Situation at the Sites of Peaceful Nuclear Explosions on the Territory of the Russian Federation. IzdAT, Moscow, 2005. (Russian).

L27 Long, S., D. Fenton, M. Cremin et al. The effectiveness of radon preventive and remedial measures in Irish homes. J Radiol Prot 33(1): 141-149 (2013).

L28 Loueyit, C.J., B. Keiffer, S. Fourcade et al. Study of the post-closure provisions for managing solid tailings from the extraction and processing of uranium ores resulting from the industrial activities of the COMUF company at Mounana, Gabon. International Symposium on the Uranium Production Cycle and the Environment, Vienna, Austria, 2–6 October 2000. International Atomic Energy Agency.

L29 Louw, I. Potential radiological impact of the phosphate industry in South Africa on the public and the environment (Paper 1). J Environ Radioact 217: 106214 (2020).

L30 Lukashenko, S.N., A.O. Aidarkhanov, A.K. Aidarkhanova et al. Topical issues in radioecology of Kazakhstan, Issue 5 Optimization of study of the Semipalatinsk test site lands for the purpose of their transfer into economic turnover. National Nuclear Center of the Republic of Kazakhstan, Pavlodar Press House, Kurchatov, 2017.

L31 Lukashenko, S.N., Y.G. Strilchuk, M.A. Umarov et al. Semipalatinsk Test Site: Present State. 978-601-7844-45-5. National Nuclear Center of the Republic of Kazakhstan, Pavlodar Press House, Kurchatov, 2018.

M1 Maguire, H., G. Fraser, J. Croft et al. Assessing public health risk in the London polonium-210 incident, 2006. Public Health 124(6): 313-318 (2010).

M2 Mahamood, N.K. and V. Prakash. Studies on indoor and outdoor radon/thoron concentration and estimation of radiological parameters from gamma dose rates along the coastal regions of Trivandrum and Kollam Districts, Kerala, India. Radiochem 61(5): 637-644 (2019).

M3 Manohar, S.B., B.S. Tomar, S.S. Rattan et al. Post shot radioactivity measurements on samples extracted from thermonuclear test site. BARC Newsletter 186: 1-6 (1999).

M4 Mares, V., T. Maczka, G. Leuthold et al. Air crew dosimetry with a new version of EPCARD. Radiat Prot Dosim 136(4): 262-266 (2009).

M5 Maringer, F.J., H. Kaineder, E. Nadschlager et al. Standards and experience in radon measurement and regulation of radon mitigation in Austria. Appl Radiat Isot 66(11): 1644-1649 (2008).

M6 Marriott, C.J., C.E. Webber and K.Y. Gulenchyn. Radiation exposure for 'caregivers' during high-dose outpatient radioiodine therapy. Radiat Prot Dosim 123(1): 62-67 (2007).

M7 Marshall, A.C. Gulf war depleted uranium risks. J Expo Sci Environ Epidemiol 18(1): 95-108 (2008).

M8 MARTAC. Rehabilitation of former nuclear test sites at Emu and Maralinga (Australia) 2003. MARTAC Report 0642773289. The Maralinga Rehabilitation Technical Advisory Committee, Canberra, 2003.

M9 Mas, J.L., E.G. San Miguel, J.P. Bolívar et al. An assay on the effect of preliminary restoration tasks applied to a large TENORM wastes disposal in the south-west of Spain. Sci Total Environ 364(1-3): 55-66 (2006).

M10 Masarik, J. and J. Beer. An updated simulation of particle fluxes and cosmogenic nuclide production in the Earth's atmosphere. J Geophys Res Atmos 114: D11103 (2009).

M11 Masson, O., G. Steinhauser, D. Zok et al. Airborne concentrations and chemical considerations of radioactive ruthenium from an undeclared major nuclear release in 2017. Proc Natl Acad Sci 116(34): 16750-16759 (2019).

M12 Mathieu, I., J. Caussin, P. Smeesters et al. Recommended restrictions after ^{131}I therapy: Measured doses in family members. Health Phys 76(2): 129-136 (1999).

M13 Mc Carron, B., X. Meng and S. Colclough. An investigation into indoor radon concentrations in certified passive house homes. Int J Environ Res Pub Health 17(11): 4149 (2020).

M14 McEwan, A.C., K.M. Matthews and L.P. Gregory. An environmental radiation survey of Christmas Island, Kiribati. Report No. 1981/9. National Radiation Laboratory, Wellington, 1981.

M15 McGrath, J.A., R. Aghamolaei, J. O'Donnell et al. Factors influencing radon concentration during energy retrofitting in domestic buildings: A computational evaluation. Build Environ 194: 107712 (2021).

M16 McLaughlin, J., M. Murray, L. Currivan et al. Long-term measurements of thoron, its airborne progeny and radon in 205 dwellings in Ireland. Radiat Prot Dosim 145(2-3): 189-193 (2011).

M17 McLaughlin, J.P. Public health and environmental aspects of DU. International Congress Series 1276: 137-140 (2005).

M18 Megumi, K., M. Abe, T. Matsunami et al. A study on seasonal variation of radon concentration in indoor air in Osaka district. J Radiat Res 36(4): 301 (1995).

M19 Mehra, R., S. Kansal and N.P. Singh. Measurement of thoron and radon progeny in outdoors of Sirsa, India, using defined solid angle absolute beta counting. Radiat Prot Dosim 141(4): 400-403 (2010).

M20 Meier, M.M., T. Berger, T. Jahn et al. Impact of the South Atlantic Anomaly on radiation exposure at flight altitudes during solar minimum. Sci Rep 13(1): 9348 (2023).

M21 Meisenberg, O., R. Mishra, M. Joshi et al. Radon and thoron inhalation doses in dwellings with earthen architecture: Comparison of measurement methods. Sci Total Environ 579: 1855-1862 (2017).

M22 Melo, D.R., L. Bertelli, S.A. Ibrahim et al. Dose coefficients for internal dose assessments for exposure to radioactive fallout. Health Phys 122(1): 125-235 (2022).

M23 Memon, T.A., K. Khan, A. Jabbar et al. Assessment of the ambient dose rate around research reactors by thermoluminescence dosimeters. Nucl Technol Radiat Prot 25(1): 41-45 (2010).

M24 Meyer, W. Impact of constructional energy-saving measures on radon levels indoors. Indoor Air 29(4): 680-685 (2019).

M25 MHLW. Radionuclides in foods - Current situation and protective measures. Ministry of Health, Labour and Welfare, Tokyo, 2021.

M26 Miklyaev, P.S. and T.B. Petrova. Studies of radon emanation from clays. Water Resources 38(7): 868-875 (2012).

M27 Miklyaev, P.S., T.B. Petrova, D.V. Shchitov et al. Radon transport in permeable geological environments. Sci Total Environ 852: 158382 (2022).

M28 Mildenberger, J. TRIUMF class IB licence renewal. CNSC Commission Member Document. Document No. 193210: Canadian Nuclear Safety Commission. TRIUMF Accelerators Inc., Ottawa, ON, 2021.

M29 Ministry of Justice and The Rt Hon Lucy Frazer KC MP. X-ray scanners stop over 1,000 illegal items entering prisons. Press release. Government of the United Kingdom. [Internet] Available from (https://www.gov.uk/government/news/x-ray-scanners-stop-over-1-000-illegal-items-entering-prisons) on 02.05.2023.

M30 Mirsaidov, U.M. Wastes from former mining and milling activities in Tajikistan. International Seminar on Uranium Legacy of Soviet Union in Central Asia: Problems and way forward, Dushanbe, Tajikistan, 20–22 November 2012.

M31 Misdaq, M.A., M. Amrane and J. Ouguidi. Concentrations of ^{222}Rn, ^{220}Rn and their decay products measured in outdoor air in various rural zones (Morocco) by using solid-state nuclear track detectors and resulting radiation dose to the rural populations. Radiat Prot Dosim 138(3): 223-236 (2010).

M32 Mishra, R., B.K. Sapra, R. Prajith et al. Inhalation exposures due to radon and thoron (^{222}Rn and ^{220}Rn): Do they differ in high and normal background radiation areas in India? J Environ Radioact 147: 125-129 (2015).

M33 Mishra, R., M. Joshi, O. Meisenberg et al. Deposition and spatial variation of thoron decay products in a thoron experimental house using the Direct Thoron Progeny Sensors. J Radiol Prot 37(2): 379-389 (2017).

M34 Mishra, R., R.P. Rout, R. Prajith et al. Dynamics and direct sensing of radon progeny. J Radioanal Nucl Chem 330(3): 1393-1396 (2021).

M35 MOE. Results of the internal exposure measurement using a whole-body counter. External Counting Survey. Ministry of the Environment, Government of Japan. [Internet] Available from (https://www.env.go.jp/en/chemi/rhm/basic-info/1st/10-07-03.html) on 12.02.2024.

M36 Moharram, B.M., M.N. Suliman, N.F. Zahran et al. ^{238}U, ^{232}Th content and radon exhalation rate in some Egyptian building materials. Annals Nucl Ener 45: 138-143 (2012).

M37 Mokrov, Y.G. and A.I. Alexakhin. Monitoring as the basis for ensuring safety of Karachay Lake closure implementation. Radioact Waste 3(4): 60-68 (2018). (Russian).

M38 Monahan, E., P. Murphy, S. Long et al. The effectiveness of passive sumps and static cowls in reducing radon levels in new build Irish dwellings. J Environ Radioact 248: 106866 (2022).

M39 Moshupya, P.M., S.C. Mohuba, T.A. Abiye et al. In situ determination of radioactivity levels and radiological doses in and around the gold mine tailing dams, Gauteng Province, South Africa. Minerals 12(10): 1295 (2022).

M40 Mrdakovic Popic, J., C.R. Bhatt, B. Salbu et al. Outdoor ^{220}Rn, ^{222}Rn and terrestrial gamma radiation levels: investigation study in the thorium rich Fen Complex, Norway. J Environ Monit 14(1): 193-201 (2012).

M41 Mrdakovic Popic, J., H. Haanes, C. Di Carlo et al. Tools for harmonized data collection at exposure situations with naturally occurring radioactive materials (NORM). Environ Int 175: 107954 (2023).

M42 Mrdakovic Popic, J., H. Knapstad, M. Nilsen et al. Regulatory control of naturally occurring radioactive material (NORM) in the Nordic countries: Report from working group Nordic NAT. 03:2023. Nordic Radiation and Nuclear Safety Series. The Swedish Radiation Safety Authority. The Radiation Safety Authorities in Denmark, Finland, Iceland, Norway and Sweden, Stockholm, 2023.

M43 Mrdakovic Popic, J., L. Urso and B. Michalik. Assessing the exposure situations with naturally occurring radioactive materials across European countries by means of the e-NORM survey. Sci Total Environ 905: 167065 (2023).

M44 Mueller, T.J., J.M. Steele and A.C. Gellender. Environmental monitoring and disposal of radioactive wastes from U.S. naval nuclear-powered ships and their support facilities. NT-20-1. United States Department of the Navy, Washington D.C., 2020.

M45 Murphy, P., A. Dowdall, S. Long et al. Estimating population lung cancer risk from radon using a resource efficient stratified population weighted sample survey protocol - Lessons and results from Ireland. J Environ Radioact 233: 106582 (2021).

M46 Musolino, S.V., N.A. Greenhouse and A.P. Hull. An estimate by two methods of thyroid absorbed doses due to BRAVO fallout in several Northern Marshall Islands. Health Phys 73(4): 651-662 (1997).

N1 Nagaoka, K., I. Hiraide, K. Sato et al. Nationwide measurements of cosmic-ray dose rates throughout Japan. Radiat Prot Dosim 132(4): 365-374 (2008).

N2 Nandakumaran, P. and N. Vinayachandran. A preliminary appraisal of radon concentration in groundwater from the High Background Radiation Area (HBRA) of Coastal Kerala. Geol Soc India 95(5): 491-496 (2020).

N3 Napier, B.A. Joint U.S./Russian studies of population exposures resulting from nuclear production activities in the southern Urals. Health Phys 106(2): 294-304 (2014).

N4 NAS. Airport passenger screening using backscatter X-ray machines: Compliance with standards. National Academies of Sciences, Engineering, Medicine. The National Academies Press, Washington, D.C., 2015.

N5 NAS. Molybdenum-99 for medical imaging. National Academies of Sciences, Engineering, Medicine. The National Academies Press, Washington, D.C., 2016.

N6 National Academy of Medical Sciences of Ukraine. Thirty five years of the Chornobyl disaster: Radiological and medical consequences, strategies of protection and revival. National Report of Ukraine 978-966-7656-14-0. (D.A. Bazyka et al., eds.). National Research Center of Radiation Medicine, Kyiv, 2022.

N7 Nazarbaev, N. and S. Hollingsworth. Scientific, technical and engineering work to ensure the safety of the former Semipalatinsk test site, Vol. III. Worldwide Promedia, London, 2017.

N8 Nazarbaev, N. and S. Hollingsworth. Scientific, technical and engineering work to ensure the safety of the former Semipalatinsk test site, Vol. II. Worldwide Promedia, London, 2017.

N9 NBH and K. Ulbak. The Thule accident: Assessment of radiation doses from terrestrial radioactive contamination. National Board of Health, Copenhagen, 2011.

N10 NCRP. Screening models for releases of radionuclides to atmosphere, surface water, and ground. NCRP Report No. 123-II. National Council on Radiation Protection and Measurements, Bethesda, 1996.

N11 NCRP. Screening of humans for security purposes using ionizing radiation scanning systems. NCRP Commentary No.16. National Council on Radiation Protection and Measurements, Bethesda, 2003.

N12 Nelson, K. and J.W. Baum. Health risk assessment of irradiated topaz. Nuclear Regulatory Commission, Washington, D.C., 1993.

N13 Nelson, V.A. Radiological survey of plants, animals, and soil in micronesia. Report No. NVO-0269-35. United States Department of Energy. Office of Scientific and Technical Information, Seattle, 1975.

N14 Németh, C., J. Somlai and B. Kanyár. Estimation of external irradiation of children due to the use of coal-slag as building material in Tatabánya, Hungary. J Environ Radioact 51(3): 371-378 (2000).

N15 Nguyen, M., E.C. Holmes and L.T. Angenent. The short-term effect of residential home energy retrofits on indoor air quality and microbial exposure: A case-control study. PLoS One 16(9): e0230700 (2021).

N16 Nguyễn, N.T.Á., D.O.N. Nguyễn-Thùy, H.Ó.N. Nguyễn-Văn et al. Radioactive thoron ^{220}Rn exhalation from unfired mud building material into room air of earthen dwellings. Front Earth Sci 9: 629241 (2021).

N17 Niedenthal, J. A history of the people of Bikini following nuclear weapons testing in the Marshall Islands: With recollections and views of elders of Bikini Atoll. Health Phys 73(1): 28-36 (1997).

N18 Njinga, R.L. and V.M. Tshivhase. Lifetime cancer risk due to gamma radioactivity in soils from Tudor Shaft mine environs, South Africa. J Radiat Res Appl Sci 9(3): 310-315 (2016).

N19 Njinga, R.L. and V.M. Tshivhase. Use of RESRAD-Onsite 7.2 code to assess environmental risk around Tudor Shaft mine tailing sites. Environ Nat Resour Res 8(3): 138-147 (2018).

N20 NNSA. China Nuclear and Radiation Safety Management System - General principles. National Nuclear Safety Administration. China Atomic Energy Authority. [Internet] Available from (http://www.caea.gov.cn/english/n6759372/c6809184/content.html) on 25.01.2024.

N21 NNSA. 2022 Annual Report. National Nuclear Safety Administration, The People's Republic of China, Beijing, 2022.

N22 NNSA. Annual reports archive. National Nuclear Safety Administration, Ministry of Ecology and Environment of the People's Republic of China. [Internet] Available from (https://nnsa.mee.gov.cn/english/resources/) on 25.01.2024.

N23 Nordyke, M.D. The Soviet program for peaceful uses of nuclear explosions. Sci Glob Secur 7(1): 1-117 (1998).

N24 Norris, R.S. and T.B. Cochran. United States Nuclear Tests July 1945 to 31 December 1992. Report No. NWD 94-1. Natural Resources Defense Council, Washington D.C., 1994.

N25 NRA. Environmental monitoring results and analyses – The 1st quarter of FY2023, Nuclear Regulation Authority, Japan, 2023.

N26 NRA. Nuclear Regulation Authority Library. [Internet] Available from (https://www.nra.go.jp/english/library/index.html#FDR) on 12.02.2024.

N27 NRC. Public Summary: The Health Effects of Exposure to Indoor Radon. in: Health Effects of Exposure to Radon: BEIR VI. National Academies Press, Washington D.C., 1999.

N28 NRC. Risk assessment of radon in drinking water. National Research Council, The National Academies Press, Washington D.C., 1999.

N29 NRC. Appendix C: Radioactivity in Guam after nuclear-weapons testing in the Pacific. pp. 359-366 in: Assessment of the Scientific Information for the Radiation Exposure Screening and Education Program. National Research Council, The National Academies Press, Washington D.C., 2005.

N30 NTI. China Submarine Capabilities. Nuclear Threat Initiative. [Internet] Available from (https://www.nti.org/analysis/articles/china-submarine-capabilities/) on 08.12.2023.

N31 Nuccetelli, C., Y. Pontikes, F. Leonardi et al. New perspectives and issues arising from the introduction of (NORM) residues in building materials: a critical assessment on the radiological behaviour. Const Build Mater 82: 323-331 (2015).

N32 Nugraha, E.D., M. Hosoda, Kusdiana et al. Comprehensive exposure assessments from the viewpoint of health in a unique high natural background radiation area, Mamuju, Indonesia. Sci Report 11(1): 14578 (2021).

N33 Nuhu, H., S. Hashim, M.S. Mohd Sanusi et al. Radiological assessment subjected to outdoor radon and thoron concentrations and terrestrial gamma radiation measurements in Perak Malaysia. Appl Radiat Isot 179: 109991 (2022).

N34 Nyambura, C., S. Tokonami, N.O. Hashim et al. Annual effective dose assessment due to radon and thoron progenies in dwellings of Kilimambogo, Kenya. J Radiat Prot Dosimetry 184(3-4): 430-434 (2019).

O1 O'Connor, B.H., A.M. Donoghue, T.J. Manning et al. Radiological assessment for bauxite mining and alumina refining. Ann Occup Hyg 57(1): 63-76 (2013).

O2 OECD. Decisions on the adoption of OECD legal instruments radiation protection standards for gaseous tritium light devices. Report No. OECD/LEGAL/0110. OECD Legal Instruments. Organisation for Economic Co-operation and Development, Vienna, 2022.

O3 OECD. Uranium 2022: Resources, production and demand. A joint report by the Nuclear Energy Agency and the International Atomic Energy Agency. Organisation for Economic Co-operation and Development, Vienna, 2023.

O4 OECD/NEA. Environmental remediation of uranium production facilities. A joint report by the OECD Nuclear Energy Agency and the International Atomic Energy Agency. Organisation for Economic Co-operation and Development, Paris, 2002.

O5 OECD/NEA. The supply of medical isotopes: An economic diagnosis and possible solutions. Organisation for Economic Co-operation and Development, Paris, 2019.

O6 Oluwatayo, I., C. Bonnie and S. John. A snapshot of United States PET cyclotron and radiopharmaceutical production operations and locations. J Nucl Med 53(suppl 1): 1085 (2012).

O7 Omori, Y., G. Prasad, A. Sorimachi et al. Long-term measurements of residential radon, thoron, and thoron progeny concentrations around the Chhatrapur placer deposit, a high background radiation area in Odisha, India. J Environ Radioact 162-163: 371-378 (2016).

O8 Omori, Y., S. Tokonami, S.K. Sahoo et al. Radiation dose due to radon and thoron progeny inhalation in high-level natural radiation areas of Kerala, India. J Radiol Prot 37(1): 111-126 (2017).

O9 OneGeology. Global lithological map. British Global Survey. [Internet] Available from (https://onegeology.org/) on 29.01.2024.

O10 ONR. The United Kingdom's seventh national report on compliance with the obligations of the Joint Convention on the Safety of Spent Fuel and on the Safety of Radioactive Waste Management. Office for Nuclear Regulation. UK Department for Business, Energy and Industrial Strategy, London, 2020.

O11 Ostroumova, E., A. Brenner, V. Oliynyk et al. Subclinical hypothyroidism after radioiodine exposure: Ukrainian-American cohort study of thyroid cancer and other thyroid diseases after the Chornobyl accident (1998-2000). Environ Health Perspect 117(5): 745-750 (2009).

O12 Othman, I. and M.S. Al-Masri. Impact of phosphate industry on the environment: A case study. J Appl Radiat Isot 65(1): 131-141 (2007).

O13 Outbakat, M.B., R. Choukr-Allah, M. El Gharous et al. Does phosphogypsum application affect salts, nutrients, and trace elements displacement from saline soils? Front Environ Sci 10 (2022).

O14 Owen, R. The Litvinenko Inquiry: Report into the death of Alexander Litvinenko. HC 695. House of Commons, London, UK, 2016.

P1 Pampuri, L., P. Caputo and C. Valsangiacomo. Effects of buildings' refurbishment on indoor air quality. Results of a wide survey on radon concentrations before and after energy retrofit interventions. Sustainable Cities and Society 42: 100-106 (2018).

P2 Pan, Z. Radiation exposures caused by the nuclear industry in China. Radiat Prot Dosim 62(4): 245-254 (1995).

P3 Pan, Z., W. Zhibo, C. Zhuzhou et al. Radiological environmental impact of the nuclear industry in China. Health Phys 71(6): 847-862 (1996).

P4 Pan, Z. and S. Liu. Radiation level in China. China Atomic Energy Publishing and Media Ltd, Beijing, 2011.

P5 Pan, Z., S. Liu and X. Su. Radiation levels and effects in China. China Atomic Energy Publishing and Media Ltd, Beijing, 2024. (Chinese).

P6 Panchenko, S.V., M.V. Vedernikova, I.I. Linge et al. Radioecological situation in regions of State Atomic Energy Corporation Rosatom enterprises location. RIBRAE RAS, 2021. (Russian).

P7 Panitskiy, A.V. and S.N. Lukashenko. Nature of radioactive contamination of components of ecosystems of streamflows from tunnels of Degelen massif. J Environ Radioact 144: 32-40 (2015).

P8 Panwar, P., M. Prasad and R.C. Ramola. Study of soil-gas and indoor radon concentration in a test village at Tehri Garhwal, India. J Radioanal Nucl Chem 330(3): 1383-1391 (2021).

P9 Paridaens, J. and H. Vanmarcke. Radiological impact of almost a century of phosphate industry in Flanders, Belgium. Health Phys 95(4): 413-424 (2008).

P10 Pasztor, L., K.Z. Szabo, G. Szatmari et al. Mapping geogenic radon potential by regression kriging. Sci Total Environ 544: 883-891 (2016).

P11 Patton Schell, T. Governing uranium in China. DIIS Report 2014:03. Stockholm International Peace Institute. Danish Institute for International Studies (DIIS), Copenhagen, Denmark, 2014.

P12 Paul, M., B. Likar, Z. Logar et al. The remediation of a uranium mining and milling site in Slovenia. pp. 229-238 in: Uranium, Mining and Hydrogeology. (B.J. Merkel and A. Hasche-Berger, eds.). Springer Berlin Heidelberg, Berlin, 2008.

P13 PCAire. Predictive Code for Aircrew Radiation Exposure (PCAIRE) system. PCAire Inc. [Internet] Available from (https://commercial.pcaire.com/) on 07.03.2024.

P14 Pereira, A.J., M.M. Godinho and L.J. Neves. On the influence of faulting on small-scale soil-gas radon variability: A case study in the Iberian uranium province. J Environ Radioact 101(10): 875-882 (2010).

P15 Pereira, R., S. Barbosa and F.P. Carvalho. Uranium mining in Portugal: A review of the environmental legacies of the largest mines and environmental and human health impacts. Environ Geochem Health 36(2): 285-301 (2014).

P16 Pereira, W.S., A. Kelecom, A.X. da Silva et al. Assessment of uranium release to the environment from a disabled uranium mine in Brazil. J Environ Radioact 188: 18-22 (2018).

P17 Peremyslova, L.M., V.A. Kostyuchenko, I.Y. Popova et al. Intake of ^{90}Sr and ^{137}Cs with the diet, internal irradiation public doses on the territory of the Karachay trace for 1967-2001. Radiat Safe Iss 3: 32-41 (2003). (Russian).

P18 Perrier, F., P. Richon and J.C. Sabroux. Temporal variations of radon concentration in the saturated soil of Alpine grassland: The role of groundwater flow. Sci Total Environ 407(7): 2361-2371 (2009).

P19 Petermann, E. and P. Bossew. Mapping indoor radon hazard in Germany: The geogenic component. Sci Total Environ 780: 146601 (2021).

P20 Petermann, E., H. Meyer, M. Nussbaum et al. Mapping the geogenic radon potential for Germany by machine learning. Sci Total Environ 754: 142291 (2021).

P21 Petoussi-Henss, N., H. Schlattl, M. Zankl et al. Organ doses from environmental exposures calculated using voxel phantoms of adults and children. Phys Med Biol 57(18): 5679-5713 (2012).

P22 Petrescu, D.C., R.M. Petrescu-Mag and A.R. Tenter. The little Chernobyl of Romania: The legacy of a uranium mine as negotiation platform for sustainable development and the role of new ethics. J Agri Environ Ethics 32(1): 51-75 (2019).

P23 Phipps, A.W., G.M. Kendall, J.W. Stather et al. Committed equivalent organ doses and committed effective doses from intakes of radionuclides. Technical Report NRPB-M-288. National Radiological Protection Board, Chilton, 1991.

P24 Pigg, S., D. Cautley and P.W. Francisco. Impacts of weatherization on indoor air quality: A field study of 514 homes. Indoor Air 28(2): 307-317 (2018).

P25 Pinto, P.V., K. Sudeep Kumara and N. Karunakara. Mass exhalation rates, emanation coefficients and enrichment pattern of radon, thoron in various grain size fractions of monazite rich beach placers. Radiat Meas 130: 106220 (2020).

P26 Pinto, R., Z. Oliveira, C. Diamantino et al. Passive treatment of radioactive mine water in Urgeirica uranium mine, Portugal. Conference Proceedings of IMWA 2016: Mining Meets Water-Conflicts and Solutions, Leipzig, Germany, 11–15 July 2016.

P27 Pires do Rio, M.A., E.C. Amaral, H.M. Fernandes et al. Environmental radiological impact associated with non-uranium mining industries: a proposal for screening criteria. J Environ Radioact 59(1): 1-17 (2002).

P28 Podtesov, G.N., A.V. Akleyev and A.Y. Davankov. Chelyabinsk Region: Elimination of Consequences of Radiation Accidents. South Ural Book Publishing House, 2006. (Russian).

P29 Pohll, G. and K. Pohlmann. Evaluation of the radionuclide tracer test conducted at the project Gnome underground nuclear test site, New Mexico. Report No. DOE/NV/11508-08. Nevada University. Desert Research Institute, Las Vegas, NV, 1996.

P30 Polivkina, Y.N., N.V. Larionova, S.N. Lukashenko et al. Assessment of the tritium distribution in the vegetation cover in the areas of underground nuclear explosions at the Semipalatinsk test site. J Environ Radioact 237: 106705 (2021).

P31 Porter, S.J. and A.S. Grigoriev. Successful Recovery and Decommissioning of Russian RTGs: A Cooperative International Effort. Conference of the Institute of Nuclear Material Management, Atlanta, GA, 24–28 July 2016. Lawrence Livermore National Laboratory.

P32 Potischman, N., S.I. Salazar, M.A. Scott et al. Methods and findings on diet and lifestyle used to support estimation of radiation doses from radioactive fallout from the trinity nuclear test. Health Phys 119(4): 390-399 (2020).

P33 Powers, C.W., J. Burger, D. Kosson et al. Amchitka independent science assessment: Biological and geophysical aspects of potential radionuclide exposure in the Amchitka marine environment. Consortium for Risk Evaluation with Stakeholders Participation II, Piscataway, NJ, 2005.

P34 Prasad, G., T. Ishikawa, M. Hosoda et al. Estimation of radon diffusion coefficients in soil using an updated experimental system. Rev Sci Instrum 83(9): 093503 (2012).

P35 Prasad, M., M. Rawat, A. Dangwal et al. Measurements of radon and thoron progeny concentrations in dwellings of Tehri Garhwal, India, using LR-115 deposition-based DTPS/DRPS technique. Radiat Prot Dosimetry 167(1-3): 102-106 (2015).

P36 Prasad, M., P. Bossew, G. Anil Kumar et al. Dose assessment from the exposure to attached and unattached progeny of radon and thoron in indoor environment. Acta Geophysica 66(5): 1187-1194 (2018).

P37 Pressyanov, D., D. Dimitrov and I. Dimitrova. Energy-efficient reconstructions and indoor radon: the impact assessed by CDs/DVDs. J Environ Radioact 143: 76-79 (2015).

P38 Prince, J.F., M.L. Smits, G.C. Krijger et al. Radiation emission from patients treated with holmium-166 radioembolization. J Vasc Interv Radiol 25(12): 1956-1963.e1951 (2014).

P39 Pyngrope, A., A. Khardewsaw, Y. Sharma et al. Study of indoor radon, thoron and their progeny in south west Khasi Hills district of Meghalaya, India. Radiat Prot Dosim 189(3): 347-353 (2020).

Q1 Qamouche, K., A. Chetaine, A. Elyahyaoui et al. Radiological characterization of phosphate rocks, phosphogypsum, phosphoric acid and phosphate fertilizers in Morocco: An assessment of the radiological hazard impact on the environment. Materials Today: Proceedings 27(4): 3234-3242 (2020).

Q2 Quindós Poncela, L.S., P.L. Fernández Navarro, J. Gómez Arozamena et al. Population dose in the vicinity of old Spanish uranium mines. Sci Total Environ 329(1): 283-288 (2004).

Q3 Quinn, V.E. Analysis of meteorological and radiological data for selected fallout episodes. Health Phys 59(5): 577-592 (1990).

R1 Rademacher, S.E. Plutonium exposures to personnel assigned to Johnston Atoll. U.S. Air Force Safety Center, Kirtland, TX, 2016.

R2 Rahman, S., N. Mati, Matiullah et al. Radon exhalation rate from the soil, sand and brick samples collected from NWFP and FATA, Pakistan. Radiat Prot Dosim 124(4): 392-399 (2007).

R3 Rajaretnam, G. and H.B. Spitz. Effect of leachability on environmental risk assessment for naturally occurring radioactive materials in petroleum oil fields. Health Phys 78(2): 191-198 (2000).

R4 Ram, R., N.D. Owen, C. Kalnins et al. Understanding the mobility and retention of uranium and its daughter products. J Hazard Mater 410: 124553 (2021).

R5 Ramachandran, T.V. Environmental thoron ^{220}Rn : A review. Int J Radiat Res 8(3): 129-147 (2010).

R6 Ramola, R.C., G. Prasad, G.S. Gusain et al. Preliminary indoor thoron measurements in high radiation background area of southeastern coastal Orissa, India. Radiat Prot Dosim 141(4): 379-382 (2010).

R7 Ramzaev, V., A. Mishine, L. Basalaeva et al. Radiostrontium hot spot in the Russian Arctic: Ground surface contamination by ^{90}Sr at the "Kraton-3" underground nuclear explosion site. J Environ Radioact 95(2-3): 107-125 (2007).

R8 Ramzaev, V., V.S. Repin and E.V. Khramtsov. Peaceful underground nuclear explosions: Current issues in radiation protection for the general public. Radiat Hygiene 2(2): 27-33 (2009). (Russian).

R9 Ramzaev, V., V. Repin, A. Medvedev et al. Radiological investigations at the "Taiga" nuclear explosion site: Site description and in situ measurements. J Environ Radioact 102(7): 672-680 (2011).

R10 Ramzaev, V.P., A.M. Biblin, V.S. Repin et al. Tritium contamination of surface and ground waters at the “Dnepr” peaceful underground nuclear explosions site. Radiat Hygiene 15(1) (2022). (Russian).

R11 Ran, Y., S. Wang, Y. Zhao et al. A review of biological effects and treatments of inhaled depleted uranium aerosol. J Environ Radioact 222: 106357 (2020).

R12 Rangaswamy, D.R., S. Suresh, E. Srinivasa et al. Estimation of radiological dose due to radon, thoron and their progeny in indoor atmosphere of Shivamogga district, Karnataka, India. J Radioanal Nucl Chem 332(6): 2379-2388 (2023).

R13 Rani, S., S. Kansal, A.K. Singla et al. Investigation of indoor ^{222}Rn, ^{220}Rn and their progeny in Punjab, northwestern India. J Radioanal Nucl Chem 332(1): 1-13 (2023).

R14 Razafindramiandra, H.A., T.H. Randriamora, M. Rasolonirina et al. Public exposure due to natural radioactivity in Madagascar uranium zone using direct and indirect method, case of Vatovory abandoned site and its surroundings. Radiat Sci Technol 3(6): 60-67 (2017).

R15 Regenspurg, S., J. Dilling, J. Mielcarek et al. Naturally occurring radionuclides and their geochemical interactions at a geothermal site in the North German basin. Environ Earth Sci 72(10): 4131-4140 (2014).

R16 RERF. US-Japan joint reassessment of atomic bomb radiation dosimetry in Hiroshima and Nagasaki. Radiation Effects Research Foundation, Hiroshima, 1987.

R17 RERF. RERF Library. Radiation Effects Research Foundation. [Internet] Available from (https://www.rerf.or.jp/en/) on 22.02.2024.

R18 Rezaie, F., M. Panahi, S.M. Bateni et al. Spatial modeling of geogenic indoor radon distribution in Chungcheongnam-do, South Korea using enhanced machine learning algorithms. Environ Int 171: 107724 (2023).

R19 Riesenfeld, E.P., T.W. Marcy, K. Reinier et al. Radon awareness and mitigation in Vermont: A public health survey. Health Phys 92(5): 425-431 (2007).

R20 Riley, W.J., A.J. Gadgil, Y.C. Bonnefous et al. The effect of steady winds on radon-222 entry from soil into houses. Atmos Environ 30(7): 1167-1176 (1996).

R21 Ringer, W. Monitoring trends in civil engineering and their effect on indoor radon. Radiat Prot Dosim 160(1-3): 38-42 (2014).

R22 Robinson, A.L., R.G. Sextro and W.J. Riley. Soil-gas entry into houses driven by atmospheric pressure fluctuations—The influence of soil properties. Atmos Environ 31(10): 1487-1495 (1997).

R23 Robison, W.L., K.T. Bogen and C.L. Conrado. An updated dose assessment for resettlement options at Bikini Atoll—a U.S. nuclear test site. Health Phys 73(1): 100-114 (1997).

R24 Robison, W.L., V.E. Noshkin, C.L. Conrado et al. Northern Marshall Islands radiological survey: Data and dose assessments. Health Phys 73(1): 37-48 (1997).

R25 Robison, W.L. and T.F. Hamilton. Radiation doses for Marshall Islands Atolls affected by U.S. nuclear testing: All exposure pathways, remedial measures, and environmental loss of ^{137}Cs. Health Phys 98(1): 1-11 (2010).

R26 Rochedo, E.R.R. and L.M.H. Vasconcellos. Effluent control for the uranium mine area at Pocos de Caldas, Brazil. Fourth International Congress on Radiological Protection, Rio de Janeiro, Brazil, 2–5 November 2005.

R27 Roessler, C.E., R. Kautz, W.E. Bolch, Jr. et al. The effect of mining and land reclamation on the radiological characteristics of the terrestrial environment of Florida's phosphate regions. Conference on Natural Radiation Environment III, Houston, TX, 23–28 April 1978.

R28 Romanov, G.N., G.P. Shejn and G.M. Aksenov. Exposure doses for the population living on East-Urals radioactive trace: Current estimates. Radiat Saf Probl (Mayak Prod Assoc Sci J) 4: 52-67 (1997). (Russian).

R29 ROSATOM. Performance of State Atomic Energy Corporation ROSATOM in 2020. State Atomic Energy Corporation Rosatom, Moscow, 2021.

R30 Rudakov, D., D. Pikarenia, O. Orlinska et al. A predictive assessment of the uranium ore tailings impact on surface water contamination: Case study of the city of Kamianske, Ukraine. J Environ Radioact 268-269: 107246 (2023).

R31 Russian Federation. Decree of the Government of the Russian Federation, Rule No. 1069 dated 19.10.2012 (as amended on 29.10.2022) Russian Federation, 2012. (Russian).

R32 Russian Federation. The sixth national report of the Russian Federation on compliance with the obligations of the Joint Convention on the Safety of Spent Fuel Management and the Safety of Radioactive Waste Management. State Atomic Energy Corporation ROSATOM, Federal Environmental, Industrial and Nuclear Supervision Service, Moscow, 2020.

S1 Sabbarese, C., F. Ambrosino and A. D'Onofrio. Development of radon transport model in different types of dwellings to assess indoor activity concentration. J Environ Radioact 227: 106501 (2021).

S2 Sahoo, B.K., B.K. Sapra, J.J. Gaware et al. A model to predict radon exhalation from walls to indoor air based on the exhalation from building material samples. Sci Total Environ 409(13): 2635-2641 (2011).

S3 Saïdou, S. Tokonami, M. Hosoda et al. From radon and thoron measurements, inhalation dose assessment to national regulation and radon action plan in Cameroon. J Radiat Prot Res 47(4): 237-245 (2022).

S4 Sainz, C., L.S. Quindos, P.L. Fernandez et al. High background radiation areas: The case of Villar de la Yegua village (Spain). Radiat Prot Dosim 125(1-4): 565-567 (2007).

S5 Sainz, C., J.L. Gutiérrez-Villanueva, I. Fuente et al. Two significant experiences related to radon in a high risk area in Spain. Nukleonika 55(4): 513-518 (2010).

S6 Sajwan, R.S., V. Joshi, N. Kumar et al. Study of radiation exposure due to indoor radon, thoron and progeny in Ghuttu, Tehri Garhwal, India. J Radioanal Nucl Chem 330(3): 1497-1507 (2021).

S7 Sakoda, A., Y. Ishimori and K. Yamaoka. A comprehensive review of radon emanation measurements for mineral, rock, soil, mill tailing and fly ash. Appl Radiat Isot 69(10): 1422-1435 (2011).

S8 Sakr, S., K. Inoue, A. Mohamed et al. Distribution of natural radionuclides in NORM samples from North Abu Rusheid area, Egypt. J Environ Radioact 266-267: 107240 (2023).

S9 Salama, E., S.U. El-Kameesy and R. Elrawi. Depleted uranium assessment and natural radioactivity monitoring in North West of Iraq over a decade since the last Gulf War. J Environ Radioact 201: 25-31 (2019).

S10 Salbu, B., M. Burkitbaev, G. Stromman et al. Environmental impact assessment of radionuclides and trace elements at the Kurday U mining site, Kazakhstan. J Environ Radioact 123: 14-27 (2013).

S11 Sancho, C. and R. García-Tenorio. Radiological evaluation of the transuranic remaining contamination in Palomares (Spain): A historical review. J Environ Radioact 203: 55-70 (2019).

S12 Sannappa, J., M.S. Chandrashekara and L. Paramesh. Spatial distribution of radon and thoron concentrations indoors and their concentrations in different rooms of buildings. Indoor Built Environ 15(3): 283-288 (2016).

S13 Sanusi, M.S.M., W. Hassan, S. Hashim et al. Tabulation of organ dose conversion factors for terrestrial radioactivity monitoring program. Appl Radiat Isot 174: 109791 (2021).

S14 Sathish, L.A., K. Nagaraja and T.V. Ramachandran. Indoor ^{222}Rn and ^{220}Rn concentrations and doses in Bangalore, India. Radiat Prot Dosim 151(2): 344-353 (2012).

S15 Sato, T. Analytical model for estimating terrestrial cosmic ray fluxes nearly anytime and anywhere in the world: Extension of PARMA/EXPACS. PLoS One 10(12): e0144679 (2015).

S16 Sato, T. Evaluation of world population-weighted effective dose due to cosmic ray exposure. Sci Rep 6: 33932 (2016).

S17 Sato, T. Analytical model for estimating the zenith angle dependence of terrestrial cosmic ray fluxes. PLoS One 11(8) (2016).

S18 Saueia, C.H. and B.P. Mazzilli. Distribution of natural radionuclides in the production and use of phosphate fertilizers in Brazil. J Environ Radioact 89(3): 229-239 (2006).

S19 Saunier, O., D. Didier, A. Mathieu et al. Atmospheric modeling and source reconstruction of radioactive ruthenium from an undeclared major release in 2017. Proc Natl Acad Sci 116(50): 24991-25000 (2019).

S20 Schiavina, M., S. Freire and K. MacManus. GHS population grid multitemporal (1975-2030), European Commission, Joint Research Centre (JRC), 2022.

S21 Schneider, S., D.C. Kocher, G.D. Kerr et al. Systematic radiological assessment of exemptions for source and byproduct materials. NUREG-1717. U.S. Nuclear Regulatory Commission, Office of Nuclear Regulatory Research, Washington, D.C., 2001.

S22 Schoengold, C.R., M.E. DeMarre and E.M. Kirkwood. Radiological effluents released from U.S. continental tests 1961 through 1992. United States Department of Energy, Las Vegas, NV, 1996.

S23 Schubert, M., A. Musolff and H. Weiss. Influences of meteorological parameters on indoor radon concentrations (^{222}Rn) excluding the effects of forced ventilation and radon exhalation from soil and building materials. J Environ Radioact 192: 81-85 (2018).

S24 Seco, S.L.R., F.P. Domingos, A. Pereira et al. Estimation of the radon production potential in sedimentary rocks: A case study in the lower and middle Jurassic of the Lusitanian Basin (Portugal). J Environ Radioact 220-221: 106272 (2020).

S25 Semwal, P., T.K. Agarwal, M. Joshi et al. Effective dose estimation of radon, thoron and their progeny concentrations in the environs of Himalayan belt, India. Intl J Environ Sci Technol 20(4): 4127-4138 (2022).

S26 Sengul, H., A.K. Ozer and M.S. Gulaboglu. Beneficiation of Mardin-Mazıdağı () calcareous phosphate rock using dilute acetic acid solutions. Chem Eng J 122(3): 135-140 (2006).

S27 Seymour, A.H. and V.A. Nelson. Radionuclides in air, water, and biota. pp.579-613. Energy Research and Development Administration, Technical Information Center, A. Environment of Amchitka Island, Alaska, 1977.

S28 Shagina, N.B., M.I. Vorobiova, M.O. Degteva et al. Reconstruction of the contamination of the Techa River in 1949-1951 as a result of releases from the "Mayak" production association. Radiat Environ Biophys 51(4): 349-366 (2012).

S29 Shagina, N.B., E.I. Tolstykh, M.O. Degteva et al. Age and gender specific biokinetic model for strontium in humans. J Radiol Prot 35(1): 87-127 (2015).

S30 Shaikh, F. Pakistan's nuclear bomb: Beyond the non-proliferation regime. Oxford Journals 78(1): 29-48 (2002).

S31 Sharma, S., A. Kumar, R. Mehra et al. Assessment of progeny concentrations of ^{222}Rn/^{220}Rn and their related doses using deposition-based direct progeny sensors. Environ Sci Pollut Res Int 25(12): 11440-11453 (2018).

S32 Sharma, S., R.K. Sharma and R.K. Singh. Mayapuri radiological catastrophe: good practices and the lessons learnt. Curr Radiopharm 15(1): 21-31 (2022).

S33 Shiozawa, Y. and T. Wadas. A targeted alpha-particle radiopharmaceutical for bone metastatic breast cancer. U.S. Army Medical Research and Materiel Command, Maryland, 2021.

S34 Shishkina, E.A., B.A. Napier, D.L. Preston et al. Dose estimates and their uncertainties for use in epidemiological studies of radiation-exposed populations in the Russian Southern Urals. PLoS One 18(8): e0288479 (2023).

S35 Sibley, T.H. and L.D. Tornberg. Amchitka radiobiological program, final report July 1970 to December 1979. United States Department of Energy, Seattle, 1982.

S36 Sikka, S.K. and A. Kakodkar. Some preliminary results of May 11-13, 1998: Nuclear detonations at Prokhran. BARC Newsletter 172: 1-4 (1998).

S37 Simion, E., I. Mihalcea, V. Cuculeanu et al. Dynamics of outdoor radon and thoron progeny concentrations in some geographical areas of Romania. Rom J Phys 58(Suppl): S251-S261 (2013).

S38 Simon, S.L. A brief history of people and events related to atomic weapons testing in the Marshall Islands. Health Phys 73(1): 5-20 (1997).

S39 Simon, S.L. and J.C. Graham. Findings of the first comprehensive radiological monitoring program of the Republic of the Marshall Islands. Health Phys 73(1): 66-85 (1997).

S40 Simon, S.L. and W.L. Robison. A compilation of nuclear weapons test detonation data for U.S. Pacific ocean tests. Health Phys 73(1): 258-264 (1997).

S41 Simon, S.L. and A. Bouville. Radiation doses to local populations near nuclear weapons test sites worldwide. Health Phys 82(5): 706-725 (2002).

S42 Simon, S.L., A. Bouville, C.E. Land et al. Radiation doses and cancer risks in the Marshall Islands associated with exposure to radioactive fallout from Bikini and Enewetak nuclear weapons tests: Summary. Health Phys 99(2): 105-123 (2010).

S43 Simon, S.L., A. Bouville, D. Melo et al. Acute and chronic intakes of fallout radionuclides by Marshallese from nuclear weapons testing at Bikini and Enewetak and related internal radiation doses. Health Phys 99(2): 157-200 (2010).

S44 Simon, S.L. Introduction to the Trinity Nuclear Test Collection of Papers. Health Phys 119(4): 389 (2020).

S45 Simon, S.L., A. Bouville, H.L. Beck et al. Estimated radiation doses received by New Mexico residents from the 1945 Trinity Nuclear Test. Health Phys 119(4): 428-477 (2020).

S46 Simon, S.L., A. Bouville, H.L. Beck et al. Dose estimation for exposure to radioactive fallout from nuclear detonations. Health Phys 122(1): 1-20 (2022).

S47 Singh, B., K. Kant and M. Garg. Radiological assessment of ^{222}Rn, ^{220}Rn, EERC, and EETC in residential dwellings of district Palwal, Southern Haryana, India. J Radioanal Nucl Chem 331(2): 701-713 (2022).

S48 Singh, B. and K. Kant. Annual effective dose due to inhalation of indoor radionuclides and their progeny measured by track etched techniques using pinhole dosimeter and deposition-based progeny sensors. J Radioanal Nucl Chem 332: 3121-3131 (2023).

S49 Singh, P., P. Singh, S. Singh et al. A study of indoor radon, thoron and their progeny measurement in Tosham region Haryana, India. J Radiat Res Appl Sci 8(2): 226-233 (2015).

S50 Singla, A.K., S. Kansal and R. Mehra. Dose distribution to individual tissues and organs due to exposure of alpha energies from radon and thoron to local population of Hanumangarh, Rajasthan, India. J Radioanal Nucl Chem 327(3): 1073-1085 (2021).

S51 SKB. Safety analysis for SFR long-term safety. Technical Report TR-14-01. Main report for the safety assessment SR-PSU. Swedish Nuclear Fuel and Waste Management Co, Stockholm, 2015.

S52 SKB. Low and intermediate level waste in SFR. Report No. R-15-15. Reference inventory for waste 2013. Swedish Nuclear Fuel and Waste Management Co, Stockholm, 2015.

S53 Skeppstrom, K. and E. Wahlin. Is thoron a problem in Swedish dwellings? Results of measurements of concentrations of thoron and its progeny. Radiat Prot Dosim 167(1-3): 107-110 (2015).

S54 Skipperud, L., A.G. Jorgensen, L.S. Heier et al. Po-210 and Pb-210 in water and fish from Taboshar uranium mining Pit Lake, Tajikistan. J Environ Radioact 123: 82-89 (2013).

S55 Slezakova, M., K. Navratilova Rovenska, L. Tomasek et al. Short- and long-term variability of radon progeny concentration in dwellings in the Czech Republic. Radiat Prot Dosim 153(3): 334-341 (2013).

S56 Smetsers, R.C.G.M., R.O. Blaauboer and S.A.J. Dekkers. Ingredients for a Dutch radon action plan, based on a national survey in more than 2500 dwellings. J Environ Radioact 165: 93-102 (2016).

S57 Sneve, M.K. Remote Control: Decommissioning RTGs. IAEA Bulletin 48(1): 42-43 (2006).

S58 Sneve, M.K. and V. Reka. Upgrading the regulatory framework of the Russian Federation for the safe decommissioning and disposal of radioisotope thermoelectric generators. Final project report. Norwegian Radiation Protection Authority, Rostechnadzor, Oslo, 2007.

S59 Song, G., X. Wang, D. Chen et al. Contribution of ^{222}Rn-bearing water to indoor radon and indoor air quality assessment in hot spring hotels of Guangdong, China. J Environ Radioact 102(4): 400-406 (2011).

S60 Sprague, B.L., K.P. Lowry, D.L. Miglioretti et al. Changes in mammography use by women's characteristics during the first 5 months of the COVID-19 pandemic. J Natl Cancer Inst 113(9): 1161-1167 (2021).

S61 Stahmer, U. Generic transportation worker dose assessment. Report No. NWMO TR-2014017. Nuclear Waste Management Organisation, Toronto, 2014.

S62 Stahmer, U. Assessing radiological dose to members of the public and workers during used nuclear fuel transportation. Eighteenth International Symposium on the Packaging and Transportation of Radioactive Materials (PATRAM) Kobe, Japan, 18–23 September 2016.

S63 Stanley, F.K.T., J.L. Irvine, W.R. Jacques et al. Radon exposure is rising steadily within the modern North American residential environment, and is increasingly uniform across seasons. Sci Rep 9(1): 18472 (2019).
S64 Steck, D.J. Annual average indoor radon variations over two decades. Health Phys 96(1): 37-47 (2009).
S65 Steck, D.J. Pre- and post- market measurements of gamma radiation and radon emanation from a large sample of decorative granite. Nineteenth International Radon Symposium: Gateway to the Future, St. Louis, MO, 20–23 September 2009. American Association of Radon Scientists and Technologists.
S66 Steck, D.J. The effectiveness of mitigation for reducing radon risk in single-family Minnesota homes. Health Phys 103(3): 241-248 (2012).
S67 Stegnar, P., I. Shishkov, M. Burkitbayev et al. Assessment of the radiological impact of gamma and radon dose rates at former U mining sites in Central Asia. J Environ Radioact 123: 3-13 (2013).
S68 Stewart, D.I., M. Csõvári, C.S. Barton et al. Performance of a functionalised polymer-coated silica at treating uranium contaminated groundwater from a Hungarian mine site. Eng Geol 85(1): 174-183 (2006).
S69 Stezhko, V.A., E.E. Buglova, L.I. Danilova et al. A cohort study of thyroid cancer and other thyroid diseases after the Chornobyl accident: Objectives, design and methods. Radiat Res 161(4): 481-492 (2004).
S70 Stocker, T., R. Purtschert, T. Wagner et al. Kohlenstoff-14, Krypton-85, Argon-37. Umweltradioaktivität und Strahlendosen in der Schweiz 2019. pp.116-127. Bundesamt für Gesundheit Abteilung Strahlenschutz Bern, 2022. (German).
S71 Stojanovska, Z., J. Januseski, P. Bossew et al. Seasonal indoor radon concentration in FYR of Macedonia. Radiat Meas 46(6-7): 602-610 (2011).
S72 Stojanovska, Z., P. Bossew, S. Tokonami et al. National survey of indoor thoron concentration in FYR of Macedonia (continental Europe–Balkan region). Radiat Meas 49: 57-66 (2013).
S73 Studenski, M.T. Effective dose to patients and staff when using a mobile PET/SPECT system. J Appl Clin Med Phys 14(3): 215-225 (2013).
S74 Sulaiman, I. and M. Omar. Environmental radon/thoron concetrations and radiation levels in Sarawak and Sabah. J Nucl Rel Technol 7(1) (2010).
S75 Sun, L.C., C.B. Meinhold, A.R. Moorthy et al. Assessment of plutonium exposure in the Enewetak population by urinalysis. Health Phys 73(1): 127-132 (1997).
S76 Sundal, A.V., C.L. Jensen, K. Anestad et al. Anomalously high radon concentrations in dwellings located on permeable glacial sediments. J Radiol Prot 27(3): 287-298 (2007).
S77 Sundal, A.V., V. Valen, O. Soldal et al. The influence of meteorological parameters on soil radon levels in permeable glacial sediments. Sci Total Environ 389(2-3): 418-428 (2008).
S78 Sundell-Bergman, S., R. Avila, I. de la Cruz et al. Assessing the impact of releases of radionuclides into sewage systems in urban environment–simulation, modelling and experimental studies studies–LUCIA. NKS Series no. 192. Nordisk Kernesikkerhedsforskning, Roskilde, 2009.
S79 Suric Mihic, M., I. Beslic, S. Davila et al. Estimation of airborne ^{106}Ru activity concentration from total beta activity of Pm10 particle fractions. Radiat Prot Dosim 189(4): 497-504 (2020).
S80 Suzuki, G., I. Yamaguchi, H. Ogata et al. A nation-wide survey on indoor radon from 2007 to 2010 in Japan. J Radiat Res 51(6): 683-689 (2010).
S81 Suzuki, Y., N. Tanaka and H. Akiyama. Attempt of Bayesian estimation from left-censored data using the markov chain monte carlo method: Exploring Cr(VI) concentrations in mineral water products. Food Safety 8(4): 67-89 (2020).
S82 Sweden. Seventh national report under the Joint Convention on the Safety of Spent Fuel Management and on the Safety of Radioactive Waste Management. DS 2020:21. Sweden's implementation of the obligations of the Joint Convention. Government Offices of Sweden, Ministry of Environment, Stockholm, 2020.
S83 Swordy, S.P. The energy spectra and anisotropies of cosmic rays. Space Sci Rev 99(1): 85-94 (2001).

S84 Symonds, P., D. Rees, Z. Daraktchieva et al. Home energy efficiency and radon: An observational study. Indoor Air 29(5): 854-864 (2019).
S85 Synnott, H., P.A. Colgan, O. Hanley et al. The effectiveness of radon remediation in Irish Schools. Health Phys 92(1): 50-57 (2007).
S86 Syuryavin, A.C., S. Park, M.M. Nirwono et al. Indoor radon and thoron from building materials: Analysis of humidity, air exchange rate, and dose assessment. Nucl Eng Technol 52(10): 2370-2378 (2020).
S87 Szerbin, P. Radon concentrations and exposure levels in Hungarian caves. Health Phys 71(3): 362-369 (1996).
T1 Taylor, N., D. Baker, S. Ciattaglia et al. Updated safety analysis of ITER. Fusion Eng Des 86(6): 619-622 (2011).
T2 Taylor, N., S. Ciattaglia, P. Cortes et al. ITER safety and licensing update. Fusion Eng Des 87(5): 476-481 (2012).
T3 Tchorz-Trzeciakiewicz, D.E. and A.T. Solecki. Seasonal variation of radon concentrations in atmospheric air in the Nowa Ruda area (Sudety Mountains) of southwest Poland. Geochem J 45: 455-461 (2011).
T4 Tchorz-Trzeciakiewicz, D.E. and A.T. Solecki. Variations of radon concentration in the atmosphere. Gamma dose rate. Atmos Environ 174: 54-65 (2018).
T5 Teegarden, B.J. Cosmic-ray production of deuterium and tritium in the Earth's atmosphere. J Geophys Res 72(19): 4863-4868 (1967).
T6 Teller, E. Plowshare. Report No. UCRL-7222. University of California, Livermore, 1963.
T7 TEPCO. Partial revision of the application for approval to amend the implementation plan for Fukushima Daiichi Nuclear Power Station as specified nuclear facility. FDEC-R4-69. Tokyo Electric Power Company Holdings Inc., Tokyo, 2022.
T8 TEPCO. Observation data - Fukushima Daiichi Nuclear Power Station. Tokyo Electric Power Company Holdings. [Internet] Available from (https://www.tepco.co.jp/en/hd/decommission/data/index-e.html) on 12.02.2024.
T9 Thiessen, K.M., F.O. Hoffman, A. Bouville et al. Parameter values for estimation of internal doses from ingestion of radioactive fallout from nuclear detonations. Health Phys 122(1): 236-268 (2022).
T10 Till, J.E., S.L. Simon, R. Kerber et al. The Utah thyroid cohort study: Analysis of the dosimetry results. Health Phys 68(4): 472-483 (1995).
T11 Titov, A.V., N.K. Shandala, D.V. Isaev et al. Radiation survey in the area of peaceful nuclear explosion "Takhta-Kugulta". Med Radiol Radiat Saf 66(2): 13-22 (2021).
T12 Tokonami, S. Characteristics of thoron (^{220}Rn) and its progeny in the indoor environment. Int J Environ Res Public Health 17(23): 8769 (2020).
T13 Tolstykh, E.I., M.O. Degteva, L.M. Peremyslova et al. Reconstruction of long-lived radionuclide intakes for Techa riverside residents: Strontium-90. Health Phys 101(1): 28-47 (2011).
T14 Tolstykh, E.I., N.G. Bugrov, V.A. Krivoshchapov et al. Results of lifetime measurements of strontium-90 content in the body of residents of the Ural region: Analysis of data for 2006–2012. Radiat Hygiene 6(1): 5-11 (2013). (Russian).
T15 Tolstykh, E.I., M.O. Degteva, N.G. Bougrov et al. Body potassium content and radiation dose from ^{40}K for the Urals population (Russia). PLoS One 11(4): e0154266 (2016).
T16 Tolstykh, E.I., L.M. Peremyslova, M.O. Degteva et al. Reconstruction of radionuclide intakes for the residents of East Urals radioactive trace (1957-2011). Radiat Environ Biophys 56(1): 27-45 (2017).
T17 Tommasone, P.F., P. Carbone, S. De Francesco et al. Rainstorm-induced soil ^{222}Rn concentration spikes observed in Southern Italy. Environ Earth Sci 73(12): 8177-8187 (2015).
T18 Tondel, M., E.M. Andersson and L. Barregard. Time trends in indoor radon concentrations in Sweden. Epidemiology 20(6): S146 (2009).
T19 Torkar, D., B. Zmazek, J. Vaupotič et al. Application of artificial neural networks in simulating radon levels in soil gas. Chem Geol 270(1-4): 1-8 (2010).

T20 Tosheva, Z., A. Kies and H. Hofmann. Radon in potable waters in Luxembourg. Nukleonika 55(4): 583-588 (2010).

T21 Trevisi, R., S. Risica, M. D'Alessandro et al. Natural radioactivity in building materials in the European Union: A database and an estimate of radiological significance. J Environ Radioact 105: 11-20 (2012).

T22 Tschiersch, J. and O. Meisenberg. Thoron exhalation from building material and related indoor concentrations. Proceedings from International Conference on Radioecology & Environmental Radioactivity Bergen, Norway, 15–20 June 2008. Norwegian Radiation Protection Authority.

T23 Tschiersch, J. and O. Meisenberg. The HMGU thoron experimental house: A new tool for exposure assessment. Radiat Prot Dosim 141(4): 395-399 (2010).

T24 Tukey, J.W. Exploratory Data Analysis Vol. 2. Addison-Wesley, Reading, MA, 1977.

T25 Tung, C.J., T.C. Chao, T.R. Chen et al. Dose reconstruction for residents living in ^{60}Co-contaminated rebar buildings. Health Phys 74(6): 707-713 (1998).

U1 Ujic, P., I. Celikovic, A. Kandic et al. Internal exposure from building materials exhaling ^{222}Rn and ^{220}Rn as compared to external exposure due to their natural radioactivity content. Appl Radiat Isot 68(1): 201-206 (2010).

U2 Ukraine. National Report on compliance with obligations under the Joint Convention on the Safety of Spent Fuel Management and on the Safety of Radioactive Waste Management, 7th review meeting. State Nuclear Regulatory Inspectorate of Ukraine, Kyiv, 2020.

U3 UN. Treaty on underground nuclear explosions for peaceful purposes (with agreed statement and protocol dated at Washington on 1 June 1990). United Nations Treaty Series 1714, No. 29638. Moscow and Washington, D.C., 1993.

U4 UN. Resolution establishing the Preparatory Commission for the Comprehensive Nuclear-Test-Ban Treaty Organization, Meeting of States Signatories. United Nations General Assembly. United Nations, New York, 1996.

U5 UN. 2022 Revision of world population prospects. United Nations Department of Economic and Social Affairs, Population Division. [Internet] Available from (https://population.un.org/wpp/)

U6 UN. Report of the scientific advisory group on the status and developments of nuclear weapons, nuclear weapon risks, the humanitarian consequences of nuclear weapons, nuclear disarmament and related issues. Second meeting of States parties to the treaty on the prohibition of nuclear weapons, 27 November–1 December 2023. Document No. TPNW/MSP/2023/8. United Nations, New York, 2023.

U7 UNEP. Depleted uranium in Bosnia and Herzegovina: Post-conflict environmental assessment. United Nations Environment Programme, Nairobi, 2003.

U8 UNSCEAR. Report of the United Nations Scientific Committee on the Effects of Atomic Radiation to the General Assembly thirteenth session. Supplement No. 17 (A/3838). United Nations Scientific Committee on the Effects of Atomic Radiation, New York, 1958.

U9 UNSCEAR. Report of the United Nations Scientific Committee on the Effects of Atomic Radiation to the General Assembly seventeenth session. Supplement No.16 (A/5216). United Nations Scientific Committee on the Effects of Atomic Radiation, New York, 1962.

U10 UNSCEAR. Ionizing radiation: Levels and effects. Volume I: Levels. UNSCEAR 1972 Report. United Nations Scientific Committee on the Effects of Atomic Radiation, 1972 Report to the General Assembly, with annexes. United Nations sales publication E.72.IX.17. United Nations, New York, 1972.

U11 UNSCEAR. Ionizing radiation: Sources and biological effects. UNSCEAR 1982 Report. United Nations Scientific Committee on the Effects of Atomic Radiation, 1982 Report to the General Assembly, with annexes. United Nations sales publication E.82.IX.8. United Nations, New York, 1982.

U12 UNSCEAR. Sources, effects and risks of ionizing radiation. UNSCEAR 1988 Report. United Nations Scientific Committee on the Effects of Atomic Radiation, 1988 Report to the General Assembly, with annexes. United Nations sales publication E.88.IX.7. United Nations, New York, 1988.

U13 UNSCEAR. Sources and effects of ionizing radiation. UNSCEAR 1993 Report. United Nations Scientific Committee on the Effects of Atomic Radiation, 1993 Report to the General Assembly,

with scientific annexes. United Nations sales publication E.94.IX.2. United Nations, New York, 1993.

U14 UNSCEAR. Sources and effects of ionizing radiation. Volume II: Effects. UNSCEAR 2000 Report. United Nations Scientific Committee on the Effects of Atomic Radiation, 2000 Report to the General Assembly, with scientific annexes. United Nations sales publication E.00.IX.4. United Nations, New York, 2000.

U15 UNSCEAR. Sources and effects of ionizing radiation. Volume I: Sources. UNSCEAR 2000 Report. United Nations Scientific Committee on the Effects of Atomic Radiation, 2000 Report to the General Assembly, with scientific annexes. United Nations sales publication E.00.IX.3. United Nations, New York, 2000.

U16 UNSCEAR. Hereditary effects of radiation. UNSCEAR 2001 Report. United Nations Scientific Committee on the Effects of Atomic Radiation, 2001 Report to the General Assembly, with scientific annex. United Nations sales publication E.01.IX.2. United Nations, New York, 2001.

U17 UNSCEAR. Effects of ionizing radiation. Volume I: Report to the General Assembly, Scientific Annexes A and B. UNSCEAR 2006 Report. United Nations Scientific Committee on the Effects of Atomic Radiation. United Nations sales publication E.08.IX.6. United Nations, New York, 2008.

U18 UNSCEAR. Effects of ionizing radiation. Volume II: Scientific Annexes C, D and E. UNSCEAR 2006 Report. United Nations Scientific Committee on the Effects of Atomic Radiation. United Nations sales publication E.09.IX.5. United Nations, New York, 2009.

U19 UNSCEAR. Sources and effects of ionizing radiation. Volume I: Sources: Report to the General Assembly, Scientific Annexes A and B. UNSCEAR 2008 Report. United Nations Scientific Committee on the Effects of Atomic Radiation. United Nations sales publication E.10.XI.3. United Nations, New York, 2010.

U20 UNSCEAR. Sources and effects of ionizing radiation. Volume II: Effects: Scientific Annexes C, D and E. UNSCEAR 2008 Report. United Nations Scientific Committee on the Effects of Atomic Radiation. United Nations sales publication E.11.IX.3. United Nations, New York, 2011.

U21 UNSCEAR. Report of the United Nations Scientific Committee on the Effects of Atomic Radiation 2010. Fifty-seventh session, includes scientific report: Summary of low-dose radiation effects on health. UNSCEAR 2010 Report. United Nations Scientific Committee on the Effects of Atomic Radiation. United Nations sales publication M.II.IX.4. United Nations, New York, 2011.

U22 UNSCEAR. Sources, effects and risks of ionizing radiation. Volume I: Report to the General Assembly and Scientific Annex A. UNSCEAR 2013 Report. United Nations Scientific Committee on the Effects of Atomic Radiation. United Nations sales publication E.14.IX.1. United Nations, New York, 2014.

U23 UNSCEAR. Sources, effects and risks of ionizing radiation. Report to the General Assembly and Scientific Annexes A and B. UNSCEAR 2012 Report. United Nations Scientific Committee on the Effects of Atomic Radiation. United Nations sales publication E.16.IX.1. United Nations, New York, 2015.

U24 UNSCEAR. Sources, effects and risks of ionizing radiation. Report to the General Assembly and Scientific Annexes A, B, C and D. UNSCEAR 2016 Report. United Nations Scientific Committee on the Effects of Atomic Radiation. United Nations sales publication E.17.IX.1. United Nations, New York, 2017.

U25 UNSCEAR. Sources, effects and risks of ionizing radiation. Report to the General Assembly and Scientific Annexes A and B. UNSCEAR 2017 Report. United Nations Scientific Committee on the Effects of Atomic Radiation. United Nations sales publication E.18.IX.1. United Nations, New York, 2018.

U26 UNSCEAR. Evaluation of data on thyroid cancer in regions affected by the Chernobyl accident. A white paper to guide the Scientific Committee's future programme of work. United Nations Scientific Committee on the Effects of Atomic Radiation. United Nations, New York, 2018.

U27 UNSCEAR. Sources, effects and risks of ionizing radiation. Report to the General Assembly and Scientific Annexes A and B. UNSCEAR 2019 Report. United Nations Scientific Committee

on the Effects of Atomic Radiation. United Nations sales publication E.20.IX.5. United Nations, New York, 2020.

U28 UNSCEAR. Sources, effects and risks of ionizing radiation. Volume III: Scientific Annex C. UNSCEAR 2020/2021 Report. United Nations Scientific Committee on the Effects of Atomic Radiation. United Nations sales publication E.21.IX.3. United Nations, New York, 2021.

U29 UNSCEAR. Sources, effects and risks of ionizing radiation. Volume II: Scientific Annex B. UNSCEAR 2020/2021 Report. United Nations Scientific Committee on the Effects of Atomic Radiation. United Nations sales publication E.21.IX.2. United Nations, New York, 2021.

U30 UNSCEAR. Sources, effects and risks of ionizing radiation. Volume IV: Scientific Annex D. UNSCEAR 2020/2021 Report. United Nations Scientific Committee on the Effects of Atomic Radiation. United Nations sales publication E.21.IX.4. United Nations, New York, 2021.

U31 UNSCEAR. Sources, effects and risks of ionizing radiation. Volume I: Report to the General Assembly and Scientific Annex A. UNSCEAR 2020/2021 Report. United Nations Scientific Committee on the Effects of Atomic Radiation. United Nations sales publication E.21.IX.1. United Nations, New York, 2021.

U32 Uosif, M.A. and A. El-Taher. Radiological assessment of Abu-Tartur phosphate, Western Desert Egypt. Radiat Prot Dosim 130(2): 228-235 (2008).

U33 Urosevic, V., D. Nikezic and S. Vulovic. A theoretical approach to indoor radon and thoron distribution. J Environ Radioact 99(12): 1829-1833 (2008).

U34 Urso, L., C. Ipbüker, K. Mauring et al. D9.62 – Methodology to quantify improvement: Guidance on uncertainty analysis for radioecological models. H2020–662287. European Joint Programme for the Integration of Radiation Protection Research, Brussels, 2019.

U35 US. National Report for the seventh review meeting of the Joint Convention on the Safety of Spent Fuel Management and on the Safety of Radioactive Waste Management. United States Department of Energy, Washington, DC, 2020.

U36 USDOE. Announced United States nuclear tests: July 1945 through December 1989. DOE/NV-209 (rev. 13). United States Department of Energy, Las Vegas, NV, 1990.

U37 USDOE. Project Chariot site assessment and remedial action final report. DOE/NV-368. Nevada Environmental Restoration Project. United States Department of Energy, Las Vegas, NV, 1994.

U38 USDOE. Defense related uranium mines: Report to Congress. United States Department of Energy, Washington, DC, 2014.

U39 USDOE. United States Nuclear Tests July 1945 through September 1992. DOE/NV-209 (rev. 16). United States Department of Energy, Las Vegas, NV, 2015.

U40 USDOE. Summary of annual site environmental reports. Calendar Year 2022. United States Department of Energy, Grand Junction, CO, 2022.

U41 USDOE. Summary of annual site environmental report radiological doses and releases 2015−2018. United States Department of Energy, Grand Junction, CO, 2022.

U42 USDOE. Nevada National Security Site Environmental Report 2022. DOE/NV/03624-1788. (T.J. Redding, ed.) United States Department of Energy, Las Vegas, NV, 2023.

U43 USDOE. Fact sheet: Gnome-coach, New Mexico, Site - A Nevada offsite, United States Department of Energy, Las Vegas, NV, 2023.

U44 USDOE. Fact sheet: Chariot, Alaska site - A Nevada offsite. U.S. Department of Energy. [Internet] Available from (https://www.energy.gov/lm/articles/chariot-alaska-site-fact-sheet) on 12.02.2024.

U45 USDOE. Fact sheet: Rulison, Colorado site - A Nevada offsite, United States Department of Energy, Las Vegas, NV, 2023.

U46 USDOE. Annual Site Environmental Reports (ASER). United States Department of Energy. [Internet] Available from (https://www.energy.gov/ehss/doe-annual-site-environmental-reports-aser) on 23.02.2024.

U47 USDON. Submarine Force Pacific (SUBPAC) commands: Attack submarines. United States Department of the Navy. [Internet] Available from (https://www.csp.navy.mil/SUBPAC-Commands/Submarines/Attack-Submarines/) on 08.12.2023.

U48 USEIA. Nuclear explained. United States Energy Information Administration. [Internet] Available from (http://eia.doe.gov/cneaf/nuclear/page/intro.html) on 07.11.2023.

U49 USEPA. Uranium location database compilation. EPA 402-R-05-009. Technologically Enhanced Naturally Occuring Radioactive Materials (TENORM). United States Environmental Protection Agency, Washington, DC, 2006.

U50 USEPA. Corrective action at Johnston Atoll. United States Environmental Protection Agency. [Internet] Available from (https://www.epa.gov/pi/corrective-action-johnston-atoll) on 14.12.2023.

U51 USFWS. Johnston Atoll National Wildlife Refuge. United States Fish & Wildlife Service. [Internet] Available from (https://www.fws.gov/refuge/johnston-atoll) on 14.12.2023.

U52 USGS. Factsheet: Radioactive elements in coal and fly ash: Abundance, forms, and environmental significance, United States Geological Survey, 1997.

U53 USMDH. Radioactive materials regulatory guide: Production of radioactive material using a cyclotron, Minnesota Department of Health, Radioactive Materials Unit. St. Paul, MN, 2008.

U54 USNRC. Environmental assessment of ionization chamber smoke detectors containing Am-241. NUREG/CR-1156. Office of Nuclear Material Safety and Safeguards, U.S. Nuclear Regulatory Commission, Washington, DC, 1979.

U55 USNRC. Systematic radiological assessment of exemptions for source and byproduct materials, U.S. Nuclear Regulatory Commission. Washington, DC, 2001.

U56 USNRC. Spent fuel transportation risk assessment. Final Report NUREG-2125. U.S. Nuclear Regulatory Commission, Washington, DC, 2012.

U57 Usoskin, I.G. and G.A. Kovaltsov. Production of cosmogenic ^{7}Be isotope in the atmosphere: Full 3-D modeling. J Geophys Res 113: D12107 (2008).

U58 Utkin, S.S. On the Techa's reservoirs cascade influence on the long-term forecast of the Techa river radioactive contamination. Radiat Hygiene 9(3): 36-42 (2016). (Russian).

V1 Vakulovsky, S.M., A.I. Nikitin, V.B. Chumichev et al. Data on radioactive contamination of the territory of settlements of the Russian Federation with ^{137}Cs, ^{90}Sr, $^{239+240}$Pu. 2020. (Russian).

V2 Valmari, T., I. Makelainen, H. Reisbacka et al. Finnish radon situation analysed using national measurement database. Radiat Prot Dosim 145(2-3): 101-106 (2011).

V3 Valmari, T., H. Arvela and H. Reisbacka. Radon in Finnish apartment buildings. Radiat Prot Dosim 152(1-3): 146-149 (2012).

V4 Vandecasteele, C.M., M. Sonck and D. Degueldre. Rejet accidentel d'iode-131 par l'IREsur le site de Fleurus: Retour d'expérience de l'autorité de sûreté belge. Radioprotection 46(2): 159-173 (2011). (French).

V5 Vandenhove, H., L. Sweeck, D. Mallants et al. Assessment of radiation exposure in the uranium mining and milling area of Mailuu Suu, Kyrgyzstan. J Environ Radioact 88(2): 118-139 (2006).

V6 Vanmarcke, H., J. Paridaens and P. Froment. Synoptique de la problématique NORM dans l'industrie belge. CK-CEN, NRG en AV-Controlatom R-3775. Mol, 2003. (French).

V7 Varshney, R., A.K. Mahur, R.G. Sonkawade et al. Evaluation and analysis of ^{226}Ra, ^{232}Th, ^{40}K and radon exhalation rate in various grey cements. Indian J Pure Appl Phys 48: 473-477 (2010).

V8 Vasilyev, A. and I. Yarmoshenko. Effect of energy-efficient measures in building construction on indoor radon in Russia. Radiat Prot Dosim 174(3): 419-422 (2017).

V9 Vasylenko, V.V., G.M. Zadorozhna, M.S. Kuriata et al. Comprehensive radiological and hygienic monitoring of particular settlements of Kyiv region in 2019. Probl Radiac Med Radiobiol 25: 188-203 (2020). (Russian).

V10 Vasylenko, V.V., M.S. Kuriata, V.V. Morozov et al. Comprehensive radiation and hygienic monitoring in population of the Rivne oblast radiologically contaminated territories. Probl Radiac Med Radiobiol 26: 124-140 (2021). (Russian).

V11 Vasylenko, V.V., M.S. Kuriata, V.V. Morozov et al. Complex radiation and hygienic monitoring of population on radiologically contaminated territories of Zhytomyr oblast in 2021. Probl Radiac Med Radiobiol 27: 150-166 (2022). (Russian).

V12 Vaupotič, J. and N. Kavasi. Preliminary study of thoron and radon levels in various indoor environments in Slovenia. Radiat Prot Dosim 141(4): 383-385 (2010).

V13 Vaupotič, J., I. Kobal and M.J. Križman. Background outdoor radon levels in Slovenia. Nukleonika 55(4): 579-582 (2010).

V14 Vaupotič, J., T. Streil, S. Tokonami et al. Diurnal variations of radon and thoron activity concentrations and effective doses in dwellings in Niška Banja, Serbia. Radiat Prot Dosim 157(3): 375-382 (2013).

V15 Veerasamy, N., R. Murugan, S. Kasar et al. Geochemical characterization of monazite sands based on rare earth elements, thorium and uranium from a natural high background radiation area in Tamil Nadu, India. J Environ Radioact 232: 106565 (2021).

V16 Vesper, B.E., M. Dooley, T.H. Mohaupt et al. Cleanup of Johnston Atoll missile launch facility. Report No. TR88-1. AFRRI Technical Report. Armed Forces Radiobiology Research Institute. U.S. Defence Technical Information Center, Bethesda, MD, 1988.

V17 Vienneau, D., S. Boz, L. Forlin et al. Residential radon - Comparative analysis of exposure models in Switzerland. Environ Pollut 271: 116356 (2021).

V18 Vinson, D.S., T.R. Campbell and A. Vengosh. Radon transfer from groundwater used in showers to indoor air. Appl Geochem 23(9): 2676-2685 (2008).

V19 Visnuprasad, A.K., G. Jaikrishnan, B.K. Sahoo et al. Contribution of thoron and progeny towards inhalation dose in a thorium abundant beach environment. Radiat Prot Dosim 178(4): 405-413 (2018).

V20 Vlasova, N.G. Methodological approach to individualized dose reconstruction of people exposed due to the accident at the Chernobyl NPP. Med Radiol Radiat Saf 58(3): 24-33 (2013).

V21 Vlasova, N.G. Doses assessment of population at long-term period after Chernobyl accident. Radiat Hygiene 7(3): 9-18 (2014). (Russian).

V22 Voitsekhovitch, O., Y. Soroka and T. Lavrova. Uranium mining and ore processing in Ukraine – radioecological effects on the Dnipro River water ecosystem and human health. pp. 206-214 in: Radionuclides in the Environment. Elsevier, 2006.

V23 Vukotic, P., Z. Stojanovska and N. Antovic. Developing a method for predicting radon concentrations above a reference level in new Montenegrin buildings. J Environ Radioact 227: 106500 (2021).

W1 Waclawek, Z. Remediation of the low-level radioactive waste tailing pond in Kowary (Poland). International Symposium on Restoration of Environments with Radioactive Residues Arlington, VA, USA, 29 November–3 December 1999. International Atomic Energy Agency

W2 Watson, S.J., A.L. Jones, W.B. Oatway et al. Ionising radiation exposure of the UK population: 2005 review. UK Health Protection Agency, Chilton, 2005.

W3 Weise, K. and W. Woger. A Bayesian theory of measurement uncertainty. Meas Sci Technol 3: 1-11 (1992).

W4 Whitcomb, R.C., Jr. Reconstruction and analysis of ^{137}Cs fallout deposition patterns in the Marshall Islands. Health Phys 82(3): 304-315 (2002).

W5 WHO. Depleted uranium: Sources, exposure and health effects. World Health Organization, Geneva, 2001.

W6 WHO. Food cluster diets. World Health Organization. [Internet] Available from (https://www.who.int/data/gho/samples/food-cluster-diets) on 02.05.2023.

W7 WHO. Guidelines for drinking-water quality: Fourth edition incorporating the first and second addenda. World Health Organization, Geneva, 2022.

W8 WHO. Global Environment Monitoring System (GEMS/Food) - Food contamination monitoring and assessment programme. World Health Organization. [Internet] Available from (https://www.who.int/teams/nutrition-and-food-safety/databases/global-environment-monitoring-system-food-contamination) on 30.04.2023.

W9 Widner, T.E. and S.M. Flack. Characterization of the world's first nuclear explosion, the Trinity test, as a source of public radiation exposure. Health Phys 98(3): 480-497 (2010).

W10 Wilkinson, W. Radiation dose assessment for transport of nuclear fuel cycle materials. Information paper. World Nuclear Transport Institute, London, 2006.

W11 Williams, G.A., R.S. O'Brien, M. Grzechnik et al. Estimates of radiation doses to the skin for people camped at Wallatinna during the UK Totem 1 atomic weapons test. Radiat Prot Dosim 174(3): 322-336 (2017).

W12 Wilson-Nichols, M.J., J.E. Wilson, L.M. McDowell-Boyer et al. Independent verification of plutonium decontamination on Johnston Atoll (1992-1996). Oak Ridge National Laboratory, Grand Junction, CO, 1998.

W13 Wilson-Nichols, M.J., P.V. Egidi, E.K. Roemer et al. Independent verification survey of the clean coral storage pile at the Johnston Atoll plutonium-contaminated soil remediation project. Oak Ridge National Laboratory, Grand Junction, CO, 2000.

W14 Winkler, R., F. Ruckerbauer and K. Bunzl. Radon concentration in soil gas: A comparison of the variability resulting from different methods, spatial heterogeneity and seasonal fluctuations. Sci Total Environ 272(1-3): 273-282 (2001).

W15 Wise, K.N. and J.R. Moroney. Public health impact of fallout from British nuclear weapons tests in Australia, 1952-1957. Report No. ARL-TR-105. Australian Radiation Laboratory, Melbourne, 1992.

W16 WNA. Nuclear reactors and radioisotopes for space. World Nuclear Association. [Internet] Available from (https://world-nuclear.org/information-library/non-power-nuclear-applications/transport/nuclear-reactors-for-space.aspx) on 11.12.2023.

W17 WNA. World uranium mining production. World Nuclear Association. [Internet] Available from (https://world-nuclear.org/information-library/Nuclear-Fuel-Cycle/Mining-of-Uranium/World-Uranium-Mining-Production) on 01.08.2024.

W18 WNA. The nuclear fuel report: Expanded summary – Global scenarios for demand and supply availability 2021-2040. World Nuclear Association, London, 2022.

W19 WNA. World nuclear performance report 2023. World Nuclear Association, London, 2023.

W20 WNTI. Frequently asked questions about nuclear transport: How many shipments take place annually. World Nuclear Transport Institute. [Internet] Available from (https://www.wnti.co.uk/industry/faqs/) on 22.06.2023.

W21 Wolf, S.F., J.K. Bates, E.C. Buck et al. Physical and chemical characterization of actinides in soil from Johnston Atoll. Environ Sci Technol 31(2): 467-471 (1997).

W22 Wu, Y., H. Sun, D. Liu et al. Levels and distribution of indoor radon concentrations in Shenzhen, China. Chinese J Radiol Med Prot 36(7): 513-516 (2016).

W23 Wu, Y., Z. Qin, X. Zhao et al. Radionuclide contents in food collected from regions surrounding retired uranium mine in Northwest of Guangxi and their committed dose to public. Occup Health 35: (2019).

W24 Wymer, D.G. and J.C. Botha. Managing the environmental impacts of low activity wastes from the South African gold mining industry. Proceedings of the 8th International Conference on Radioactive Waste Management and Environmental Remediation (ASME 2001), Bruges, Belgium, 30 September–4 October 2001.

W25 Wysocka, M., S. Chalupnik, B. Michalik et al. Environmental impact of coal mining on the natural environment in Poland. Proceedings of the International Symposium on Technologically enhanced natural radiation (TENR II), Rio de Janeiro, Brazil, 12–17 September 1999.

X1 Xiang, L., P.-h. Liu, X.-f. Jiang et al. Health risk assessment and spatial distribution characteristics of heavy metal pollution in rice samples from a surrounding hydrometallurgy plant area in No. 721 uranium mining, East China. J Geochem Explor 207: 106360 (2019).

X2 Xie, D., M. Liao, H. Wang et al. A study of diurnal and short-term variations of indoor radon concentrations at the University of Michigan, USA and their correlations with environmental factors. Ind Built Environ 26(8): 1051-1061 (2016).

X3 Xu, L., L. Ge, Y. Gu et al. Investigation of indoor radon concentration and radiation levels in Chengdu area. China Environ Sci 33(2): 351-356 (2013).

Y1 Yao, Y., B. Chen and W. Zhuo. Reanalysis of residential radon surveys in China from 1980 to 2019. Sci Total Environ 757: 143767 (2021).

Y2 Yarmoshenko, I., A. Vasilyev, G. Malinovsky et al. Variance of indoor radon concentration: Major influencing factors. Sci Total Environ 541: 155-160 (2016).

Y3 Yarmoshenko, I., A. Onishchenko, G. Malinovsky et al. Radon time series in four flats in energy efficient multi-storey building. Radiat Prot Dosim 191(2): 228-232 (2020).

Y4 Yarmoshenko, I., M. Zhukovsky, A. Onishchenko et al. Factors influencing temporal variations of radon concentration in high-rise buildings. J Environ Radioact 232: 106575 (2021).

Y5 Yarmoshenko, I.V., A.V. Vasilyev, A.D. Onishchenko et al. Indoor radon problem in energy efficient multi-storey buildings. Radiat Prot Dosim 160(1-3): 53-56 (2014).

Y6 Yarmoshenko, I.V., G.P. Malinovsky, M.V. Zhukovsky et al. Comparison of measures on protection against accidental radiation and indoor radon exposure in Muslyumovo, Techa River. Radiat Prot Dosim 177(1-2): 125-129 (2017).

Y7 Yarmoshenko, I.V., A.D. Onishchenko, G.P. Malinovsky et al. Modeling and justification of indoor radon prevention and remediation measures in multi-storey apartment buildings. Results Eng 16: 100754 (2022).

Y8 Yasuda, H. JISCARD EX Personal Edition User's Manual. Ver.1.0. National Institute of Radiological Sciences, Chiba, 2008.

Y9 Yukihara, E.G. and S. Estier. Ergebnisse der Ganzkörpermessungen. in: Umwelradioaktivität und Strahlendosen in der Schweiz 2019. Bundesamt für Gesundheit, Abteilung Strahlenschutz, Bern, 2019. (German).

Z1 Zeevaert, T., L. Sweeck and H. Vanmarcke. The radiological impact from airborne routine discharges of a modern coal-fired power plant. J Environ Radioact 85(1): 1-22 (2006).

Z2 Zhang, L., C. Liu and Q. Guo. Measurements of thoron and radon progeny concentrations in Beijing, China. J Radiol Prot 28(4): 603-607 (2008).

Z3 Zhang, L. and Q. Guo. Observation and analysis of atmospheric radon in Qingdao, China. J Radiol Prot 31(1): 129-134 (2011).

Z4 Zhang, L., Y. Wang and Q. Guo. One-Year continuous measurement of outdoor radon progeny concentration in Beijing area. J Radiat Prot Res 45(3): 95-100 (2020).

Z5 Zhang, Z., F. Wen, X. Xu et al. ^{210}Po content in vegetables eaten by residents and estimation of internal exposure dose. Chinese J Radiol Health 29 (2020).

Z6 Zheng, X., Q. Sun, X. Jing et al. Evolution of pore structure and radon exhalation characterization of porous media grouting. Sci Total Environ 865: 161352 (2023).

Z7 Zhou, L., J. Berquist, Y. Li et al. Passive soil depressurization in Canadian homes for radon control. Build Environ 188: 107487 (2021).

Z8 Zhou, Y., N. Yu, J. Wang et al. Review of the 5·7 Nanjing ^{192}Ir source radiological accident. Radiat Med Prot 3(4): 190-195 (2022).

Z9 Zhukovsky, M., M. Vasyanovich, A. Onishchenko et al. Anomalously high unattached fraction of ^{220}Rn decay products in the atmosphere of monazite storage facility. Appl Radiat Isot 151: 1-6 (2019).

Z10 Zhukovsky, M.V. and A.V. Vasilyev. Mechanisms and sources of radon entry in buildings constructed with modern technologies. Radiat Prot Dosim 160(1-3): 48-52 (2014).

Z11 Zhuo, W., T. Iida, J. Moriizumi et al. Simulation of the concentrations and distributions of indoor radon and thoron. Radiat Prot Dosim 93(4): 357-368 (2001).

Z12 Zippel, C., J. Ermert, M. Patt et al. Cyclotrons operated for nuclear medicine and radiopharmacy in the German speaking D-A-CH countries: An update on current status and trends. Front Nucl Med 2: 850414 (2022).

Z13 Zoran, M.A., M.R. Dida, A.T. Zoran et al. Outdoor ^{222}Radon concentrations monitoring in relation with particulate matter levels and possible health effects. J Radioanal Nucl Chem 296(3): 1179-1192 (2012).

Z14 Zunić, Z.S., K. Kozak, G. Ciotoli et al. A campaign of discrete radon concentration measurements in soil of Niška Banja town, Serbia. Radiat Meas 42(10): 1696-1702 (2007).

Z15 Zunić, Z.S., I.V. Yarmoshenko, A. Birovljev et al. Radon survey in the high natural radiation region of Niska Banja, Serbia. J Environ Radioact 92(3): 165-174 (2007).

unscear.org

This publication contains:

VOLUME II

Scientific annex with appendix

Scientific annex

Annex B: Evaluation of public exposure to ionizing radiation

EVALUATING RADIATION SCIENCE FOR INFORMED DECISION-MAKING

In 1955 the United Nations General Assembly established the Scientific Committee on the Effects of Atomic Radiation (UNSCEAR) in response to concerns about the effects of ionizing radiation on human health and the environment. At that time fallout from atmospheric nuclear weapons tests was reaching people through air, water and food. UNSCEAR was to collect and evaluate information on the levels and effects of ionizing radiation. Its first reports laid the scientific grounds on which the Partial Test Ban Treaty prohibiting atmospheric nuclear weapons testing was negotiated in 1963.

Over the decades, UNSCEAR has evolved to become the world authority on the global levels and effects of exposure to ionizing radiation. UNSCEAR's independent and objective evaluations of the science are to provide for—but not address—informed policymaking and decision-making related to radiation risks and protection.

ISBN 978-92-1-003331-2

9 789210 033312

2519504